THE STUDY OF OPTIMAL MODEL REFERENCE ADAPTIVE CONTROL OF A CONTINUOUS STIRRED TANK REACTOR USING AN ON-LINE HYBRID COMPUTER

by

YUNG-CHENG CHAO

M.Sc., University of Wisconsin

A Thesis

submitted in fulfilment of the requirements

for the degree of Doctor of Philosophy

The Department of Chemical Engineering

The University of Aston in Birmingham,

Birmingham, U.K.

June 1972.

SUMMARY

A general algorithm and theory of optimal model reference adaptive control (OMRAC) for processes with n-state variables has been developed, and its need was strongly supported by the results of a comprehensive literature survey and analysis. The theory has been tested on a fully and a partially simulated continuous stirred tank reactor using two state variables and, in both cases, has given satisfactory results. A hybrid computer has been used for both operations, and in the partially simulated case a well-stirred vessel with its auxiliary heat transfer equipment was used as the real plant item.

OMRAC is a combination of two schemes, viz. the optimal model reference (OMR) scheme and the optimal adaptive control (OAC) scheme. The optimal model reference scheme is generated by an optimal control law, $m^*(t)$ with constant parameters to generate optimal state variable profiles or trajectories, $\theta^r(t)$. The optimal adaptive control scheme is generated by a modified optimal control law, $U^*(t)$ with constant parameters to minimise the difference between the optimal state variable profiles, $\theta^r(t)$, and the real process variables, $\theta(t)$, in the presence of unmeasurable changing parameters.

The theoretical development of OMRAC has been confirmed for a range of possible operating conditions both in complete simulation tests and also in experimental on-line operation of the partially simulated system. The operation of the on-line hybrid computer control system was successful and gave a reliable performance

provided care was taken in the computer programming and precautions for linear interface design and output response sensitivity were implemented.

DEDICATION

to

My Mother

and

My Wife

A C K N O W L E D G E M E N T S

The author wishes to express his sincere thanks to the following:-

Mr.A.R.Cooper of the Department of Chemical Engineering, for his kind help, encouragement and supervision.

Dr.B.Gay of the Department of Chemical Engineering, for his kind help.

Mr.N.Roberts, Chief Technician of the Department of Chemical Engineering, and his staff for their technical assistance.

The National Science Council, Republic of China, for the research fellowship.

I N D E X

Page

INDEX TO TABLES

INDEX TO FIGURES

CHAPTER 1. INTRODUCTION

On the existing equipment for a continuous stirred tank reactor (CSTR), the heat release of an exothermic reaction is partially simulated in the reactor by means of immersion heaters. A study of such a "Partial Simulation Technique" has been made by Buxton at the end of 1970 (80). As an extension of this research work, the following three points have been considered:

1. All of the original parameters of the system were assumed to be constant, i.e. it was not adaptive.
2. The original control system was designed to incorporate continuous three mode feedback control, i.e. it was not optimal control.
3. For the original complete and partial simulation a conventional temperature controller was used, i.e. it was not on-line computer control.

By including a combination of developments to overcome the above three limitations, a single complete system was proposed for the present research work, and strong support is given as a result of a comprehensive literature survey.

The major objectives of this research work were:

1. Theoretical development of the optimal model reference adaptive control (OMRAC) system combined with the more complicated general optimal PID control laws.
2. Complete simulation of the developed OMRAC system applied to a CSTR using the combined TR-10 and TR-48 hybrid computers.
3. On-line computer system design and operation of developed OMRAC applied to a CSTR using TR-10 and TR-48 hybrid computers.

All this research work can be represented by a complete block diagram shown in Fig.1.1.

From Fig.1.1. this research is divided into two parts:

Part I. Theoretical and complete simulation work (Chapters 3, 4, 5,6, and 7).

Part II On-line computer control work (Chapters 8, 9, 10 and 11).

A comprehensive literature survey is shown in Chapter 2, and two systematic summary tables and the discussion indicate the features of originality of this research work.

As an extension of the basic concept of my previous work, (see 2.4.2) [67], a general algorithm and theory of OMRAC system was developed theoretically and complicated general optimal PID control laws for the optimal adaptive control (OAC) scheme were derived in detail and are shown in Chapter 3.

From the theoretical development, the OMRAC scheme is combined with the OMR scheme and the OAC scheme.

Based on Pontryagin's maximum principle, the mathematical derivation both of the OMR scheme and the OAC scheme for a CSTR are shown in Chapters 4 and 5 respectively. A total of twenty-eight non-linear algebraic equations to determine all of the coefficients of different optimal PID control laws were solved by digital computer (Appendix 1). The overall three OMRAC schemes are shown in Chapter 6.

From Chapters 3, 4, 5 and 6 a complete simulation of the developed OMRAC system applied to a CSTR using TR-10 and TR-48 hybrid computers is shown in Chapter 7. All hybrid computer programming with all sealed computer variable equations of the overall OMRAC scheme were designed and programmed in detail and are shown in Figs. 7.1 to 7.6 while the corresponding potentiometer and amplifier settings for each figure and the static checks are shown in Tables 7.2 to 7.7. A total of sixty-nine plotted figures for different operating cases with different conditions are shown in Figs. 7.7. to 7.54. and in Appendix 2. Analysis and discussion of all the theoretical results are shown at the end of this chapter.

In Part I, the theoretical development of OMRAC has been positively proved, and the further work of on-line hybrid computer system design and operation in combination with a partially simulated CSTR is studied and shown in Part II.

On-line computer OMRAC system is shown in Chapter 8.

The overall functional diagram and the modified experimental apparatus designed for the on-line computer OMRAC system are shown in Fig. 8.1 and all calibrations of experimental apparatus are shown in Appendix 4.

The requirements of interface system design as for any industrial transmitter is that the terminal relation between the computer side and the process side must be extremely linear.
To meet this requirement, the interface system was designed in detail and is shown in Fig. 8.2. All on-line computer programming of the OMRAC scheme with the interface system designs were programmed in detail and are shown in Fig. 8.3.

A continuous test run of on-line operation is shown in Chapter 9. The purpose was to test the overall performance of the on-line system and to find successful operating procedures and techniques to produce reliable and reproducible on-line computer OMRAC

All operation and analysis of on-line computer OMRAC is shown in Chapter 10.

A total of sixty-eight plotted figures for different operating cases with different conditions are shown in Figs. 10.1 to 10.68. Comparison and analysis of process response, phase-plane trajectories, optimal control laws, optimal PID control, OMRAC stability, and experimental data calculations are discussed in detail.

For a quantitative analysis and evaluation of OMRAC both for complete simulation and on-line operation, a new term "Optimal Adaptivity" is introduced in Chapter 11. Overall, sixteen three dimensional figures of optimal adaptivity are shown in Figs. 11.1 to 11.16 and the analysis and discussion follow.

An overall systematic conclusion and suggestion for future OMRAC system work are discussed in detail in Chapter 12.

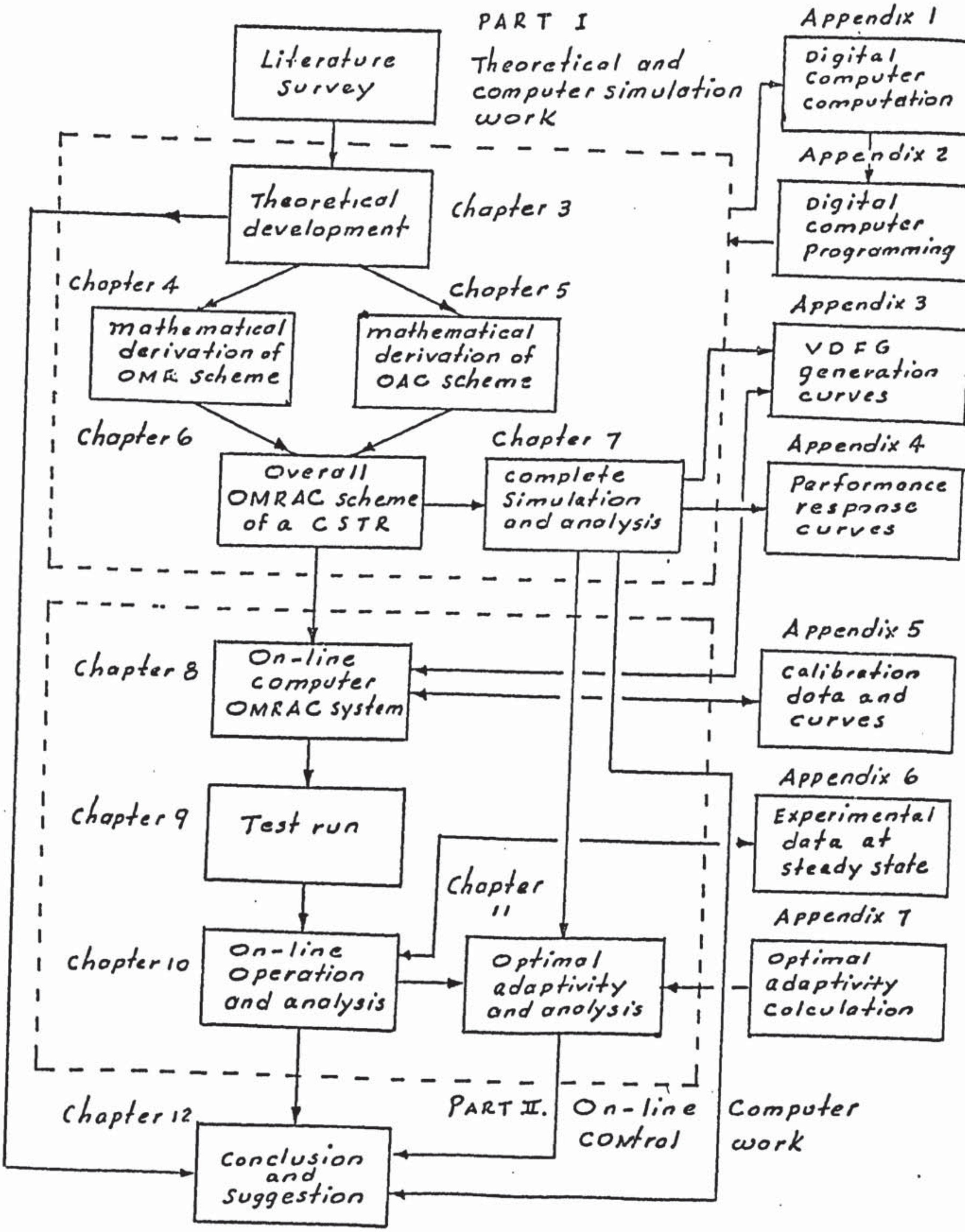

where: OMR = Optimal model reference

OAC = Optimal adaptive control

OMRAC = Optimal model reference adaptive control

Figure 1.1 Block diagram of overall research work on OMRAC of a CSTR using an on-line hybrid computer

CHAPTER 2

LITERATURE SURVEY ON ADAPTIVE CONTROL

For the past decade, adaptive control has been combined with optimal control to give a challenging new area of automatic control research[16,17].

This chapter presents a comprehensive literature survey, brief review, systematic summary and discussion of adaptive control systems. The major sources are based on a series report from William's I/EC Chemical Engineering Fundamental Review of Computers and Process Control between 1958 and 1970[1-11], four surveys and reviews[12,13,14,17], two text-books[15,16], several reference books[18-24], and forty articles up to the present time[31 ~ 71].

In this chapter, the following six sections are considered:

2.1 Basic concept, definition and classification.

2.2 General brief review of adaptive control system from known surveys and text-books.

2.3 General survey of adaptive control systems from current papers, excluding Chemical Engineering.

2.4 General Survey of adaptive control systems in Chemical Engineering.

2.5 Summary of the current literature on adaptive control systems:

   (i) A summary of the current literature on adaptive control systems (Table I).

(ii) A summary of current literature on model reference adaptive control systems (Table II).

2.6 Discussion.

2.1 Basic concept, definition and classifications

Since Draper and Li[18] published the first research paper on adaptive control in 1951 (sometimes called self-optimizing control[17]) the definition and classification of adaptive control systems have not been unified until the present time. In this section definitions are proposed upon which the whole research work will be based, and classification is given for all of the systematic survey, summary and discussion in this chapter.

2.1.1. Basic concept

In chemical processes, frequently the optimal operating conditions will be influenced by some of the uncontrollable and unmeasurable parameters and load variables such as inlet concentration, temperature profile, catalysis activity, flow and mixing pattern, overall heat transfer rate, mass transfer rate and ambient external conditions. If any process operates in the presence of such an unmeasurable, uncontrollable parameter or load variable the optimal operating condition of the process can still adapt by self-adjustment or self-modification; this is the basic concept of adaptation.

Actually adaptation which is the ability of self-adjustment and self-modification in response to changing conditions of environment or structure is a fundamental attribute of living organisms[12].

2.1.2 Definition

Many definitions, varying from the specific to very general, have been advanced for adaptive control by workers such as Mishkin and Braun[15], Eveleigh[13,16], Shinners[14] and Lee, Adams and Gaines[19]. Here one general definition from Shinners is introduced as follows:

An adaptive control system is basically a feedback control system which automatically achieves a desired response or performance index in the presence of extreme change in the controlled system's parameters and major external disturbance.

From the above definition, an adaptive control system should contain the following characteristics:

(1) The system operates under a changing situation.

(2) The master control loop is always a feedback control system

(3) The system has a set of adjustable controller parameters; in servomechanisms it is always gain, filter time constant, while in process control it is the settings Kc, Ti, Td of the PID controller.

(4) Ability to determine system performance index (PI) (index of performance, figure of merit, objective function) or desired operating point or response.

(5) Ability to maintain a good quality of control with respect to certain PI by automatic adjustment of the set of adjustable parameters (Fig. 2.1).

In this research work, the modified definition of adaptive control system which is extended and based on my previous research work[67] will be defined as follows:

Adaptive control is the optimal control of a process in the presence of unmeasurable and uncontrollable parameters and load variables; the optimal control law can be modified by an adaptive controller in which different types of adaptation can be generated (Fig.2.2).

Adaptive control defined as above may be called optimal adaptive control, the differences between these two definitions are:

(i) clear emphasis that the changed process situation arises from unmeasurable and uncontrollable parameters or load variables.

(ii) Adjustment is achieved directly by optimal control system instead of by a conventional control system.

(iii) Adjustment is achieved directly by a modified optimal control law instead of by conventional adjustment of the parameters of PID controller.

2.1.3. Classifications:

The authors of three excellent surveys[12-14] suggested their different classifications of adaptive control systems from the different points of view and approaches which are used in analysis and design.

Aseltine, Manici and Sarture[12] suggested the separation of the adaptive system into five classes:

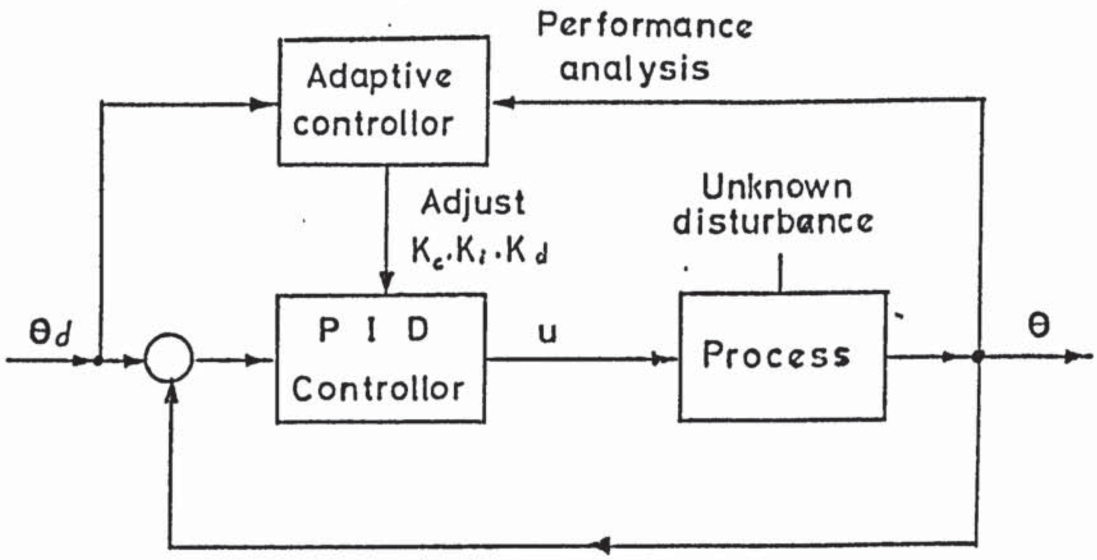

Figure 2.1 Adaptive control system by usual definition

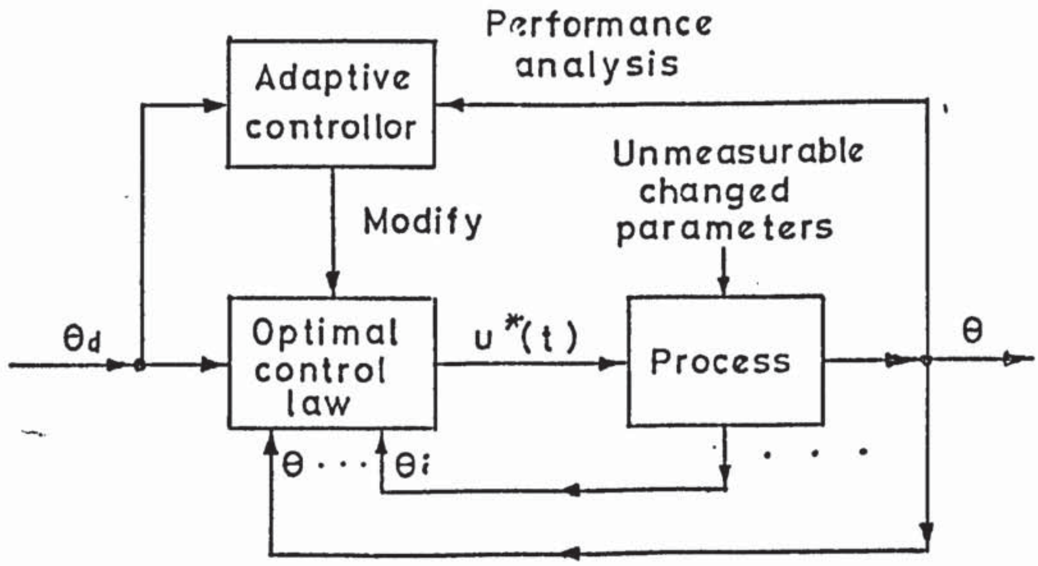

Figure 2.2 Adaptive control system by modified definition

(1) Passive or environment adaptation;

(2) Input adaptation;

(3) Extremum adaptation;

(4) System variable adaptation;

(5) System characteristic adaptation.

For the first two classes, the system adaptation is based on different locations of disturbance (environment and input). For the third class, the system adaptation is based on operating optimal performance. For the last two classes the system adaptation is based on different locations of measurement (variables and transfer functions). This classification is thus not unified.

Eveleigh[13] suggested separation of the adaptive system into four classes:

(1) Input adaptive

(2) Plant adaptive

(3) Parameter adaptive

(4) Signal synthesis adaptive.

For the first two classes, the system adaptation is based on different locations of the disturbance (input and plant). The classifications of (3) and (4) are to distinguish between direct parameter adjustment and signal synthesis adaptive systems.

So this classification is not unified either.

Shinners[14] suggested four classes:

(1) Model reference adaptive control system

(2) Non-linear adaptive control system

(3) Impulsive-response adaptive control system

(4) Digital computer controlled adaptive control system.

For class (1), the system adaptation is based on a very important type of adaptation. For class (2), the system adaptation is based on the non-linear element of the system. For class (3), the system adaptation is based on one kind of identification method[16]. For class (4), the system is adapted by using a digital computer to compute the forcing function required to obtain the desired response by iterative operation.

All of these four classes are based on different approaches and so this is not a unified classification.

According to the basic type and idea of adaptation in most of the past adaptive control research work, it is desirable to suggest a unified classification of adaptive control systems divided into the following three general classes from which all systematic survey, summary and discussion in this chapter will arise:

(1) Model Reference adaptive control

(2) Identification adaptive control

(3) System characteristic and optimization adaptive control

(1) <u>Model Reference Adaptive Control</u>: The master control system response is compared to a known model reference assumed to have the desired response characteristics. The observed response error signal is used to adjust one or more parameters in the master

control system by the adaptive controller, thereby forcing its response to approach that of the model (Fig.2.3).

(2) Identification Adaptive Control: Using some form of test signal input, the system is to be adapted by identification of characteristics of the unknown changed parameters or system transfer function or some equivalent form of information (Fig.2.4).

(3) System characteristic and optimization adaptive control: The system is to be adapted by using system characteristics and/or any optimization techniques to automatically adjust the parameters to achieve optimal performance without definite model reference and identification functions (Fig.2.1).

2.2. General brief review of adaptive control from known survey and text-books.

There are four general surveys and reviews of adaptive control(12,13,14,17). As a matter of interest the first form of adaptive control was referred to as an optimal control system by Draper and Li(18) in 1951, who reported the automatic adjustment of gasoline engine spark timing and fuel mixing to minimise manifold pressure.

2.2.1. Aseltine, Manici and Sarture(12) gave their survey in 1958. A total of 35 research articles, mostly from AIEE, IRE and ASME between 1951 and 1958 and divided into five classes (see Section 1.1.3) has been reviewed and useful

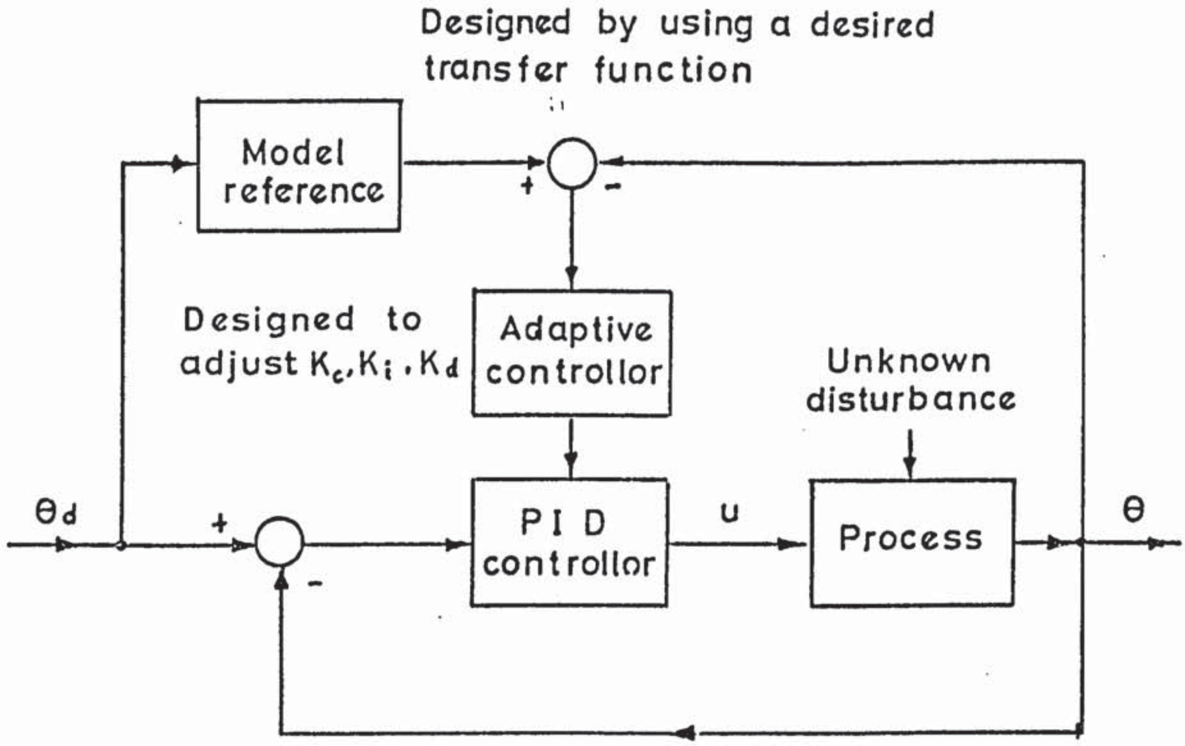

Figure 2.3 General type of model reference adaptive control system

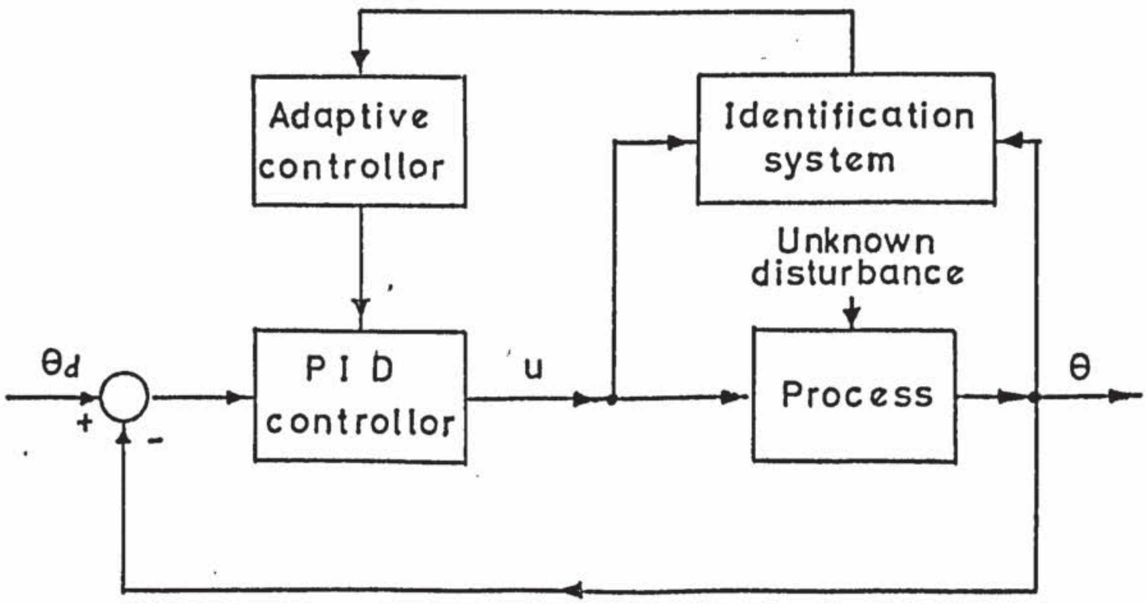

Figure 2.4 General type of identification adaptive control system

systematic Tables 2.1 and 2.2 for the characteristics of adaptive control systems have been prepared.

2.2.2 Oldenburger(17) gave a comprehensive survey both for optimal control and self-optimizing control (adaptive control). Over three hundred published articles and books, mostly from AIEE, IRE, AEEE, ASME and Automation and Remote Control, exist but no brief review and systematic summary or analysis of adaptive control from this survey was possible.

2.2.3. Shinners(14) also gave a brief review both for optimal control and adaptive control. The author introduced the basic concept of adaptivity, the types of adaptive control (See Section 1.1.3) and several examples of each type were illustrated.

It must be pointed out that the model reference adaptive control system shown in Fig.2.3, was first designed by M.I.T. Instrumentation Laboratory for use as an adaptive pilot(25). The model is based upon pilot preference, airframe limitations, performance, objective, etc. The gains in the yaw orientation loop, the roll stabilisation loop and the roll-damping loop are automatically adjusted by adaptive control.

2.2.4. Eveleigh(13) gave a more complete general review of adaptive control and most material in this review has been written in his later published book(16). This is only one of the recently published books on adaptive control systems.

The author emphasised both in his review and in his book that the adaptive control may be broken down into three major functions:

(i) Identification,

(ii) decision, and

(iii) modification.

Identification is defined as the process by which the system is characterised or by which the PI value is measured.

In the decision process, the PI measurements are used to decide how system performance is related to the desired optimum.

Modification is the process of changing the system parameters toward the optimal setting.

Decision and modification are the required basic functions to develop an adaptive controller shown on all five previous figures (Fig. 2.1 ～ Fig.2.5) respectively.

The definition of identification shown above is different from that shown in Chapter 7 of the present author's book. Identification shown in Chapter 7 is defined "exclusively as the process of measuring a system transfer function or some equivalent form of information". It is almost the same as the proposed type 2 classification (see Section 2.1.3.).

Actually identification as shown above will be divided into two parts:

(1) Identification of the system which will belong to type 2 classification.

(2) Identification of PI values which will belong to Type 3 classification.

However, "model reference", the most basic function of adaptive control, was still not included in the author's three major functions.

From the above discussion, the suggested new classification of the three basic types of adaptive control seems reasonable for the representation of all systems.

2.2.5. Several useful techniques in adaptive control

Based upon Eveleigh's book and other reference books, Several useful techniques used in adaptive control will be discussed.

A. Identification problem

Although a variety of identification methods are discussed, the three chosen for emphasis are (1) cross-correlation, (2) pulse transfer function method and (3) quasi-linearisation.

(1) Identification using cross-correlation provides direct information about the system. The output of the cross-correlation results in a point on the impulse response for the system. Additional points on the impulse response may be obtained by introducting additional cross-correlation channels having appropriate delays. This method is limited to linear systems.

(2) The pulse transfer function method is most appropriate in digital systems.

(3) Quasi-linearisation, a form of gradient method, is similar to the second variation procedure for solving boundary value problems. The basic concept is small signal linearization of the system response about a nominal path through state space. This method is an effective identification procedure which applies to both linear and non-linear systems

Sage[23] in his text-book discussed both continuous and discrete system identification and modeling using quasi-linearisation.

My previous research work[67] developed an identification function by using Z-transform and least square techniques to identify the time varying gain of a second order process.

B. <u>Steepest descent (or ascent) approach to adaptive control</u>

The steepest descent (or ascent) technique has been used for static optimization in different fields[26,27].

The strategy for a steepest descent adaptive system is identical to that used for static optimization[28]. Thus assume a PI response surface in n-dimensional parameter space with a well-defined minimum as the optimum point. Let the starting point in parameter space be

$$P_o = (a_1, a_2, - - - - a_n)$$

The operating procedure is as follows:

(1) Measure the value of $(\partial(PI)/\partial a_n)$ by perturbation of the a_n falue and observation of the results. Store the results.

(2) Form the vector:

Slope of path $P_o \longrightarrow P_1$

$$Z = \sum_{i=1}^{n} I_i \frac{\partial (PI)}{\partial a_i}$$

where I_i = standard unit vector in n space

and Z = slope of path $P_o \rightarrow P_1$

(3) Adjust the system's location by moving to the new parameter position:

$$P_1 = P_o + k Z$$

where k = adaptive gain

(4) Repeat the process until the optimum value of PI is reached.

PI response surface representative of adaptive control has been emphasised by Eveleigh in his review.
My previous published paper(30) has also discussed the PI response surface generated by steepest descent and approached by using an analogue computer.

C. <u>Sinusoidal-perturbation approach to adaptive control</u>

Figure 2.5 shows a representative variation of PI with adjustable parameter m, the effect of sinusoidal-perturbation for offset in both directions from the optimum is also illustrated.

Let:

$$m(t) = m_1 + c_1 \sin \omega t \qquad (1\text{-}1)$$

the first order Taylor's series approximation for PI, J(m,t) is given by

$$J(m_1,t) = J(m_1)t + J'(m_1)c_1 \sin t + J''(m)\frac{(c_1 \sin\omega t)^2}{2} \qquad (1\text{-}2)$$

$$+ \ldots\ldots\ldots$$

where $J'(m_1) = \left(\frac{\partial J}{\partial m}\right) m = m_1$, the slope of the PI curve.

The fundamental frequency component of $J(m_1,t)$ is proportional in magnitude to the slope of J at $m = m_1$, and it changes sign (shifts phase 180°) at $m = m^*$. Thus both the magnitude and sign of $(\partial J/\partial m)$ at $m = m_1$ are contained in the w_1 component of $J(m_1,t)$, and an adaptive loop error signal can be derived from the output using a standard (correlation) detector.

Draper and Li(18) first used this technique, Eveleigh discussed the general stability analysis of such techniques(29), while Box(61), Alpeter(69) and Price(70) all used such techniques on chemical reactors and will be discussed later.

The first book of adaptive control written by Mishkin and Braun was published in 1961, and gives the general principles and knowledge for adaptive control. There are a few optimal control text books(19-22, 24) containing some knowledge and techniques of adaptive control which are valuable for reference.

2.3. General survey of adaptive control system from current systems excluding the Chemical Engineering field.

All the material selected in this section was contained in twenty nine articles (1963-1972) and is connection on the survey of model reference. This survey may be linked with the several earlier surveys discussed in Section 1.2, to give a more complete survey of adaptive control systems.

According to the suggested classification discussed in Section 2.1.3, there are three classes:

Class 1: Model reference adaptive control system,

Class 2: Identification adaptive control system.

Class 3: System characteristic and optimization adaptive control system.

2.3.1. Model Reference Adaptive Control System (Class I)

Model reference system has proved to be one of the most popular and reliable methods in the growing field of adaptive control. The general definition and functional figure has been discussed and shown in Section 2.1.3. A total of twenty articles have been reviewed.

Halbert(31) used the hybrid computer to simulate an aircraft adaptive control system. The proposed adaptive technique utilises predicted as well as measured past information on aircraft behaviour to calculate optimum controller parameters. The optimal performance is determined by a systematic search procedure in parameter space. The search programme is under the direction of the logic elements and employs an analog computer model of the aircraft system solved at high speed for prediction purposes. Kwai(32) presented a technique for controlling two parameters with a known range of variation to give the desired dynamic performance of the system. Desired damping is used as

Model I, and desired natural frequency is used as Model 2. The equalised maximum overshoot (or under shoot) criterion and the equalised response areas criterion are employed. A second order system is considered in detail. A simulation study is made on a general purpose digital computer.

White[33] proposed a simple criterion which permits variation in the optimum adaptive parameters to be calculated as the input-signal varies. The approximate equations for the adapting system are formed by using a parameter perturbation technique. The equations are then used to give an estimate of the stability of the adaptive loop. The whole of the theoretical work is supported by extensive analogue-simulation studies.

Dressler[34] proposed a simple adaptation technique derived analytically. By solving the differential equations of the reference model and the adaptive control system, an expression was obtained showing the explicit functional dependence of the performance error on the adaptive parameter.

Graupe and Cassir[35] described a model reference adaptive control system where extrapolation techniques are used for identification and for error-prediction at discrete time intervals. The system employs rectangular adaption pulses of finite duration to minimise a cost-function of predicted square errors.

Pearson and Noonan[36] proposed a modified gradient procedure for the discrete adjustment of parameter in a model reference adaptive control problem.

Wilkie and Perkins(37) proposed the transformed state variables to pursue dynamically similar models. The parameter vector is adjusted to minimise the effect of the variable plant parameters on the system response.

Bristal, Inaloglu and Steadman,(38) proposed a response pattern or shape as the model reference instead of a particular desired response for adaptive control.

Powell(39) employs an adaptive model to estimate the state, dynamic and future trajectories of an unknown plant. By using a speeded-up model, control is automatically synthesised to minimise a performance index.

Price(40) proposed an accelerated gradient method which is capable of adapting rapidly to plant parameter variations. It is based upon the objective of improving the stability characteristics of a gradient type model reference adaptive control system. A design procedure is developed for an nth order linear plant. It is applied to the control of pitch motion for an airframe; simulation results comparing the technique with conventional gradient methods are presented.

Buxton and Powell(41) described the results of a simulated study carried out to demonstrate the feasibility of a self-adaptive automatic carrier landing system. The mean square error index was used as PI, and a suitable gradient algorithm was used as the adaptive control block.

Monopoli(42) proposed a reduction of order technique which is useful in controller design for single input, single output, linear plants which have transfer functions with zeros and parameters which vary slowly compared with the response time of the plant.

Park[43] and Monopoli[44] proposed the Liapunov direct method (i.e. the second method) to design a model reference adaptive control system and has the advantage over the MIT rule, designed by Osburn, Whitaker and Kezer[45] that the asymptotic stability is a by-product of the design.

From the introduction by Park and Monopoli, this technique was improved and extended by a number of authors, as follows:

Winsor and Roy[46] extended the technique to a broader class of linear, time-invariant plants for n state variables and r control variables.

Landau[47] extended so that more general results may be obtained in the problem of analysis and synthesis of model reference adaptive control systems from the point of view of stability, using Porov's results in the field of hyperstable systems.

Gromyko and Sankovskii[48] applied the Liapunov direct method to the construction of adaptive systems of the model by combined active(parametric)and passive(signal)adjustments.

Gilbart, Monopoli and Price[49] extended a modified Liapunov design technique for model reference adaptive control systems and showed the result in improved system convergence.

Shahein, Ghonaimy and Shen[50] presented two methods for accelerating the convergence in model reference adaptive control systems. The adaptive loop, incorporating feedback, can be synthesised either directly from a Liapunov function or indirectly from the minimisation of a Liapunov function along the steepest descent path.

The model refenence adaptive control system has been well developed using the Liapunov direct method in recent years. Here a simple introduction to the technique is given:

Consider the simple model reference adaptive control system (Fig.2.6),where the problem is to find a suitable adaptive loop to adjust K_c so that $K_c K_v$ is eventually equal to the model gain K, although it is initially different from K. Using a tentative Liapunov function:

$$V = e^2 + \lambda x^2 \quad (\lambda \text{ constant} > 0) \qquad (1\text{-}3)$$

where V = Liapunov function,

e = response error,

$x = K - K_c K_v$,

K_c = controller gain

K_v = control value gain

then $$\dot{x} = - K_v \dot{K}_c \qquad (1\text{-}4)$$

$$\frac{dV}{dt} = 2e\dot{e} + 2\lambda x\dot{x}$$

$$= 2e\left[-\frac{e}{L} + \frac{x\theta_d(t)}{L}\right] + 2\lambda x\dot{x} \qquad (1\text{-}5)$$

where $\theta_d(t)$ = input

L = time constant

Now let

$$\dot{x} = - e\theta_d(t)/\lambda t \qquad (1\text{-}6)$$

so that

$$\frac{dV}{dt} = - 2\ddot{e}^2/L \leqslant 0 \quad \text{for any value of } e \qquad (1\text{-}7)$$

Liapunov's theorem states that a system is stable if a scalar function $V(x_1, x_2, \ldots\ldots x_n)$ is found with the following properties:

1. Outside the origin, $V(x_1, x_2, \ldots x_n) > 0$
2. $V(0) = 0$
3. $V(x_1, x_2, \ldots x_n)$ is continuous and has continuous first partial derivatives in a region R about the origin
4. $\dot{V} = \frac{\partial V(x_i, x_2, \ldots x_n)}{\partial t} \leqslant 0$ in R

Hence, equation (1-6) is a necessary condition for stability of the adaptive control system.

From equations (1-4) and (1-6):

$$\dot{K}_c = \frac{e\theta_d(t)}{\lambda K_v t} \qquad (1\text{-}8)$$

or

$$K_e = \left[\frac{B'}{s}\right] \left[e \cdot \theta_d(t)\right] \qquad (1\text{-}9)$$

where

$$B' = \frac{1}{\lambda K_v t} \qquad (1\text{-}10)$$

This gives a new system represented by a Liapunov function and shown in Fig. 2.6.

4

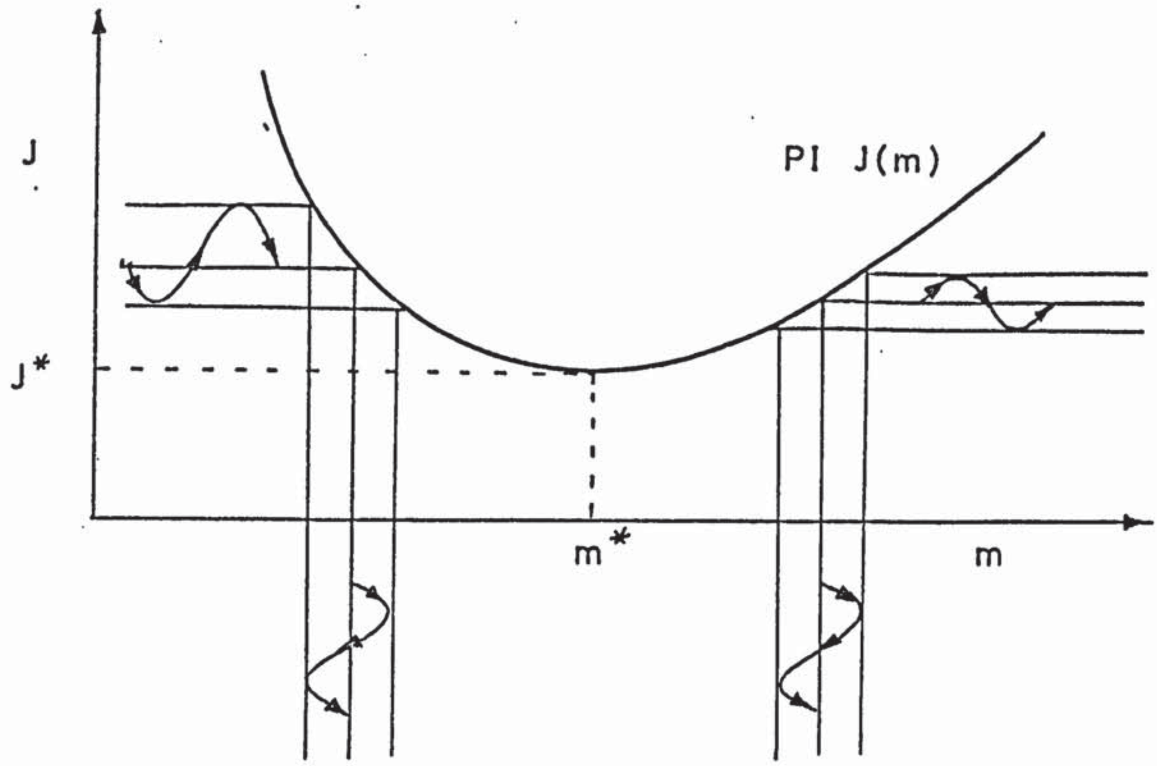

Figure 2.5 The effect of sinusoidal pertubation upon a PI function

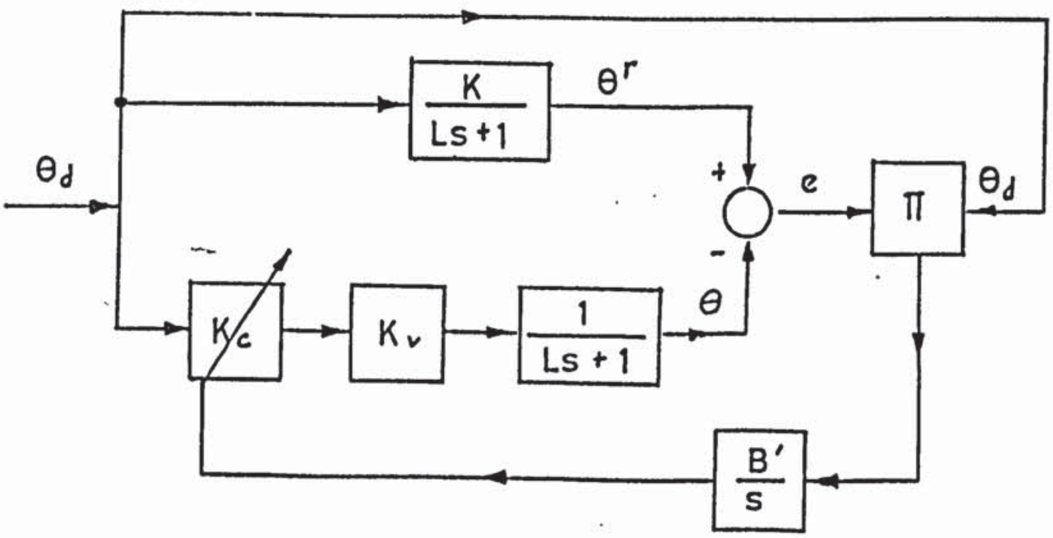

Figure 2.6 Liapunov method for model reference adaptive control

2.3.2. Identification Adaptive Control System (Class 2)

Two approaches to identification are normally used. System variable identification attempts to minimise some arbitrary error criterion by identification of the system variables. System characteristic identification or plant identification requires the determination of some information about the system such as transfer function, impulse response, damping ratio of a dominant part of the poles, or the magnitude and phase of the system output in response to a test signal.

A total of four articles are reviewed.

Womack and Watt[51] proposed an identification method which is achieved by a high frequency sinusoidal test signal. A linear control system with two variable parameters is considered, and the adaptive system is simulated by analogue computer.

Kershow[52] proposed a plant identification in which the adaptive scheme is based on measured transfer characteristics and includes an impulse transfer function computer to calculate the transfer function of the plant from the transient response to a driving signal.

Puri[53] proposed an identification algorithm based upon discrete orthogonal functions and used it to identify the flight motion parameters. This research deals with a digital autopilot design for flight path control. Three subroutines were contained in the adaptive control computer: identification subroutine, optimal synthesis subroutine and adaptive compensation subroutine.

Obradovic (54) proposed an adaptive and optimal time control method for processes with time varying coefficients. The method is primarily based on the area formed between the curves presenting the input and output variables of a controlled process. The method permits the process identification in terms of an equivalent linear transfer function with time delay during a real control transient.

2.3.3. System characteristics and Optimization adaptive control systems (Class 3)

Any adaptive control system without definite model reference and identification functions but using system characteristics and/or optimization techniques to generate an adaptive controller belongs to Class 3.

A total of five articles are reviewed.

Banham and Smith(55) suggest that by a linear representation of the non-linear system a controller can be designed with adaptive features, and provides optimum compensation for transient system requirements. The adaptive feature is used to adjust the controller parameters K_c and T_i required to maintain an optimum combination of closed lopp system response and stability over the designed range of process operation. The method was applied to a forced draft blower.

Aoki(56) proposed the concept relating to loss of performance in certain adaptive control systems. These concepts are useful in determining or in bounding the possible loss in the adaptive control system where certain parameters are not known precisely. The connection with the minimax principle of statistical decision theory was also pointed out by him.

Pearson and Sarachik[57] did work related to an approach introduced by Kulikowski[58] for adaptive optimal control of non-linear systems. In this approach, the plant dynamics are represented by an operator which transforms the input time functions into corresponding output time functions.

Pearson[59] in another similar work extended and modified the approach to adaptive optimal control proposed by Kulikowski. Emphasis was placed upon optimizing the steady-state system performance in which the desired output of the plant is a periodic function of time.

Pearson[60] proposed a modified gradient procedure for making discrete-time changes in the adjustable parameter of a continuous-time non-linear system during normal operating conditions. The algorithm employs the best available estimate of the unknown plant parameters as well as an estimate of the disturbance state and the outlet variables.

2.4. General Survey of adaptive control systems applied in Chemical Engineering

A general survey of adaptive control systems applied in the Chemical Engineering field is given in this separate section, and a total of eleven articles (1962-1971) are reviewed.

2.4.1. Model Reference Adaptive Control System (Class 1)

Marcus and Hougen(61) proposed a model reference adaptive control scheme applied to a simulated heat exchanger control system. Automatic self-adjustment of parameters of a PID controller was achieved to maintain the dynamic performance in the presence of a wide variation of process parameters; shell-side flow rate and tube-side inlet temperature were considered.

Crandall and Stevens(62) applied model reference adaptive control to a continuous stirred tank reactor. The performance index was the integral of the square of the derivation of the output composition from a value determined by a reference model.(or response error). The adaptive controller was incorporated with an automatic identification scheme and decision process, and operated in the presence of disturbances in cooling water temperature and/or catalyst activity.

Casciano and Staffin(63) proposed an adaptive control scheme which used desired first order differential equations as model references. The adaptive loop was operative only during a transient and corrected only in the direction of mismatch between process and model. A first order process with varying time constant and two mode controller (P and I) were considered. The effects on system stability with a pure time delay, or an additional pole in the process are presented.

Ryan and Crandall(64) developed a method for applying classical minimisation techniques to forms of algebraic performance indices for use in optimal adaptive control systems. Essentially, the derivative of a general objective function is constrained to be equal to the integrand of a desired integral performance index. Derivatives of the objective function can be taken with respect to the controllable parameters, set equal to zero, and solved for the setting which minimises the performance index over a period of time. The method has been applied to a stirred tank reactor, and a two mode (PI) and three mode (PID) controller were used. The adaptive control system adjusted the controller settings periodically.

Ahlgren and Stevens(65) developed a normalised version of the model reference adaptive control system including suitable procedures for adjusting adaptive control gains and demonstrated excellent adaptive performance for a simulated stirred tank reactor. The three constants in a conventional PID controller were simultaneously adjusted to accomplish this adaptation.

2.4.2. Identification Adaptive Control Systems (Class 2)

Most identification methods require that a small test signal be superimposed on the input signal. The following two identification methods gave different approaches to this.

Mellichamp. Coughanowr and Koppel(66) proposed an identification scheme. The method employed a small identification tank which followed the first order control tank to identify process gain accurately in spite of unknown load changes. An identification control adaptive system can be designed to maintain control loop gain within the system's limits, thus maintaining good control characteristics.

The disadvantage of such a procedure is the necessary duplication of equipment and the necessity of driving the identification flow system output in both directions from the control set-point.

Chao and Huang[67] proposed a method for the optimal design of adaptive control systems which consisted of three parts. First, an optimal control law of the time invariant process is derived. Second, Z- transform and least square techniques are used to develop an identification method which treats the time-varying gain of a second order process. Finally the above two parts are combined to design an adaptive control system which not only adapts to changes of environment but also keeps the system approaching the optimal state.

The results of analog computer simulation of optimal control and digital computer simulation of adaptive control are given. The effects of sampling time and weight factor on stability of the adaptive control system are discussed briefly (Fig.2.7).

In this report, the authors have introduced a more important concept: instead of adjustment of parameters of a conventional PID controller by modification of the optimal control law, an extension of such a concept using a new

5

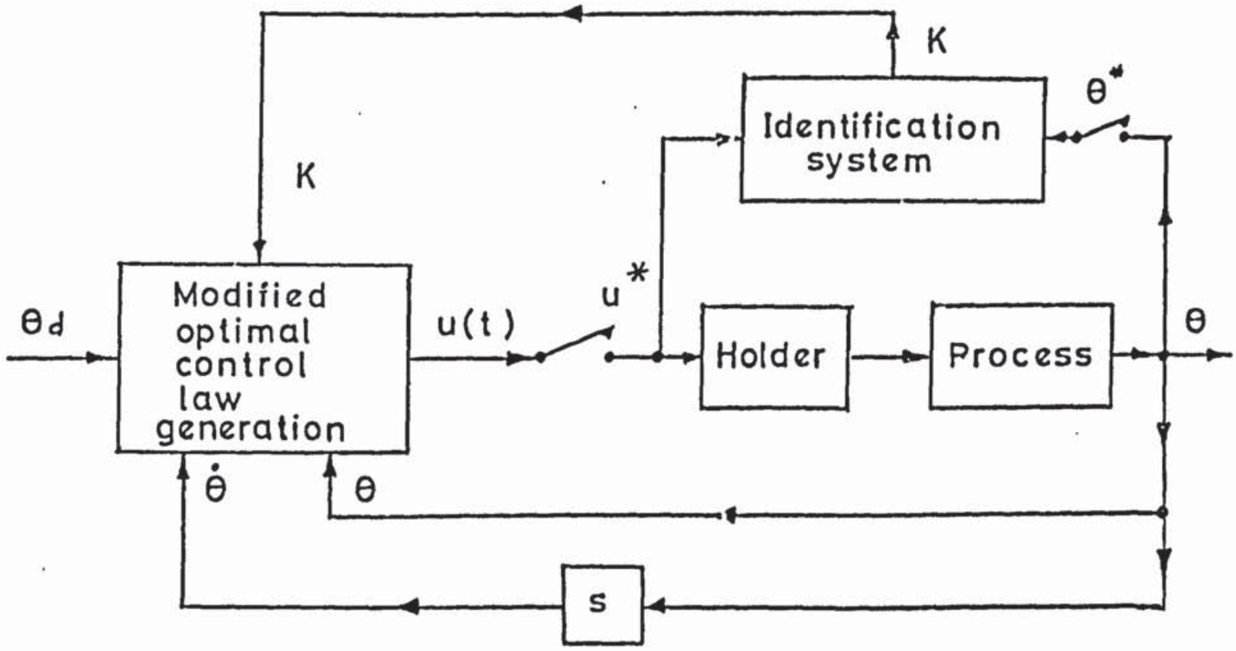

Figure 2.7 Optimal adaptive control by identification

algorithm and theory of so called "Optimal Model Reference Adaptive Control" is developed in this research (see Section 2.6 and Chapter 3).

2.4.3. System Characteristics and Optimization Adaptive Control Systems (Class 3)

There are three articles(68-70) in which the sinusoidal perturbation method is applied for adaptive control, and the final article(71) studied an optimal sensitivity and adaptive control system.

Box and Chanmugam(68) proposed a method of adaptive optimization in which the operating conditions are continuously modified by the sinusoidal perturbation method, so as to be at the optimal level at all times. Starting from a simple concept of evolutionary operation, an analogous method is developed. A detailed analysis of the effects of process dynamics in the case of a consecutive reaction system is given.

Hoyer, White, Foley and Altpeter(69) gave the general theory underlying multivariable sinusoidal perturbation adaptive optimization (SPAO). Process characteristics which indicate possible SPAO application are designated and techniques pertinent to the application of SPAO in chemical process control are discussed, The influence of the nature of the response surface and disturbance characteristics of dynamic behaviour of an extremum seeking adaptive optimizer is examined. System modifications which may yield significant improvement in overall optimizer performance are delineated.

These techniques have been successfully applied to two pilot plants, a gas fired furnace and a fixed bed catalytic reactor, thus conclusively demonstrating the efficiency of this variant of adaptive optimization.

Price and Rippin[70] also applied the sinusoidal perturbation method of extremum seeking to an actual laboratory scale chemical process. The principle differences between this work and that carried out at Wisconsin[69] are the form of objective function used and the dynamics of the system are also more complicated. The process can be made to follow automatically changes in the position of the best operating point if a continuous estimate of the gradient of the objective function with respect to each controller variable is available. These gradients were estimated from the response of the system to sinusoidal perturbations in the controller process variables about the current operating point. The digital computer simulation was used, and the contour plots were prepared using the off-line mode.

Weinrich and Lapidus[71] proposed two general approaches to examine the sensitivity of optimal control systems to parameter variation. The first for open-loop systems involves augmenting the performance index with sensitivity terms and minimising the combined index. The second approach, an adaptive-type controller, involves estimating those parameter variations that have caused observed state deviations and adjusting the control policy in response to this measurement.

In this paper the work is illustrated by numerical examples.

2.5. A summary of the current literature on adaptive control systems

Based upon the above general search of a total of forty articles in the recent literature on adaptive control systems (1962 ~ 1972), two summary tables were prepared and are systematically explained and listed below:

2.5.1. Table 2.1. A general summary of the current literature on the adaptive control system

Content of Table 2.1.:

Column I. Classification of adaptive control system

(1) Model reference

(2) Identification

(3) System characteristics and optimization.

Column II Function of system

(1) Process control

(2) Servomechanism (Engine, machine, aircraft missiles, satellite, etc.)

(3) General mathematics

Column III Type of master control system

(1) Conventional control system

(2) Optimal control system

Column IV Type of Adjusted parameters of master controller

(1) Gain, filter time constant, etc.
(always used in servomechanism field)

(2) K_c, T_i, T_d, of conventional PID controller
(always used in Process control field).

(3) Signal synthesis

(4) Optimal control law modifications

Column V Major type of study

(1) Theoretical

(2) Experimental

(3) Both

Column VI Results and solution

(1) Experimental

(2) Analytical

(3) Analogue (or Hybrid) computer

(4) Digital computer

(5) On-line computer operation.

2.5.2. Table 2.2. <u>A general summary of the current literature of model reference adaptive control systems</u> - (additional information)

The following further information about model reference adaptive control systems is added:

I. Model reference

II. Performance index

III. Adaptive controller.

Table 2.1. A general summary of the current literature on adaptive control systems

Reference No.	I			II			III		IV				V			VI				
	1	2	3	1	2	3	1	2	1	2	3	4	1	2	3	1	2	3	4	5
31 Halbert	*				*		*		*				*					*		
32 Kwai	*				*		*		*				*						*	
33 White	*					*	*		*				*					*		
34 Drassler	*					*	*		*				*					*		
35 Graupe & Cassir	*					*		*			*					*			*	
36 Pearson & Noonan	*					*							*							
37. Wilkie & Parkins	*					*	*						*							
38 Inaloglu & Steadman	*			*			*			*			*			*				
39 Powell	*					*		*			*		*					*		
40 Price	*					*	*		*				*					*		
41 Buxton & Powell	*				*		*		*						*			*		
42 Monopoli	*					*	*				*		*							
43 Parks	*					*	*		*				*							
44 Monopoli	*					*	*		*				*							
45 Osburn, Whitaker & Kezar	*					*	*		*				*							
46 Winsor & Roy	*					*	*		*				*							
47 Landau	*					*	*				*		*				*	*		
48 Gromyko & Sankovskii	*					*	*		*				*					*		
49 Gilbart Monopoli & price	*					*	*		*				*					*		

Table 2.1. (continued)

Reference No.	I			II			III		IV				V			VI				
	1	2	3	1	2	3	1	2	1	2	3	4	1	2	3	1	2	3	4	5
50 Shahein Ghonaimy & Shen	*					*	*		*				*					*		
51.Womack & Watt		*				*	*		*				*					*		
52 Kershow		*		*			*			*			*					*	*	
53 Puri		*			*		*		*				*							
54 Obradovic		*				*	*			*			*					*		
55 Banham & Smith			*		*		*			*					*			*		
56 Aoki			*			*		*			*		*				*			
57 Pearson & Sarachik			*			*		*			*		*				*			
59 Pearson			*			*		*			*		*				*			
60 Pearson			*			*	*		*				*							
61 Marcus & Hougen	*			*			*			*			*					*		
62 Crandall & Stevens	*			*			*			*					*	*				
63 Casciano & Staffin	*			*			*			*			*					*		
64 Ryan & Crandall	*			*			*			*			*						*	
65 Ahlgren & Stevens	*			*			*			*			*						*	
66 Mallichamp Coughanowr & Koppel		*		*			*			*					*	*		*		
67 Chao & Huang		*		*				*				*	*					*	*	
68 Box & Chanmugam			*	*			*			*			*						*	

Table 2.1. (continued)

Reference No.	I			II			III		IV				V			VI				
	1	2	3	1	2	3	1	2	1	2	3	4	1	2	3	1	2	3	4	5
69 Hoyer, White, Foley & Altpeter			*	*			*			*			*							
70 Price & Rappin			*	*			*			*					*	*				*
71 Weinrich & Lapidus			*	*				*				*	*						*	

Table 2.2. A general summary of current literature of model reference adaptive control systems (Additional information)

Reference No	Model reference	Performance index	Adaptive controller
31 Halbert	desired transfer function	integral of response error	systematic search
32 Kwai	1. desired damping 2. desired frequency	1. equalised max. overshoot 2. equalised response area	Known range of variations
33 White	desired transfer function	$PI = \int \frac{\partial e}{\partial k} e\,dt = 0$	A simple criterion
34 Drassler	desired transfer function	response error	Gradient approach
35 Graupe & Cassir	desired transfer function	cost function of product square error	extrapolation technique
36 Pearson	desired transfer function	integral square error	modified gradient method
37 Wilkie & Perkins	desired dynamic equation	response error	transformed state variables
38 Inaloglu & Steadman	desired dynamic response pattern	response error	response pattern
39 Powell	adapted model to estimate state dynamic and future trajectory of unknown plant	function of predicted trajectory of the system error	speed-up modeller
40 Price	desired dynamic equation	response error	accelerated gradient technique
41 Buxton & Powell	idealised air-plane behaviour	mean square error	gradient algorithm
42 Monopoli	desired dynamic equation	response error vector	a reduction of order
43 Park	desired transfer function	response error	Liapunov function
44 Monopoli	desired transfer function	response error	Liapunov function

Table 2.2 (continued)

Reference No	Model reference	Performance index	Adaptive controller
45 Osburn, Whitaker & Kezar	desired transfer function	integral of error square	MIT rule generated from minimised PI
46 Winsor & Roy	desired plant equation	response error	Liapunov function
47 Landau	desired dynamic equation	response error	Popov function
48 Gromyko & Sankovskii	desired dynamic equation	response error	Liapunov function with active and passive adjustment
49. Gilbart Monopoli & Price	desired dynamic equation	response error	Modified Liapunov function
50 Shahein Ghoniamy & Shen	desired dynamic equation	response error	steepest descent path
61 Marcus & Hougen	dynamic performance equation	response error	minimise PI
62 Crandall & Stevens	desired transfer function	integral of response error square	minimise PI incorporated with identification scheme
63 Casciano & Staffin	desired transfer function	response error	steady state correction from PI
64 Ryan & Crandall	desired dynamic equation	$PI = J(e)\Big\|_{t_1}^{t_2}$ J = objective function	minimise PI
63 Ahlgren & Stevens	desired dynamic equation	integral response error square	minimise PI

2.6. Discussion

2.6.1. Most major research work an adaptive control is seen from Table 2.1 to be theoretical. Both theoretical and experimental approaches with different optimal control and optimal adaptive control operations are emphasised throughout the present research work.

2.6.2. From Table 2.1, there is only one article[70] on the use of on-line digital computer operation, and none on on-line hybrid computer operation which is used in the present research work as the major important activity.

2.6.3. From Table 2.1, there are only two articles which propose the modification of the optimal control law generated by the master control loop and using identification (Class 2)[67] and estimation (Class 3)[71] respectively. However no such use in combination with model reference (Class 1) has been reported.

2.6.4. From Table 2.2, almost all model reference adaptive control uses some desired dynamic response equation. In the present research, the model reference adaptive control is generated by the optimal control law to form the optimal profile or optimal trajectory of the state variables.

2.6.5. From Table 2.2, almost every adaptive controller of model reference adaptive control is developed by different individual techniques. There is no general principle or theory upon which they are based. As an extension of the basic concept from my previous work (See Section 2.4.2.) a general algorithm and theory of optimal model reference adaptive control systems is developed theoretically in Chapter 3.

P A R T I

THEORETICAL AND COMPLETE SIMULATION WORK

(CHAPTER 3 TO CHAPTER 7)

CHAPTER 3

THEORETICAL DEVELOPMENT OF GENERAL SCHEME FOR OPTIMAL MODEL REFERENCE ADAPTIVE CONTROL (OMRAC)

3.1. General algorithm and theory of OMRAC

As an extension of the basic concept for modification of optimal control law from my previous work (sed 2.4.2.), a general algorithm and theory of OMRAC is shown below:

3.1.1. Algorithm

OMRAC contains two cascade optimal control systems, generated in such a way that the first optimal control system is generated with constant normal parameters as the optimal model reference scheme which produces the optimal state variable profile or trajectory (e.g. optimal concentration profile in a CSTR), while the second optimal system is generated with unmeasurable and uncontrollable changed parameters and variables of real process as the optimal adaptive control scheme which receives the optimal state variable profile from the model reference scheme as input function. Any response error between the current state variable of the real process and the model reference scheme, will force the optimal adaptive control scheme's desired performance index to be a minimum by a modified optimal control law. Thus the current process state variable will always be following the optimal model reference scheme as closely as possible.

3.1.2. Theory

OMRAC is made up from two schemes, viz: Optimal Model Reference (OMR) scheme and Optimal Adaptive Control (OAC) scheme. Thus:

OMRAC = OMR + OAC

1. The OMR scheme is generated by an optimal control law, $m^*(t)$ with constant parameters to generate an optimal state variable profile or trajectory, $\theta^r(t)$ as OMR.
2. The OAC scheme is generated by a modified optimal control law, $U^*(t)$ with constant parameters to minimise the function of $\theta^r(t) - \theta(t)$ in the presence of unmeasurable changed parameters, and:

$$U^*(t) = m^*(t) + \phi^*(t) \qquad (3\text{-}1)$$

where $\phi^*(t)$ is the derived optimal PID control law

Optimal PID control law in"WEAK FORM":

$$\begin{aligned}\phi^*(t) = {} & \sum_{i=1}^{n-1} \alpha_i (C,K,P^*) \left[\theta_i^r(t) - \theta_i(t)\right] \\ & + \sum_{i=1}^{n-1} \beta_i (C,K,P^*) \int_{t_o}^{t_f} \left[\theta_i^r(t) - \theta_i(t)\right] dt \\ & + \sum_{i=1}^{n-1} \gamma_i (C,K,P^*) \frac{d}{dt}\left[\theta_i^r(t) - \theta_i(t)\right] \qquad (3\text{-}2)\end{aligned}$$

Optimal PID control law in "STRONG FORM":

$$\phi^*(t) = \left(\phi^*(t)\right)_{\text{weak form}} + \sum_{i=1}^{n-1} \Delta p \Delta \theta_i \left(\frac{\partial \alpha_i}{\partial P}\right)_{P=P^*} + \int_{t_o}^{t_f} \left(\sum_{i=1}^{n-1} \Delta p \Delta \theta_i \left(\frac{\partial \beta_i}{\partial P}\right)_{P=P^*}\right) dt + \sum_{i=1}^{n-1} \left(\frac{\partial \gamma_i}{\partial P}\right)_{P=P^*} \frac{d}{dt}\left(\Delta p \Delta \theta_i\right) \quad (3\text{-}3)$$

$$\left.\begin{aligned} &\text{For Optimal P} \; ; \; \beta_i = \gamma_i = 0 \\ &\text{For Optimal P + I} \; : \; \gamma_i = 0 \end{aligned}\right\} \quad (3\text{-}4)$$

where θ_i = n state process variables in the presence of unmeasurable changed paramaters

$\alpha_i, \beta_i, \gamma_i$ = optimal control law coefficients

C = all constants

K = all weighting factors

and P^* = all constant normal parameters

Based upon the above algorithm and theory, a general scheme and mechanism on OMRAC is established (see Fig.3.1).

A brief comparison of the above developed OMRAC with the general type of model reference adaptive control (MRAC) is shown in Figs. 2.3 and 2.6. from the literature survey and in the following table:

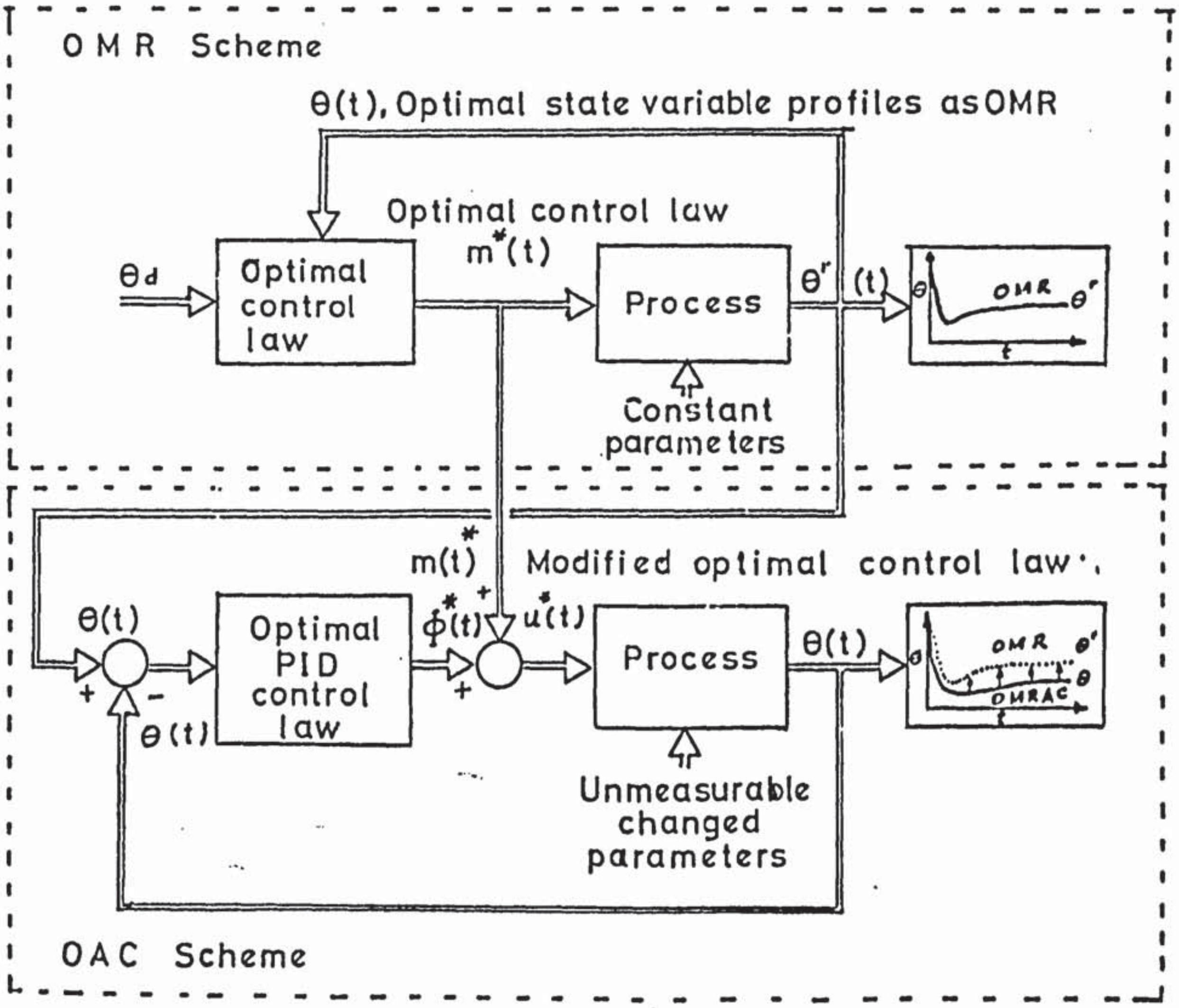

OMR Scheme + OAC Scheme ⇒

OMRAC Scheme

Figure 3.1 General scheme of optimal model reference adaptive control (OMRAC)

Table 3.1. A brief comparison between OMRAC and MRAC

		MRAC	OMRAC
1.	General Principle	Usually there is no general principle or theory upon which they are based	A general theory for n-state variable process has been developed in the present work
2.	Model reference	Usually designed for a desired transfer function	Designed by OMR scheme
3.	Adaptive system	Usually designed to adjust the conventional PID controller's parameters	Designed by OAC scheme with modified optimal PID control laws
4.	Overall control system	Usually designed by conventional feedback control loop	Designed by two cascade optimal control loops

3.2. Optimal Control System

Let the general process equations containing two state variables be:

$$\frac{d\theta_1}{dt} = f_1\,(\theta_1, \theta_2, \theta_{L1}, \theta_{L2}, m_1, m_2) \qquad (3\text{-}5)$$

$$\frac{d\theta_2}{dt} = f_2\,(\theta_1, \theta_2, \theta_{L1}, \theta_{L2}, m_1, m_2) \qquad (3\text{-}6)$$

where θ_1, θ_2 = state variables

θ_{L1}, θ_{L2} = load variables

m_1, m_2 = control variables

with initial and final conditions:

$$\theta_1(t_o) = \theta_{10}, \theta_2(t_o) = \theta_{20} \quad (3\text{-}7\text{-}1)$$

$$\theta_1(t_f) = \theta_{1f}, \theta_2(t_f) = \theta_{2f} \quad (3\text{-}7\text{-}2)$$

The process is controlled and operated always at its steady state conditions: $(\theta_1(t_f), \theta_2(t_f))$ or $(\theta_{1f}, \theta_{2f})$.

Let the performance index be:

$$J(m_1, m_2) = \int_{t_o}^{t_f} F(\theta_1, \theta_2, \theta_{L1}, \theta_{L2}, \dot{m}_1, m_2)\, dt \quad (3\text{-}8)$$

control variables m_1 and m_2 are subject to the following constraints:

$$|m_1| \leqslant M_1 \quad (3\text{-}9\text{-}1)$$

$$|\dot{m}_2| \leqslant M_2 \quad (3\text{-}9\text{-}2)$$

Define the functional equation:

$$f(\theta_1, \theta_2) = \underset{(\dot{m}_1, m_2)}{\text{Min}} \left[J(m_1, m_2) \right] \quad (3\text{-}10)$$

or

$$f(\theta_1, \theta_2) = J(m_1^*, m_2^*)$$

$$= \int_{t_o}^{t_f} F(\theta_1, \theta_2, \theta_{L1}, \theta_{L2}, m_1^*, m_2^*)\, dt \quad (3\text{-}11)$$

where :

$f(\theta_1, \theta_2)$ = minimum performance index, a function of state variables, subject to the process equations (3-5) and (3-6) with boundary conditions (3-7) and generated by the optimal control law (m_1^*, m_2^*)

$m_1^*\ m_2^*$ = the optimal control law and is derived by any optimal control technique - maximum principle[72-74] and dynamic programming[74-76] are suggested here - and is a function of current state variables θ_1, θ_2, load variables θ_{L1}, θ_{L2}, and subject to the constraints shown below

$$m_1^* = m_1^* \ (\theta_1, \theta_2, \theta_{L1}, \theta_{L2}) \tag{3-12}$$

$$m_2^* = m_2^* \ (\theta_1, \theta_2, \theta_{L1}, \theta_{L2}) \tag{3-13}$$

Substituting the optimal control law into process equations (3-5) and (3-6), solving and eliminating time t, the optimal phase plane trajectory $\left[\theta_1^*(t); \theta_2^*(t)\right]$ for any fixed boundary condition is determined and shown in Fig.3.2.

3.3. Optimal model reference (OMR) Scheme

According to Theory I statement: OMR is generated by an optimal state variable profile or trajectory. Which one should be used as OMR is discussed in detail.

The optimal control system is in optimality only when all parameters in the system are unchanged but for most chemical processes in operation, the unmeasurable parameters (or uncontrolled variables) are always changed (see 2.1.1.). Then the new optimal phase plane trajectory will differ from the original one, and there is a close relation between state variables and parameters at final steady state, that is:

$$\theta_1(t_f) = h\left[\theta_2(t_f);\ C_1,\ C_2, --- C_r;\ P_1,\ P_2,\ ----P_s\right] \qquad (3\text{-}14)$$

where:

$\theta_1(t_f),\ \theta_2(t_f) = \theta_{1s},\ \theta_{2s}$ = final steady state variables

$C_1,\ C_2, --- C_r$ = constants

$P_1,\ P_2, --- P_s$ = parameters.

From equation 3-14, it is clear that, due to unmeasurable changed parameters, $\theta_2(t_f)$ must be changed when it is desired that $\theta_1(t_f)$ should be kept constant and vice-versa.

For a CSTR, the final steady state is shown in equation (3-15).

$$C_s = \frac{F\ C_o}{F + aVAe^{-E/RT_s}} \qquad (3\text{-}15)$$

where:

$C_s,\ T_s$ = reactor concentration and temperature at final steady state as state variables

V, E, R = constants

F, a = inlet charge flowrate and catalyst activity as parameters

C_o = Inlet concentration as load variable.

For any change in F, a or C_o, the reactor steady state temperature must change to maintain constant reactor steady state concentration C_s which is the object of the control and T_s cannot be predicted before the load and/or parameter changes are known. This is illustrated in Fig.3.3.

From Fig.3.3 a CSTR usually contains two optimal paths (C^*, T^*), and when unmeasured parameters change, T mustchange to maintain C on its original optimal path (C^*). So for a two state variable process, OMR is a single optimal state variable profile or optimal concentration profile in a CSTR (See Fig.3.4).

In general for an N state variable process, OMR has N-1 (maximum) individual optimal state variable profile, or a single N-1 (maximum) state variable trajectory.

Thus:

1. If N = 2 N -1 = 1 (maximum), and then OMR is only a single optimal profile (Fig.3.4).
2. If N = 3 N - 1 = 2 (maximum), and then OMR can be one or two optimal profiles according to the number of θ^r used in the function equation of the OAC scheme (equation 3-22) or a two state variable trajectory (Fig.3.5).

For on-line computer control, when an optimal phase plane trajectory is used as the OMR scheme, there is no real time problem between the time response of the real process operation and the computer operation, because time has been eliminated from the trajectory (Fig.3.5). However when an optimal state variable profile is used as the OMR scheme, since there is time response,

·7

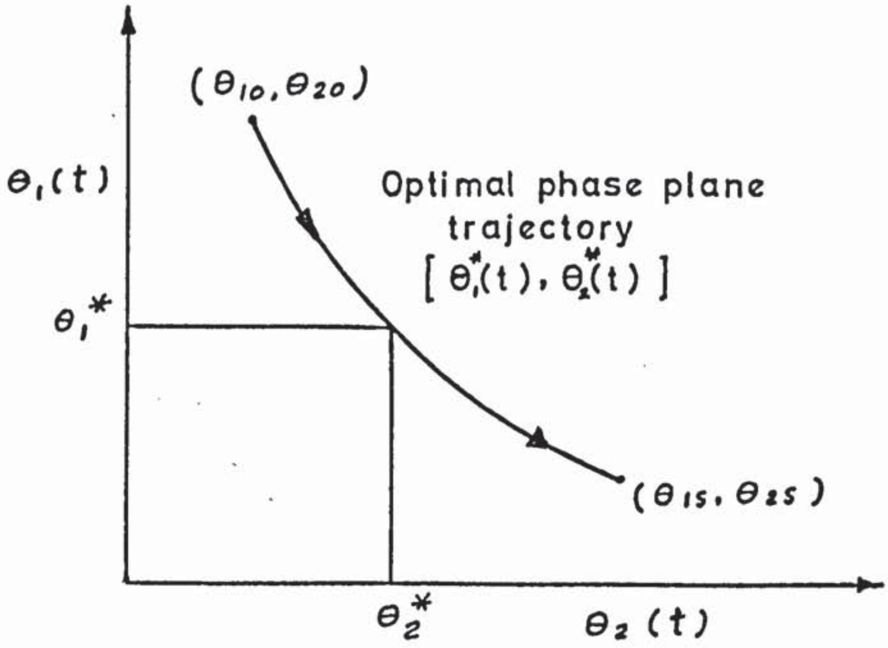

Figure 3.2 Optimal phase plane trajectory

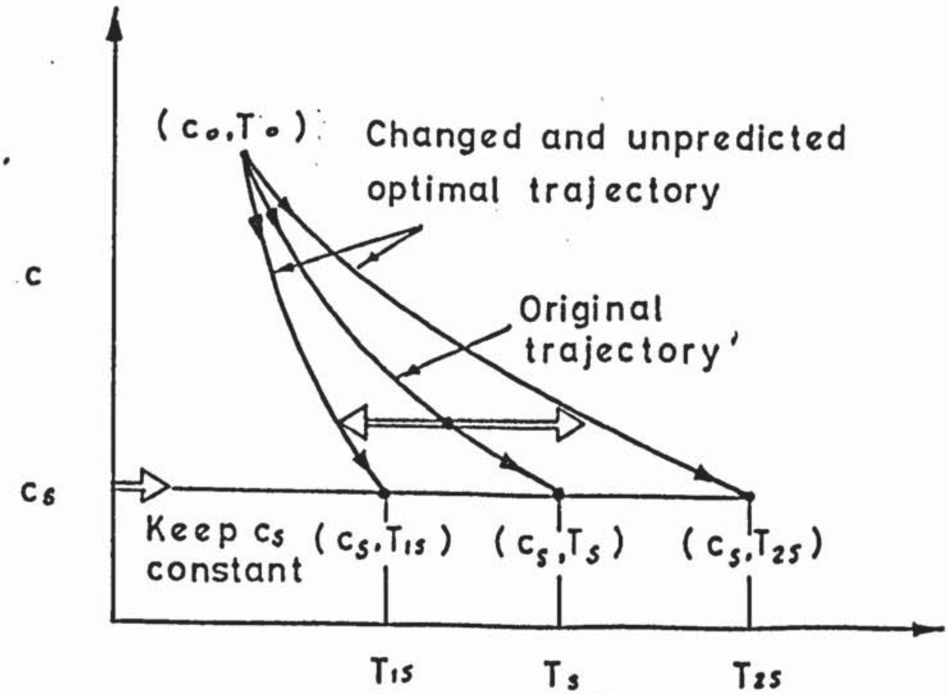

Figure 3.3 Changed and unpredicted optimal phase plane trajectory

8

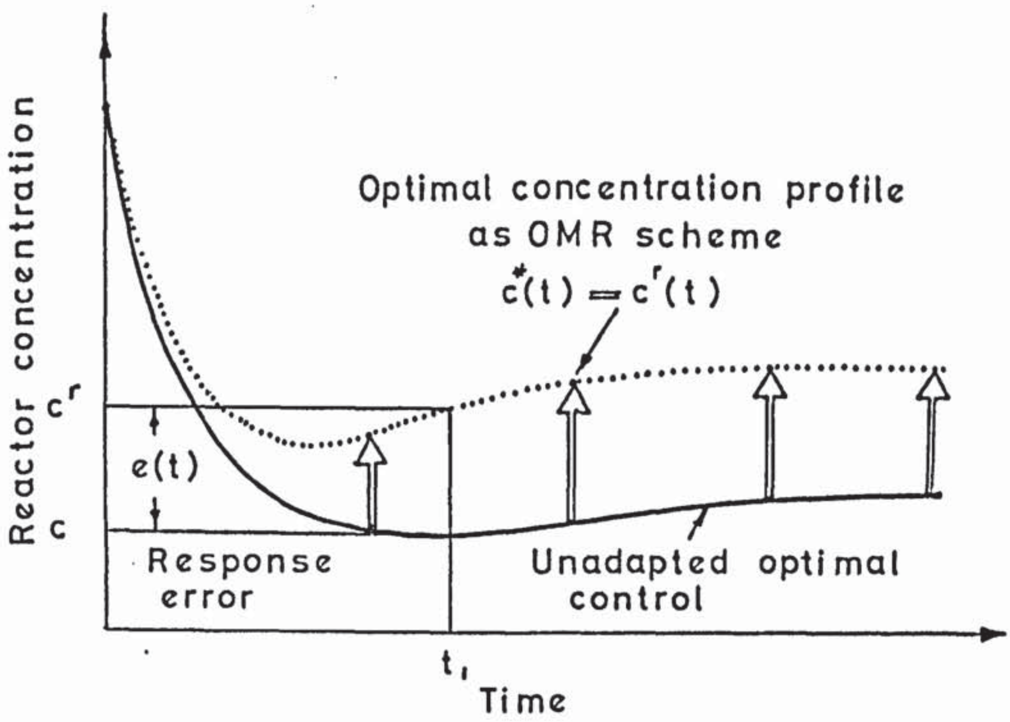

Figure 3.4 Optimal state variable profile as OMR scheme

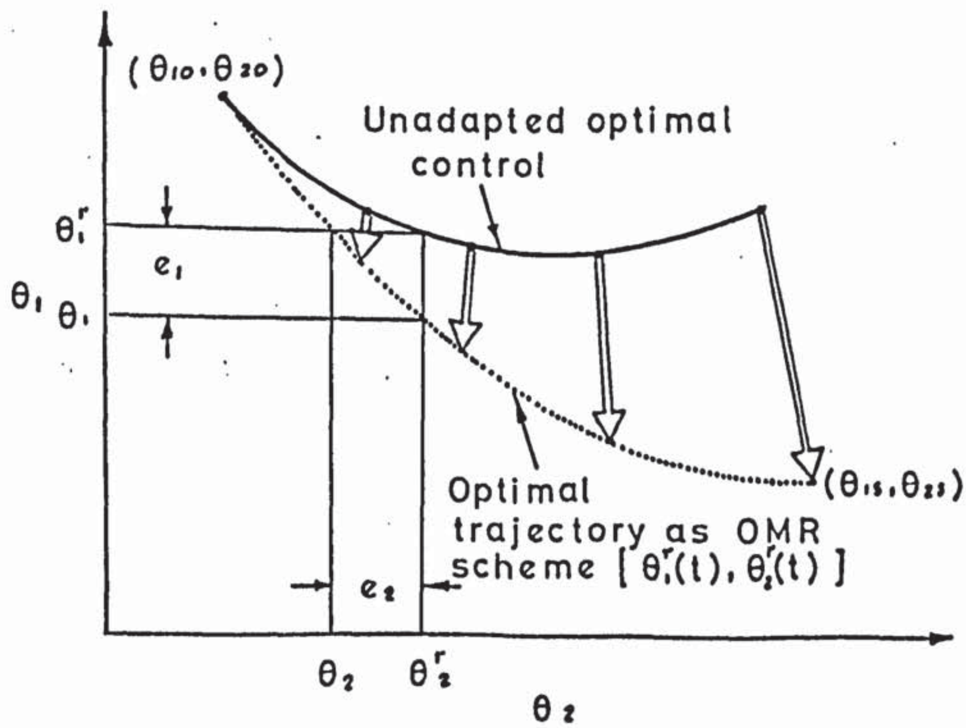

Figure 3.5 Optimal phase plane trajectory as OMR scheme

the real time problem must be carefully considered. That means the state variable from the model reference must be synchronised with the same state variable measured from the real process operation and this is the chief difference between them. In the present research work by using Hybrid and analogue computers for on-line control, real-time operation will be produced by putting the time scale factor equal to unity and measuring in seconds.

3.4. Optimal adaptive control (OAC) scheme

A second optimal control system was generated and called the OAC scheme. The OMR scheme either from optimal trajectory or from optimal profile can be treated as the set-point input of the OAC scheme. Any response error of the current state variables from OMR due to unmeasurable changed parameters for other uncontrollable variables will be forced by the OAC scheme to the minimum of a given desired performance index by a modified optimal control law.

The OAC scheme is developed in detail in the following section.

3.4.1. Modified optimal control law by "Optimal P"

Let the system equations be the same as for the OMR scheme

$$\frac{d\theta_1}{dt} = f_1 (\theta_1, \theta_2, \theta_{L1}, \theta_{L2}, U_1, U_2) \quad (3\text{-}16).$$

$$\frac{d\theta_2}{dt} = f_1 (\theta_1, \theta_2, \theta_{L1}, \theta_{L2}, U_1, U_2) \quad (3\text{-}17)$$

where:

θ_1, θ_2 = state variables

θ_{L1}, θ_{L2} = load variables

U_1, U_2 = control variables

with initial and final conditions the same as for the OMR scheme,

i.e. $\theta_1(t_o) = \theta_{10}, \theta_2(t_o) = \theta_{20}$ (3-18-1)

$\theta_1(t_f) = \theta_{1f}, \theta_2(t_f) = \theta_{2f}$ (3-18-2)

The process is controlled to follow the input from the OMR scheme and finally is operated at its steady state conditions: $(\theta_1(t_f), \theta_2(t_f))$, or $(\theta_{1f}, \theta_{2f})$.

From (3.3) actually only one state variable either θ_1^r or θ_2^r will be selected, according to which one is desired to be controlled and used for the OMR scheme. Here let θ_1 be that selected for OMR:

Then the performance index will be

$$J\ (U_1, U_2) = \int_{t_o}^{t_f} (\theta_1^r, \theta_1, \theta_{\ell 1}, \theta_{\ell 2}, U_1, U_2)\ dt \qquad (3\text{-}19)$$

with U_1 and U_2 subject to the same constraints as in the OMR scheme:

$$|U_1| \leqslant M_1 \qquad (3\text{-}20\text{-}1)$$

$$|U_2| \leqslant M_2 \qquad (3\text{-}20\text{-}2)$$

Define the equation

$$f(\theta_1, \theta_1^r) = \min_{(U_1,U_2)} \left[J(U_1, U_2) \right] \quad (3\text{-}21)$$

or

$$f(\theta_1, \theta_1^r) = J(U_1^*, U_2^*)$$

$$= \int_{t_o}^{t_f} F(\theta_1, \theta_1^r, \theta_{L1}, \theta_{L2}, U_1^*, U_2^*)\, dt \quad (3\text{-}22)$$

where

$f(\theta_1, \theta_1^r)$ = the minimum performance index, a function of the state variable θ_1, and the state input variable θ_1^r, subject to the process equations (3-16) and (3-17) with boundary conditions (3-18) generated by the derived optimal control law (U_1^*, U_2^*).

U_1^*, U_2^* = the optimal control law of the OAC scheme, which is derived by any optimal control technique and is a function of the current state variables, input variable, load variables, and unmeasurable changed parameters, is subject to the constraints (3-20) and is shown below:

$$U_1^* = U_1^*(\theta_1^r; \theta_1, \theta_2; \theta_{L1}, \theta_{L2}; P_1, P_2, \text{----} P_r) \quad (3\text{-}23)$$

$$U_2^* = U_2^*(\theta_1^r; \theta_1, \theta_2; \theta_{L1}, \theta_{L2}; P_1, P_2, \text{----} P_r) \quad (3\text{-}24)$$

where P_1, P_2, ---P_r are the unmeasurable changed parameters. The theoretical approach of the modified optimal control law is derived in detail as follows:

Following Denn and Douglas(77), the optimal control law of a two state variable set of linearised process equations subject to a quadratic objective function within fixed boundary conditions and derived by the maximum principle is:

$$U^*(t) = -\alpha_1 \theta_1(t) - \alpha_2 \theta_2(t) \qquad (3\text{-}25)$$

where

$\theta_1(t)$ = current state variable

$\theta_2(t)$ = current state variable

α_1 = optimal control law coefficient = $\alpha_1(C,K,P)$

α_2 = optimal control law coefficient = $\alpha_2(C,K,P)$

C = all process constants

K = all weighting factors used in the objective function

P = all process parameters (in the present case P is constant)

The above form of optimal control law has also been shown by Tou(79) but was derived by Dynamic Programming.

Extension of equation (3-25) in general form with n state variables (n-1) selected input variables, load variables and with unmeasurable changed parameters, leads to the following general form:

$$U^*(t) = -\left[\sum_{i=1}^{n} \alpha_i \theta_i(t) + \sum_{i=1}^{n-1} \beta_i \theta_i^r(t) + \sum_{i=1}^{\upsilon} \gamma_i \theta_{Li}(t)\right] \qquad (3\text{-}26)$$

where: $\alpha_i = \alpha_i(C,K,P) \quad i = 1,2,----n$ (3-27-1)

$\beta_i = \beta_i(C,K,P) \quad i = 1,2,----n-1$ (3-27-2)

$\gamma_i = \gamma_i(C,K,P) \quad i = 1,2,----$ (3-27-3)

$\alpha_i, \beta_1, \gamma_i$ are the optimal control law coefficients determined by the maximum principle and shown in Chapter 4 in detail

when: $\theta_i(t) = \theta_i^r(t) \quad i = 1,2,---n-1, \; t_o \leq t \leq t_f$ (3-28)

then the response of the OAC scheme is the same as the same process and boundary conditions which leads to the same optimal control law (see equations (3-1) and (3-2))

$$\left(U^*(t)\right)_{\theta_i(t) = \theta_i^r(t)} = m^*(t) \tag{3-29}$$

then equation (3-26) becomes:

$$\left(U^*(t)\right)_{\theta_i(t) = \theta_i^r(t)} = -\left(\sum_{i=1}^{n-1} (\alpha_i + \beta_i)\theta_i^r(t) + \sum_{i=1}^{v} \gamma_i \theta_{Li}(t) + \alpha_n \theta_n(t)\right) = m^*(t)$$

or

$$m^*(t) + \sum_{i=1}^{n-1} (\alpha_i + \beta_i)\theta_i^r(t) = -\left(\alpha_n \theta_n(t) + \sum_{i=1}^{v} \gamma_i \theta_{Li}(t)\right) \tag{3-30}$$

substituting equation (3-30) into equation (3-26) gives:

$$U^*(t) = m^*(t) + \sum_{i=1}^{n-1} \alpha_i \left(\theta_i^r(t) - \theta_i(t)\right) \tag{3-31}$$

where $\theta_i^r(t) - \theta_i(t) = e_i(t)$

= response error

$\alpha_i = \alpha_i(C,K,P)$ (3-27-1)

Let: $P = P^* + \Delta P$

where: P = unmeasurable changed parameters

P^* = parameters at normal value or value at steady state condition

ΔP = change of parameters or perturbation of parameters from their normal value

Then equation (3-27-1) becomes:

$$\alpha_i = \alpha_i(C,K,P^* + \Delta P) \tag{3-32}$$

By a Taylor's series expansion and omitting the second and higher order terms, equation (3-32) becomes:

$$\alpha_i = \alpha(C,K,P^*) + \Delta P\left(\frac{\partial \alpha_i}{\partial P}\right)_{P=P^*} \tag{3-33}$$

Substituting equation (3-33) into equation (3-31) gives:

$$U^*(t) = m^*(t) + \sum_{i=1}^{n-1} \alpha_i(C,K,P^*)\left(\theta_i^r(t) - \theta_i(t)\right)$$
$$+ \sum_{i=1}^{n-1} \Delta P \Delta \theta_i \left(\frac{\partial \alpha_i}{\partial P}\right)_{P=P^*} \tag{3-34}$$

In equation (3-34), the term $\Delta P \Delta \theta_i$ is a second order perturbation; if the unmeasurable changed parameter is within a certain range of the normal value, the last term of equation (3-34) can be justifiably omitted. Then the theoretical approach of the modified optimal control law for the OAC scheme will be:

$$\boxed{U^*(t) = m^*(t) + \sum_{i=1}^{n-1} \alpha_i(C,K,P^*)\left(\theta_i^r(t) - \theta_i(t)\right)} \tag{3-35}$$

Equation (3-35) has the same form as equation (3-31) except for the change of P to P*.

Equation (3-35) states that: the difference between the optimal control law of the OAC scheme and the optimal control law of the OMR scheme is proportional to the response error, and all the coefficients α_i will be determined with constant normal parameters.

Also since equation (3-35) is very similar to conventional proportional control, this modified optimal control law will be called "Optimal P".

3.4.2. Modified optimal control law by "Optimal P + I"

By using the same approach, the modified optimal control law can be derived for more complicated forms, just the same as the conventional controller modes.

In the literature, only Shih[79] introduced the integral action into optimal control. Here it has been derived by a different kind of approach and has been extended to all combinations of the Optimal PID system and the full complications of the theoretical approach have been applied in the subsequent work on complete simulation and on-line computer control operation (see Chapter 7 and Part II).

Let the general form of optimal control law be:

$$U^*(t) = -\left(\sum_{i=1}^{n} \alpha_i \theta_i(t) + \sum_{i=1}^{n-1} \beta_i \theta_i^r(t) + \sum_{i=1}^{\nu} \gamma_i \theta_{Li}(t) + \sum_{i=1}^{n-1} \int_{t_o}^{t_f} \delta_i \left[\theta_i(t) - \theta_i^r(t) \right] dt \right) \quad (3\text{-}36)$$

where $\alpha_i = \alpha_i (C,K,P) \quad i = 1,2,----n$ (3-37-1)

$\beta_i = \beta_i (C,K,P) \quad i = 1,2,----n-1$ (3-37-2)

$\gamma_i = \gamma_i (C,K,P) \quad i = 1,2,----$ (3-37-3)

$\delta_i = \delta_i (C,K,P) \quad i = 1,2,----n-1$ (3-37-4)

All $\alpha_i, \beta_i, \gamma_i$ and δ_i the optimal law coefficients can be determined by the maximum principle as shown in Chapter 5 in detail.

When $\theta_i(t) = \theta_i^r(t); \quad i = 1,2,----n-1; \quad t_o \leq t \leq t_f$

$$\left(U^*(t)\right)_{\theta_i(t) = \theta_i^r(t)} = m^*(t)$$

$$= -\left(\sum_{i=1}^{n-1} (\alpha_i + \beta_i)\theta_i^r(t) + \sum_{i=1}^{\nu} \gamma_i \theta_{Li}(t) + \alpha_n \theta_n(t)\right) \quad (3\text{-}38)$$

Hence

$$m^*(t) + \sum_{i=1}^{n-1} (\alpha_i + \beta_i)\theta_i^r(t) = -\left(\sum_{i=1}^{\nu} \gamma_i \theta_{Li} + \alpha_n \theta_n(t)\right) \quad (3\text{-}39)$$

Substituting equation (3-39) into equation (3-36) and simplifying:

$$U^*(t) = m^*(t) + \sum_{i=1}^{n-1} \alpha_i \left(\theta_i^r(t) - \theta_i(t)\right)$$

$$+ \sum_{i=1}^{n-1} \int_{t_o}^{t_f} \delta_i \left(\theta_i^r(t) - \theta_i(t)\right) dt \quad (3\text{-}40)$$

Let

$$P = P^* + \Delta P$$

Then $\alpha_i = \alpha_i (C,K,P^* + \Delta P)$ (3-41-1)

$\delta_i = \delta_i (C,K,P^* + \Delta P)$ (3-41-2)

Expansion of equation (3-41) by a Taylor's series and neglecting the second and higher order terms:

$$\alpha_i = \alpha_i(C,K,P^*) + \Delta P \left(\frac{\partial \alpha_i}{\partial P}\right)_{P=P^*} \qquad (3\text{-}42\text{-}1)$$

$$\delta_i = \delta_i(C,K,P^*) + \Delta P \left(\frac{\partial \delta_i}{\partial P}\right)_{P=P^*} \qquad (3\text{-}42\text{-}2)$$

Substituting equation (3-42) into equation (3-40) gives:

$$U^*(t) = m^*(t) + \sum_{i=1}^{n-1} \alpha_i(C,K,P^*)\left(\theta_i^r(t) - \theta_i(t)\right)$$

$$+ \sum_{i=1}^{n-1} {}_i(C,K,P^*) \int_{t_o}^{t_f} \left(\theta_i^r(t) - \theta_i(t)\right) dt$$

$$+ \left(\sum_{i=1}^{n-1} \Delta P \Delta \theta_i \frac{\partial \alpha_i}{\partial P}_{P=P^*} + \int_{t_o}^{t_f} \left(\sum_{i=1}^{n-1} \Delta P \Delta \theta_i \left(\frac{\partial \delta_i}{\partial P}\right)_{P=P^*}\right) dt\right) \qquad (3\text{-}43)$$

In equation 3-44), neglecting the second order perturbation terms, the theoretical approach of the modified optimal control law for the OAC scheme will be:

$$U^*(t) = m^*(t) + \sum_{i=1}^{n-1} \alpha_i(C,K,P^*)\left(\theta_i^r(t) - \theta_i(t)\right) + \sum_{i=1}^{n-1} \delta_i(C,K,P^*) \int_{t_o}^{t_f} \left(\theta_i^r(t) - \theta_i(t)\right) dt \qquad (3\text{-}44)$$

Equation (3-44) has the same form as equation (3-40) except for the change of P to P*.

Equation (3-44) states that: the difference between the optimal control law of the OAC scheme and the optimal control law of OMR scheme is proportional to the response error and its integral and all the coefficients α_i and δ_i will be determined with constant normal parameters.

Also equation (3-44) is very similar to conventional P + I control and so this modified optimal control law will be called "Optimal P + I".

3.4.3. Modified optimal control law by "Optimal P + I + D"

Let the general form of optimal control law be:

$$U^*(t) = -\left(\sum_{i=1}^{n} \alpha_i \theta_i(t) + \sum_{i=1}^{n-1} \beta_i \theta_i^r(t) + \sum_{i=1}^{v} \gamma_i \theta_{Li}(t) + \sum_{i=1}^{n-1} \int_{t_0}^{t_f} \delta_i \left(\theta_i(t) - \theta_i^r(t) \right) dt + \sum_{i=1}^{n-1} \frac{d}{dt} \zeta_i \left(\theta_i(t) - \theta_i^r(t) \right) \right) \quad (3\text{-}45)$$

where:

$$\alpha_i = \alpha_i(C,K,P) \quad i = 1,2,----n \quad (3\text{-}46\text{-}1)$$

$$\beta_i = \beta_i(C,K,P) \quad i = 1,2,----n-1 \quad (3\text{-}46\text{-}2)$$

$$\gamma_i = \gamma_i(C,K,P) \quad i = 1,2,---- v \quad (3\text{-}46\text{-}3)$$

$$\delta_i = \delta_i(C,K,P) \quad i = 1,2,----n-1 \quad (3\text{-}46\text{-}4)$$

$$\zeta_i = \zeta_i(C,K,P) \quad i = 1,2,----n-1 \quad (3\text{-}46\text{-}5)$$

All α_i, β_i, γ_i, δ_i, and ζ_i, the optimal law coefficients can be determined by the maximum principle and is shown in Chapter 5 in detail.

When: $\theta_i(t) = \theta_i^r(t)$; $i = 1,2,----n-1$; $t_o \leq t \leq t_f$

$$\left[U^*(t)\right]_{\theta_i(t) = \theta_i^r(t)} = m^*(t)$$

$$= -\left(\sum_{i=1}^{n-1} (\alpha_i + \beta_i)\theta_i^r(t) + \sum_{i=1}^{v} \gamma_i \theta_{Li}(t) + \alpha_n \theta_n(t)\right) \quad (3\text{-}47)$$

$$\text{or } m^*(t) + \sum_{i=1}^{n-1} (\alpha_i + \beta_i)\theta_i^r(t) = -\left(\sum_{i=1}^{v} \gamma_i \theta_{Li}(t) + \alpha_n \theta(t)\right) \quad (3\text{-}48)$$

Substituting equation (3-48) into equation (3-45) and simplifying:

$$U^*(t) = m_i^*(t) + \sum_{i=1}^{n-1} \alpha_i\left(\theta_i^r(t) - \theta_i(t)\right)$$

$$+ \sum_{i=1}^{n-1} \int_{t_o}^{t_f} \delta_i\left(\theta_i^r(t) - \theta_i(t)\right) dt$$

$$+ \sum_{i=1}^{n-1} \frac{d}{dt} \zeta_i\left(\theta_i^r(t) - \theta_i(t)\right) \quad (3\text{-}49)$$

Let: $P = P^* + \Delta P$

$$\alpha_i = \alpha_i(C,K,P^* + \Delta P) \quad (3\text{-}50\text{-}1)$$

$$\delta_i = \delta_i(C,K,P^* + \Delta P) \quad (3\text{-}50\text{-}2)$$

$$\zeta_i = \zeta_i(C,K,P^* + \Delta P) \quad (3\text{-}50\text{-}3)$$

Expansion of equation (3-50) by a Taylor's series and neglecting the second and higher order terms:

$$\alpha_i = \alpha_i(C,K,P^*) + \Delta P\left(\frac{\partial \alpha_i}{\partial P}\right)_{P=P^*} \quad (3\text{-}51\text{-}1)$$

$$\delta_i = \delta_i(C,K,P^*) + \Delta P\left(\frac{\partial \delta_i}{\partial P}\right)_{P=P^*} \quad (3\text{-}51\text{-}2)$$

$$\zeta_i = \zeta_i(C,K,P^*) + \Delta P\left(\frac{\partial \zeta_i}{\partial P}\right)_{P=P^*} \quad (3\text{-}51\text{-}3)$$

Substituting equation (3-51) into equation (3-49) gives:

$$
\begin{aligned}
U^*(t) = m^*(t) &+ \sum_{i=1}^{n-1} \alpha_i\,(C,K,P^*)\left(\theta_i^r(t) - \theta_i(t)\right) \\
&+ \sum_{i=1}^{n-1} \delta_i(C,K,P^*) \int_{t_o}^{t_f} \left(\theta_i^r(t) - \theta_i(t)\right) dt \\
&+ \sum_{i=1}^{n-1} \zeta_i(C,K,P^*)\ \frac{d}{dt}\left(\theta_i^r(t) - \theta_i(t)\right) \\
&+ \sum_{i=1}^{n-1} \Delta P \Delta \theta_i \left(\frac{\partial \alpha_i}{\partial P}\right)_{P=P^*} + \int_{t_o}^{t_f} \left(\sum_{i=1}^{n-1} \Delta P \Delta \theta_i \left(\frac{\partial \delta_i}{\partial P}\right)_{P=P^*}\right) dt \\
&+ \sum_{i=1}^{n-1} \left(\frac{\partial \zeta_i}{\partial P}\right)_{P=P^*} \frac{d}{dt}\left(\Delta P \Delta \theta_i\right)
\end{aligned}
\qquad (3\text{-}52)
$$

In equation (3-52), neglecting the second order perturbation terms, then the theoretical approach of the modified optimal control law for the OAC scheme will be:

$$
\boxed{
\begin{aligned}
U^*(t) = m^*(t) &+ \sum_{i=1}^{n-1} \alpha_i\,(C,K,P^*)\left(\theta_i^r(t) - \theta_i(t)\right) \\
&+ \sum_{i=1}^{n-1} \delta_i\,(C,K,P^*) \int_{t_o}^{t_f} \left(\theta_i^r(t) - \theta_i(t)\right) dt \\
&+ \sum_{i=1}^{n-1} \zeta_i\,(C,K,P^*)\ \frac{d}{dt}\left(\theta_i^r(t) - \theta_i(t)\right)
\end{aligned}
}
\qquad (3\text{-}53)
$$

Equation (3-53) has the same form as equation (3-40) except for the change of P to P*.

Equation (3-53) states that: the difference between the optimal control law of the OAC scheme and the optimal law of the OMR scheme is proportional to response error, its integral and its derivative and all the coefficients α_i, δ_i and ζ_i will be determined with constant normal parameters.

Also equation (3-53) is very similar to conventional P + I + D control, and so this modified optimal control law will be called "Optimal P + I + D".

3.4.4. Discussion

(1) Equations (3-35), (3-44) and (3-53) are modified optimal control laws represented by "Optimal P, P + I and P + I + D" respectively. Since the second order perturbation terms have been neglected, they may be called "Weak Form" of the modified optimal control law.

(2) Equations (3-34), (3-43) and (3-52) are also modified optimal control laws represented by "Optimal P, P + I and P + I + D" respectively. Since they contain the second order perturbation terms, they may be called "Strong Form" of the modified optimal control law.

(3) Because of the presence of unmeasurable changed parameters the comparatively weak form can easily be developed and operated. Hence the "weak form" was used throughout this research work.

CHAPTER 4

MATHEMATICAL DERIVATION OF THE OMR SCHEME FOR A CONTINUOUS STIRRED TANK REACTOR (C.S.T.R.).

4.1. Assumptions for the derivation

For justification of the mathematical derivation of a partially simulated CSTR, all assumptions used are the same as in Buxton's Ph.D.Thesis[80] and are listed below:

(1) The partially simulatedCSTR is designed and based on a simple non-reversible first order exothermic chemical reaction.

(2) Water in the reactor is well mixed by a mixer whose speed is adjusted by a variac.

(3) Since the operating temperature of the reactor is only about $30^{\circ}C$, heat losses from reactor to vessel to surroundings are neglected.

(4) Since the percentage of total heat absorbed by the immersion heater coil is about 1% of the input to the reactor, then the immersion heater time lag is neglected.

(5) Since the time delay in the cooling coil is about 1.3 sec. for 10 litre/min flowrate, then time delay in the cooling coil is neglected. Actually by using an additional new electric temperature transmitter for outlet cooling coil to give a direct ΔT measurement (refer to PartII) this effect of time delay in the cooling has been eliminated.

(6) Since the time constant in the coding coil is below 1.0 sec. for 10 litre/min flow rate, then the time constant in cooling coil is neglected.

(7) Since the changing of the control valve with positioner from fully closed to fully open takes about 5 sec. the time delay in the control valve is neglected.

(8) Since electrical measurement devices both for temperature and flow are used, the time delay is always less then 1 sec., and these are neglected.

(9) Since all interface signals used between the computers and process are electrical the time delay between them is neglected.

The total operating time of every actual on-line operation is about 600 sec. (refer to Part II), so all the above assumptions are reasonable.

4.2. Process Mathematical model

For a simple first order non-reversible exothermic reaction in a CSTR, the dynamic material and energy equations are shown below:

$$\frac{dC}{dt} = \frac{F}{V}(C_o - C) - aAe^{-E/RT}C \qquad (4\text{-}1)$$

$$\frac{dT}{dt} = \frac{F}{V}(T_o - T) + \frac{aA(-\Delta H)e^{-E/RT}C}{\rho C_p} - \frac{Q_c}{\rho C_p V} \qquad (4\text{-}2)$$

initial conditions: $C = C(t_o)$; $T = T(t_o)$ (4-3--1)

final conditions: $C = C(t_f)$; $T = T(t_f)$ (4-3-2)

where

C_o = inlet concentration (mol/litre)

C = concentration in reactor (mol/litre)

F = inlet flowrate to reactor (litre/min)

V = reactor effective volume (litres)

a = catalyst activity (% of original value)

A = constant of Arrhenius equation (1/sec)

E = reaction energy, a constant (cal/mol)

R = gas constant (cal/mol^{o}K)

T = reactor temperature (^{o}C)

T_o = inlet temperature(^{o}C)

$(-\Delta H)$ = change of enthalpy on reaction (cal/mol)

ρ = density of reactant (g/cm^3)

C_p = specific heat of reactant (cal/g.deg C)

Q_c = heat removed by cooling coil water (cal/sec)

In equations (4-1) and (4-2), let

state variables = C, T.

control variable = Q_c

load variables: C_o, T_o

parameters: a, F.

Note: In the actual on-line operation, since it is difficult to manually operate an exact step change of T_o, it will be kept constant, and a, F, used as the unmeasurable and uncontrollable changed parameters and C_o used as the load variable.

Equations (4-1) and (4-2) are generalised as follows:

$$\frac{dC}{dt} = G\,(C_o, T_o, C, T, Q_c) \qquad (4\text{-}4)$$

$$\frac{dT}{dt} = H\,(C_o, T_o, C, T, Q_c) \qquad (4\text{-}5)$$

In the research work, the optimal control law is derived from the process mathematical model linearised about the steady state operating points by Pontryagin's maximum principle, while for complete simulation and on-line operation the original non-linear equations of the process itself (4-1), (4-2) will still be used. (See Chapters 6, 7 8 and Part II)

Linearused equations from (4-4) and (4-5) about the steady state operating point are shown below

$$\frac{d\theta_1}{dt} = a_{11}\theta_1 + a_{12}\theta_2 + d_{11}\theta_{L1} = f_1(\theta_1, \theta_2, \theta_{L1}) \qquad (4\text{-}6)$$

$$\frac{d\theta_2}{dt} = a_{21}\theta_1 + a_{22}\theta_2 + d_{22}\theta_{L2} + bm = f_2(\theta_1, \theta_2, \theta_{L2}, m) \qquad (4\text{-}7)$$

with initial conditions

$$\theta_1(t_o) = \theta_{10} \qquad (4\text{-}8\text{-}1)$$

$$\theta_2(t_o) = \theta_{20} \qquad (4\text{-}8\text{-}2)$$

final conditions

$$\theta_1(t_f) = \theta_{1f} \qquad (4\text{-}9\text{-}1)$$

$$\theta_2(t_f) = \theta_{2f} \qquad (4\text{-}9\text{-}2)$$

where

$$\theta_1 = C - C_s = \Delta C \qquad (4\text{-}10\text{-}1)$$

$$\theta_2 = T - T_s = \Delta T \qquad (4\text{-}10\text{-}2)$$

$$\theta_{L1} = C_o - C_{os} = \Delta C_o \qquad (4\text{-}10\text{-}3)$$

$$\theta_{L2} = T_o - T_{os} = \Delta T_o \qquad (4\text{-}10\text{-}4)$$

$$m = Q_c - Q_{cs} = \Delta Q_c \qquad (4\text{-}10\text{-}5)$$

subscript s = steady state

$$a_{11} = \left(\frac{\partial G}{\partial C}\right)_s = -\frac{F}{V} - aAe^{-\frac{E}{RT_s}} \qquad (4\text{-}11\text{-}1)$$

$$a_{12} = \left(\frac{\partial G}{\partial C}\right)_s = \frac{aAE}{RT_s^2} e^{\frac{-E}{RT_s}} C_s \quad (4\text{-}11\text{-}2)$$

$$d_{11} = \left(\frac{\partial G}{\partial C_o}\right)_s = \frac{F}{V} \quad (4\text{-}11\text{-}3)$$

$$a_{21} = \left(\frac{\partial H}{\partial C}\right)_s = \frac{aA(-\Delta H)e^{-\frac{E}{RT_s}}}{\rho C_p} \quad (4\text{-}11\text{-}4)$$

$$a_{22} = \left(\frac{\partial H}{\partial T}\right)_s = -\frac{F}{V} - \frac{aA(-\Delta H)}{\rho C_p}\left(\frac{E}{RT_s^2} e^{-\frac{E}{RT_s}}\right) C_s \quad (4\text{-}11\text{-}5)$$

$$d_{22} = \left(\frac{\partial H}{\partial T_o}\right)_s = \frac{F}{V} \quad (4\text{-}11\text{-}6)$$

$$b = \left(\frac{\partial H}{\partial Q_c}\right)_s = -\frac{1}{\rho C_p V} \quad (4\text{-}11\text{-}7)$$

4.3. Optimal control system

The system will be operated by generation of an optimal concentration profile in a CSTR from any initial condition to the desired steady state with changed load variables and with constant parameters.

Since the optimal concentration profile will be generated, so the performance index is suggested as follows:

$$J_{(m)} = \int_{t_o}^{t_f} \left[K_1(\theta_d - \theta_1)^2 + K_2 \theta_2^2 + m^2 \right] dt \quad (4\text{-}12)$$

where θ_d = Set point of $\theta_1(t)$, or desired concentration of new steady state condition

K_1, K_2 = weighting factors

Define the functional equation

$$f(\theta_d, \theta_1, \theta_2) = \underset{(m)}{\text{Min}} \left\{ \int_{t_o}^{t_f} \left[K_1(\theta_d - \theta_1)^2 + K_2\theta_2^2 + m^2 \right] dt \right\}$$

$$= \int_{t_o}^{t_f} \left[K_1(\theta_d - \theta_1)^2 + K_2{\theta_2}^2 + m^{*2} \right] dt \qquad (4\text{-}13)$$

Equation (4-13) is an expression of the optimal control law $m^*(t)$ which can minimise the performance index equation (4-12) and which is subject to the linearised process equations (4-6) and (4-7) with boundary conditions given by equation (4-8) and (4-9). Here we assume m is free to vary without restriction and the constraint will be discussed in the next section.

Using the maximum principle, let a new variable $\theta_3(t)$ as performance index be introduced

$$\theta_3(t) = \int_{t_o}^{t_f} \left[K_1 (\theta_d - \theta_1)^2 + K_2 \theta_2^2 + m^2 \right] dt \qquad (4\text{-}14)$$

or

$$\frac{d\theta_2}{dt} = K_1 (\theta_d - \theta_1)^2 + K_2\theta_2^2 + m^2 = f_3(\theta_d, \theta_1, \theta_2, m) \qquad (4\text{-}15)$$

then the original performance index becomes:

$$S(t_f) = C_3 \theta_3(t_f) \qquad (4\text{-}16)$$

where $S(t_f)$ = performance index using a different simple form

$$C_3 = \lambda_3(t_f) = 1 \tag{4-17}$$

$\lambda(t)$ = adjoint variable defined later

From the maximum principle a Hamiltonian equation is introduced as follows:

$$H(\theta_1, \theta_2, m, \lambda) = \sum_{i=1}^{3} \lambda_i f_i$$

$$= \lambda_1 \left[a_{11}\theta_1 + a_{12}\theta_2 + d_{11}\theta_{L1} \right]$$

$$+ \lambda_2 \left[a_{21}\theta_1 + a_{22}\theta_2 + d_{22}\theta_2 + bm \right]$$

$$+ \lambda_3 \left[k_1(\theta_d - \theta_1)^2 + K_2\theta_2^2 + m^2 \right] \tag{4-18}$$

where λ_1, λ_2, and λ_3 are adjoint variables given by the following equation

$$\frac{d\lambda_i}{dt} = -\left(\frac{\partial H}{\partial \theta_i}\right) \tag{4-19}$$

or: $$\frac{d\lambda_1}{dt} = -\frac{\partial H}{\partial \theta_1} = -a_{11}\lambda_1 - a_{21}\lambda_2 + 2K_1(\theta_d - \theta_1)\lambda_3 \tag{4-20}$$

$$\frac{d\lambda_2}{dt} = -\frac{\partial H}{\partial \theta_2} = -a_{12}\lambda_1 - a_{22}\lambda_2 - 2K_2\theta_2\lambda_3 \tag{4-21}$$

$$\frac{d\lambda_3}{dt} = -\frac{\partial H}{\partial \theta_2} = 0 \tag{4-22}$$

Since $\frac{d\lambda_3}{dt} = 0$, $\lambda_3(t_f) = 1$

Hence $$\lambda_3(t) = 1 \tag{4-23}$$

Substituting $\lambda_3(t)$ into equations (4-18), (4-20) and (4-21) gives:

$$H(\theta_1, \theta_2, m, \lambda) = (a_{11}\theta_1 + a_{12}\theta_2 + d_{11}\theta_{L1})\lambda_1$$

$$+ (a_{21}\theta_1 + a_{22}\theta_2 + d_{22}\theta_{L2} + bm)\lambda_2$$

$$+ (K_1(\theta_d - \theta_1)^2 + K_2\theta_2^2 + m^2) \qquad (4\text{-}24)$$

$$\frac{d\lambda_1}{dt} = - a_{11}\lambda_1 - a_{21}\lambda_2 + 2K_1(\theta_d - \theta_1) \qquad (4\text{-}25)$$

$$\frac{d\lambda_2}{dt} = - a_{21}\lambda_1 - a_{22}\lambda_2 - 2K_2\theta_2 \qquad (4\text{-}26)$$

The optimal control law will be determined by the condition that:

$$\frac{\partial H}{\partial m} = 0 \qquad (4\text{-}27)$$

so $$b\lambda_2 + 2m = 0$$

or $$m^*(t) = - (\tfrac{b}{2})\lambda_2(t) \qquad (4\text{-}28)$$

Substituting equation (4-28) into equation (4-7) and rewriting equation (4-6):

$$\frac{d\theta_1}{dt} = a_{11}\theta_1 + a_{12}\theta_2 + d_{11}\theta_{L1} \qquad (4\text{-}6)$$

$$\frac{d\theta_2}{dt} = a_{21}\theta_1 + a_{22}\theta_2 + d_{22}\theta_{L2} - \frac{b^2}{2}\lambda_2 \qquad (4\text{-}29)$$

Since the boundary conditions of the state variables $\theta_1(t)$ and $\theta_2(t)$ are fixed and shown in equations (4-8) and (4-9) which are based upon steady state operation, so the boundary conditions of $\lambda_1(t)$ and $\lambda_2(t)$ will be free [73,77]; or:

Initial conditions:

$$\lambda_1(t_o) = \text{free} \qquad (4\text{-}30\text{-}1)$$

$$\lambda_2(t_o) = \text{free} \qquad (4\text{-}30\text{-}2)$$

Final conditions:

$$\lambda_1(t_f) = \text{free} \qquad (4\text{-}31\text{-}1)$$

$$\lambda_2(t_f) = \text{free} \qquad (4\text{-}31\text{-}2)$$

Since both $\lambda_1(t)$ and $\lambda_2(t)$ are free boundary conditions, then $\lambda_1(t)$ and $\lambda_2(t)$ can be set to be any function between the time: $t_o \leq t \leq t_f$, and subject to the equations (4-6), (4-29), (4-25) and (4-26). Hence, following Denn and Douglas[77], as an extension let the solution of $_1(t)$ and $_2(t)$ take the form:

$$\lambda_1(t) = \alpha_{11}\theta_1(t) + \alpha_{12}\theta_2(t) + \alpha_{13}\theta_d(t) + \alpha_{14}\theta_{L1}(t) + \alpha_{15}\theta_{22}(t) \qquad (4\text{-}32)$$

$$\lambda_2(t) = \alpha_{12}\theta_1(t) + \alpha_{22}\theta_2(t) + \alpha_{23}\theta_d(t) + \alpha_{24}\theta_{L1}(t) + \alpha_{25}\theta_{L2}(t) \qquad (4\text{-}33)$$

where: $\theta_1(t)$, $\theta_2(t)$, $\theta_d(t)$, $\theta_{L1}(t)$ and $\theta_{L2}(t)$ are state variables, desired set-point variable and load variables respectively are all measurable

and $\alpha_{11}, \alpha_{12}, \alpha_{13}, \alpha_{14}, \alpha_{15}, \alpha_{22}, \alpha_{23}, \alpha_{24}$ and α_{25} are coefficients to be determined in section 5 in detail.

Substituting $\lambda_2(t)$ into equation (4-28), the optimal control law of the OMR scheme will be:

$$m^*(t) = -\frac{b}{2}\Big[\alpha_{12}\theta_1(t) + \alpha_{22}\theta_2(t) + \alpha_{23}\theta_d(t) + \alpha_{24}\theta_{L1}(t) + \alpha_{25}\theta_{L2}(t)\Big] \tag{4-34}$$

Then solving equations (4-6) and (4-7) with known $m^*(t)$, the optimal concentration profile for OMR will be obtained as:

$$\theta_1^*(t) \equiv \theta_1^r(t) \qquad t_o \leq t \leq t_f \tag{4-35}$$

4.4. Consideration of constraints

In the derivation of section 3, it was assumed that $m^*(t)$ was free to vary without any restriction. However $m^*(t)$ operates with the following constraints:

From equation (4-10-5):

$$m^*(t) = Q_c^* - Q_{cs}$$

$$\text{or} \quad Q_c^*(t) = m^* + Q_{cs} \tag{4-36}$$

where:

Q_{cs} = Cooling coil heat removal rate at steady state

$Q_c^*(t)$ = optimal cooling coil heat removal rate

$Q_c^*(t)$ is limited by the cooling water flowrate which is controlled by a pneumatic control valve, i.e.

$$(Q_c)_{min} \leq Q_c^* \leq (Q_c)_{max} \tag{4-37}$$

where:

$(Q_c)_{min}$ = minimum heat removal rate when the control valve is closed and $(Q_c)_{max}$ = maximum heat removal rate when the control valve is wide open

According to the statement of the maximum principle, it will be known from (72,77,78) that:

Along the minimum (or maximum) path, the Hamiltonian is stationary when the optimal control law is unconstrained, and a minimum (or maximum) when the optimal control law lies at a constraint. In other words, the necessary condition for the performance index to be at a minimum (or maximum) is that $m^*(t)$ lies in the interior of the region of $m(t)$, or:

$$M_{min} < m^*(t) < M_{max}$$

$$\frac{\partial H}{\partial m} = 0 \quad \text{at } m(t) = m^*(t)\,;\; t_o \leq t \leq t_f \qquad (4\text{-}38)$$

when $m^*(t)$ lies at the boundary of the constraints:

$$H = \text{Min} \quad \text{at} \quad m^*(t) = M_{min} \qquad (4\text{-}39\text{-}1)$$

or

$$H = \text{Max} \quad \text{at } m^*(t) = M_{max} \qquad (4\text{-}39\text{-}2)$$

Hence $m^*(t)$ can be treated as a limiter between M_{min} and M_{max}.

4.5. Determination of the coefficients: α_{12}, α_{22}, $\dot{\alpha}_{23}$, α_{24} and α_{25}.

Differentiating equations (4-32) and 4-33), neglecting the derivatives of θ_d, θ_{L1} and θ_{L2}, and substituting equations

(4-6), (4-7) and (4-34) into the equations, gives

$$\frac{d\lambda_1}{dt} = \alpha_{11}(a_{11}\theta_1 + a_{12}\theta_2 + d_{11}\theta_{L1}) + \alpha_{12}\Big[a_{21}\theta_1 + a_{22}\theta_2$$

$$+ d_{22}\theta_{L2} - \frac{b^2}{2}(\alpha_{12}\theta_1 + \alpha_{22}\theta_2 + \alpha_{23}\theta_d + \alpha_{24}\theta_{L1} + \alpha_{25}\theta_{L2})\Big]$$

$$= (a_{11}\alpha_{11} + a_{21}\alpha_{12} - \frac{b^2}{2}\alpha_{12}^2)\theta_1$$

$$+ (a_{12}\alpha_{11} + a_{22}\alpha_{12} - \frac{b^2}{2}\alpha_{12}\alpha_{22})\theta_2$$

$$+ (d_{11}\alpha_{11} - \frac{b^2}{2}\alpha_{12}\alpha_{24})\theta_{L1}$$

$$+ (d_{22}\alpha_{12} - \frac{b^2}{2}\alpha_{12}\alpha_{25})\theta_{L1} - (\frac{b^2}{2}\alpha_{12}\alpha_{23})\theta_d \qquad (4\text{-}40)$$

$$\frac{d\lambda_2}{dt} = \alpha_{12}(a_{11}\theta_1 + a_{12}\theta_2 + d_{11}\theta_{L1}) + \alpha_{22}\Big[(a_{21}\theta_1 + a_{22}\theta_2 + d_{22}\theta_{L2}$$

$$- \frac{b^2}{2}(\alpha_{21}\theta_1 + \alpha_{22}\theta_2 + \alpha_{23}\theta_d + \alpha_{24}\theta_{L1} + \alpha_{25}\theta_{L2})\Big]$$

$$= (a_{11}\alpha_{12} + a_{21}\alpha_{22} - \frac{b^2}{2}\alpha_{12}\alpha_{22})\theta_1$$

$$+ (a_{12}\alpha_{12} + a_{22}\alpha_{22} - \frac{b^2}{2}\alpha_{22}^2)\theta_2$$

$$+ (d_{11}\alpha_{12} - \frac{b^2}{2}\alpha_{22}\alpha_{24})\theta_{L1}$$

$$+ (d_{22}\alpha_{22} - \frac{b^2}{2}\alpha_{22}\alpha_{25})\theta_{L2} - (\frac{b^2}{2}\alpha_{22}\alpha_{23})\theta_d \qquad (4\text{-}41)$$

Substituting equations (4-32) and (4-33) into equations (4-25 and (4-26) gives:

$$\frac{d\lambda_1}{dt} = - a_{11}(\alpha_{11}\theta_1 + \alpha_{12}\theta_2 + \alpha_{13}\theta_d + \alpha_{14}\theta_{L1} + \alpha_{15}\theta_{L2})$$

$$- a_{21}(\alpha_{12}\theta_1 + \alpha_{22}\theta_2 + \alpha_{23}\theta_d + \alpha_{24}\theta_{L1} + \alpha_{25}\theta_{L2})$$

$$+ 2K_1(\theta_d - \theta_1)$$

$$= (-a_{11}\alpha_{11} - a_{21}\alpha_{12} - 2K_1)\,\theta_1$$

$$+ (-a_{11}\alpha_{12} - a_{21}\alpha_{22})\,\theta_2$$

$$+ (-a_{11}\alpha_{13} - a_{21}\alpha_{23} + 2K_1)\,\theta_d$$

$$+ (-a_{11}\alpha_{14} - a_{21}\alpha_{24})\,\theta_{L1}$$

$$+ (-a_{11}\alpha_{15} - a_{21}\alpha_{25})\,\theta_{L2} \qquad (4\text{-}42)$$

$$\frac{d\lambda_2}{dt} = -a_{12}(\alpha_{11}\theta_1 + \alpha_{12}\theta_2 + \alpha_{13}\theta_d + \alpha_{14}\theta_{L1} + \alpha_{15}\theta_{L2})$$

$$- a_{22}(\alpha_{12}\theta_1 + \alpha_{22}\theta_2 + \alpha_{23}\theta_d + \alpha_{24}\theta_{L1} + \alpha_{25}\theta_{L2})$$

$$- 2K_2\,\theta_2$$

$$= (-a_{12}\alpha_{11} - a_{22}\alpha_{12})\,\theta_1$$

$$+ (-a_{12}\alpha_{12} - a_{22}\alpha_{22} - 2K_2)\,\theta_2$$

$$+ (-a_{12}\alpha_{13} - a_{22}\alpha_{23})\,\theta_d$$

$$+ (-a_{12}\alpha_{14} - a_{22}\alpha_{24})\,\theta_{L1}$$

$$+ (-a_{12}\alpha_{15} - a_{22}\alpha_{25})\,\theta_{L2} \qquad (4\text{-}43)$$

From the above four equations (4-40), (4-41), (4-42) and (4-43) equating both sides of $d\lambda_1/dt$ and $d\lambda_2/dt$; the coefficients of θ_1, θ_2, θ_d, θ_{L1} and θ_{L2} are identical. Thus:

$$(a_{11}\alpha_{11} + a_{21}\alpha_{12} - \frac{b^2}{2}\alpha_{12}^2) = (-a_{11}\alpha_{11} - a_{21}\alpha_{12} - 2K_1) \qquad (4\text{-}44)$$

$$(a_{12}\alpha_{11} + a_{22}\alpha_{12} - \frac{b^2}{2}\alpha_{12}\alpha_{22}) = (-a_{11}\alpha_{12} - a_{21}\alpha_{22}) \qquad (4\text{-}45)$$

$$(-\frac{b^2}{2}\alpha_{12}\alpha_{23}) = (-a_{11}\alpha_{13} - a_{21}\alpha_{23} + 2K_1) \qquad (4\text{-}46)$$

$$(d_{11}\alpha_{11} - \frac{b^2}{2}\alpha_{12}\alpha_{24}) = (-a_{11}\alpha_{14} - a_{21}\alpha_{24}) \qquad (4\text{-}47)$$

$$(d_{22}\alpha_{12} - \frac{b^2}{2}\alpha_{12}\alpha_{25}) = (-a_{11}\alpha_{15} - a_{21}\alpha_{25}) \tag{4-48}$$

$$(a_{11}\alpha_{12} + a_{21}\alpha_{22} - \frac{b^2}{2}\alpha_{12}\alpha_{22}) = (-a_{12}\alpha_{11} - a_{22}\alpha_{12}) \tag{4-49}$$

$$(a_{12}\alpha_{12} + a_{22}\alpha_{22} - \frac{b^2}{2}\alpha_{22}^2) = (-a_{12}\alpha_{12} - a_{22}\alpha_{22} - 2K_2) \tag{4-50}$$

$$(-\frac{b^2}{2}\alpha_{22}\alpha_{23}) = (-a_{12}\alpha_{13} - a_{22}\alpha_{23}) \tag{4-51}$$

$$(d_{11}\alpha_{12} - \frac{b^2}{2}\alpha_{22}\alpha_{24}) = (-a_{12}\alpha_{14} - a_{22}\alpha_{24}) \tag{4-52}$$

$$(d_{22}\alpha_{22} - \frac{b^2}{2}\alpha_{22}\alpha_{25}) = (-a_{12}\alpha_{15} - a_{22}\alpha_{25}) \tag{4-53}$$

In the above ten equations, equation (4-45) is identical to equation (4-49), and rearranging all of the nine independent equations gives:

$$K_1 + a_{11}\alpha_{11} + a_{21}\alpha_{12} - \frac{b^2}{4}\alpha^2_{12} = 0 \tag{4-54}$$

$$a_{12}\alpha_{11} + (a_{11} + a_{22})\alpha_{12} + a_{21}\alpha_{22} - \frac{b^2}{2}\alpha_{12}\alpha_{22} = 0 \tag{4-55}$$

$$-2K_1 + a_{11}\alpha_{13} + a_{21}\alpha_{23} - \frac{b^2}{2}\alpha_{12}\alpha_{23} = 0 \tag{4-56}$$

$$d_{11}\alpha_{11} + a_{11}\alpha_{14} + a_{21}\alpha_{24} - \frac{b^2}{2}\alpha_{12}\alpha_{24} = 0 \tag{4-57}$$

$$d_{22}\alpha_{12} + a_{11}\alpha_{15} + a_{21}\alpha_{25} - \frac{b^2}{2}\alpha_{12}\alpha_{25} = 0 \tag{4-58}$$

$$K_2 + a_{12}\alpha_{12} + a_{22}\alpha_{22} - \frac{b^2}{4}\alpha^2_{22} = 0 \tag{4-59}$$

$$a_{12}\alpha_{13} + a_{22}\alpha_{23} - \frac{b^2}{2}\alpha_{22}\alpha_{23} = 0 \tag{4-60}$$

$$d_{11}\alpha_{12} + a_{12}\alpha_{14} + a_{22}\alpha_{24} - \frac{b^2}{2}\alpha_{22}\alpha_{24} = 0 \tag{4-61}$$

$$a_{12}\alpha_{15} + d_{22}\alpha_{22} + a_{22}\alpha_{25} - \frac{b^2}{2}\alpha_{22}\alpha_{25} = 0 \tag{4-62}$$

From the above nine non-linear algebraic equations nine unknown coefficients can be solved by a Newton-Raphson iteration method using a digital computer (See Appendix 1).

CHAPTER 5

MATHEMATICAL DERIVATION OF THE OAC SCHEME FOR A CONTINUOUS STIRRED TANK REACTOR

5.1. Optimal adaptive control (OAC) system

Rewriting the linearised process equations gives :

$$\frac{d\theta_1}{dt} = a_{11}\theta_1 + a_{12}\theta_2 + d_{11}\theta_{L1} = f_1\ (\theta_1, \theta_2, \theta_{L1}) \qquad (5\text{-}1)$$

$$\frac{d\theta_2}{dt} = a_{21}\theta_1 + a_{22}\theta_2 + d_{22}\theta_{L2} + bU = f_2\ (\theta_1, \theta_2, \theta_{L2}, U) \qquad (5\text{-}2)$$

where

$$U = \Delta Q = Q_c - Q_{cs} \qquad (5\text{-}3)$$

with the initial and final conditions

$$\theta_1(t_o) = \theta_{10} \qquad (5\text{-}4\text{-}1)$$

$$\theta_2(t_o) = \theta_{20} \qquad (5\text{-}4\text{-}2)$$

$$\theta_1(t_f) = \theta_{1f} \qquad (5\text{-}5\text{-}1)$$

$$\theta_2(t_f) = \theta_{2f} \qquad (5\text{-}5\text{-}2)$$

The system is operated and controlled to follow the input response of the optimal concentration profile generated from the OMR scheme, $\theta_1^r(t)$ and forced to the final steady state in the presence of unmeasurable changed parameters or laod variables.

The proposed performance index is as follows:

$$J\ (U) = \int_{t_o}^{t_f} \left[K_3\ (\theta_1^r - \theta_1)^2 + U^2 \right] dt \qquad (5\text{-}6)$$

where: $\theta_1^r(t) = \theta_1{}^*(t)$ = the optimal concentration profile generated from the OMR scheme

and K_3 = weighting factor.

Define the functional equation as:

$$f\ (\theta_1, \theta_1^r) = \underset{(U)}{\text{Min}} \int_{t_o}^{t_f} \left[K_3\ (\theta_1^r - \theta_1)^2 + U^2 \right]\ dt \qquad (5\text{-}7)$$

or

$$f\ (\theta_1, \theta_1^r) = \int_{t_o}^{t_f} \left[K_3\ (\theta_1^r - \theta_1)^2 + U^{*2} \right]\ dt \qquad (5\text{-}8)$$

Equation (5-8) states that the minimum performance index is a function of θ_1 and θ_1^r, subject to the process equations (5-1) and (5-2) with boundary conditions (5-4) and (5-5) and generated by the optimal control law $U^*(t)$, in the presence of unmeasurable changed parameters or load variables. Here the constraints within $U^*(t)$ will be considered with the same conditions as discussed in (4.4)

Using the maximum principle, let the new variable $\theta_3(t)$ be introduced as performance index:

$$\theta_3(t) = \int_{t_o}^{t} \left[K_3\ (\theta_1^r - \theta_1)^2 + U^2 \right] dt \qquad (5\text{-}9)$$

or $$\frac{d\theta_3}{dt} = K_3(\theta_1^r - \theta_1)^2 + U^2 = f_3\ (\theta_1, \theta_1^r, U) \qquad (5\text{-}10)$$

Then the original performance index becomes:

$$S(t_f) = C_3\, \theta_3(t_f) \qquad (5\text{-}11)$$

where

$S(t_f)$ = performance index

$C_3 = \lambda_3(t_f) = 1$

From the maximum principle a Hamiltonian equation is introduced as follows :

$$H(\theta_1, \theta_2, U, \lambda) = \sum_{i=1}^{3} \lambda_i f_i$$

$$= \lambda_1 \left[a_{11}\theta_1 + a_{12}\theta_2 + d_{11}\theta_{L1} \right]$$
$$+ \lambda_2 \left[a_{21}\theta_1 + a_{22}\theta_2 + d_{22}\theta_{L1} + bU \right]$$
$$+ \lambda_3 \left[K_3 (\theta_1^r - \theta_1)^2 + U^2 \right] \qquad (5\text{-}12)$$

where λ_1, λ_2 and λ_3 are adjoint variables, and are subject to the following equations:

$$\frac{d\lambda_i}{dt} = -\left(\frac{\partial H}{\partial \theta_i}\right)$$

or

$$\frac{d\lambda_1}{dt} = -\frac{\partial H}{\partial \theta_1} = -a_{11}\lambda_1 - a_{21}\lambda_2 + 2K_3 (\theta_1^r - \theta_1)\lambda_3 \qquad (5\text{-}13)$$

$$\frac{d\lambda_2}{dt} = -\frac{\partial H}{\partial \theta_2} = -a_{12}\lambda_1 - a_{22}\lambda_2 \qquad (5\text{-}14)$$

$$\frac{d\lambda_3}{dt} = -\frac{\partial H}{\partial \theta_3} = 0 \qquad (5\text{-}15)$$

$$\therefore \frac{d\lambda_3}{dt} = 0 \ ; \ \lambda_3(t_f) = 1 \quad \therefore \quad \lambda_3(t) = 1 \qquad (5\text{-}16)$$

Substituting $\lambda_3(t)$ into equations (5-12) and (5-13), and rewriting equation (5-4):

$$H(\theta_1, \theta_2, U, \lambda) = \left[a_{11}\theta_1 + a_{12}\theta_2 + d_{11}\theta_{L1} \right] \lambda_1$$
$$+ \left[a_{21}\theta_1 + a_{22}\theta_2 + d_{22}\theta_{L2} + bU \right] \lambda_2$$
$$+ \left[K_3 (\theta_1^r - \theta_1)^2 + U^2 \right] \qquad (5\text{-}17)$$

$$\frac{d\lambda_1}{dt} = - a_{11}\lambda_1 - a_{21}\lambda_2 + 2K_3 (\theta_1^r - \theta_1) \qquad (5\text{-}18)$$

$$\frac{d\lambda_2}{dt} = - a_{12}\lambda_1 - a_{22}\lambda_2 \qquad (5\text{-}14)$$

The optimal control law will be determined from the condition that:

$$\frac{\partial H}{\partial U} = 0$$

or $$b\lambda_2 + 2U = 0$$

$$\therefore \quad U^*(t) = - (\tfrac{b}{2}) \lambda_2(t) \qquad (5\text{-}19)$$

Since the system will be forced to operate around the steady state under fixed boundary conditions, the boundary value of $\lambda_1(t)$ and $\lambda_2(t)$ will be free:

Initial conditions:

$$\lambda_1(t_o) = \text{free} \qquad (5\text{-}20\text{-}1)$$

$$\lambda_2(t_o) = \text{free} \qquad (5\text{-}20\text{-}2)$$

Final conditions:

$$\lambda_1(t_f) = \text{free} \qquad (5\text{-}21\text{-}1)$$

$$\lambda_2(t_f) = \text{free} \qquad (5\text{-}21\text{-}2)$$

Since the above free boundary conditions are for both $\lambda_1(t)$ and $\lambda_2(t)$, they can be set to be any function between the time $t_o \leq t \leq t_f$, and subject to the equations (5-1), (5-2), (5-18), (5-14) and (5-19).

By using the same general derived principles and techniques described in Chapters 3 and 4, the more complicated optimal PID of the OAC scheme and the corresponding coefficients will be determined in the following sections.

5.2. Optimal P of OAC scheme

Let

$$\lambda_1(t) = \beta_{11}\theta_1(t) + \beta_{12}\theta_2(t) + \beta_{13}\theta_1^r(t) + \beta_{14}\theta_{L1}(t) + \beta_{15}\theta_{L2}(t) \quad (5\text{-}22)$$

$$\lambda_2(t) = \beta_{12}\theta_1(t) + \beta_{22}\theta_2(t) + \beta_{23}\theta_1^r(t) + \beta_{24}\theta_{L1}(t) + \beta_{25}\theta_{L2}(t) \quad (5\text{-}23)$$

where:

$\theta_1(t)$, $\theta_2(t)$, $\theta_1^r(t)$, $\theta_{L1}(t)$, and $\theta_{L2}(t)$

are state variables, model reference input variable, and load variables respectively and can be measurable and β_{11}, β_{12}, β_{13}, β_{14}, β_{15}, β_{22}, β_{23}, β_{24} and β_{25} are coefficients to be determined.

After all necessary coefficients have been determined, substituting $\lambda_2(t)$ of equation (5-23) into equation (5-19), then the optimal control law will be:

$$U^*(t) = -\frac{b}{2}\ \beta_{12}\theta_1(t) + \beta_{22}\theta_2(t) + \beta_{23}\theta_I^r(t) + \beta_{24}\theta_{L1}(t) + \beta_{25}\theta_{L2}(t) \quad (5\text{-}24)$$

when $\theta_1(t) = \theta_1^r(t)$; $t_o \leq t \leq t_f$

then the response of the OAC scheme is the same as the OMR scheme, since both schemes contain the same process and boundary conditions and both optimal control laws are also the same. Thus:

$$\left[U^*(t) \right]_{\theta_1 = \theta_1^r} = m^*(t)$$

$$= -\frac{b}{2} \left[(\beta_{12} + \beta_{23}) \theta_1^r(t) + \beta_{22}\theta_2(t) + \beta_{24}\theta_{L1}(t) + \beta_{25}\theta_{L2}(t) \right] \quad (5\text{-}25)$$

or

$$m^*(t) + \frac{b}{2} (\beta_{12} + \beta_{23}) \theta_1^r(t) = -\frac{b}{2} \left[\beta_{22}\theta_2(t) + \beta_{24}\theta_{L1}(t) + \beta_{25}\theta_{L2}(t) \right] \quad (5\text{-}26)$$

Substituting equation (5-26) into equation (5-24), simplifying and applying the perturbation principle shown in Optimal P of the OAC scheme in (3.4.1.) (Chapter 3), leads to:

$$U^*(t) = m^*(t) + \frac{b}{2} \beta_{12} \left[\theta_1^r(t) - \theta_1(t) \right] \quad (5\text{-}27)$$

where

$\beta_{12} = \beta_{12}(C, K, P^*)$

= optimal P coefficient

C = all process constants

K = all wwighting factors

P^* = all process parameters with normal value

Equation (5-27) states that: the optimal control law of the OAC scheme is proportional to the perturbation of the Optimal control law from the OMR scheme and the corresponding coefficient β_{12} will be determined with constant normal parameters.

Comparing equation (5-27) with equation (3-35) in Chapter 3 (3.4.1.), shows that equation (5-27) is a special case of equation (3-35), the general optimal P of the OAC scheme.

5.3. Determination of Optimal P coefficient, β_{12}.

Differentiating equations (5-22) and (5-23), neglecting the derivatives of θ_1^r, θ_{L1} and θ_{L2} and substituting equations (5-1), (5-2) and (5-24) into the differentiated equations, gives:

$$\frac{d\lambda_1}{dt} = \beta_{11}(a_{11}\theta_1 + a_{12}\theta_2 + d_{11}\theta_{L1}) + \beta_{12}\Big[a_{21}\theta_1 + a_{22}\theta_2$$
$$d_{22}\theta_{L2} - \frac{b^2}{2}(\beta_{12}\theta_1 + \beta_{22}\theta_2 + \beta_{23}\theta_1^r + \beta_{24}\theta_{L1} + \beta_{25}\theta_{L2})\Big]$$
$$= (a_{11}\beta_{11} + a_{21}\beta_{12} - \frac{b^2}{2}\beta_{12})\,\theta_1$$
$$+ (a_{12}\beta_{11} + a_{22}\beta_{12} - \frac{b^2}{2}\beta_{12}\beta_{22})\,\theta_2$$
$$- (\frac{b^2}{2}\beta_{12}\beta_{23})\,\theta_1^r + d_{11}\beta_{11} - \frac{b^2}{2}\beta_{12}\beta_{24})\,\theta_{L1}$$
$$+ (d_{22}\beta_{12} - \frac{b^2}{2}\beta_{12}\beta_{25})\,\theta_{L2} \qquad (5\text{-}28)$$

$$\frac{d\lambda_2}{dt} = \beta_{12}(a_{11}\theta_1 + a_{12}\theta_2 + d_{11}\theta_{L1}) + \beta_{22}\Big[a_{21}\theta_1 + a_{22}\theta_2$$
$$+ d_{22}\theta_{L2} - \frac{b^2}{2}(\beta_{12}\theta_1 + \beta_{22}\theta_2 + \beta_{23}\theta_1^r + \beta_{24}\theta_{L1} + \beta_{25}\theta_{L2})\Big]$$
$$= (a_{11}\beta_{12} + a_{21}\beta_{22} - \frac{b^2}{2}\beta_{12}\beta_{22})\quad 1$$
$$+ (a_{12}\beta_{12} + a_{22}\beta_{22} - \frac{b^2}{2}\beta_{22}^2)\quad 2$$
$$- (\frac{b^2}{2}\beta_{22}\beta_{23})\,\theta_1^r + (d_{11}\beta_{12} - \frac{b^2}{2}\beta_{22}\beta_{24})\,\theta_{L1}$$
$$+ (d_{22}\beta_{22} - \frac{b^2}{2}\beta_{22}\beta_{25})\,\theta_{L2} \qquad (5\text{-}29)$$

Substituting equations (5-22) and (5-23) into equations (5-18) and (5-14), gives:

$$\frac{d\lambda_1}{dt} = - a_{11} (\beta_{11}\theta_1 + \beta_{12}\theta_2 + \beta_{13}\theta_1^r + \beta_{14}\theta_{L1} + \beta_{15}\theta_{L2})$$

$$- a_{21} (\beta_{12}\theta_1 + \beta_{22}\theta_2 + \beta_{23}\theta_1^r + \beta_{24}\theta_{L1} + \beta_{25}\theta_{L2})$$

$$+ 2K_3 (\theta_1^r - \theta_1)$$

$$= (- a_{11}\beta_{11} - a_{21}\beta_{12} - 2K_3)\,\theta_1$$

$$+ (- a_{11}\beta_{12} - a_{21}\beta_{22})\,\theta_2$$

$$+ (- a_{11}\beta_{13} - a_{21}\beta_{23} + 2K_3)\,\theta_1^r$$

$$+ (- a_{11}\beta_{14} - a_{21}\beta_{24})\,\theta_{L1}$$

$$+ (- a_{11}\beta_{15} - a_{21}\beta_{25})\,\theta_{L2} \qquad (5\text{-}30)$$

$$\frac{d\lambda_2}{dt} = - a_{12} (\beta_{11}\theta_1 + \beta_{12}\theta_2 + \beta_{13}\theta_1^r + \beta_{14}\theta_{L1} + \beta_{15}\theta_{L2})$$

$$- a_{22} (\beta_{12}\theta_1 + \beta_{22}\theta_2 + \beta_{23}\theta_1^r + \beta_{24}\theta_{L1} + \beta_{25}\theta_{L2})$$

$$= (- a_{12}\beta_{11} - a_{22}\beta_{12})\,\theta_1$$

$$+ (- a_{12}\beta_{12} - a_{22}\beta_{22})\,\theta_2$$

$$+ (- a_{12}\beta_{13} - a_{22}\beta_{23})\,\theta_1^r$$

$$+ (-a_{12}\beta_{14} - a_{22}\beta_{24})\,\theta_{L1}$$

$$+ (- a_{12}\beta_{15} - a_{22}\beta_{25})\,\theta_{L2} \qquad (5\text{-}31)$$

From the above four equations (5-28), (5-29), (5-30) and (5-31), equating both sides of $\frac{d\lambda_1}{dt}$ and $\frac{d\lambda_2}{dt}$, the coefficients of θ_1, θ_2, θ_1^r, θ_{L1} and θ_{L2} are identical. Thus:

$$(a_{11}\beta_{11} + a_{21}\beta_{12} - \frac{b^2}{2}\beta_{12}^2) = (-a_{11}\beta_{11} - a_{21}\beta_{12} - 2K_3) \tag{5-32}$$

$$(a_{12}\beta_{11} + a_{22}\beta_{12} - \frac{b^2}{2}\beta_{12}\beta_{22}) = (-a_{11}\beta_{12} - a_{21}\beta_{22}) \tag{5-33}$$

$$(-\frac{b^2}{2}\beta_{12}\beta_{23}) = (-a_{11}\beta_{13} - a_{21}\beta_{23} + 2K_3) \tag{5-34}$$

$$(d_{11}\beta_{11} - \frac{b^2}{2}\beta_{12}\beta_{24}) = (-a_{11}\beta_{14} - a_{21}\beta_{24}) \tag{5-35}$$

$$(d_{22}\beta_{12} - \frac{b^2}{2}\beta_{12}\beta_{25}) = (-a_{11}\beta_{15} - a_{21}\beta_{25}) \tag{5-36}$$

$$(a_{11}\beta_{12} + a_{21}\beta_{22} - \frac{b^2}{2}\beta_{12}\beta_{22}) = (-a_{12}\beta_{11} - a_{22}\beta_{12}) \tag{5-37}$$

$$(a_{12}\beta_{12} + a_{22}\beta_{22} - \frac{b^2}{2}\beta_{22}^2) = (-a_{12}\beta_{12} - a_{22}\beta_{22}) \tag{5-38}$$

$$(-\frac{b^2}{2}\beta_{22}\beta_{23}) = (-a_{12}\beta_{13} - a_{22}\beta_{23}) \tag{5-39}$$

$$(d_{11}\beta_{12} - \frac{b^2}{2}\beta_{22}\beta_{22}) = (-a_{12}\beta_{14} - a_{22}\beta_{24}) \tag{5-40}$$

$$(d_{22}\beta_{22} - \frac{b^2}{2}\beta_{22}\beta_{25}) = (-a_{12}\beta_{15} - a_{22}\beta_{25}) \tag{5-41}$$

In the above ten equations, equation (5-33) is identical to equation (5-37). Rearrangement of the remaining nine independent equations yields:

$$K_3 + a_{11}\beta_{11} + a_{21}\beta_{12} - \frac{b^2}{4}\beta_{12}^2 = 0 \tag{5-42}$$

$$a_{12}\beta_{11} + (a_{11} + a_{22})\beta_{12} + a_{21}\beta_{22} - \frac{b^2}{2}\beta_{12}\beta_{22} = 0 \tag{5-43}$$

$$-2K_3 + a_{11}\beta_{13} + a_{21}\beta_{23} - \frac{b^2}{2}\beta_{12}\beta_{23} = 0 \tag{5-44}$$

$$d_{11}\beta_{11} + a_{11}\beta_{14} + a_{21}\beta_{24} - \frac{b^2}{2}\beta_{12}\beta_{24} = 0 \tag{5-45}$$

$$d_{22}\beta_{12} + a_{11}\beta_{15} + a_{21}\beta_{25} - \frac{b^2}{2}\beta_{12}\beta_{25} = 0 \quad (5\text{-}46)$$

$$d_{12}\beta_{12} + a_{22}\beta_{22} - \frac{b^2}{4}\beta_{22}^2 = 0 \quad (5\text{-}47)$$

$$a_{12}\beta_{13} + a_{22}\beta_{23} - \frac{b^2}{2}\beta_{22}\beta_{23} = 0 \quad (5\text{-}48)$$

$$d_{11}\beta_{12} + a_{12}\beta_{14} + a_{22}\beta_{24} - \frac{b^2}{2}\beta_{22}\beta_{24} = 0 \quad (5\text{-}49)$$

$$d_{22}\beta_{22} + a_{12}\beta_{15} + a_{22}\beta_{25} - \frac{b^2}{2}\beta_{22}\beta_{25} = 0 \quad (5\text{-}50)$$

From the above nine non-linear algebraic equations nine unknown coefficients can be solved. Equations (5-42) to (5-50) are in the same form as equations (4-54) to (4-62) of the OMR scheme, because both schemes are derived with the same optimal proportional control action. Solving equations (5-42), (5-43) and (5-47), the coefficient β_{12} will be determined by a Newton-Raphson iteration method using a digital computer (see Appendix 1).

5.4. Optimal P + I of OAC scheme

Let:

$$\lambda_1 = \beta_{11}\theta_1 + \beta_{12}\theta_2 + \beta_{13}\theta_1^r + \beta_{14}\theta_{L1} + \beta_{15}\theta_{L2} + \beta_{16}\int_{t_o}^{t}(\theta_1 - \theta_1^r)\,dt + \epsilon_1\int_{t_o}^{t}\left[\int_{t_o}^{t}(\theta_1 - \theta_1^r)\,dt\right]dt + \ldots \quad (5\text{-}51)$$

$$\lambda_2 = \beta_{21}\theta_1 + \beta_{22}\theta_2 + \beta_{23}\theta_1^r + \beta_{24}\theta_{L1} + \beta_{25}\theta_{L1} + \beta_{26}\int_{t_o}^{t}(\theta_1 - \theta_1^r)\,dt + \epsilon_2\int_{t_o}^{t}\left[\int_{t_o}^{t}(\theta_1 - \theta_1^r)\,dt\right]dt + \ldots \quad (5\text{-}52)$$

In the process control field, the integral control action is only represented by the single integration of the error variables and any double or higher integration is never used. This is because the use of integral control can eliminate offset, but it can also easily introduce unstable tendencies into the system if a large coefficient is selected; this is because the output of the integral controller always increases when the error is present. So in general it is not necessary to use double or higher integration in integral control. But actually in the broad physical sense, the double and higher integration of error variable must exist and is presented in equations (5-51) and (5-52).

Also in the derivation of Optimal P + I the single integration form is of interest and the double and higher integrals were neglected. Equation (5-51) and (5-52) then become:

$$\lambda_1 = \beta_{11}\theta_1 + \beta_{12}\theta_2 + \beta_{13}\theta_1^r + \beta_{14}\theta_{L1} + \beta_{15}\theta_{L2} + \beta_{16}\int_{t_o}^{t} (\theta_1 - \theta_1^r)\, dt \qquad (5\text{-}53)$$

$$\lambda_2 = \beta_{21}\theta_1 + \beta_{22}\theta_2 + \beta_{23}\theta_1^r + \beta_{24}\theta_{L1} + \beta_{25}\theta_{L2} + \beta_{26}\int_{t_o}^{t} (\theta_1 - \theta_1^r)\, dt \qquad (5\text{-}54)$$

where:

β_{ij} = coefficients to be determined

$i = 1, 2$

$j = 1, 2, \ldots\ldots 6$

But in later derived procedures (see next section) for the first order derivatives of λ_1 and λ_2, i.e. $\dot{\lambda}_1$ and $\dot{\lambda}_2$ from equations (5-53) and (5-54), the integral form is automatically lost, and the coefficients β_{16} and β_{26} are always equal to zero (see next section's discussion). Hence the suggested strategy for derivation of Optimal P + I is that when $\dot{\lambda}_1$ and $\dot{\lambda}_2$ occur and the single integral form is to be retained, then the double integration should be introduced with the selection of comparatively small weighting factors ϵ_1 and ϵ_2 (see section 5)

After all the necessary coefficients have been determined, substituting $\lambda_2(t)$ of equation (5-54) into equation (5-19), then the optimal control law will be:

$$U^*(t) = -\frac{b}{2}\Big[\beta_{21}\theta_1 + \beta_{22}\theta_2 + \beta_{23}\theta_1^r + \beta_{24}\theta_{L1} + \beta_{25}\theta_{L2} + \beta_{26}\int_{t_o}^{t}(\theta_1 - \theta_1^r)\,dt\Big] \qquad (5\text{-}55)$$

when $\theta_1(t) = \theta_1^r(t)$; $t_o \leq t \leq t_f$

then:

$$\Big[U^*(t)\Big]_{\theta_1 = \theta_1^r} = m^*(t)$$

$$= -\frac{b}{2}\Big[(\beta_{21} + \beta_{23})\theta_1^r + \beta_{22}\theta_2 + \beta_{24}\theta_{L1} + \beta_{25}\theta_{L2}\Big] \qquad (5\text{-}56)$$

or:

$$m^*(t) + \frac{b}{2}(\beta_{21} + \beta_{23})\theta_1^r$$

$$= -\frac{b}{2}(\beta_{22}\theta_2 + \beta_{24}\theta_{L1} + \beta_{25}\theta_{L2}) \qquad (5\text{-}57)$$

Substituting equation (5-57) into equation (5-55) and simplifying and applying the perturbation principle shown in Optimal P + I of the OAC scheme in (3.4.2) leads to:

$$U^*(t) = m^*(t) + \frac{b}{2}\left\{ \beta_{21}\left[\theta_1^r(t) - \theta_1(t)\right] + \beta_{26}\int_{t_o}^{t}\left[\theta_1^r(t) - \theta_1(t)\right] dt \right\} \tag{5-58}$$

where: $\beta_{21} ; \beta_{26} = \beta_{21}(C,K,P^*) ; \beta_{26}(C,K,P^*)$

= Optimal P + I coefficients

C = process constants

K = weighting factors

P* = process parameters with normal value

Equation (5-58) states that: the optimal control law of the OAC scheme is proportional to the perturbation and the integral of perturbation of the optimal control law from the OMR scheme and the corresponding coefficients β_{21} and β_{26} will be determined with normal parameters.

Comparing equation (5-58) with equation (3-44) in Chapter 3 (3.4.2), shows that equation (5-58) is a special case of equation (3-44) the general Optimal P + I of the OAC scheme.

5.5. Determination of Optimal P + I coefficients β_{21} and β_{26}

Differentiation of equations (5-51) and (5-52) and neglecting the derivatives of θ_1^r, θ_{L1} and θ_{L2}:

$$\frac{d\lambda_1}{dt} = \beta_{11}\frac{d\theta_1}{dt} + \beta_{12}\frac{d\theta_2}{dt} + \beta_{16}(\theta_1 - \theta_1^r) + \epsilon_1\int_{t_o}^{t}(\theta_1 - \theta_1^r)\,dt \qquad (5\text{-}59)$$

$$\frac{d\lambda_2}{dt} = \beta_{21}\frac{d\theta_1}{dt} + \beta_{22}\frac{d\theta_2}{dt} + \beta_{26}(\theta_1 - \theta_1^r) + \epsilon_2\int_{t_o}^{t}(\theta_1 - \theta_1^r)\,dt \qquad (5\text{-}60)$$

Substituting equations (5-1), (5-2) and (5-55) into equations (5-59) and (5-60) yields:

$$\begin{aligned}
\frac{d\lambda_1}{dt} = {} & \beta_{11}(a_{11}\theta_1 + a_{12}\theta_2 + d_{11}\theta_{L1}) \\
& + \beta_{12}\Big(a_{21}\theta_1 + a_{22}\theta_2 + d_{22}\theta_{L2} - \frac{b^2}{2}(\beta_{21}\theta_1 + \beta_{22}\theta_2) \\
& \quad + \beta_{23}\theta_1^r + \beta_{24}\theta_{L1} + \beta_{25}\theta_{L2} + \beta_{26}\int_{t_o}^{t}(\theta_1 - \theta_1^r)\,dt\Big) \\
& + \beta_{16}(\theta_1 - \theta_1^r) + \epsilon_1\int_{t_o}^{t}(\theta_1 - \theta_1^r)\,dt \\
= {} & (a_{11}\beta_{11} + a_{21}\beta_{12} + \beta_{16} - \frac{b^2}{2}\beta_{12}\beta_{21})\,\theta_1 \\
& + (a_{12}\beta_{11} + a_{22}\beta_{12} - \frac{b^2}{2}\beta_{12}\beta_{22})\,\theta_2 \\
& - (\frac{b^2}{2}\beta_{12}\beta_{23} + \beta_{16})\,\theta_1^r \\
& + (d_{11}\beta_{11} - \frac{b^2}{2}\beta_{12}\beta_{24})\,\theta_{L1} \\
& + (d_{22}\beta_{12} - \frac{b^2}{2}\beta_{12}\beta_{25})\,\theta_{L2} \\
= {} & (-\frac{b^2}{2}\beta_{12}\beta_{26} + \epsilon_1)\int_{t_o}^{t}(\theta_1 - \theta_1^r)\,dt
\end{aligned} \qquad (5\text{-}61)$$

$$\frac{d\lambda_2}{dt} = \beta_{21}(a_{11}\theta_1 + a_{12}\theta_2 + d_{11}\theta_{L1})$$

$$+ \beta_{22}\Big[a_{21}\theta_1 + a_{22}\theta_2 + d_{22}\theta_{L2} - \frac{b^2}{2}(\beta_{21}\theta_1 + \beta_{22}\theta_2$$

$$+ \beta_{23}\theta_1^r + \beta_{24}\theta_{L1} + \beta_{25}\theta_{L2} + \beta_{26}\int_{t_o}^{t} (\theta_1 - \theta_1^r)\, dt \Big]$$

$$+ \beta_{26}(\theta_1 - \theta_1^r) + \epsilon_2 \int_{t_o}^{t_1} (\theta_1 - \theta_1^r)\, dt$$

$$= (a_{11}\beta_{21} + a_{22}\beta_{22} - \frac{b^2}{2}\beta_{21}\beta_{22} + \beta_{26})\,\theta_1$$

$$+ (a_{12}\beta_{21} + a_{22}\beta_{22} - \frac{b^2}{2}\beta_{22}^2)\,\theta_2$$

$$- (\frac{b^2}{2}\beta_{22}\beta_{23} + \beta_{26})\,\theta_1^r$$

$$+ (d_{11}\beta_{21} - \frac{b^2}{2}\beta_{22}\beta_{24})\,\theta_{L1}$$

$$+ (d_{22}\beta_{22} - \frac{b^2}{2}\beta_{22}\beta_{25})\ _{L2}$$

$$+ (-\frac{b^2}{2}\beta_{22}\beta_{26} + \epsilon_2)\int_{t_o}^{t} (\theta_1 - \theta_1^r)\, dt \qquad (5\text{-}62)$$

Substituting equations (5-53) and (5-54) into equations (5-18) and (5-14) gives:

$$\frac{d\lambda_1}{dt} = a_{11}(\beta_{11}\theta_1 + \beta_{12}\theta_2 + \beta_{13}\theta_1^r + \beta_{14}\theta_{L1} + \beta_{15}\theta_{L2} + \beta_{16}\int_{t_o}^{t} (\theta_1 - \theta_1^r)\, dt$$

$$- a_{21}(\beta_{21}\theta_1 + \beta_{22}\theta_2 + \beta_{23}\theta_1^r + \beta_{24}\theta_{L1} + \beta_{25}\theta_{L2} + \beta_{26}\int_{t_o}^{t} (\theta_1 - \theta_1^r)\, dt$$

$$+ 2K_3\,(\theta_1^r - \theta_1)$$

$$= (-a_{11}\beta_{11} - a_{21}\beta_{21} - 2K_3)\theta_1 + (-a_{11}\beta_{12} - a_{21}\beta_{22})\theta_2$$

$$+ (-a_{11}\beta_{13} - a_{21}\beta_{23} + 2K_3)\theta_1^r + (-a_{11}\beta_{14} - a_{21}\beta_{24})\theta_{L1}$$

$$+ (-a_{11}\beta_{15} - a_{21}\beta_{25})\theta_{L2} + (-a_{11}\beta_{16} - a_{21}\beta_{26})\int_{t_o}^{t}(\theta_1 - \theta_1^r)\,dt \tag{5-63}$$

$$\frac{d\lambda_2}{dt} = -a_{12}(\beta_{11}\theta_1 + \beta_{12}\theta_2 + \beta_{13}\theta_1^r + \beta_{14}\theta_{L1} + \beta_{15}\theta_{L2} + \beta_{16}\int_{t_o}^{t}(\theta_1 - \theta_1^r)dt$$

$$- a_{22}(\beta_{21}\theta_1 + \beta_{22}\theta_2 + \beta_{23}\theta_1^r + \beta_{24}\theta_{L1} + \beta_{25}\theta_{L2} + \beta_{26}\int_{t_o}^{t}(\theta_1 - \theta_1^r)dt$$

$$= (-a_{12}\beta_{11} - a_{22}\beta_{21})\theta_1 + (-a_{12}\beta_{12} - a_{22}\beta_{22})\theta_2$$

$$+ (-a_{12}\beta_{13} - a_{22}\beta_{23})\theta_1^r + (-a_{12}\beta_{14} - a_{22}\beta_{24})\theta_{L1}$$

$$+ (-a_{12}\beta_{15} - a_{22}\beta_{25})\theta_{L2} + (-a_{12}\beta_{16} - a_{22}\beta_{26})\int_{t_o}^{t}(\theta_1 - \theta_1^r)\,dt \tag{5-64}$$

From the above four equations (5-61), (5-62), (5-63) and (5-64), equating both sides of $\frac{d\lambda_1}{dt}$ and $\frac{d\lambda_2}{dt}$ the coefficients of θ_1, θ_2, θ_1^r, θ_{L1}, θ_{L2} and $\int_{t_o}^{t}(\theta_1 - \theta_1^r)\,dt$ are indetical. Thus:

$$(a_{11}\beta_{11} + a_{21}\beta_{12} - \frac{b^2}{2}\beta_{12}\beta_{21} + \beta_{16}) = (-a_{11}\beta_{11} - a_{21}\beta_{21} - 2K_3) \tag{5-65}$$

$$(a_{12}\beta_{11} + a_{22}\beta_{12} - \frac{b^2}{2}\beta_{12}\beta_{22}) = (-a_{11}\beta_{12} - a_{21}\beta_{22}) \tag{5-66}$$

$$(-\frac{b^2}{2}\beta_{12}\beta_{22} - \beta_{16}) = (-a_{11}\beta_{13} - a_{21}\beta_{23} + 2K_3) \tag{5-67}$$

$$(d_{11}\beta_{11} - \frac{b^2}{2}\beta_{12}\beta_{24}) = (- a_{11}\beta_{14} - a_{21}\beta_{24}) \tag{5-68}$$

$$(d_{22}\beta_{12} - \frac{b^2}{2}\beta_{12}\beta_{25}) = (- a_{11}\beta_{15} - a_{21}\beta_{25}) \tag{5-69}$$

$$(- \frac{b^2}{2}\beta_{12}\beta_{26} + \epsilon_1) = (- a_{11}\beta_{16} - a_{21}\beta_{26}) \tag{5-70}$$

$$(a_{11}\beta_{21} + a_{21}\beta_{22} - \frac{b^2}{2}\beta_{21}\beta_{22} + \beta_{26}) = (- a_{12}\beta_{11} - a_{22}\beta_{21}) \tag{5-71}$$

$$(a_{12}\beta_{21} + a_{21}\beta_{22} - \frac{b^2}{2}\beta_{22}^2) = (- a_{12}\beta_{12} - a_{22}\beta_{22}) \tag{5-72}$$

$$(- \frac{b^2}{2}\beta_{22}\beta_{23} - \beta_{26}) = (- a_{12}\beta_{13} - a_{22}\beta_{23}) \tag{5-73}$$

$$(d_{11}\beta_{21} - \frac{b^2}{2}\beta_{22}\beta_{24}) = (- a_{12}\beta_{14} - a_{22}\beta_{24}) \tag{5-74}$$

$$(d_{22}\beta_{22} - \frac{d^2}{2}\beta_{22}\beta_{25}) = (- a_{12}\beta_{15} - a_{22}\beta_{25}) \tag{5-75}$$

$$(- \frac{b^2}{2}\beta_{22}\beta_{26} + \epsilon_2) = (- a_{21}\beta_{16} - a_{22}\beta_{26}) \tag{5-76}$$

After rearrangement and simplification of the above twelve equations (5-65) to (5-76), the following set of equations is obtained:

$$2K_3 + 2a_{11}\beta_{11} + a_{21}\beta_{12} + a_{21}\beta_{21} - \frac{b^2}{2}\beta_{12}\beta_{21} + \beta_{16} = 0 \tag{5-77}$$

$$a_{12}\beta_{11} + (a_{11} + a_{22})\beta_{12} + a_{21}\beta_{22} - \frac{b^2}{2}\beta_{12}\beta_{22} = 0 \tag{5-78}$$

$$-2K_3 + a_{11}\beta_{13} - \beta_{16} + a_{21}\beta_{23} - \frac{b^2}{2}\beta_{12}\beta_{23} = 0 \tag{5-79}$$

$$d_{11}\beta_{11} + a_{11}\beta_{14} + a_{21}\beta_{24} - \frac{b^2}{2}\beta_{12}\beta_{24} = 0 \tag{5-80}$$

$$d_{22}\beta_{12} + a_{11}\beta_{15} + a_{21}\beta_{25} - \frac{b^2}{2}\beta_{12}\beta_{25} = 0 \tag{5-81}$$

$$a_{11}\beta_{16} + a_{21}\beta_{26} - \frac{b^2}{2}\beta_{12}\beta_{26} + \epsilon_1 = 0 \tag{5-82}$$

$$a_{12}\beta_{11} + (a_{11} + a_{22})\beta_{21} + a_{21}\beta_{22} - \frac{b^2}{2}\beta_{21}\beta_{22} + \beta_{26} = 0 \quad (5\text{-}83)$$

$$a_{12}\beta_{12} + a_{12}\beta_{21} + 2a_{22}\beta_{22} - \frac{b^2}{2}\beta^2_{22} = 0 \quad (5\text{-}84)$$

$$a_{12}\beta_{13} + a_{22}\beta_{23} - \beta_{26} - \frac{b^2}{2}\beta_{22}\beta_{23} = 0 \quad (5\text{-}85)$$

$$a_{12}\beta_{14} + d_{11}\beta_{21} + a_{22}\beta_{24} - \frac{b^2}{2}\beta_{22}\beta_{24} = 0 \quad (5\text{-}86)$$

$$a_{12}\beta_{15} + d_{22}\beta_{22} + a_{22}\beta_{25} - \frac{b^2}{2}\beta_{22}\beta_{25} = 0 \quad (5\text{-}87)$$

$$a_{12}\beta_{16} + a_{22}\beta_{26} - \frac{b^2}{2}\beta_{22}\beta_{26} + \epsilon_2 = 0 \quad (5\text{-}88)$$

For determination of β_{21} and β_{26}, equations (5-77), (5-78), (5-82), (5-83), (5-84) amd (5-88) among the above twelve non-linear equations must be solved by a Newton-Raphson iteration method by digital computer (see Appendix 1).

Among the above derived twelve non-linear algebraic equations, equations (5-82) and (5-87) are the more important ones to determine the coefficients β_{16} and β_{26} of Optimal P + I OAC scheme, as discussed below:

Rewriting these two equations gives:

$$a_{11}\beta_{16} + a_{21}\beta_{26} - \frac{b^2}{2}\beta_{12}\beta_{26} + \epsilon_1 = 0 \quad (5\text{-}82)$$

$$a_{12}\beta_{16} + a_{22}\beta_{26} - \frac{b^2}{2}\beta_{22}\beta_{26} + \epsilon_2 = 0 \quad (5\text{-}88)$$

ϵ_1 and ϵ_2 are comparatively small values relative to all of the other weighting factors. So let $\epsilon_1 = \epsilon_2 = \epsilon$, and assume the coefficients β_{12} and β_{22} have been determined from other equations. Then β_{12} and β_{22} are determined coefficients (or constants) in these two equations, and thus equations (5-82) and (5-88) become:

$$a_{11}\beta_{16} + a_{21}\beta_{26} - (\frac{b^2}{2}\beta_{12})\beta_{26} + \epsilon = 0 \quad (5\text{-}89)$$

$$a_{12}\beta_{16} + a_{22}\beta_{26} - (\frac{b^2}{2}\beta_{22})\beta_{26} + \epsilon = 0 \quad (5\text{-}90)$$

Solving for β_{26} gives :

$$\beta_{26} = \frac{(a_{12} - a_{11})}{(a_{11}a_{22} - a_{12}a_{21}) - \frac{b^2}{2}(a_{11}\beta_{22} - a_{12}\beta_{12})} \quad (5\text{-}91)$$

Equation (5-91) shows clearly that:

(1) Equation (5-91) is a simple linear algebraic equation with constant slope which passes through zero when $\epsilon = 0$.

(2) For a given set of process constants and parameters, the slope of equation (5-91) must be constant

(3) β_{26} must be equal to zero when ϵ is equal to zero. This is the condition of general single integral control (see equation (5-51) and (5-52)).

(4) Since ϵ is a small weighting factor which can arbitrarily start from a zero value, the condition for the general type of single integral control is the special case of the derived Optimal P + I system

5.6. Optimal P + I + D of OAC scheme

Let:

$$\lambda_1 = \beta_{11}\theta_1 + \beta_{12}\theta_2 + \beta_{13}\theta_1^r + \beta_{14}\theta_{L1} + \beta_{15}\theta_{L2}$$

$$+ \left[\beta_{16}\int_{t_o}^{t} (\theta_1 - \theta_1^r)dt + \epsilon_1 \int_{t_o}^{t}\int_{t_o}^{t} (\theta_1 - \theta_1^r)\, dtdt\right] + \beta_{17}\frac{d}{dt}(\theta_1 - \theta_1^r)$$

(5-92)

and

$$\lambda_2 = \beta_{21}\theta_1 + \beta_{22}\theta_2 + \beta_{23}\theta_3 + \beta_{24}\theta_{L1} + \beta_{25}\theta_{L2}$$

$$+ \beta_{26}\int_{t_o}^{t} (\theta_1 - \theta_1^r)\, dt + \epsilon_2 \int_{t_o}^{t}\int_{t_o}^{t} (\theta_1 - \theta_1^r)\, dtdt + \beta_{27}\frac{d}{dt}(\theta_1 - \theta_1^r)$$

(5-93)

When the double integral are neglected, equations (5-92) and (5-93) become:

$$\lambda_1 = \beta_{11}\theta_1 + \beta_{12}\theta_2 + \beta_{13}\theta_1^r + \beta_{14}\theta_{L1} + \beta_{15}\theta_{L2} + \beta_{16}\int_{t_o}^{t} (\theta_1 - \theta_1^r)\, dt$$

$$+ \beta_{17}\frac{d}{dt}(\theta_1 - \theta_1^r) \qquad (5\text{-}94)$$

and

$$\lambda_2 = \beta_{21}\theta_1 + \beta_{22}\theta_2 + \beta_{23}\theta_1^r + \beta_{24}\theta_{1L} + \beta_{25}\theta_{L2} + \beta_{26}\int_{t_o}^{t} (\theta_1 - \theta_1^r)\, dt$$

$$+ \beta_{27}\frac{d}{dt}(\theta_1 - \theta_1^r) \qquad (5\text{-}95)$$

where β_{ij} = coefficient to be determined

$i = 1, 2$

$j = 1, 2, \ldots\ldots 7$

The derivation of optimal integral control coefficients is suggested by the same strategy as before. After all necessary coefficients have been determined, substituting $\lambda_2(t)$ into equation (5.19), will then give the optimal law:

$$U^* = -\frac{b}{2}\Big[\beta_{21}\theta_1 + \beta_{22}\theta_2 + \beta_{23}\theta_1^r + \beta_{24}\theta_{L1} + \beta_{25}\theta_{L2} + \beta_{26}\int_{t_o}^{t}(\theta_1 - \theta^r)\,dt + \beta_{27}\frac{d}{dt}(\theta_1 - \theta_1^r)\Big] \qquad (5\text{-}96)$$

When $\theta_1(t) = \theta_1^r(t); \quad t_o \leq t \leq t_f$

$$\Big[\ U^*(t)\ \Big]_{\theta_1 = \theta_1^r} = m^*(t) \qquad (5\text{-}97)$$

Then:

$$m^*(t) = -\frac{b}{2}\Big[(\beta_{21} + \beta_{23})\theta_1^r + \beta_{22}\theta_2 + \beta_{24}\theta_{L1} + \beta_{25}\theta_{L2}\Big] \qquad (5\text{-}98)$$

or

$$m^*(t) + \frac{b}{2}(\beta_{21} + \beta_{23})\theta_1^r = -\frac{b}{2}(\beta_{22}\theta_2 + \beta_{24}\theta_{L1} + \beta_{25}\theta_{L2}) \qquad (5\text{-}99)$$

Substituting equation (5-99) into equation (5-96), simplifying and applying the perturbation principle shown in Optimal P + I + D of the OAC scheme in (3.4.3) yields:

$$U^*(t) = m^*(t) + \frac{b}{2}\Big\{\beta_{21}\Big[\theta_1^r(t) - \theta_1(t)\Big] + \beta_{26}\int_{t_o}^{t}\Big[\theta_1^r(t) - \theta_1(t)\Big]dt + \beta_{27}\frac{d}{dt}\Big[\theta_1^r(t) - \theta_1(t)\Big]\Big\}$$

where: $\beta_{21}, \beta_{26}, \beta_{27} = \beta_{21}(C,K,P^*),\ \beta_{26}(C,K,P^*),\ \beta_{27}(C,K,P^*)$

= Optimal P + I + D Coefficients

C = Process constants

K = Weighting factors

P* = Process parameters with normal value

(5-100)

Equation (5-100) states that: the optimal control law of the OAC scheme is proportional to the perturbation integral of the perturbation, and derivative of the perturbation of the optimal control law from the OMR scheme and the corresponding coefficients β_{21}, β_{26} and β_{27} will be determined with normal parameters.

Comparing equation (5-100) with equation (3-53) in Chapter 3 (3.4.3) shows that equation (5-100) is a special case of equation (3-53), the general Optimal P + I + D of the OAC scheme.

5.7. Determination of Optimal P + I + D coefficients β_{21}, β_{26} and β_{27}

Differentiation of equations (5-92) and (5-93), neglecting the first derivatives of θ_{L1}, θ_{L2} and the second derivative of $(\theta_1 - \theta_1^r)$, gives:

$$\frac{d\lambda_1}{dt} = \beta_{11}\frac{d\theta_1}{dt} + \beta_{12}\frac{d\theta_2}{dt} + \beta_{13}\frac{d\theta_1^r}{dt} + \beta_{16}(\theta_1 - \theta_1^r) + \epsilon_1\int_{t_o}^{t}(\theta_1 - \theta_1^r)dt \tag{5-101}$$

$$\frac{d\lambda_2}{dt} = \beta_{21}\frac{d\theta_1}{dt} + \beta_{22}\frac{d\theta_2}{dt} + \beta_{23}\frac{d\theta_1^r}{dt} + \beta_{26}(\theta_1 - \theta_1^r) + \epsilon_2\int_{t_o}^{t}(\theta_1 - \theta_1^r)dt \tag{5-102}$$

Substituting equations (5-1), (5-2), and (5-96) into (5-101) and (5-102) and letting

$$\frac{d}{dt}(\theta_1 - \theta_1^r) = \frac{d\theta_1}{dt} - \frac{d\theta_1^r}{dt} \tag{5-103}$$

gives:

$$\frac{d\lambda_1}{dt} = \beta_{11}(a_{11}\theta_1 + a_{12}\theta_2 + d_{11}\theta_{L1})$$

$$+ \beta_{12}\Big[a_{21}\theta_1 + a_{22}\theta_2 + d_{22}\theta_{L2} - \frac{b^2}{2}(\beta_{21}\theta_1 + \beta_{22}\theta_2$$

$$+ \beta_{23}\theta_1^r + \beta_{24}\theta_{L1} + \beta_{25}\theta_{L2} + \beta_{26}\int_{t_o}^{t}(\theta_1 - \theta_1^r)\,dt$$

$$+ \beta_{27}(a_{11}\theta_1 + a_{12}\theta_2 + d_{11}\theta_{L1}) - \beta_{27}\frac{d\theta_1^r}{dt})\Big]$$

$$+ \beta_{13}\frac{d\theta_1^r}{dt} + \beta_{16}(\theta_1 - \theta_1^r) + \epsilon_1\int_{t_o}^{t}(\theta_1 - \theta_1^r)\,dt \qquad (5\text{-}104)$$

After rearrangement and simplification, equation (5-104) becomes:

$$\frac{d\lambda_1}{dt} = (a_{11}\beta_{11} + a_{21}\beta_{12} - \frac{b^2}{2}\beta_{12}\beta_{21} - \frac{b^2}{2}a_{11}\beta_{12}\beta_{27} + \beta_{16})\theta_1$$

$$+ (a_{12}\beta_{11} + a_{22}\beta_{12} - \frac{b^2}{2}\beta_{12}\beta_{22} - \frac{b^2}{2}a_{12}\beta_{12}\beta_{27})\theta_2$$

$$+ (-\frac{b^2}{2}\beta_{12}\beta_{23} - \beta_{16})\theta_1^r$$

$$+ (d_{11}\beta_{11} - \frac{b^2}{2}\beta_{12}\beta_{24} - \frac{b^2}{2}d_{11}\beta_{12}\beta_{27})\theta_{L1}$$

$$+ (d_{22}\beta_{12} - \frac{b^2}{2}\beta_{12}\beta_{25})\theta_{L2}$$

$$+ (-\frac{b^2}{2}\beta_{12}\beta_{26} + \epsilon_1)\int_{t_o}^{t}(\theta_1 - \theta_1^r)\,dt$$

$$+ (\frac{b^2}{2}\beta_{12}\beta_{27} + \beta_{13})\frac{d\theta_1^r}{dt} \qquad (5\text{-}105)$$

Similarly:

$$\frac{d\lambda_2}{dt} = \beta_{21}(a_{11}\theta_1 + a_{12}\theta_2 + d_{11}\theta_{L1})$$

$$+ \beta_{22}\Big[a_{11}\theta_1 + a_{22}\theta_2 + d_{22}\theta_{L2} - \frac{b^2}{2}(\beta_{21}\theta_1 + \beta_{22}\theta_2$$

$$+ \beta_{23}\theta_1^r + \beta_{24}\theta_{L1} + \beta_{25}\theta_{L2} + \beta_{26}\int_{t_o}^{t}(\theta_1 - \theta_1^r)\,dt$$

$$+ \beta_{27}(a_{11}\theta_1 + a_{12}\theta_2 + d_{11}\theta_{L1}) - \beta_{27}\frac{d\theta_1^r}{dt})\Big]$$

$$+ \beta_{23}\frac{d\theta_1^r}{dt} + \beta_{26}(\theta_1 - \theta_1^r) + \epsilon_2\int_{t_o}^{t}(\theta_1 - \theta_1^r)\,dt \qquad (5\text{-}106)$$

After rearrangement and simplification, equation (5-106) becomes:

$$\frac{d\lambda_2}{dt} = a_{11}\beta_{21} + a_{21}\beta_{22} - \frac{b^2}{2}\beta_{21}\beta_{22} - \frac{b^2}{2}a_{11}\beta_{22}\beta_{27} + \beta_{26})\,\theta_1$$

$$+ (a_{12}\beta_{21} + a_{22}\beta_{22} - \frac{b^2}{2}a_{12}\beta_{22}\beta_{27})\,\theta_2$$

$$+ (-\frac{b^2}{2}\beta_{22}\beta_{23} - \beta_{26})\,\theta_1^r$$

$$+ (d_{11}\beta_{21} - \frac{b^2}{2}\beta_{22}\beta_{24} - \frac{b^2}{2}d_{11}\beta_{22}\beta_{27})\,\theta_{L1}$$

$$+ (d_{22}\beta_{22} - \frac{b^2}{2}\beta_{22}\beta_{25})\,\theta_{L2}$$

$$+ (-\frac{b^2}{2}\beta_{22}\beta_{26} + \epsilon_2)\int_{t_o}^{t}(\theta_1 - \theta_1^r)\,dt$$

$$+ (\frac{b^2}{2}\beta_{22}\beta_{27} + \beta_{23})\frac{d\theta_1^r}{dt} \qquad (5\text{-}107)$$

Substituting equations (5-94) and (5-95) into equations (5-18) and (5-4), gives:

$$
\begin{aligned}
\frac{d\lambda_1}{dt} &= - a_{11}\Big[\beta_{11}\theta_1 + \beta_{12}\theta_2 + \beta_{13}\theta_1^r + \beta_{14}\theta_{L1} + \beta_{15}\theta_{L2} \\
&\quad + \beta_{16}\int_{t_o}^{t} (\theta_1 - \theta_1^r)\, dt - \beta_{17}\frac{d\theta_1^r}{dt} + \beta_{17}(a_{11}\theta_1 + a_{12}\theta_2 \\
&\quad + d_{11}\theta_{L1})\Big] - a_{21}\Big[\beta_{21}\theta_1 + \beta_{22}\theta_2 + \beta_{23}\theta_1^r \\
&\quad + \beta_{24}\theta_{L1} + \beta_{25}\theta_{L2} + \beta_{26}\int_{t_o}^{t} (\theta_1 - \theta_1^r)\, dt - \beta_{27}\frac{d\theta_1^r}{dt} \\
&\quad + \beta_{27}(a_{11}\theta_1 + a_{12}\theta_2 + d_{11}\theta_{L1})\Big] + 2K_3(\theta_1^r - \theta_1) \\
&= (- a_{11}\beta_{11} - a_{21}\beta_{21} - 2K_3 - a_{11}^2\beta_{17} - a_{11}a_{21}\beta_{27})\,\theta_1 \\
&\quad + (- a_{11}\beta_{12} - a_{21}\beta_{22} - a_{11}a_{12}\beta_{17} - a_{12\ 21}\beta_{27})\,\theta_2 \\
&\quad + (- a_{11}\beta_{13} - a_{21}\beta_{23} + 2K_3)\,\theta_1^r \\
&\quad + (- a_{11}\beta_{14} - a_{21}\beta_{24} - a_{11}d_{11}\beta_{17} - a_{21}d_{11}\beta_{27})\,\theta_{L1} \\
&\quad + (- a_{11}\beta_{15} - a_{21}\beta_{25})\,\theta_{L2} \\
&\quad + (- a_{11}\beta_{16} - a_{21}\beta_{26})\int_{t_o}^{t} (\theta_1 - \theta_1^r)\, dt \\
&\quad + (a_{11}\beta_{17} + a_{21}\beta_{27})\frac{d\theta_1^r}{dt}
\end{aligned}
\tag{5-108}
$$

$$\frac{d\lambda_2}{dt} = - a_{12} \ \beta_{11}\theta_1 + \beta_{12}\theta_2 + \beta_{13}\theta_1^r + \beta_{14}\theta_{L1} + \beta_{15}\theta_{L2}$$

$$+ \beta_{16}\int_{t_o}^{t} (\theta_1 - \theta_1^r)\, dt + \beta_{17}(a_{11}\theta_1 + a_{12}\theta_2 + d_{11}\theta_{L1})$$

$$- \beta_{17} \frac{d\theta_1^r}{dt} - a_{22} \ \beta_{21}\theta_1 + \beta_{22}\theta_2 + \beta_{23}\theta_1^r$$

$$+ \beta_{24}\theta_{L1} + \beta_{25}\theta_{L2} + \beta_{26}\int_{t_o}^{t} (\theta_1 - \theta_1^r)\, dt$$

$$+ \beta_{27} (a_{11}\theta_1 + a_{12}\theta_2 + d_{11}\theta_{L1}) - \beta_{27} \frac{d\theta_1^r}{dt}$$

$$= (- a_{12}\beta_{11} - a_{11}a_{12}\beta_{17} - a_{22}\beta_{21} - a_{11}a_{22}\beta_{27})\, \theta_1$$

$$+ (- a_{12}\beta_{12} - a_{12}^2\beta_{17} - a_{22}\beta_{22} - a_{12}a_{22}\beta_{27})\, \theta_2$$

$$+ (- a_{12}\beta_{13} - a_{22}\beta_{23})\, \theta_1^r$$

$$+ (- a_{12}\beta_{14} - a_{12}d_{11}\beta_{17} - a_{22}\beta_{24} - a_{22}d_{11}\beta_{27})\, \theta_{L1}$$

$$+ (- a_{12}\beta_{15} - a_{22}\beta_{25})\, \theta_{L2}$$

$$+ (- a_{12}\beta_{16} - a_{22}\beta_{26})\int_{t_o}^{t} (\theta_1 - \theta_1^r)\, dt$$

$$+ (a_{12}\beta_{17} + a_{22}\beta_{27}) \ \frac{d\theta_1^r}{dt} \qquad (5\text{-}109)$$

From the above four equations (5-105), (5-107), (5-108) and (5-109), equating both sides of $\frac{d\lambda_1}{dt}$ and $\frac{d\lambda_2}{dt}$, the coefficients of θ_1, θ_2, θ_1^r and θ_{L2}, $\int_{t_o}^{t} (\theta_1 - \theta_1^r)$ and $\frac{d\theta_1^r}{dt}$ are identical.

Thus:

$$a_{11}\beta_{11} + a_{21}\beta_{12} - \frac{b^2}{2}\beta_{12}\beta_{21} - \frac{b^2}{2}a_{11}\beta_{12}\beta_{27} + \beta_{16}$$

$$= - a_{11}\beta_{11} - a_{21}\beta_{21} - 2K_3 - a_{11}^2\beta_{17} - a_{11}\alpha_{21}\beta_{27} \quad (5\text{-}110)$$

$$a_{12}\beta_{11} + a_{22}\beta_{12} - \frac{b^2}{2}\beta_{12}\beta_{22} - \frac{b^2}{2}a_{12}\beta_{12}\beta_{27}$$

$$= - a_{11}\beta_{12} - a_{21}\beta_{22} - a_{11}a_{12}\beta_{17} - a_{12}a_{12}\beta_{27} \quad (5\text{-}111)$$

$$- \frac{b^2}{2}\beta_{12}\beta_{23} - \beta_{16} = - a_{11}\beta_{13} - a_{21}\beta_{23} + 2K_3 \quad (5\text{-}112)$$

$$d_{11}\beta_{11} - \frac{b^2}{2}\beta_{12}\beta_{24} - \frac{b^2}{2}d_{11}\beta_{12}\beta_{27}$$

$$= - a_{11}\beta_{14} - a_{21}\beta_{24} - a_{11}d_{11}\beta_{17} - a_{21}d_{11}\beta_{27} \quad (5\text{-}113)$$

$$d_{22}\beta_{12} - \frac{b^2}{2}\beta_{12}\beta_{25} = - a_{11}\beta_{15} - a_{21}\beta_{25} \quad (5\text{-}114)$$

$$- \frac{b^2}{2}\beta_{12}\beta_{26} + \epsilon_1 = - a_{11}\beta_{16} - a_{21}\beta_{26} \quad (5\text{-}115)$$

$$\frac{b^2}{2}\beta_{12}\beta_{27} + \beta_{13} = a_{11}\beta_{17} + a_{21}\beta_{27} \quad (5\text{-}116)$$

$$a_{11}\beta_{21} + a_{21}\beta_{22} - \frac{b^2}{2}\beta_{21}\beta_{22} - \frac{b^2}{2}a_{11}\beta_{22}\beta_{27} + \beta_{26}$$

$$= - a_{12}\beta_{11} - a_{11}a_{12}\beta_{17} - a_{22}\beta_{21} - a_{11}a_{22}\beta_{27} \quad (5\text{-}117)$$

$$a_{12}\beta_{21} + a_{22}\beta_{22} - \frac{b^2}{2}\beta_{22}^2 - \frac{b^2}{2}a_{12}\beta_{22}\beta_{27}$$

$$= - a_{12}\beta_{12} - a_{12}^2\beta_{17} - a_{22}\beta_{22} - a_{12}\alpha_{22}\beta_{27} \quad (5\text{-}118)$$

$$-\frac{b^2}{2}\beta_{22}\beta_{23} - \beta_{26} = -a_{12}\beta_{13} - a_{22}\beta_{23} \qquad (5\text{-}119)$$

$$d_{11}\beta_{21} - \frac{b^2}{2}\beta_{22}\beta_{24} - \frac{b^2}{2}d_{11}\beta_{22}\beta_{27}$$

$$= -a_{12}\beta_{14} - a_{12}d_{11}\beta_{17} - a_{22}\beta_{24} - a_{22}d_{11}\beta_{27} \qquad (5\text{-}120)$$

$$d_{22}\beta_{22} - \frac{b^2}{2}\beta_{22}\beta_{25} = -a_{12}\beta_{15} - a_{22}\beta_{25} \qquad (5\text{-}121)$$

$$-\frac{b^2}{2}\beta_{22}\beta_{26} + \epsilon_2 = -a_{12}\beta_{16} - a_{22}\beta_{26} \qquad (5\text{-}122)$$

$$\frac{b^2}{2}\beta_{22}\beta_{27} + \beta_{23} = a_{12}\beta_{17} + a_{22}\beta_{27} \qquad (5\text{-}123)$$

After rearrangement and simplification of the above fourteen equations (5-110) to (5-123), yields:

$$2K_3 + 2a_{11}\beta_{11} + a_{21}\beta_{12} + \beta_{16} + a_{11}^2\beta_{17} + a_{21}\beta_{21}$$
$$+ a_{11}a_{21}\beta_{27} - \frac{b^2}{2}\beta_{12}\beta_{21} - \frac{b^2}{2}a_{11}\beta_{12}\beta_{27} = 0 \qquad (5\text{-}124)$$

$$a_{12}\beta_{11} + (a_{11} + a_{22})\beta_{12} + a_{11}a_{12}\beta_{17} + a_{21}\beta_{22}$$
$$+ a_{12}a_{21}\beta_{27} - \frac{b^2}{2}\beta_{12}\beta_{22} - \frac{b^2}{2}a_{12}\beta_{12}\beta_{27} = 0 \qquad (5\text{-}125)$$

$$-2K_3 + a_{11}\beta_{13} - \beta_{16} + a_{21}\beta_{23} - \frac{b^2}{2}\beta_{12}\beta_{23} = 0 \qquad (5\text{-}126)$$

$$d_{11}\beta_{11} + a_{11}\beta_{14} + a_{11}d_{11}\beta_{17} + a_{21}\beta_{14} + a_{21}d_{11}\beta_{27}$$
$$-\frac{b^2}{2}\beta_{12}\beta_{24} - \frac{b^2}{2}d_{11}\beta_{12}\beta_{27} = 0 \qquad (5\text{-}127)$$

$$d_{22}\beta_{12} + a_{11}\beta_{15} + a_{21}\beta_{25} - \frac{b^2}{2}\beta_{12}\beta_{25} = 0 \qquad (5\text{-}128)$$

$$a_{11}\beta_{16} + a_{21}\beta_{26} - \frac{b^2}{2}\beta_{12}\beta_{26} + \epsilon_1 = 0 \qquad (5\text{-}129)$$

$$\beta_{13} - a_{11}\beta_{17} - a_{21}\beta_{27} + \frac{b^2}{2}\beta_{12}\beta_{27} = 0 \qquad (5\text{-}130)$$

$$a_{12}\beta_{11} + a_{11}a_{12}\beta_{17} + (a_{11} + a_{22})\beta_{21} + a_{21}\beta_{22} + \beta_{26}$$

$$+ a_{11}a_{22}\beta_{27} - \frac{b^2}{2}\beta_{21}\beta_{22} - \frac{b^2}{2} a_{11}\beta_{22}\beta_{27} = 0 \qquad (5\text{-}131)$$

$$a_{12}\beta_{12} + a_{12}^2\beta_{17} + a_{12}\beta_{21} + 2a_{22}\beta_{22} + a_{12}a_{22}\beta_{27}$$

$$- \frac{b^2}{2}\beta_{22}^2 - \frac{b^2}{2} a_{12}\beta_{22}\beta_{27} = 0 \qquad (5\text{-}132)$$

$$a_{12}\beta_{13} + a_{22}\beta_{23} - \beta_{26} - \frac{b^2}{2}\beta_{22}\beta_{23} = 0 \qquad (5\text{-}133)$$

$$a_{12}\beta_{14} + a_{12}d_{11}\beta_{17} + d_{11}\beta_{21} + a_{22}\beta_{24} + a_{22}d_{11}\beta_{27}$$

$$- \frac{b^2}{2}\beta_{22}\beta_{24} - \frac{b^2}{2} d_{11}\beta_{22}\beta_{27} = 0 \qquad (5\text{-}134)$$

$$a_{12}\beta_{15} + d_{22}\beta_{22} + a_{22}\beta_{25} - \frac{b^2}{2}\beta_{22}\beta_{25} = 0 \qquad (5\text{-}135)$$

$$a_{12}\beta_{16} + a_{22}\beta_{26} - \frac{b^2}{2}\beta_{22}\beta_{26} + \epsilon_2 = 0 \qquad (5\text{-}136)$$

$$-a_{12}\beta_{17} - a_{22}\beta_{27} + \beta_{23} + \frac{b^2}{2}\beta_{22}\beta_{27} = 0 \qquad (5\text{-}137)$$

For determination of β_{21}, β_{26} and β_{27}, equations (5-124), (5-125), (5-126), (5-129), (5-130), (5-131), (5-132), (5-133), (5-136 and (5-137) among the above fourteen non-linear equations must be solved by a Newton-Raphson iteration method using a digital computer (see Appendix 1)

CHAPTER 6

STRUCTURE OF THE GENERAL SCHEMES OF OMRAC FOR A CONTINUOUS STIRRED TANK REACTOR

From Theory II : (Chapter 3 : 3.1.2)

OMRAC Scheme = OMR Scheme + OAC Scheme.

For the combination of the OMR and the Oac Schemes derived in detail in Chapters 4 and 5 respectively, the structure of general OMRAC schemes for a CSTR is established and used for the further work on hybrid computer programming both for complete simulation and for on-line operation.

6.1. General Scheme I

OMR Scheme:

Optimal control action : Optimal P

Optimal control law (equation (4-34))

$$m^*(t) = \frac{b}{2}\Big[\alpha_{12}\theta_1(t) + \alpha_{22}\theta_2(t) + \alpha_{23}\theta_d(t) + \alpha_{24}\theta_{L1}(t) + \alpha_{25}\theta_{L2}(t)\Big] \qquad (6\text{-}1)$$

OAC Scheme:

Optimal control action : Optimal P

Optimal control law (equation (5-27))

$$U^*(t) = m^*(t) + \frac{b}{2}\,\beta_{12}\Big[\theta_1^r(t) - \theta_1(t)\Big] \qquad (6\text{-}2)$$

The structure of the general scheme I of OMRAC is shown in Fig. 6.1.

9

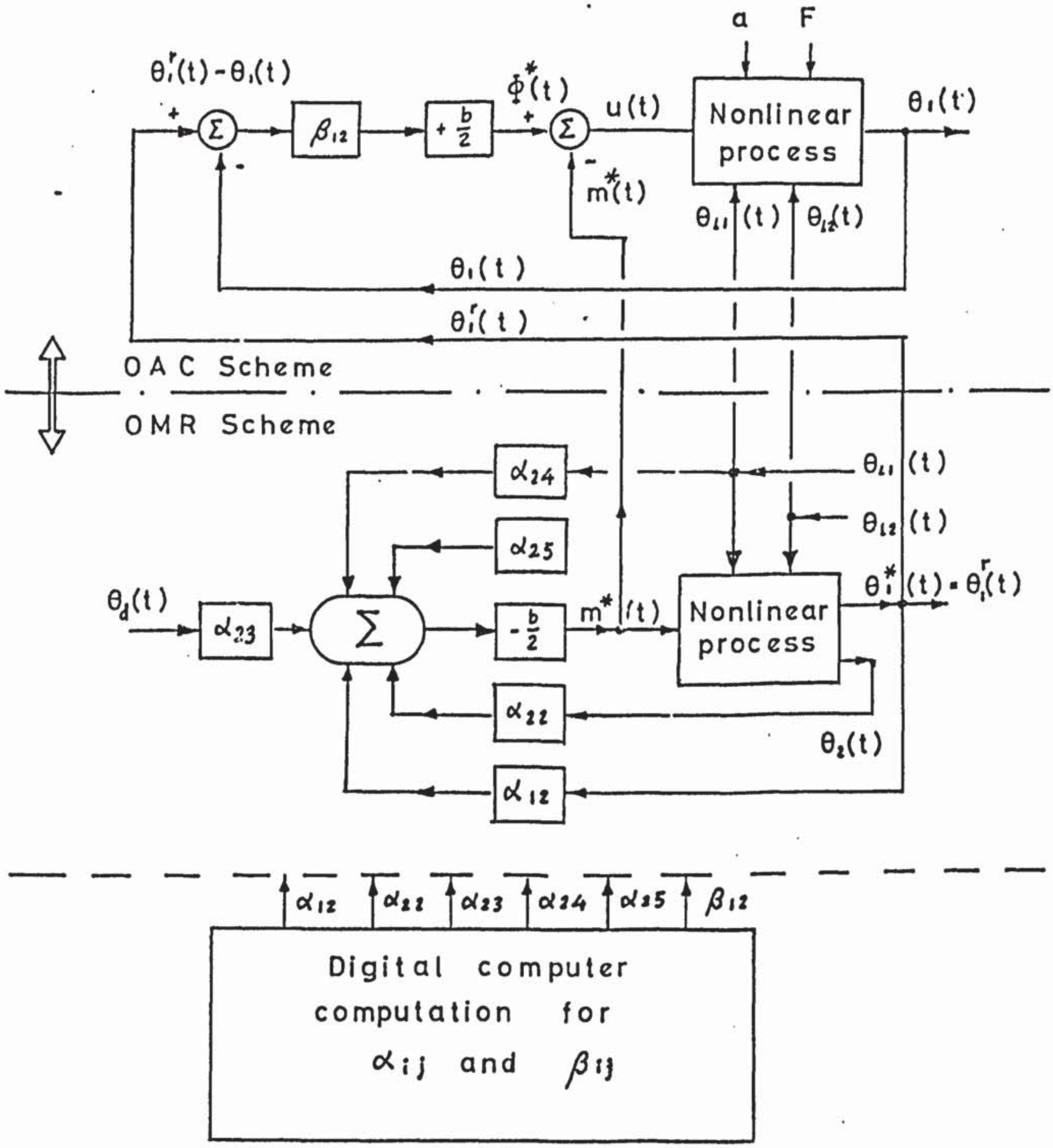

Figure 6·1 Structure of General scheme I of OMRAC

6.2. General Scheme II

OMR Scheme:

Optimal control action: Optimal P

Optimal control law (equation (4-34)):

$$m^*(t) = -\frac{b}{2}\Big[\alpha_{12}\theta_1(t) + \alpha_{22}\theta_2(t) + \alpha_{23}\theta_d(t) + \alpha_{24}\theta_{L1}(t) + \alpha_{25}\theta_{L2}(t)\Big] \qquad (6\text{-}2)$$

OAC Scheme:

Optimal control action : Optimal P + I

Optimal control law (equation (5-58)):

$$U^*(t) = m^*(t) + \frac{b}{2}\left\{\beta_{21}\Big[\theta_1^r(t) - \theta_1(t)\Big] + \beta_{26}\int_{t_o}^{t}\Big[\theta_1^r(t) - \theta_1(t)\Big]dt\right\} \qquad (6\text{-}3)$$

The structure of general scheme II of OMRAC is shown in Fig.6.2.

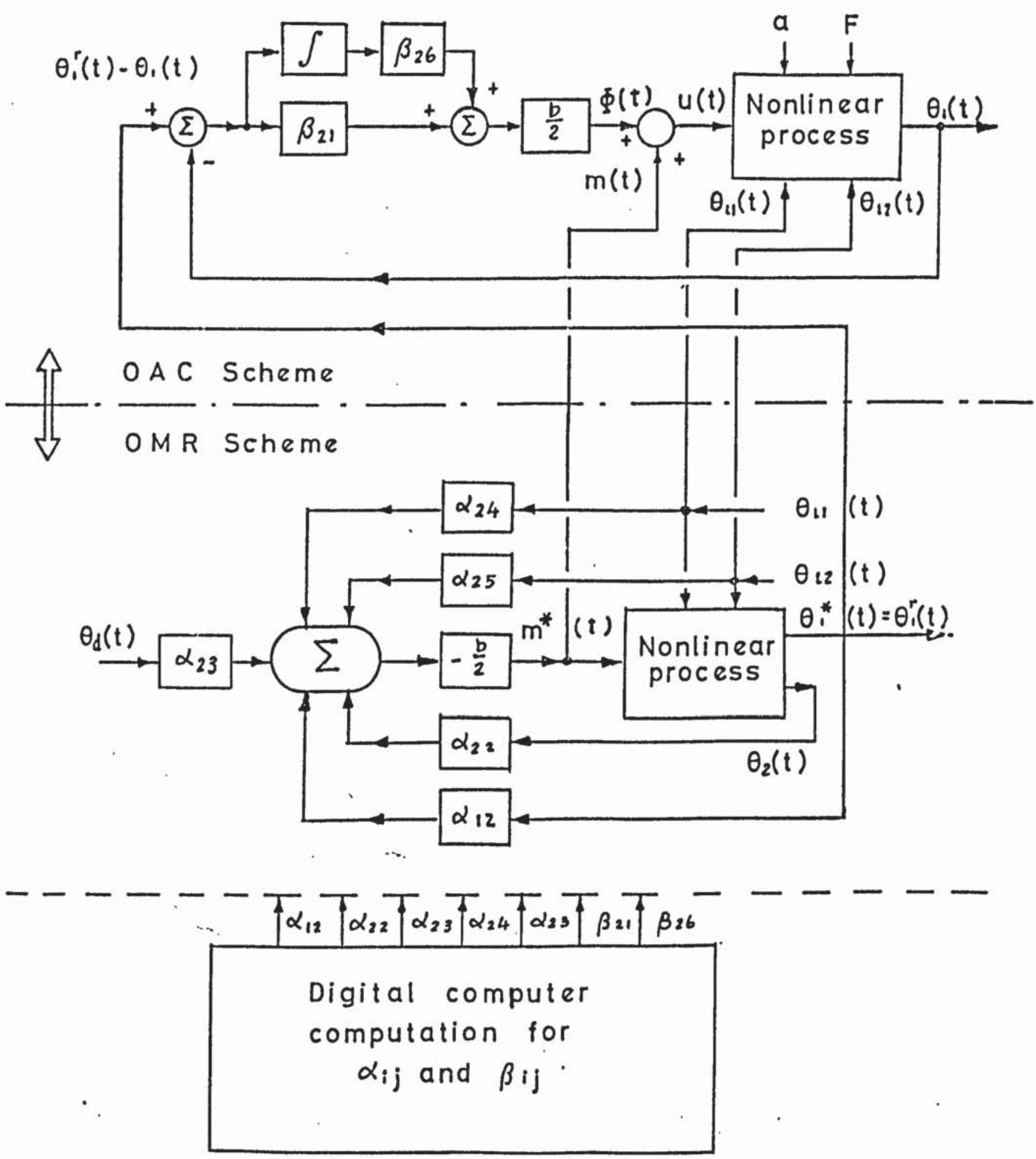

Figure 6·2 Structure of General scheme II of OMRAC

6.3. General Scheme III

OMR Scheme

Optimal control action : Optimal P

Optimal control law (equation (4-34)):

$$m^*(t) = -\frac{b}{2}\left[\alpha_{12}\theta_1(t) + \alpha_{22}\theta_2(t) + \alpha_{23}\theta_d(t) + \alpha_{24}\theta_{L1}(t) + \alpha_{25}\theta_{L2}(t)\right] \quad (6\text{-}1)$$

OAC Scheme

Optimal control action : Optimal P + I + D

Optimal control law (equation 5-100)):

$$U^*(t) = m^*(t) + \frac{b}{2}\left\{\beta_{21}\left[\theta_1^r(t) - \theta_1(t)\right] + \beta_{26}\int_{t_o}^{t}\left[\theta_1^r(t)-\theta_1(t)\right]dt + \beta_{27}\frac{d}{dt}\left[\theta_1^r(t)-\theta_1(t)\right]\right\} \quad (6\text{-}4)$$

The structure of the general scheme III of OMRAC is shown in Fig.6.3.

Note: The values of β_{21} and β_{26} in Optimal P + I + D are different from those in Optimal P + I, because of the different set of equations (Chapter 5).

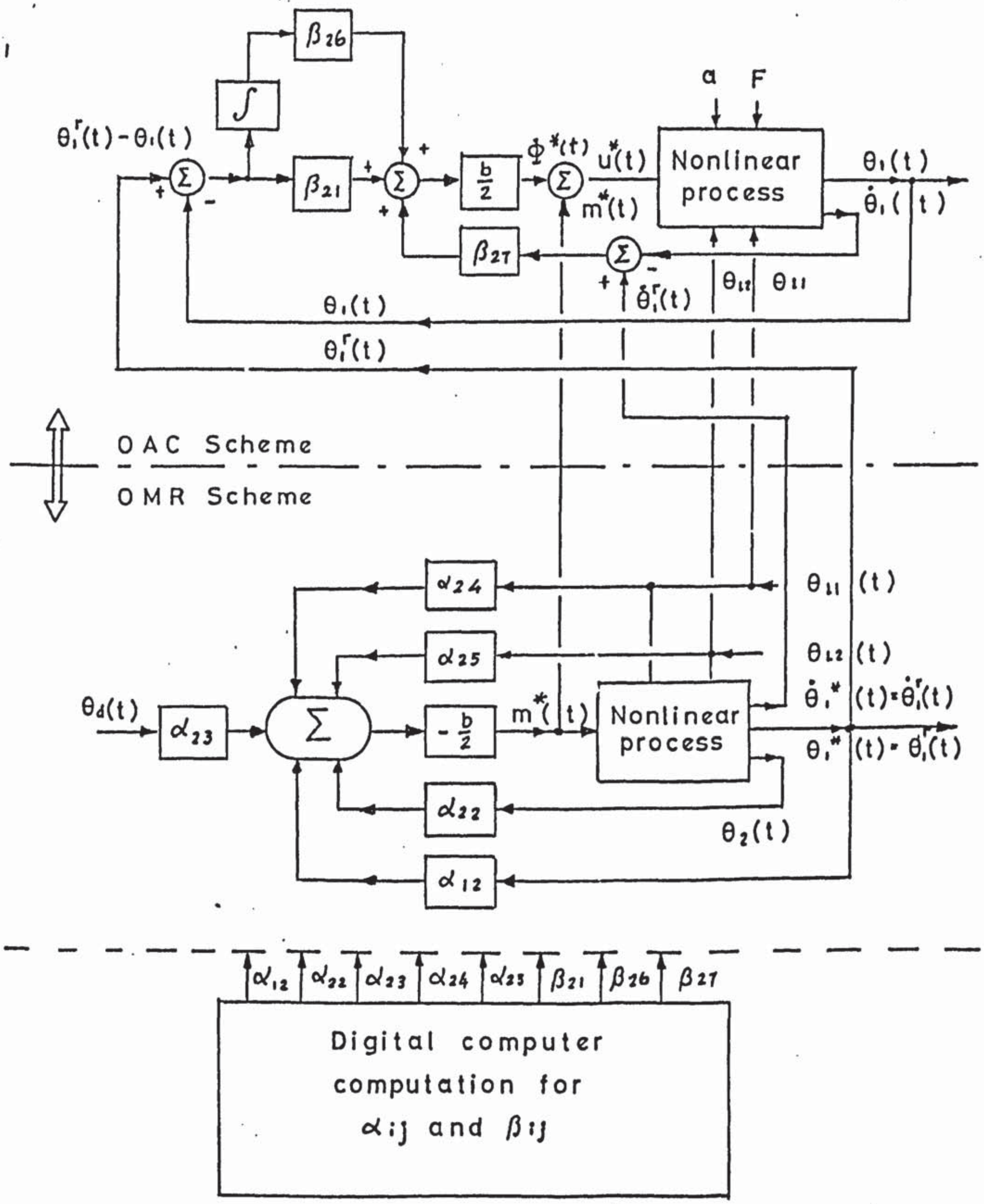

Figure 6.3 Structure of General scheme III of OMRAC

CHAPTER 7

COMPLETE SIMULATION ON OMRAC FOR A CSTR USING THE TR-10 AND TR-48 ANALOGUE AND HYBRID COMPUTERS

7.1. General case consideration for a partially simulated CSTR

The terms "complete simulation" and "partial simulation" have been defined by Buxton in his Ph.D.Thesis[80] (p:vii) as shown below:

Complete simulation:

This term is used when the entire process is modelled and then implemented on a computer to obtain a solution.

Partial simulation:

This term is used when some of the process exists in real plant whilst a particular part of it is chosen to be modelled and simulated on a computer. The computer operates on-line to the real equipment and the two operate together, thus representing the whole of the process for the purpose of the investigation.

The process equations of a CSTR may be rewritten as follows:

$$\frac{dC}{dt} = \frac{F}{V}(C_o - C) - aKC \qquad (7\text{-}1)$$

$$\frac{dT}{dt} = \frac{F}{V}(T_o - T) + \frac{aKC(-\Delta H)}{\rho C_p} - \frac{Q_c}{\rho C_p V} \qquad (7\text{-}2)$$

where $K = A e^{-\frac{E}{RT}}$ is the reaction rate (sec^{-1}) (7-3)

and the heat generation of an exothermic reaction, Q_g is:

$$Q_g = (-\Delta H)\ V\ aKC \qquad (7\text{-}4)$$

For partial simulation applied to a CSTR, equation (7-1) and part of equation (7-2) are simulated directly on the analogue computer and the heat is generated in the reactor by means of immersion heaters. The reactor temperature can be controlled by a feedback control loop containing a detecting element (thermocouple), a three mode conventional PID controller and a control valve to control the cooling water flowrate. The heat generation system using an immersion heater is designed to be actuated by a servomechansim. Complete and partial simulation for a step change applied to the reactor at the steady state was studied by means of the EAL TR-10 analogue computer and was reported by Buxton at the end of 1970.

Since for partial simulation of a CSTR, the reaction constants such as A and E in equation (7-3) can be arbitrarily selected in a certain reasonable range, other values ($-\Delta H$), K and Q_g can be calculated from operating experimental data.

By using Buxton's experiments 6 and 7 (p.337[80] the operating experimental data is shown as follows:

T_s	=	reactor temperature as steady state	=	$30^{o}C$
T_c	=	reactor inlet charge temperature	=	$19^{o}C$
T_{cl}	=	cooling water inlet temperature	=	$19^{o}C$
T_{cs}	=	cooling water outlet temperature at steady state	=	$27^{o}C$
C_s	=	reactor concentration at steady state	=	0.097 mol/litre
m_c	=	cooling water flowrate	=	2.15 litre/min
C_o	=	inlet concentration	=	1.0 mol/litre
F	=	reacter charge flowrate	=	3.0 litre/min

A	=	constant in Arrhenius equation	= $6.3 \times 10^{15}\ \frac{1}{sec}$
E	=	reaction energy, a constant	= 24000 cal/mol
R	=	gas constant	= 1.987 cal/mol.deg.K
V	=	reactor effective volume	= 16 litre
C_p	=	specific heat of reactant	= 1 cal/gm.deg C
ρ	=	density of reactant	= 1 gm/cm^3

Heat from immersion heater Q_g = 842 cal/sec

Reaction rate constant K = 0.032 1/sec

Change of enthalpy $(-\Delta H)$ = 18600 cal/mol.

Using the above experimental data at steady state, several simple calculations and checks can be made and are shown below:

1. Check on steady state concentration:

At steady state, equation (7-1) becomes:

$$0 = \frac{F}{V}(C_o - C_s) - aKC_s \tag{7-5}$$

$$K = Ae^{-\frac{E}{RT}} = 6.3 \times 10^{15} \exp\left[-\frac{24000}{1.987(273 + 30)}\right]$$

$$= 6.3 \times 10^{15} \exp(-39.8433)$$

$$= 0.0314 \quad (1/sec) \tag{7-6}$$

then

$$0 = \frac{3}{16 \times 60}(1 - C_s) - 1 \times 0.0314 \times C_s$$

$$\therefore \quad C_s = 0.08985 \cong 0.09 \text{ mol/litre}$$

i.e. the theoretical value of C_s = 0.09 (mol/litre)

and the experimantal value of C_s = 0.097 (mol/litre)

2. Check on Q_g.

$$Q_g = \rho_c C_{pc} F_c \ (T_{cs} - T_{c1}) + \rho \ C_p F(T_s - T_o) \quad (7\text{-}7)$$

$$= \frac{2.15 \times 1000}{60} (27-19) + \frac{3.0 \times 1000}{60} (30-19)$$

$$= 837 \text{ cal/sec.}$$

3. Check on $(-\Delta H)$

$$-\Delta H = \frac{Q_g}{V \ K \ C_s} = \frac{837}{16 \times 0.0314 \times 0.09} \quad (7\text{-}8)$$

$$= 18511 \text{ cal/mol.}$$

The above simple checks show quite good agreement between the partially simulated technique and the theoretical one.

From the above analysis, a general case of the research work on OMRAC for a partially simulated CSTR which was used both for complete simulation and on-line computer operation will be given below:

Operating steady state conditions:

C_s = 0.09 mol/litre

T_s = 30^oC

Operating normal inlet conditions:

C_o = 1.0 mol/litre

F = 3.0 litre/min.

Process physical constants:

V = 16.0 litre

ρ = 1.0 mol/cm^3

C_p = 1.0 cal/g.deg C

Reactant constants

$$A = 6.3 \times 10^{15} \text{ 1/sec.}$$

$$E = 24{,}000 \text{ cal/mol}$$

$$R = 1.987 \text{ cal/mol deg K}$$

7.2. Magnitude scaling and time scaling

All analogue and hybrid computer programming must be unified and represented by scaled computer variables and related equations through all the work both for complete simulation and on-line computer operation (see Part II)

7.2.1. Magnitude scaling

The estimated maximum value of variables and their scaled computer variables are tabulated in Table 7.1.

Table 7.1. Magnitude scaling

Process variables	Estimated max. value	Scaled computer variables (machine unit or mu) (1 mu = IO volt)
C (mol/litre)	C_m = 1.0 (mol/litre)	$\left[\frac{C}{C_m}\right]$
C_o (mol/litre)	C_m = 1.0 (mol/litre)	$\left[\frac{C_o}{C_m}\right]$
C_{os} (mol/litre)	C_m = 1.0 (mol/litre)	$\left[\frac{C_{os}}{C_m}\right]$
C_s (mol/litre)	C_m = 1.0 (mol/litre)	$\left[\frac{C_s}{C_m}\right]$
C_r (mol/litre)	C_m = 1.0 (mol/litre)	$\left[\frac{C_r}{C_m}\right]$

Table 7.1. Magnitude scaling (continued)

Process variable	Estimated max. value	Scaled computer variable (mu)
C_{rs} (mol/litre)	C_m = 1.0 (mol/litre)	$\left[\frac{C_{rs}}{C_m}\right]$
C_d (mol/litre)	C_m = 1.0 (mol/litre)	$\left[\frac{C_d}{C_m}\right]$
C_{ds} (mol/litre)	C_m = 1.0 (mol/litre)	$\left[\frac{C_{ds}}{C_m}\right]$
$\Delta C = \theta_1$ (mol/litre)	C_m = 1.0 (Mol/litre)	$\left[\frac{\Delta C}{C_m}\right]$
$\Delta C_o = \theta_2$ (mol litre)	C_m = 1.0 (mol/litre)	$\left[\frac{\Delta C_o}{C_m}\right]$
ΔC_r (mol/litre)	C_m = 1.0 (mol/litre)	$\left[\frac{\Delta C_r}{C_m}\right]$
ΔC_d (mol/litre)	C_m = 1.0 (mol/litre)	$\left[\frac{\Delta C_d}{C_m}\right]$
$\dot{C}$ (mol/litre-sec)	$\dot{C}_m$ = 0.1 (mol/litre-sec)	$\left[\frac{\dot{C}_m}{\dot{C}_m}\right]$
$\dot{C}_r$ (mol/litre-sec)	$\dot{C}_m$ = 0.1 (mol/litre-sec)	$\left[\frac{\dot{C}_r}{\dot{C}_m}\right]$
$\Delta\dot{C}$ (mol/litre-sec)	$\dot{C}_m$ = 0.1 (mol/litre-sec)	$\left[\frac{\Delta\dot{C}}{\dot{C}_m}\right]$
T (°C)	T_m = 100 (°C)	$\left[\frac{T}{T_m}\right]$
T (°C)	T_m' = 40 (°C)	$\left[\frac{T}{T_m'}\right]$
T (°C)	T_m'' =39.25(°C)	$\left[\frac{T}{T_m''}\right]$
T_o (°C)	T_m = 100 (°C)	$\left[\frac{T_o}{T_m}\right]$
T_s (°C)	T_m = 100 (°C)	$\left[\frac{T_s}{T_m}\right]$
$\Delta\dot{T}$ (°C/sec)	$\dot{T}_m$ = 1.0 (°C/sec)	$\left[\frac{\Delta\dot{T}}{\dot{T}_m}\right]$

Table 7.1. Magnitude scaling (continued)

Process variable	Estimated Max.Value	Scaled computer variable (mu)
ΔT (^oC)	T_m = 100 (^oC)	$\left[\frac{\Delta T}{T_m}\right]$
$\dot{T}$ (^oC/sec)	$\dot{T}_m$ = 1.0 (^oC/sec)	$\left[\frac{\dot{T}}{\dot{T}_m}\right]$
K (1/sec)	K_m = 0.1 (1/sec)	$\left[\frac{K}{K_m}\right]$
F (litre/min)	F_m = 5.0 (litre/min)	$\left[\frac{F}{F_m}\right]$
a (dimensionless)	a_m = 1.0 (dimensionless)	$\left[\frac{a}{a_m}\right]$
Q_c (Kcal/min) or (60 Kcal/h)	Q_{cm} = 100 (60 Kcal/h)	$\left[\frac{Q_c}{Q_{cm}}\right]$
Q_{cs} (Kcal/min) or (60 Kcal/h)	Q_{cm} = 100 (60 Kcal/h)	$\left[\frac{Q_{cs}}{Q_{cm}}\right]$
m* (Kcal/min) or (60 Kcal/h)	Q_{cm} = 100 (60 Kcal/h)	$\left[\frac{m^*}{Q_{cm}}\right]$
U* (Kcal/min) or (60 Kcal/h)	Q_{cm} = 100 (60 Kcal/h)	$\left[\frac{U^*}{Q_{cm}}\right]$
F_c (litre/min)	F_{cm} = 10 (litre/min)	$\left[\frac{F_c}{F_{cm}}\right]$
Q_g (Kcal/h x 10^{-3})	Q_{gm} = 10 (Kcal/h x 10^{-3})	$\left[\frac{Q_g}{Q_{gm}}\right]$

7.2.2. Time Scaling

$$\tau = \beta t \quad (7\text{-}9)$$

where

τ = machine time (sec)

t = process real time (sec)

β = time scale factor

For complete simulation work :

$$\beta = 0.1$$

For on-line computer operation :

$$\beta = 1.0$$

7.3. Modified Linearisation coefficients

Linearised equations (4-6) and (4-7) which omitted T_o term, can be written as follows:

$$\Delta\dot{C} = a_{11}\,\Delta C + a_{12}\,\Delta T + d_{11}\,\Delta C_o \qquad (7\text{-}10)$$

$$\Delta\dot{T} = a_{21}\,\Delta C + a_{22}\,\Delta T + b\,\Delta Q_c \qquad (7\text{-}11)$$

The scaled computer equations based on the information contained in Table 7.1, are

$$\left[\frac{\Delta\dot{C}}{\dot{C}_m}\right] = \left(\frac{a_{11}C_m}{\dot{C}_m}\right)\left[\frac{\Delta C}{C_m}\right] + \left(\frac{a_{12}T_m}{\dot{C}_m}\right)\left[\frac{\Delta T}{T_m}\right] + \left(\frac{d_{11}C_m}{\dot{C}_m}\right)\left[\frac{\Delta C_o}{C_m}\right] \qquad (7\text{-}12)$$

$$\left[\frac{\Delta\dot{T}}{\dot{T}_m}\right] = \left(\frac{a_{21}\cdot C_m}{\dot{T}_m}\right)\left[\frac{\Delta C}{C_m}\right] + \left(\frac{a_{22}\cdot T_m}{\dot{T}_m}\right)\left[\frac{\Delta T}{T_m}\right] + \left(\frac{b\cdot Q_{cm}}{\dot{T}_m}\right)\left[\frac{\Delta Q_c}{Q_{cm}}\right] \qquad (7\text{-}13)$$

The original linearised coefficients of equations (7-10) and (7-11) can be determined by given constants shown at the end of Section 1, then:

$$a_{11} = -\frac{F}{V} - A\exp\left(-\frac{E}{RT_s}\right)$$

$$= -\left(\frac{3}{60} \times \frac{1}{16}\right) - 0.0314 = -0.0345 \qquad (7\text{-}14\text{-}1)$$

$$a_{12} = \left(-\frac{E}{RT_o^2}\right) A \exp\left(-\frac{E}{RT_s}\right) \cdot C_s$$

$$= \frac{39.8433}{303} \times 0.0314 \times 0.09 = 0.00037 \qquad (7\text{-}14\text{-}2)$$

$$a_{21} = \frac{(-\Delta H) A \exp\left(-\frac{E}{RT_s}\right)}{\rho C_p \times 1000}$$

$$= \frac{18511 \times 0.0314}{1 \times 1 \times 1000} = 0.5812 \qquad (7\text{-}14\text{-}3)$$

$$a_{22} = -\frac{F}{V} - \frac{(-\Delta H) A \exp\left(-\frac{E}{RT_s^2}\right) C_s}{\rho C_p}$$

$$= -\left(\frac{3}{60} \times \frac{1}{60}\right) - \left(\frac{18511 \times 0.0314}{1 \times 1 \times 1000}\right)\left(\frac{39.8433}{303}\right)(0.09)$$

$$= -0.00995 \cong -0.01 \qquad (7\text{-}14\text{-}4)$$

$$b = -\frac{1}{\rho C_p V} \cdot \frac{1}{60} = \frac{-1}{1 \times 1 \times 16 \times 60} = 0.0011 \qquad (7\text{-}14\text{-}5)$$

$$d_{11} = \frac{F}{V} \cdot \frac{1}{60} = \frac{3}{16} \cdot \frac{1}{60} = 0.003 \qquad (7\text{-}14\text{-}6)$$

Substituting all of the above calculated coefficients and estimated maximum values into equations (7-12) and (7-13) then gives:

$$\left[\frac{\Delta \dot{C}}{\dot{C}_m}\right] = \left(\frac{-0.0345 \times 1.0}{0.1}\right)\left[\frac{\Delta C}{C_m}\right] + \left(\frac{0.00037 \times 100}{0.1}\right)\left[\frac{\Delta T}{T_m}\right]$$

$$+ \left(\frac{0.003 \times 1.0}{0.1}\right)\left[\frac{\Delta C_o}{C_m}\right]$$

$$= -(0.345)\left[\frac{\Delta C}{C_m}\right] + 0.37\left[\frac{\Delta T}{C_m}\right] + 0.03\left[\frac{\Delta C_o}{C_m}\right] \qquad (7\text{-}15)$$

$$\left[\frac{\Delta\dot{T}}{\dot{T}_m}\right] = \left(\frac{0.58 \times 1}{1}\right)\left[\frac{\Delta C}{C_m}\right] + \left(\frac{-0.01 \times 100}{1.00}\right)\left[\frac{\Delta T}{T_m}\right]$$

$$+ \left(\frac{-0.0011 \times 100}{1.0}\right)\left[\frac{\Delta Q_c}{Q_{cm}}\right]$$

$$= + (0.58)\left[\frac{\Delta C}{C_m}\right] - (1.0)\left[\frac{\Delta T}{T_m}\right] - (0.11)\left[\frac{\Delta Q_c}{Q_{cm}}\right] \quad (7\text{-}16)$$

From scaled computer variable equations (7-15) and (7-16) the modified linearised coefficients will be:

$$\left.\begin{aligned} a'_{11} &= -0.345 = D(1) \\ a'_{12} &= +0.37 = D(2) \\ a'_{21} &= +0.58 = D(3) \\ a'_{22} &= -1.00 = D(4) \\ b' &= -0.11 = D(5) \\ d'_{11} &= +0.03 = D(6) \end{aligned}\right\} \quad (7.17)$$

The above set of modified linearisation coefficients can be used as D(i) defined in Appendix 1 for all digital computer programming as "READ INPUT" to compute all optimal control law coefficients α_{ij} and β_{ij} both for the OMR scheme and the OAC scheme.

Then all computed values of α_{ij} and β_{ij} will be potentiometer setting values in the analogue and hybrid computer programming and is discussed in the following section.

7.4. Programming the computer

7.4.1. OMR Scheme computer programming

From equations (7-1) and (7-2) and the corresponding equations (7-19) and (7-20), the scaled computer variable equations of the OMR scheme are shown below:

$$\left[\frac{\dot{C}}{\dot{C}_m}\right] = \left(\frac{F}{60.V}\right)\left(\frac{C_m}{\dot{C}_m}\right)\left[\frac{C_o}{C_m}\right] - \left(\frac{F}{60V}\right)\left(\frac{C_m}{\dot{C}_m}\right)\left[\frac{C}{C_m}\right]$$

$$- \left(\frac{a_s\ K_m\ C_m}{\dot{C}_m}\right)\left[\frac{K}{K_m}\right]\left[\frac{C}{C_m}\right]$$

$$= \left(\frac{3}{60 \times 16}\right)\left(\frac{1}{1}\right)\left[\frac{c_o}{C_m}\right] - \left(\frac{3}{60 \times 16}\right)\left(\frac{1}{1}\right)\left[\frac{C}{C_m}\right]$$

$$- \left(\frac{1 \times .1 \times 1}{0.1}\right)\left[\frac{K}{K_m}\right]\left[\frac{C}{C_m}\right] \qquad (7\text{-}18)$$

$$\left[\frac{\dot{T}}{\dot{T}_m}\right] = \left(\frac{F}{60V}\right)\left(\frac{T_m}{\dot{T}_m}\right)\left[\frac{T_o}{T_m}\right] - \left(\frac{F}{60V}\right)\left(\frac{T_m}{\dot{T}_m}\right)\left[\frac{T}{T_m}\right]$$

$$- \left(\frac{a_s\ K_m\ C_m\ \ H}{C_p\ \dot{T}_m x1000}\right)\left[\frac{K}{K_m}\right]\left[\frac{C}{C_m}\right]$$

$$- \left(\frac{Q_{cm}}{C_p V\ 60\ .\ \dot{T}_m}\right)\left[\frac{Q_c}{Q_{cm}}\right]$$

$$= \left(\frac{3}{60 \times 16}\right)\left(\frac{100}{1.0}\right)\left[\frac{T_o}{T_m}\right] - \left(\frac{3}{60 \times 16}\right)\left(\frac{100}{1.0}\right)\left[\frac{T}{T_m}\right]$$

$$- \left(\frac{1.0 \times 0.1 \times 1.0 \times 18511}{1.0 \times 1.0 \times 1.0 \times 1000}\right)\left[\frac{K}{K_m}\right]\left[\frac{C}{C_m}\right]$$

$$- \left(\frac{100}{1.0 \times 1.0 \times 16 \times 60 \times 1.0}\right)\left[\frac{Q_c}{Q_{cm}}\right] \qquad (7\text{-}19)$$

Simplifying equations (7-18) and (7-19) gives :

$$\left[\frac{\dot{C}}{\dot{C}_m}\right] = 0.031\left[\frac{C_o}{C_m}\right] - 0.031\left[\frac{C}{C_m}\right] - 1.0\left[\frac{K}{K_m}\right]\left[\frac{C}{C_m}\right] \qquad (7\text{-}20)$$

$$\left[\frac{\dot{T}}{\dot{T}_m}\right] = 0.31\left[\frac{T_o}{T_m}\right] - 0.31\left[\frac{T}{T_m}\right] - 1.85\left[\frac{K}{K_m}\right]\left[\frac{C}{C_m}\right]$$

$$- 0.11\left[\frac{Q_c}{Q_{cm}}\right] \qquad (7\text{-}21)$$

The optimal control law of the OMR scheme from Chapter 6 equation (6-1) gives:

$$\left[\frac{Q_c}{Q_{cm}}\right] = \left[\frac{Q_{cs}}{Q_{cm}}\right] + \left[\frac{m^*}{Q_{cm}}\right] ; \tag{7-22}$$

and $$\left[\frac{m^*}{Q_{cm}}\right] = -\frac{b'}{2}\left(\alpha_{12}\left[\frac{\Delta C}{C_m}\right] + \alpha_{22}\left[\frac{\Delta T}{T_m}\right] + \alpha_{23}\left[\frac{\Delta C_d}{C_m}\right] + \alpha_{24}\left[\frac{\Delta C_o}{C_m}\right]\right) \tag{7-23}$$

where:

$$\left[\frac{\Delta C}{C_m}\right] = \left[\frac{C}{C_m}\right] + \left[\frac{C_s}{C_m}\right] = \left[\frac{C}{C_m}\right] - \left[\frac{.09}{1.0}\right] = \left[\frac{C}{C_m}\right] - 0.9\ v \tag{7-24}$$

$$\left[\frac{\Delta T}{T_m}\right] = \left[\frac{T}{T_m}\right] - \left[\frac{T_s}{T_m}\right] = \left[\frac{T}{T_m}\right] - \left[\frac{30}{100}\right] = \left[\frac{T}{T_m}\right] - 3.0\ v \tag{7-25}$$

$$\left[\frac{\Delta C_d}{C_m}\right] = \left[\frac{C_d}{C_m}\right] - \left[\frac{C_{ds}}{C_m}\right] = \left[\frac{C_d}{C_m}\right] - \left[\frac{.09}{1.0}\right] = \left[\frac{C_d}{C_m}\right] - 0.9\ v \tag{7-26}$$

$$\left[\frac{\Delta C_o}{C_m}\right] = \left[\frac{C_o}{C_m}\right] + \left[\frac{C_{os}}{C_m}\right] = \left[\frac{C_o}{C_m}\right] - \left[\frac{1.0}{1.0}\right] = \left[\frac{C_o}{C_m}\right] - 10\ V \tag{7-27}$$

$\left[\frac{Q_{cs}}{Q_{cm}}\right]$ calculated by trial and error from equations (7-20) and (7-21) at steady state, is

$$\left[\frac{Q_{cs}}{Q_{cm}}\right] = -\ 0.753\ \text{mu} = -\ 7.53\ \text{volt.}$$

Using the above scaled computer variable equations (7-20) to (7-27) the computer diagram of the OMR scheme is shown in Fig.7.1.

7.4.2. OAC scheme computer programming:

Process scaled computer variable equations:

$$\left[\frac{\dot{C}}{\dot{C}_m}\right] = \left(\frac{F_m}{60\ V}\right)\left(\frac{C_m}{\dot{C}_m}\right)\left[\frac{C_o}{C_m}\right]\left[\frac{F}{F_m}\right] - \left(\frac{F_m}{60V}\right)\left(\frac{C_m}{\dot{C}_m}\right)\left[\frac{C}{C_m}\right]\left[\frac{F}{F_m}\right]$$

$$-\left(\frac{a_m\ K_m\ C_m}{\dot{C}_m}\right)\left[\frac{a}{a_m}\right]\left[\frac{K}{K_m}\right]\left[\frac{C}{C_m}\right]$$

$$= \left(\frac{5}{60 \times 16}\right)\left(\frac{1}{0.1}\right)\left[\frac{C_o}{C_m}\right]\left[\frac{F}{F_m}\right] - \left(\frac{5}{60 \times 16}\right)\left(\frac{1}{0.1}\right)\left[\frac{C}{C_m}\right]\left[\frac{F}{F_m}\right]$$

$$-\left(\frac{1.0 \times 0.1 \times 1.0}{0.1}\right)\left[\frac{a}{a_m}\right]\left[\frac{K}{K_m}\right]\left[\frac{C}{C_m}\right] \qquad (7.28)$$

$$\left[\frac{\dot{T}}{\dot{T}_m}\right] = \left(\frac{F_m}{60V}\right)\left(\frac{T_m}{\dot{T}_m}\right)\left[\frac{T_o}{T_m}\right]\left[\frac{F}{F_m}\right] - \left(\frac{F_m}{60V}\right)\left(\frac{T_m}{\dot{T}_m}\right)\left[\frac{T}{T_m}\right]\left[\frac{F}{F_m}\right]$$

$$-\left(\frac{a_m\ K_m\ C_m\ \Delta H}{\rho\ C_p\ T_m \times 1000}\right)\left[\frac{a}{a_m}\right]\left[\frac{K}{K_m}\right]\left[\frac{C}{C_m}\right]$$

$$-\left(\frac{Q_{cm}}{\rho C_p\ V \times 60} \cdot \frac{1}{T_m}\right)\left[\frac{Q_c}{Q_{cm}}\right]$$

$$= \left(\frac{5}{60 \times 16}\right)\left(\frac{1.0}{1.0}\right)\left[\frac{F}{F_m}\right]\left[\frac{T_o}{T_m}\right] - \left(\frac{5}{60 \times 16}\right)\left(\frac{100}{1.0}\right)\left[\frac{F}{F_m}\right]\left[\frac{T}{T_m}\right]$$

$$-\left(\frac{1.0 \times 0.1 \times 1.0 \times 18511}{1.0 \times 1.0 \times 1.0 \times 1000}\right)\left[\frac{a}{a_m}\right]\left[\frac{K}{K_m}\right]\left[\frac{C}{C_m}\right]$$

$$-\left(\frac{100}{1.0 \times 1.0 \times 16 \times 60 \times 1}\right)\left[\frac{Q_c}{Q_{cm}}\right] \qquad (7\text{-}29)$$

Simplifying equations (7-28) and (7-29) gives

$$\left[\frac{\dot{C}}{\dot{C}_m}\right] = 0.052\left[\frac{C_o}{C_m}\right]\left[\frac{F}{F_m}\right] - 0.052\left[\frac{C}{C_m}\right]\left[\frac{F}{F_m}\right]$$

$$-\ 1.0\left[\frac{a}{a_m}\right]\left[\frac{K}{K_m}\right]\left[\frac{C}{C_m}\right] \qquad (7\text{-}30)$$

$$\left[\frac{T}{T_m}\right] = 0.52\left[\frac{T_o}{T_m}\right]\left[\frac{F}{F_m}\right] - 0.52\left[\frac{T}{T_m}\right]\left[\frac{F}{F_m}\right] - 1.85\left[\frac{a}{a_m}\right]\left[\frac{K}{K_m}\right]\left[\frac{C}{C_m}\right] - 0.11\left[\frac{Q_c}{Q_{cm}}\right] \quad (7.31)$$

Optimal control law for the OAC scheme:

From Chapter 6, equations (6-2), (6-3) and (6-4) give the following relationship which is developed below for the combinations of control modes used in the work.

$$\left[\frac{Q_c}{Q_{cm}}\right] = \left[\frac{Q_{cs}}{Q_{cm}}\right] + \left[\frac{U^*}{Q_{cm}}\right] \quad (7\text{-}32)$$

1. Optimal P control:

$$\left[\frac{U^*}{Q_{cm}}\right] = \left[\frac{m^*}{Q_{cm}}\right] + 0.055\,\beta_{12}\left(\left[\frac{\Delta C_r}{C_m}\right] - \left[\frac{\Delta C}{C_m}\right]\right) \quad (7\text{-}33)$$

$$\text{Now}\left[\frac{\Delta C_r}{C_m}\right] = \left[\frac{C_r}{C_m}\right] - \left[\frac{C_{rs}}{C_m}\right] \quad (7\text{-}34)$$

$$\left[\frac{\Delta C}{C_m}\right] = \left[\frac{C}{C_m}\right] - \left[\frac{C_s}{C_m}\right] \quad (7\text{-}35)$$

$$\text{and}\left[\frac{C_{rs}}{C_m}\right] = \left[\frac{C_s}{C_m}\right] \quad (7\text{-}36)$$

$$\therefore \left[\frac{U^*}{Q_{cm}}\right] = \left[\frac{m^*}{Q_{cm}}\right] + 0.055\,\beta_{12}\left(\left[\frac{C_r}{C_m}\right] - \left[\frac{C}{C_m}\right]\right) \quad (7\text{-}37)$$

2. Optimal P + I control

$$\left[\frac{U^*}{Qcm}\right] = \left[\frac{m^*}{Q_{cm}}\right] + 0.055\left(\beta_{21}\left(\left[\frac{C_r}{C_m}\right] - \left[\frac{C}{C_m}\right]\right) + \beta_{26}\int_{t_o}^{t}\left(\left[\frac{C_r}{C_m}\right] - \left[\frac{C}{C_m}\right]\right) dt\right) \quad (7\text{-}38)$$

3. <u>Optimal P + I + D Control</u>

$$\left[\frac{U^*}{Q_{cm}}\right] = \left[\frac{m^*}{Qcm}\right] + 0.055\left(\beta_{21}\left(\left[\frac{C_r}{C_m}\right]-\left[\frac{C}{Cm}\right]\right)\right.$$

$$+ \beta_{26}\int_{t_o}^{t}\left(\left[\frac{C_r}{C_m}\right] - \left[\frac{C}{C_m}\right]\right) dt$$

$$\left. + \beta_{27}\left(\left[\frac{C_r}{C_m}\right] - \left[\frac{C}{C_m}\right]\right)\right) \qquad (7\text{-}39)$$

Using the above scaled computer variable equations (7.30), (7-31), (7-32), (7-37), (7-38) and (7-39), the computer diagram of the OAC scheme is shown in Fig.7.2.

The computer diagram of the optimal PID control law is shown in Fig.7.3

By using the same equations (7-22) to (7-27), the computer diagram for the unadapted optimal control operation is shown in Fig.7.4.

The computer diagram for performance response is shown in Fig.7.5. Performance response (PR) is defined as the integral of the response square error

$$\text{i.e.} \quad PR = \int_{t_o}^{t}\left(\left[\frac{C_r}{C_m}\right]-\left[\frac{C}{C_m}\right]\right)^2 dt \qquad (7\text{-}40)$$

and is used in "Optimal Adaptivity" for quantitative analysis of OMRAC (See Chapter 11, Part II)

The higher and lower limits of constraint can be estimated from Buxton's experimental data at steady state (Section 1)

$$a \leqslant \left[\frac{U^*}{Q_{cm}}\right] \leqslant b \qquad (7\text{-}41)$$

where

$a = 1.72$ volt

$b = + 6.28$ volt

The computer diagram for optimal control law constraints is shown in Fig.7.6.

7.4.3. VDGF Programming on $\left[\frac{T}{T_m}\right]$ vs. $\left[\frac{K}{K_m}\right]$

The Arrhenius equation (7-3) is used both for the OMR scheme and the OAC scheme and should be carefully programmed as follows:

From equation (7-3) :

$$K = 6.3 \times 10^5 \exp\left(- \frac{24000}{1.987\ (273 + T)}\right) \qquad (7\text{-}42)$$

Let

$$K_m = A \exp\left(- \frac{E}{RT_m'}\right) \text{ where } T_m' = {}^{\circ}K \qquad (7\text{-}43)$$

$$T_m' = 40^{\circ}C = 317\ {}^{\circ}K$$

then

$$\frac{K}{K_m} = \exp\left(\frac{24000}{1.987 \times 313} - \frac{24000}{1,987\ (273 + T)}\right) \qquad (7\text{-}44)$$

Programming of equations (7-42) and (7-44) on the digital computer is shown in Appendix 1-10 and 1-11 and from the computer results:

$T = 39^{\circ}C$, $K = 0.969$

$T_m' = 40^{\circ}C$, $K = 0.1097$

$T_m'' = 39.25^{\circ}C$, $K = 0.10$

Then the VDFG can be programmed as follows

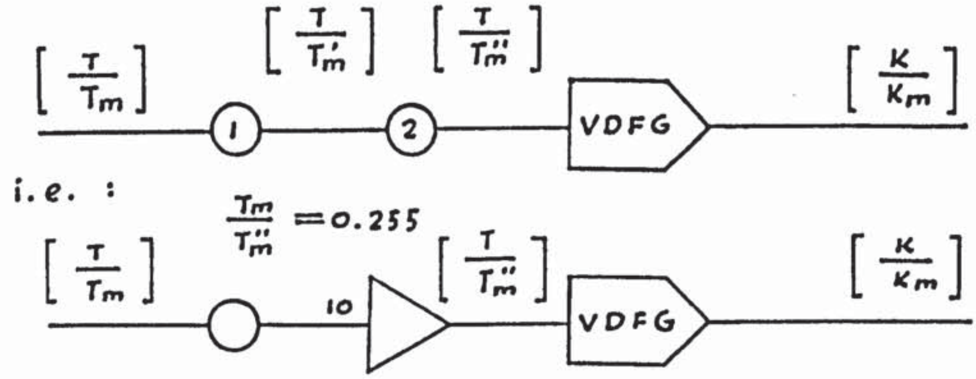

VDFG - 2 on TR-48 was programmed for the OMR scheme

VDFG - 1 on TR-48 was programmed for the OAC scheme

(see Appendix Fig.A3.1)

7.5. Potentiometer and Amplifier assignments

Potentiometer and amplifier assignments of the overall OMRAC scheme are tabulated as follows: -

Table 7.2. Potentiometer setting assignment sheet for the OMR scheme (Fig.7.1)

Table 7.3. Amplifier Assignment sheet for the OMR scheme (Fig.7.1).

Table 7.4. Potentiometer setting assignment sheet for the OAC scheme (Fig.7.2)

Table 7.5. Potentiometer setting assignment sheet for the OAC scheme (Figs. 7.3, 7.4, 7.5, and 7.6)

Table 7.6. Amplifier Assignment sheet for the OAC scheme (Fig.7.2)

Table 7.7. Amplifier assignment sheet for the OAC scheme (Figs. 7.3, 7.4, 7.5 and 7.6).

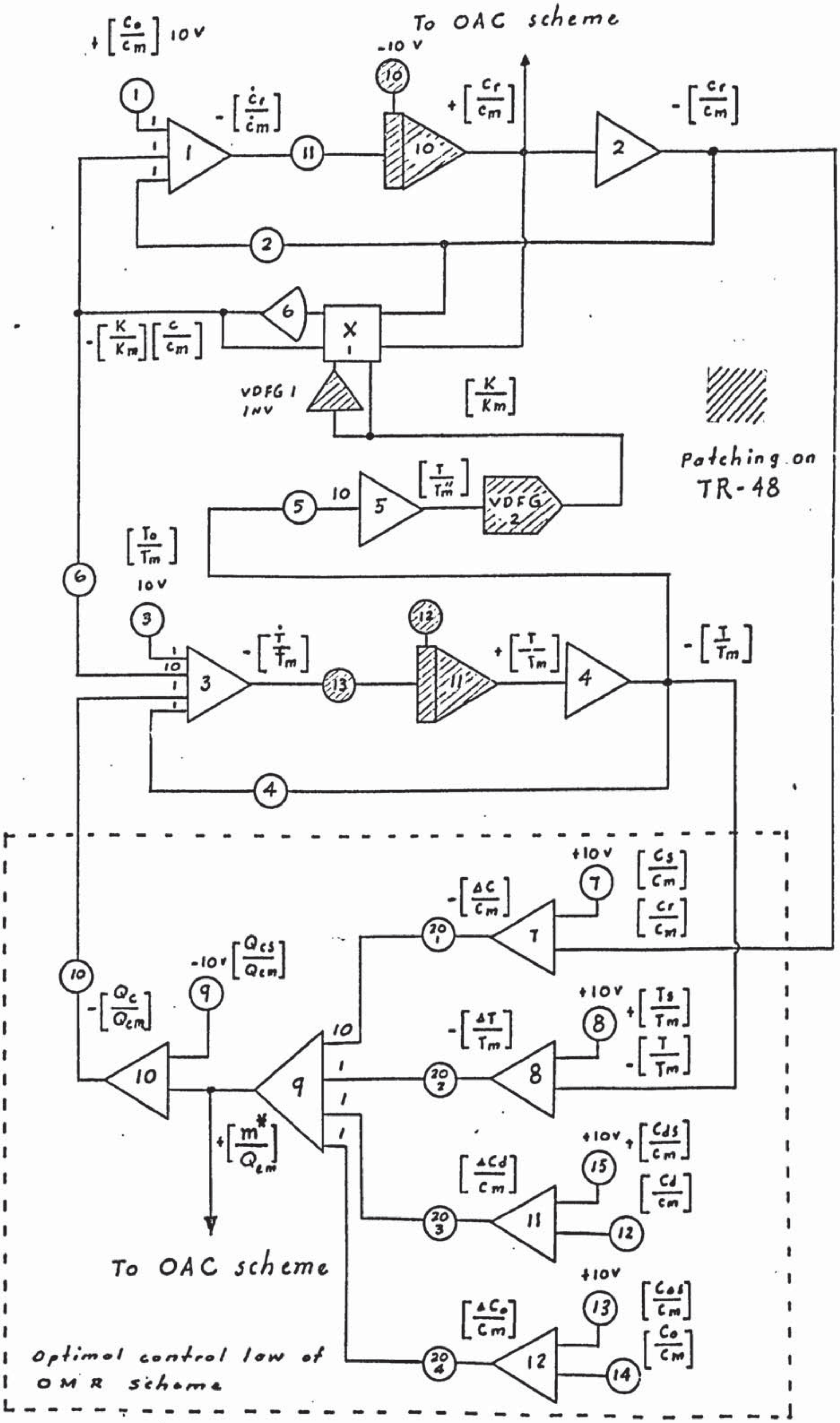

Figure 7.1 Compute diagram of OMR scheme
(on TR-10)

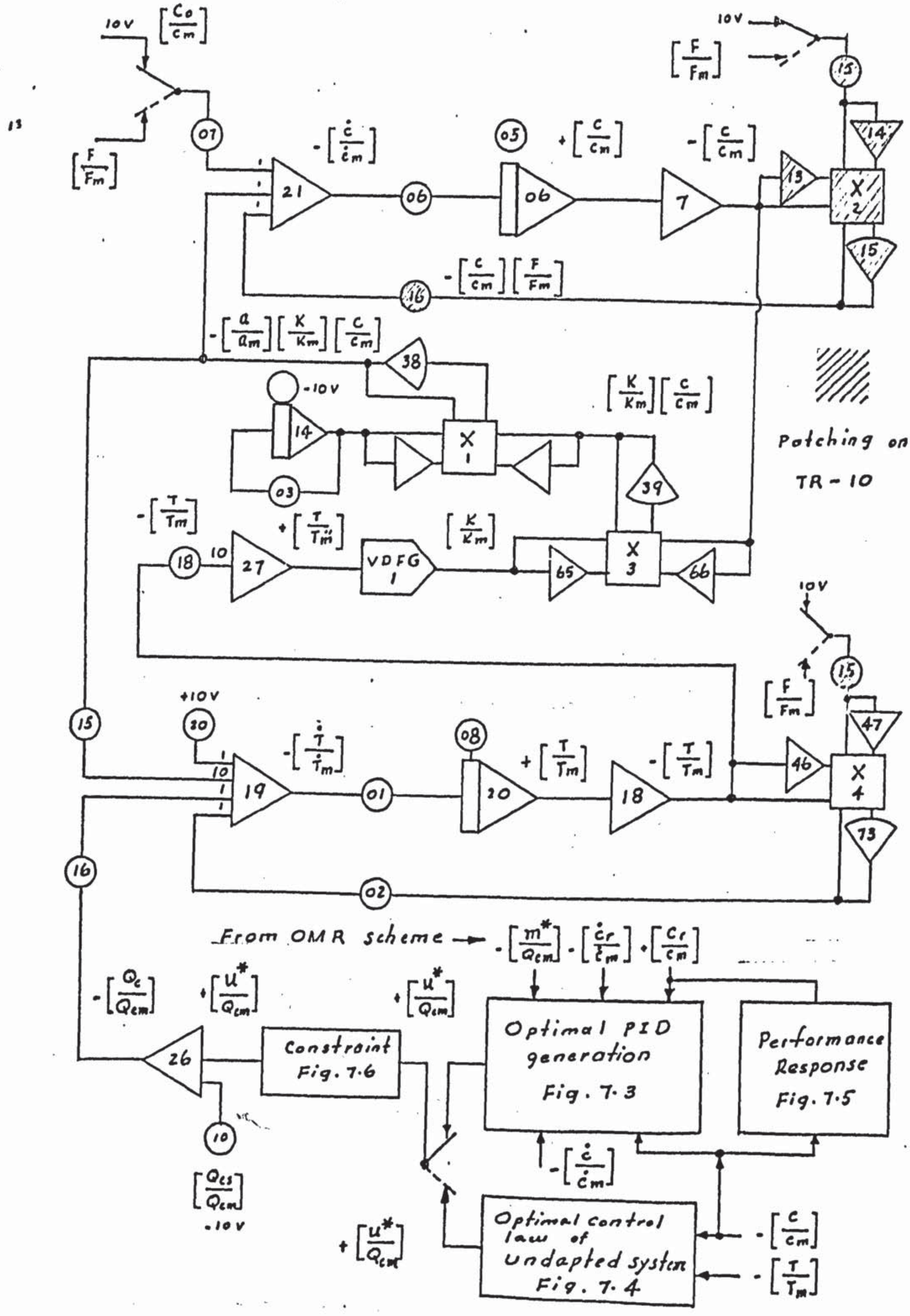

Figure 7.2 Computer diagram of OAC scheme (on TR-48)

14

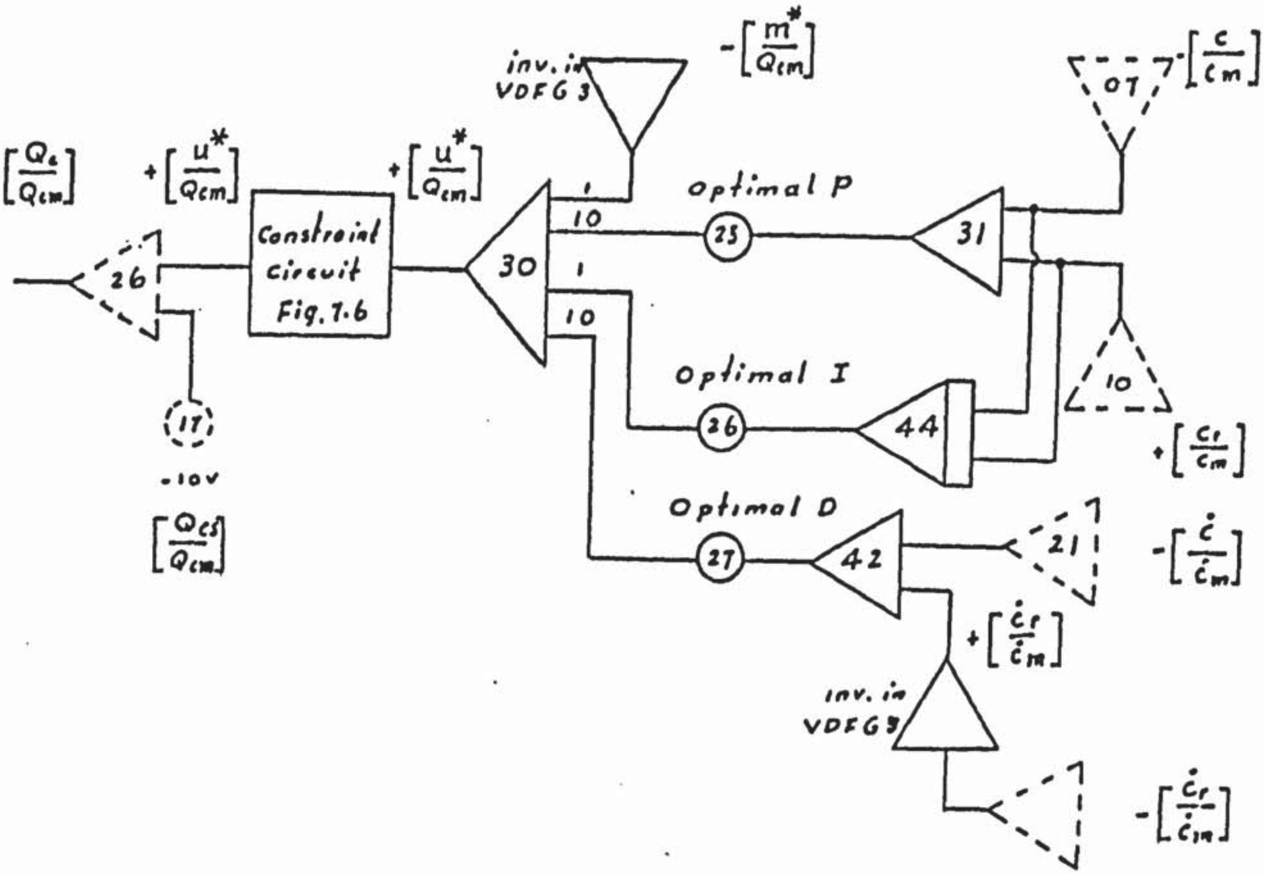

Figure 7.3 Computer diagram of optimal PID control law generation

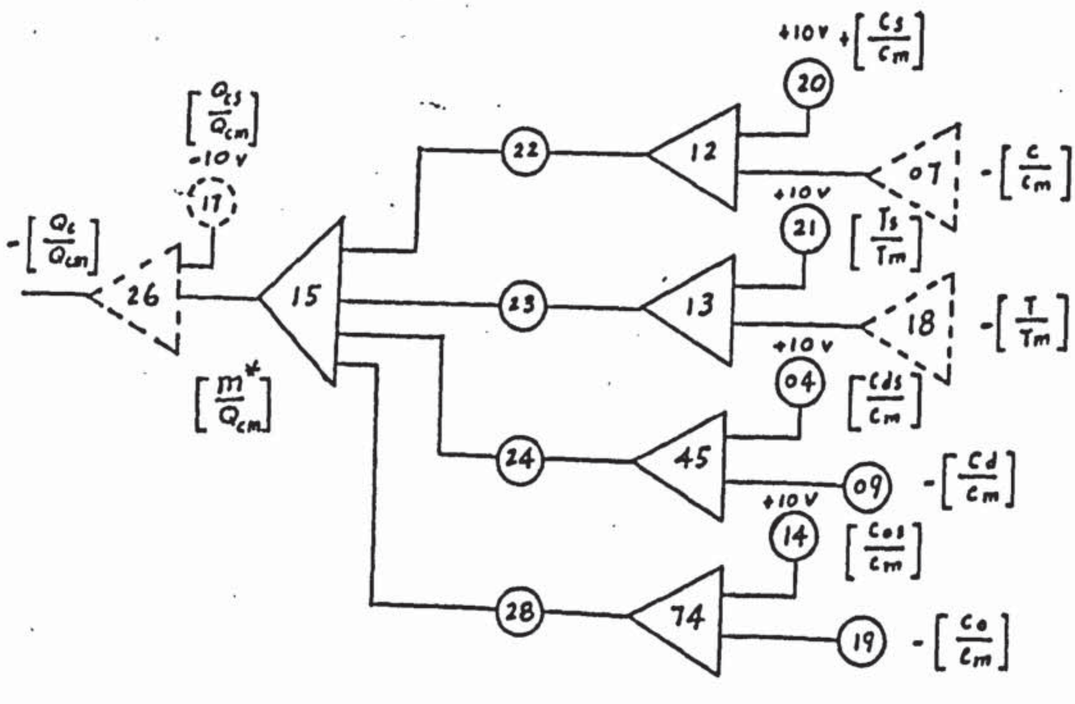

Figure 7.4 Computer diagram of OMR optimal control law generation

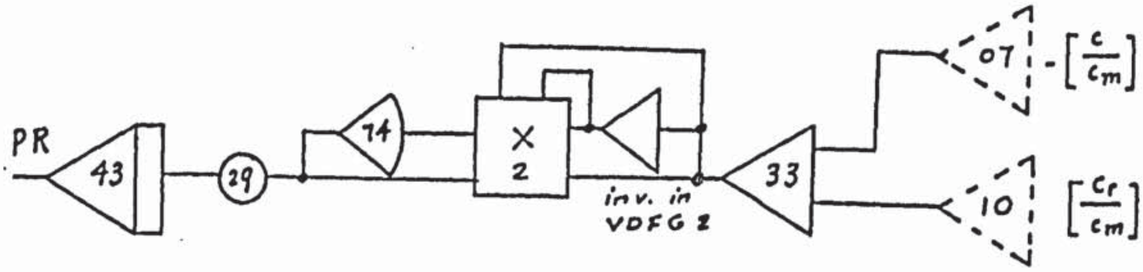

Figure 7.5 Computer diagram of performance response (PR)

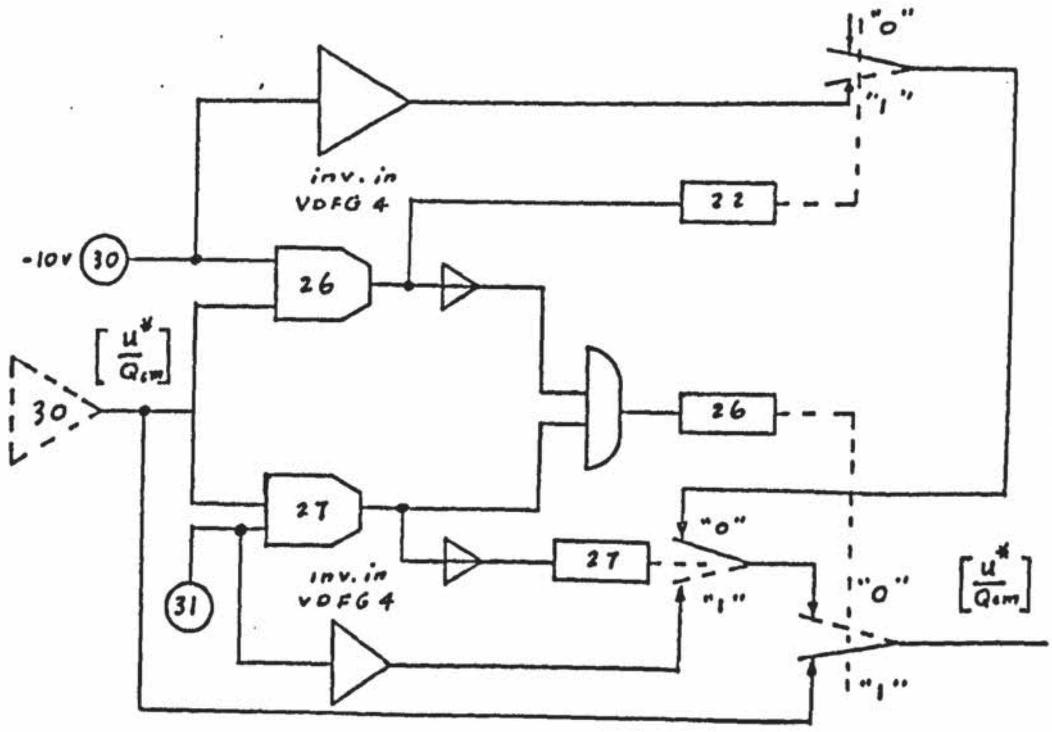

Figure 7.6 Computer diagram of optimal control law constraints

TABLE 7.2.

Potentiometer assignment sheet for the OMR Scheme

(Fig. 7.1)

Computer used	Pot No.	Parameter description	Setting static check	Notes
TR-10	1		0.031	eq.(7-20)
"	2		0.031	eq. (7-20)
"	3	$\left[\frac{T_o}{T_m}\right] \times 0.31$	0.062	eq. (7-21)
"	4		0.31	eq. (7-21)
"	5		0.255	Section 7.4.3.
"	6		0.185	eq. (7-21)
"	7	$\left[\frac{C_s}{C_m}\right]/10$	0.09	eq. (7-24)
"	8	$\left[\frac{T_s}{T_m}\right]/10$	0.30	eq. (7-25)
"	9	$\left[\frac{Q_{cs}}{Q_{cm}}\right]/10$	0.753	eq. (7-22)
"	10		0.11	eq. (7-21)
"	11	$\left[\frac{C_{ds}}{C_m}\right]/10$	0.09	eq. (7-26)
"	12	$\left[\frac{C_d}{C_m}\right]/10$	0.09	Let C_d be unchanged
"	13	$\left[\frac{C_{os}}{C_m}\right]/10$	1.0	eq. (7-27)
"	14	$\left[\frac{C_o}{C_m}\right]/10$	1.0	Let C_o be unchanged
"	20-1	0.055_{11}	0.28	See Appendix 2.7
"	20-2	0.055_{22}	0.8	"
"	20-3	0.055_{23}		"
"	20-4	0.055_{24}		"

TABLE 7.2. (continued)

Computer used	Pot No.	Parameter description	Setting static check	Notes
TR-48	10	$\left[\frac{C(o)}{C_m}\right]$ /10	0.135	
"	11	$\left(\dot{C}_m/C_m \beta\right)$	1.0	β = 0.1
"	12	$\left[\frac{T(o)}{T_m}\right]$ /10	0.33	
"	13	$\left(\dot{T}/T_m \beta\right)$	0.1	β = 0.1

TABLE 7.3.

Amplifier assignment sheet for the OMR scheme (Fig.7.1)

Computer used	AMP No.	FB	Output variables	Static check (Volt)	Notes
TR-48	10	$\int$	$+\left[\frac{C}{C_m}\right]$	+ 1.35	
"	11	$\int$	$+\left[\frac{T}{T_m}\right]$	+ 3.3	
TR-10	1	Σ	$-\left[\frac{\dot{C}}{\dot{C}_m}\right]$	-(.31-.042-.61) = 0.342	
"	2	Inv.	$-\left[\frac{C}{C_m}\right]$	- 1.35	
"	3	Σ	$-\left[\frac{\dot{T}}{\dot{T}_m}\right]$	-(.62-1.03-1.1 +1.0) = 0.51	
"	4	Inv.	$-\left[\frac{T}{T_m}\right]$	- 3.3	
"	5	Amp.	$+\left[\frac{T}{T_m''}\right]$	3.3x2.55 = 8.415	
TR-48		VDFG	$+\left[\frac{K}{K_m}\right]$	4.5	To multiplier 1, TR-10
TR-10	6	HG	$-\left[\frac{K}{K_m}\right]\left[\frac{C}{C_m}\right]$	-4.5x1.35/10 = -.61	From multiplier 1, TR-10
"	7	Σ	$-\left[\frac{\Delta C_r}{C_m}\right]$	-(-1.35+.9) = +.45	
"	8	Σ	$-\left[\frac{\Delta T}{T_m}\right]$	-(-3.3+3)= + .3	
"	11	Σ	$-\left[\frac{\Delta C_d}{C_m}\right]$	0	Let there be no change
"	12	Σ	$-\left[\frac{\Delta C_o}{C_m}\right]$	0	"

TABLE 7.3. (Continued)

Computer used	Amp No.	FB	Output variables	Static check (volt)	Notes
TR-10	9	Σ	$+\left[\frac{m^*}{Q_{cm}}\right]$	$-(+4.5\times2.8+.3\times8)$ $= -1.5$	Let $K_1=K_2$ $= 8$
"	10	Σ	$-\left[\frac{Q_c}{Q_{cm}}\right]$	$-(-1.5-7.5)$ $= +9.03$	

TABLE 7.4.

Potentiometer assignment sheet for the OAC scheme

(Fig. 7.2)

Computer used	Pot No.	Parameter description	Setting static check	Notes
TR-48	00		0.062	eq.(7-31), let F before change
"	01	$\left(\dot{T}_m/T_m\beta\right)$	0.1	β = 0.1
"	02		0.52	eq. (7-31), let F before change
"	03	decay constant		by different setting
"	05	$\left[\frac{C(0)}{C_m}\right]/10$	0.135	
"	06	$\left(\dot{C}_m/C_m\beta\right)$	1.0	β = 0.1
"	07		0.031	eq. (7-30), let F before change
"	08	$\left[\frac{T(o)}{T_m}\right]/10$	0.33	
"	15		0.185	eq. (7-31)
"	16		0.11	eq. (7-31)
"	17		0.753	eq. (7-22)
"	18		0.255	section 7.4.3.
TR-10	15	$\left[\frac{F}{F_m}\right]/10$	0.6	
"	16		0.052	eq. (7-30)

TABLE 7.5

Potentiometer assignment sheet for the OAC scheme

(Figs. 7.3, 7.4, 7.5 and 7.6)

Computer used	Pot No.	Parameter description	Setting static check	Notes
		Figure 3		
TR-48	25	Optimal P	0.055 x 21	See Appendix 2-7
"	26	" I	0.055 x 26	"
"	27	" D	0.055 x 27	"
		Figure 4		
TR-48	20		0.09	eq.(7-24)
"	21		0.3	eq.(7-25)
"	04		0.09	eq.(7-26)
"	09		0.09	let C_d be unchanged
"	14		1.0	eq.(7-27)
"	19		1.0	Let C_o be unchanged
"	22		0.055 x 21	See Appendix 2-7
"	23		0.055 x 22	"
"	24		0.055 x 23	"
"	28		0.055 x 24	"
		Figure 5		
TR-48	29		0.1	due to condition
		Figure 6		
TR-48	30		0.628	eq.(7-41)
"	31		0.172	eq.(7-41)

TABLE 7.6.

Amplifier assignment sheet for the OAC scheme (Fig. 7.2)

Computer used	Amp No.	FB	Output variables	Static check (volt)	Notes
TR-48	06	$\int$	$+\left[\frac{C}{C_m}\right]$	+ 1.35	
"	07	inv.	$-\left[\frac{C}{C_m}\right]$	- 1.35	
"	21	Σ	$-\left[\frac{\dot{C}}{\dot{C}_m}\right]$	-(.31-.042-.61) = 0.342	before any change
TR-10	13	inv.	$+\left[\frac{C}{C_m}\right]$	+ 1.35	
"	14	inv.	$-\left[\frac{F}{F_m}\right]$	- 6.0	F before change
"	15	HG	$-\left[\frac{C}{C_m}\right]\left[\frac{F}{F_m}\right]$	(1.35x6.0)/10 = -0.81	"
TR-48	20	$\int$	$+\left[\frac{T}{T_m}\right]$	3.3	
"	18	inv.	$-\left[\frac{T}{T_m}\right]$	- 3.3	
"	19	Σ	$-\left[\frac{\dot{T}_m}{\dot{T}_m}\right]$	-(,62-1.03-1.1 +1.0) = 0.51	
"	46	inv.	$+\left[\frac{T}{T_m}\right]$	+ 3.3	
"	47	inv.	$-\left[\frac{F}{F_m}\right]$	- 6.0	F before change
"	73	HG	$-\left[\frac{T}{T_m}\right]\left[\frac{F}{F_m}\right]$	-(3.3)(+6.0)/10 = 1.98	"
"	27	Amp	$+\left[\frac{T}{T_m''}\right]$	3.3x2.55 = 8.415	
"		VDFG	$\left[\frac{K}{K_m}\right]$	4.5	

TABLE 7.6. (continued)

Computer used	Amp No.	FB	Output variables	Static check (volt)	Notes
TR-48	65	Inv.	$-\left[\frac{K}{K_m}\right]$	- 4.5	
"	66	inv.	$+\left[\frac{C}{C_m}\right]$	+ 1.35	
"	39	HG	$-\left[\frac{K}{K_m}\right]\left[\frac{C}{C_m}\right]$	-(4.5)(1.35)/10 = -0.61	
"	14	$\int$	$\left[\frac{a}{a_m}\right]$	1.0	before change
"	VDFG-1 inv	inv.	$-\left[\frac{a}{a_m}\right]$	- 1.0	Inv. in VDFG-1
"	VDFG-1 inv.	inv.	$+\left[\frac{K}{K_m}\right]\left[\frac{C}{C_m}\right]$	+ 0.61	Inv.in VDFG-1
"	38	HG	$-\left[\frac{a}{a_m}\right]\left[\frac{K}{K_m}\right]\left[\frac{C}{C_m}\right]$	- 0.61	
"	26		$-\left[\frac{Q_c}{Q_{cm}}\right]$	-(-1.5-7.5) = +9.03	

TABLE 7.7

Computer used	Amp No.	FB	Output variable	Static check (volt)	Notes
			Figure 3		
TR-48	31	Σ	response error	0	Before operation
"	44	∫	integral of response error	0	"
"	VDFG-3 inv.	Inv.	$+\left[\frac{\dot{C}_r}{\dot{C}_m}\right]$	- 0.342	Inv. in VDFG-3
"	42	Σ	derivative of response error	0	before operation
"	VDFG-3 Inv.	Inv.	$-\left[\frac{m^*}{Q_{cm}}\right]$	+ 1.50	Inv. in VDFG-3
"	30	Σ	$+\left[\frac{U^*}{Q_{cm}}\right]$	- 1.50	
			Figure 4		
TR-48	12	Σ	$-\left[\frac{\Delta C}{C_m}\right]$	+ 0.45	
"	13	Σ	$-\left[\frac{\Delta T}{C_m}\right]$	+ 0.3	
"	45	Σ	$-\left[\frac{\Delta C_d}{C_m}\right]$	0	Let there be no change
"	74	Σ	$-\left[\frac{\Delta C_o}{C_m}\right]$	0	"
"	15	Σ	$+\left[\frac{m^*}{Q_{cm}}\right]$	- 1.5	Let $K_1 = K_2 = 8$

TABLE 7.7 (continued)

Computer used	Amp No.	FB	Output variable	Static check (volt)	Notes
			Figure 5		
TR-48	33		response error	0	before operation
"	VDFG-2 Inv.	Inv.	- response error	0	Inv. in VDFG-2
"	74	HG	(response error)^2	0	
"	43	$\int$	Performance response (PR)	0	"
			Figure 6		
	VDFG-4 inv.	Inv.	b	6.28	Inv. in VDFG-4
	VDFG-4 inv.	Inv.	a	- 1.72	"

7.6. Operation of the complete simulation

In all operations both for complete simulation and on-line computer control (work in Part II), the results both from theoretical and practical OMRAC operation can be compared almost case by case, figure by figure and curve by curve

7.6.1. Operating possibilities

All of the different kinds of operating conditions of OMRAC can be listed as follows:

(1) Unmeasurable parameter change: F decrease

(2) Unmeasurable parameter change: F increase

(3) Unmeasurable parameter change: a exponential decay

(4) Unmeasurable combined parameter change : F increase

and a exponential decay

(5) Optimal P of OAC

(6) Optimal P + I of OAC

(7) Optimal P + I + D of OAC

(8) Different initial conditions, $C(t_o)$ and $T(t_o)$

(9) Different OMR

(10) Different set point, C_d

(11) Different inlet concentration, C_o.

For more effective planning operations to cover the whole field shown above, the following two rules were obeyed:

1. All cases were operated with Optimal P of OAC except (6) and (7).
2. All cases except (1), (2), (3) and (4) were operated with more effective unmeasurable combined parameter changes:

   F : increase ; a : exponential decay (see later).

Following these two rules, ten groups of operation (i.e. (1), (2), (3), (4), (6), (7), (8), (9), (10) and (11) of the above list were used throughout the research work.

Within each group several cases were studied (see next section).

7.6.2. Kinds of figure plotted for each case.

Four kinds of figure for each case were plotted.

(1) Kind A : Reactor concentration dynamic response, C vs t

(2) Kind B : Phase plane trajectory, C vs T

(3) Kind C : Optimal control law generation, U* vs t

(4) Kind D : Performance response, $\int e^2 dt$ vs t

7.6.3. Types of different operations for each figure

Four different kinds of operation for each figure as shown below was used:

1. Unadapted system operation (US) (without control)
2. Unadapted Optimal control operation (UOC) (optimal control applied to unadapted system)
3. OMR Operation
4. OMRAC Operation

7.7. Discussion and analysis of the theoretical results from the complete simulation

7.7.1. Computer OMRAC operation (Table 7.8)

General operating conditions

(1) Initial condition: (In the 1st quadrant from the original steady state, Section 7.1)

$C(t_o) = 0.135$ mol/litre ; $T(t_o) = 33^oC$

(2) Final desired concentration

$C(t_f) = 0.09$ Mol/litre

(3) OMR : $K_1 = 8$, $K_2 = 8$

(4) OAC: Optimal P $K_3 = 100, 200, 500$ and 1000.

TABLE 7.8.

Computer OMRAC operation for complete simulation

Group	Case	Operating condition	Kind of Plot	Figure
1	1.1	F decrease 10%	A	7.7
		"	B	7.8
		"	C	7.9
		"	D	A.4.1.
	1.2	F decrease 20%	A	7.10
		"	C	7.11
		"	D	A.4.2.
	1.3	F decrease 30%	A	7.12
		"	C	7.13
		"	D	A.4.3.
	1.4	F decrease 40%	A	7.14
		"	C	7.15
		"	D	A.4.4.
2	2.1	F increase 10%	A	7.16
		"	B	7.17
		"	C	7.18
		"	D	A.4.5.
	2.2	F increase 20%	A	7.19
		"	C	7.20
		"	D	A.4.6.
3	3.1	a exponential decay 20%	A	7.21
		"	D	A.4.7.

TABLE 7.8. (continued)

Group	Case	Operating condition	Kind of plot	Figure
3	3.2	a exponential decay 30%	A	7.22
		"	C	7.23
		"	D	A.4.8.
	3.3	a exponential decay 40%	A	7.24
		"	B	7.25
		"	D	A.4.9.
4	4.1.	Combined parameter change:	A	7.26
		(F increase 10%	B	7.27
		(		
		(a decay 20%	C	7.28
		"	D	A.4.10.
5	5.1	(Group 4 (Optimal P + I		
		K_3 = 100, ϵ = 0,1,2,3,4.	A	7.29
		"	C	7.30
		"	D	A.4.11.
	5.2	K_3 = 200		
		ϵ = 0,1,2,3,4,8,15	A	7.31
		"	B	7.32
		"	C	7.33
		"	D	A.4.12.
6		(Group 4 (Optimal P+ I + D		
	6.1	K = 1, ϵ = 0.5,1.0,1.5,2.0	A	7.34
		"	D	A.4.13.

TABLE 7.8. (continued)

Group	Case	Operating condition	Kind of plot	Figure
6	6.2	K = 3, ϵ = 0.5,1.0,1.5,2.0	A	7.35
		"	B	7.36
		"	C	7.37
		"	D	A.4.14
7		(Group 4 (Different initial conditions		
	7.1	($C(t_o)$ = 0.15 mol/litre)	A	7.38
		($T(t_o)$ = 28°C)	B	7.39
		((2nd quadrant))	C	7.40
		( )	D	A.4.15
	7.2	($C(t_o)$ = 0.07 mol/litre)	A	7.41
		($T(t_o)$ = 27°C)	B	7.42
		((3rd quadrant))	C	7.43
		( )	D	A.4.16
	7.3	($C(t_o)$ = 0.06 mol/litre)	A	7.44
		($T(t_o)$ = 34°C)	B	7.45
		((4th quadrant))	D	A.4.17
8		(Group 4 (Different OMR		
	8.1	(OAR Optimal P K_3 = 200)	A	7.46
		((1) $K_1 = K_2 = 4$)	B	7.47
		((2) $K_1 = K_2 = 8$)	D	A.4.18
		((3) $K_1 = K_2 = 15$)		

TABLE 7.8 (continued)

Group	Case	Operating condition	Kind of plot	Figure
9	9.1	(Group 4 (different set point, C_d	A	7.48
		(OAC Optimal P, K_3 = 200) ( )	B	7.49
		((1) C_d:0.09 — 0.10 mol/) (litre)	C	7.50
		( ) ((2) C_d:0.09 — 0.08 mol/) (litre)	D	A.4.19
10		(Group (Different inlet (concentration		
	10.1	(C_o as load variable) ( )	A	7.51
		((1) C_o:1.0 — 0.9 mol/) (litre)	B	7.52
		( ) ((2) C_o:1.0 — 1.1 mol/) (litre)	D	A.4.20
	10.2	(C_o as parameter) ( )	A	7.53
		((1) C_o:1.0 — 0.9 mol/) (litre)	B	7.54
		( ) ((2) C_o:1.0 — 1.1 mol/) (litre)	D	A.4.21

7.7.2. An unusual shape of curve was found in Figs. 7.12 and 7.14 for which an explanation is offered in comparison with the curves obtained from other similar conditions. In these figures (cases 1.3 and 1.4) F decrease 30% and 40%, for "US" (Unadapted System) operation, C decreases with an unusual shape. This is due to the large percentage decrease of F, causing a large percentage increase of T and producing a large effect from the non-linear term: $aAe^{-\left(\frac{E}{RT}\right)}$. The same effect occurs with a large percentage decrease of a in the exponential decay (30% - 40%) where $a = e^{-ct}$ (see Figs. 7.22 and 7.24).

This feature does not arise in OMRAC due to the large increase of F_c which forces T to decrease.

7.7.3. For any individual or combination of unmeasurable changed parameters and with the different possible operating conditions from group 1 —— group 10), all dynamic response curves and phase-plane trajectories follow a distinct smooth, regular and effective order:

$$(US)_c \rightarrow (UOC)_c \rightarrow \overset{\text{OMRAC}}{\begin{pmatrix} K_3 = 100 \rightarrow & K_3 = 200 \rightarrow \\ K_3 = 500 \rightarrow & K_3 = 1000 \end{pmatrix}_c} \rightarrow (OMR)_c$$

where $\rightarrow$ = more offset from OMR.

7.7.4. All optimal law U* and m* also follow a smooth, regular effective order:

$$\overset{\text{OMRAC}}{\left(K_3=1000 \rightarrow K_3=500 \rightarrow K_3=200 \rightarrow K_3=100\right)_{U^*}} \rightarrow (UOC)_{m^*} \rightarrow (OMR)_{m^*}$$

when K_3 increases, $|U^* - m^*|$ increases

7.7.5. Performance response : $PR = \int e^2 dt$

shows the effective order:

$$(UOC)_{PR} > \overset{\text{OMRAC}}{\left(K_3=100 > K_3=200 > K_3=500 > K_3=1000\right)_{PR}} > 0$$

For the theoretical case:

when $C(t) = C_r(t)$; $t_o \leq t \leq t_f$

then PR = 0

7.7.6. From the above facts, the response of OMRAC is always better than UOC and is more effective and approaches OMR more closely as a limit as the weighting factor is increased.

7.7.7. From all dynamic response curves and phase plane trajectories, OMRAC displays excellent asmptotic stability.

7.7.8. The adaptation of OMRAC seems to have no limitation for any operating conditions shown in 7.7.1. The only limitation is the constraint of the optimal control law U*, which corresponds to the control valve capacity for cooling water flowrate.

7.7.9. Optimal P + I and Optimal P + I + D of OMRAC can produce greater improvement tham Optimal P only, and Optimal PID has the same general properties as the conventional PID controller (see Groups 5 and 6).

7.7.10. All of the above discussion is based on a qualitative analysis of OMRAC. For the quantitative analysis of OMRAC, a new term "OPTIMAL ADAPTIVITY" is introduced and discussed in detail in Chapter 11, Part II.

7.7.11. From all of the above discussion and analysis the theoretical development of OMRAC has been positively supported and proved, and the further work of on-line hybrid computer operation in combination with a partially simulated CSTR is studied and shown in Part II.

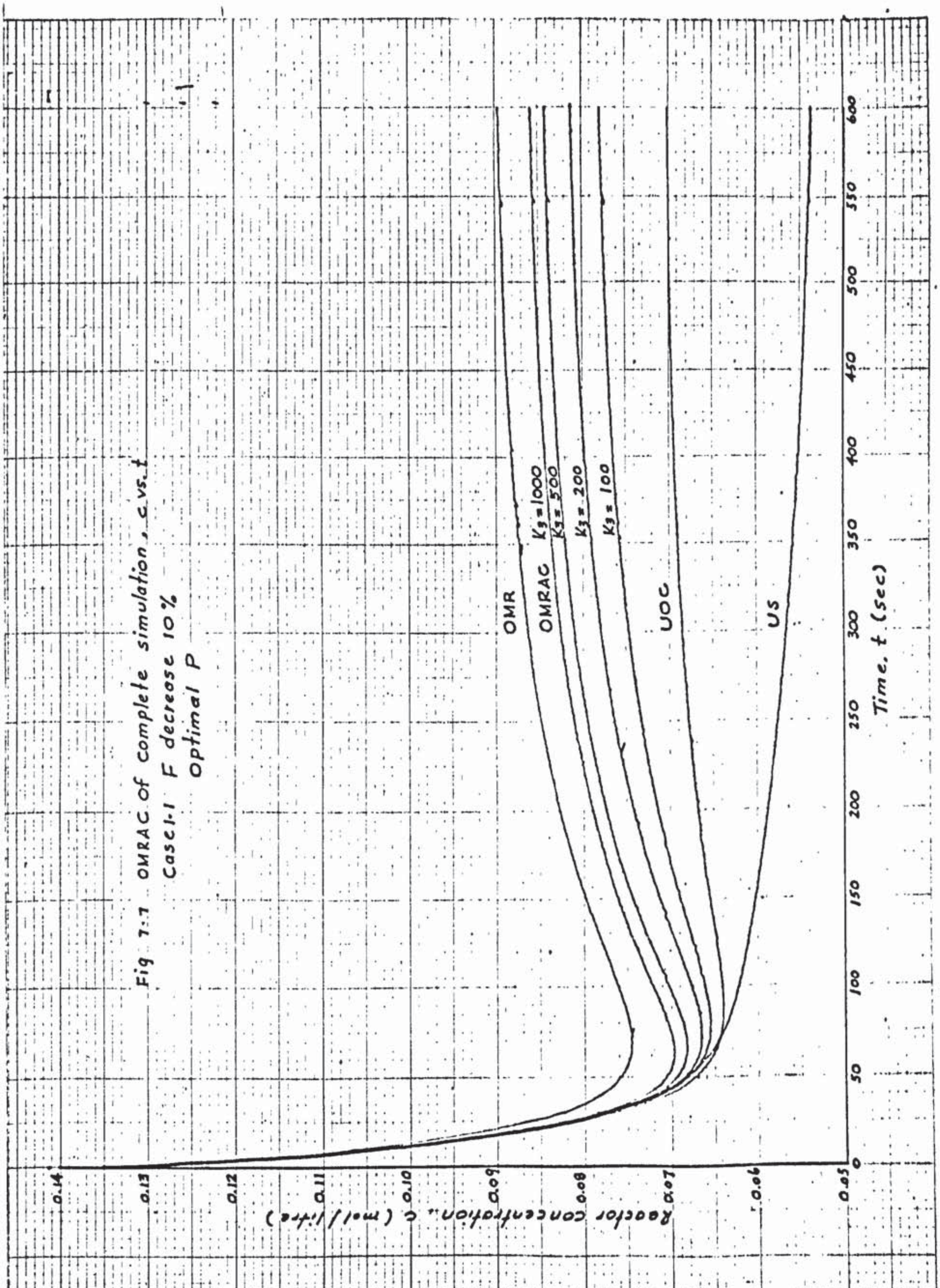

Fig 7.7 OMRAC of complete simulation, c vs. t
Case 1.1 F decrease 10%
Optimal P

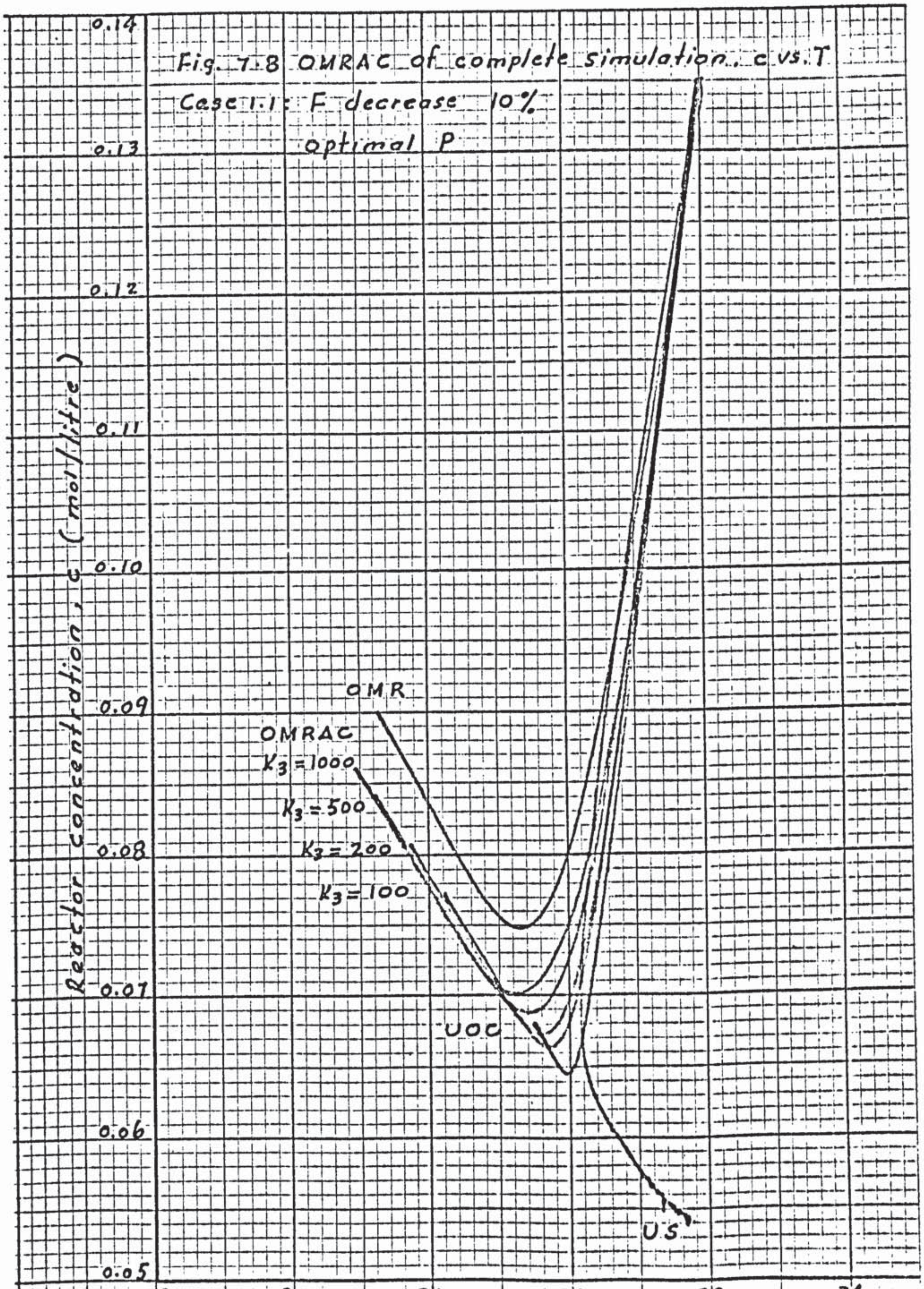

Fig. 7.8 OMRAC of complete simulation, c vs. T
Case 1.1: F decrease 10%
optimal P
0.14
0.13
0.12
0.11
0.10
0.09
0.08
0.07
0.06
0.05
Reactor concentration, c (mol/litre)
OMR
OMRAC
$K_3 = 1000$
$K_3 = 500$
$K_3 = 200$
$K_3 = 100$
UOC
US
29
30
31
32
33
34
Reactor temperature, T (°C)

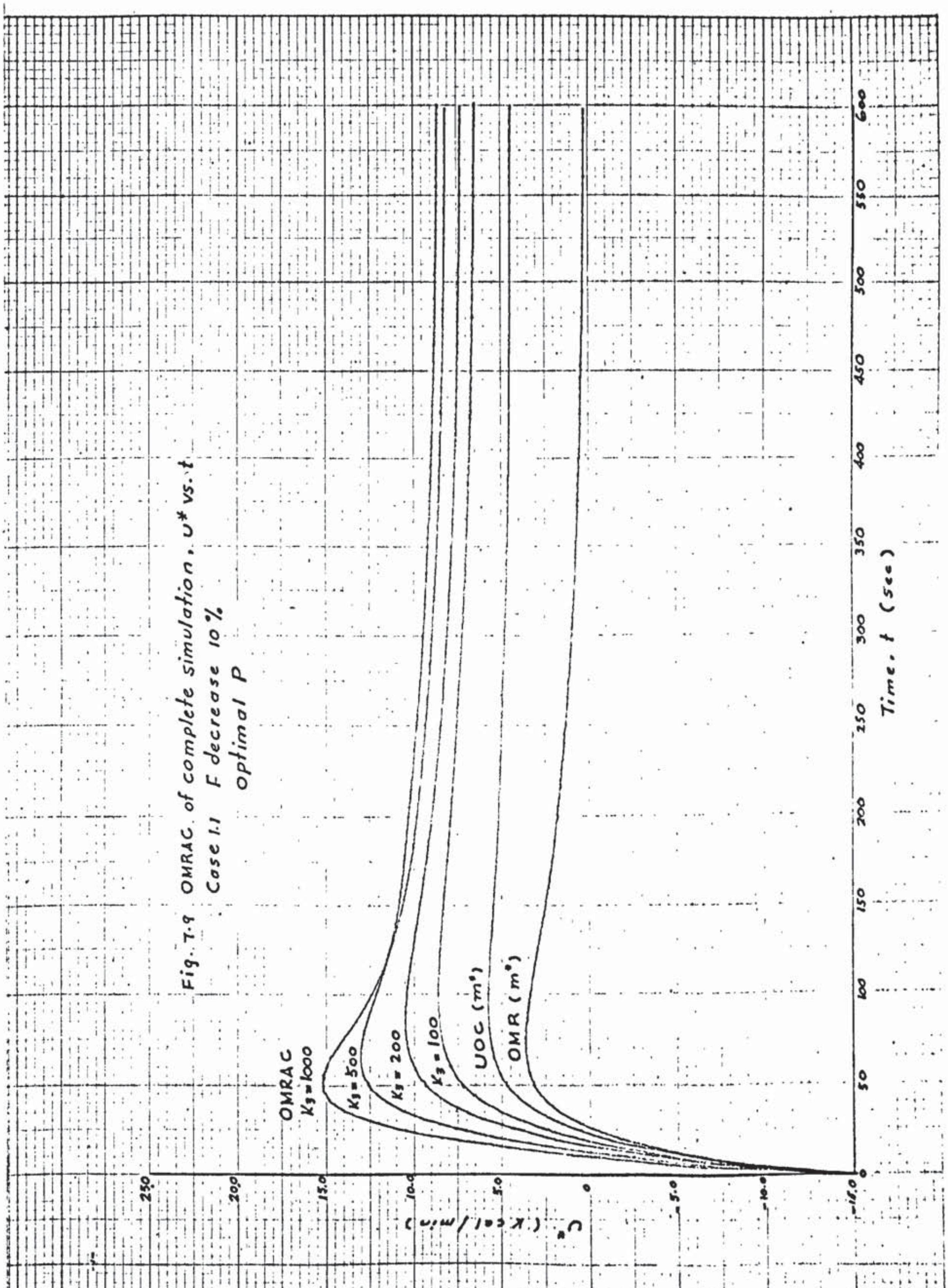

Fig. T-9 OMRAC of complete simulation, u^* vs. t
Case 1.1 F decrease 10%
optimal P

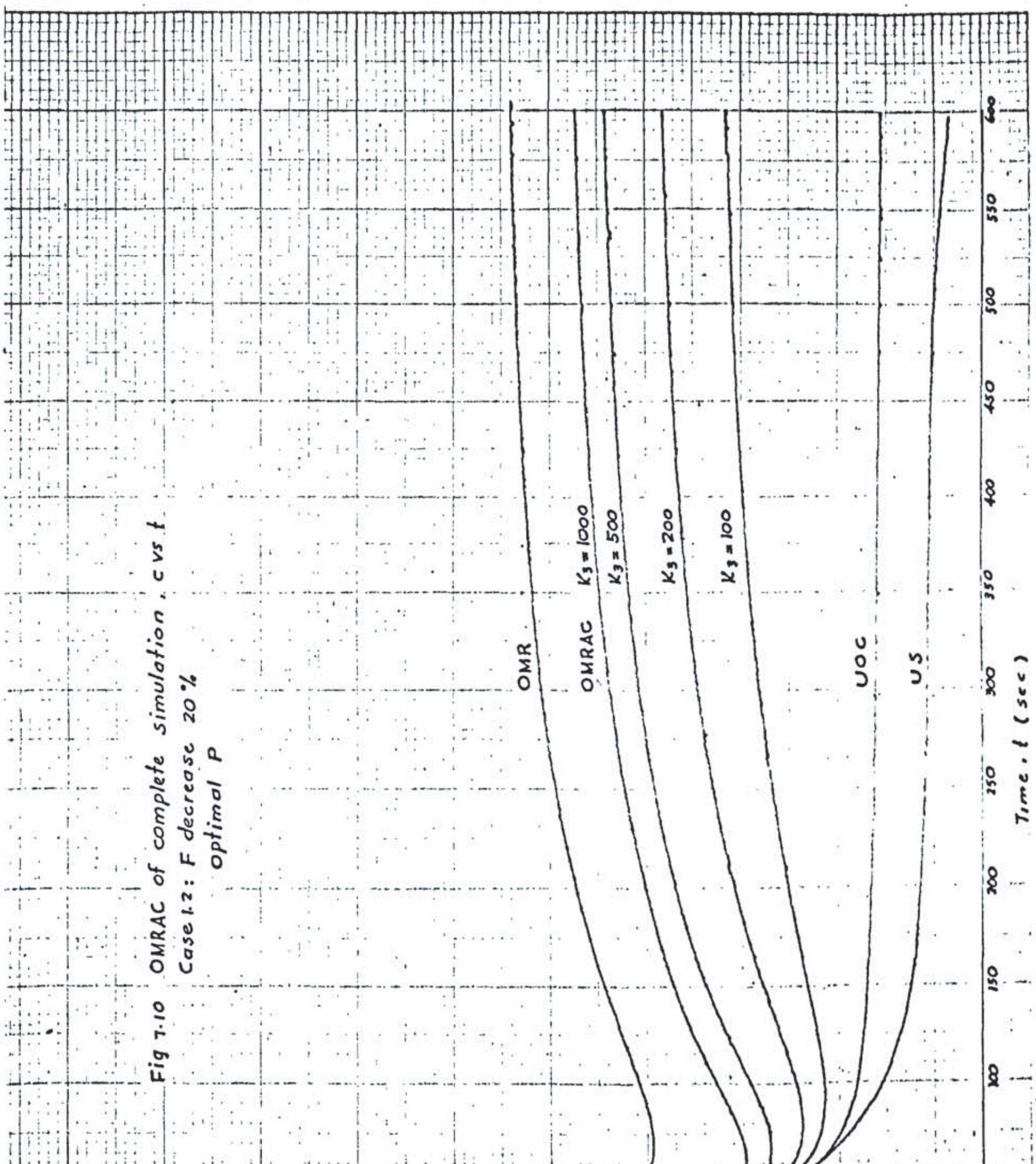

Fig 7.10 OMRAC of complete simulation, c vs t
Case 1.2: F decrease 20%
optimal P

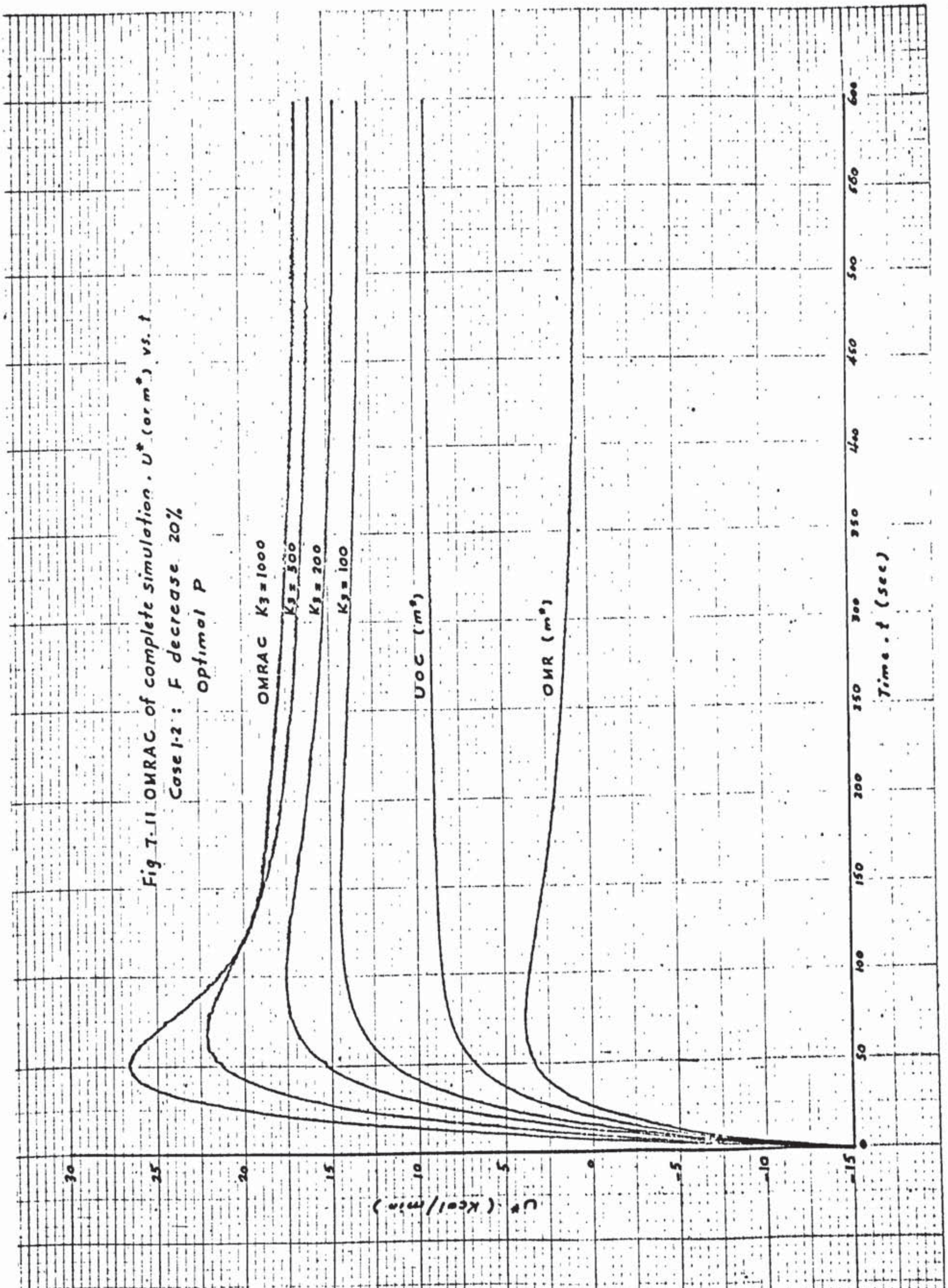
Fig T-11 OMRAC of complete simulation. U* (or m*) vs. t
Case I-2: F decrease 20%
optimal P
OMRAC K3=1000
K3=500
K3=200
K3=100
UOC (m*)
OMR (m*)
Time, t (sec)
U* (Kcal/min)
30
25
20
15
10
5
0
-5
-10
-15
0
50
100
150
200
250
300
350
400
450
500
550
600

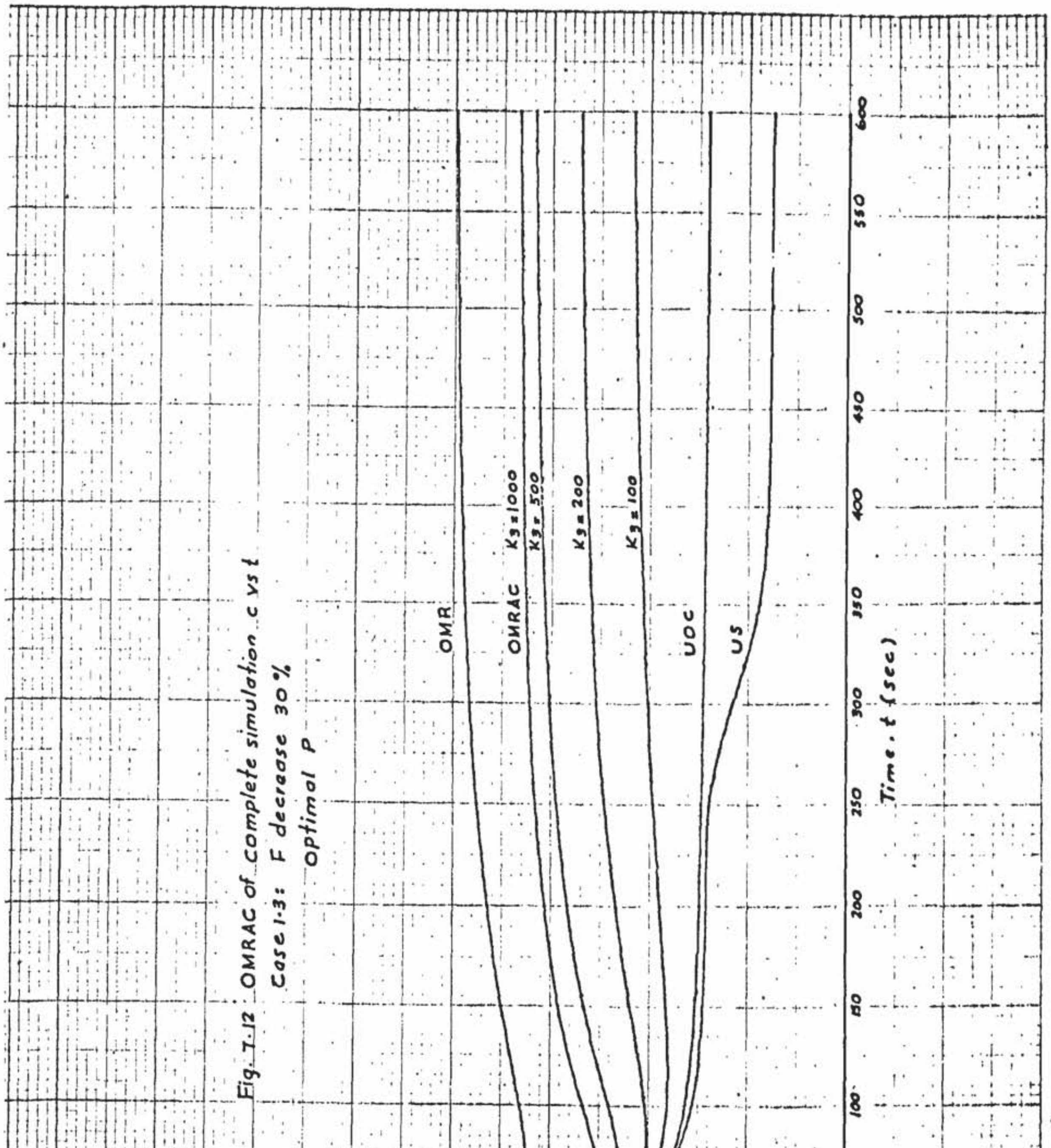

Fig. 7.12 OMRAC of complete simulation c vs t
Case 1.3: F decrease 30%
optimal P

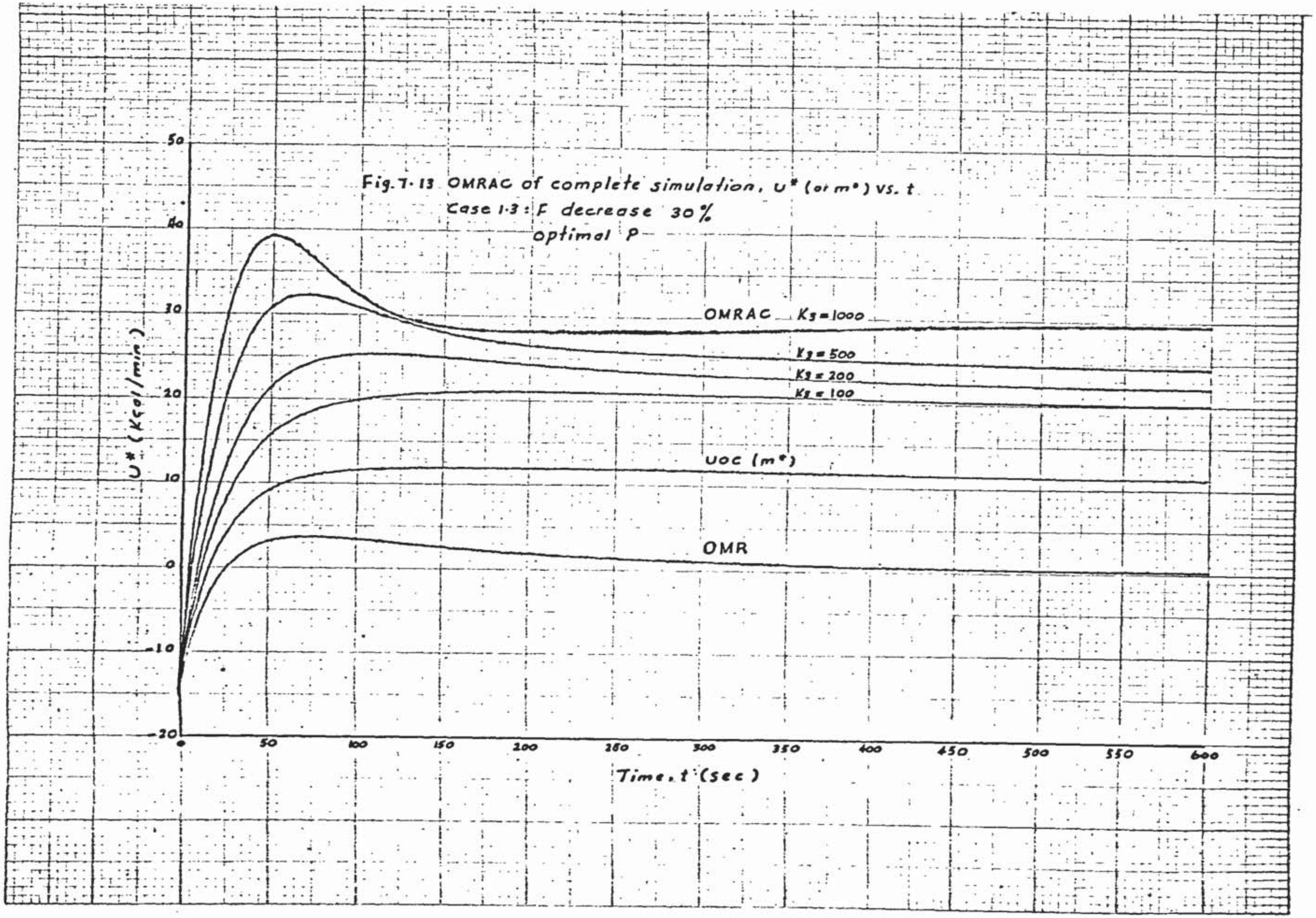

Fig. 7-13 OMRAC of complete simulation, U* (or m*) vs. t
Case 1-3: F decrease 30%
optimal P

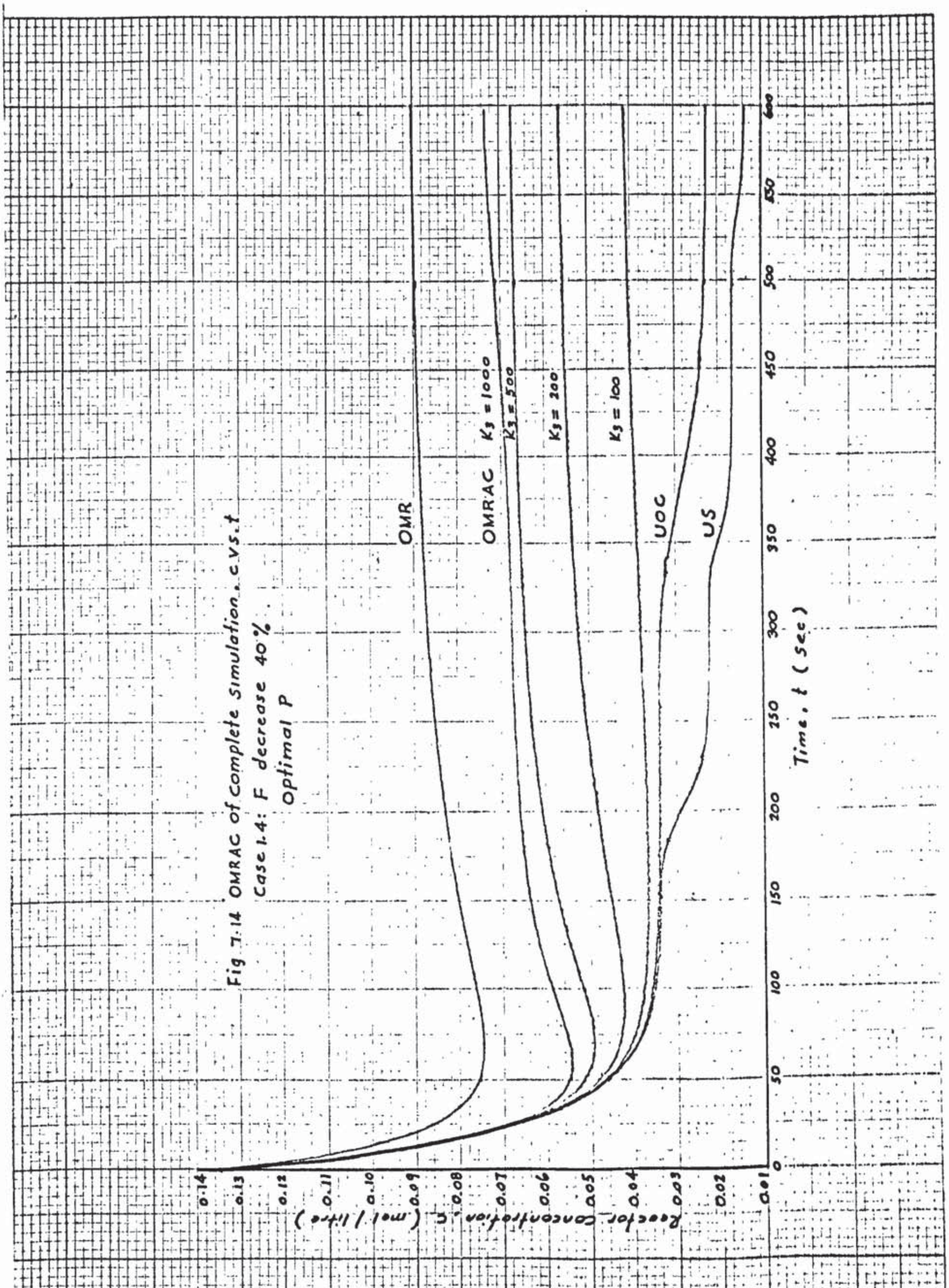

Fig 7.14 OMRAC of complete simulation, c vs. t
Case 1.4: F decrease 40%
optimal P

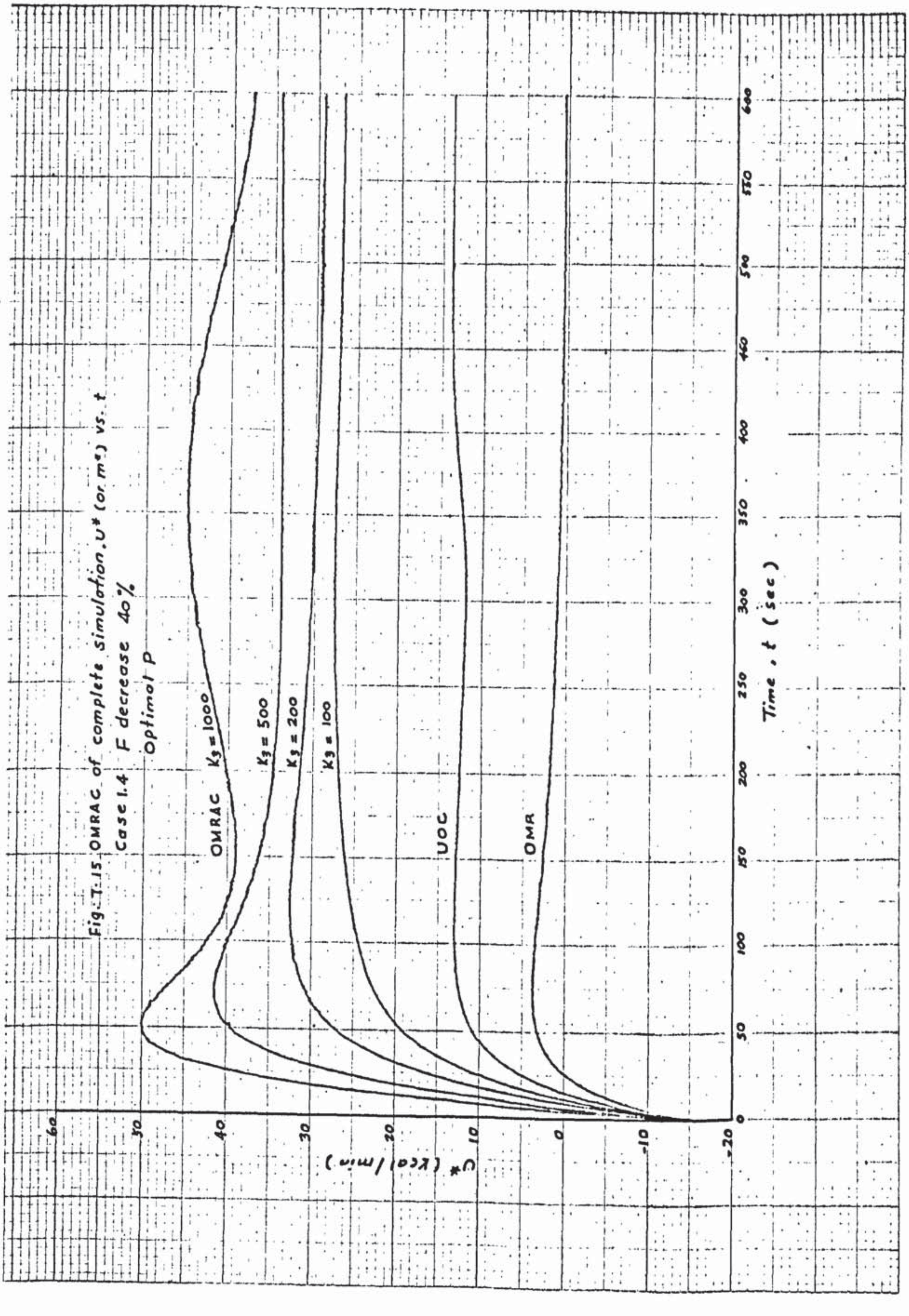
Fig. T.15 OMRAC of complete simulation, U* (or m*) vs. t
Case 1.4 F decrease 40%
Optimal P
OMRAC K3 = 1000
K3 = 500
K3 = 200
K3 = 100
UOC
OMR
U* (kcal/min)
60
50
40
30
20
10
0
-10
-20
Time, t (sec)
0
50
100
150
200
250
300
350
400
450
500
550
600

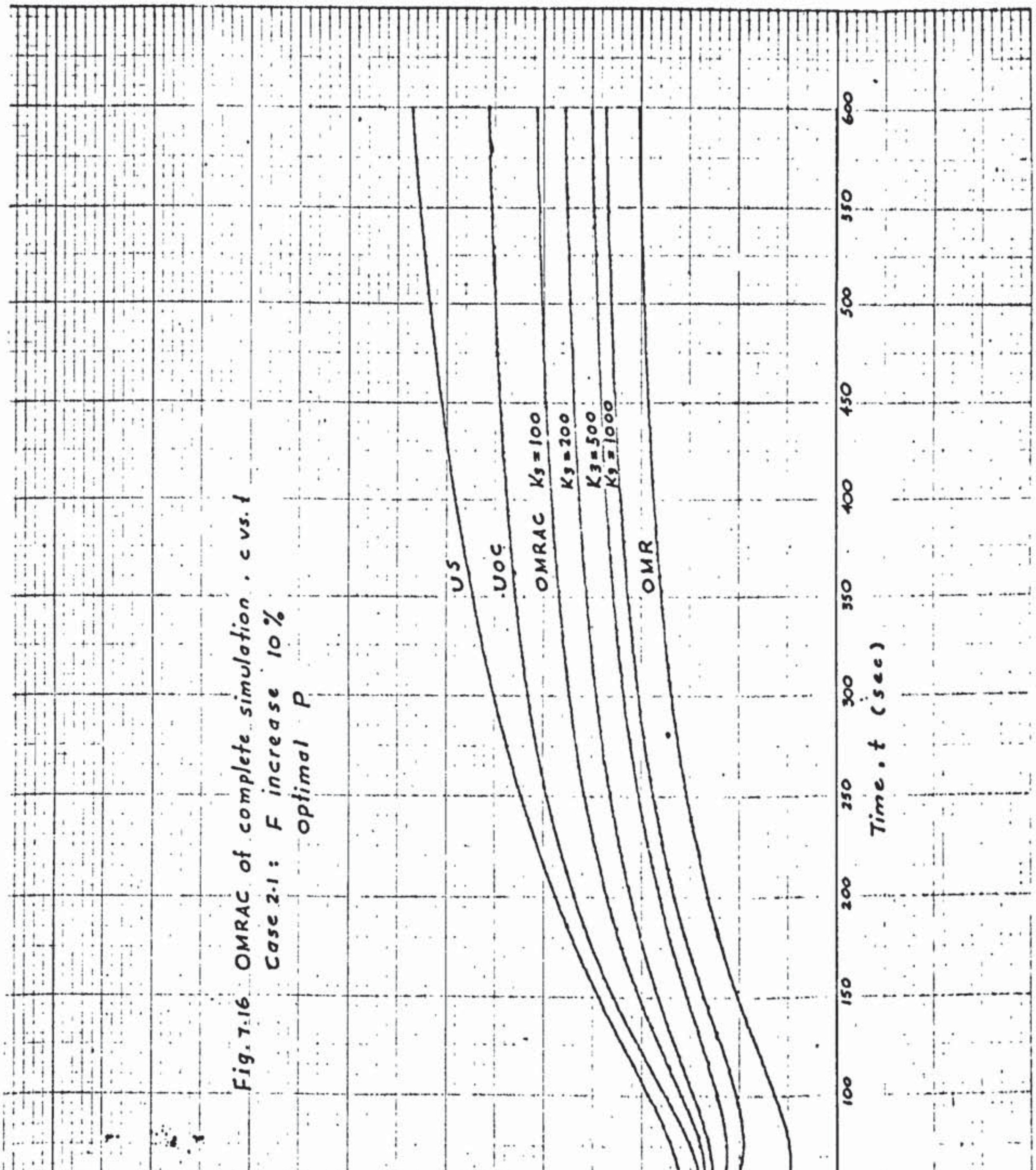

Fig. 7.16 OMRAC of complete simulation, c vs. t
Case 2.1: F increase 10%
optimal P

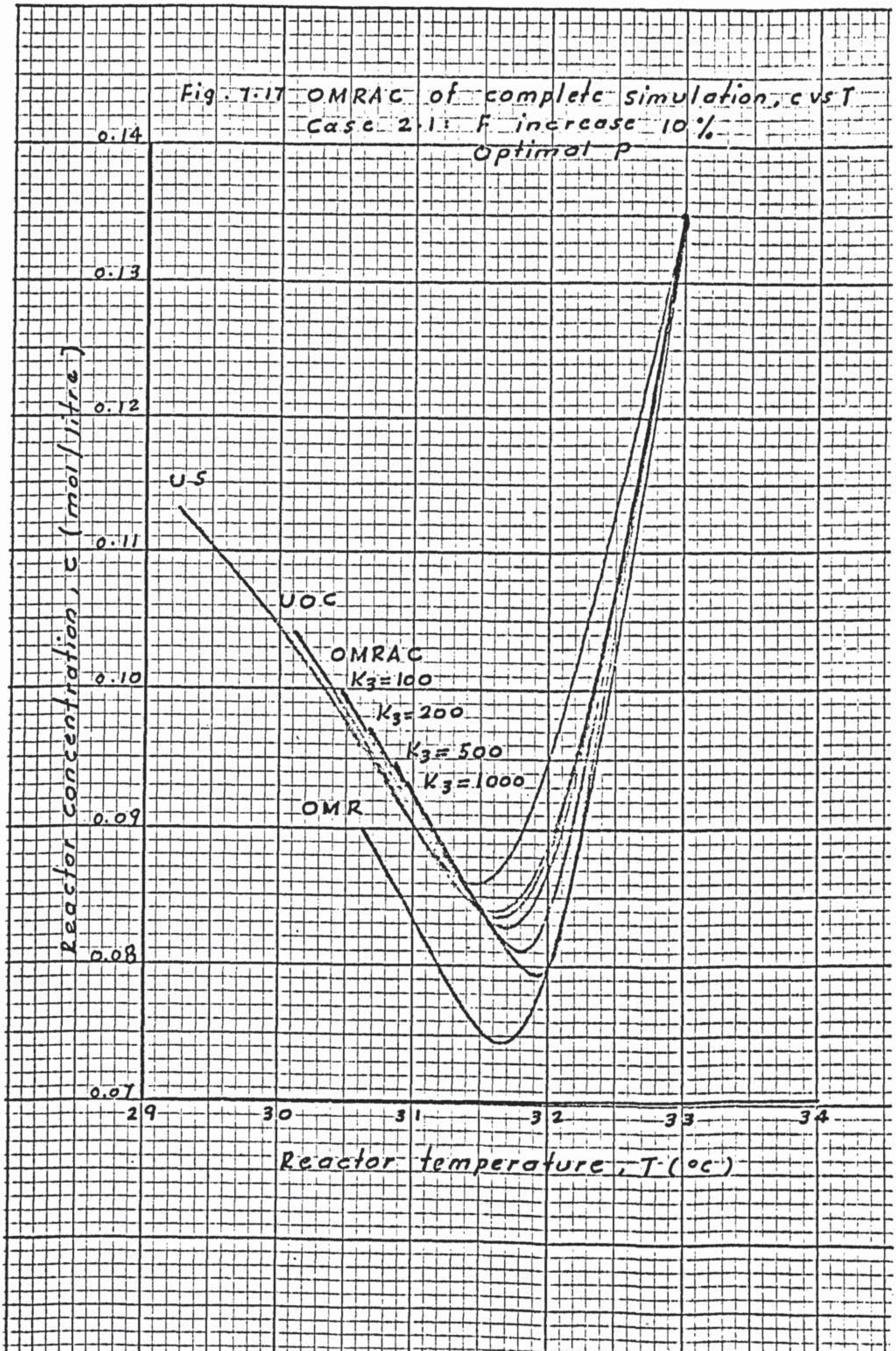
Fig. 7.17 OMRAC of complete simulation, c vs T
Case 2.1: F increase 10%
Optimal P
0.14
0.13
0.12
0.11
0.10
0.09
0.08
0.07
US
UOC
OMRAC
K3=100
K3=200
K3=500
K3=1000
OMR
29
30
31
32
33
34
Reactor concentration, c (mol/litre)
Reactor temperature, T (oc)

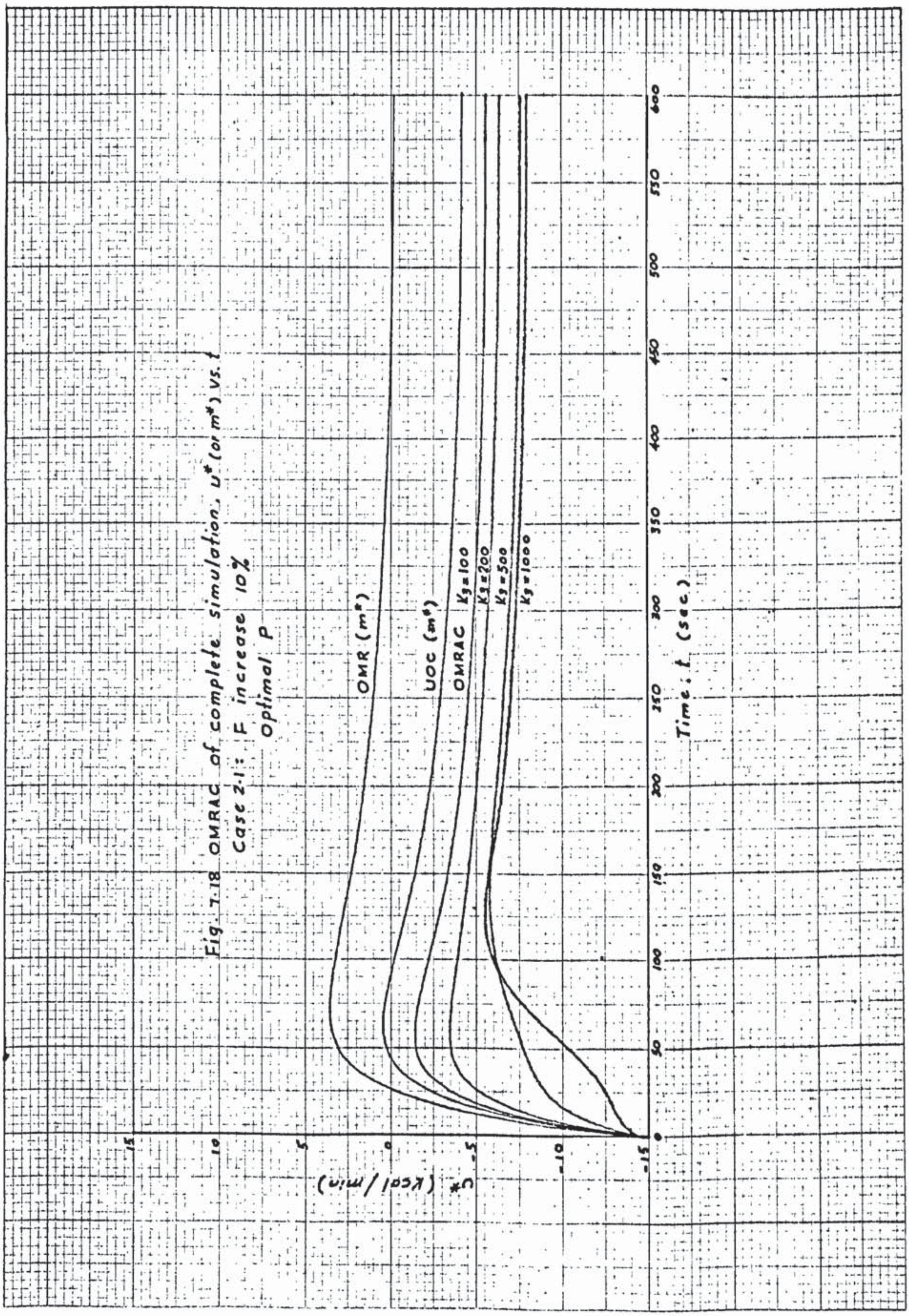

Fig. 7.18 OMRAC of complete simulation, u* (or m*) vs. t

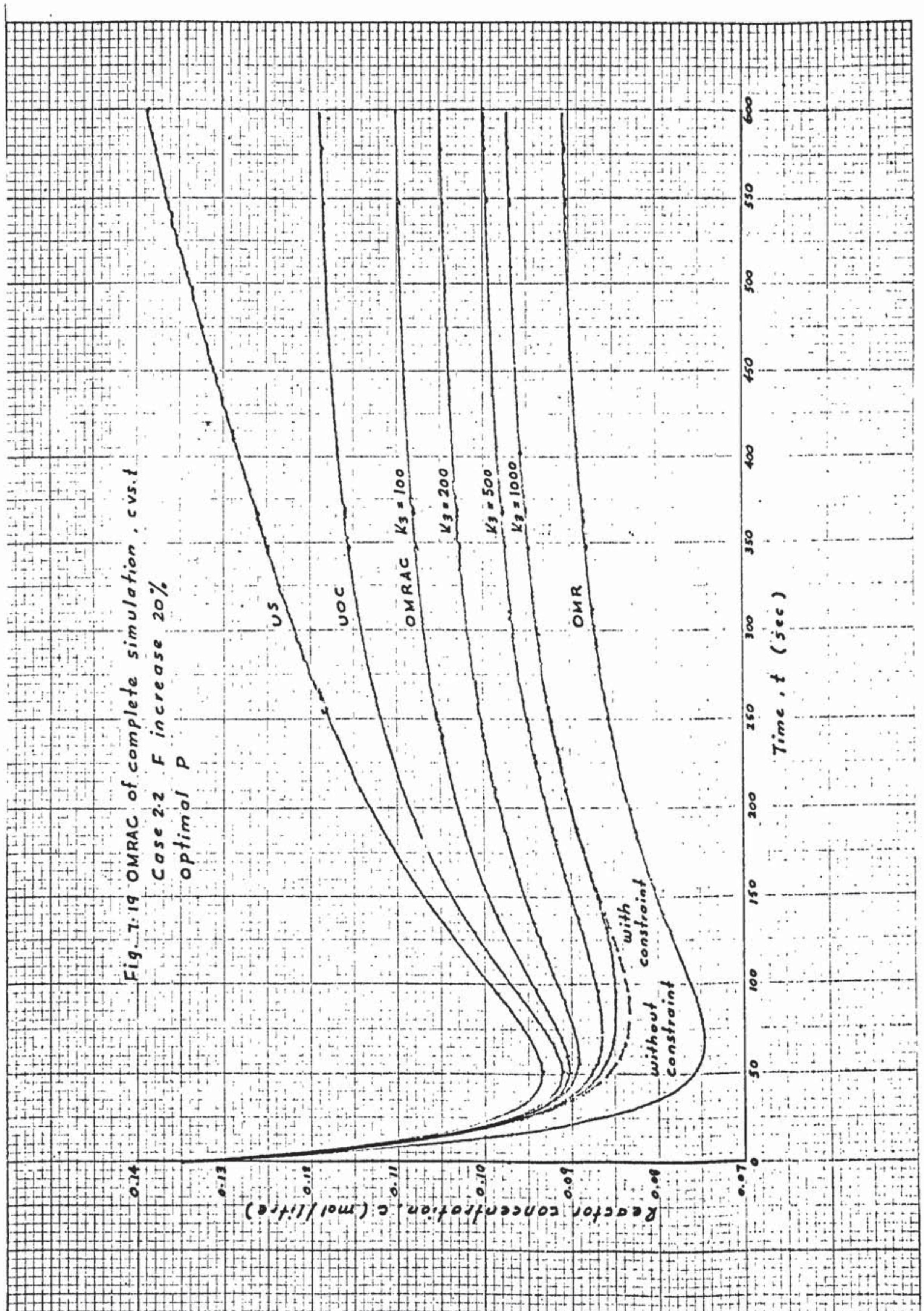

Fig. 7.19 OMRAC of complete simulation, c vs. t
Case 2.2 F increase 20%
optimal P

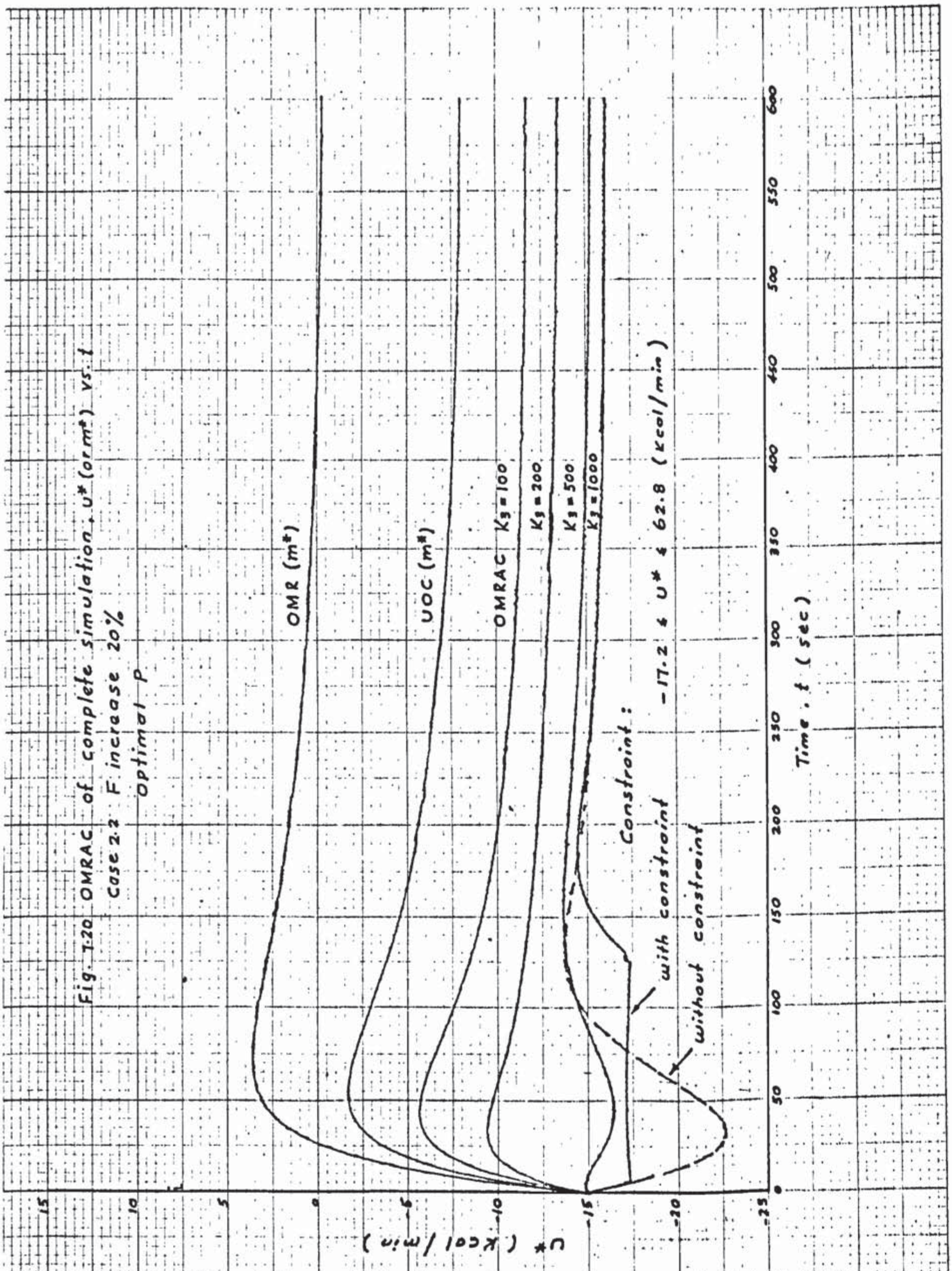

Fig. 7.20 OMRAC of complete simulation, U* (or m*) vs. t
Case 2.2 F increase 20%
optimal P

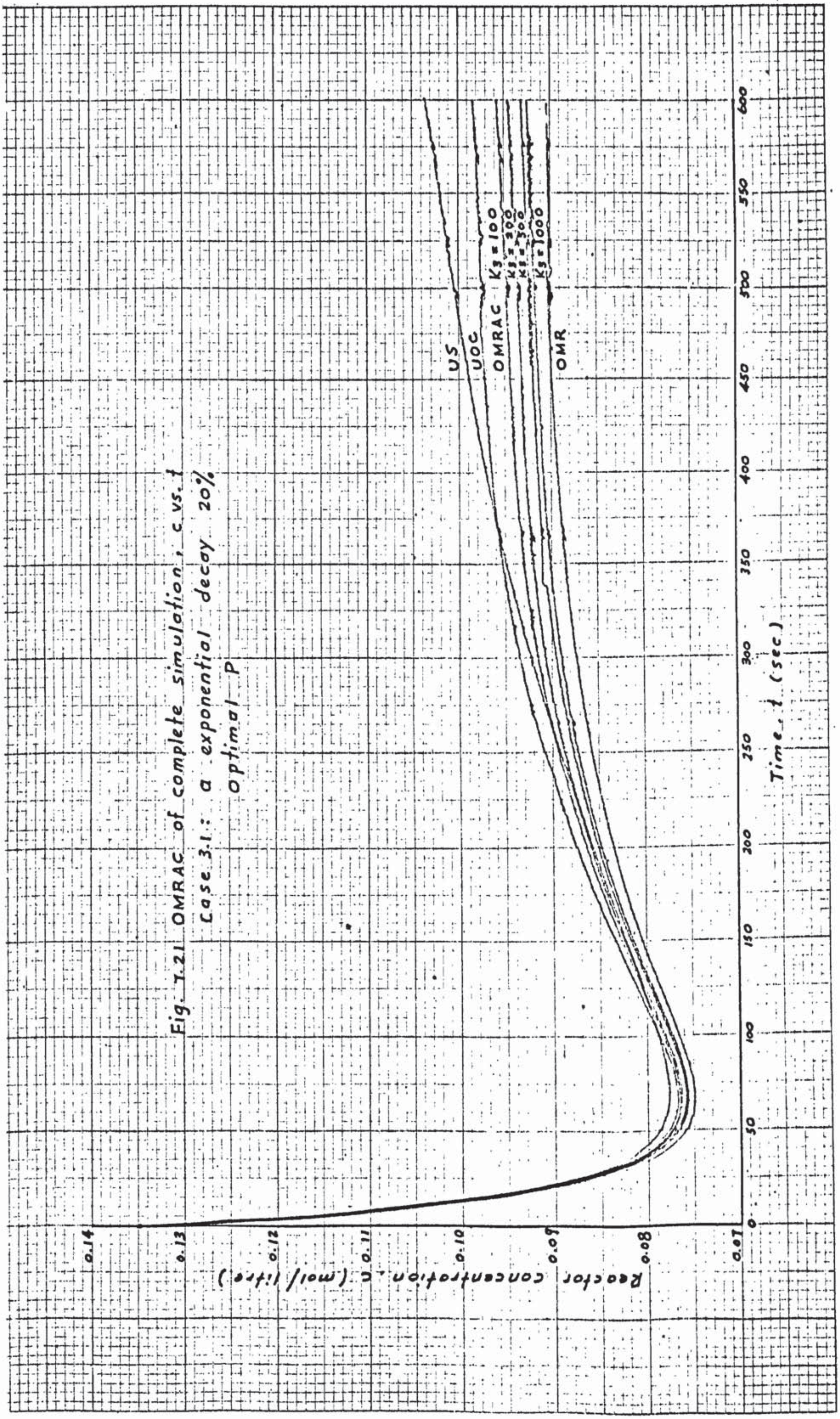

Fig. 7.21 OMRAC of complete simulation, c vs. t
Case 3.1: a exponential decay 20%
optimal P

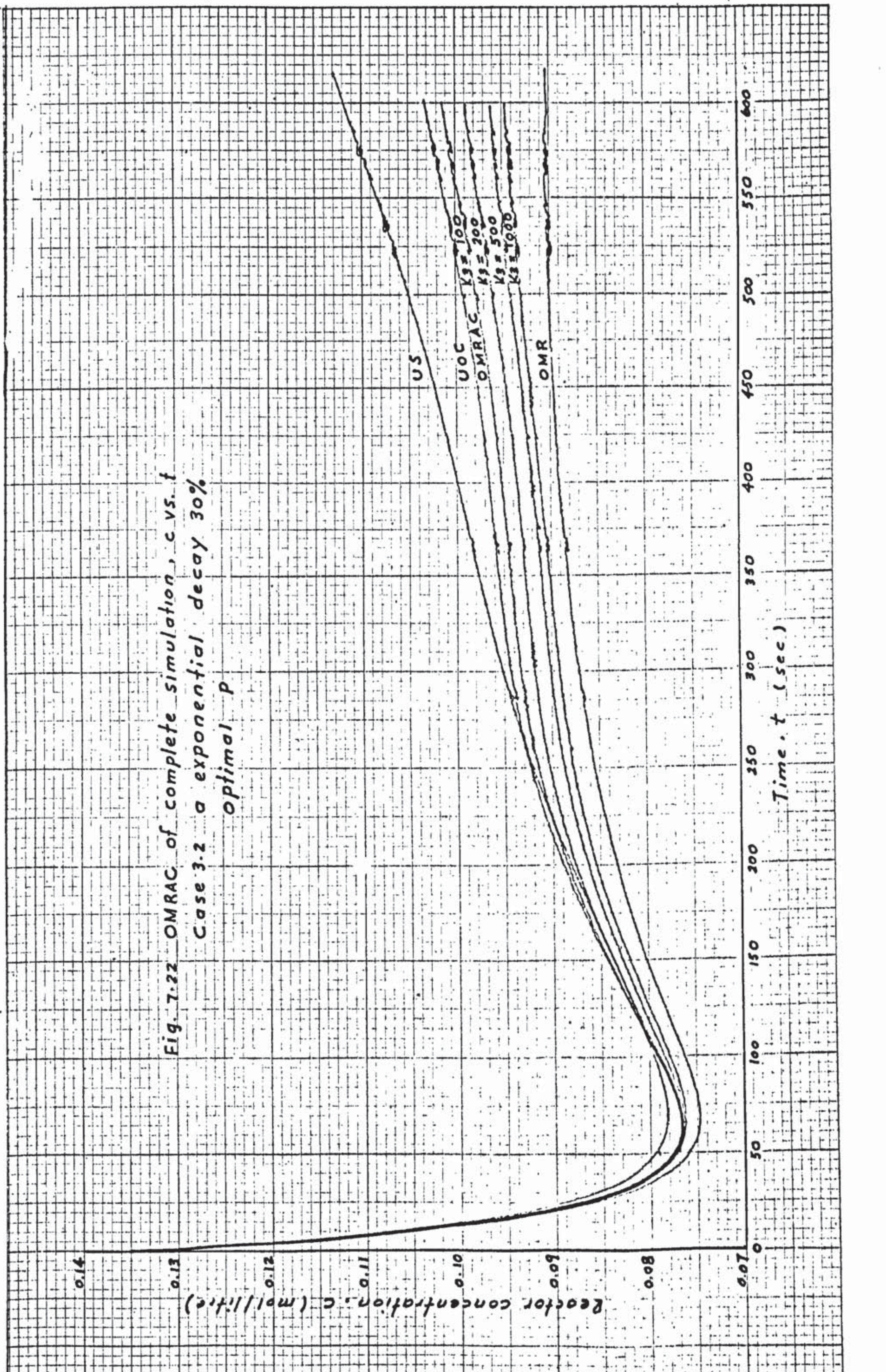

Fig. 7.22 OMRAC of complete simulation, c vs. t
Case 3.2 a exponential decay 30%
optimal P

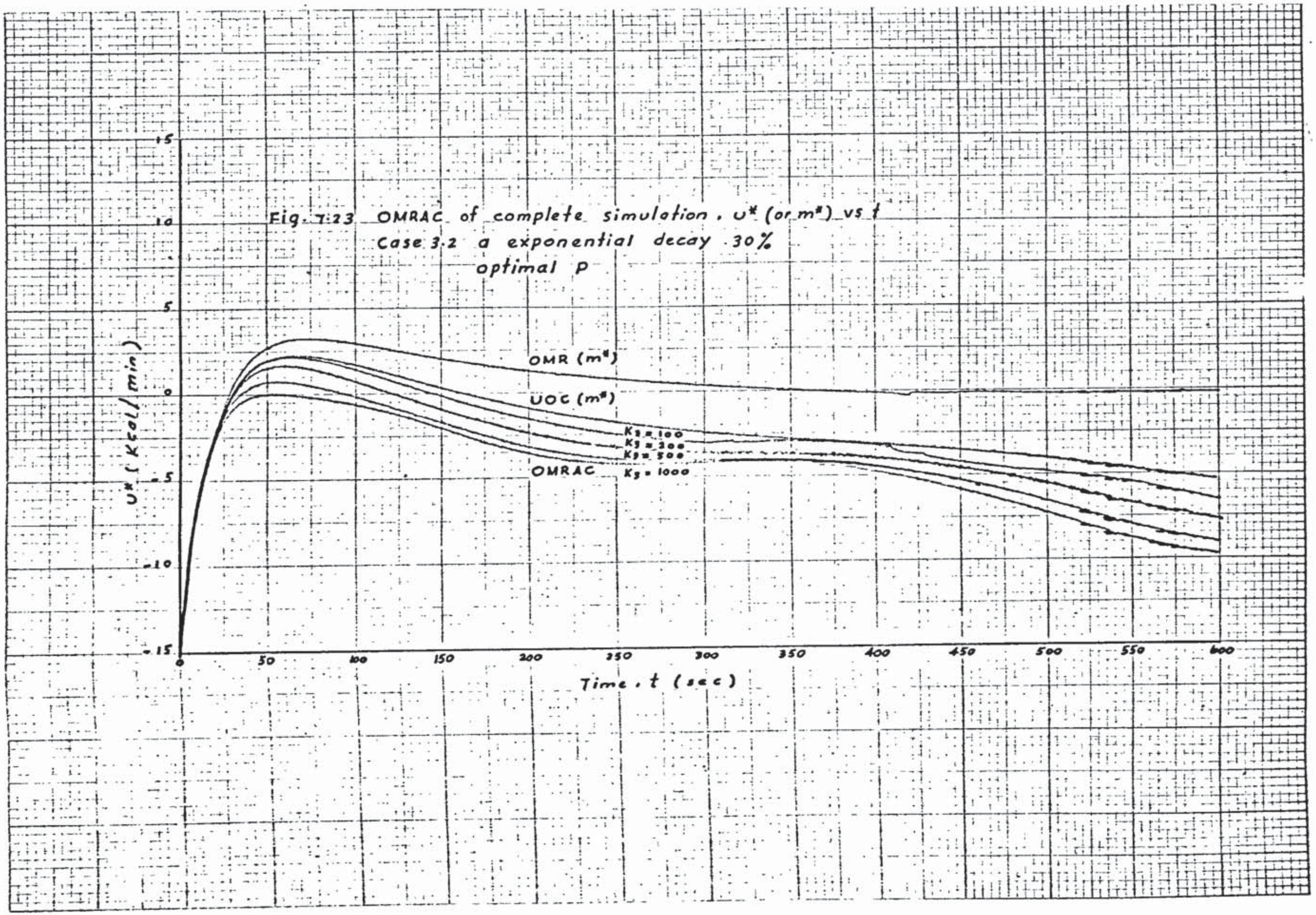

Fig. 7.23 OMRAC of complete simulation, U* (or m*) vs t
Case 3.2 a exponential decay 30%
optimal P

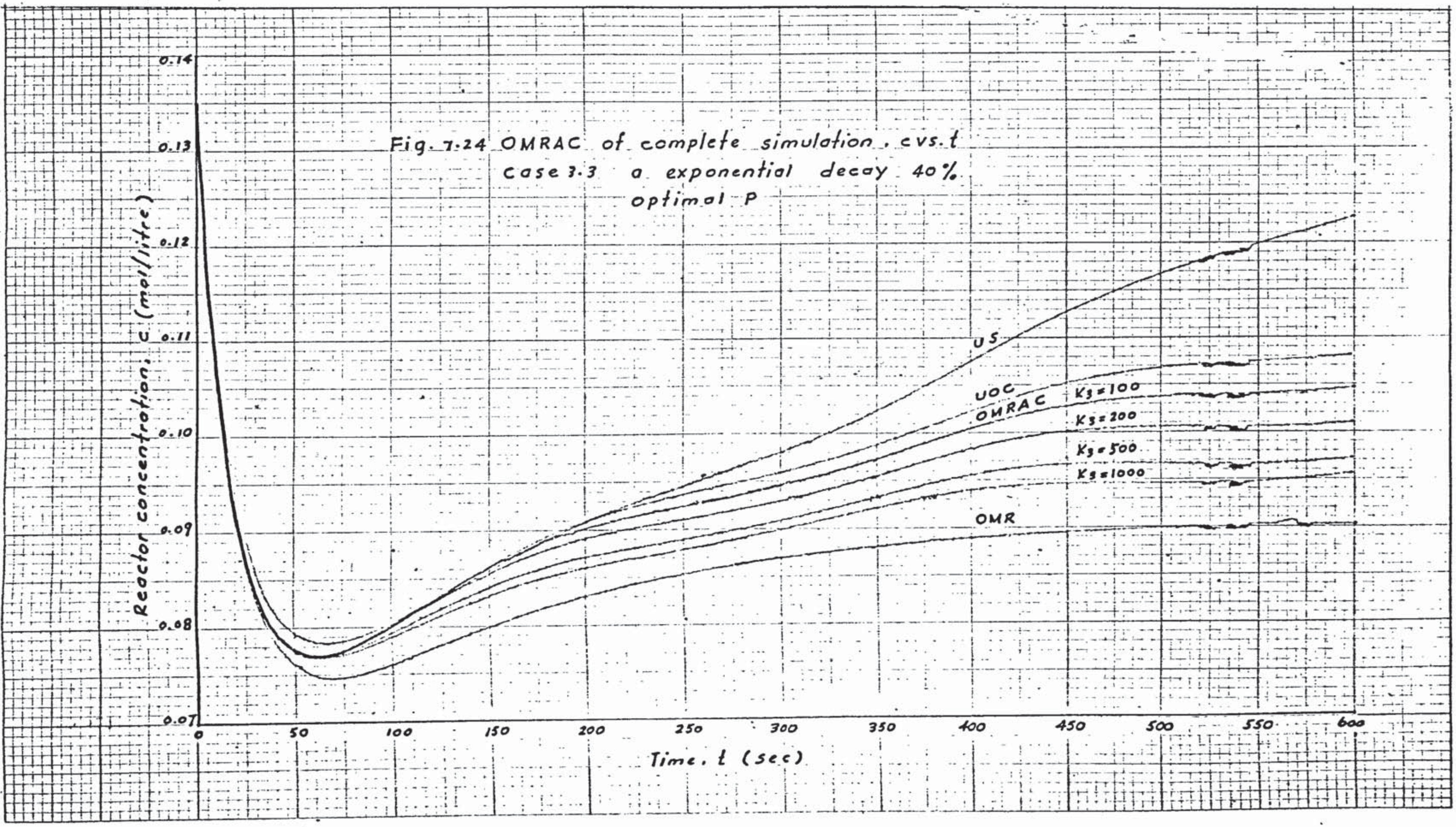

Fig. 7.24 OMRAC of complete simulation, c vs. t
case 3.3 a exponential decay 40%
optimal P

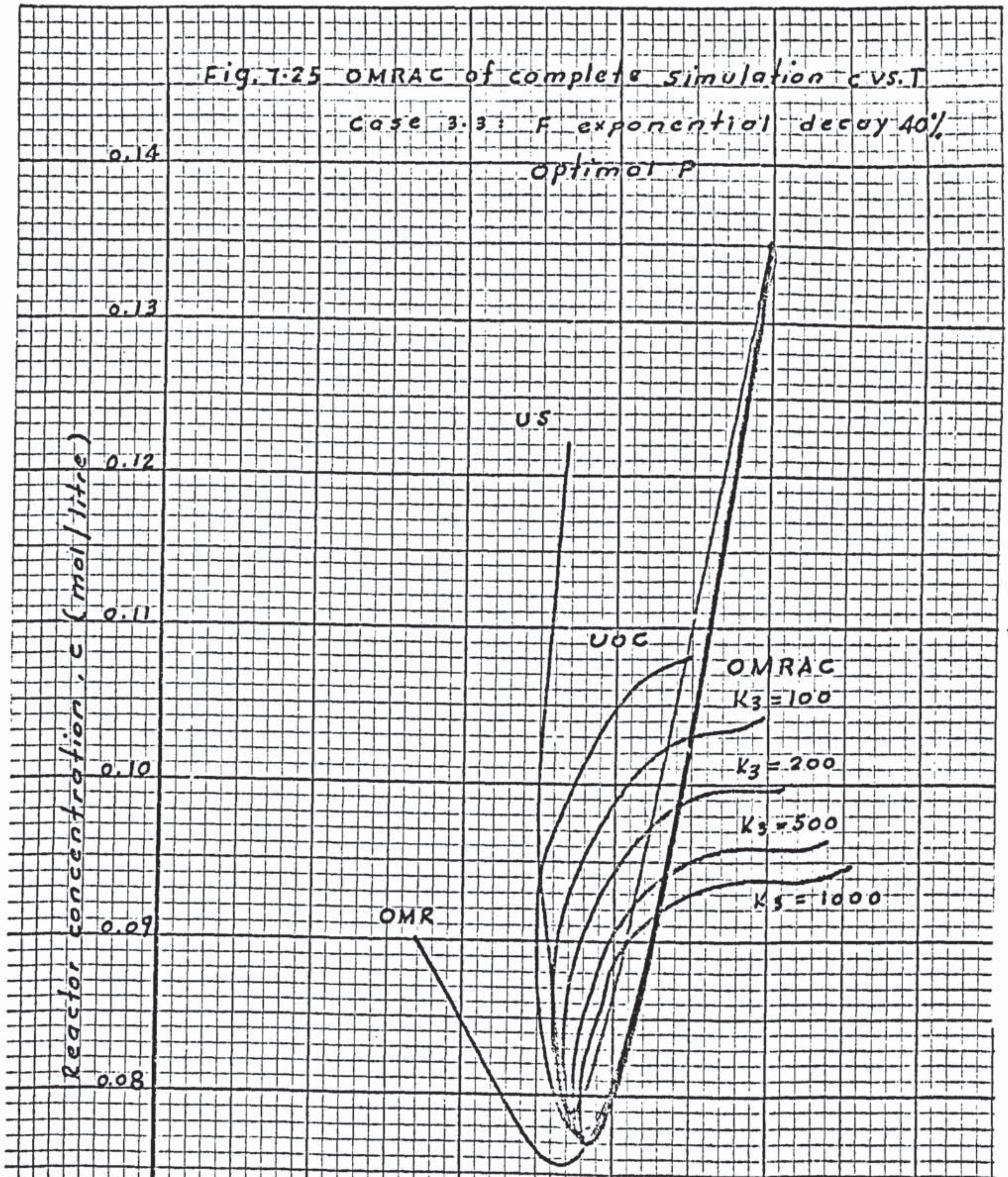
Fig. 7·25 OMRAC of complete simulation c vs. T
Case 3·3: F exponential decay 40%
optimal P
0.14
0.13
0.12
0.11
0.10
0.09
0.08
0.07
US
UOC
OMRAC
K3 = 100
K3 = 200
K3 = 500
K5 = 1000
OMR
29
30
31
32
33
34
Reactor concentration, c (mol/litre)
Reactor temperature, T (°c)

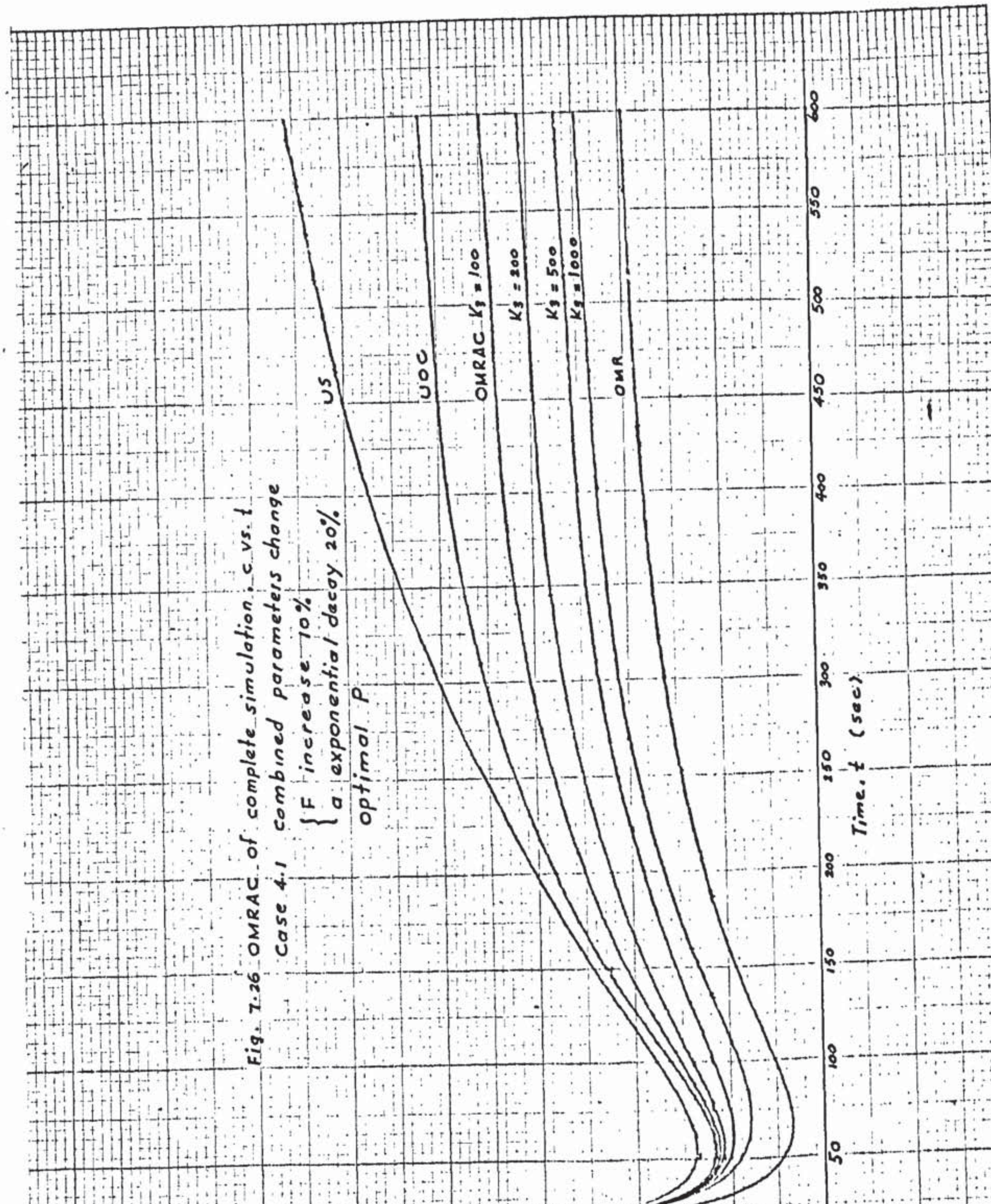

Fig. 7.26 OMRAC of complete simulation, c vs. t
Case 4.1 combined parameters change
{ F increase 10%
{ a exponential decay 20%
optimal P

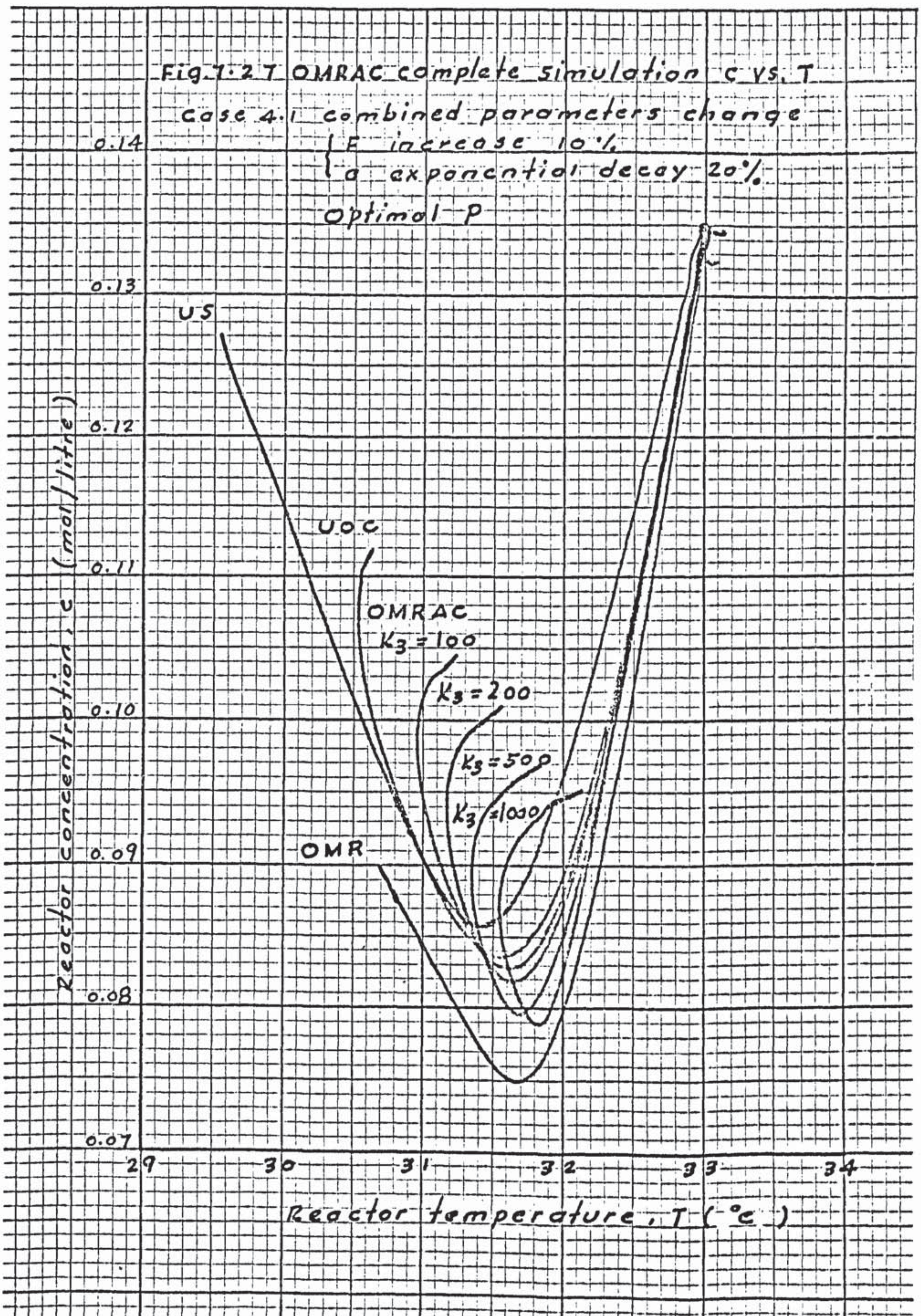
Fig. 7.27 OMRAC complete simulation c vs. T
case 4.1 combined parameters change
{ F increase 10%
{ a exponential decay 20%
Optimal P
US
UOC
OMRAC
K3 = 100
K3 = 200
K3 = 500
K3 = 1000
OMR
0.14
0.13
0.12
0.11
0.10
0.09
0.08
0.07
29
30
31
32
33
34
Reactor concentration, c (mol/litre)
Reactor temperature, T (°C)

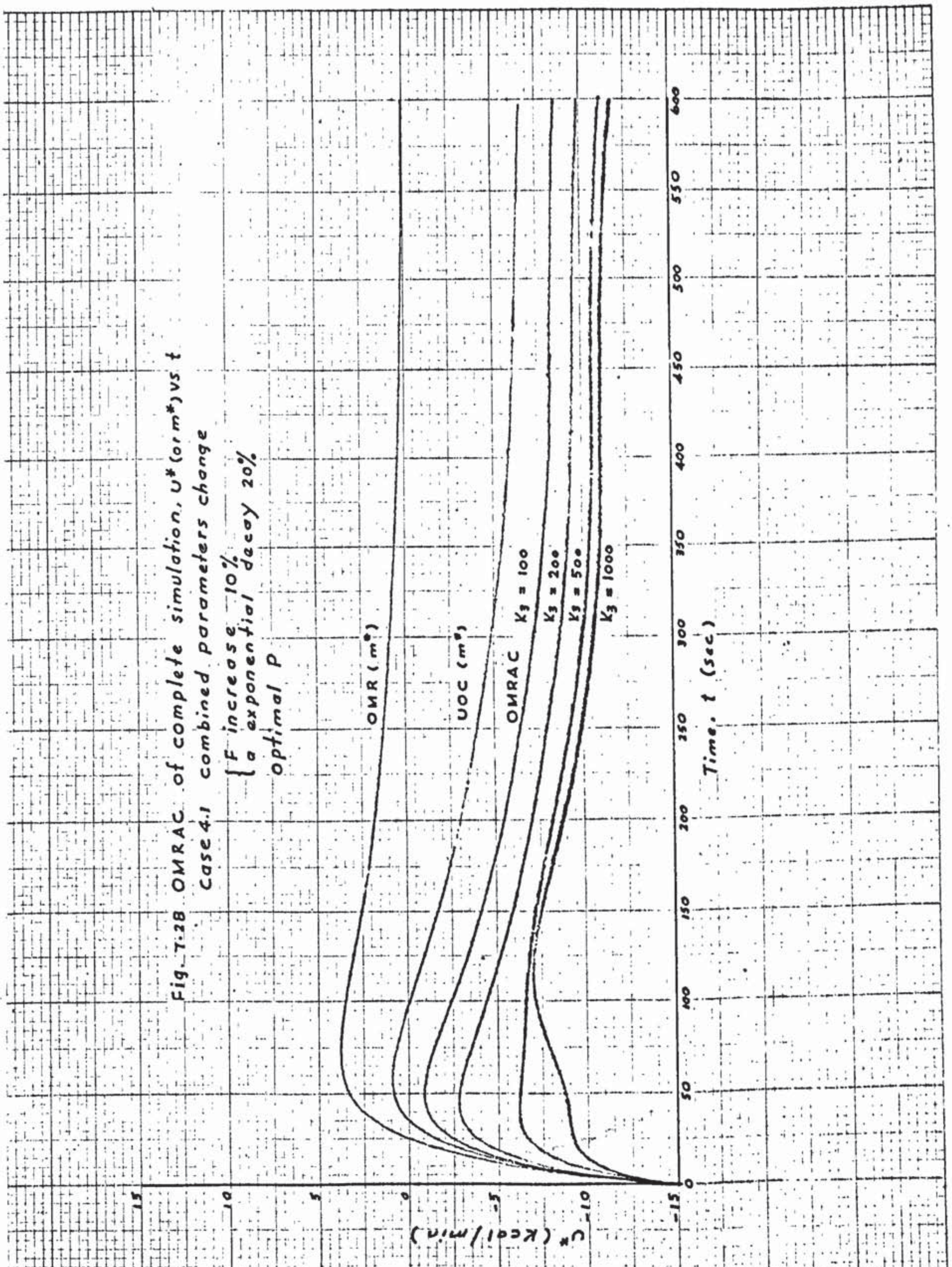

Fig. 7.28 OMRAC of complete simulation, U* (or m*) vs t
Case 4.1 combined parameters change
{ F increase 10%
{ a exponential decay 20%
optimal P

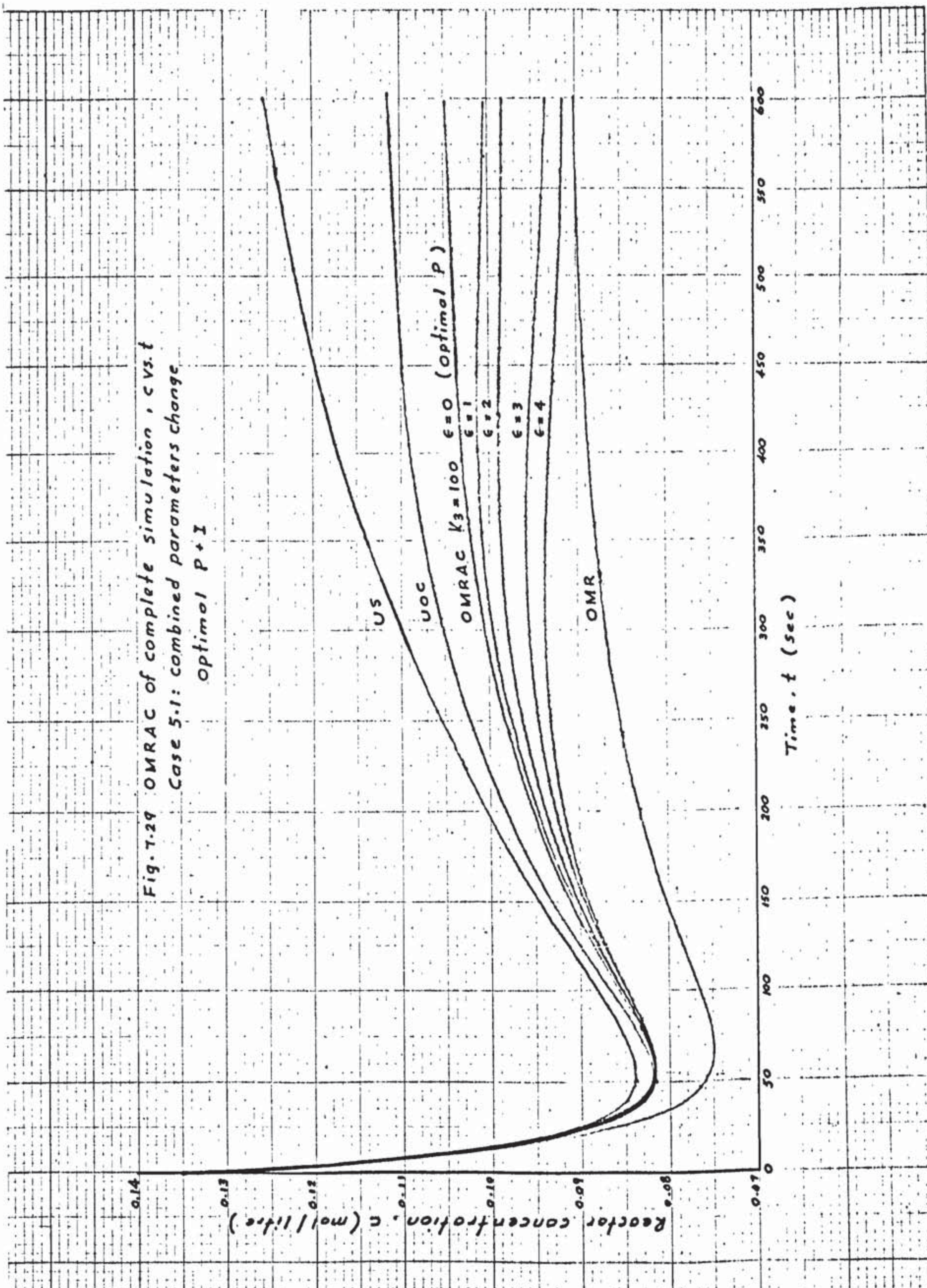

Fig. 7.29 OMRAC of complete simulation, c vs. t
Case 5.1: combined parameters change
optimal P + I

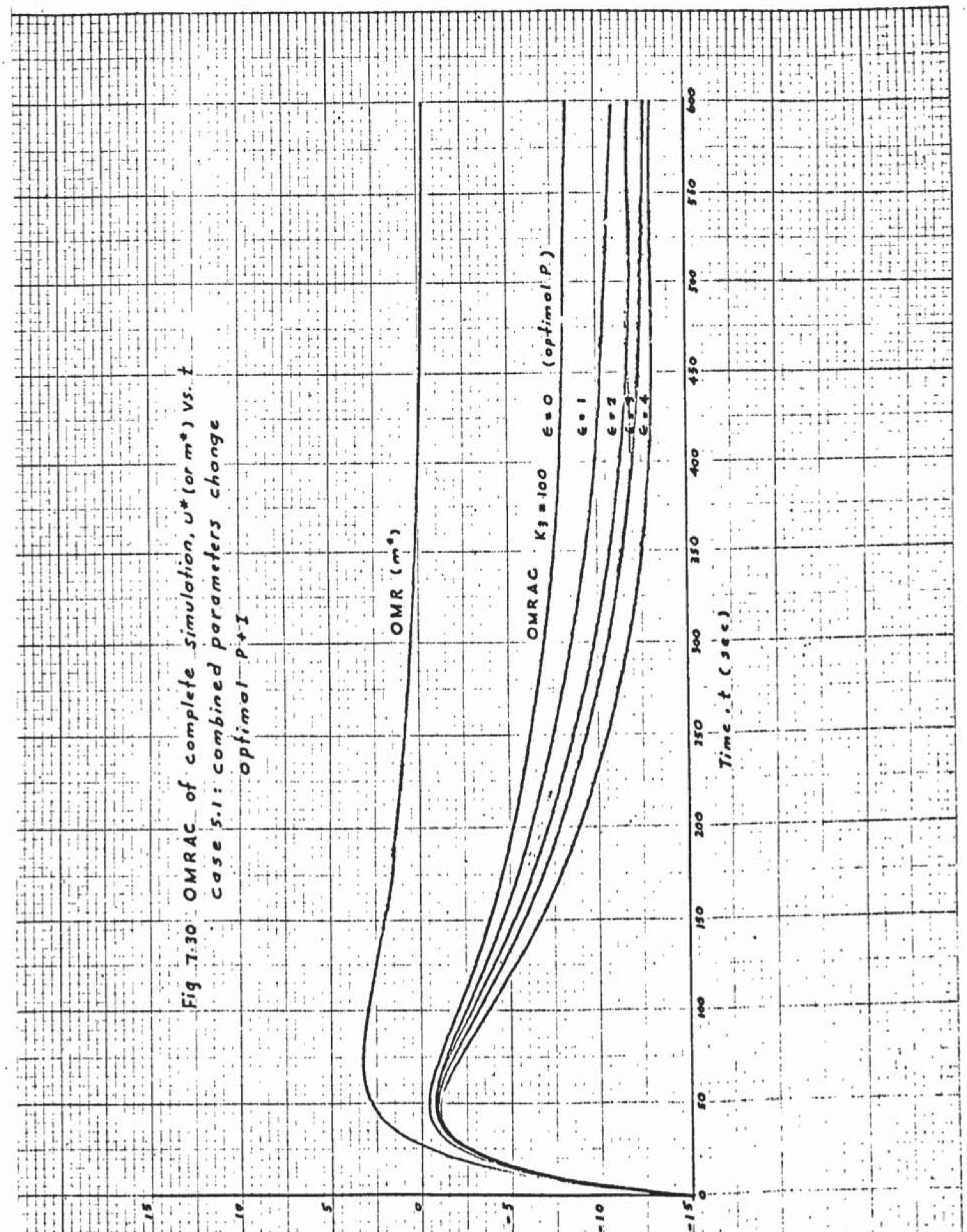

Fig 7.30 OMRAC of complete simulation, u^* (or m^*) vs. t
case 5.1: combined parameters change
optimal P+I

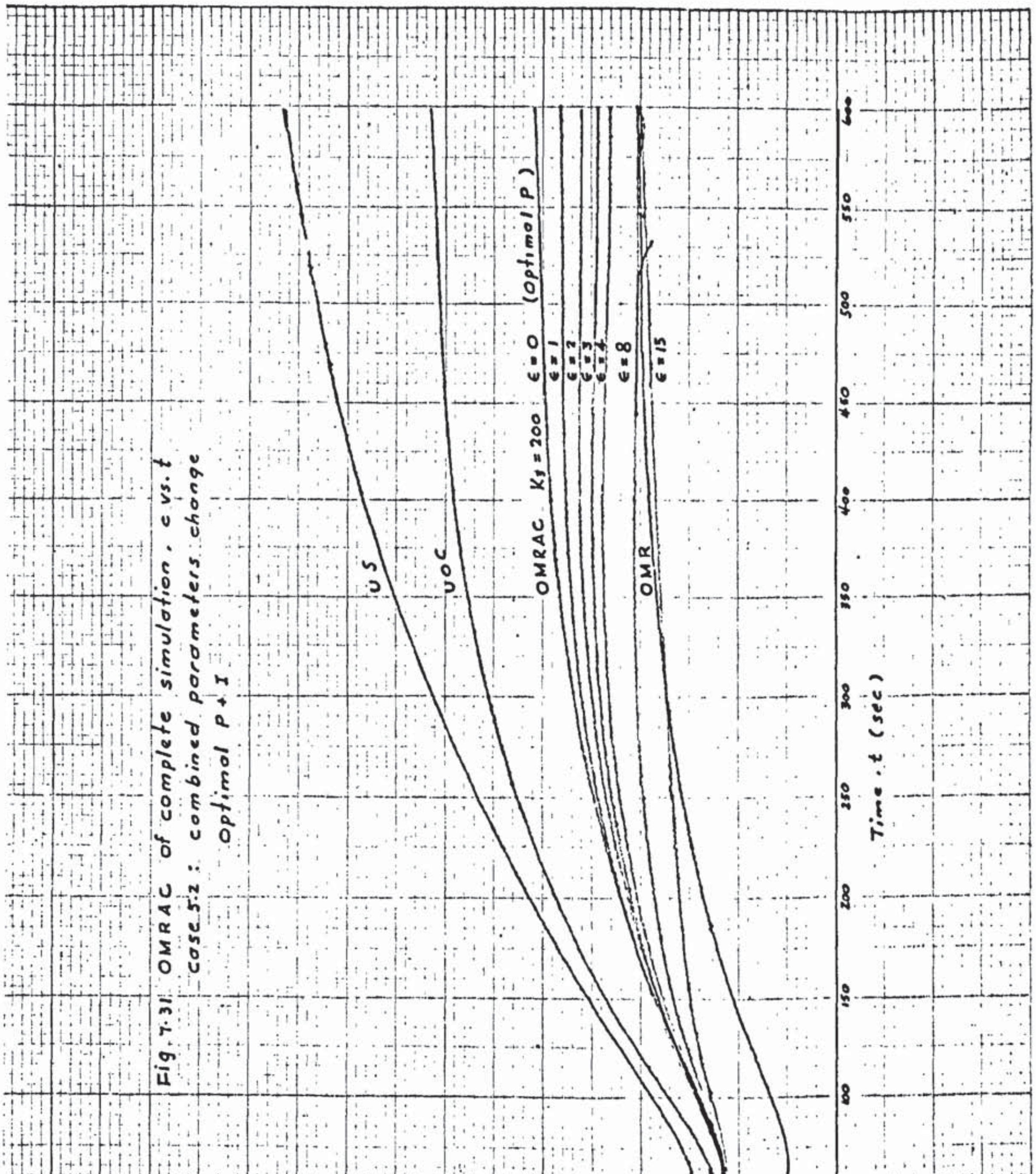
Fig. 7.31 OMRAC of complete simulation, c vs. t
case 5.2 : combined parameters change
optimal P + I
US
UOC
OMRAC Ks = 200 ε = 0 (optimal P)
ε = 1
ε = 2
ε = 3
ε = 4
ε = 8
ε = 15
OMR
Reactor concentration, c (mol/litre)
0.14
0.13
0.12
0.11
0.10
0.09
0.08
0.07
Time, t (sec)
0
50
100
150
200
250
300
350
400
450
500
550
600

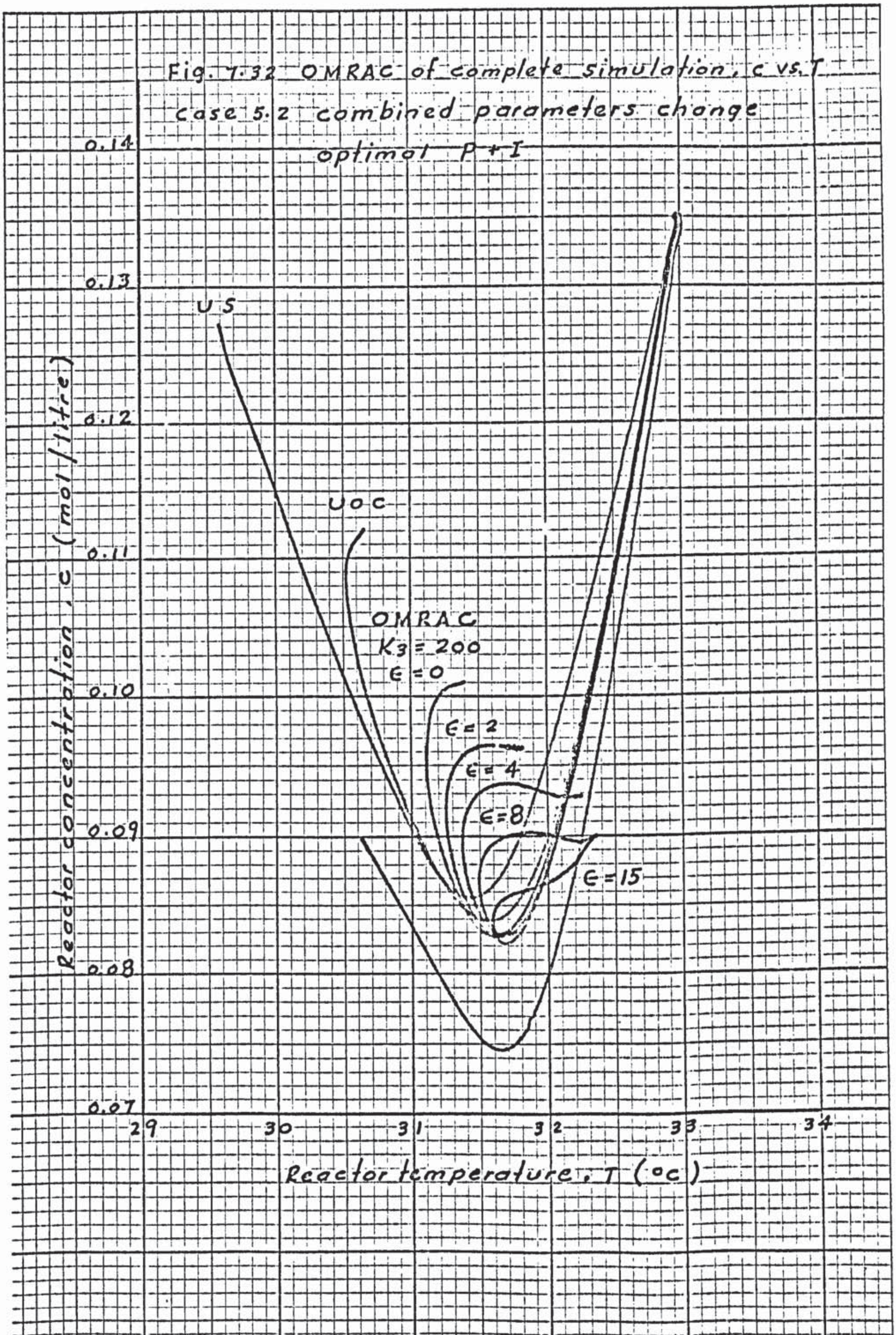
Fig. 7.32 OMRAC of complete simulation, c vs. T
case 5.2 combined parameters change
optimal P+I
0.14
0.13
0.12
0.11
0.10
0.09
0.08
0.07
US
UOC
OMRAC
K3 = 200
ϵ = 0
ϵ = 2
ϵ = 4
ϵ = 8
ϵ = 15
29
30
31
32
33
34
Reactor concentration, c (mol/litre)
Reactor temperature, T (°C)

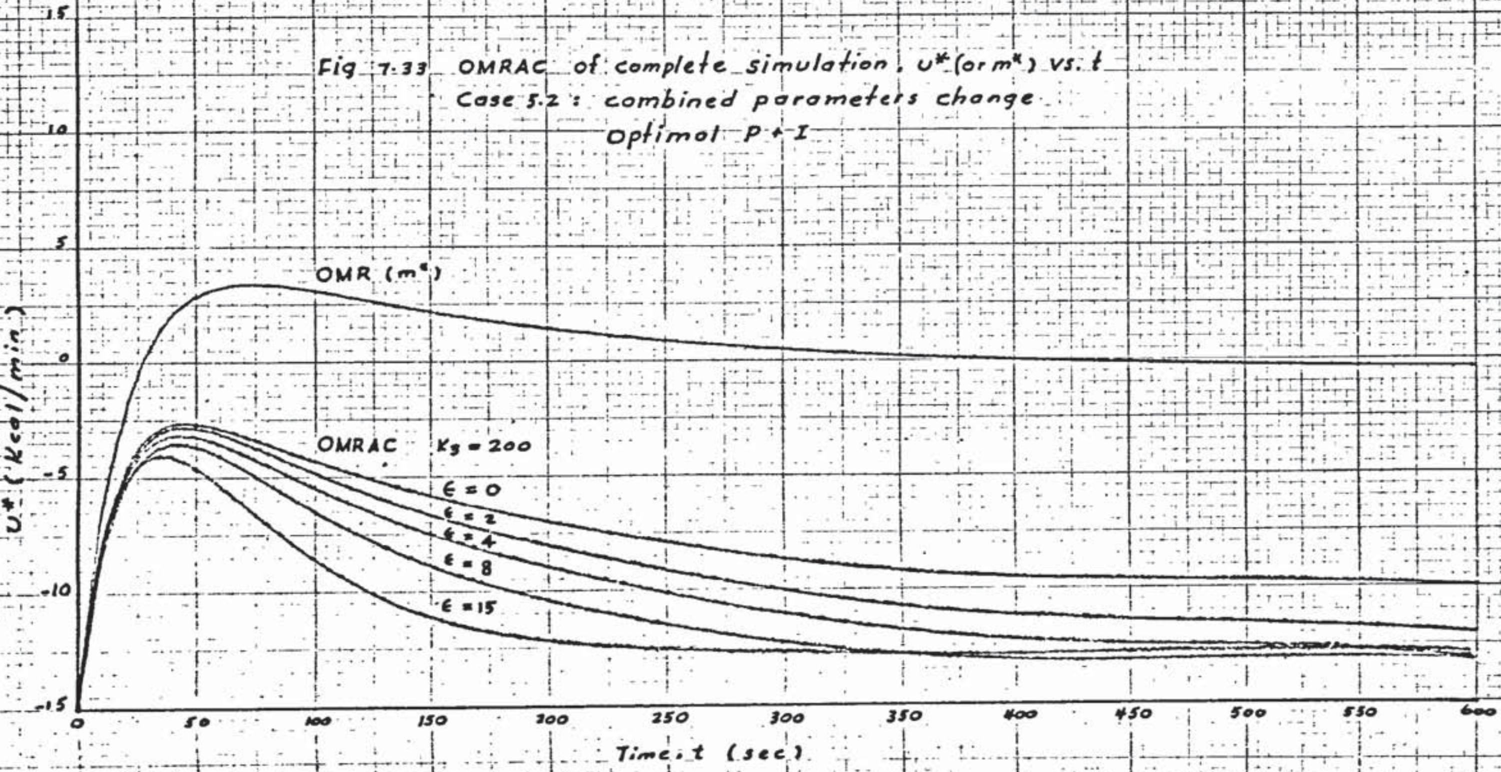

Fig 7.33 OMRAC of complete simulation, U* (or m*) vs. t
Case 5.2 : combined parameters change
Optimal P + I

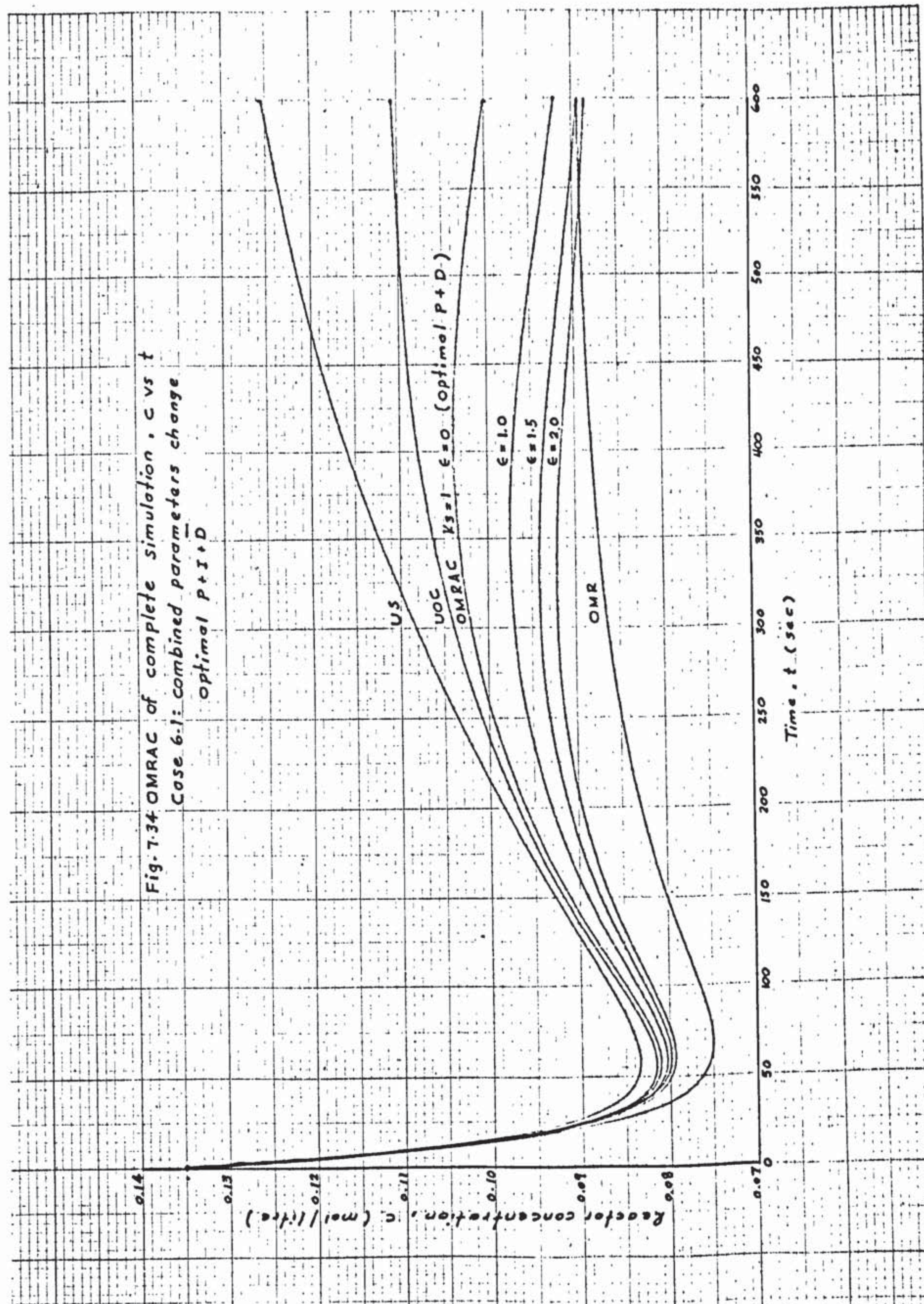
Fig. 7.34 OMRAC of complete simulation, c vs t
Case 6.1: combined parameters change
optimal P+I+D
US
UOC
OMRAC $K_3=1$ $\epsilon=0$ (optimal P+D)
$\epsilon=1.0$
$\epsilon=1.5$
$\epsilon=2.0$
OMR
Reactor concentration, c (mol/litre)
0.14
0.13
0.12
0.11
0.10
0.09
0.08
0.07
Time, t (sec)
0
50
100
150
200
250
300
350
400
450
500
550
600

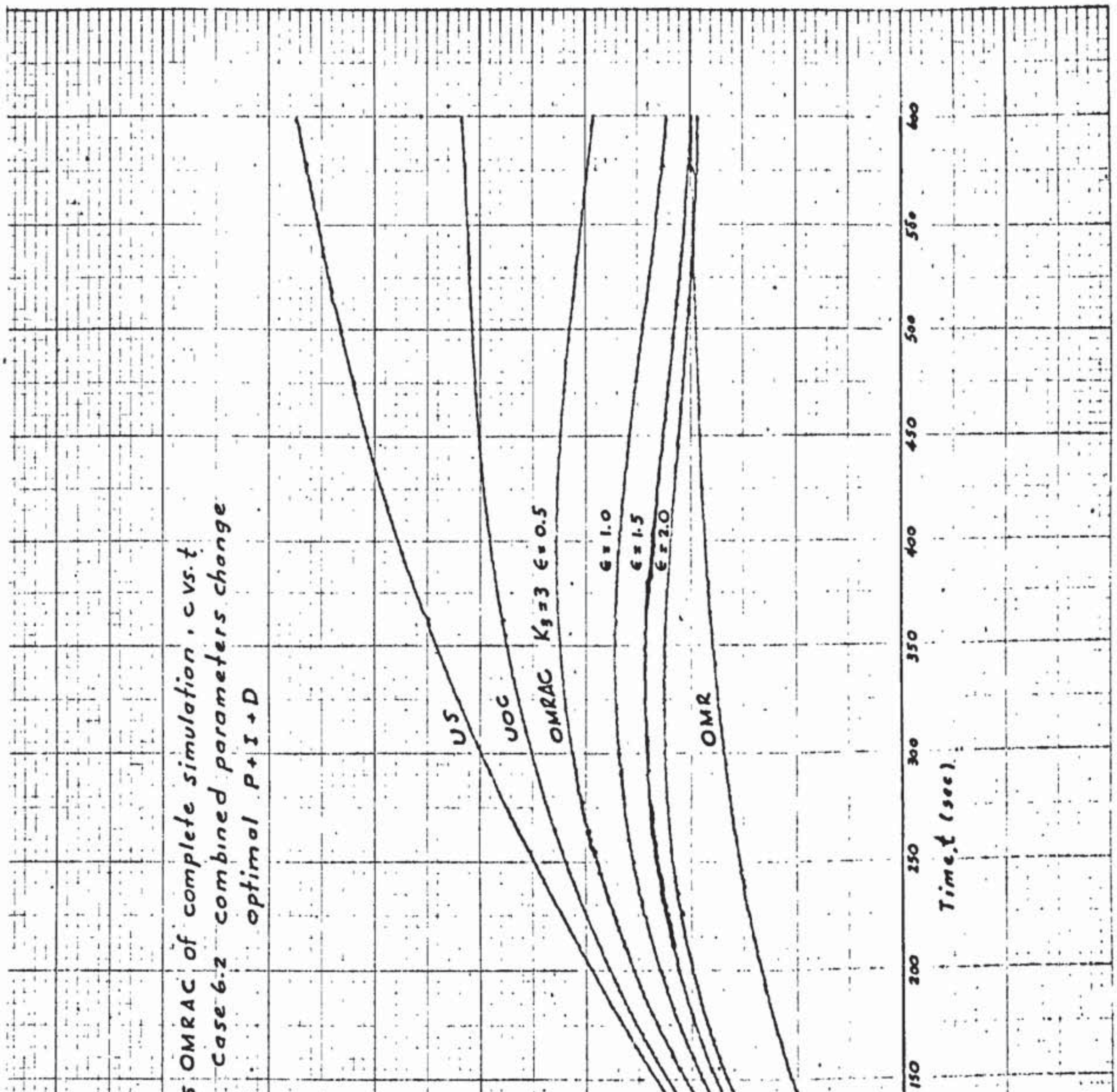

Fig. 7.35 OMRAC of complete simulation, c vs. t
Case 6.2 combined parameters change
optimal P + I + D

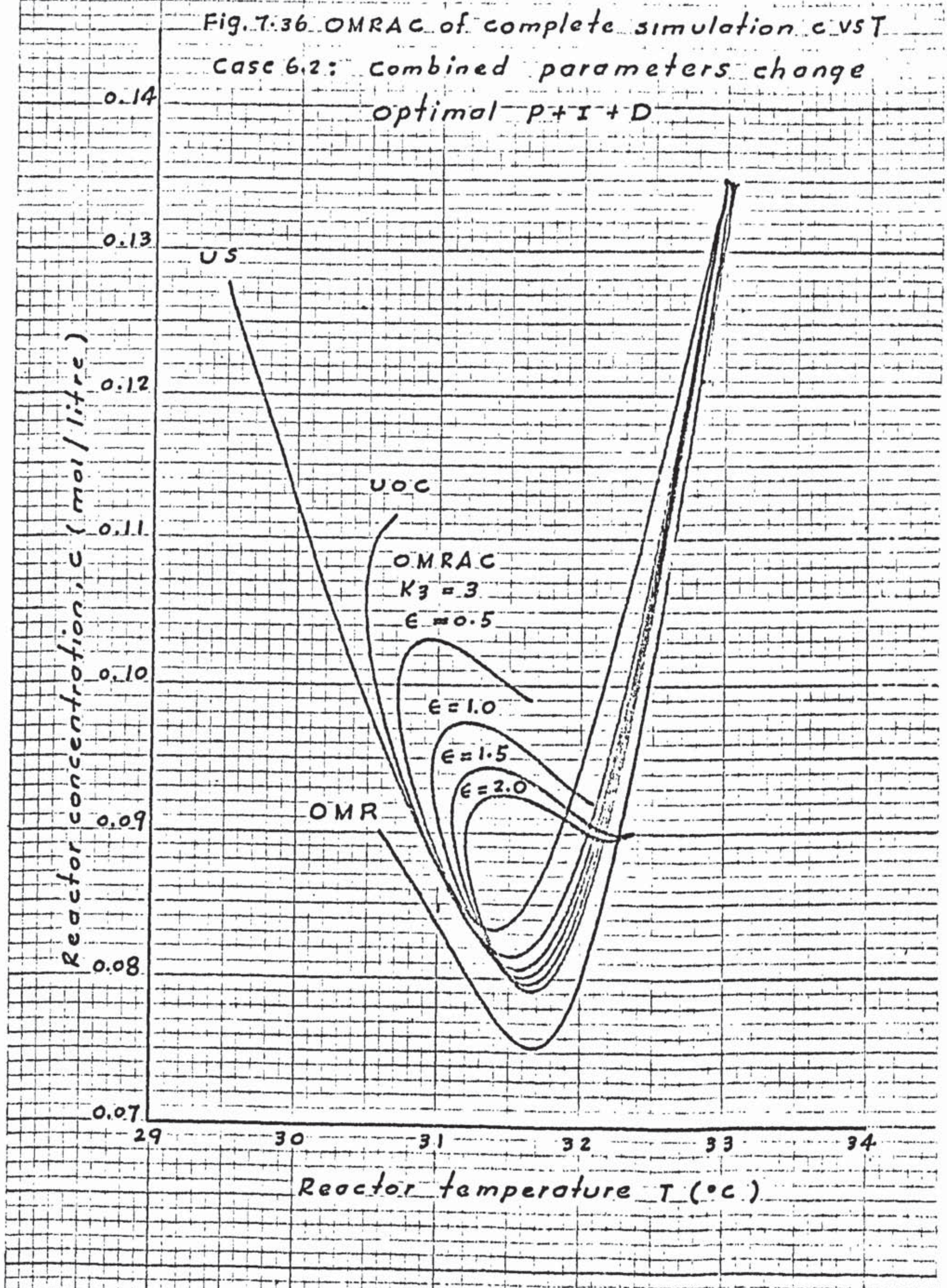
Fig. 7.36 OMRAC of complete simulation c vs T
Case 6.2: Combined parameters change
optimal P+I+D
0.14
0.13
0.12
0.11
0.10
0.09
0.08
0.07
US
UOC
OMRAC
K3 = 3
ε = 0.5
ε = 1.0
ε = 1.5
ε = 2.0
OMR
29
30
31
32
33
34
Reactor concentration, c (mol/litre)
Reactor temperature T (°C)

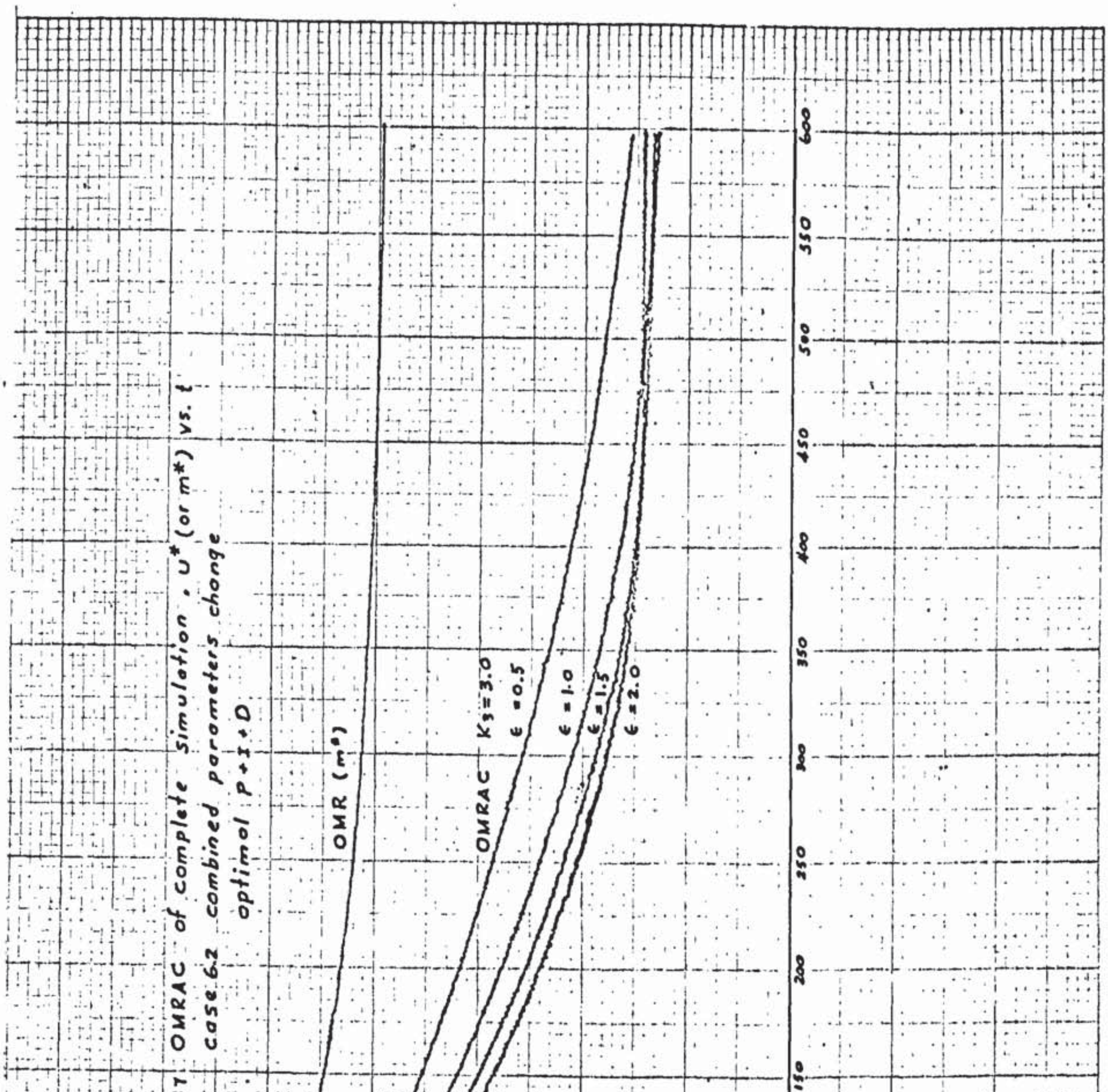

Fig.7.37 OMRAC of complete simulation, U* (or m*) vs. t
case 6.2 combined parameters change
optimal P+I+D

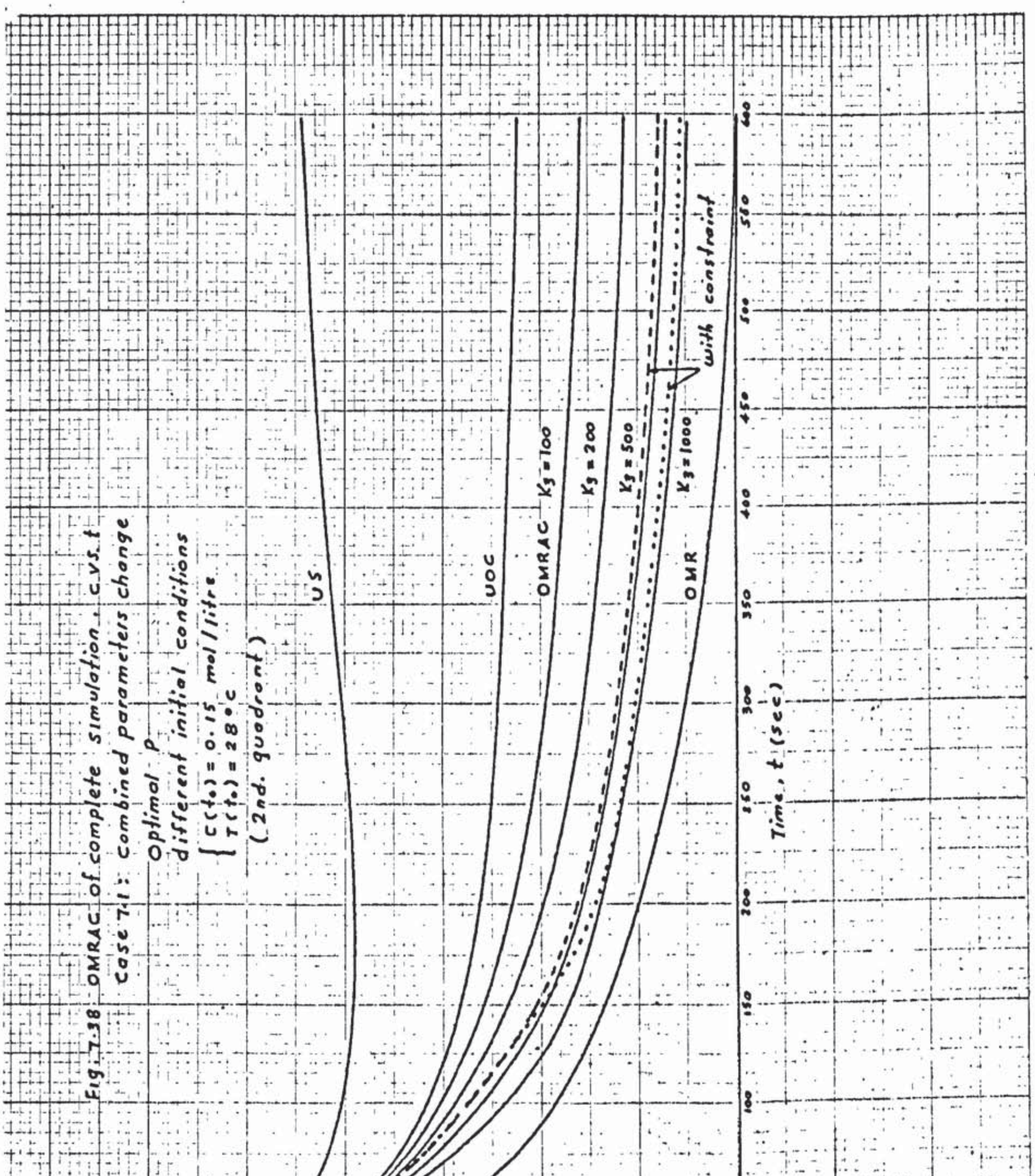

Fig. 7.38 OMRAC of complete simulation, C vs. t
Case 7.1: combined parameters change
Optimal P
different initial conditions
$C(t_0) = 0.15$ mol/litre
$T(t_0) = 28\,^\circ C$
(2nd. quadrant)

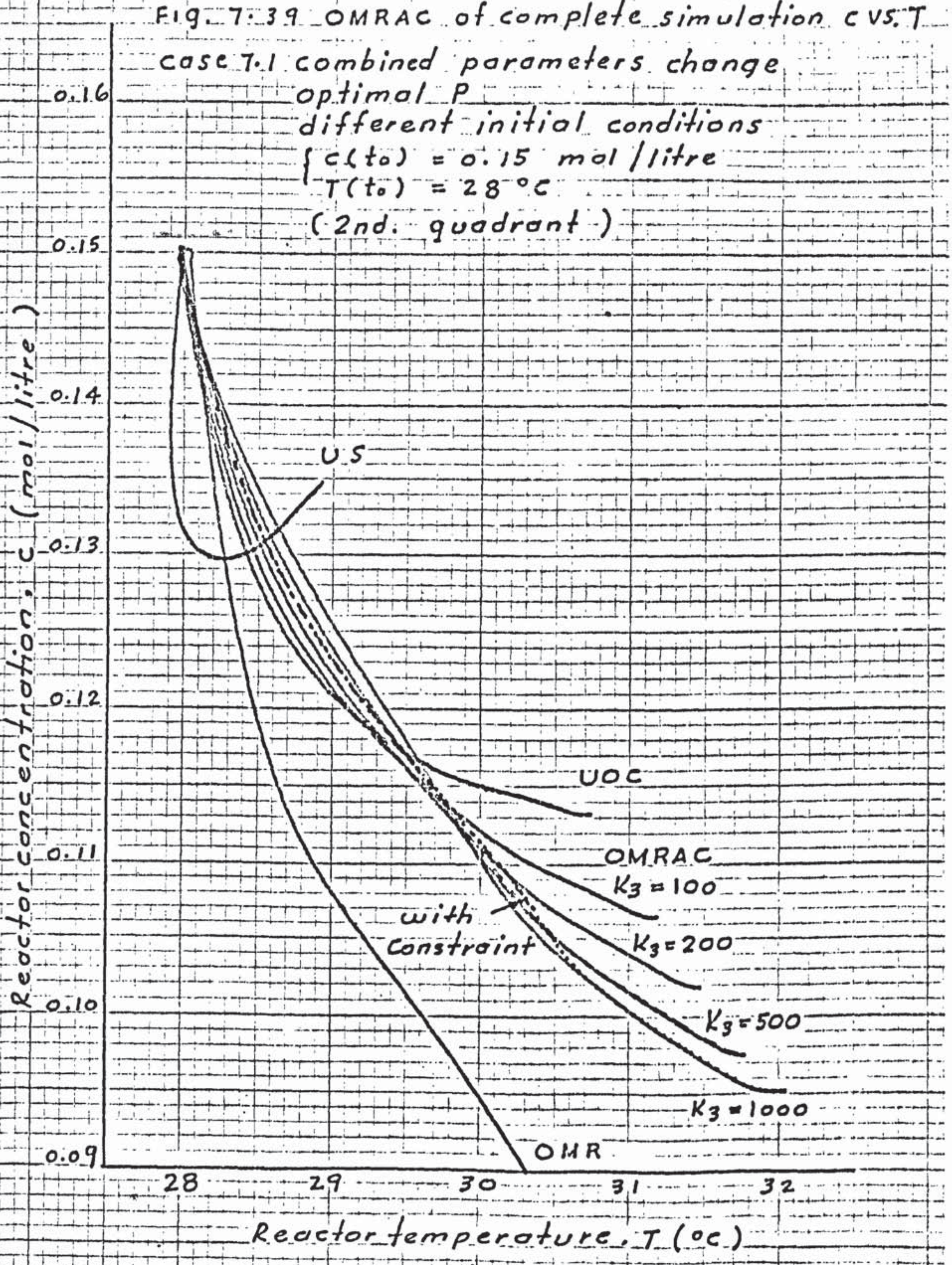
Fig. 7.39 OMRAC of complete simulation c vs. T
case 7.1 combined parameters change
optimal P
different initial conditions
c(to) = 0.15 mol/litre
T(to) = 28 °C
(2nd. quadrant)
0.16
0.15
0.14
0.13
0.12
0.11
0.10
0.09
Reactor concentration, c (mol/litre)
US
UOC
OMRAC
K3 = 100
with
Constraint
K3 = 200
K3 = 500
K3 = 1000
OMR
28
29
30
31
32
Reactor temperature, T (oc)

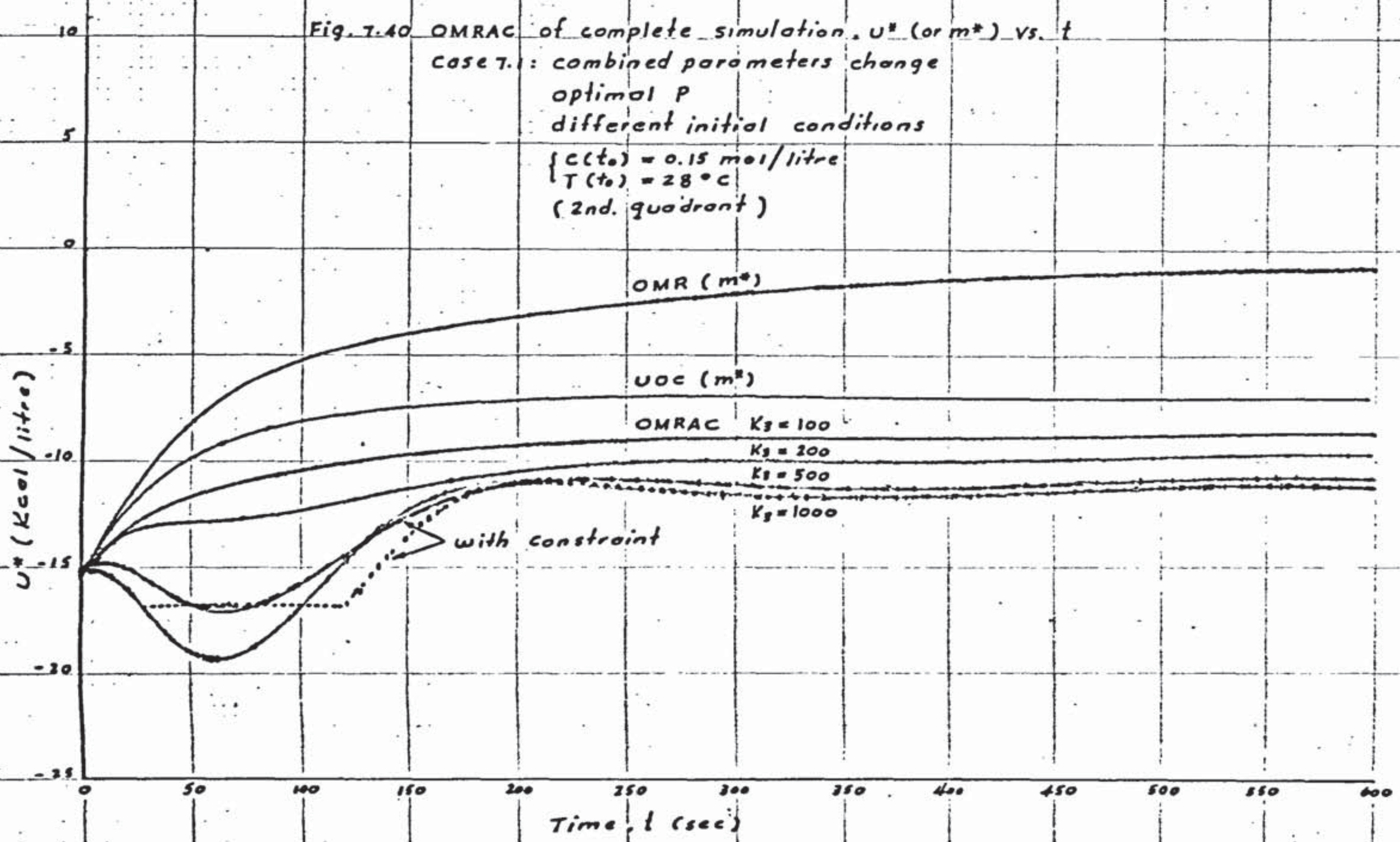

Fig. 7.40 OMRAC of complete simulation, U* (or m*) vs. t
case 7.1: combined parameters change
optimal P
different initial conditions
{ C(t₀) = 0.15 mol/litre
{ T(t₀) = 28 °C
(2nd. quadrant)

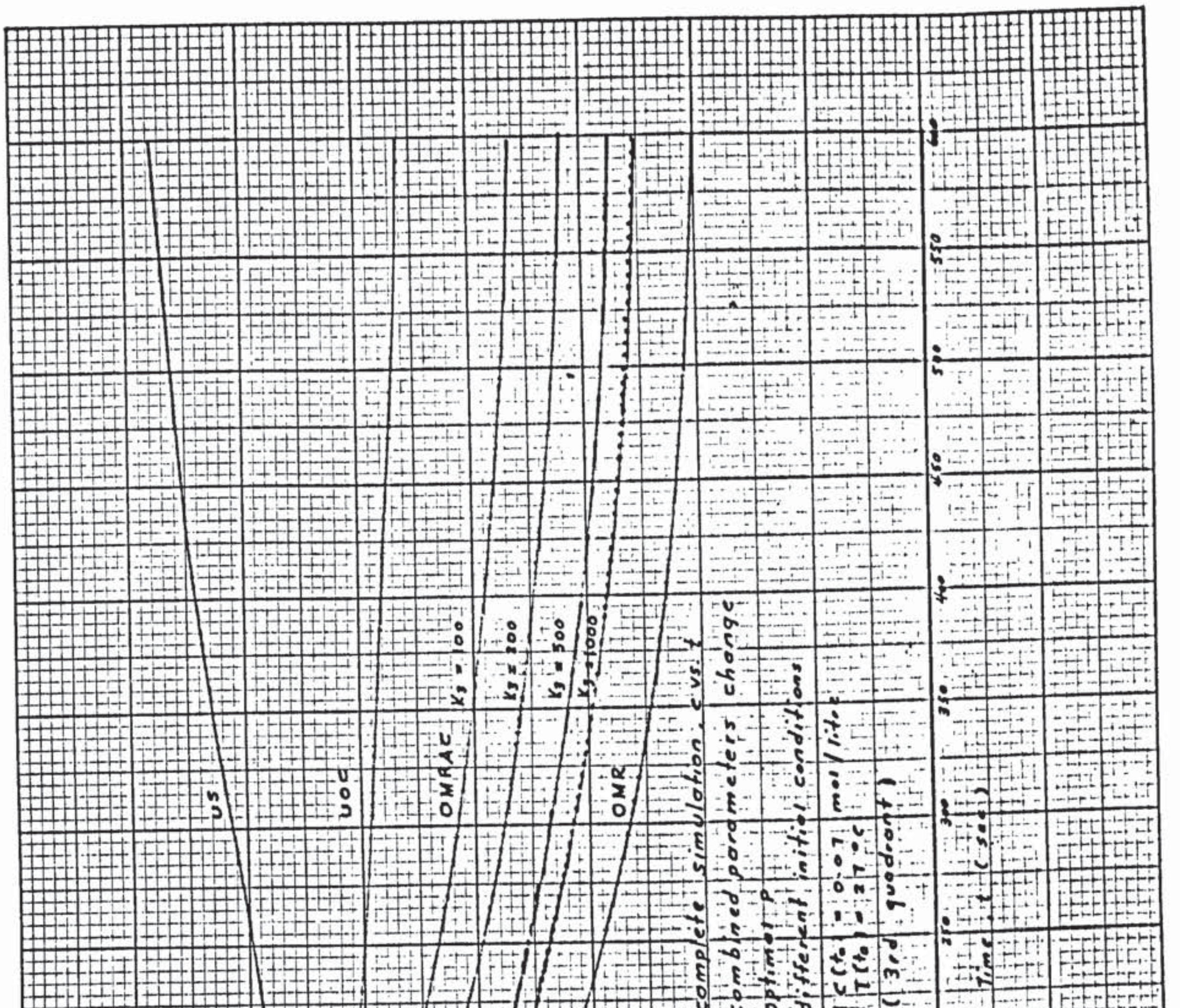

Fig. 7.41 OMRAC of complete simulation, c vs. t
Case 7.1: combined parameters change
optimal p
different initial conditions
$c(t_0) = 0.07$ mol/litre
$T(t_0) = 27$ °C
(3rd quadrant)

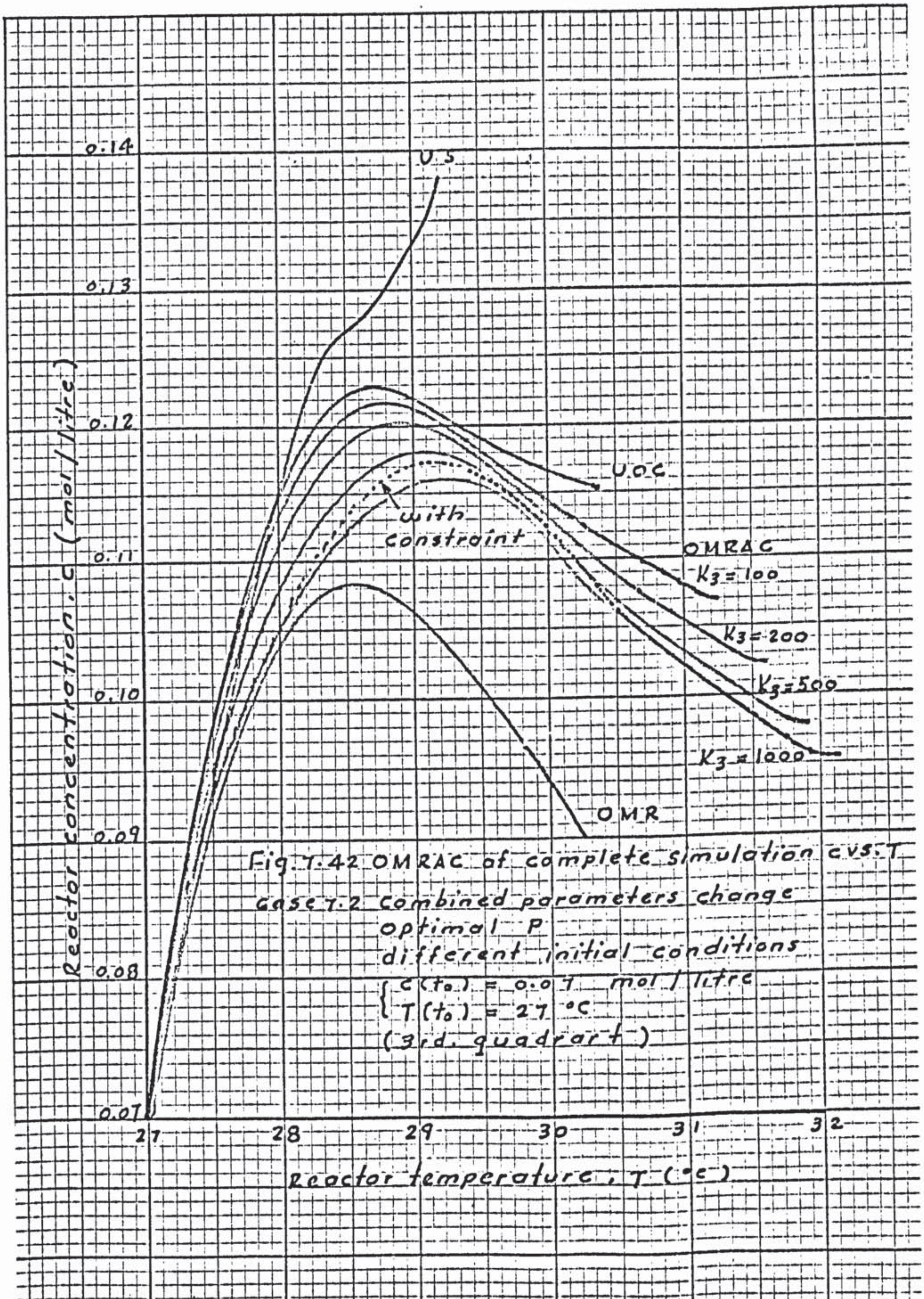

Fig. 7.42 OMRAC of complete simulation c vs. T

case 7.2 combined parameters change

optimal P

different initial conditions

$\begin{cases} c(t_o) = 0.07 \text{ mol/litre} \\ T(t_o) = 27 \text{ °C} \end{cases}$

(3rd. quadrant)

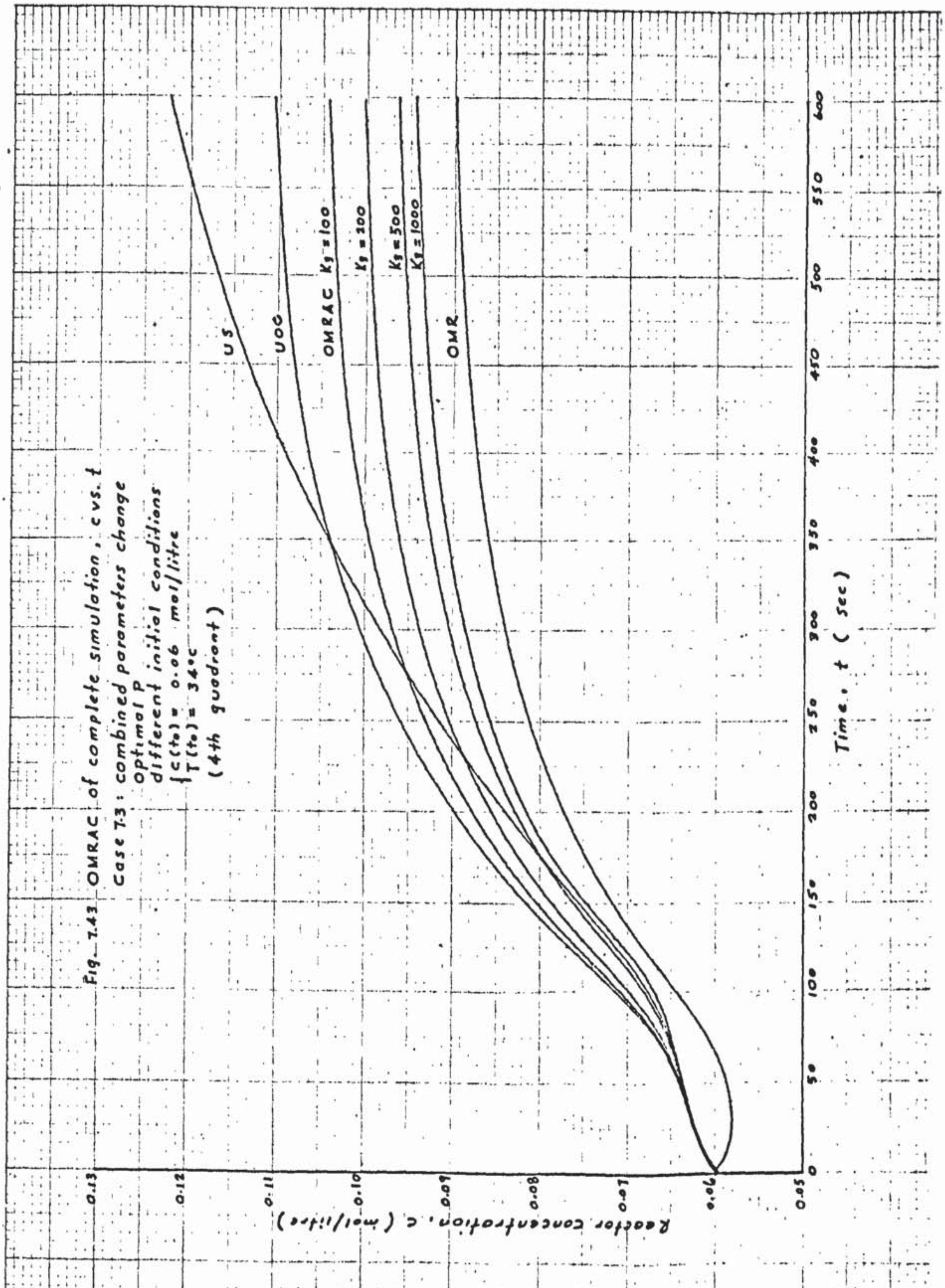

Fig. 7.43 OMRAC of complete simulation, c vs. t
Case 7.3: combined parameters change
optimal P
different initial conditions
$\{ c(t_0) = 0.06$ mol/litre
$T(t_0) = 34°c$
(4th quadrant)

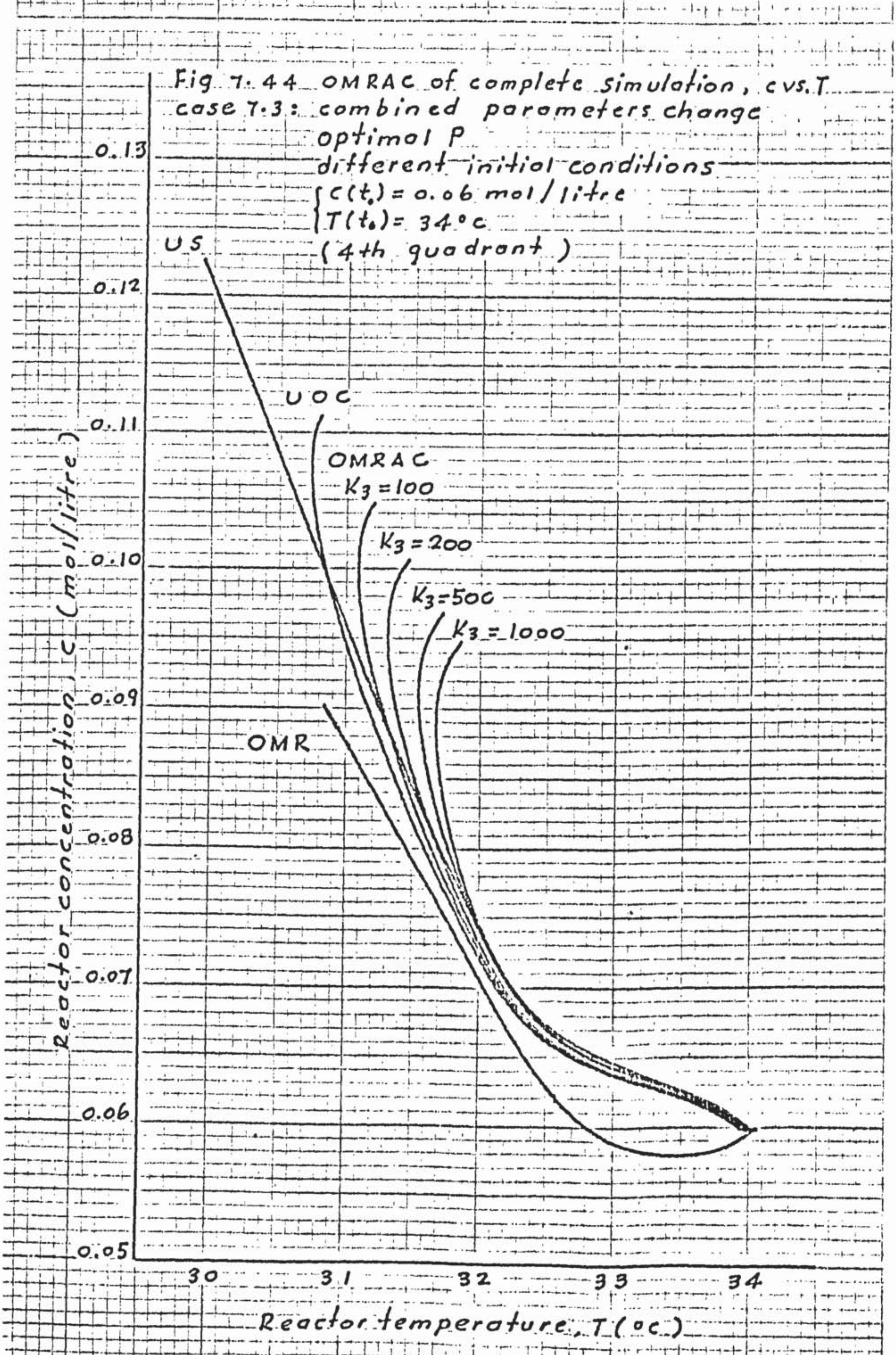
Fig. 7.44 OMRAC of complete simulation, c vs. T
case 7.3: combined parameters change
optimal P
different initial conditions
c(t₀) = 0.06 mol/litre
T(t₀) = 34°c
(4th quadrant)
US
UOC
OMRAC
K3 = 100
K3 = 200
K3 = 500
K3 = 1000
OMR
0.13
0.12
0.11
0.10
0.09
0.08
0.07
0.06
0.05
30
31
32
33
34
Reactor concentration, c (mol/litre)
Reactor temperature, T (°c)

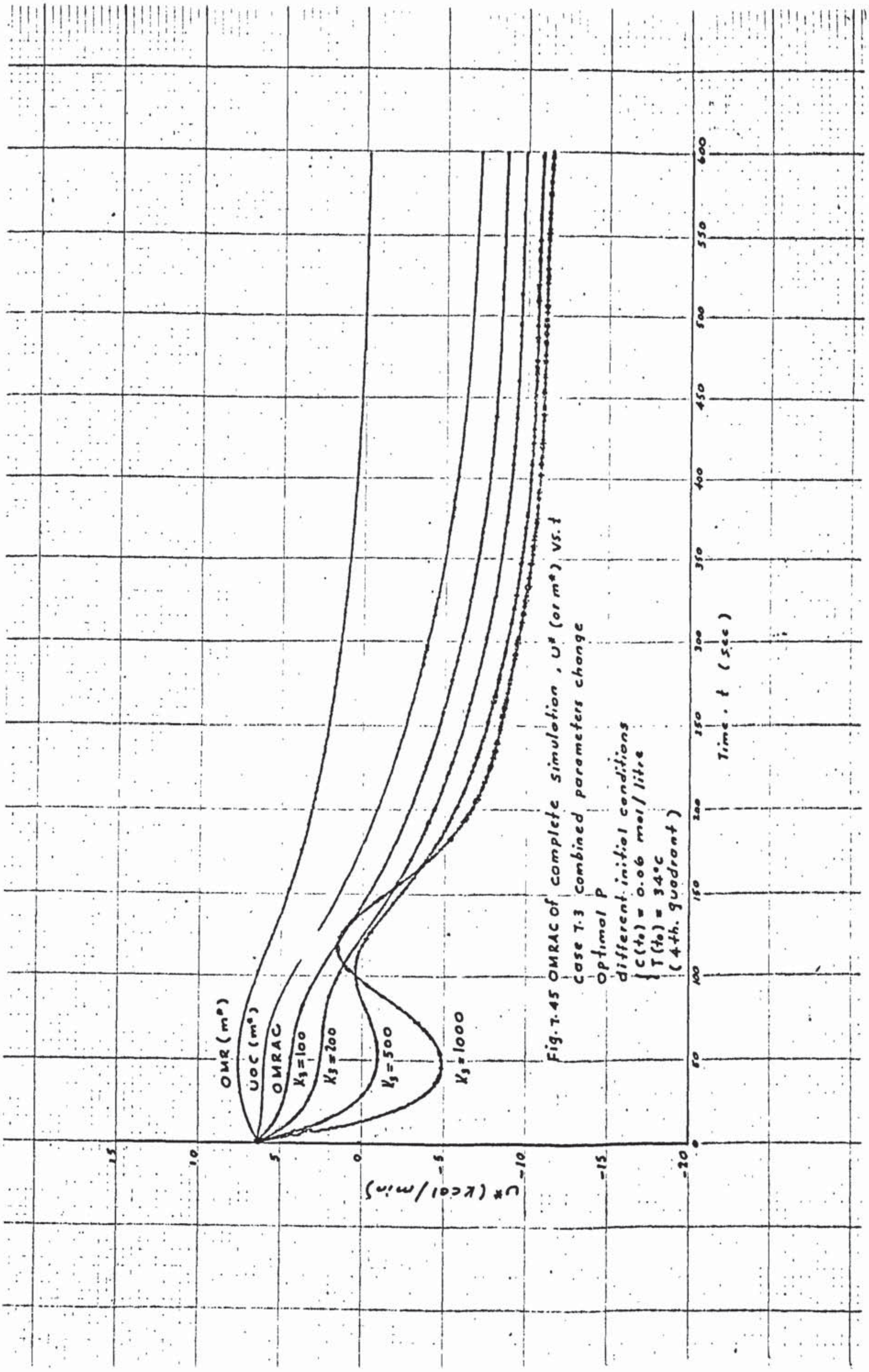

Fig. T.45 OMRAC of complete simulation, U* (or m*) vs. t
case T.3 combined parameters change
optimal P
different initial conditions
C(t0) = 0.06 mol/litre
T(t0) = 34°C
(4th. quadrant)

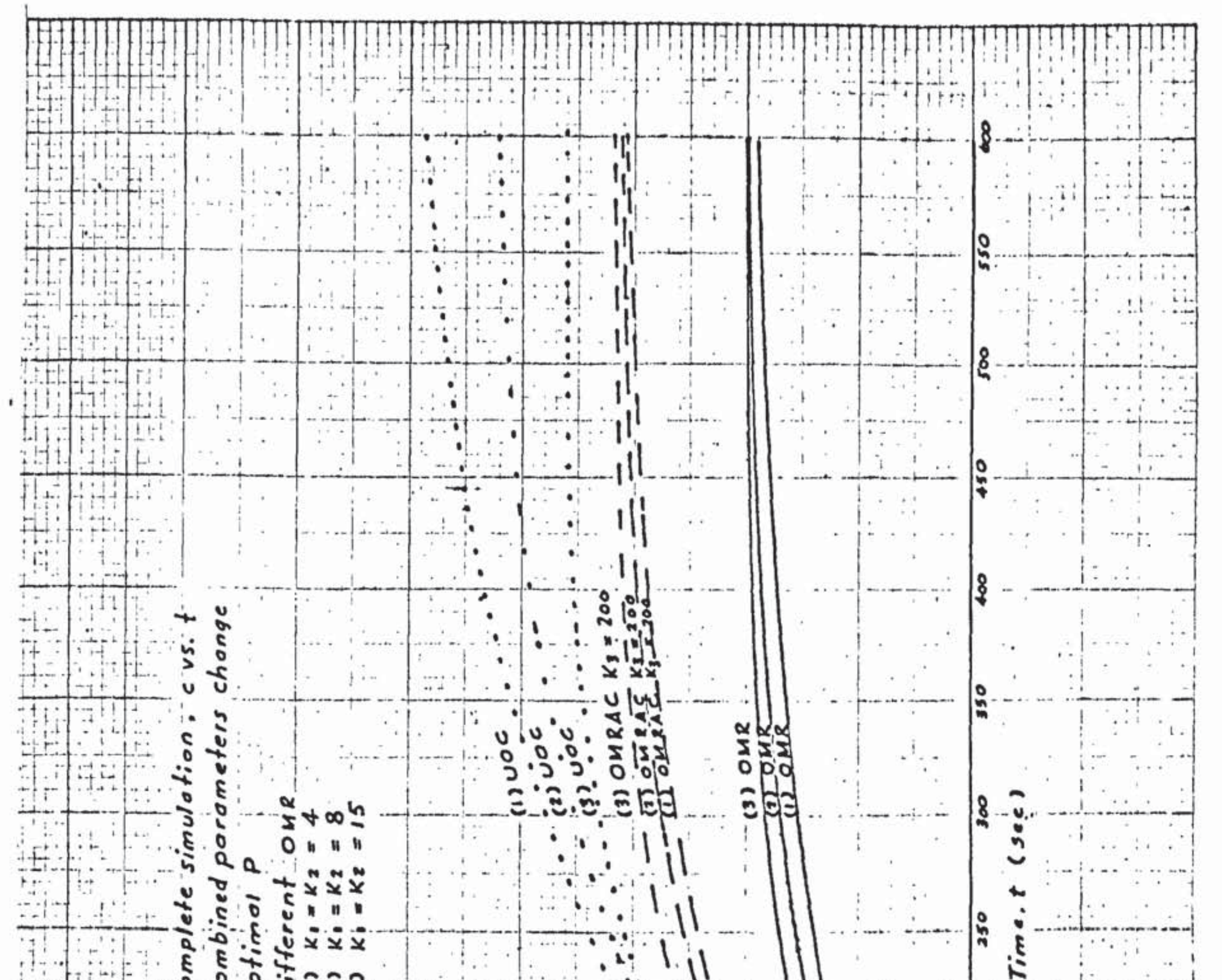

Fig. 7.46 OMRAC of complete simulation, c vs. t

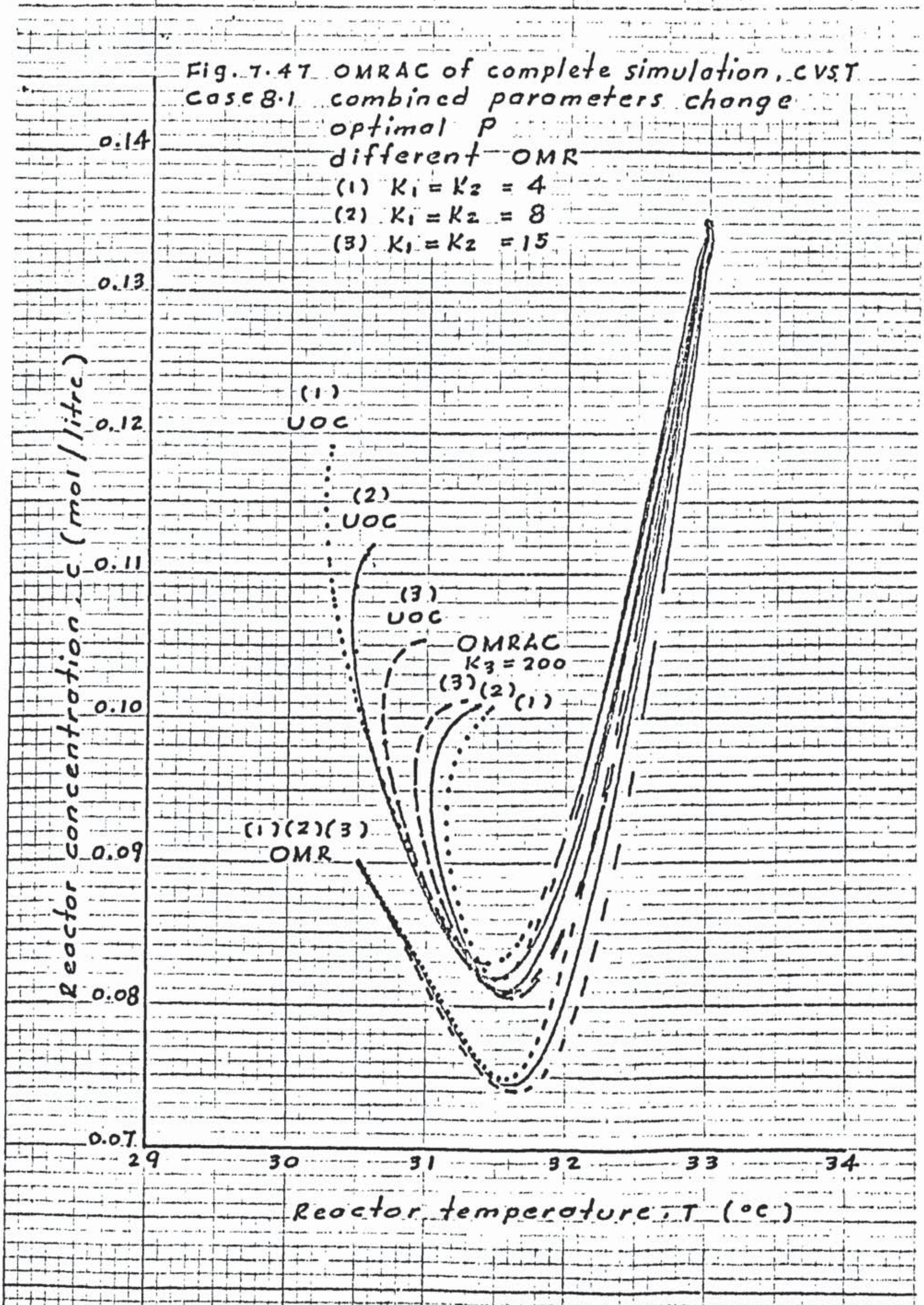
Fig. 7.47 OMRAC of complete simulation, CVST
case 8.1 combined parameters change
optimal P
different OMR
(1) $K_1 = K_2 = 4$
(2) $K_1 = K_2 = 8$
(3) $K_1 = K_2 = 15$
0.14
0.13
0.12
0.11
0.10
0.09
0.08
0.07
(1) UOC
(2) UOC
(3) UOC
OMRAC
$K_3 = 200$
(3) (2) (1)
(1)(2)(3) OMR
29
30
31
32
33
34
Reactor concentration, C (mol/litre)
Reactor temperature, T (°C)

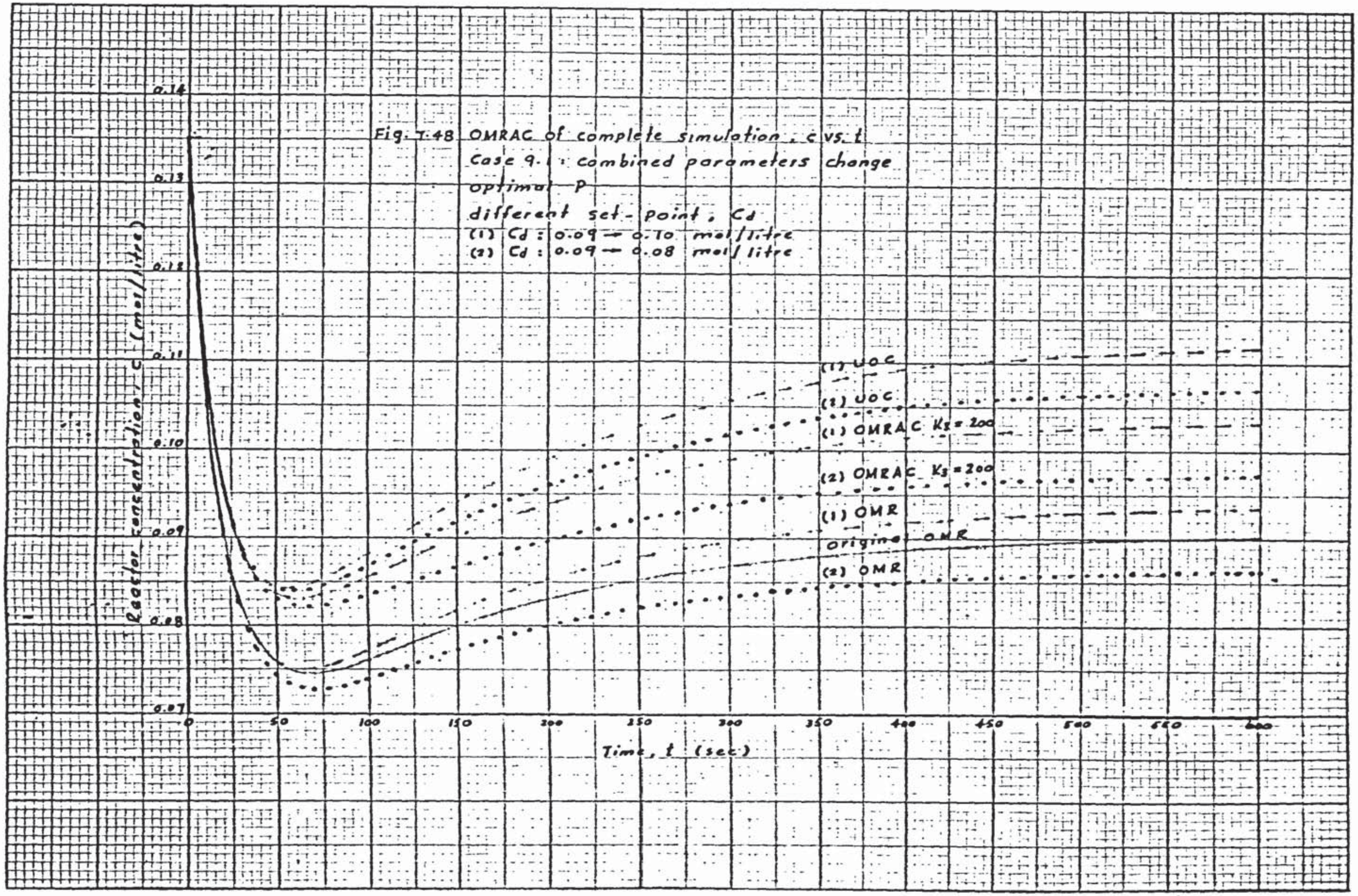

Fig. 7.48 OMRAC of complete simulation, c vs. t
Case 9.1 : combined parameters change
optimal P
different set-point, Cd
(1) Cd : 0.09 → 0.10 mol/litre
(2) Cd : 0.09 → 0.08 mol/litre

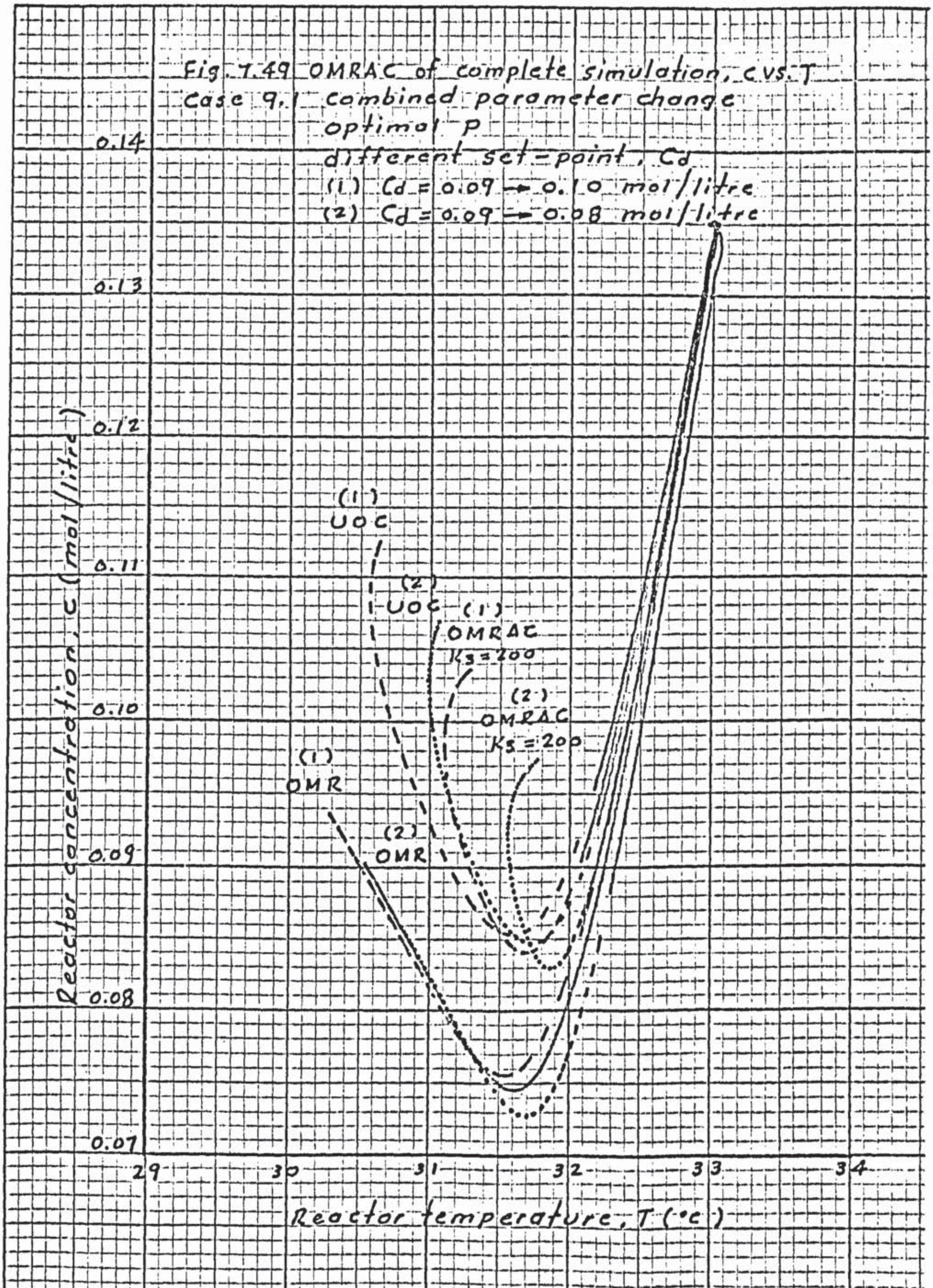

Fig. 7.49 OMRAC of complete simulation, c vs. T
Case 9.1 combined parameter change
optimal P
different set-point, Cd
(1) Cd = 0.09 → 0.10 mol/litre
(2) Cd = 0.09 → 0.08 mol/litre
0.14
0.13
0.12
0.11
0.10
0.09
0.08
0.07
(1) UOC
(2) UOC
(1) OMRAC Ks = 200
(2) OMRAC Ks = 200
(1) OMR
(2) OMR
Reactor concentration, c (mol/litre)
29
30
31
32
33
34
Reactor temperature, T (°c)

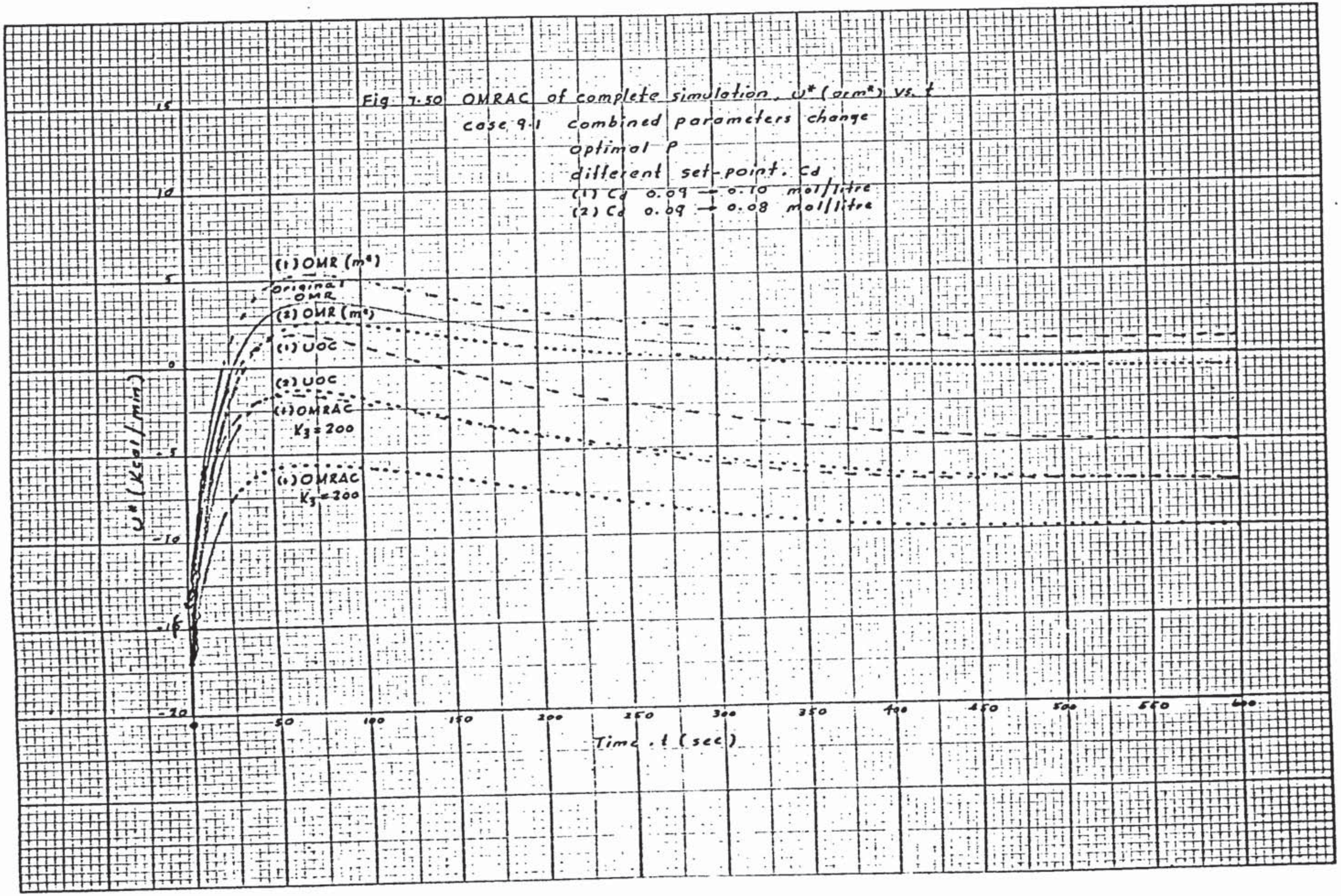

Fig 7.50 OMRAC of complete simulation, U* (orm*) vs. t
case 9.1 combined parameters change
optimal P
different set-point, Cd
(1) Cd 0.09 → 0.10 mol/litre
(2) Cd 0.09 → 0.08 mol/litre

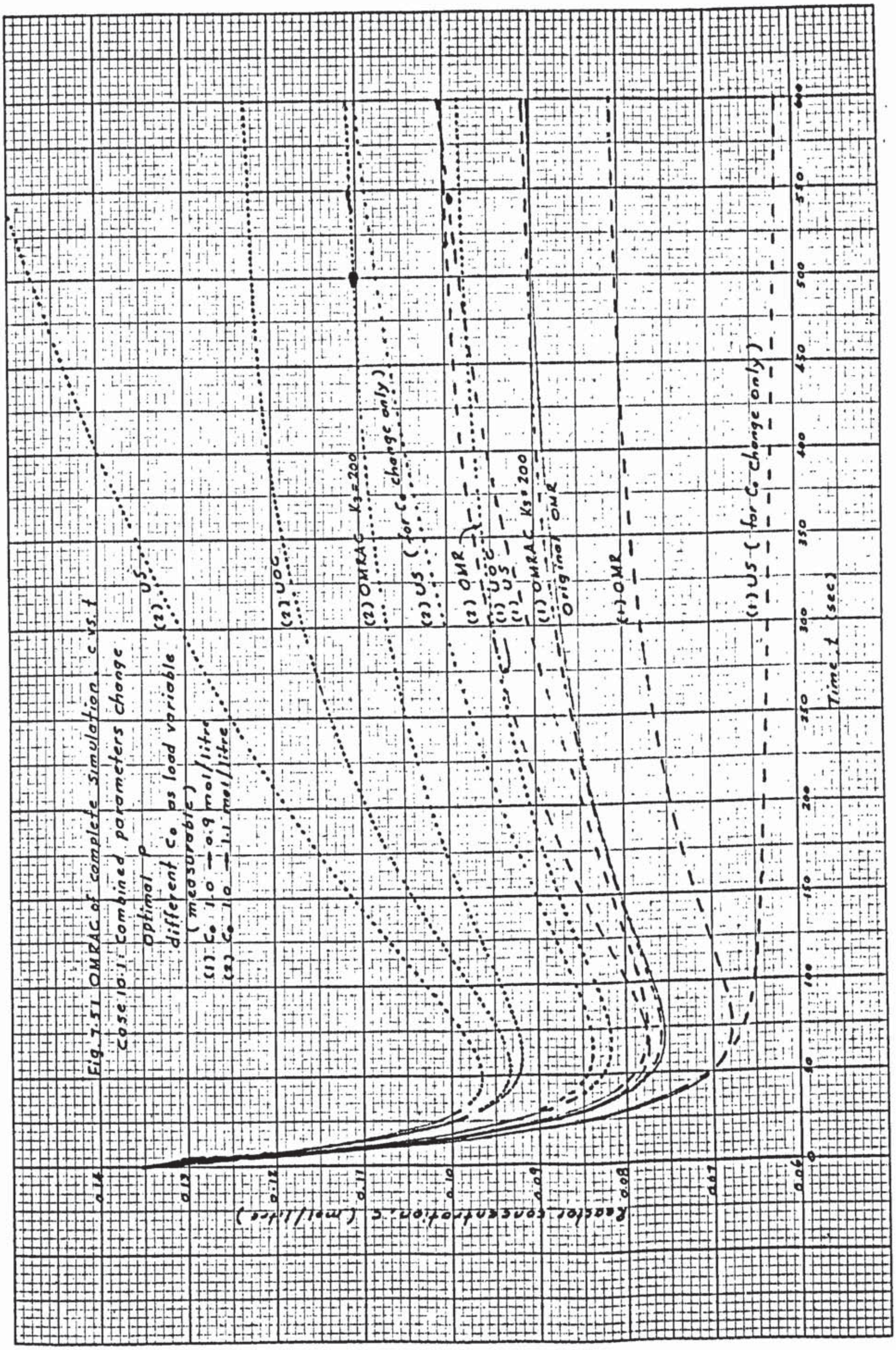

Fig. 7.51 OMRAC of complete simulation c vs. t

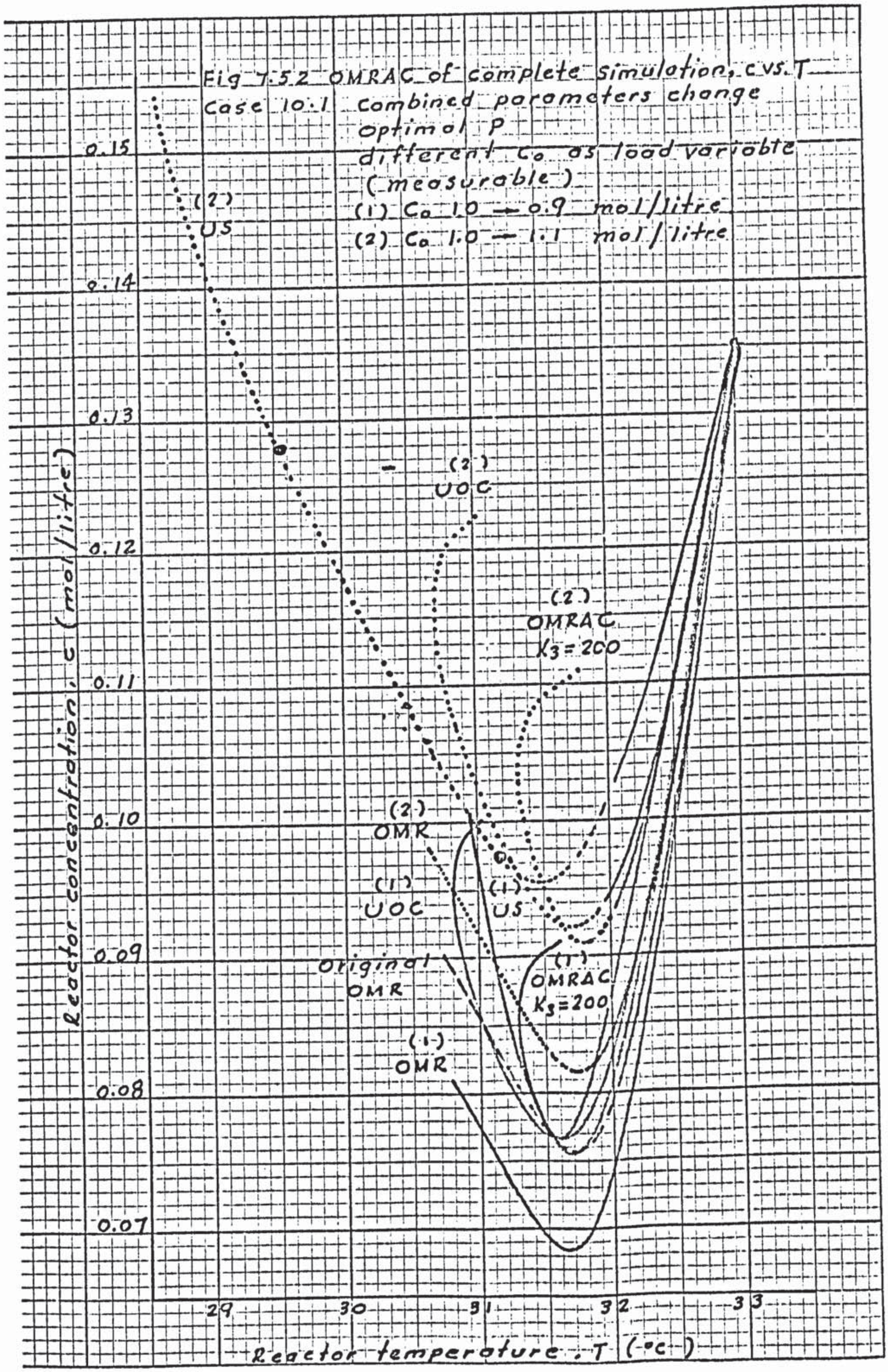

Fig 7.52 OMRAC of complete simulation, c vs. T
Case 10.1 combined parameters change
optimal P
different C_o as load variable
(measurable)
(1) C_o 1.0 → 0.9 mol/litre
(2) C_o 1.0 → 1.1 mol/litre
0.15
0.14
0.13
0.12
0.11
0.10
0.09
0.08
0.07
(2) US
(2) UOC
(2) OMRAC K_3 = 200
(2) OMR
(1) UOC
(1) US
Original OMR
(1) OMRAC K_3 = 200
(1) OMR
29
30
31
32
33
Reactor concentration, c (mol/litre)
Reactor temperature, T (°C)

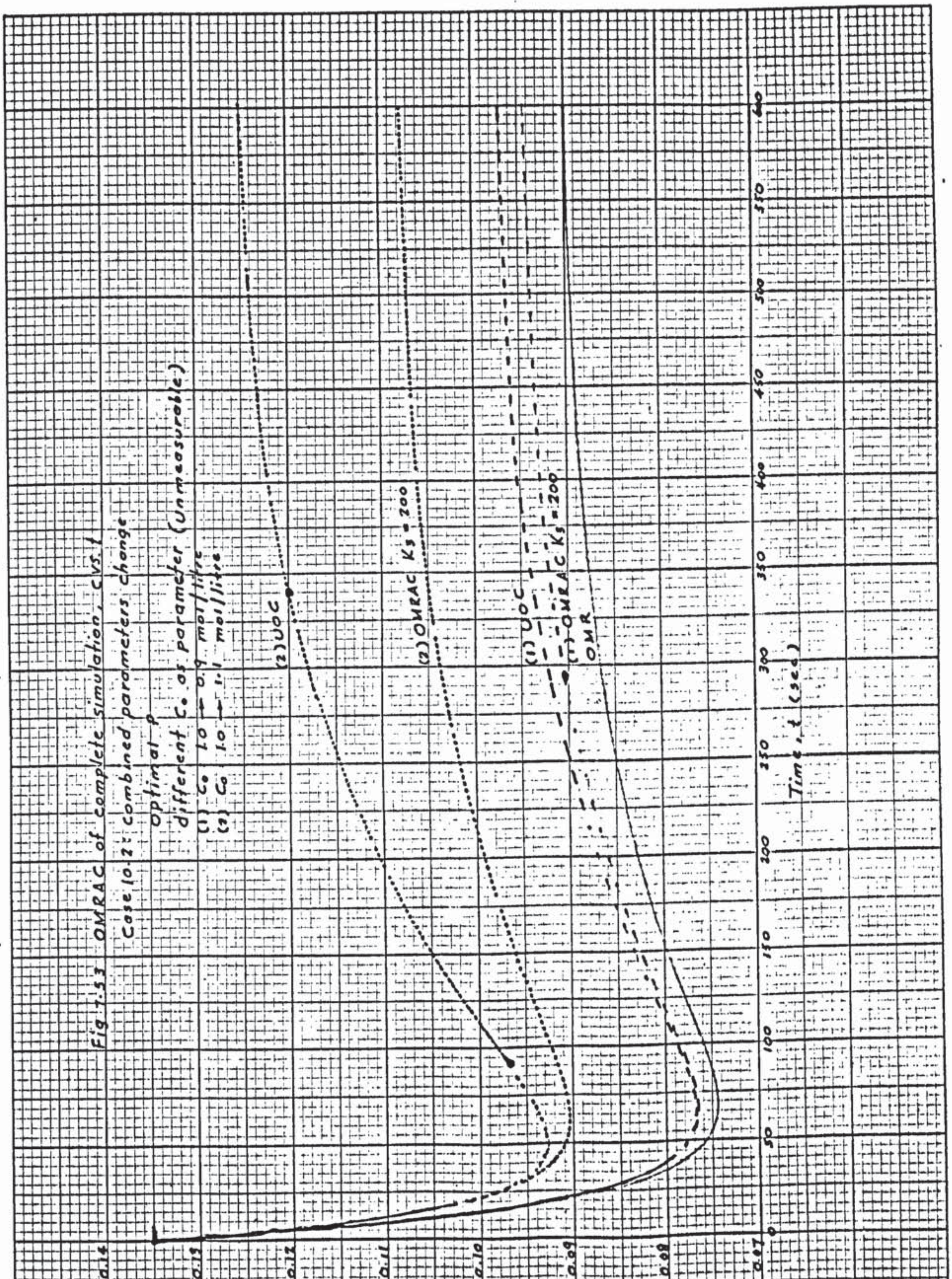
Fig 7.53 OMRAC of complete simulation, C vs. t
Case 10.2: combined parameters change
optimal ρ
different C₀ as parameter (Unmeasurable)
(1) C₀ 1.0 → 0.9 mol/litre
(2) C₀ 1.0 → 1.1 mol/litre
(2) UOC
(2) OMRAC Ks = 200
(1) UOC
(1) OMRAC Ks = 200
OMR
Reactor concentration, c (mol/litre)
0.14
0.13
0.12
0.11
0.10
0.09
0.08
0.07
Time, t (sec)
0
50
100
150
200
250
300
350
400
450
500
550
600

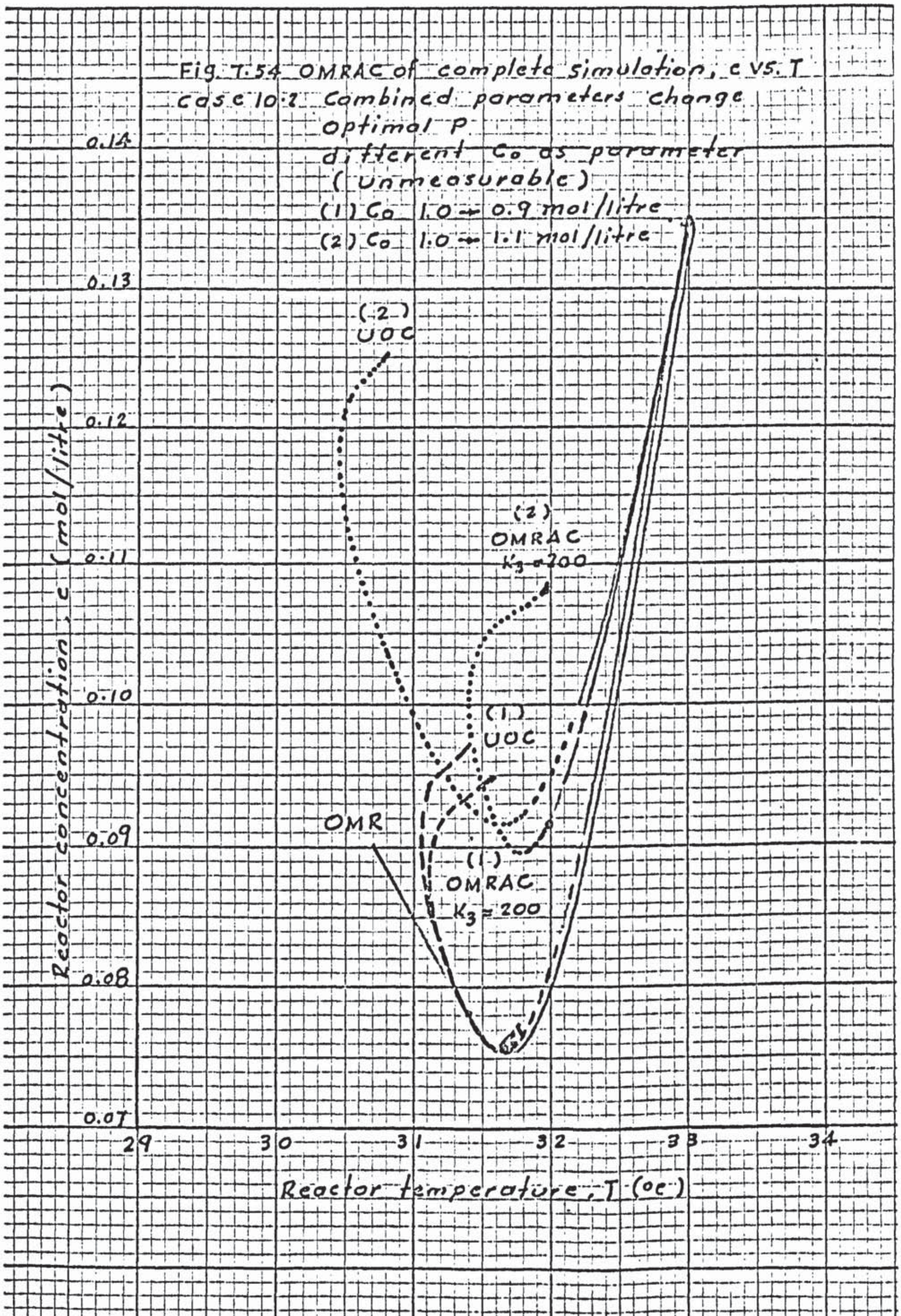
Fig. 7.54 OMRAC of complete simulation, c vs. T
case 10.2 Combined parameters change
optimal P
different Co as parameter
(unmeasurable)
(1) Co 1.0 → 0.9 mol/litre
(2) Co 1.0 → 1.1 mol/litre
0.14
0.13
0.12
0.11
0.10
0.09
0.08
0.07
(2)
UOC
(2)
OMRAC
K3 = 200
(1)
UOC
OMR
(1)
OMRAC
K3 = 200
29
30
31
32
33
34
Reactor concentration, c (mol/litre)
Reactor temperature, T (oC)

P A R T II

ON-LINE COMPUTER CONTROL WORK

(Chapter 8 to Chapter 11)

CHAPTER 8

ON-LINE COMPUTER OMRAC SYSTEM

8.1. Modified experimental apparatus

8.1.1. Functional and modified apparatus diagram

The overall functional diagram for operating the on-line hybrid computer OMRAC system is shown in Fig.8.1.

The material balance equation (7-1) and part of the energy balance equation (7-2) of a CSTR are simulated directly on the hybrid computer. Heat is generated in the reactor by means of immersion heaters at a rate controlled by a position servomechanism technique[81]; this was developed by Buxton[80]. For on-line computer OMRAC operation, additional and modified equipment and instruments were necessary. Using the techniques of complete simulation (Chapter 7), the optimal control law generated by the OMRAC scheme by the computer is transmitted through the interface system to operate the control valve directly, and the cooling water flowrate F_c is adjusted for adaptation to the unmeasurable parameter changes and other disturbances.

The modified experimental apparatus designed for the on-line computer OMRAC system is shown on Fig. 8.2 and three corresponding photographs show the actual operating system.

8.1.2. Modification and calibration of experimental apparatus

1. F_c system

F_c is transferred from $\left[\frac{Q_c}{Q_{cm}}\right]$ or $\left[\frac{F_c}{Q_{cm}}\right]$ (computer side, 0 to 10 volt) to F_c (process side, 0 to 10

16

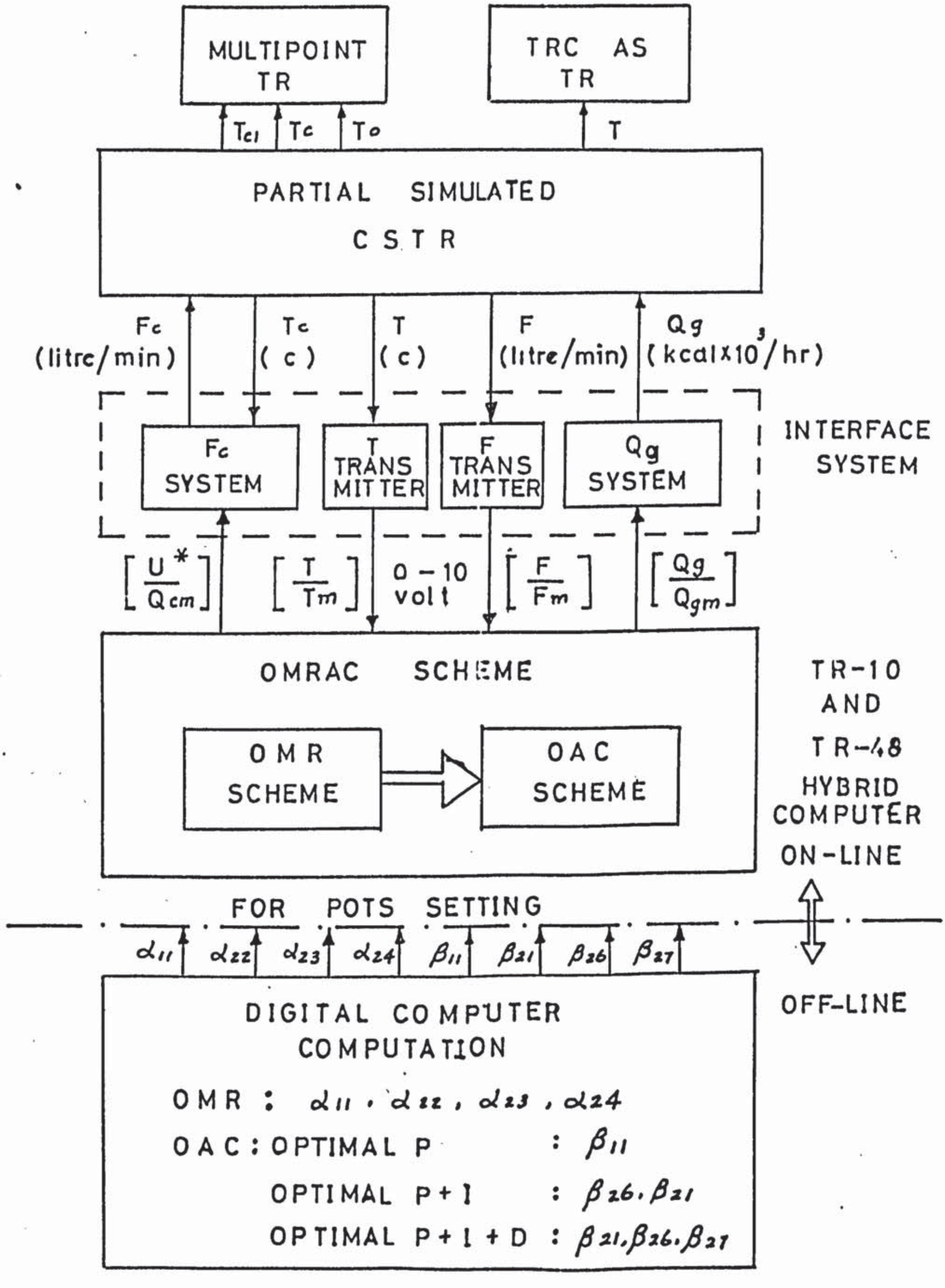

Figure 8.1 Functional diagram of on-line computer OMRAC system

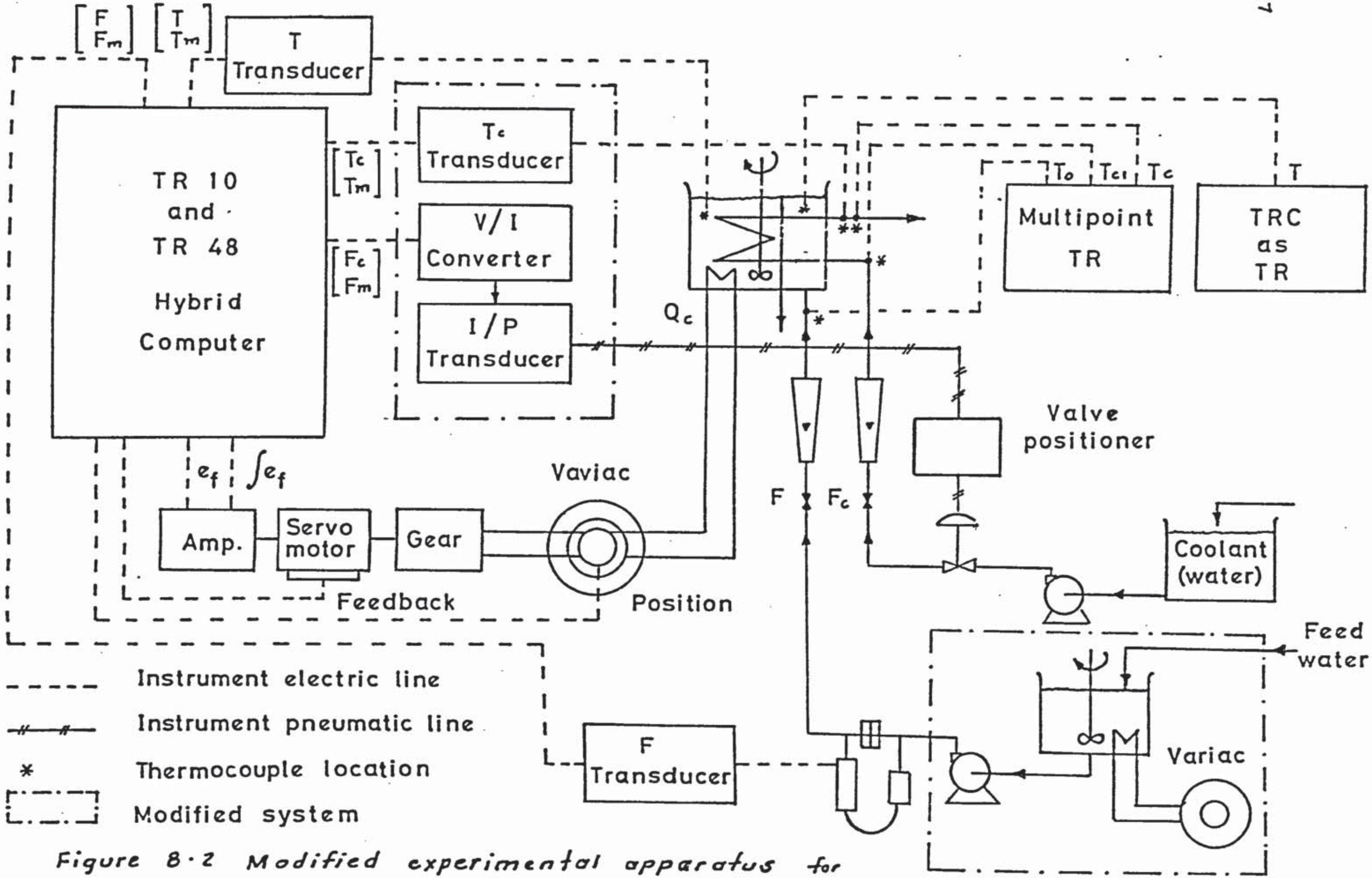

Figure 8·2 Modified experimental apparatus for on-line computer OMRAC system

ON-LINE COMPUTER OPERATING EQUIPMENT

(1) Overall system

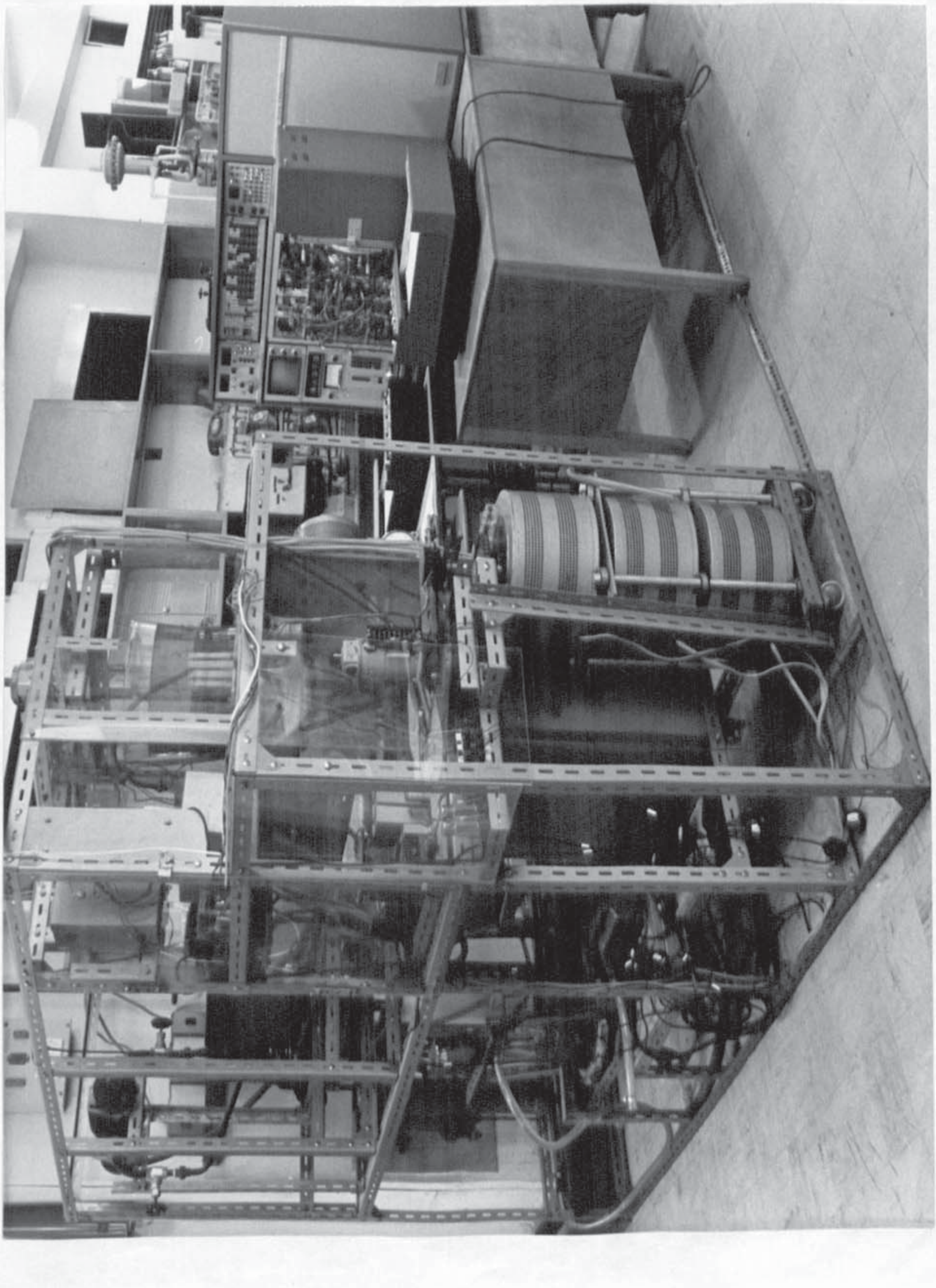

ON-LINE COMPUTER OPERATING EQUIPMENT

(2) Modified partial simulation equipment

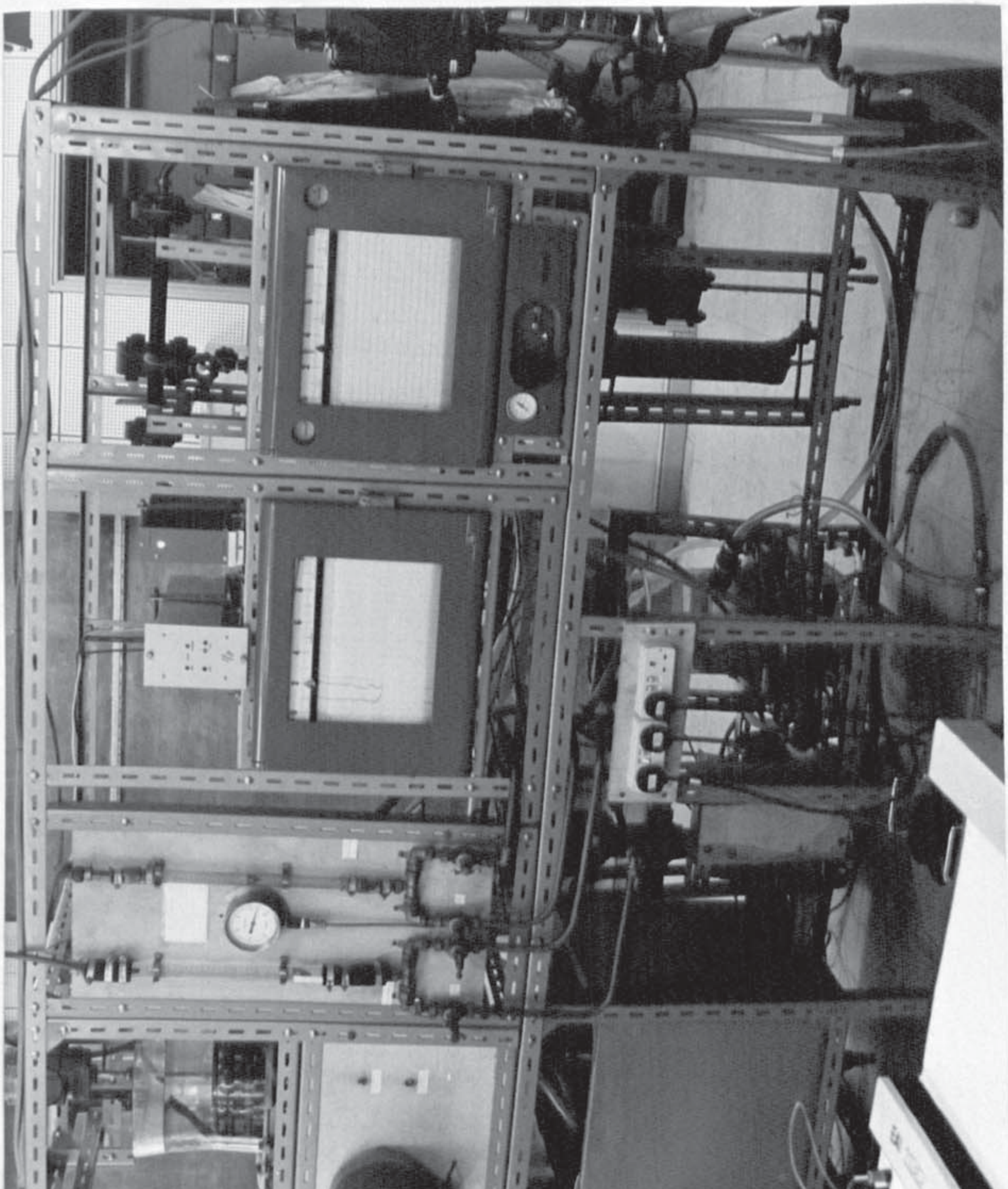

ON-LINE COMPUTER OPERATING EQUIPMENT

(3) TR-10 and TR-48 analogue and hybrid computer

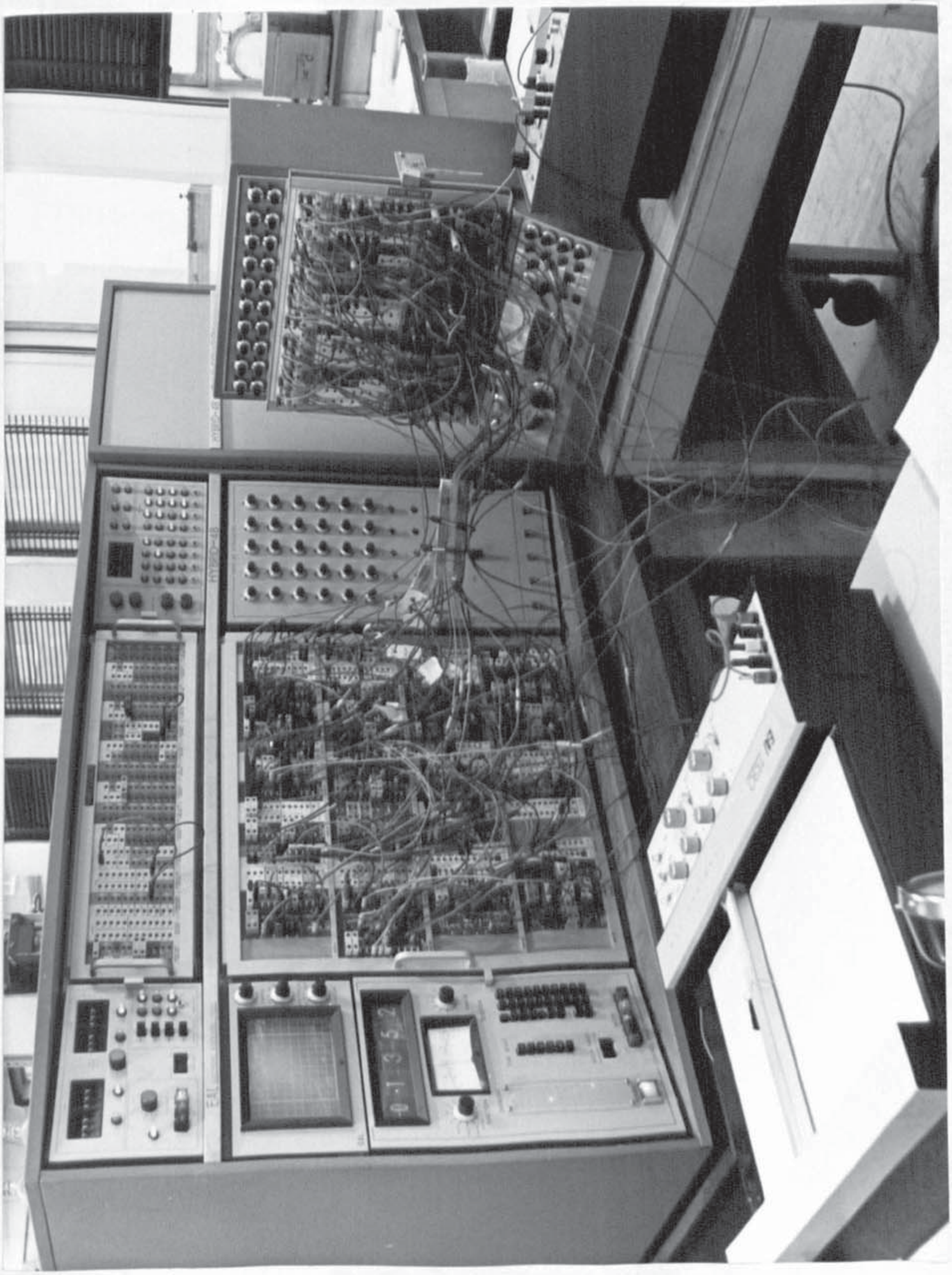

litre/min) and as an important major interface aspect of on-line computer OMRAC will be discussed in detail in the next Section (8.2).

2. Heat generation system (Q_g)

Q_g is transferred from $\left[\frac{Q_g}{Q_{gm}} \right]$ (computer side, 0-10 volt) to actual Q_g (process side, 0-10 Kcal x 10^3/h) through the position servomechanism and immersion heaters. The calibration of the existing Q_g system is given in detail in the next section (8.2).

From the existing heat generation system, the following items were modified:

(1) A new field-controlled dc servomotor with generator was installed, (Servo and Electronic Sales Ltd., Type : 67883), since the existing motor was not in good condition.

(2) Two gears between the servomotor and variac were replaced to double the gear ratio:

original : 23 : 23, i.e. 1 : 1

new : 38 : 18, i.e. 2.1 : 1

and hence to double the available torque to position the variac more smoothly.

(3) The switch and fuse location of the position servomechanism system was changed to prevent overloading and damage to the motor (Fig.8.3).

3. Rendering of inlet feed temperature independent of seasonal variations.

The inlet feed water temperature is significantly influenced during cold weather and causes the control

18

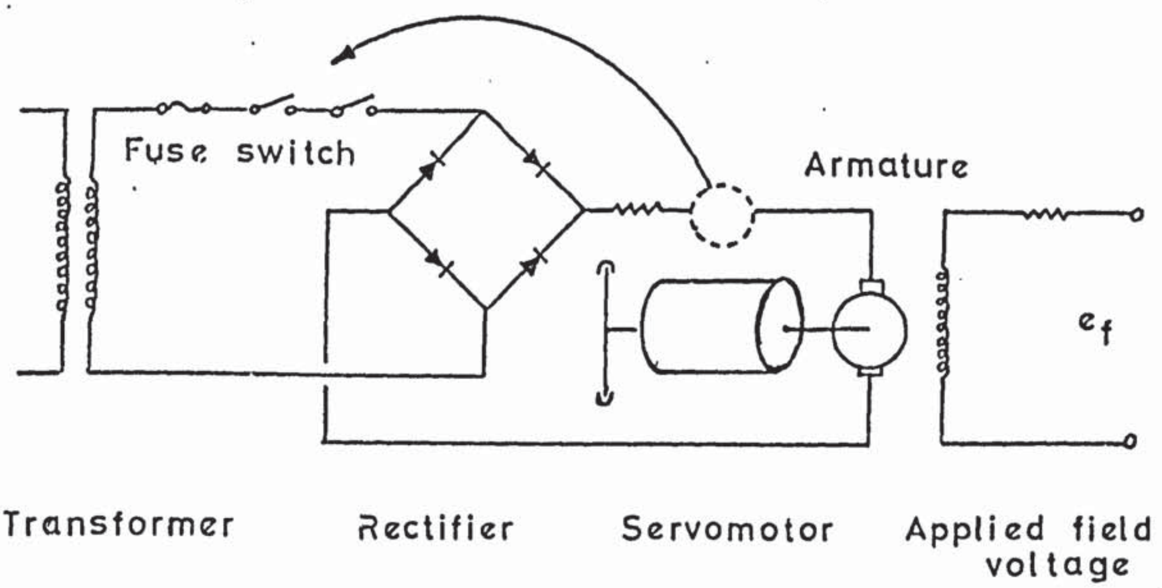

Figure 8·3 change switch and fuse location on field controlled servomotor valve to operate near to the closed position (rotameter reading of F_c off lower end of scale) at steady state. Hence a small water tank with adjustable immersion heater and pump were added (Fig.8.2 and photograph) so that the temperature of the inlet feed water could be increased to produce a suitable operating range of coding water flowrate F_c through the control valve at steady state.

4. Calibration of the original two rotameters the one for inlet feed flowrate F, and the other for cooling water flowrate F_c (see Appendix, Tables A.5.1. and 5.2. and Figs. A.5.1. and A.5.2.).

5. Calibration of the original flow transmitter: (model: Elliott electrical manometer, 438-77).

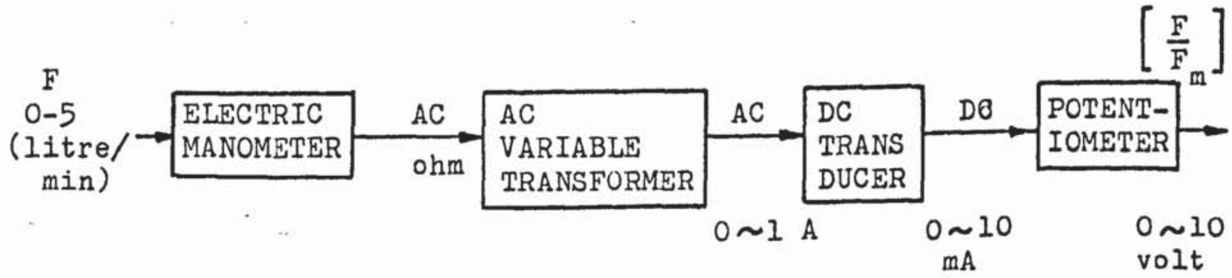

(See Appendix, Table A.5.3. and Fig. A.5.3.)

6. Repair and calibration of all original thermocouples:

Material:

Nickel chromium Alloy T1 (+) 0.0148" diameter

Nickel Aluminium Alloy T2 (-) 0.0148" diameter

Number of thermocouples:

(1) Feed water temperature, T_c to TR

(2) Cooling water inlet temperature, T_{c1} to TR

(3) Cooling water outlet temperature, T_c to TR

(4) Reactor temperature, T to TRC used as TR

(Appendix, Table A.5.4 and Fig. A.5.4).

7. Calibration of temperature transmitters.

(1) Existing Reactor temperature transmitter

(Model: Elliott TDC 21)

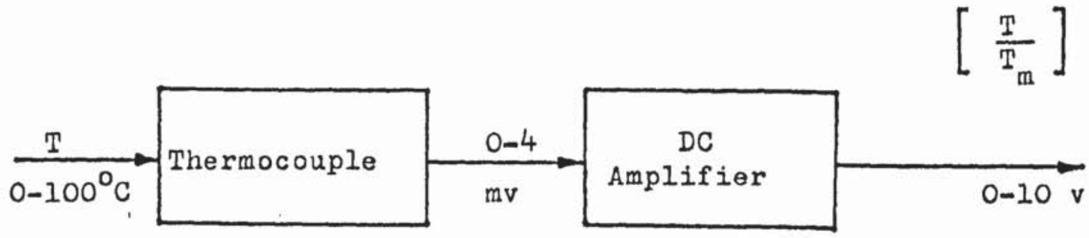

(with ice box for cold junction)

(2) New cooling water outlet temperature transmitter

(Model: Elliott M45/mv)

(with ice box for cold junction)

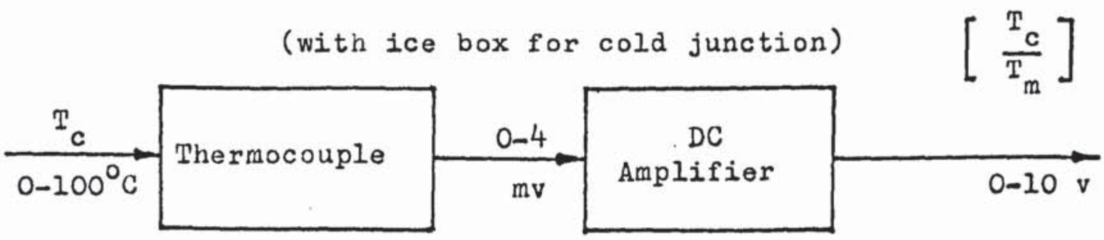

(Appendix, Table A.5.5 and Fig.A.5.5)

8.2. Interface system design

From Figs. 8.1 and 8.2 in Section 1, the major interface transfers for on-line computer OMRAC operation are F_c and Q_g. Q_g is specially used for the partially simulated CSTR, and F_c is used to transfer any complicated optimal control law (adapted or unadapted) to pneumatic pressure to operate the control value and adjust F_c directly. So F_c is the more important major interface system for any on-line computer control. The requirement of interface system design like for any industrial transmitters or transducers, is that the terminal relation between input (computer side) and output(process side) must be extremely linear. To meet this requirement the interface system was designed in detail as follows:

8.2.1. F_c system

The detailed block and functional diagram of the F_c system was designed and is shown in Fig.8.4.

Fig.8.4. clearly shows that the major purpose of the added VDFG is to produce an excellent linear relation between $\left[\frac{F_c}{F_m} \right]$ and F_c by suitably programming of the VDFG (see 8.2.1. (5)).

The components of the F_c system are discussed below:

1. Voltage to current (V/I) converter (Lee Dickens Model C5740)

   input : 0 to 10 volts

   output : 0 to 20 ma

   The calibration curve is shown in Appendix, Table A.5.6. and Fig. A.5.6.

2. Current to pneumatic pressure (I/P) transducer (Honeywell model 3120/01)

   input : 0 to 20 ma

   output : 3 to 15 psig or 1 - 13 psig

   The calibration is shown in Appendix, Table A.5.7. and Fig.A.5.7. and the combined V/I and I/P calibration curve is shown in Appendix, Table A.5.8. and Fig.A.5.8.

3. Control valve and valve positioner.

   The major advantages of the valve positioner are:

   (1) to produce more power which can decrease or eliminate the control valve hysterisis effect.

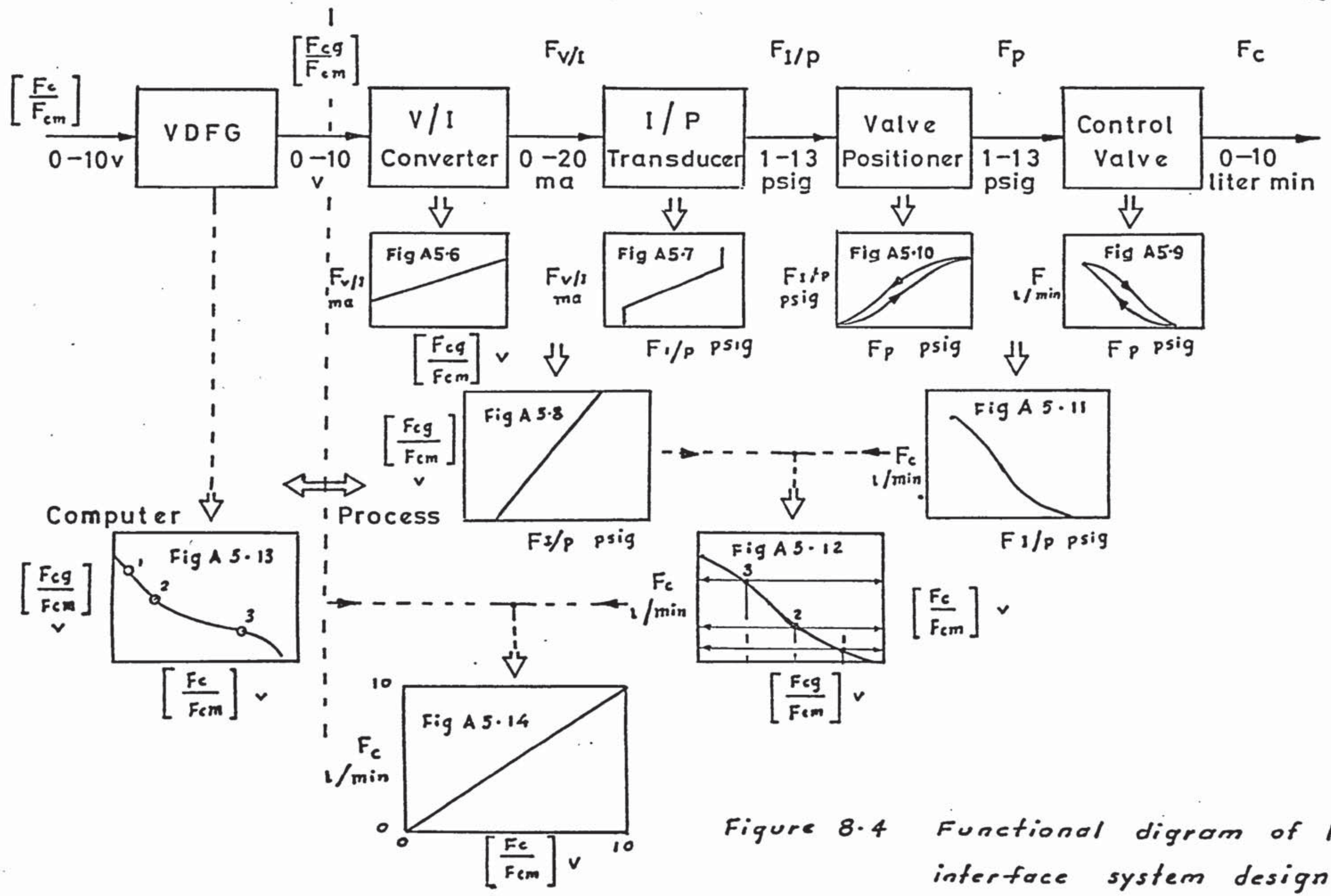

Figure 8·4 Functional digram of Fc interface system design

(2) to produce quick response which can decrease or eliminate the control valve time lag.

Without the valve positioner, the characteristic of the control valve in response to applied pneumatic pressure always possessed a hysterisis effect as shown in Appendix, Table A.5.9. and Fig. A.5.9.

When the valve positioner was added, the calibration curve of the positioner (Appendix, Table A.5.10 and Fig.A.5.10) can just compensate for the hysterisis of the control valve and the combined effect is shown in Appendix, Table A.5.11 and Fig. A.5.11, in which the hysterisis effect is almost eliminated.

4. Resultant function.

On combination of all components: V/I converter, I/P transducer, valve positioner and control valve, the resultant function between $\left[\frac{F_{cg}}{F_{cm}}\right]$ (computer side) and F_c (process side) is a non-linear curve (Appendix, Table A.5.12 and Fig. A.5.12).

5. VDFG programming.

Using the resultant function, a compensation curve of F_c interface system on VDFG can be plotted as shown in Appendix Fig.A.5.13., and this curve is programmed in detail on the TR-48 VDFG-3 (Appendix Fig. A.3.2.).

Thus for the final F_c system, the signal from the computer transmitted through the generated VDFG and then a series function of monitoring instruments, gave an excellent linear relation between $\left[\frac{F_c}{F_{cm}} \right]$ and the F_c obtained is shown in Appendix Table A.5.13 and Fig.A.5.14.

8.2.2. Q_g system

The detailed block and functional diagram for Q_g is shown on Fig.8.5, and the components are discussed below:

(1) The calibration of variac position including servo-mechanism components, amplifier, servomotor and gears, or $\left[\frac{Q_{gg}}{Q_{gm}} \right]$ from computer versus variac reading (VR), is shown in Appendix Table A.5.14 and Fig.A.5.15.

(2) The calibration of immersion heater, or VR versus Q_g is shown in Appendix Table A.5.15 and Fig.A.5.16. Q_g is calculated from experimental data while F and ΔT from the following:

$$Q_g = V\,(-\Delta H)\,KC$$

$$= \rho_c\, C_{pc}\, F_c\, (\Delta T_c) + \rho\, C_p\, F\,(\Delta T) \qquad (8\text{-}1)$$

$$F_c = 0 \quad \text{for the rest:}$$

$$Q_g = F\,\Delta T \quad \left(\frac{\text{Kcal}}{\text{min}}\right)$$

$$= 0.06\, F\, \Delta T \quad (\text{Kcal} \times 10^3/\text{h}) \qquad (8\text{-}2)$$

It is seen in Fig.A.5.17 that only a small hysterisis effect remained.

(3) The calibration of the combined variac position and immersion heater or $\left[\frac{Q_{gg}}{Q_{gm}} \right]$ versus Q_g is shown in Appendix Fig. A.5.17.

20.

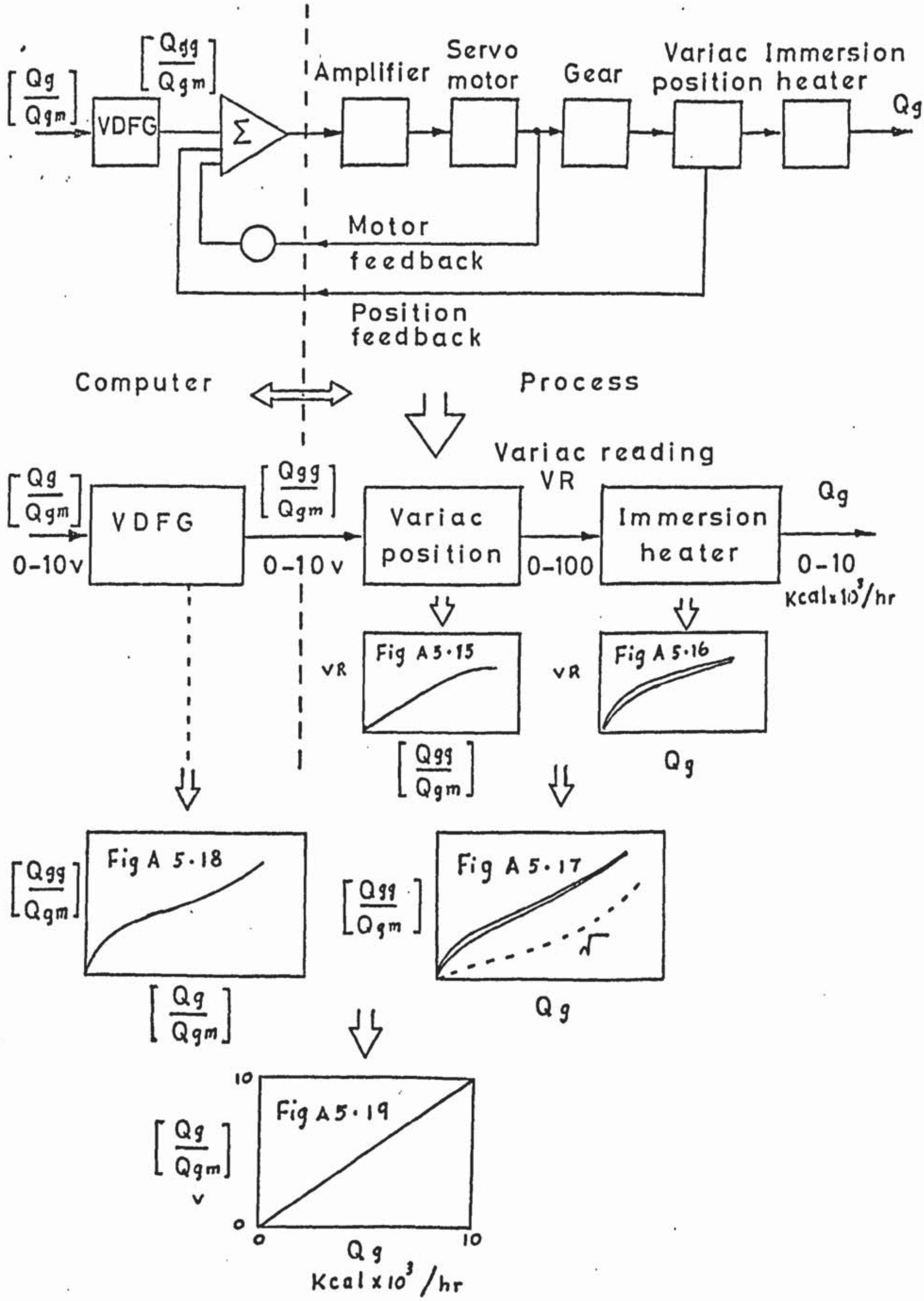

Figure 8·5 Functional digram of Qg interface system design

From Fig.A.5.17 the resultant response curve is apparently non-linear. Buxton suggested that using a square root, or the output from $\sqrt{[Q_{gg}/Q_{gm}]}$ would give an approximately linear relationship with Q_g (see Buxton's Ph.D.Thesis, Fig.A.11, p.316, and this curve is reproduced and shown in Fig.A.4.18). However, from the experimental data, $\sqrt{[Q_{gg}/Q_{gm}]}$ is also non-linear (Fig.A.5.17). Hence using the technique shown in the above section, an additional VDFG was used instead of the square root function

(4) VDFG programming

From the average value of two small hysterises calibration curves from Fig.A.5.16, a new compensated function was generated on a VDFG as shown in Appendix Fig.A.5.18 and was programmed on the TR-10 DFG (Appendix Fig.A.3.3.)

For the final Q_g, the signal from the computer was transmitted through the DFG and a series of monitoring equipment and an excellent linear relation between $[Q_g/Q_{gm}]$ and Q_g was obtained (Appendix Table A.5.16 and Fig.A.5.19)

8.3. Programming the computer.

8.3.1. OMR scheme computer programming

The computer diagram of the OMR scheme is as shown in Chapter 7, Complete Simulation (7.4.1. and Fig.7.1.) The only difference is that the time scale factor β is equal to

1.0 or

$$\tau = \beta \; t \quad = \quad t \tag{8-3}$$

Thus the computer time is equal to the process real time and the same as in the OAC scheme.

8.3.2. OAC scheme computer programming

The computer diagram of the OAC scheme is shown in Fig.8.6. Several important components and parts shown in Fig.8.6 are noted below:

1. The computer diagram of optimal PID generation is as in Chapter 7: Complete Simulation (7.4.2. and Fig.7.3), and the only differences are:
   (i) no constraint circuit since the control valve can be treated as a limiter between minimum and maximum flowrate of F_c (see 4.4).
   (ii) $\left[\frac{U^*}{Q_{cm}} \right]$ from Amp.30 is directly connected to F_c program (Fig.8.8).
2. The computer diagram of the optimal control law generated for the unadapted system is the same as in Chapter 7: Complete Simulation (7.4.2 and Fig. 7.4) and the only differences are:
   (i) $\left[\frac{T}{T_m} \right]$ signal is connected to the reactor temperature transmitter
   (ii) $\left[\frac{m^*}{Q_{cm}} \right]$ from Amp.15 is directly connected to F_c program (Fig.8.8).
3. $\left[\frac{T}{T_m} \right]$ signal is connected to the reactor temperature transmitter (8.1.2 (7)).
4. $\left[\frac{F}{F_m} \right]$ signal is connected to the feed flow transmitter (8.1.2. (5))

5. The computer programming of the Q_g interface system is discussed in section 8.3.3.

6. The computer programming of the F_c interface system is discussed in section 8.3.4.

8.3.3. Q_g system computer programming

From the functional diagram (Fig. 8.5), the computer programming of the Q_g system is shown in Fig.8.7.

The relation between $\left[\frac{a}{a_m}\right]\left[\frac{K}{K_m}\right]\left[\frac{C}{C_m}\right]$ and $\left[\frac{Q_g}{Q_{gm}}\right]$ is calculated below

$$Q_g = (-\Delta H)\ V\ a\ K\ C$$

$$= \left(\frac{cal}{mol}\right)(litre)\left(\frac{1}{sec}\right)\left(\frac{mol}{litre}\right) = \left(\frac{cal}{sec}\right)$$

$$= \frac{3600}{1000 \times 1000}\ \left(\frac{Kcal \times 10^3}{h}\right)$$

$$\text{or}\ \left[\frac{Q_g}{Q_{gm}}\right] = \left(\frac{3600}{1000 \times 1000}\right)\frac{(-\Delta H)(V)(a_m)(K_m)(C_m)}{Q_{gm}}\left[\frac{a}{a_m}\right]\left[\frac{K}{K_m}\right]\left[\frac{C}{C_m}\right]$$

$$= \left(\frac{3600}{1000 \times 1000}\right)\frac{(18511)(16)(1)(0.1)(1.0)}{10}\left[\frac{a}{a_m}\right]\left[\frac{K}{K_m}\right]\left[\frac{C}{C_m}\right]$$

$$\therefore \left[\frac{Q_g}{Q_{gm}}\right] = 10.66\left[\frac{a}{a_m}\right]\left[\frac{K}{K_m}\right]\left[\frac{C}{C_m}\right] \qquad (8-4)$$

The values of (0.1066) x (10) x (10) are the settings on Pot 00 and Amp. 18 and 19 shown in Fig.8.7.

In Fig.8.7, sw-1 is used as the switch to solve for the initial value for on-line operation discussed in detail in Chapter 9 (9.4)

In Fig. 8.7, for Buxton's original design of position servomechanism, both e_f and $\int e_f dt$ are used as input to amplifier and servomotor as applied field voltage. Since the change to a new servomotor and gear ratio (see 8.1.2.) both inputs (e_f) and ($e_f + \int e_f dt$) can produce the same smooth and sensitive operation, and so only e_f was used as the input to simplify the on-line operation.

8.3.4. F_c system computer programming

From the functional diagram (Fig.8.6), the computer programming of the F_c system is shown in Fig.8.8.

In Fig.8.8, three switches are operated according to the following rules:

	sw-2	sw-3	sw-4
1. Operation for adjusted initial condition (before start)	R	L	R or L
2. Unadapted system operation (US)	L	L	R or L
3. Unadapted Optimal control operation (UOC)	L	R	L
4. Optimal adaptive control operation (OMRAC)	L	R	R

where R = right : L = left

The relation between $\left[\frac{Q_c}{Q_{cm}}\right]$ $\left(\text{or } \left[\frac{U^*}{Q_{cm}}\right] \text{ and} \left[\frac{m^*}{Q_{cm}}\right]\right)$ and $\left[\frac{F_c}{Q_{cm}}\right]$ is calculated below:

$$Q_c = \rho_c C_{pc} F_c \Delta T_c$$

$$= \left(\frac{gm}{cm^3}\right)\left(\frac{cal}{gm \times {}^oC}\right)\left(\frac{litre}{min}\right)\left(\frac{1000\ cm^3}{litre}\right)({}^oC)$$

$$= 1000\left(\frac{cal}{min}\right) = 1\left(\frac{Kcal}{min}\right) \qquad (8\text{-}5)$$

$$\text{or} \quad \left[\frac{Q_c}{Q_{cm}}\right] = \frac{(F_{cm})(T_m)}{(Q_{cm})}\left[\frac{F_e}{F_{cm}}\right]\left[\frac{\Delta T_c}{T_m}\right]$$

$$= \frac{(10)(100)}{100}\left[\frac{F_c}{F_{cm}}\right]\left[\frac{\Delta T_c}{T_m}\right] \qquad (8\text{-}6)$$

$$\therefore \left[\frac{Q_c}{Q_{cm}}\right] = 10\left[\frac{F_c}{F_{cm}}\right]\left[\frac{\Delta T_c}{T_m}\right] \qquad (8\text{-}6)$$

$$\text{or} \quad \left[\frac{F_c}{F_{cm}}\right] = \frac{0.1\left[\frac{Q_c}{Q_{cm}}\right]}{\left[\frac{\Delta T_c}{T_m}\right]} \qquad (8\text{-}7)$$

$$\therefore \left[\frac{Q_c}{Q_{cm}}\right] = \left[\frac{Q_{cs}}{Q_{cm}}\right] + \left[\frac{U^*}{Q_{cm}}\right]$$

$$\therefore \left[\frac{F_c}{F_{cm}}\right] = \frac{0.1\left[\frac{Q_{cs}}{Q_{cm}}\right]}{\left[\frac{\Delta T_c}{T_m}\right]} + \frac{0.1\left[\frac{U^*}{Q_{cm}}\right]}{\left[\frac{\Delta T_c}{T_m}\right]} \qquad (8\text{-}8)$$

$$\text{or} \quad \left[\frac{F_c}{F_{cm}}\right] = \left[\frac{F_{cs}}{F_{cm}}\right]_{final} + \frac{0.1\left[\frac{U^*}{Q_{cm}}\right]}{\left[\frac{\Delta T_c}{T_m}\right]} \qquad (8\text{-}9)$$

when unadapted optimal control is applied, then

$$\left[\frac{F_c}{F_{cm}}\right] = \left[\frac{F_{cs}}{F_{cm}}\right]_{final} + \frac{0.1\left[\frac{m^*}{Q_{cm}}\right]}{\left[\frac{\Delta T_c}{T_m}\right]} \qquad (8\text{-}10)$$

where

$\left[\frac{F_{cs}}{F_{cm}}\right]_{final}$ = actual cooling water flowrate at the final steady state of on-line computer operation and converted into volts.

In the original design, equation (8-7) was used for programming the computer, but the actual accurate value of $\left[\frac{Q_{cs}}{Q_{cm}}\right]_{final}$ of the on-line computer operation was very difficult to obtain, so finally equations (8-9) and (8-10) were developed and chosen for programming the computer (Fig.8.8) by introduction of an iterative operation technique; the accurate value of $\left[\frac{F_{cs}}{F_{cm}}\right]_{final}$ is obtained and discussed in detail in Chapter 9 (9.5 and 9.6).

21

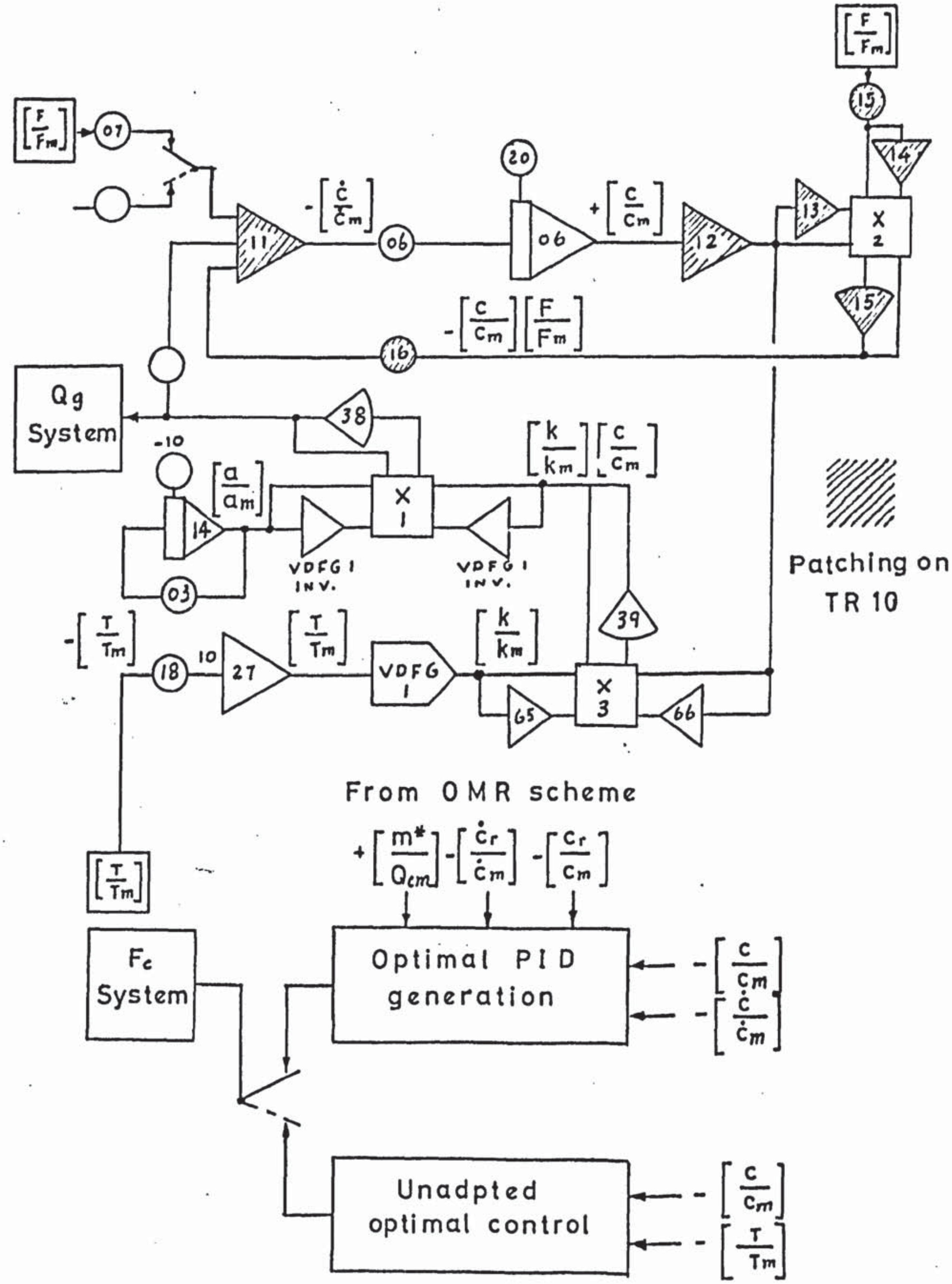

Figure 8·6 Computer diagram of on-line OAC scheme (on TR-48).

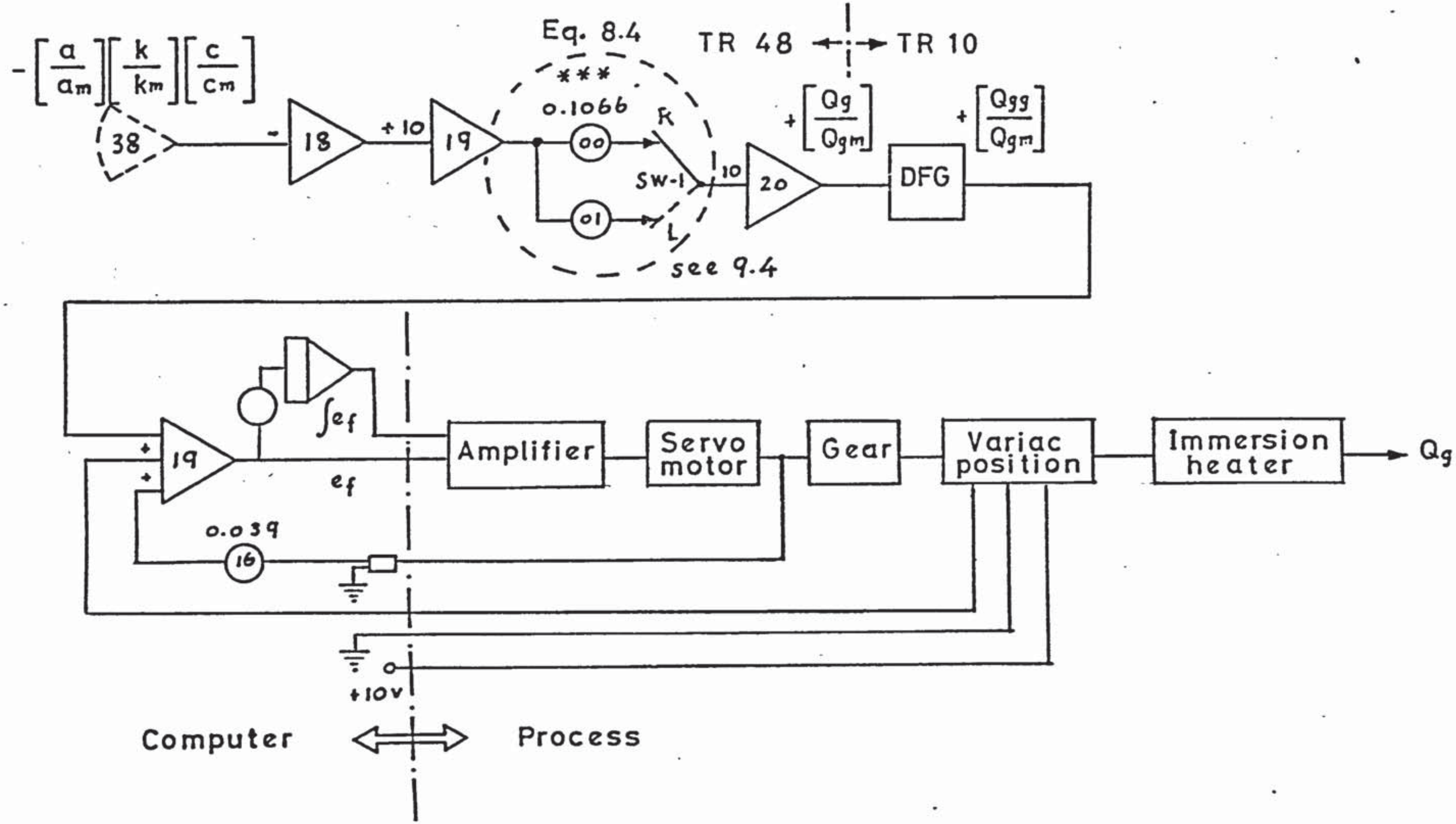

Figure 8·7 Computer diagram of Q g interface system

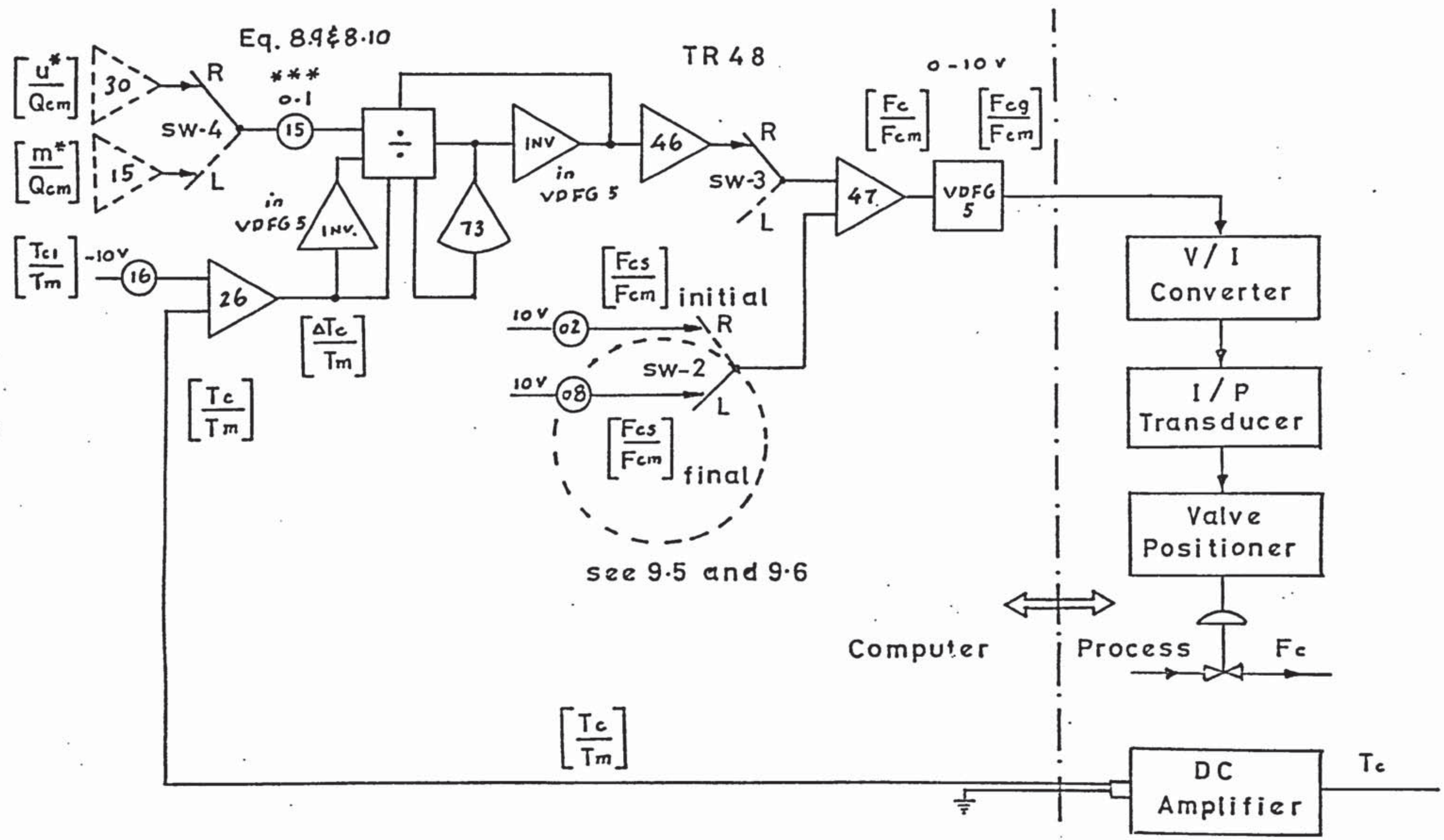

Figure 8·8 Computer diagram of F_c interface system

CHAPTER 9

COMMISSIONING OF ON-LINE COMPUTER OPERATION

9.1. Test Run

Before successful operation of the on-line computer OMRAC, a continuous test run of on-line operation was considered vital. The purpose was to test the overall performance of the on-line system and to find successful operating procedures and techniques to produce reliable and reproducible on-line computer operation for OMRAC.

From previous work including complete simulation shown in Chapter 7 and interface design and on-line computer programming shown in Chapter 8, a rigid foundation for on-line operation has been established. But from a long duration test run, several operating difficulties were found and are listed below:

1. The joining of two computers for real time on-line operation (discussed in 9.2)
2. Smooth plot of fluctuating reactor temperature (discussed in 9.3).
3. Effect on initial temperature setting on partially simulated CSTR (discussed in 9.4).
4. Determination of $\left[\frac{F_{cs}}{F_{cm}}\right]_{final}$ on partially simulated CSTR (discussed in 9.5).
5. Effect if F step change on partially simulatedCSTR (discussed in 9.6).

It should be pointed out that the difficulties (2), (3), (4) and (5) shown above exist and are amplified because of the very narrow operating ranges on the X-Y plotter used in this whole research work compared with a wide operating range used in Buxton's

Ph.D. Thesis[80] which were:

Temperature 0 - 40 $^{\circ}$C or 10.0 deg C/inch

Concentration 0 - 4 $\frac{\text{mol}}{\text{litre}}$ or 0.05 $\frac{\text{mol}}{\text{litre}}$/inch

In the present research the operating ranges on the X-Y plotter were:

Temperature 30 - 34°C or 1.0 deg C/inch

Concentration 0.06 - 0.14 $\frac{\text{mol}}{\text{litre}}$ or 0.01 $\frac{\text{mol}}{\text{litre}}$/inch

Since the operating range in this research decreased by a factor of 10 in temperature and 5 in concentration, then the sensitivity was also increased tenfold in temperature and fivefold in concentration. That means that the overall sensitivity in this research work is 50 times that of Buston's.

In general, a more narrow range of operation can produce more sensitive and accurate response results but also produces many more operating difficulties than wide range operation.

All difficulties shown above are discussed and details of their solution given in the following sections of this chapter.

9.2. Two computers joined for on-line operation.

The difficulties of analogue computer operation increase in the following order:

(TR-10) → normal operation → (TR-10) → on-line operation → (TR-10 + TR-48) → normal operation → (TR-10 + TR-48) on-line operation

In the previous complete simulation work (Chapter 7) the programming of OMR and OAC was patched on the TR-10 and TR-48 respectively (Figs. 7.1 and 7.2). Usually the dynamic response of OMR and OAC with constant parameters was approximately the same (operating time approximately 60 sec). This gives a useful dynamic check before each operation. But for on-line slow operation (operating time approximately 600 sec.) the dynamic response of the OMR patched on the TR-10 was still kept approximately the same, but the dynamic response of the OAC patched on the TR-48 was apparently changed. This may be due to the performance of each computer.

After the main part of OAC programming was re-patched on the TR-10 (Fig.8.6) then this difficulty was overcome.

For on-line operation with joined TR-10 and TR-48 computers, the following simple rules for patching and checking were followed:

(1) The performance of each component of both computers was checked.

(2) All integrators were patched on TR-48.

(3) All reference voltages (± 10v) used on TR-10 were taken from the TR-48.

(4) All voltages of OMRAC programming were checked with the same digital voltmeter on the TR-48.

(5) The major parts of the OMR and OAC programming were patched on the same computer as each other.

(6) Static checks of each group of all OMRAC patching circuits was made (Tables 7.2 to 7.7.)

(7) Static check of each input from process equipment and output to process equipment (Figs. 8.6, 8.7 and 8.8). was made.

(8) Dynamic check of OMR and OAC with constant parameter was made (usually these two responses will be approximately the same.

All static and dynamic checks shown in (6), (7) and (8) are important preparatory procedures before every on-line operation.

9.3. Smooth plot of fluctuating reactor temperature

$\left[\frac{T}{T_m}\right]$ from the existing temperature transmitter is varying within $\pm 0.1^\circ C$. Apparently it is impossible to plot a smooth phase-plane curve with the X-Y plotter for such a narrow operating range (See 9.1). Thus a filter technique was used (Fig.9.1.) and the smoother out reactor temperature is also shown in Fig.9.1.

By using this simple technique, all phase-plane trajectories of on-line computer OMRAC were plotted and are shown in Chapter 10.

9.4. Effect of initial temperature setting for partially simulated CSTR

From Chapter 7, Table 2, the initial conditions of on-line operation are:

$$C(t_o) = 0.135 \text{ mol/litre} \quad \text{or} \quad \left[\frac{C(t_o)}{C_m}\right] = 0.135 \text{ mu.}$$

$$T(t_o) = 33^\circ C \quad \text{or} \quad \left[\frac{T(t_o)}{T_m}\right] = 0.33 \text{ mu}$$

$C(t_o)$ was set on the computer and $T(t_o)$ on the process. While this appears straightforward from the test run, the $T(t_o)$ setting gave considerable trouble and is discussed in detail.

To illustrate the operational situation a simple calculation was made from experimental data of the test run:

(1) At initial conditions: $\left[\frac{K}{K_m}\right] = 0.45$ mu, $\left[\frac{C(t_o)}{C_m}\right] = .135$ mu from equation (8-4):

$$\left[\frac{Q_g}{Q_{gm}}\right] = 10.66 \left[\ 1\ \right]\left[.45\right]\left[.135\right] = 0.648 \text{ mu} = 6.48 \text{ v.}$$

$$= 6.48 \text{ Kcal} \times 10^3/\text{h}$$

from Fig.A.4.17, then

$$\left[\frac{Q_g}{Q_{gm}}\right] \cong 80 \text{ variac reading (VR)}$$

(2) Corresponding to VR = 80

$$F_c = \frac{Q_g - F\Delta T}{T_c} = \frac{6480 - 3 \times 60 \times (33 - 17.5)}{15}$$

$$= 4.9 \text{ litre/min.}$$

(3) From experimental data at final steady state

F_c = 1.54 litre/min

VR = 54.

The following possible methods for setting up initial temperature ($T(t_o) = 33^{\circ}C$) are suggested:

Method 1: Set variac reading directly from computer (see Fig.8.7); set $F_c \doteq$ 1.54 litre/min when reactor temperature is at $T(t_o) = 33^{\circ}C$ (or VR $\doteq$ 80); then start to operate the computer. Theoretically after operating, the reactor temperature should decrease immediately (Fig.9.2). But in fact, the temperature will still increase first and then decrease as shown in Fig.9.2. and the corresponding concentration response curves without and with optimal control (parameters constant) are also shown in Figs. 9.3 and 9.4 respectively.

Method 2: Manually set the variac reading at 60, until the initial steady state is obtained $T(t_o) = 33^oC$ and then start to operate the computer.

In fact the variac reading will be increased at the beginning from 60 to 80 and then decreased. Thus, more heat must be generated by the immersion heater, so that the reactor temperature also increases first and then decreases as shown in Figs.92, 9.3 and 9.4.

Method 3: Set variac reading at 80 and F_c = 4.9 litre/min (the calculated initial steady state condition), until $T(t_o) = 33^oC$, and then start to operate the computer.

In fact, the variac reading now decreases but F_c immediately drops from 4.9 litre/min to $\simeq$ 1.54 litre/min followed by a large heat release. Thus the reactor temperature also increases then decreases; this fact is the same in Method 2.

None of the above methods can make the reactor temperature decrease immediately after starting, and there is an apparent large offset from the theoretical response curves (Figs. 9.2, 9.3 and 9.4)

<u>Switching method</u>:

Eventually a switching shift technique was used and solved this difficulty. The operating procedure is shown below:

(1) Manually set the variac reading at an appropriate value (usually 60)

(2) Computer operates F_c from $\left[\frac{F_{cs}}{F_{cm}}\right]_{initial}$ directly (see Fig.8.8) .

(3) Adjust $\left[\frac{F_{cs}}{F_{cm}}\right]_{initial}$ to give the initial steady state, $T(t_o) = 33^oC$.

(4) Set SW-1 in Fig.8.7 to L position to make $e_f = 0$.

(5) Start to operate the computer. The variac reading will immediately decrease.

(6) Shift the switch SW-1 from L to R (normal condition) at a certain time determined by experiments.

The result is shown in Figs. 9.2 to 9.4 and it is much better and very close to the theoretical response curves.

9.5. Determination of $\left[\frac{F_{cs}}{F_{cm}}\right]_{final}$

$\left[\frac{F_{cs}}{F_{cm}}\right]_{final}$ has been defined in 8.3.4. as actual cooling water flowrate at final steady state of on-line computer operation, converted to volts and set on Pot 08 in Fig.8.8. To set an accurate $\left[\frac{F_{cs}}{F_{cm}}\right]_{final}$ value before operation an iteration method was used as follows:

1st iteration: Set $\left[\frac{F_{cs}}{F_{cm}}\right]_{final} = \left[\frac{F_{cs}}{F_{cm}}\right]_{initial}$

operate and find F_c at final steady state

as $\left[\frac{F_{cs}}{F_{cm}}\right]_{f1}$

2nd iteration: Set $\left[\frac{F_{cs}}{F_{cm}}\right]_{f1} = \left[\frac{F_{cs}}{F_{cm}}\right]_{f}$

operate and find F_c at final steady state

as $\left[\frac{F_{cs}}{F_{cs}}\right]_{f2}$

3rd iteration: Set $\left[\frac{F_{cs}}{F_{cm}}\right]_{f2} = \left[\frac{F_{cs}}{F_{cm}}\right]_{f1}$

operate and find F_c at final steady state until:

$$\left[\frac{F_{cs}}{F_{cm}}\right]_{fi} \longrightarrow \left[\frac{F_{cs}}{F_{cm}}\right]_{f(i-1)} .$$

then set $\left[\frac{F_{cs}}{F_{cm}}\right]_{fi}$ as $\left[\frac{F_{cs}}{F_{cm}}\right]_{final}$ on Pot 08.

By using this iteration method to determine an accurate value of $\left[\frac{F_{cs}}{F_{cm}}\right]_{final}$ and the switching method for initial value setting, then more reliable (close to theoretical) and reproducible on-line computer operation was obtained and is shown in Figs.9.5 and 9.6 and the corresponding curves in Figs. 9.3 and 9.4.

9.6. Effect of Feed flowrate step change on partially simulated CSTR

For on-line computer OMRAC operation when feed flowrate (F) decreases (or increases) by a step change, using switching and iteration methods discussed in 9.4 and 9.5, the process dynamic response (not optimal control, nor OMRAC) for on-line computer operation should be close to the theoretical process dynamic response with the same step change shown in Chapter 7. However, the results apparently gave certain differences (see Chapter 10, Figs.10.1 and 10.2) which need to be explained.

A <u>compensation technique</u> was introduced for comparison of the following two different operations:

1. Completely simulated operation:

   When F decreases and is set on the computer before operation the computer is started, there is no effect on the whole system.

2. Partially simulated operation:

When F decreases and is set on the process, it produces an implicit effect. This effect does not influence the dynamic response but it can influence the initial steady state. i.e. If F decreases, the reactor temperature at the initial steady state increases and vice versa.

The best way to compensate for such an effect is to decrease or increase the value of $\left[\frac{F_{cs}}{F_{cm}}\right]_{initial}$ according to whether F decreases or increases.

The accurately compensated $\left[\frac{F_{cs}}{F_{cm}}\right]_{final}$ is obtained either by approximate simple energy balance calculation or by the iteration method shown in 9.5. The iteration method is preferred because the compensated $\left[\frac{F_{cs}}{F_{cm}}\right]_{final}$ can be measured directly.

By using the compensated $\left[\frac{F_{cs}}{F_{cm}}\right]_{final}$ (set on Pot 08 in Fig. 8.8), the final dynamic response of on-line computer operation is in excellent agreement with the theoretical results shown in Chapter 10.

Two types of on-line computer operation for a partially simulated CSTR were defined as follows:

<u>Type 1</u>: without compensation was called:
Partial Simulated Process On-line Operation
or Type 1 Operation.

<u>Type 2</u>: with compensation was called:
Approach to Real Process On-line Operation
or Type 2 Operation.
(see Chapter 10)

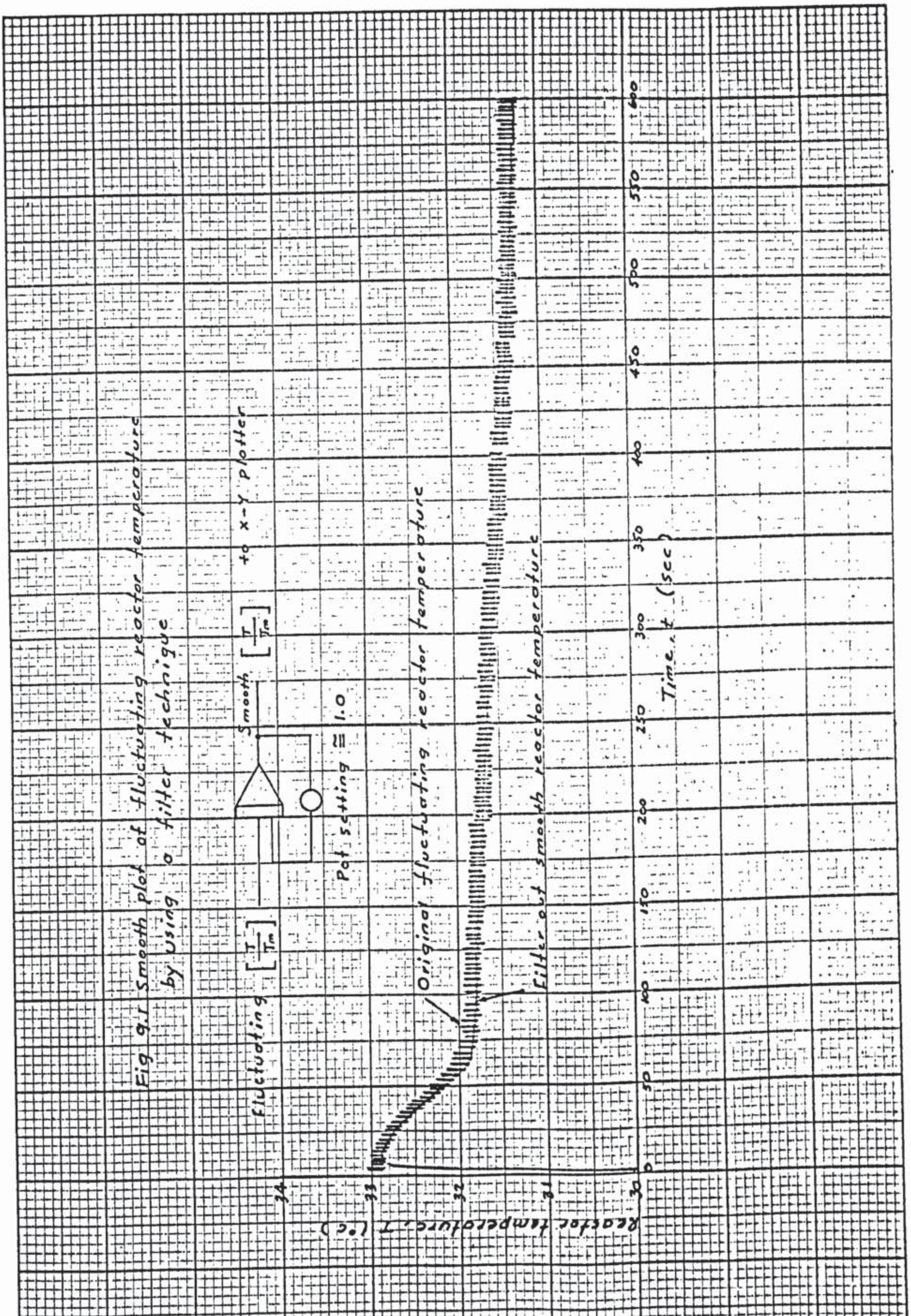

Fig 9.1 Smooth plot of fluctuating reactor temperature by using a filter technique

Fig. 9.2 Development of initial temperature setting for on-line operation T vs. t (unadapted operation)

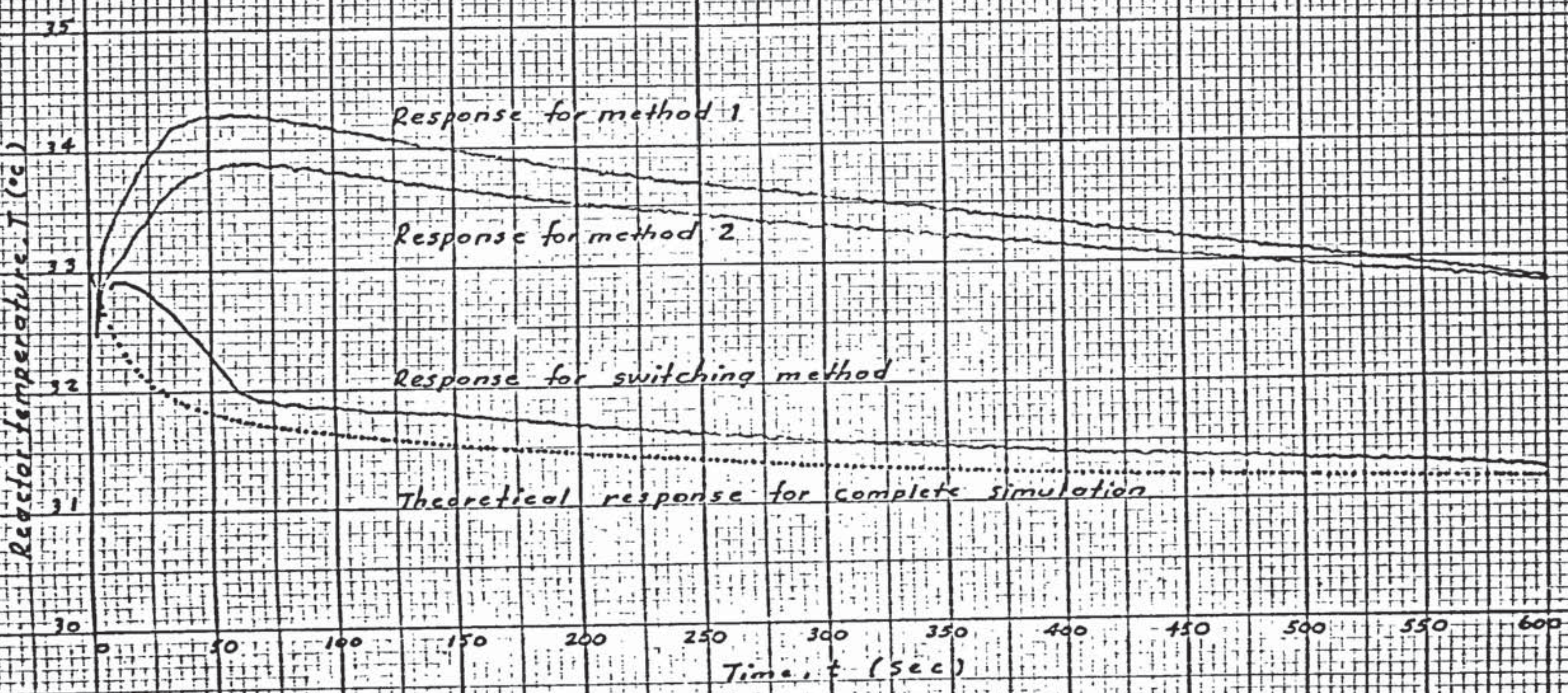

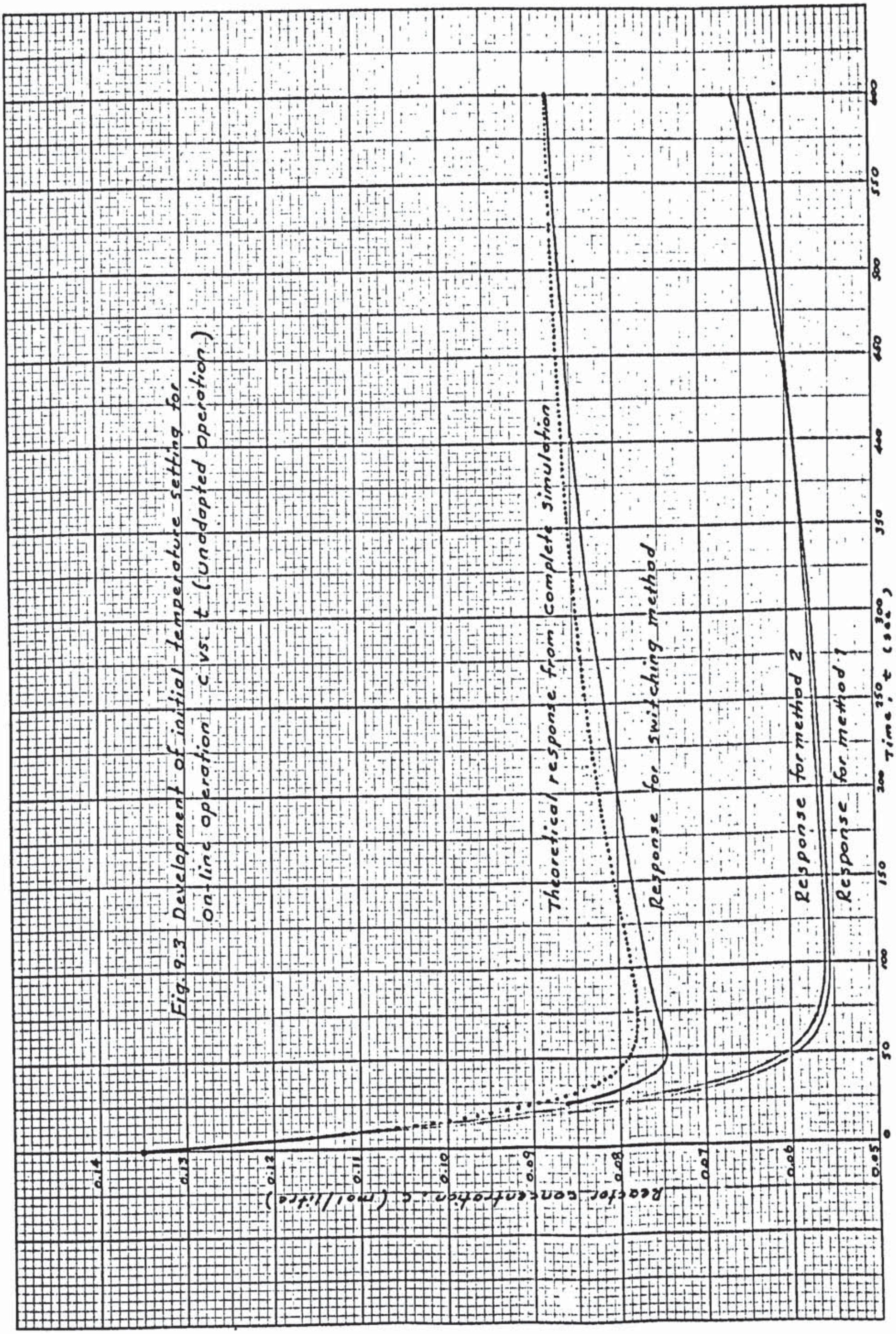

Fig. 9.3 Development of initial temperature setting for on-line operation c vs. t (unadapted operation)

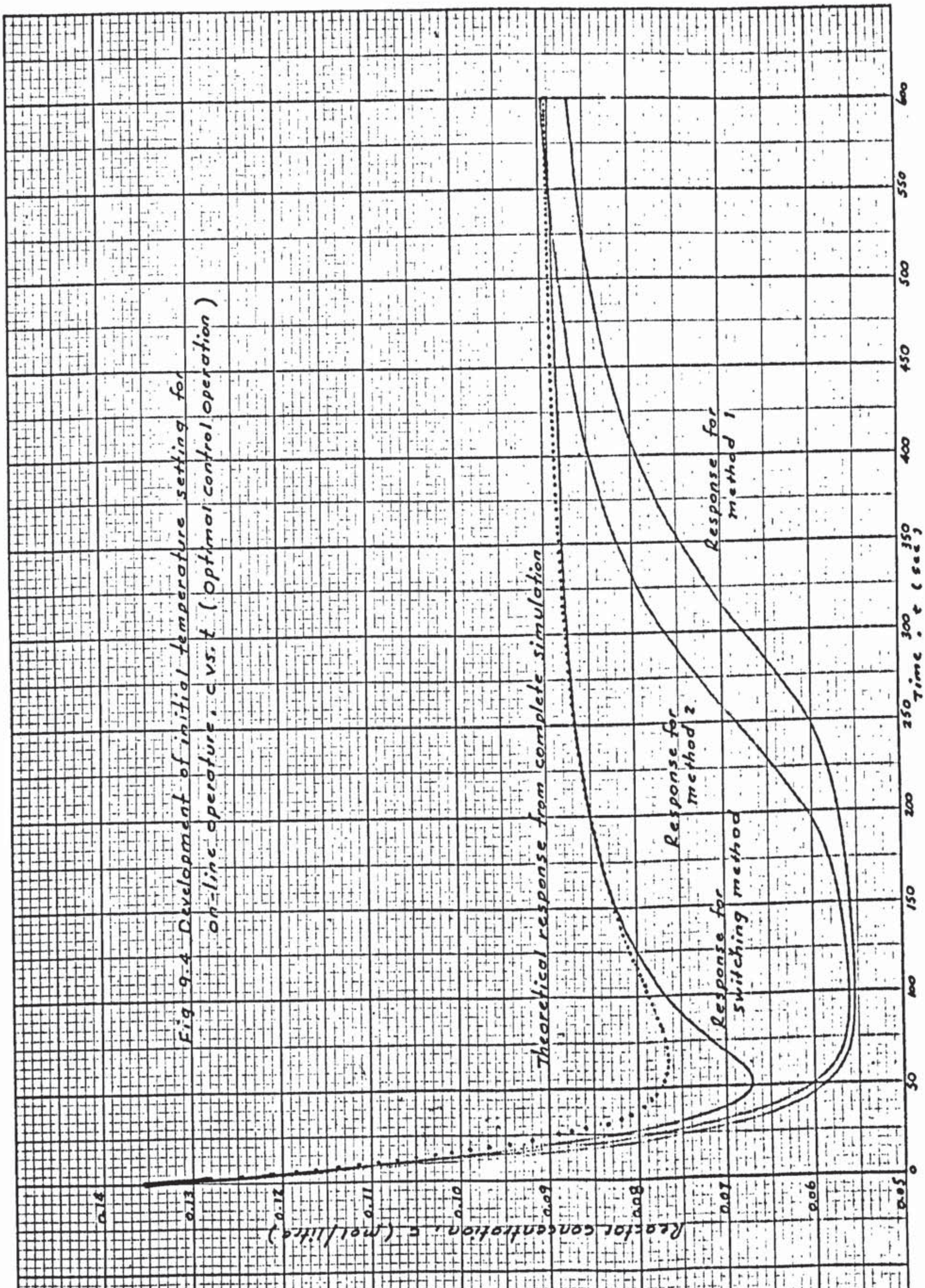

Fig 9.4 Development of initial temperature setting for on-line operator. c vs. t (Optimal control operation)

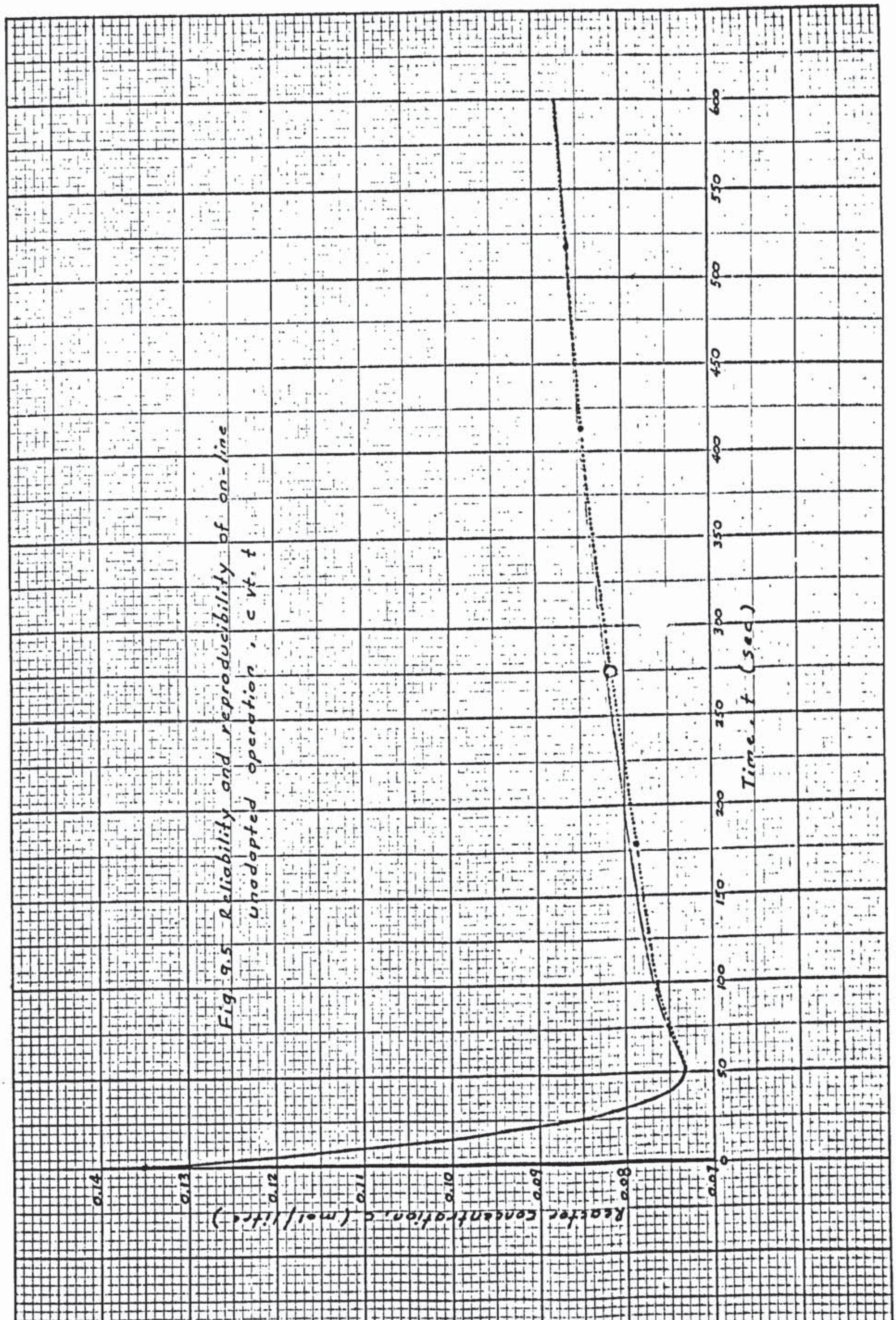

Fig 9.5 Reliability and reproducibility of on-line unadapted operation, c vt. t

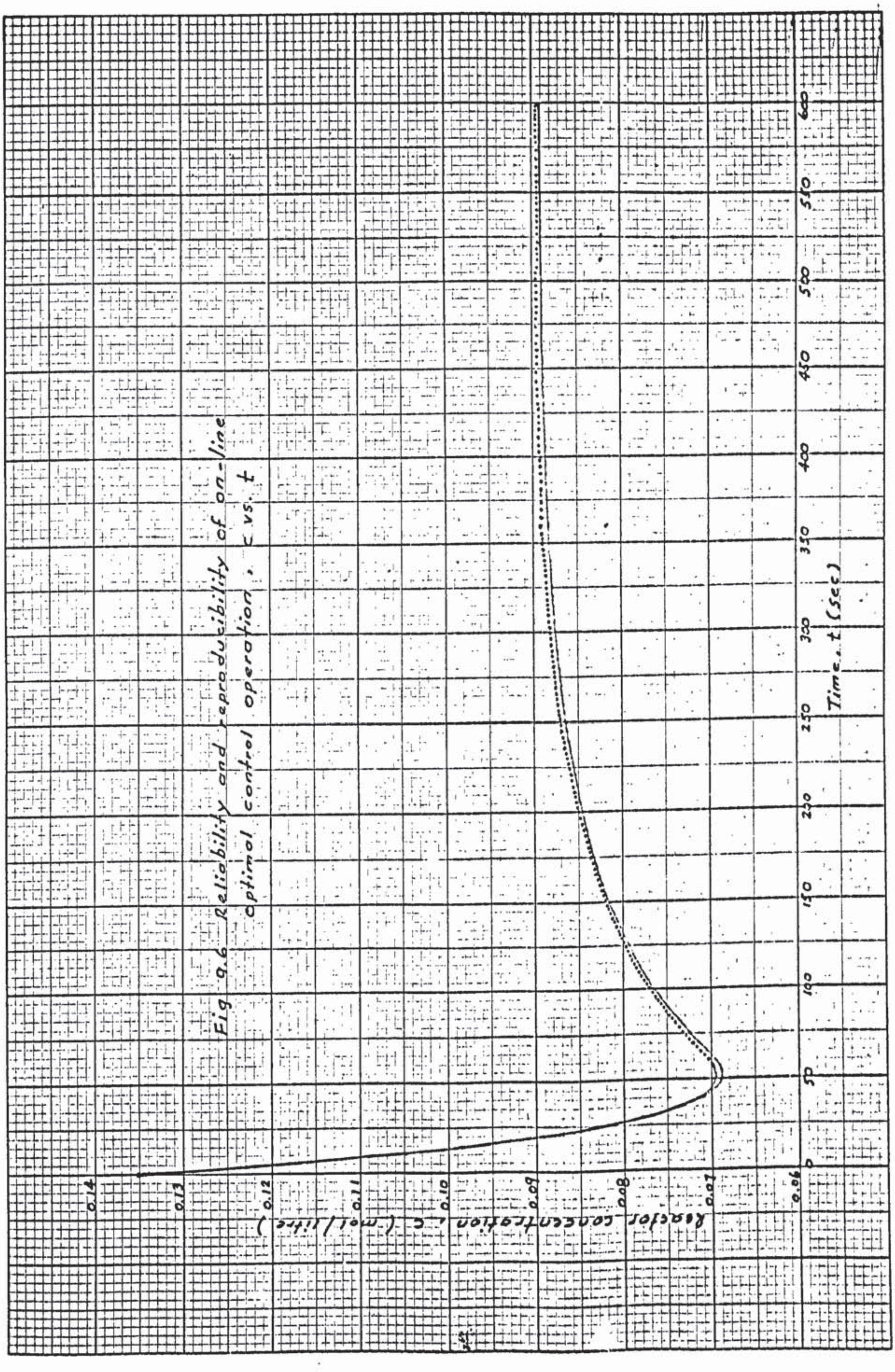

Fig 9.6 Reliability and reproducibility of on-line optimal control operation, c vs. t

CHAPTER 10

OPERATION AND ANALYSIS OF ON-LINE COMPUTER OMRAC

10.1. On-line computer OMRAC operation

In Chapter 8, a rigid on-line computer OMRAC system design was presented and in Chapter 9, the solutions of all difficulties for on-line computer operation with a very narrow operating range are given. All kinds of operating cases and groups, all kinds of figure plotting for each case, and all types of different operations within each figure are almost the same as in Chapter 7 (7.6). Thus the results from the theoretical complete simulation (Chapter 7) and the practical on-line operation of OMRAC can be compared almost case by case, figure by figure and curve by curve.

All tests of on-line computer operation of OMRAC are shown in Table 10.1.

General operating conditions: (same as in 7.7.1)

(1) Initial conditions (1st quadrant)

$C(t_o) = 0.135 \frac{\text{mol}}{\text{litre}}$; $T(t_o) = 33^\circ C$

(2) Final desired reactor concentration

$C(t_f) = 0.09 \frac{\text{mol}}{\text{litre}}$

(3) OMR : $K_1 = K_2 = 8$

(4) OAC ; Optimal P $K_3 = 100, 200, 500$ and 1000.

TABLE 10.1.

On-line computer OMRAC operation

Group	Case	Operation conditions	Type of operation	Kind of figure	Figure
1	1.1	F decrease 10%	1	A	10.1
		"	1	B	10.2
		"	1	C	10.3
	1.2	F decrease 20%	1	A	10.4
		"	1	C	10.5
	1.3	F decrease 10%	2	A	10.6
		"	2	B	10.7
		"	2	C	10.8
	1.4	F decrease 20%	2	A	10.9
		"	2	C	10.10
2	2.1	F increase 10%	2	A	10.11
		"	2	B	10.12
		"	2	C	10.13
	2.2	F increase 20%	2	A	10.14
		"	2	C	10.15
	2.3	F increase 20%	1	A	10.16
		"	1	C	10.17
3	3.1	a exponential decay 20%	2	A	10.18
		"	2	C	10.19
	3.2	a exponential decay 30%	2	A	10.20
		"	2	C	10.21
	3.3	a exponential decay 40%	2	A	10.22
		"	2	B	10.23
		"	2	C	10.24

Table 10.1 (continued)

Group	Case	Operation conditions	Type of operation	Kind of figure	Figure
3	3.4	a exponential decay 40% (for high weighting factors)	2	A	10.25
		"	2	C	10.26
4	4.1	Combined parameters change ((F decrease 10% (a decay 20%	1	A	10.27
			1	C	10.28
	4.2	"	2	A	10.29
		"	2	B	10.30
		"	2	C	10.31
5		(Group 4) (Optimal P+I)			
	5.1	K_3 = 100, ϵ = 0, 1, 2, 3	2	A	10.32
		"	2	C	10.33
	5.2	K_3 = 100, ϵ = 0.0, 0.2, 0.4, 0.6, 0.8, 1.0	2	A	10.34
		"	2	B	10.35
		"	2	C	10.36
	5.3.	K_3 = 200, ϵ = 0.0, 0.2, 0.4, 0.6, 0.8, 1.0	2	A	10.37
		"	2	B	10.38
6		(Group 4) (Optimal P + I + D)			
	6.1.	K_3 = 1, ϵ = 0.1, 0.2, 0.3, 0.4.	2	A	10.39
		"	2	B	10.40

TABLE 10.1 (continued)

Group	Case	Operation conditions	Type of operation	Kind of Figure	Figure
6	6.2	($K = 1$, $\epsilon = 0.4$ (40 min. operation	2	A	10.41
		"	2	B	10.42
	6.3	$K_3 = 10$, $\epsilon = 0.0, 0.04, 0.08, 0.12$	2	A	10.43
		"	2	B	10.44
		"	2	C	10.45
	6.4	($K_3 = 10$, $\epsilon = 0.12$ ((40 min. operation	2	A	10.46
		"	2	B	10.47
	6.5	$K_3 = 20$, $\epsilon = 0.0, 0.04, 0.08, 0.12$	2	A	10.48
		"	2	B	10.49
7		(Group 4) (different initial) (conditions)			
	7.1	($C(t_o) = 0.15$ mol/litre)	2	A	10.50
		($T(t_o) = 28^oC$)	2	B	10.51
		((2nd quadrant))	2	C	10.52
	7.2	($C(t_o) = 0.07$ mol/litre)	2	A	10.53
		($T(t_o) = 27^oC$)	2	B	10.54
		((3rd quadrant))	2	C	10.55
	7.3	($C(t_o) = 0.06$ mol/litre)	2	A	10.56
		($T(t_o) = 34^oC$)	2	B	10.57
		((4th quadrant))	2	C	10.58

TABLE 10.1 (continued)

Group	Case	Operation conditions	Type of operation	Kind of Figure	Figure
8		(Group 4 (different OMR			
	8.1	(OAC : Optimal P) (K_3= 200) ( ) ((I) $K_1 = K_2 = 4$) ( ) ((II) $K_1 = K_2 = 15$)	2 2	A B	10.59 10.60
9		(Group 4 (different set point			
	9.1	(OAC : Optimal P) (K_3 = 200) ( ) ((I) C_d : 0.10 mol/) (litre) ((II) C_d : 0.08 mol/) litre	2 2	A B	10.61 10.62
10		(Group 4 (different inlet (concentration			
	10.1	(C_o as load variable) ( ) (C_o : 0.9 mol/litre)	2 2	A B	10.63 10.64
	10.2	(C_o as load variable) ( ) (C_o : 1.1 mol/litre)	2 2	A B	10.65 10.66
	10.3	(C_o as parameter) ( ) ((I) C_o = 0.9 mol/) (litre) ((II) C_o = 1.1 mol/) (litre)	2 2	A B	10.67 10.68

10.2. Comparison of Type 1 and Type 2 on-line operation

From definition (9.6) Type 1 operation is only for the partially simulated process without compensation. Actually this type of dynamic response does not exist on the real process and Type 2 operation called approach to real process operation applies to the partially simulated process but with compensation. From all experiments on on-line operation, the dynamic response and phase-plane trajectories of Type 2 operation are different from Type 1 operation, but in good agreement with the theoretical results of complete simulation.

Since a very narrow operating range has been planned and used, the highly sensitive performance of different on-line operations such as: UC, UOC, OMRAC, and OMR of a CSTR can be plotted respectively for comparison with the theoretical results. (Figs. 7.7 to 7.54 and Figs. 10.1 to 10.68).

Thus partial simulation techniques have been extended to a highly sensitive and accurate performance operation from Buxton's original design by using compensation combined with switching and iteration methods.

10.3. Comparison and analysis of process dynamics response and phase-plane trajectories

10.3.1. For any individual and combined unmeasurable parameters with different possible conditions (from Group 1 to Group 10), all dynamic response curves and phase-plane trajectories of on-line operation are in good agreement with the theoretical results and also follow a definite smooth, regular and effective order as shown below:

$$(US) \rightarrow (UOC) \rightarrow \overset{\text{OMRAC}}{(K_3=100 \rightarrow 200 \rightarrow 500 \rightarrow 1000)} \longrightarrow (OMR)$$

where $\rightarrow$ indicates more offset from OMR

10.3.2. From the dynamic response curves of on-line operation with the same test conditions as in the theoretical results, the response of OMRAC is always better than UOC and approaches OMR as a limit as the weighting factor is increased.

10.3.3. From the dynamic response curves of on-line operation with the same test conditions as in the theoretical results, the adaptation of OMRAC has no limitations for any operating conditions. The only limitation is the constraints of the optimal control law which corresponds to the control valve minimum and maximum capacity for cooling water flowrate.

10.3.4. From all phase-plane trajectories of on-line operation, the final steady state point of OMRAC is changed, and approaches the desired reactor concentration of OMR as a limit when the weighting factor K_3 is increased; it never returns to the original steady state point of OMR, because of the change of parameters. This phenomenon was illustrated earlier in Chapter 3. (3.3 and Fig.3.3.)

10.3.5. In general all process responses of on-line operation are comparatively more sensitive than the theoretical responses from complete simulation.

10.4. Comparison and analysis of optimal control law

10.4.1. All optimal control laws for the complete simulation and on-line operation are plotted by the X-Y plotter with different units : Kcal/min for complete simulation; U^* and m^* and litre/min for on-line operation, F_c.

The relation between then has been discussed in (8.3.4.) from equation (8-9):

$$\left[\frac{F_c}{F_{cm}}\right] = \left[\frac{F_{cs}}{F_{cm}}\right] + \frac{0.1\left[\frac{U^*}{Q_{cm}}\right]}{\left[\frac{\Delta T_c}{T_m}\right]}$$

$$\text{or} \quad F_c = (F_{cs})_{final} + \left(\frac{0.1\ F_{cm} \times T_m}{Q_{cm}}\right)\left(\frac{U^*}{\Delta T_c}\right)$$

Simplifying gives:

$$F_c = (F_{cs})_{final} + \frac{U^*}{\Delta T_c} \qquad (10\text{-}1)$$

$$\text{and} \quad F_c = (F_{cs})_{final} + \frac{m^*}{\Delta T_c} \qquad (10\text{-}2)$$

where $(F_{cs})_{final}$ = cooling water flowrate at the final steady state.

In fact both $(F_{cs})_{final}$ and T_c are slightly different in each experiment, but such changes are comparatively small and shown in Appendix 6 (Tables A.6.1 to A.6.10). So the dynamic response curves both for U^* (or m^*) and F_c can be compared and evaluated correspondingly.

10.4.2. All of the optimal control laws both for theoretical and on-line operation may be arranged in the following order of effectiveness:

OMRAC

$$\left(K_3 = 1000 \rightarrow 500 \rightarrow 200 \rightarrow 100\right)_{U^*} \rightarrow \left(\text{UOC}\right)_{m^*} \rightarrow \left(\text{OMR}\right)_{m^*}$$

and F_c and F_c and F_c

10.4.3. In general the response of F_c for on-line operation is more sensitive than U* (or m*) in theoretical complete simulation. This effect will influence the process response discussed in 10.3.5.

10.4.4. The response of the optimal P + I + D control law always fluctuates since a large value of β_{27} is produced (Appendix A.2.7 and Fig. 10.45).

10.5. Comparison and analysis of optimal PID control

10.5.1. Optimal P+I and Optimal P + I + D of OMRAC for on-line operation can produce the same improved performance as Optimal P alone in complete simulation.

Optimal integral control (optimal P + I or P + I + D) in on-line operation is more sensitive than the corresponding theoretical cases and the optimal integral control weighting factor ϵ is much smaller when used for on-line operation, and is discussed below:

10.5.2. For Optimal P + I

In complete simulation : The performance in cases 5.1 and 5.2 (Figs. 7.29 to 7.33) is always excellent as ϵ increases.

Case 5.1.	Case 5.2
K_3 = 100	K_3 = 200
= 0, 1, 2, 3, 4	= 0, 1, 2, 3, 4, 8 and 15
$\left(\frac{K_3}{\varepsilon}\right)_{min} = \frac{100}{4} = 25$	$\left(\frac{K_3}{\varepsilon}\right)_{min} = \frac{200}{15} = 13.3$

where $\left(\frac{K_3}{\varepsilon}\right)_{min}$ is the minimum weighting factor ratio between K_3 and used for Optimal integral control adjustment.

. In on-line operation : The performance in cases 5.2 and 5.3 (Figs. 7.34 to 7.38) is much better than in case 5.1 (Figs. 7.32 and 7.33).

Case 5.1.	Case 5.2	Case 5.3
K_3 = 100	K_3 = 100	K_3 = 200
= 0, 1, 2, 3.	= 0, .2, .4, .8, 1.0.	= 0, .2, .4, .8, 1.0.
$\left(\frac{K_3}{\varepsilon}\right)_{min} = 33.3$	$\left(\frac{K_3}{\varepsilon}\right)_{min} = 100$	$\left(\frac{K_3}{\varepsilon}\right)_{min} = 200$

From the above analysis of Optimal P + I, for complete simulation the performance of the OMRAC is always excellent even if $\left(\frac{K_3}{\varepsilon}\right)_{min}$ decreases to 13.3. But for on-line operation, the best value of $\left(\frac{K_3}{\varepsilon}\right)$ is kept around 100 or

$$\left(\frac{K_3}{\varepsilon}\right) \simeq 100$$

10.5.3. For Optimal P + I + D

In complete simulation : The performance in cases 6.1 and 6.2 (Figs. 7.34 to 7.37) is always excellent as increases

Case 6.1.	Case 6.2.
K_3 = 1.0 = 0.5, 1, 1.5, 2.0 $\left(\frac{K_3}{\epsilon}\right)_{min}$ = 0.5	K_3 = 3.0 = 0, .5, 1.5, 2.0 $\left(\frac{K_3}{\epsilon}\right)_{min}$ = 1.5

In on-line operation : The performance in cases 6.3. and 6.3 (Figs. 10.43 to 10.49) is much better than case 6.1 (Figs. 1039 and 10.40).

Case 6.1.	Case 6.3.	Case 6.5.
K_3 = 1.0 = .1, .2, .3, .4 $\left(\frac{K_3}{\epsilon}\right)_{min}$ = 2.5	K_3 = 10.0 = 0, .04, .08, .12 $\left(\frac{K_3}{\epsilon}\right)_{min}$ = 83.8	K_3 = 10.0 = 0, .04, .08, .12 $\left(\frac{K_3}{\epsilon}\right)_{min}$ = 186.6

Note. When $\epsilon = 0$, it reduces to Optimal P + D control.

From the above analysis of Optimal P + I + D for complete simulation the performance of OMRAC is alwasy excellent even if $\left(\frac{K_3}{\epsilon}\right)_{min}$ decreases to 1.5. But for on-line operation, the best value of $\left(\frac{K_3}{\epsilon}\right)$ is kept around

$$\left(\frac{K_3}{\epsilon}\right) \simeq 80$$

In general for Optimal PID control of on-line operation the best value of $\left(\frac{K_3}{\varepsilon}\right)$ will be:

$$\left(\frac{K_3}{\varepsilon}\right) \simeq 80 - 100 \qquad (10\text{-}3)$$

10.6. Comparison and analysis of OMRAC stability

10.6.1. In the process control field all techniques used for system stability analysis such as Routh-Hurwitz, Nyquist and Liapunov stability criterion give the theoretical prediction for stability analysis from the derived system equations, and by using such techniques the system stability cannot make predictions for on-line operation. The most straightforward method to determine the system stability of on-line OMRAC is by direct use of the many dynamic response curves and phase-plane trajectories obtained from the X - Y plotter.

From the general definition of process stability (73), the comparison and analysis of OMRAC stability is shown below.

10.6.2. In general the system stability both for theoretical complete simulation and on-line operation possesses the following order of effectiveness:

$$(\text{OMR}) \leftarrow \overset{\text{OMRAC}}{\left[K_3 = 1000 \leftarrow 500 \leftarrow 200 \leftarrow 100\right]} \leftarrow (\text{UOC}) \leftarrow (\text{US})$$

where $\leftarrow$ indicates increasing stability.

10.6.3. Since the response of optimal control law in on-line operation of the process is always more sensitive than the theoretical case (10.3.3. and 10.4.3.) then in general the theoretical system response of OMRAC is always more stable than on-line operation but the latter can still possess excellent asymptotic stability in different operating conditions.

10.6.4. From Group 7 since different initial conditions are selected from the four different quadrants around the original final steady state (or $C(t_f) = 0.09$ mol/litre; $T(t_f) = 30^oC$), all response curves of OMRAC (Figs.10.50 to 10.58) still possess excellent asymptotic stability; thus, by definition, on-line OMRAC is asymptotically stable in the large.

10.6.5. Stability in Optimal PID control

From Section 5 analysis (10.5.2. and 10.5.3) the Optimal PID operation of OMRAC will maintain excellent stability when the weighting factor ratio is set as in equation 10-3, or:

$$\frac{K_3}{\epsilon} \simeq 80 - 100$$

There are several interesting figures of Optimal P + I + D obtained over a long time of operation (20 min. for dynamic response. Figs. 10.41, 10.46 and 40 min. for phase-plane, Figs. 10.42 and 10.47). For comparison of the stability of each pair of figures (10.41 and 10.46, 10.42 and 10.47), the latter one $\frac{K_3}{\epsilon} = 83.3$ is much more stable than the first $\frac{K_3}{\epsilon} = 2.5$.

10.7. Q_g and $(-\Delta H)$ calculations from experimental data

All experimental data of the final steady state conditions for on-line operation are shown in the Appendix, Tables 6.1 to 6.10.

From the many on-line experimental tests, Q_g and $(-\Delta H)$ were calculated and checked as follows:

Q_g : Q_g values can be checked for each operating case by using the following different calculations:

(1) Q_g calculated from equation (8-4)

$$Q_g = 10.66\ Q_{gm}\left[\frac{a}{a_m}\right]\left[\frac{K}{K_m}\right]\left[\frac{C}{C_m}\right]\left(\frac{\text{Kcal x } 10^3}{h}\right)$$

or

$$Q_g = 29613.48\left[\frac{a}{a_m}\right]\left[\frac{K}{K_m}\right]\left[\frac{C}{C_m}\right]\left(\frac{\text{cal}}{\text{sec}}\right) \qquad (10\text{-}4)$$

where $\left[\frac{a}{a_m}\right]\left[\frac{K}{K_m}\right]\left[\frac{C}{C_m}\right]$ is in machine units or mu.

(2) Q_g calculated directly from variac reading by using the calibration curve (Fig. A.4.16)

(3) Q_g calculated from equation (7-7)

$$Q_g = \rho_c C_{pc} F_c \Delta T_c + \rho\, C_p\, F\,(T - T_i)$$

$$\text{or} \quad Q_g = 16.7\left(F_c\, \Delta T + F\,(T - T_i)\right)\left(\frac{\text{cal}}{\text{sec}}\right) \qquad (10\text{-}5)$$

$(-\Delta H)$: $(-\Delta H)$ value was checked from the previously calculated theoretical value (18511 $\frac{\text{cal}}{\text{g.mole}}$) (7.4 and ~~Fig~~. 7.8) as follows

From equation (7-8)

$$(-\Delta H) = \frac{(Q_g)_{AV}}{aVKC_s} = \frac{(Q_g)_{AV}}{16a_m \cdot K_m \cdot C_m\left[\frac{a}{a_m}\right]\left[\frac{K}{K_m}\right]\left[\frac{C}{C_m}\right]}$$

$$\text{OR} \quad (-\Delta H) = \frac{(Q_g)_{AV}}{1.6\left[\frac{a}{a_m}\right]\left[\frac{K}{K_m}\right]\left[\frac{C}{C_m}\right]} \qquad (10\text{-}6)$$

where $(Q_g)_{AV} = \left[(Q_g)_1 + (Q_g)_2 + (Q_g)_3 \right] / 3$

All calculated Q_g and $(-\Delta H)$ values are shown in Tables 10.2 to 10.11 and the following ten tables show that:

(1) Q_g values calculated from three different kinds of method for all different on-line operations, are in excellent agreement for each operating case.

(2) $(-\Delta H)$ values in all different cases for on-line operation are in excellent agreement with the originally calculated theoretical value of:

$$(-\Delta H) = 18511 \ \frac{cal}{mol}$$

TABLE 10.2

Q_g and (- ΔH) values calculated from on-line experimental data for cases 1.1 and 1.2

(Theoretical value of (- ΔH) = 18511 $\frac{cal}{mol}$)

	Q_g cal/sec				(- ΔH) $\frac{cal}{mol}$
	(1)	(2)	(3)	(Q_g)AV	
Case 1.1					
US	823	822	834	826.33	18570
UOC	800	806	816	807.33	18680
OMRAC					
K_3 = 100	823	823	822	822.33	18488
K_3 = 200	823	822	825	823.33	18510
K_3 = 500	823	822	827	824.0	18525
K_3 = 1000	823	822	832	825.6	18562
Case 1.2					
US	823	833	814	823.33	18510
UOC	823	833	813	823.0	18503
OMRAC					
K_3 = 100	823	828	823	824.67	18540
K_3 = 200	823	828	817	822.67	18495
K_3 = 500	823	822	824	823.0	18503
K_3 = 1000	823	822	824	823.0	18503

TABLE 10.3.

Q_g and $(-\Delta H)$ values calculated from on-line experimental data for cases 1.3 and 1.4

(Theoretical value of $(-\Delta H) = 18511 \frac{cal}{mol}$)

	Q_g cal/sec				$(-\Delta H) \frac{cal}{mol}$
	(1)	(2)	(3)	$(Q_g)_{AV}$	
Case 1.3					
US	800	806	808	804.67	18626
UOC	817	822	824	821.0	18591
OMRAC					
K_3 = 100	823	828	827	826.0	18570
K_3 = 200	823	822	829	824.67	18540
K_3 = 500	829	828	831	829.33	18512
K_3 = 1000	829	828	833	830.0	18527
K_3 = 4000	829	828	834	830.33	18534
Case 1.4					
US	710	722	693	708.33	18446
UOC	794	791	795	793.33	18501
OMRAC					
K_3 = 100	806	805	812	808.0	18566
K_3 = 200	823	833	806	820.67	18450
K_3 = 500	823	833	811	822.33	18487
K_3 = 1000	829	840	812	827.0	18460

TABLE 10.4

Q_g and $(-\Delta H)$ values calculated from on-line experimental data for Cases 2.1, 2.2 and 2.3. (Theoretical value of $(-\Delta H) = 18511 \frac{cal}{mol}$)

	Q_g cal/sec				$(-\Delta H)$ $\frac{cal}{mol}$
	(1)	(2)	(3)	$(Q_g)_{AV}$	
Case 2.1.					
US	918	917	928	921.0	18569
UOC	918	917	911	915.33	18454
OMRAC					
K_3 = 100	918	917	925	920.0	18548
K_3 = 200	918	917	935	923.0	18609
K_3 = 500	918	917	927	920.67	18562
K_3 = 1000	918	917	922	919.0	18528
Case 2.2.					
US	977	970	995	980.67	18573
UOC	977	970	1007	984.67	18648
OMRAC					
K_3 = 100	977	970	998	981.67	18592
K_3 = 200	977	970	992	979.67	18554
K_3 = 500	977	970	990	979.0	18542
K_3 = 1000	977	970	996	981.0	18580
Case 2.3					
US	977	970	996	981.0	18580
UOC	977	970	993	980.0	18560
OMRAC					
K_3 = 100	977	970	1005	984.0	18636
K_3 = 200	977	970	998	981.67	18592
K_3 = 500	977	970	1004	983.67	18630
K_3 = 1000	977	970	997	981.33	18586

TABLE 10.5

Q_g and $(-\Delta H)$ values calculated from on-line experimental data for cases 3.1, 3.2 and 3.3. (Theoretical value of $(-\Delta H) = 18511 \frac{cal}{mol}$)

	Q_g cal/sec				$(-\Delta H)$ $\frac{cal}{mol}$
	(1)	(2)	(3)	$(Q_g)_{AV}$	
Case 3.1					
US	823	833	828	828.0	18615
UOC	823	833	827	827.67	18608
OMRAC					
K_3 = 100	823	828	830	827.0	18593
K_3 = 200	823	833	813	823.0	18503
K_3 = 500	823	833	818	824.67	18540
K_3 = 1000	823	833	817	824.33	18533
Case 3.2.					
US	800	791	812	801.0	18542
UOC	817	822	823	820.67	18584
OMRAC					
K_3 = 100	823	828	828	826.33	18578
K_3 = 200	823	833	823	824.67	18540
K_3 = 500	823	833	814	823.33	18510
K_3 = 1000	823	833	817	824.33	18533
Case 3.3					
US	817	822	814	817.67	18516
UOC	817	822	814	817.67	18516
OMRAC					
K_3 = 100	823	830	822	825.0	18548
K_3 = 200	823	830	819	824.0	18525
K_3 = 500	823	830	828	827.0	18593
K_3 = 1000	829	838	831	832.67	18586

TABLE 10.6

Q_g and $(-\Delta H)$ values calculated from on-line experimental data for cases 4.1 and 4.2. (Theoretical value of $(-\Delta H) = 18511 \frac{cal}{mol}$)

	Q_g cal/sec				$(-\Delta H) \frac{cal}{mol}$
	(1)	(2)	(3)	$(Q_g)_{AV}$	
Case 4.1					
US	918	917	928	921.0	18569
UOC	918	917	928	921.0	18569
OMRAC					
K_3 = 100	918	923	919	920.0	18548
K_3 = 200	918	923	918	919.67	18541
K_3 = 500	930	931	930	930.33	18518
K_3 = 1000	930	931	936.	932.33	18557
K_3 = 4000	930	931	941	934.0	18590
Case 4.2.					
US	912	917	904	911.0	18486
UOC	912	917	904	911.0	18486
OMRAC					
K_3 = 100	918	917	913	916.0	18468
K_3 = 200	918	923	909	916.67	18481
K_3 = 500	918	923	900	913.67	18421
K_3 = 1000	918	926	907	917.0	18487
K_3 = 4000	918	931	906	918.33	18515

TABLE 10.7

Q_g and $(-\Delta H)$ values calculated from on-line experimental data for cases 5.1, 5.2 and 5.3. (Theoretical value of $(-\Delta H) = 18511 \frac{cal}{mol}$)

	Q_g = cal/sec				$(-\Delta H) \frac{cal}{mol}$
	(1)	(2)	(3)	$(Q_g)_{AV}$	
Case 5.1					
OMRAC					
K_3 = 100					
ε = 0	918	917	926	920.33	18555
ε = 1	918	917	937	924.0	18629
ε = 2	918	917	941	925.33	18656
ε = 3	918	917	944	926.33	18676
Case 5.2					
OMRAC					
K_3 = 100					
ε = 0	918	931	910	919.67	18542
ε = 0.2	918	931	913	920.67	18560
ε = 0.4	918	931	910	919.67	18542
ε = 0.6	918	931	920	923.0	18609
ε = 0.8	918	931	909	919.33	18535
ε = 1.0	918	931	909	919.33	18535
Case 5.3					
OMRAC					
K_3 = 200					
ε = 0	918	917	920	918.33	18515
ε = 0.2	918	917	935	923.33	18616
ε = 0.4	918	917	917	917.33	18495
ε = 0.6	918	917	943	926.0	18670
ε = 0.8	918	917	929	921.33	18575
ε = 1.0	918	917	938	924.33	18636

TABLE.10.8

Q_g and $(-\Delta H)$ values calculated from on-line experimental data for Cases 6.1, 6.3 and 6.5 (Theoretical value of $(-\Delta H) = 18511 \frac{cal}{mol}$)

	Q_g cal/sec				$(-\Delta H) \frac{cal}{Mol}$
	(1)	(2)	(3)	$(Q_g)_{AV}$	
Case 6.1					
UOC	918	931	910	919.67	18541
OMRAC					
K_3 = 1.0					
ϵ = 0.1	918	931	916	921.67	18582
ϵ = 0.2	918	931	930	926.33	18676
ϵ = 0.3	918	931	917	922.0	18589
ϵ = 0.4	918	931	922	923.67	18622
Case 6.3	918	923	911	918.0	18508
OMRAC					
K_3 = 10					
ϵ = 0	918	928	920	922.0	18589
ϵ = 0.04	918	928	919	921.67	18582
ϵ = 0.08	918	928	928	924.67	18642
ϵ = 0.12	918	928	927	924.33	18635
Case 6.5					
UOC	918	923	913	918.0	18508
OMRAC					
K_3 = 20					
ϵ = 0	918	928	915	923.0	18607
ϵ = 0.04	918	928	915	920.33	18555
ϵ = 0.08	918	928	919	921.67	18582
ϵ = 0.12	918	928	918	921.33	18575

TABLE 10.9

Q_g and $(-\Delta H)$ values calculated from on-line experimental data for Cases 7.1, 7.2 and 7.3 (Theoretical value of $(-\Delta H) = 18511 \frac{cal}{mol}$)

	Q_g cal/sec				$(-\Delta H)\ \frac{cal}{mol}$
	(1)	(2)	(3)	$(Q_g)_{AV}$	
Case 7.1					
US	918	917	924	919.67	18541
UOC	918	928	925	920.0	18548
OMRAC					
K_3 = 100	918	928	913	919.67	18542
K_3 = 200	918	928	915	920.33	18555
K_3 = 500	918	928	923	923.0	18609
K_3 = 1000	918	928	900	915.33	18454
Case 7.2					
US	817	822	812	819.0	18546
UOC	829	833	832	831.33	18556
OMRAC					
K_3 = 100	859	850	868	859.0	18513
K_3 = 200	859	850	881	863.33	18606
K_3 = 500	859	850	888	865.67	18656
K_3 = 1000	859	850	865	858.0	18491
Case 7.3					
US	888	889	890	889.0	18521
UOC	918	917	905	913.33	18414
OMRAC					
K_3 = 100	918	917	942	925.67	18662
K_3 = 200	918	917	935	923.33	18615
K_3 = 500	918	917	933	922.67	18602
K_3 = 1000	918	917	922	919.0	18528

TABLE 10.10

Q_g and $(-\Delta H)$ values calculated from on-line experimental data for Cases 8.1 and 9.1

(Theoretical value of $(-\Delta H) = 18511 \frac{cal}{mol}$)

	Q_g cal/sec				$(-\Delta H) \frac{cal}{mol}$
	(1)	(2)	(3)	$(Q_g)_{AV}$	
Case 8.1					
(I)					
$K_1 = K_2 = 4$					
UOC	888	889	874	883.67	18410
OMRAC $K_3 = 200$	918	917	913	916.0	18468
(II)					
$K_1 = K_2 = 15$					
UOC	918	917	908	914.33	18434
OMRAC $K_3 = 200$	918	917	906	913.67	18421
Case 9.1					
(I)					
$C_d = 0.10$ mol /litre					
UOC	888	917	855	886.67	18472
OMRAC $K_3 = 200$	918	917	909	914.67	18440
(II)					
$C_d = 0.08$ mol /litre					
UOC	888	917	861	888.67	18514
OMRAC $K_3 = 200$	918	917	915	916.67	18481

TABLE 10.11

Q_g and $(-\Delta H)$ values calculated from on-line experimental data for Cases 10.1, 10.2 and 10.3

(Theoretical value of $(-\Delta H) = 18511 \frac{cal}{mol}$)

	Q_g cal/sec				$(-\Delta H) \frac{cal}{mol}$
	(1)	(2)	(3)	$(Q_g)_{AV}$	
Case 10.1					
US	829	830	839	832.67	18586
UOC	859	861	854	858.0	18491
OMRAC $K_3 = 200$	859	861	862	860.67	18549
Case 10.2					
US	977	985	983	981.66	18592
UOC	1007	1000	1005	1004.0	18456
OMRAC $K_3 = 200$	1007	1000	1011	1006.0	18493
Case 10.3					
(I) $C_o = 0.9$ mol / litre					
UOC	829	827	845	833.67	18608
OMRAC $K_3 = 200$	829	827	853	836.33	18668
(II) $C_o = 1.1$ mol / litre					
UOC	1007	1000	996	1001.0	18401
OMRAC $K_3 = 200$	1007	1000	1016	1007.67	18523

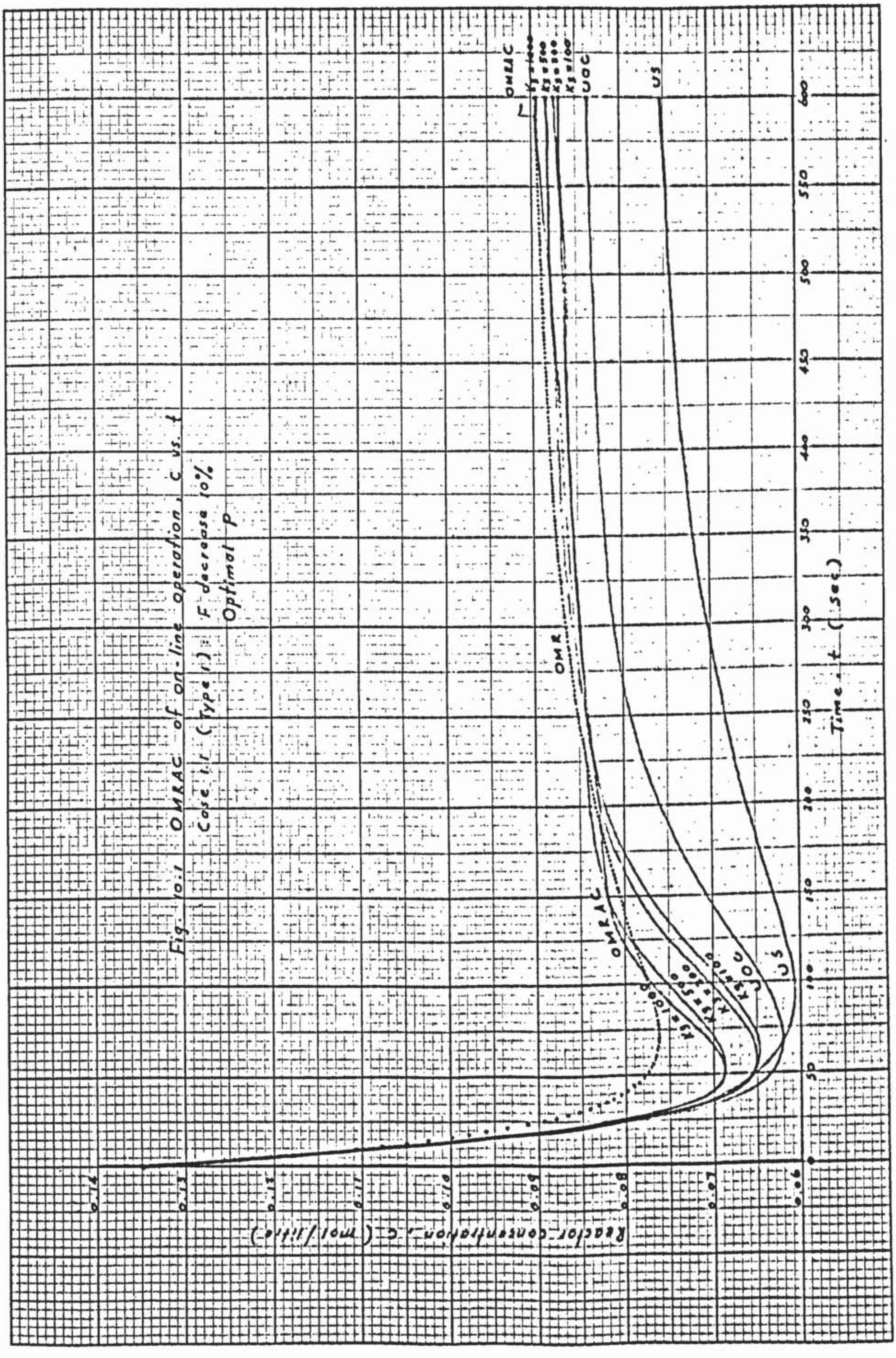
Fig. 10.1 OMRAC of on-line operation, C vs. t
Case 1.1 (Type 1): F decrease 10%
Optimal P
Reactor concentration, c (mol/litre)
Time, t (sec)
0.14
0.13
0.12
0.11
0.10
0.09
0.08
0.07
0.6
50
100
150
200
250
300
350
400
450
500
550
600
OMRAC
OMR
UOC
US

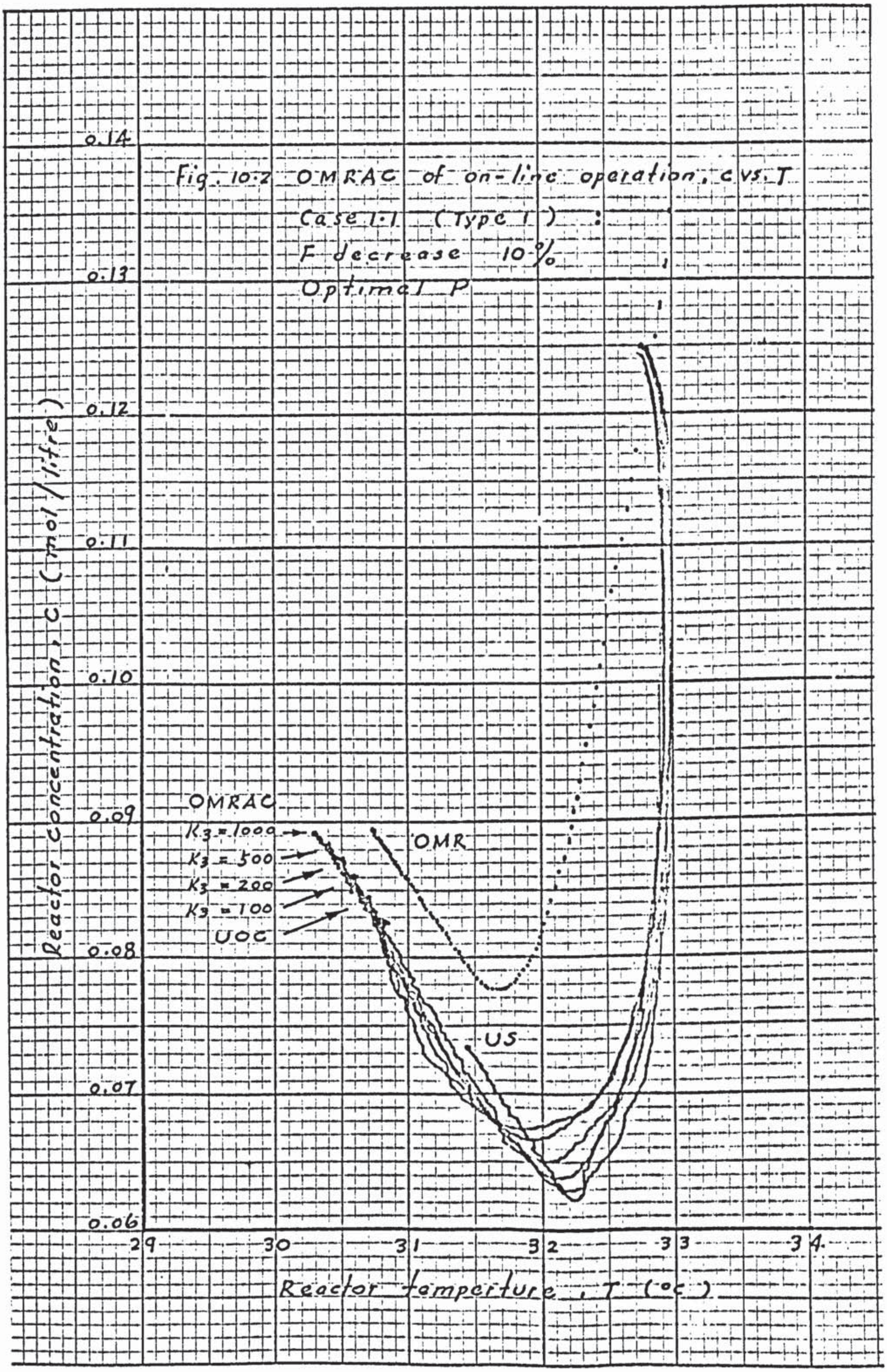
Fig. 10.2 OMRAC of on-line operation, c vs. T
Case 1.1 (Type 1) :
F decrease 10%
Optimal P
0.14
0.13
0.12
0.11
0.10
0.09
0.08
0.07
0.06
Reactor concentration, C (mol / litre)
OMRAC
$K_3 = 1000$
$K_3 = 500$
$K_3 = 200$
$K_3 = 100$
UOC
OMR
US
29
30
31
32
33
34
Reactor temperature, T (°C)

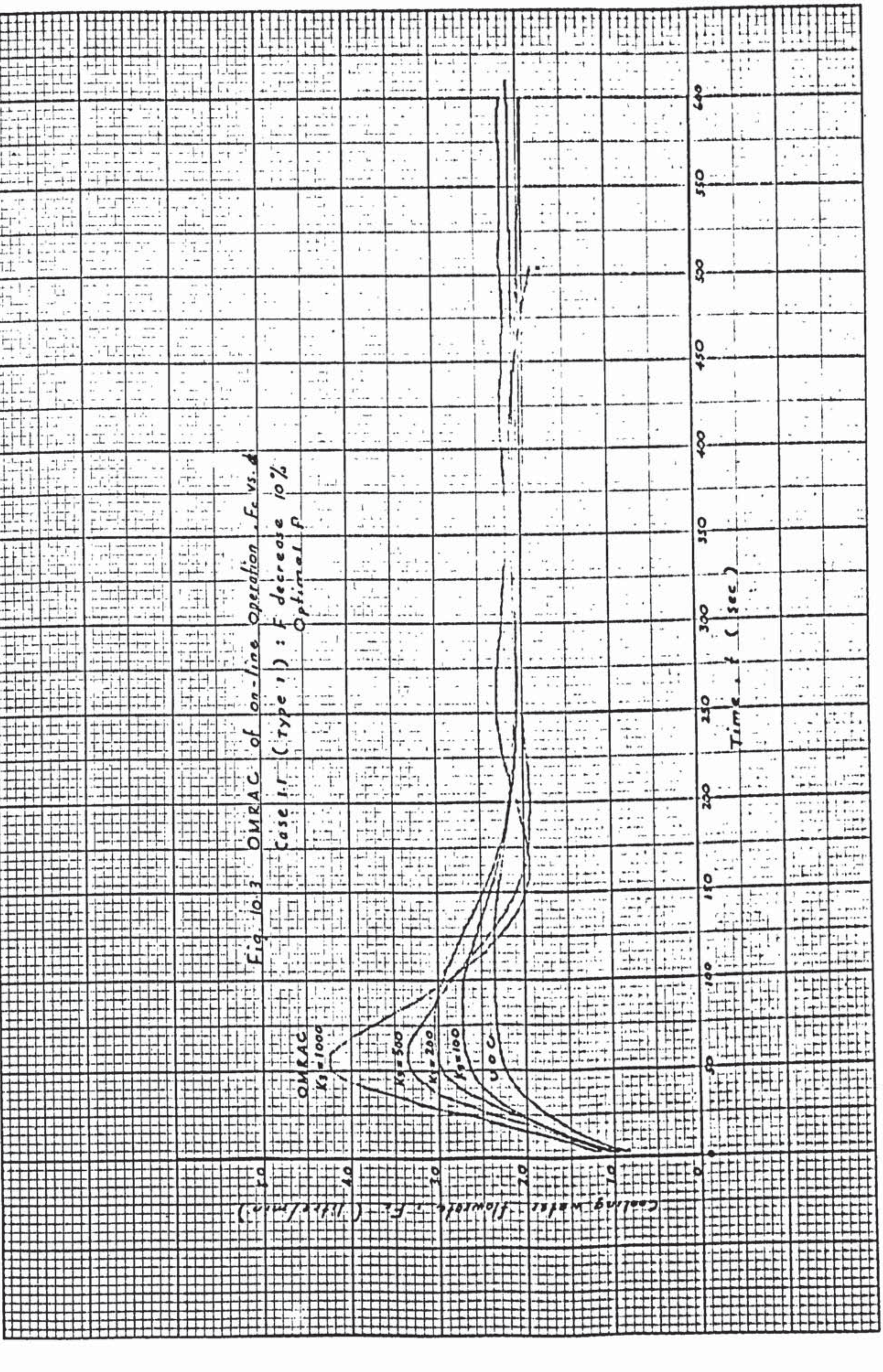

Fig. 10.3 OMRAC of on-line operation, Fc vs. t
Case 1.1 (Type 1): F decrease 10%
Optimal ρ

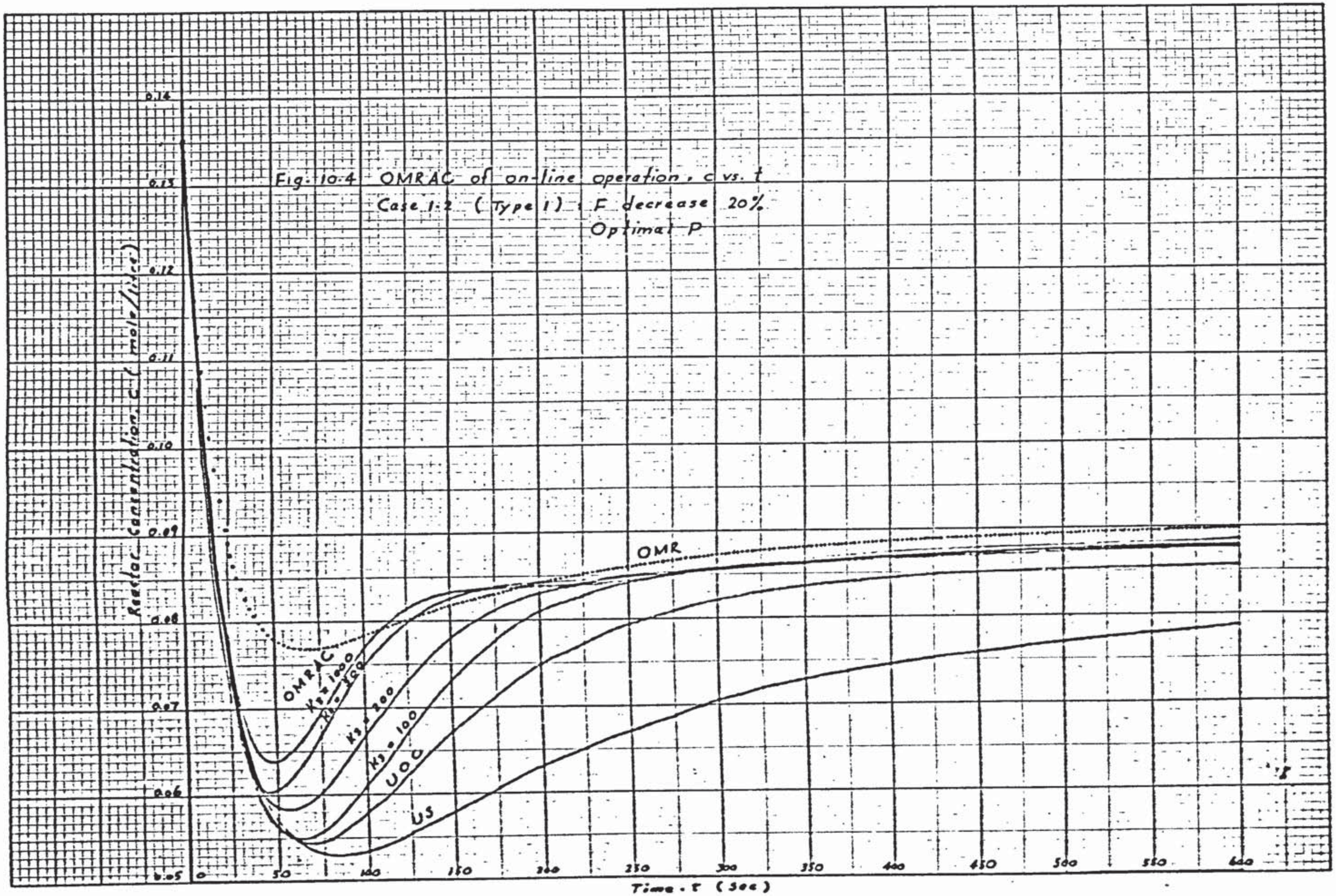

Fig. 10.4 OMRAC of on-line operation, c vs. t
Case 1.2 (Type 1) : F decrease 20%
Optimal P

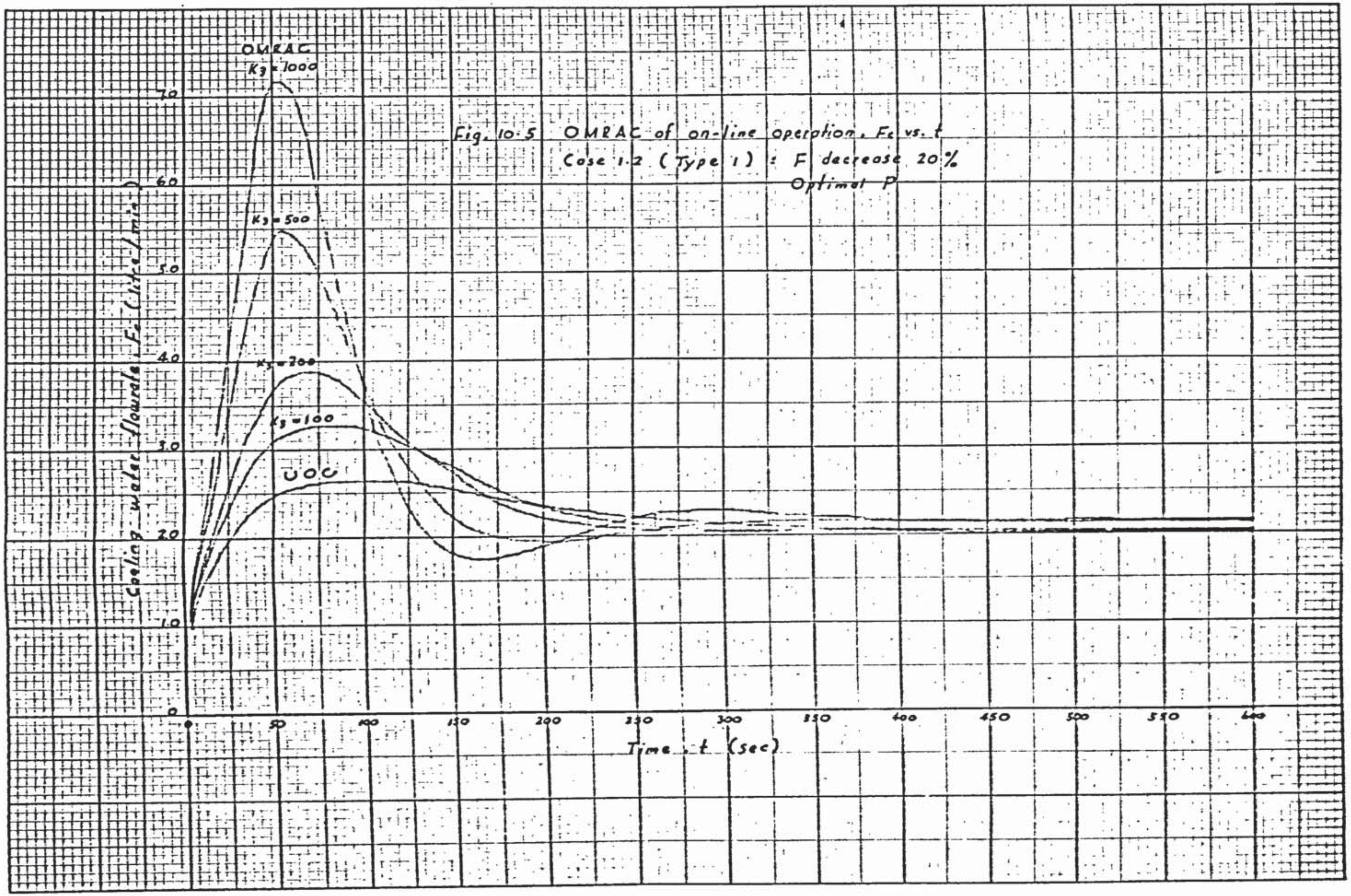

Fig. 10.5 OMRAC of on-line operation, F_c vs. t
Case 1.2 (Type 1) : F decrease 20%
Optimal P

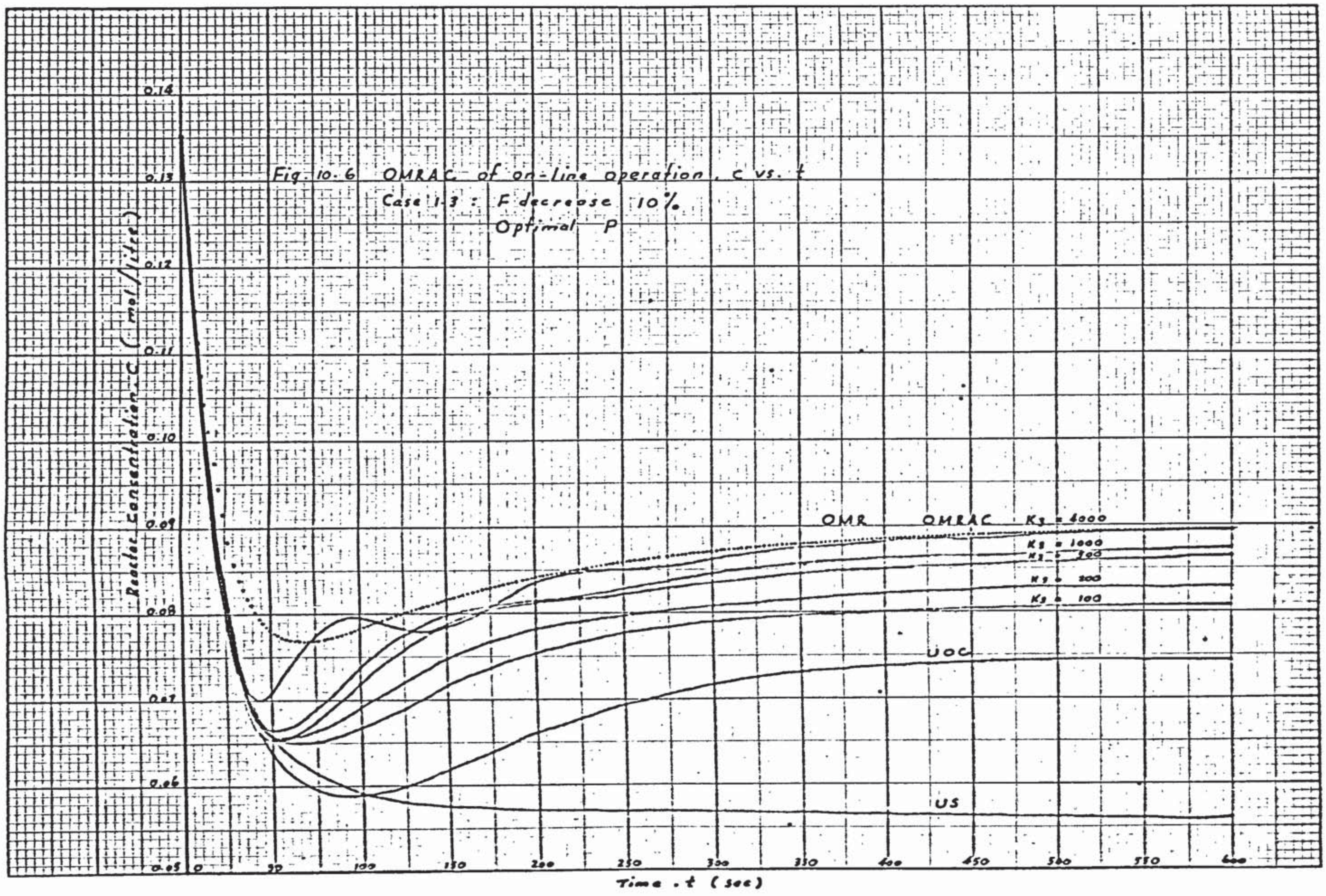

Fig. 10.6 OMRAC of on-line operation, c vs. t
Case 1-3 : F decrease 10%
Optimal P

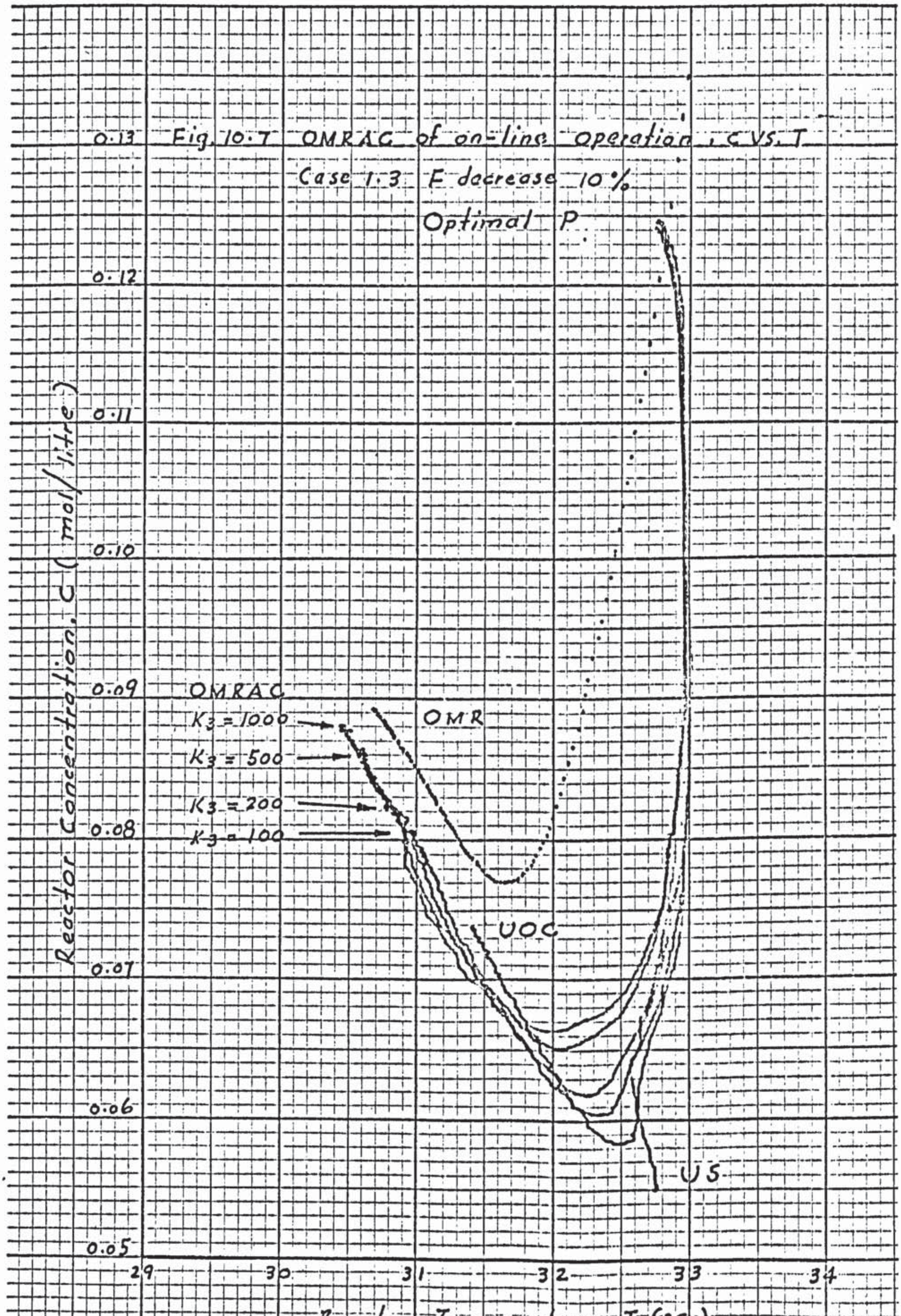
Fig. 10.7 OMRAC of on-line operation, C vs. T
Case 1.3 F decrease 10%
Optimal P
OMRAC
K3 = 1000
K3 = 500
K3 = 200
K3 = 100
OMR
UOC
US
Reactor Concentration, C (mol/litre)
Reactor Temperature, T (°c)
0.13
0.12
0.11
0.10
0.09
0.08
0.07
0.06
0.05
29
30
31
32
33
34

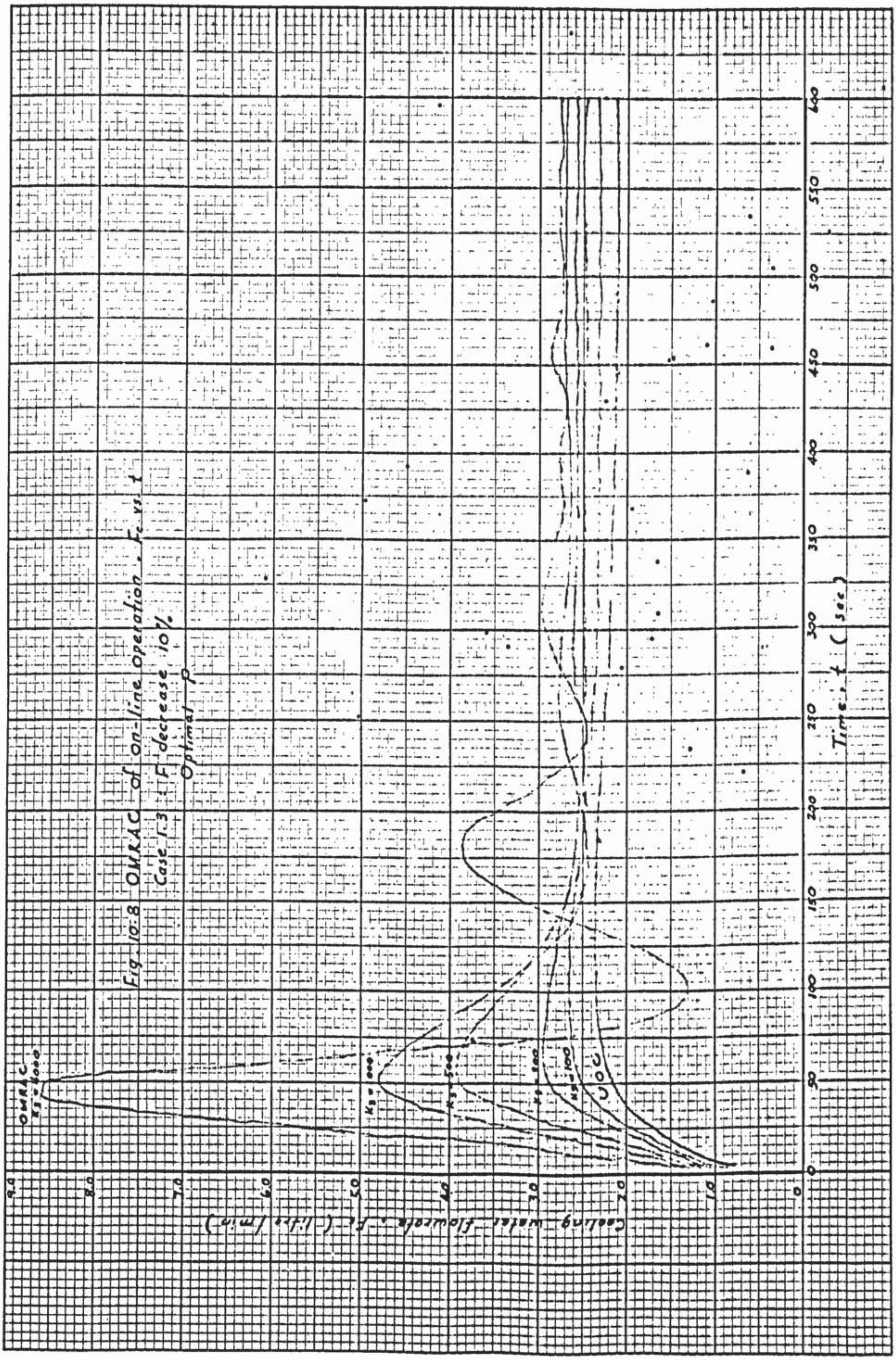

Fig. 10.8 OMRAC of on-line operation, Fc vs. t
Case 1.3 : F decrease 10%
Optimal P

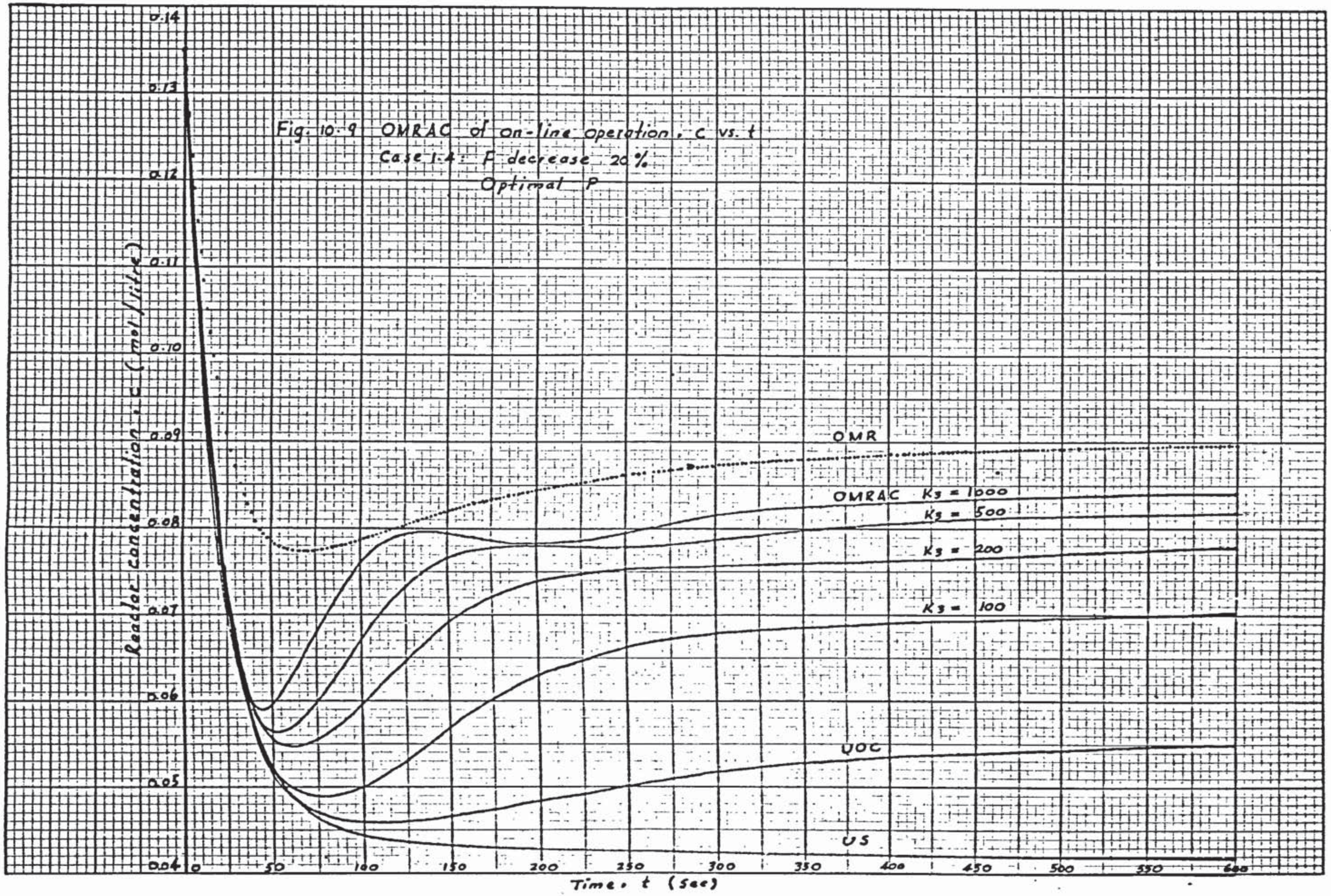

Fig. 10.9 OMRAC of on-line operation, c vs. t
Case 1.4: F decrease 20%
Optimal P

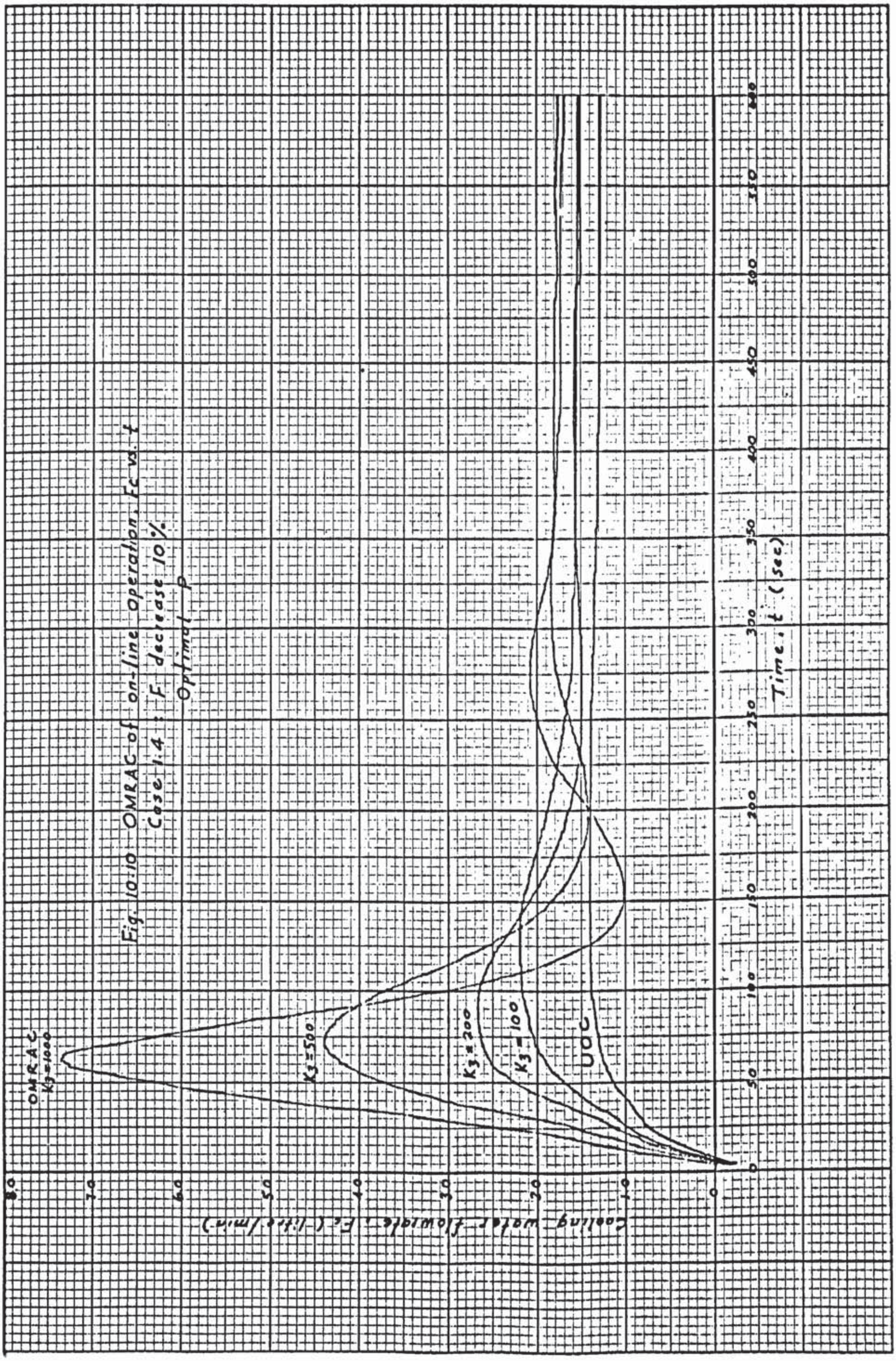

Fig. 10.10 OMRAC of on-line operation, Fc vs. t
Case 1.4: F decrease 10%
Optimal P

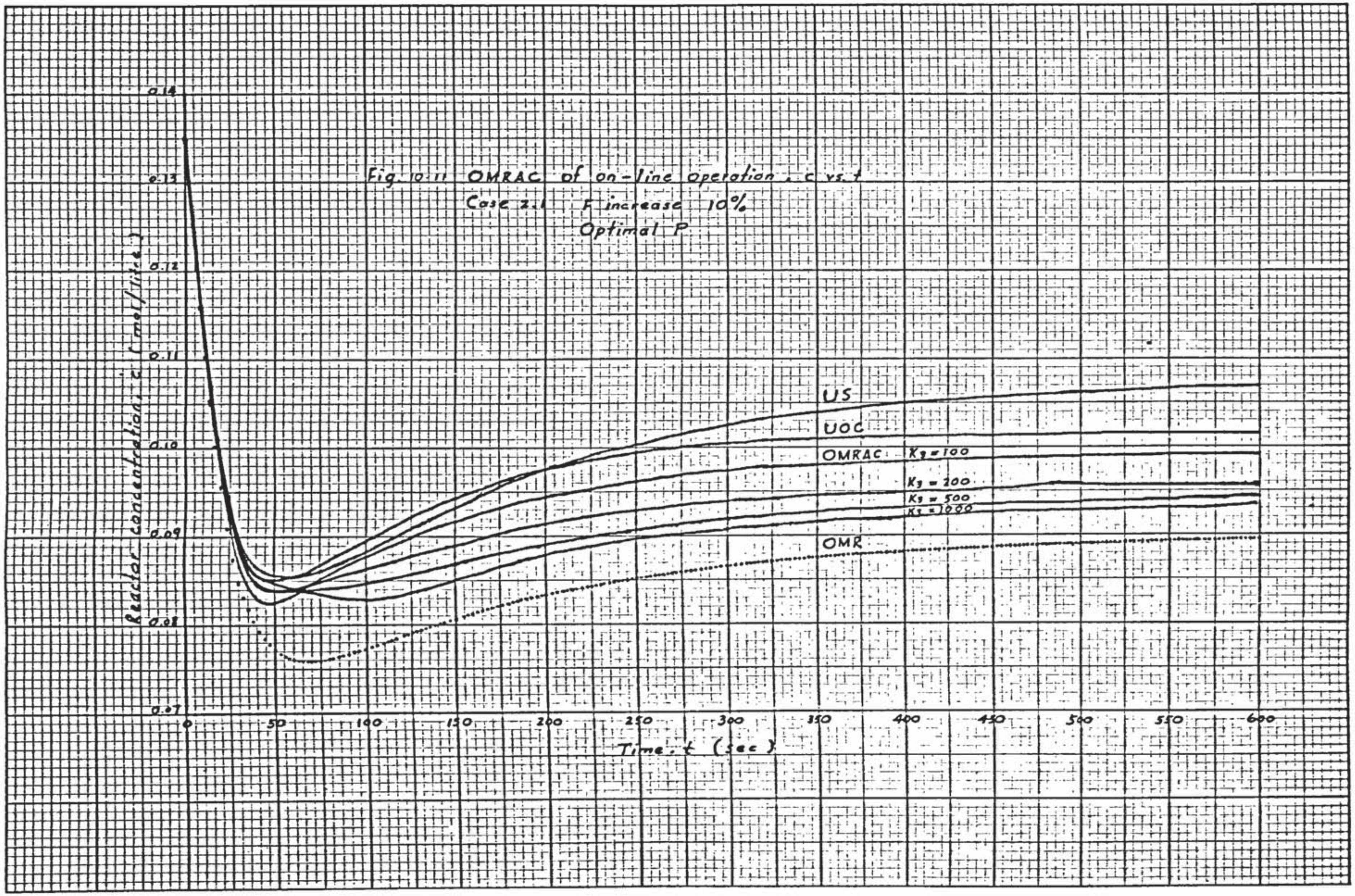

Fig. 10.11 OMRAC of on-line operation, c vs. t
Case 2.1 F increase 10%
Optimal P

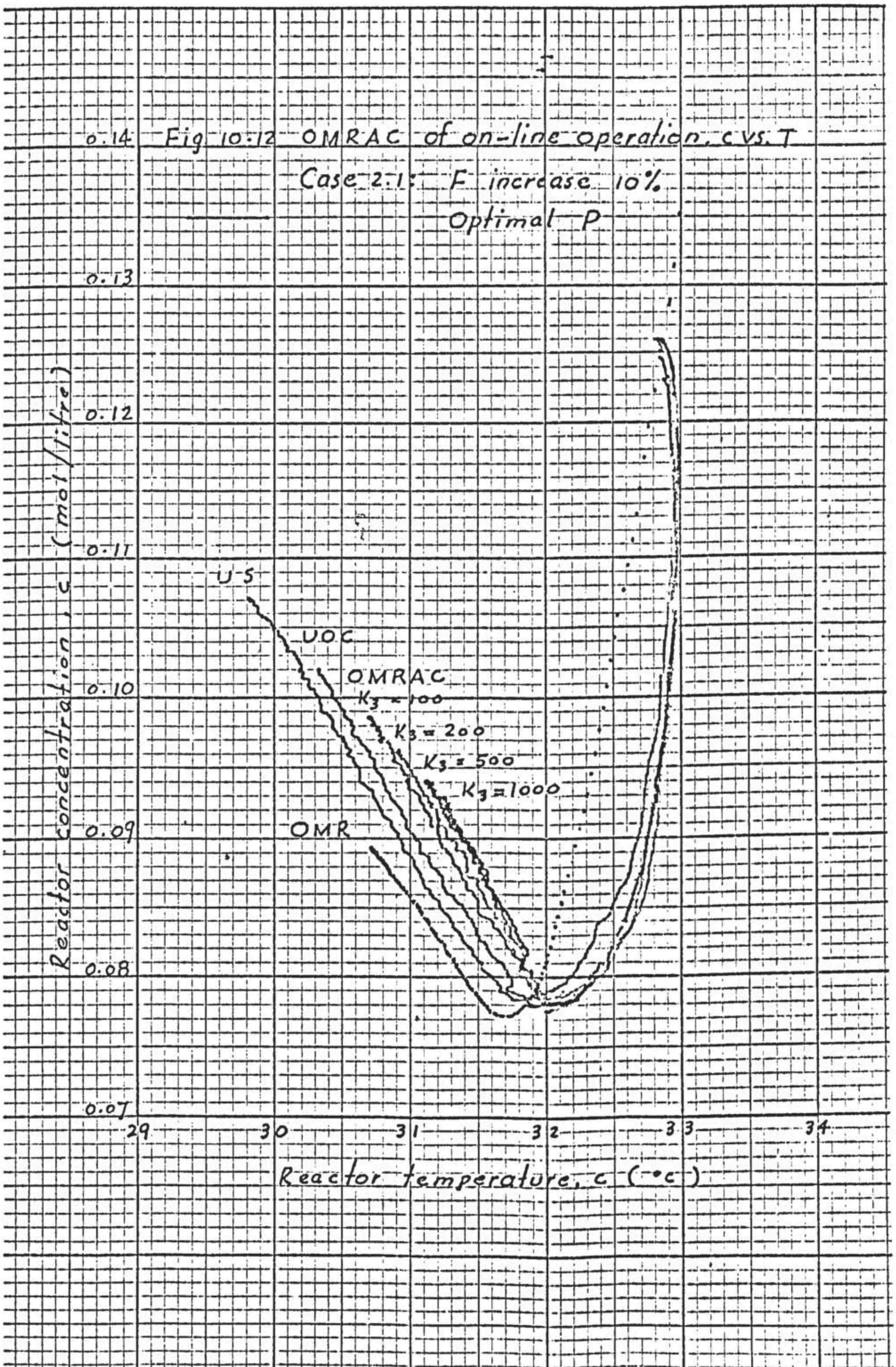
Fig 10:12 OMRAC of on-line operation, c vs. T
Case 2.1: F increase 10%
Optimal P
0.14
0.13
0.12
0.11
0.10
0.09
0.08
0.07
Reactor concentration, c (mol/litre)
U-S
UOC
OMRAC
K3 = 100
K3 = 200
K3 = 500
K3 = 1000
OMR
29
30
31
32
33
34
Reactor temperature, c (°c)

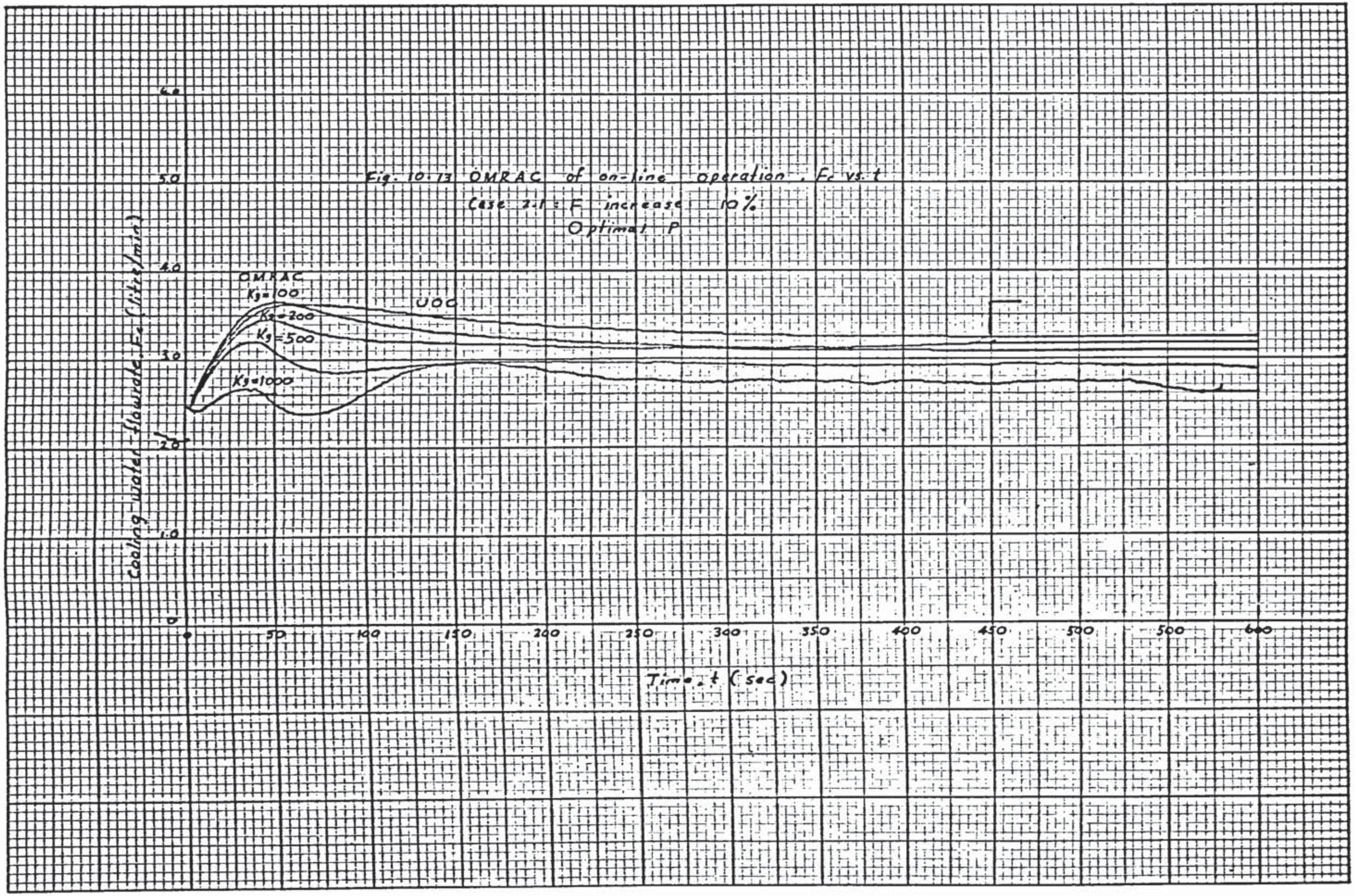

Fig. 10.13 OMRAC of on-line operation, Fc vs. t
Case 2.1: F increase 10%
Optimal P
OMRAC
Kg=100
Kg=200
Kg=500
Kg=1000
UOC
Cooling water flowrate, Fc (liter/min)
Time, t (sec)
0
1.0
2.0
3.0
4.0
5.0
6.0
50
100
150
200
250
300
350
400
450
600

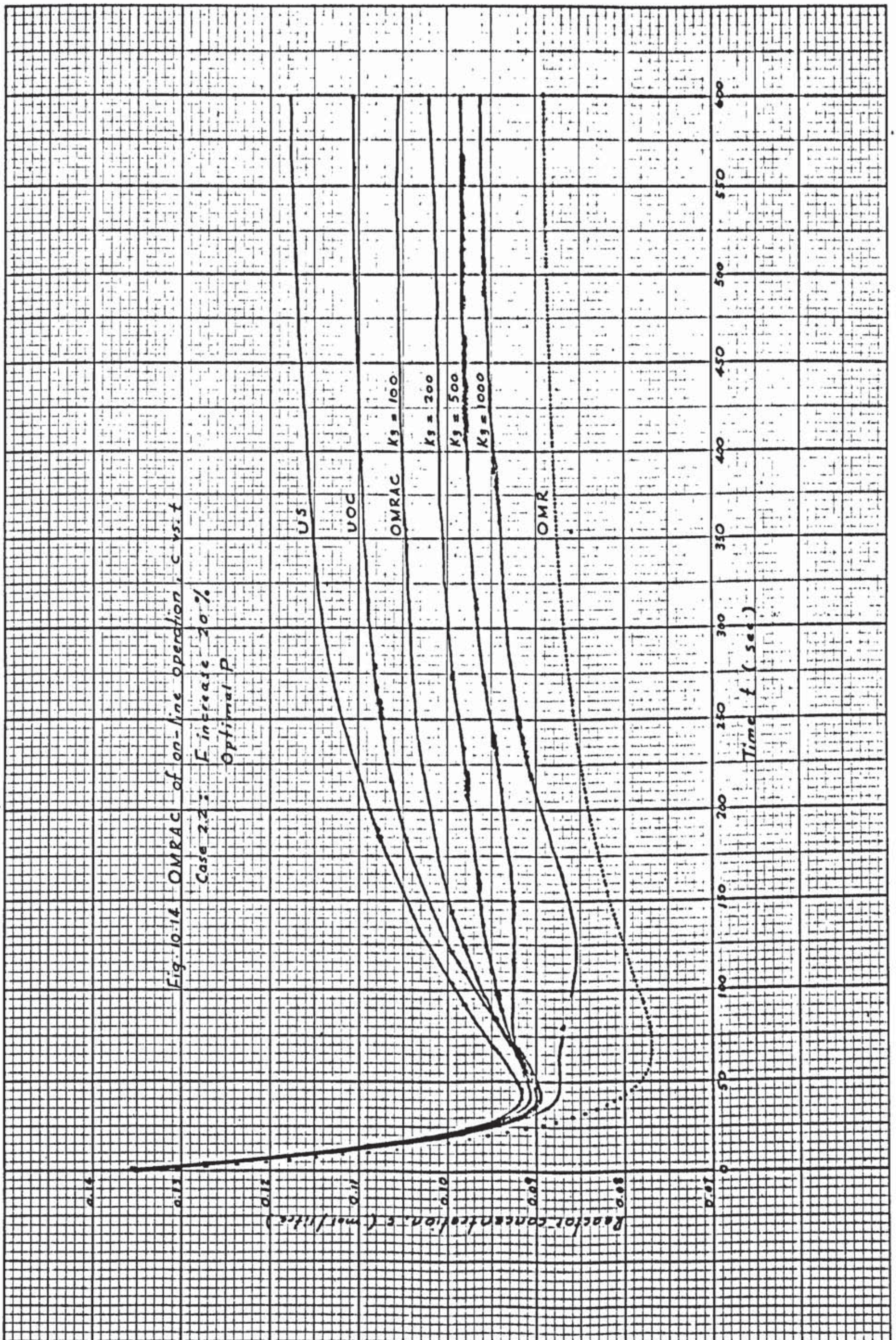

Fig. 10.14 OMRAC of on-line operation, c vs. t

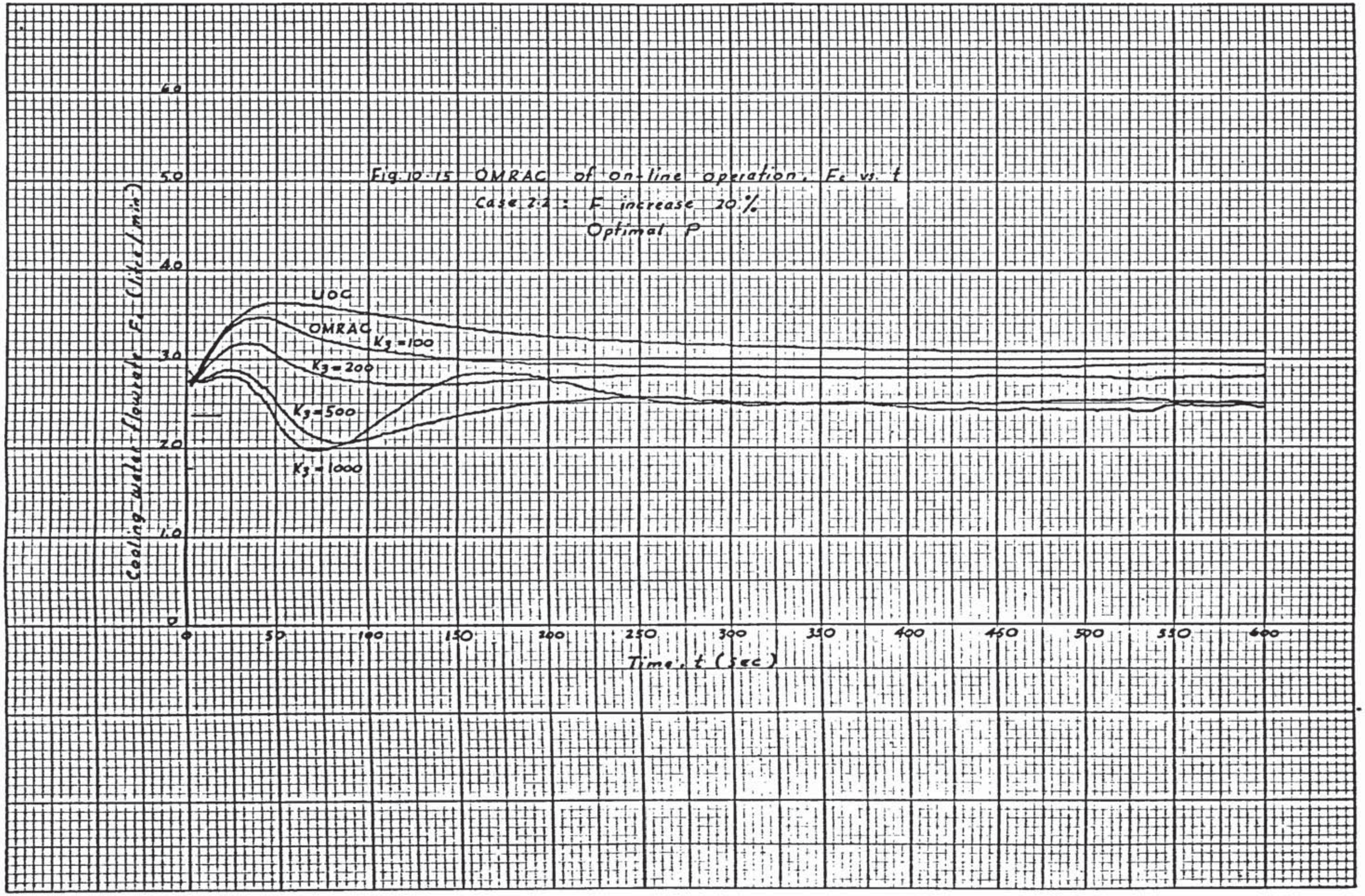

Fig. 10-15 OMRAC of on-line operation, F_c vs. t
Case 2.2 : F increase 20%
Optimal P

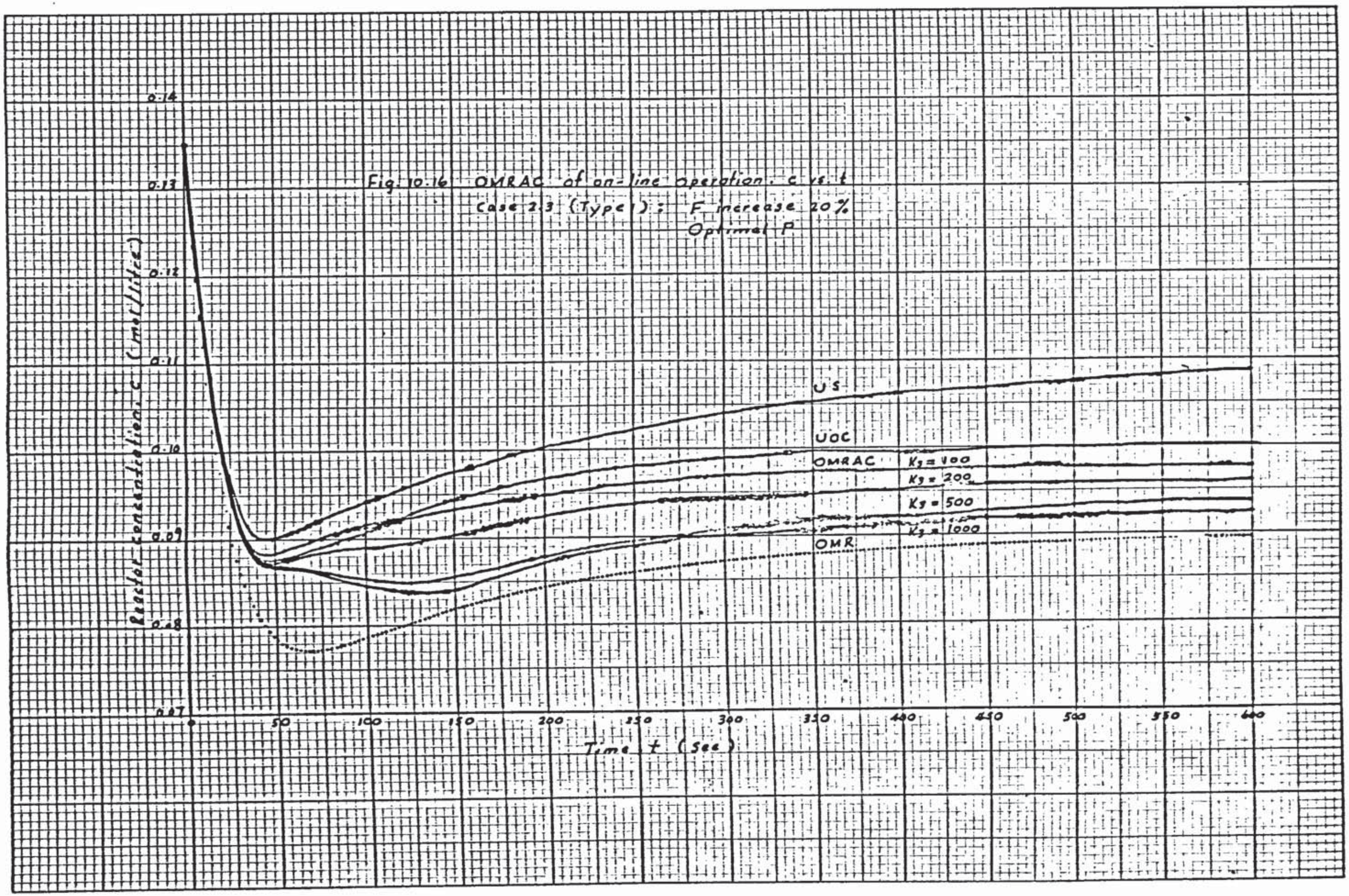

Fig. 10.16 OMRAC of on-line operation: c vs. t
Case 2.3 (Type I): F increase 20%
Optimal P

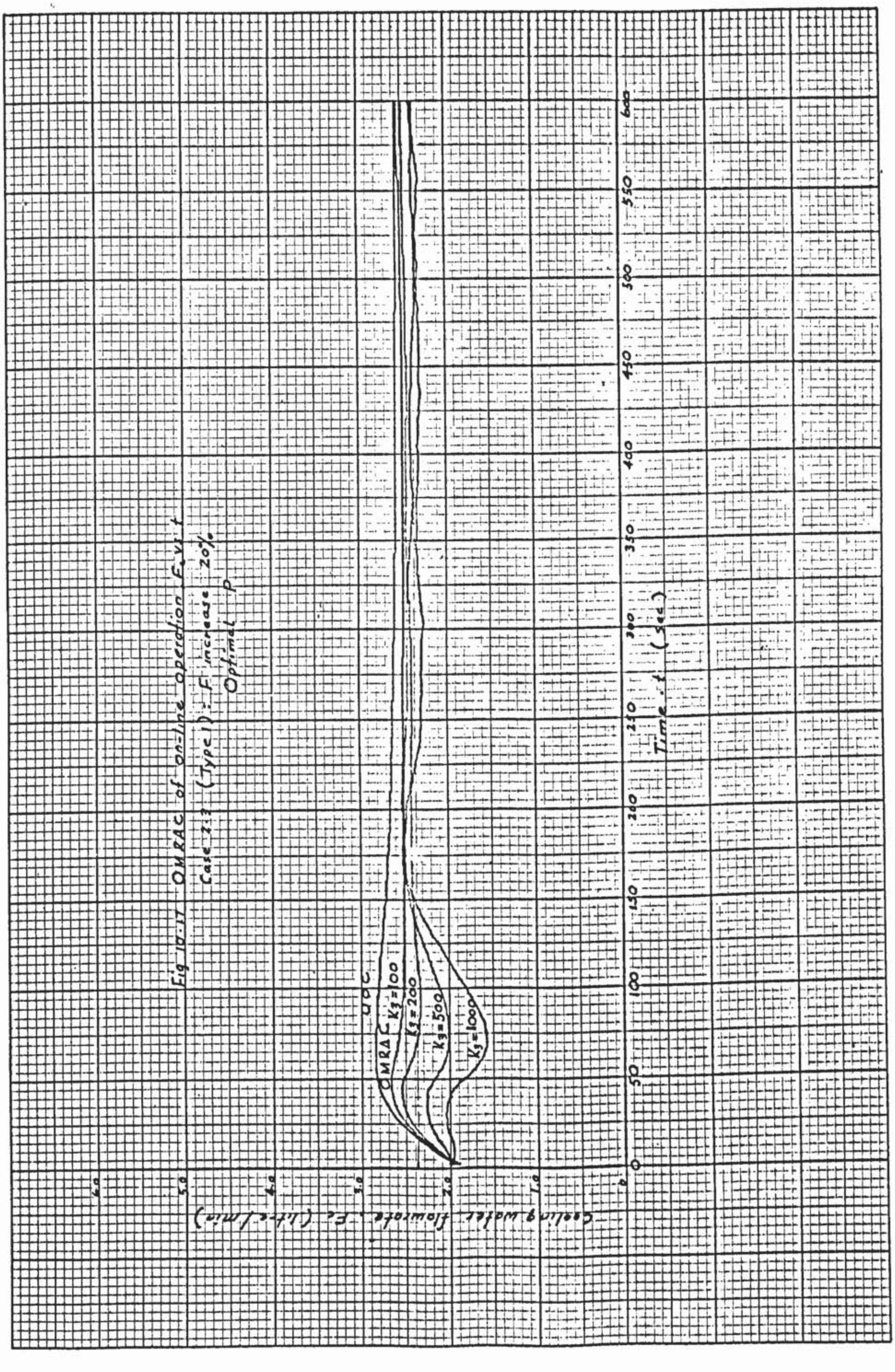

Fig 10.17 OMRAC of on-line operation F_c vs t
Case 2.3 (Type 1): F increase 20%
Optimal P

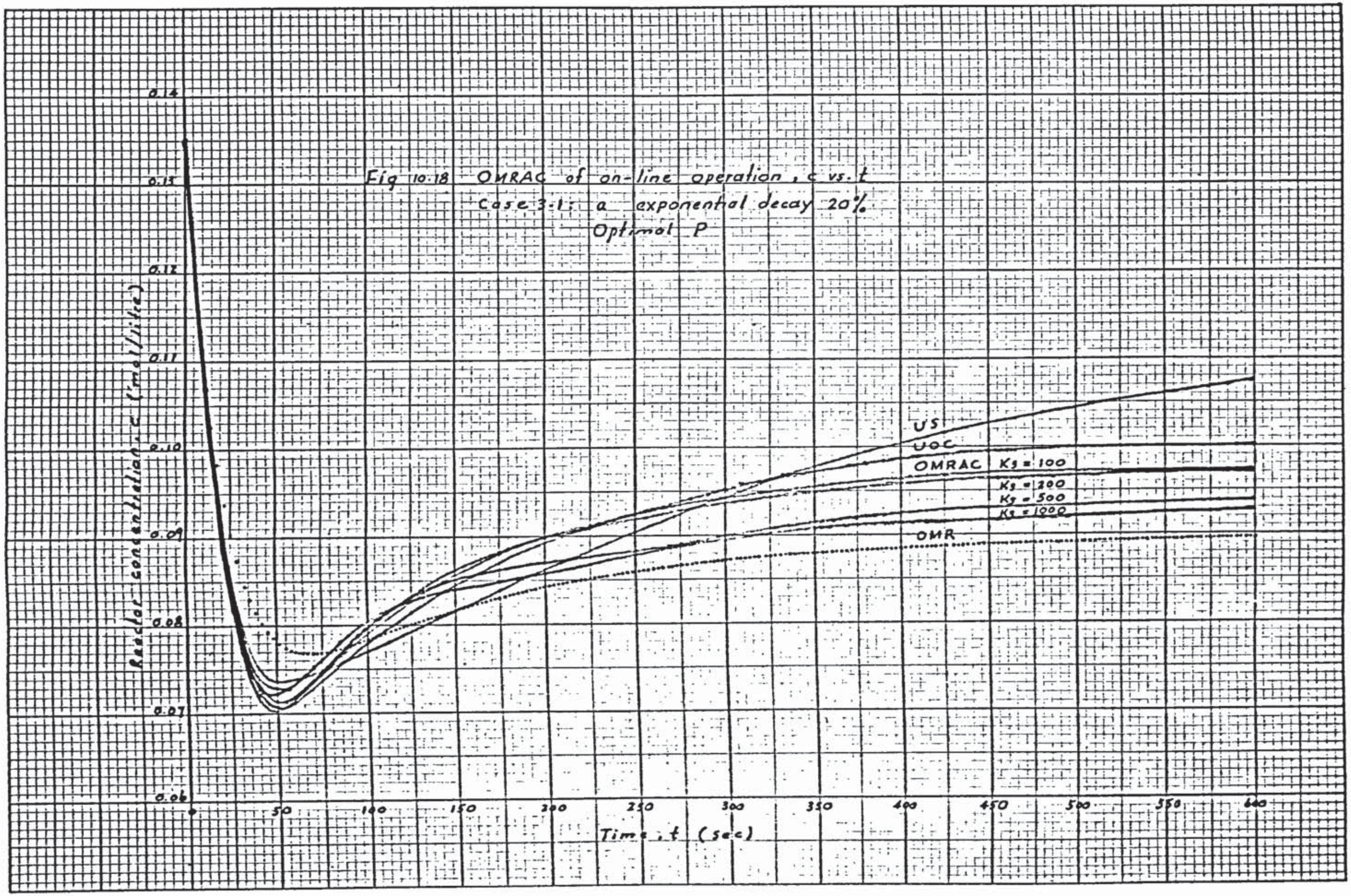

Fig 10.18 OMRAC of on-line operation, c vs. t
Case 3.1: a exponential decay 20%
Optimal P

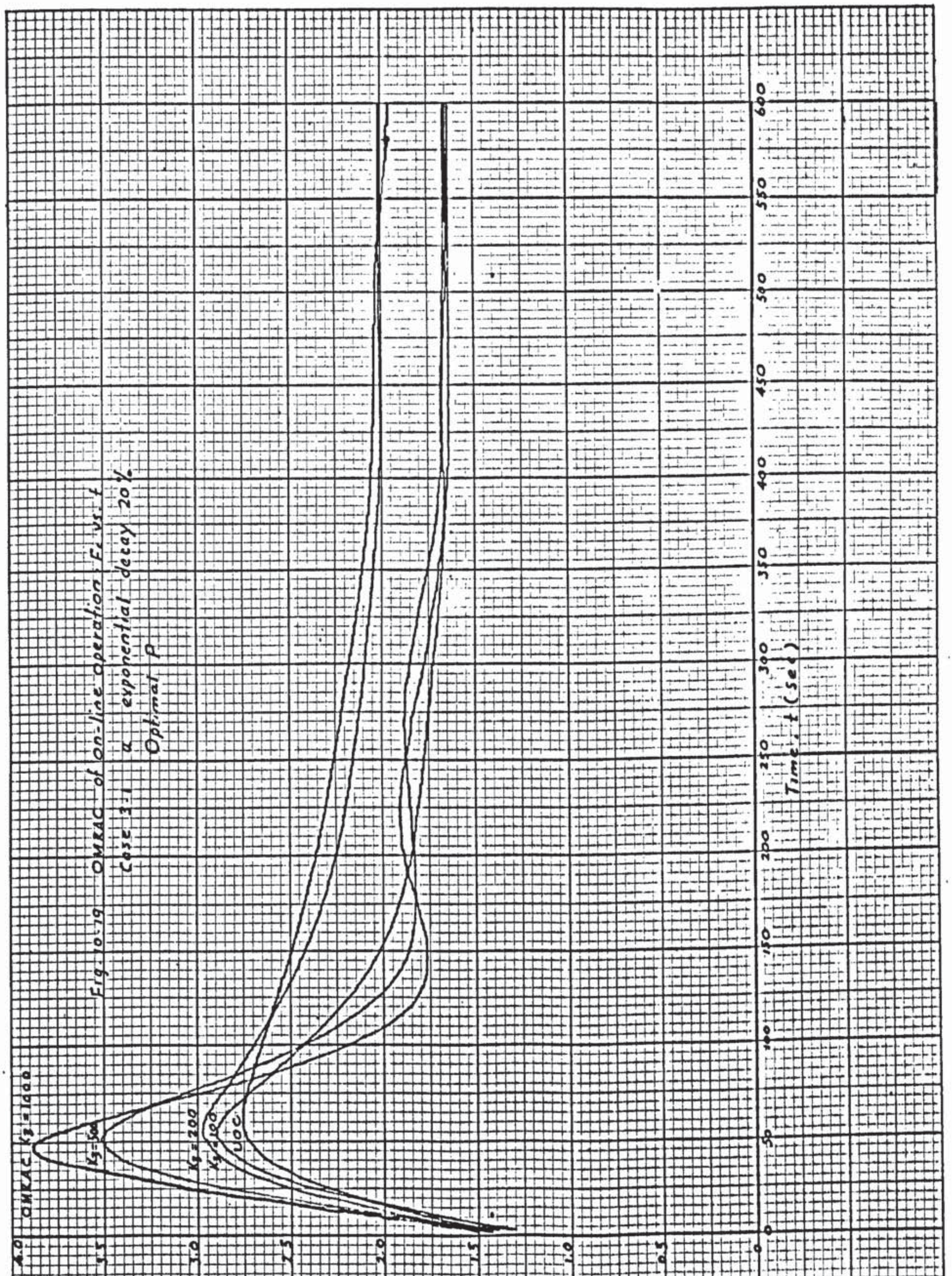
Fig. 10.19 OMRAC of on-line operation F_c vs. t
Case 3.1 α exponential decay 20%
Optimal P
OMRAC K3=1000
K3=500
K3=200
K3=100
UOC
Cooling water flowrate, Fc (liter/min)
Time, t (sec)
0
0.5
1.0
1.5
2.0
2.5
3.0
3.5
4.0
0
50
100
150
200
250
300
350
400
450
500
550
600

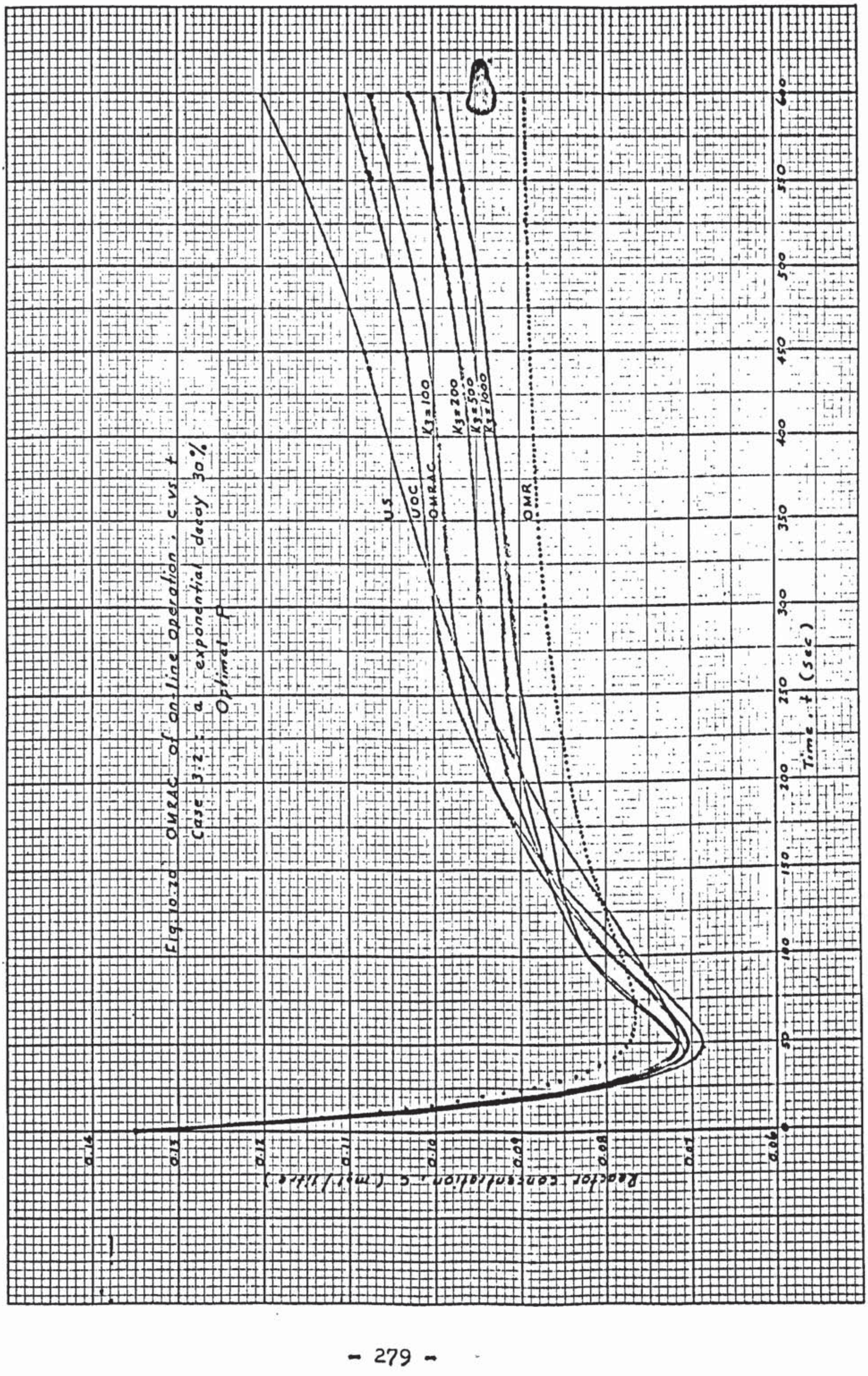

Fig.10.20 OMRAC of on-line operation, c vs. t
Case 3.2: a exponential decay 30%
Optimal p

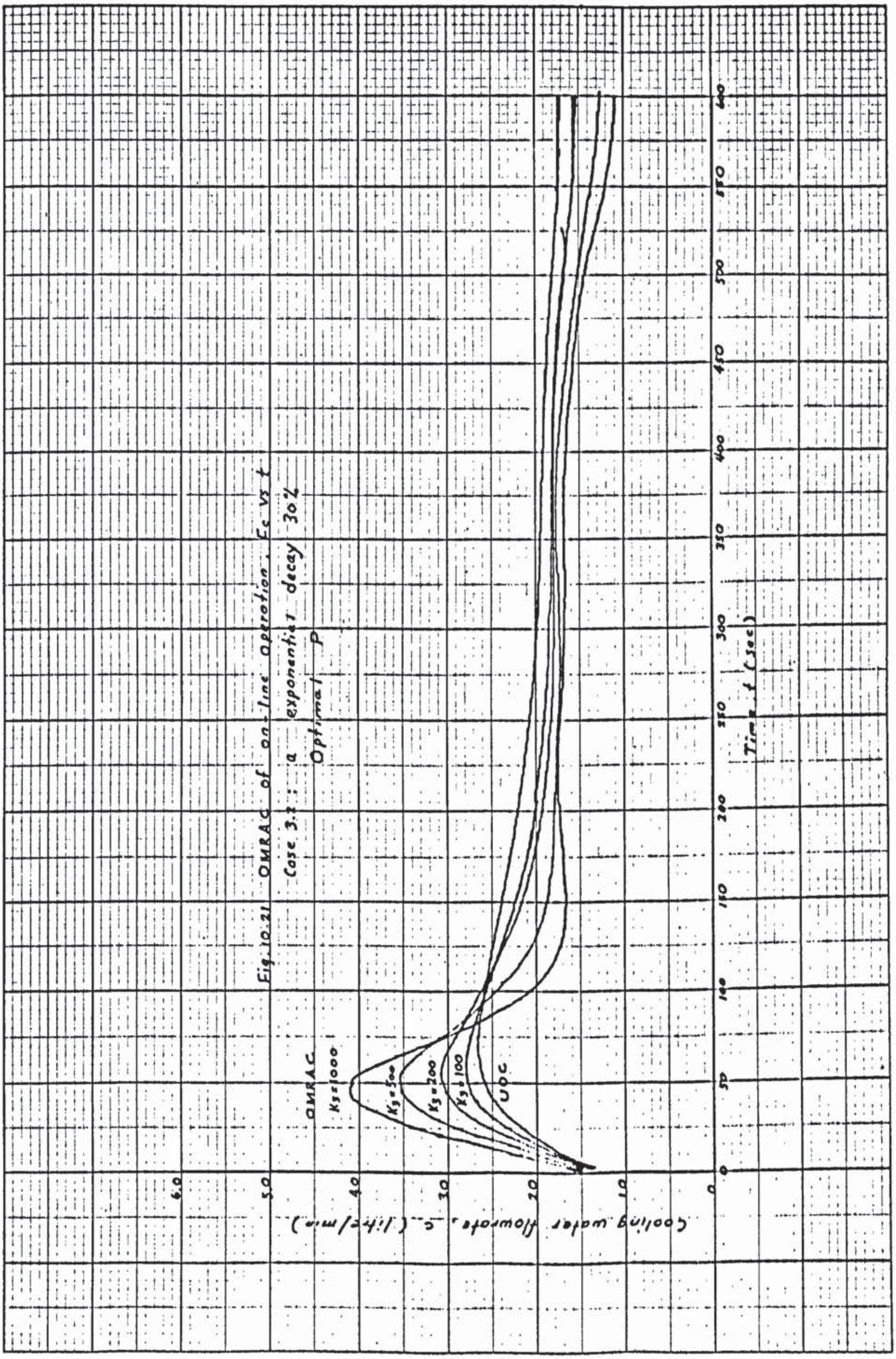

Fig. 10.21 OMRAC of on-line operation, Fc vs t
Case 3.2: a exponential decay 30%
Optimal P

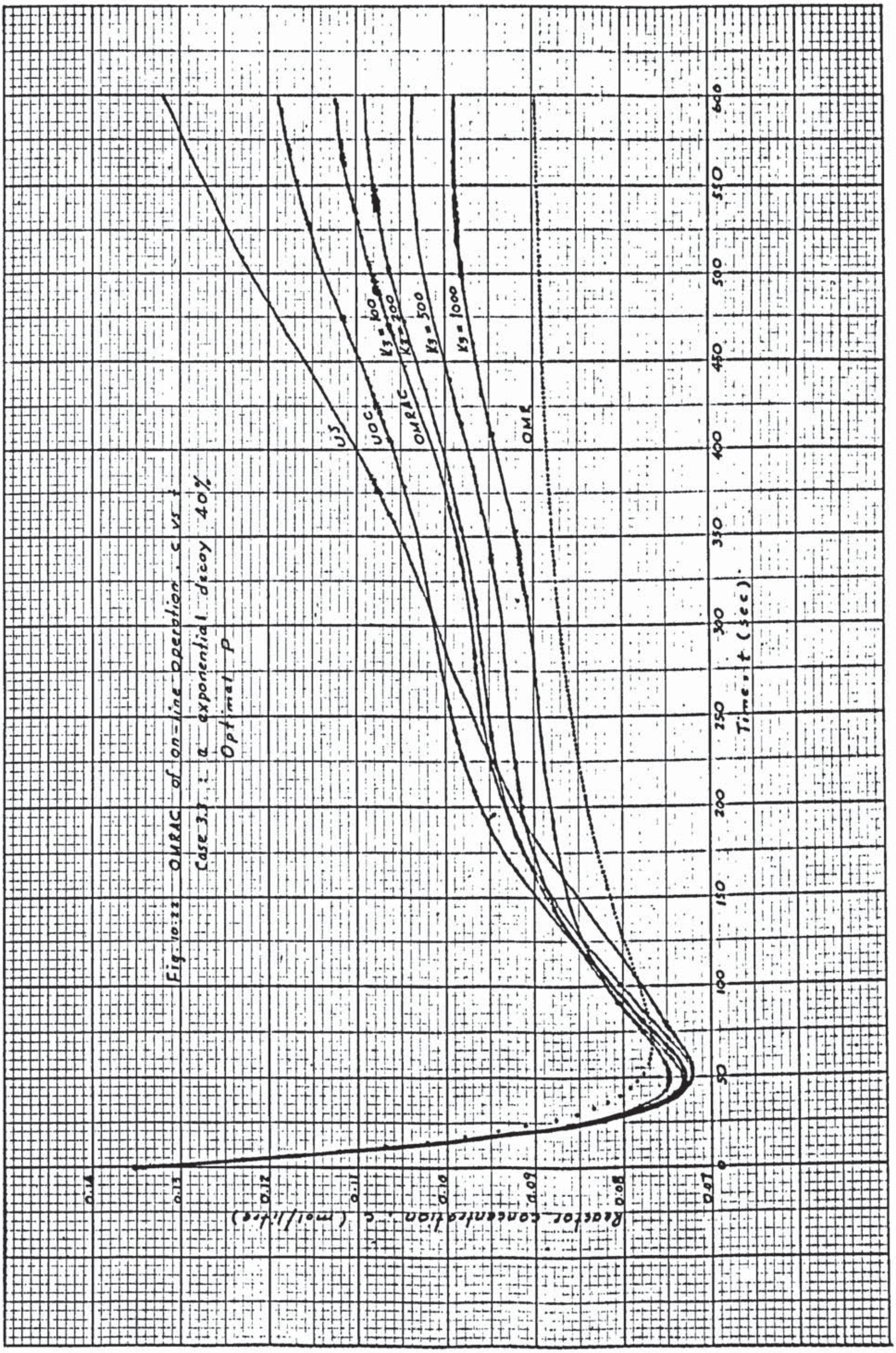

Fig. 10.22 OMRAC of on-line operation. c vs t
Case 3.3 : a exponential decay 40%
Optimal P
US
UOC
OMRAC
OMS
K3 = 100
K3 = 200
K3 = 500
K3 = 1000
Time: t (sec)
Reactor concentration: c (mol/litre)
0
50
100
150
200
250
300
350
400
450
500
550
600
0.14
0.13
0.12
0.11
0.10
0.09
0.08
0.07

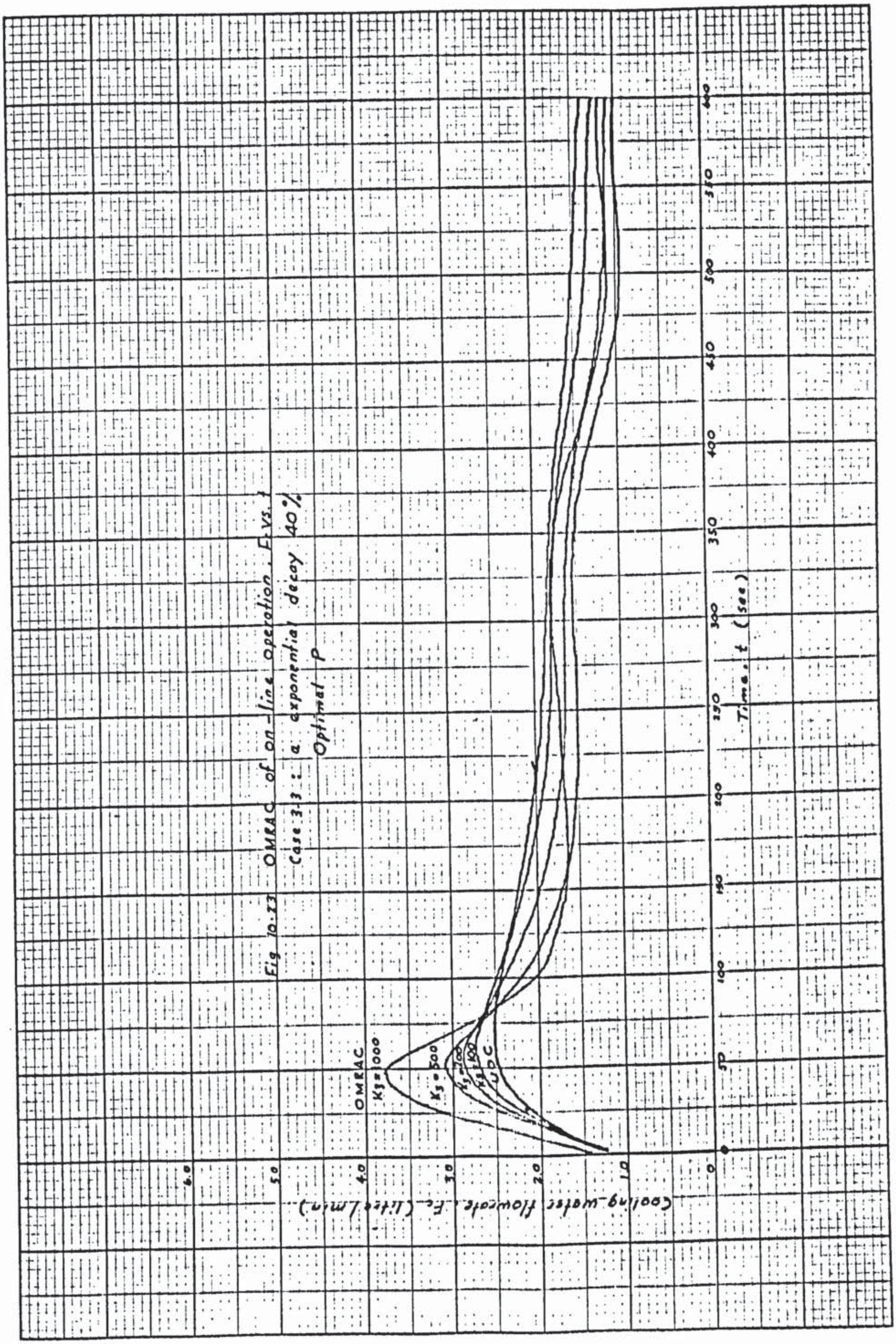

Fig 10.33 OMRAC of on-line operation, F_c vs. t
Case 3.3 : a exponential decay 40%
Optimal P
OMRAC
K_s=1000
K_s=500
K_s=200
K_s=100
UDC
Time, t (sec)
Cooling water flowrate, F_c (liter/min)
0
50
100
150
200
250
300
350
400
450
500
550
600
1.0
2.0
3.0
4.0
5.0
6.0

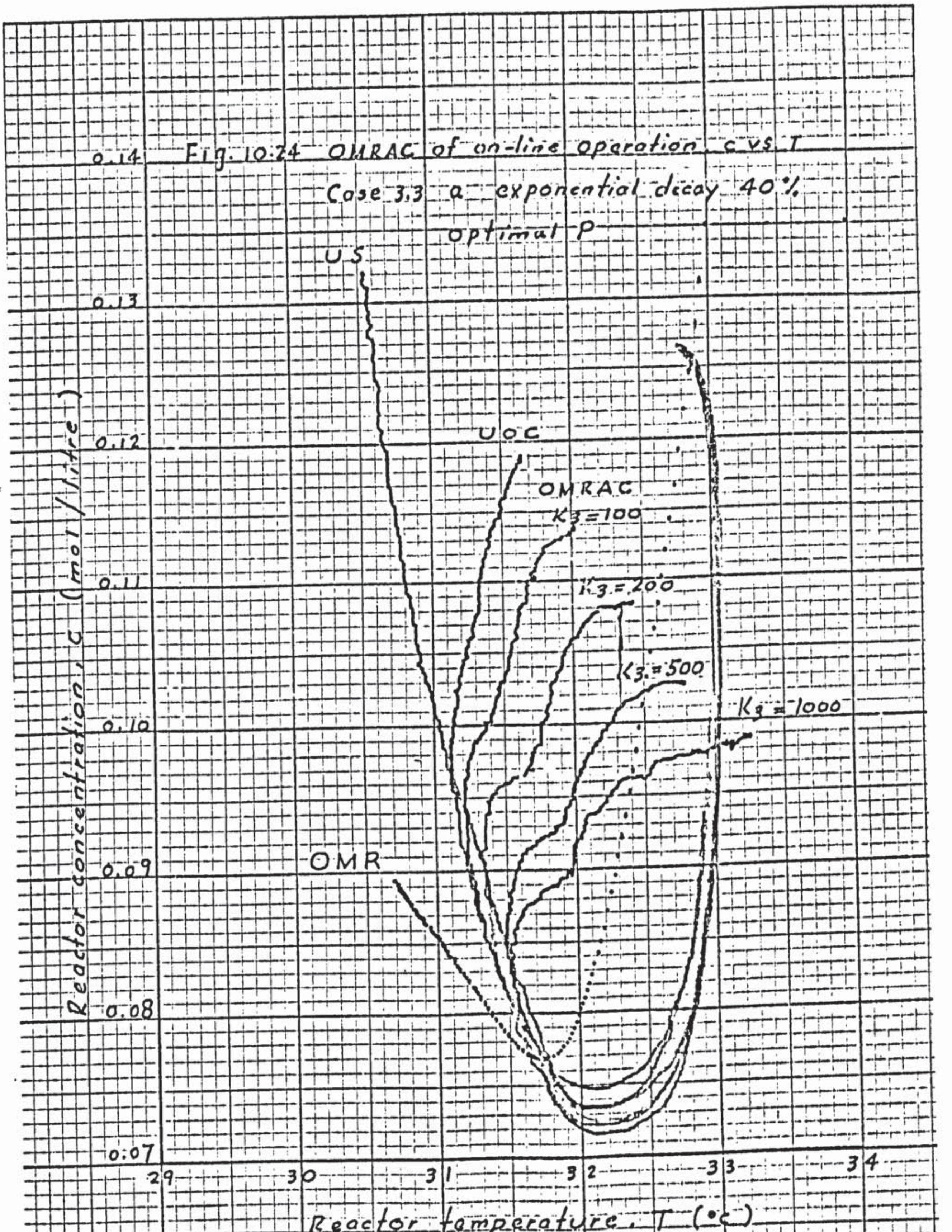
Fig. 10.24 OMRAC of on-line operation. c vs. T
Case 3.3 a exponential decay 40%
optimal P
US
UOC
OMRAC
K3=100
K3=200
K3=500
K3=1000
OMR
0.14
0.13
0.12
0.11
0.10
0.09
0.08
0:07
29
30
31
32
33
34
Reactor concentration, c (mol/litre)
Reactor temperature, T (°c)

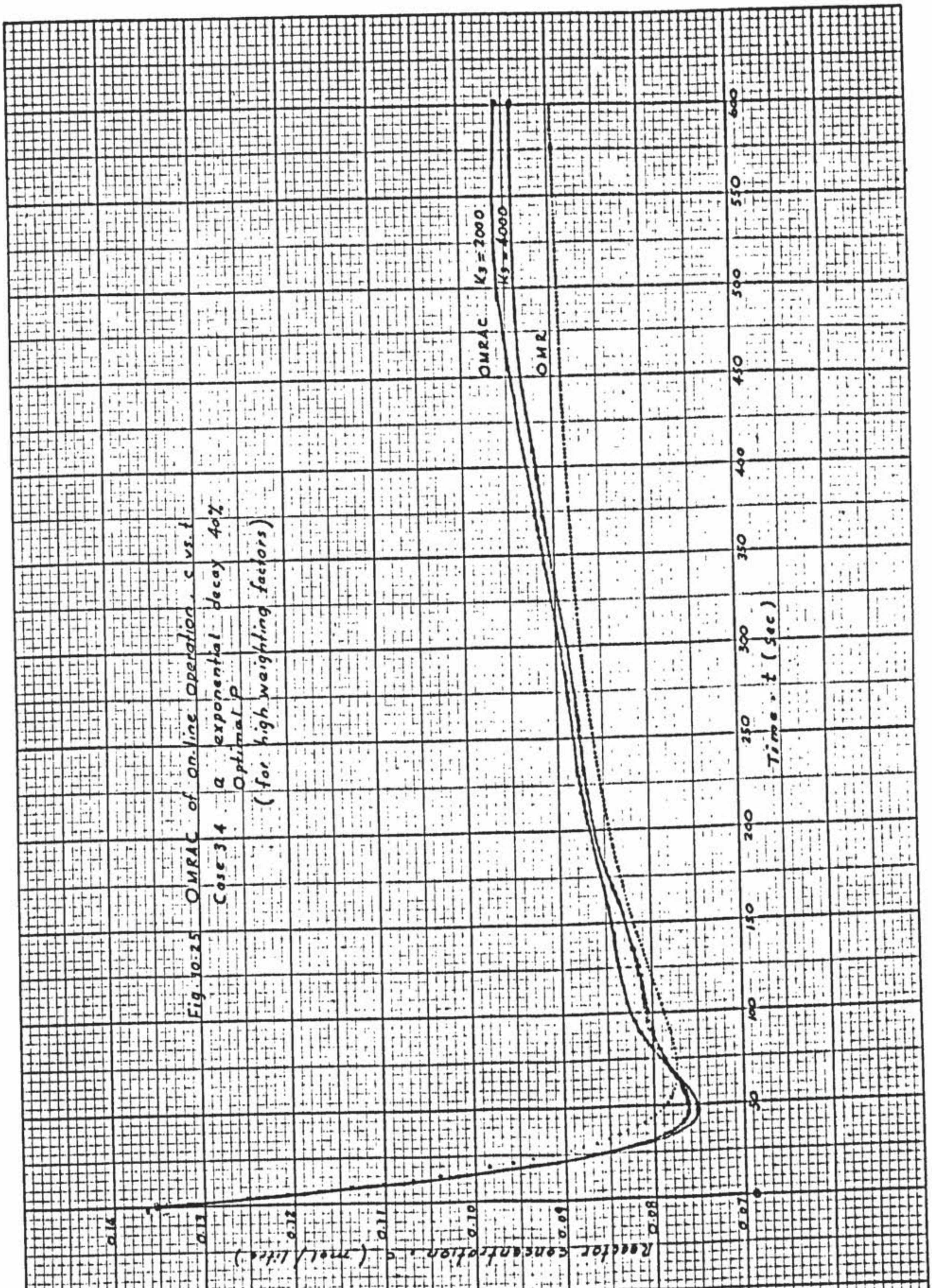

Fig. 10.25 OMRAC of on-line operation, c vs. t
Case 3.4 a exponential decay 40%
Optimal ρ
(for high weighting factors)

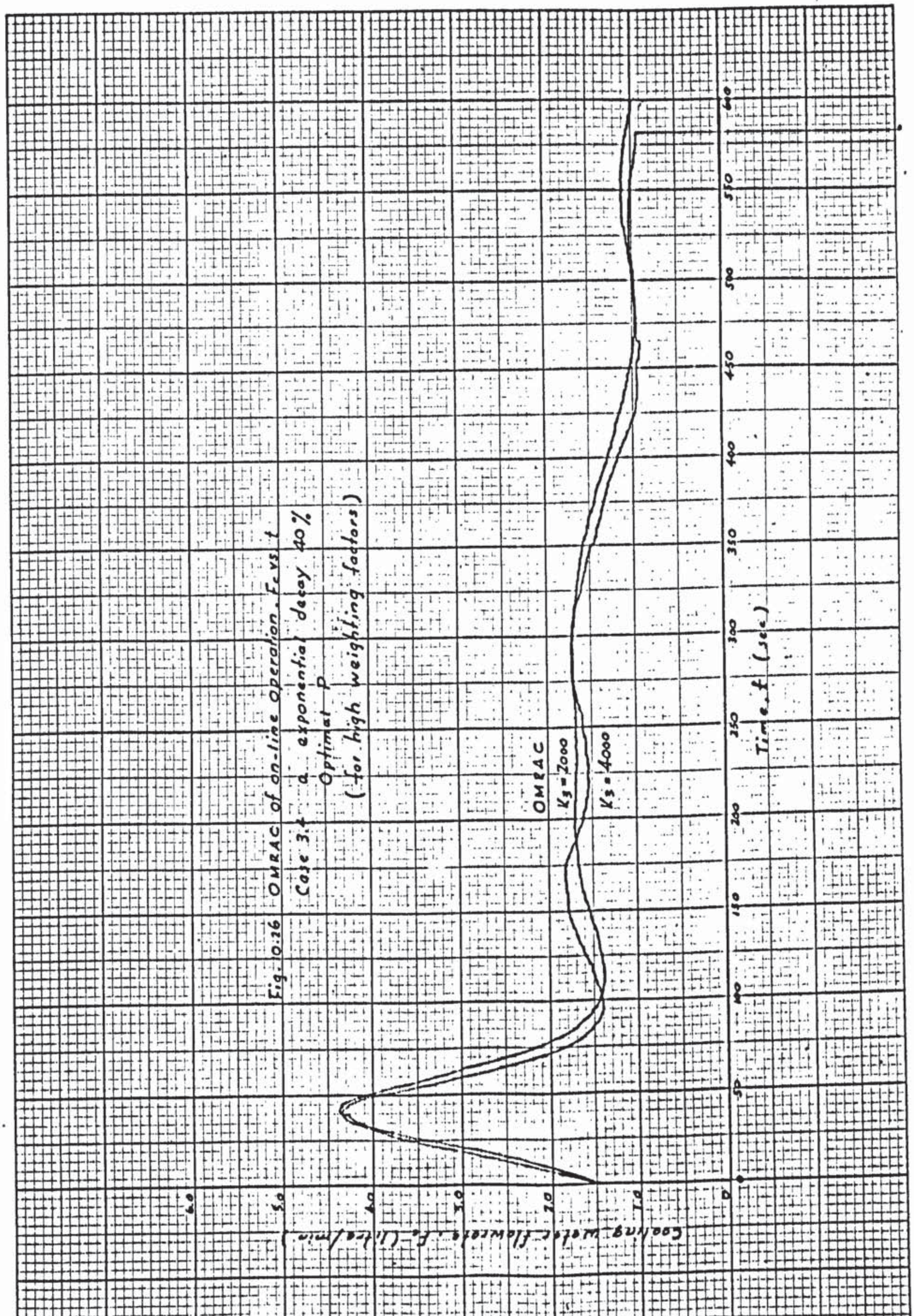

Fig. 0.26 OMRAC of on-line operation, Fc vs. t
Case 3.4 a. exponential decay 40%
Optimal P
(for high weighting factors)
OMRAC
K3 = 2000
K3 = 4000
Time, t (sec)
0
50
100
150
200
250
300
350
400
450
500
550
600
1.0
2.0
3.0
4.0
5.0
6.0

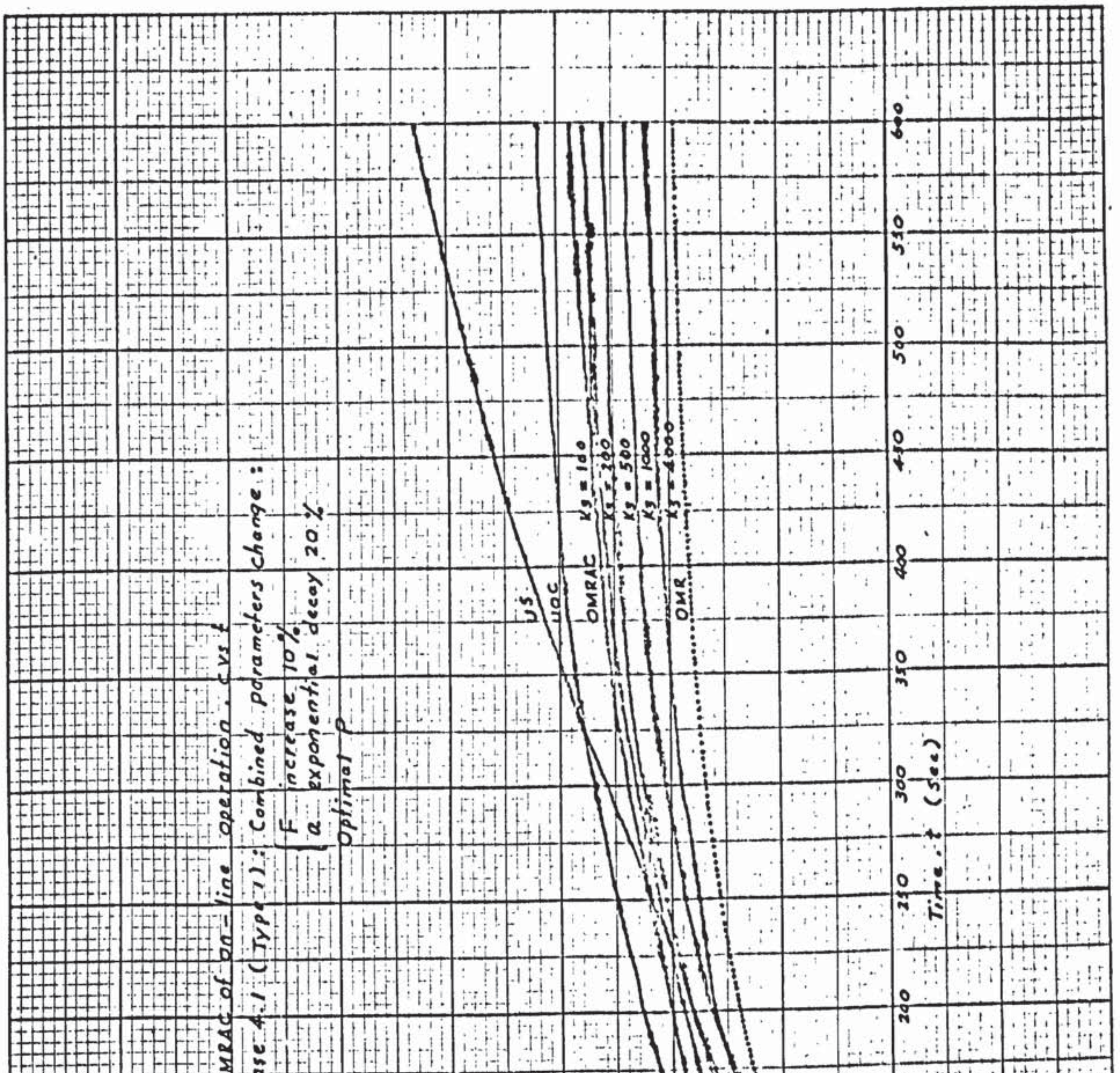

Fig. 10.37 OMRAC of on-line operation, C vs t

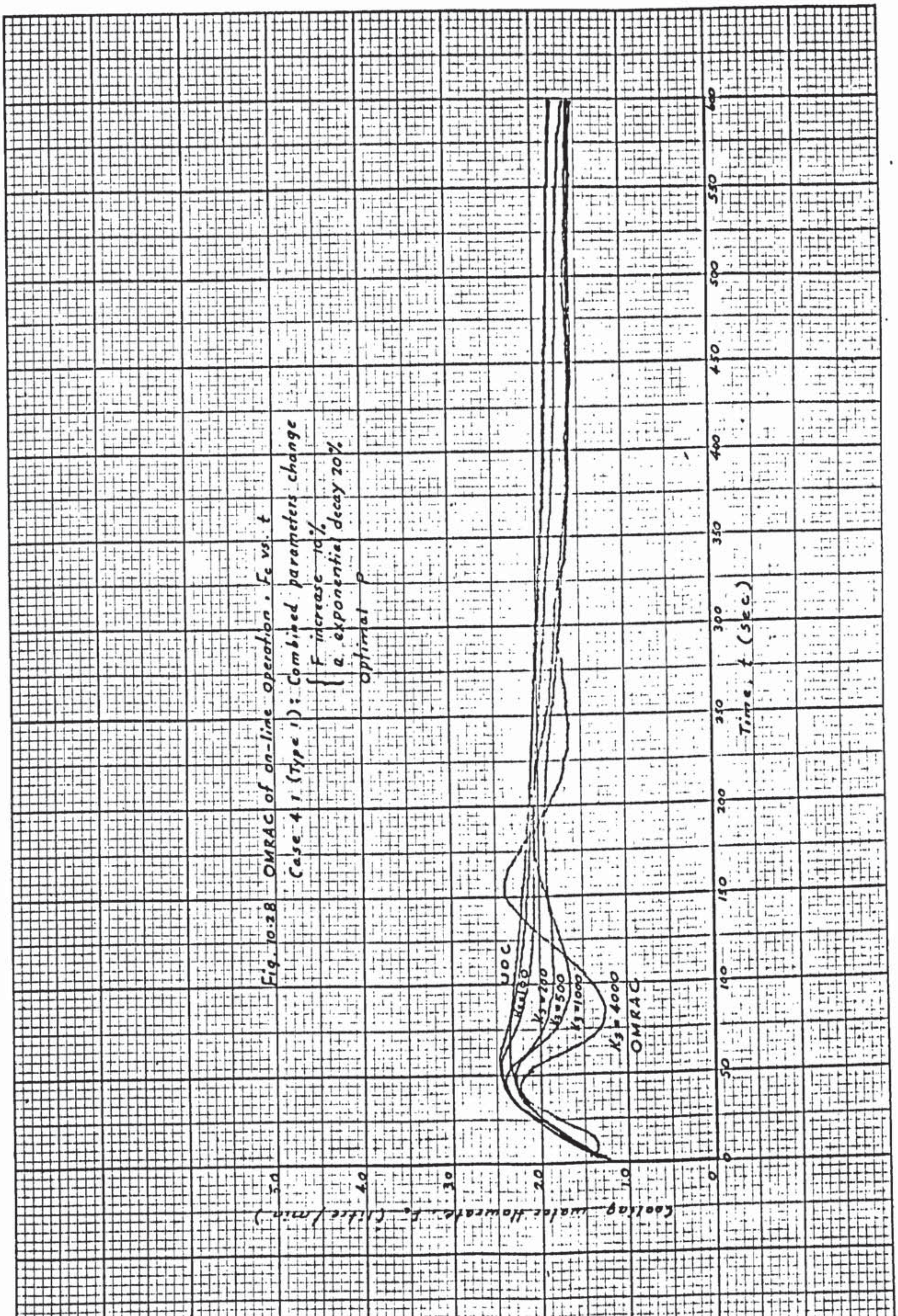

Fig. 10.28 OMRAC of on-line operation. Fc vs. t

Case 4.1 (Type I): Combined parameters change

F increase 10%

a exponential decay 20%

Optimal ρ

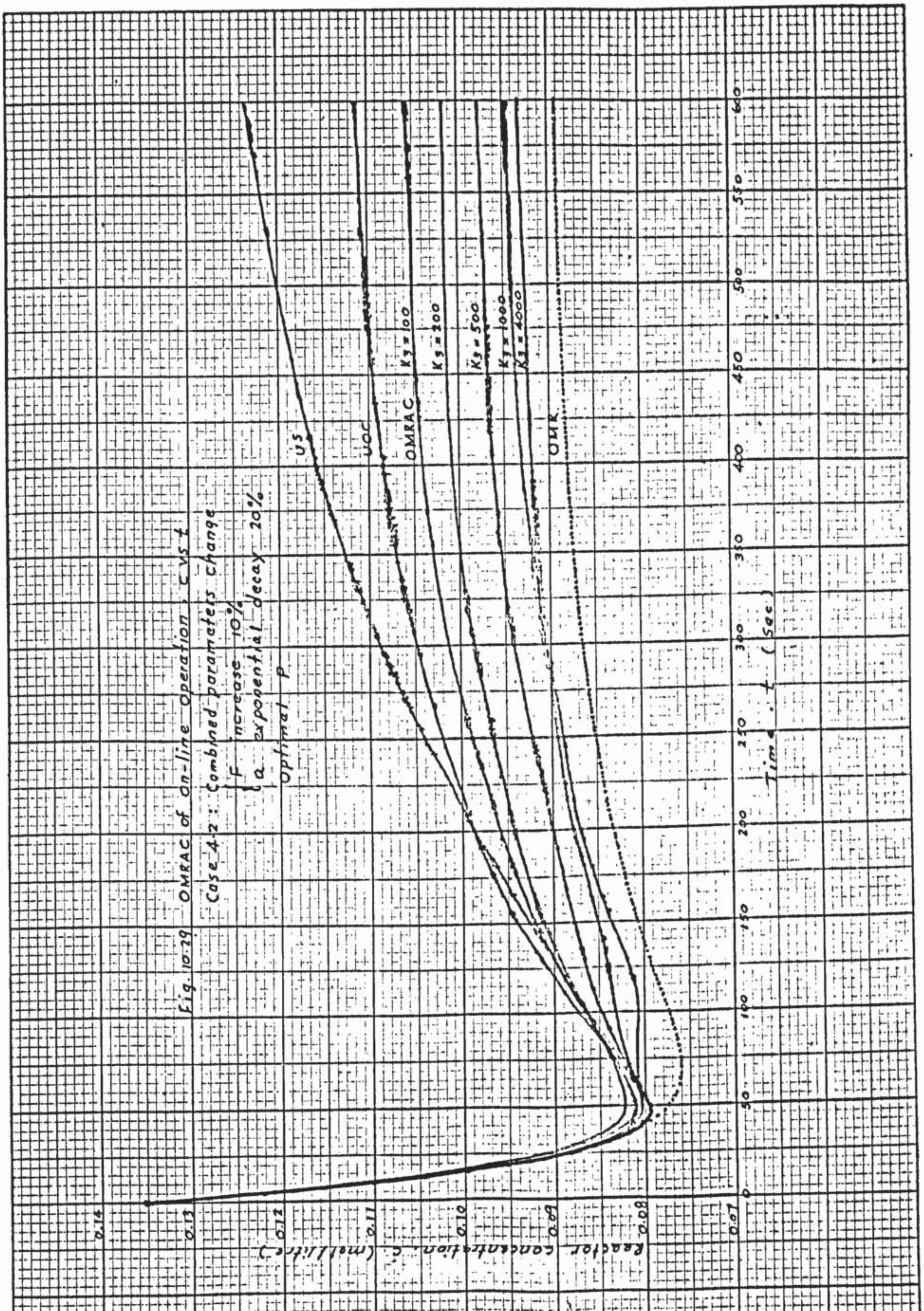

Fig. 10.29 OMRAC of on-line operation C vs t
Case 4.2: Combined parameters change
F increase 10%
a exponential decay 20%
Optimal P
US
UOC
OMRAC
OMRAC K3 = 100
K3 = 200
K3 = 500
K3 = 1000
K3 = 4000
OUK
Reactor concentration, C (mol/litre)
Time, t (sec)
0.07
0.08
0.09
0.10
0.11
0.12
0.13
0.14
0
50
100
150
200
250
300
350
400
450
500
550
600

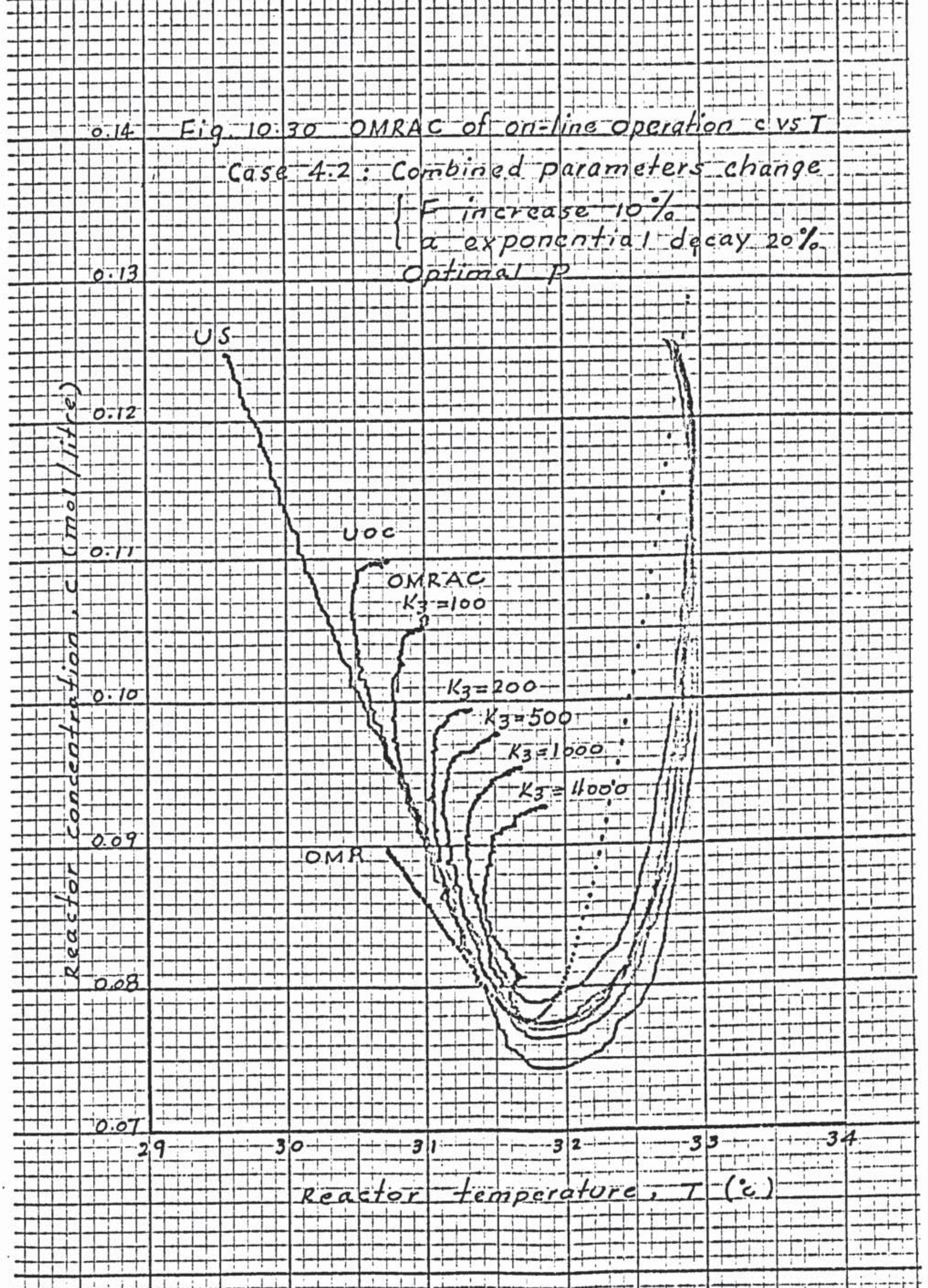
Fig. 10.30 OMRAC of on-line operation c vs T
Case 4.2 : Combined parameters change
F increase 10%
a exponential decay 20%
Optimal P
US
UOC
OMRAC
K3=100
K3=200
K3=500
K3=1000
K3=11000
OMR
0.14
0.13
0.12
0.11
0.10
0.09
0.08
0.07
29
30
31
32
33
34
Reactor concentration, c (mol/litre)
Reactor temperature, T (°c)

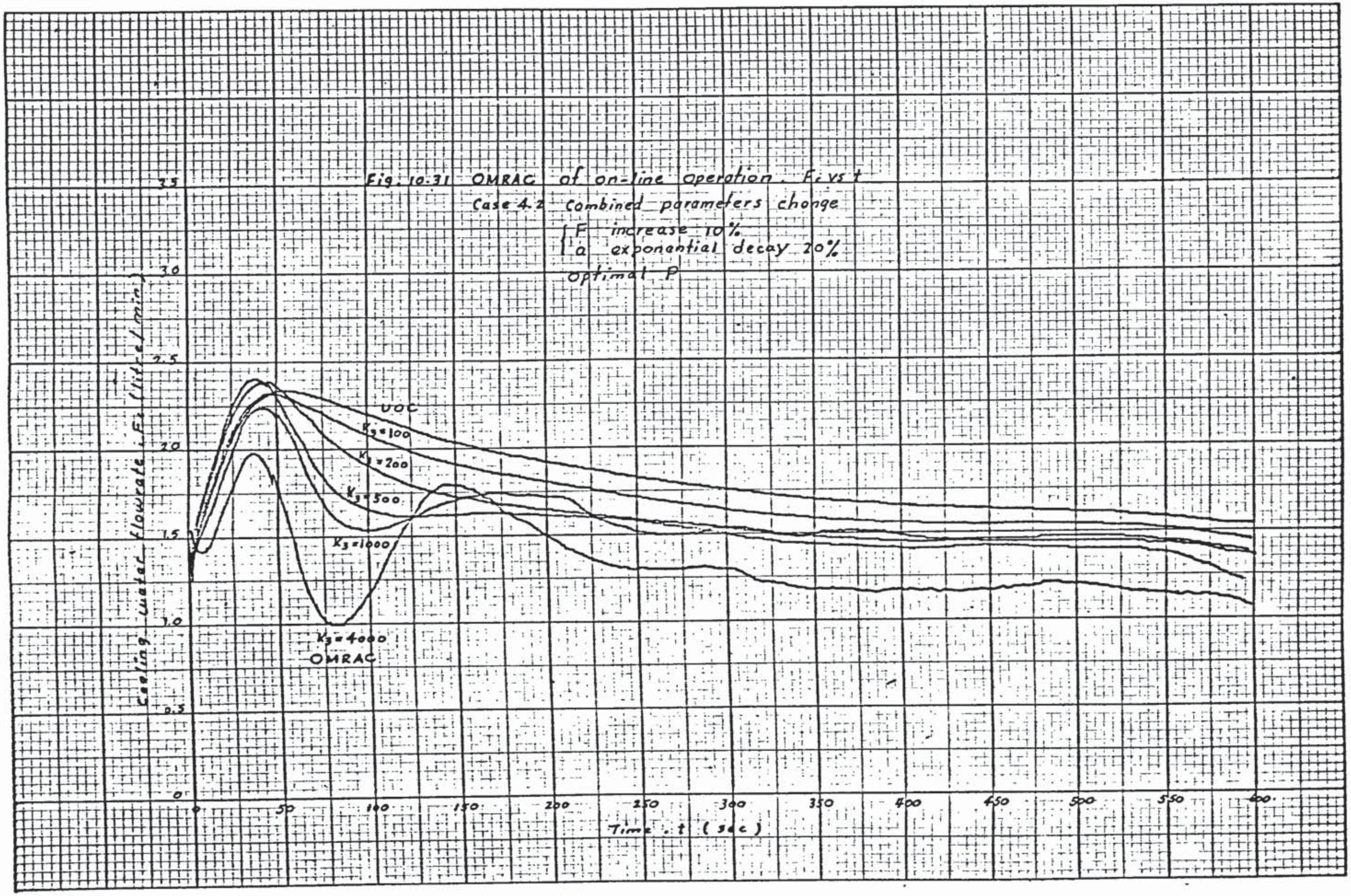

Fig. 10.31 OMRAC of on-line operation. F_c vs t
Case 4.2 Combined parameters change
F increase 10%
a exponential decay 20%
optimal P
UOC
K_3=100
K_3=200
K_3=500
K_3=1000
K_3=4000
OMRAC
Cooling water flowrate, F_c (litre/min)
Time, t (sec)
0
0.5
1.0
1.5
2.0
2.5
3.0
3.5
50
100
150
200
250
300
350
400
450
500
550
600

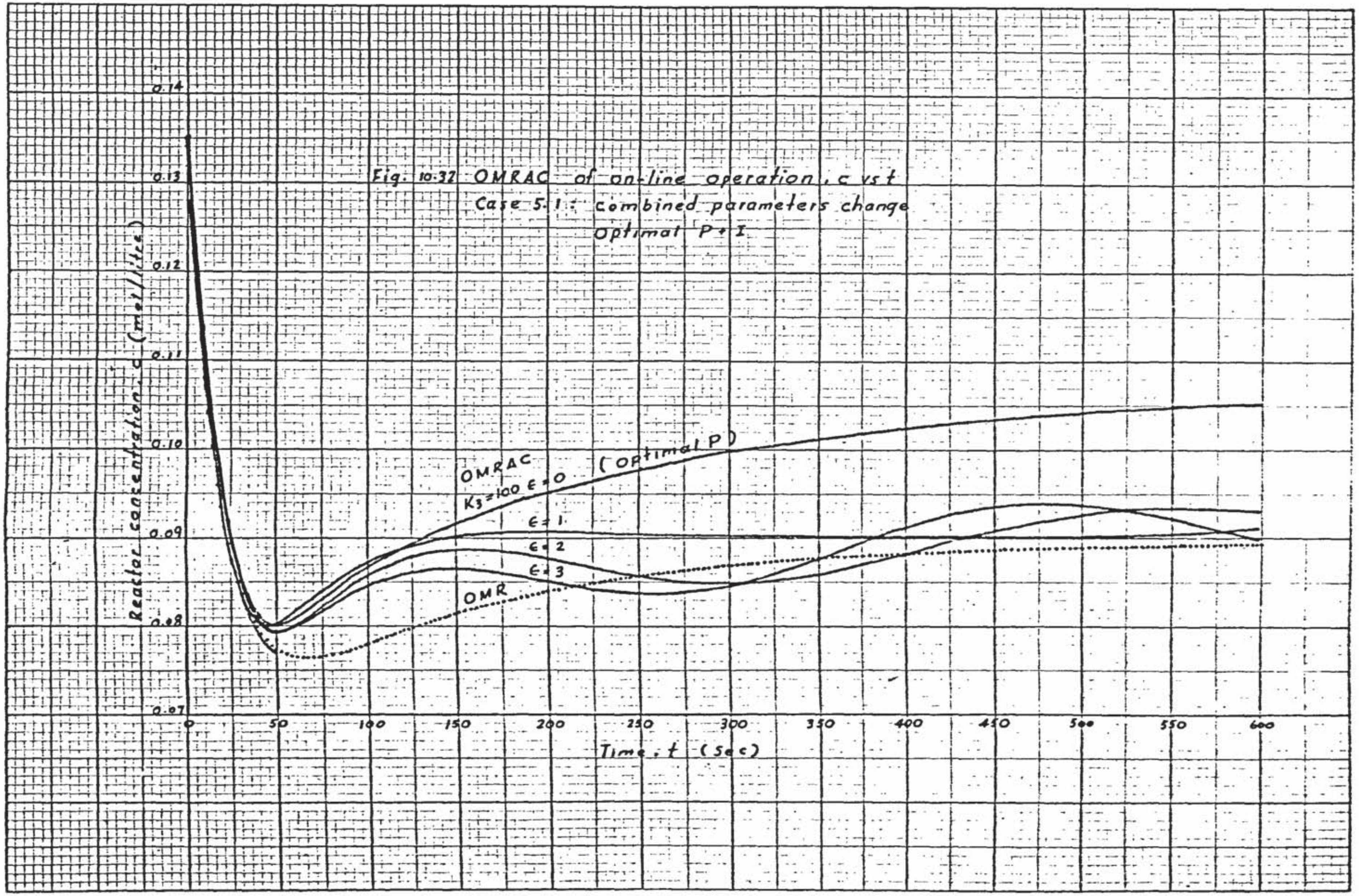
Fig. 10.32 OMRAC of on-line operation, c vs t
Case 5.1: combined parameters change
Optimal P+I
OMRAC
K3=100 ε=0 (Optimal P)
ε=1
ε=2
ε=3
OMR
Reactor concentration, c (mol/liter)
0.14
0.13
0.12
0.11
0.10
0.09
0.08
0.07
0
50
100
150
200
250
300
350
400
450
500
550
600
Time, t (Sec)

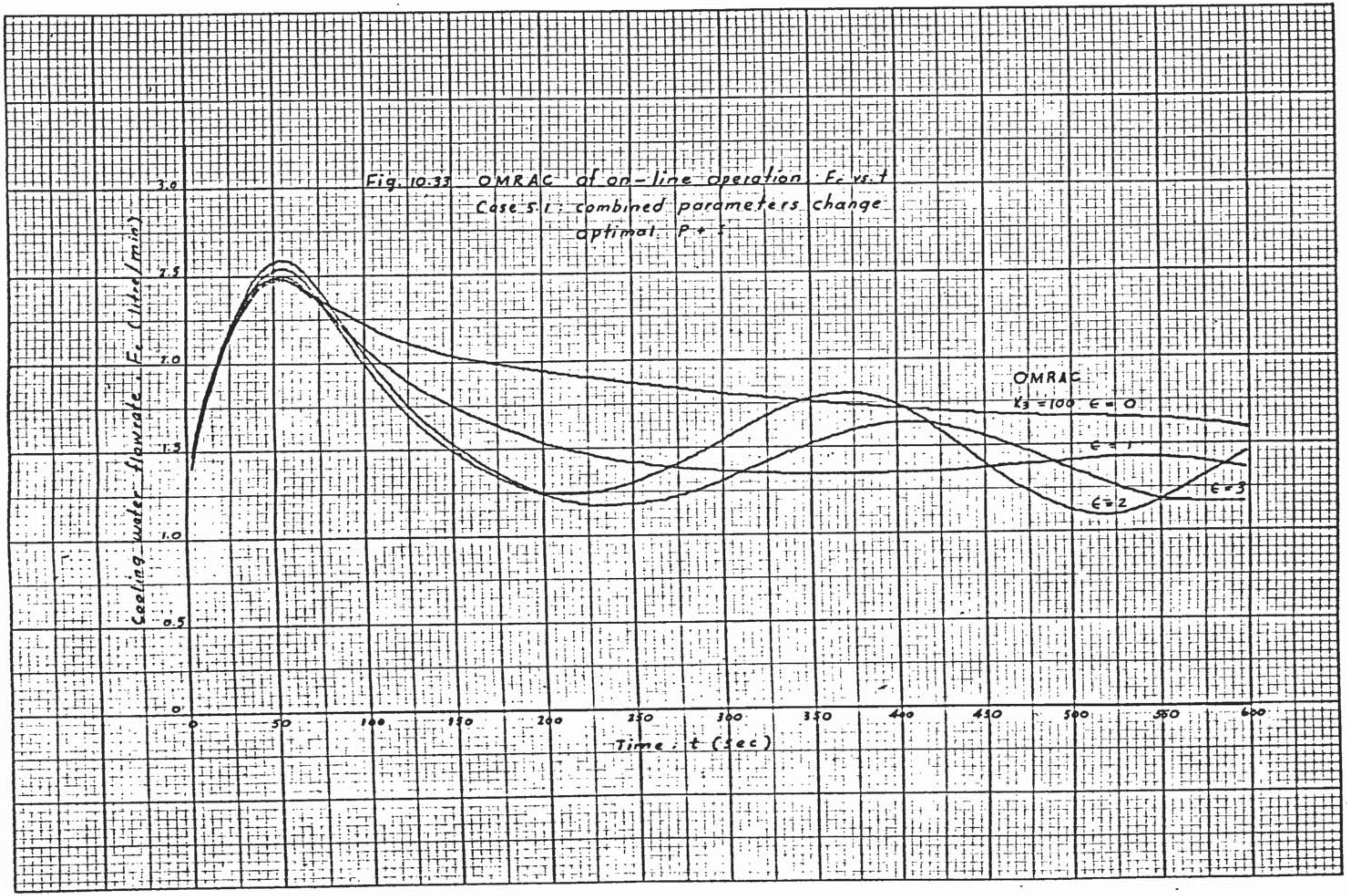

Fig. 10.33 OMRAC of on-line operation F_c vs. t
Case 5.1: combined parameters change
optimal P + I

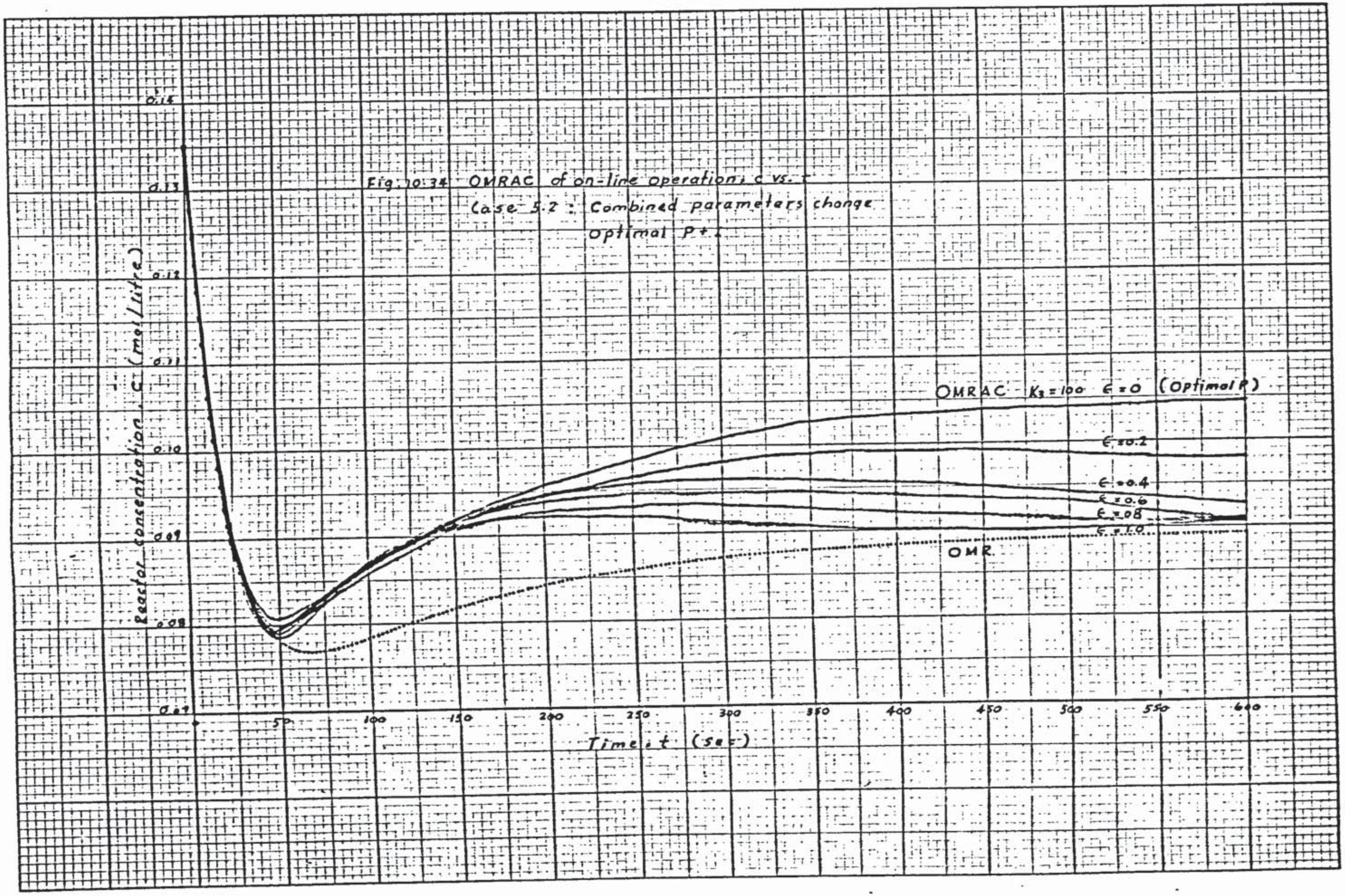

Fig. 10.34 OMRAC of on-line operation; c vs. t
Case 5.2 : Combined parameters change
Optimal P+.

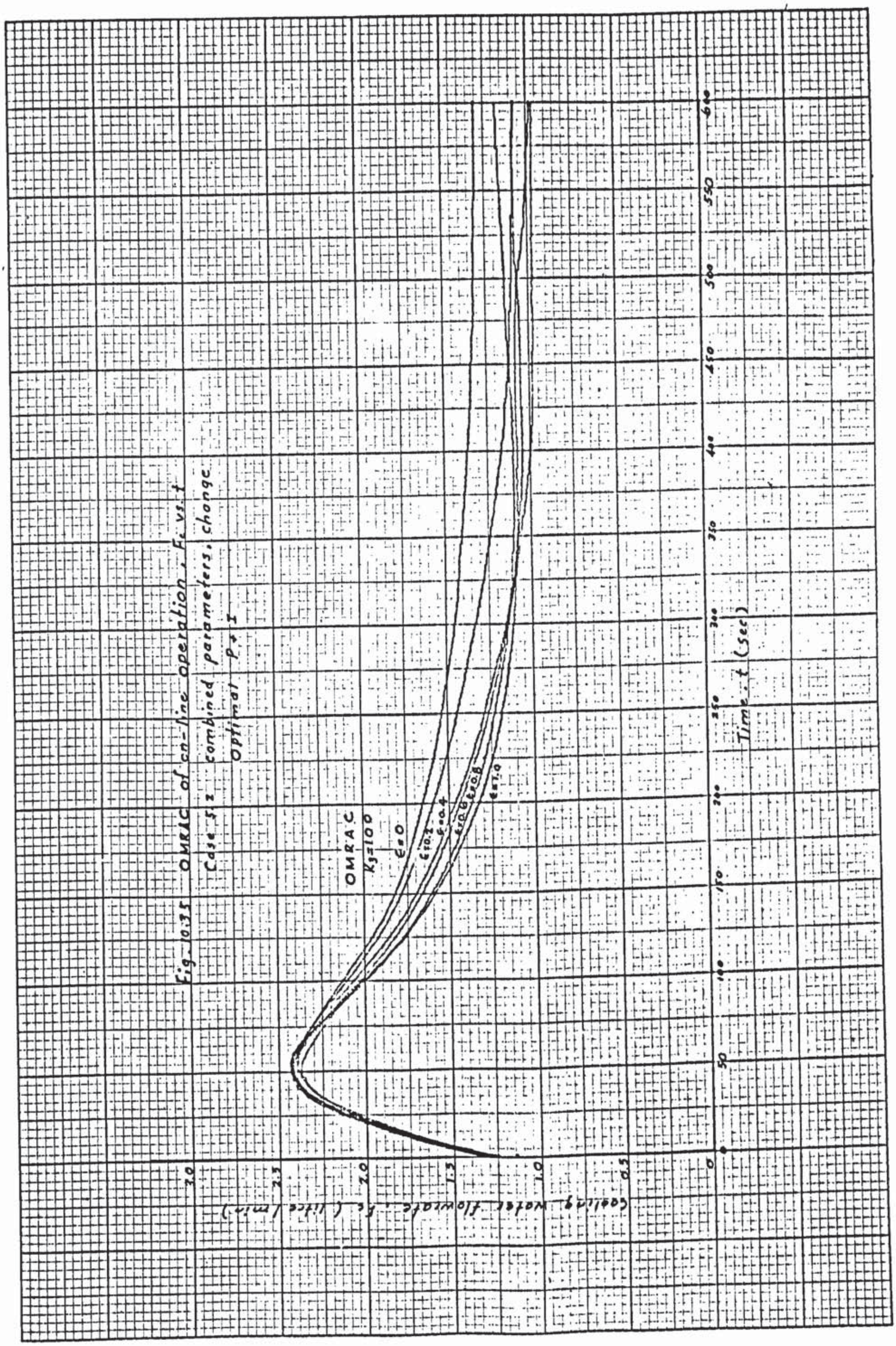

Fig. 10.35 OMRAC of on-line operation, F_c vs. t
Case 5.2 combined parameters, change
optimal P+I

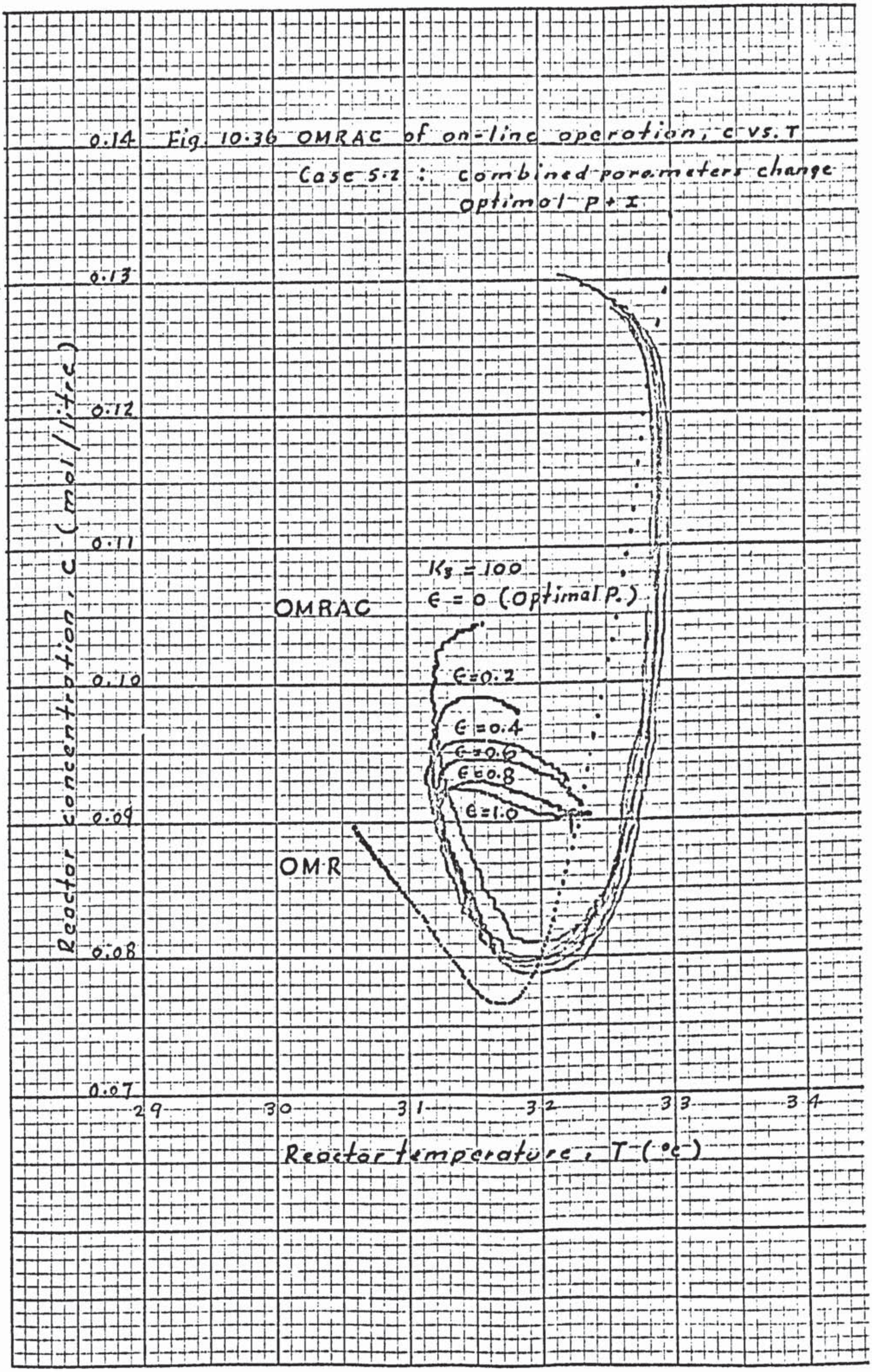
0.14
Fig. 10.36 OMRAC of on-line operation, c vs. T
Case 5.2 : combined parameters change
optimal P + I
0.13
0.12
0.11
0.10
0.09
0.08
0.07
Reactor concentration, c (mol/litre)
Kg = 100
ϵ = 0 (Optimal P.)
OMRAC
ϵ=0.2
ϵ=0.4
ϵ=0.6
ϵ=0.8
ϵ=1.0
OMR
29
30
31
32
33
34
Reactor temperature, T (°c)

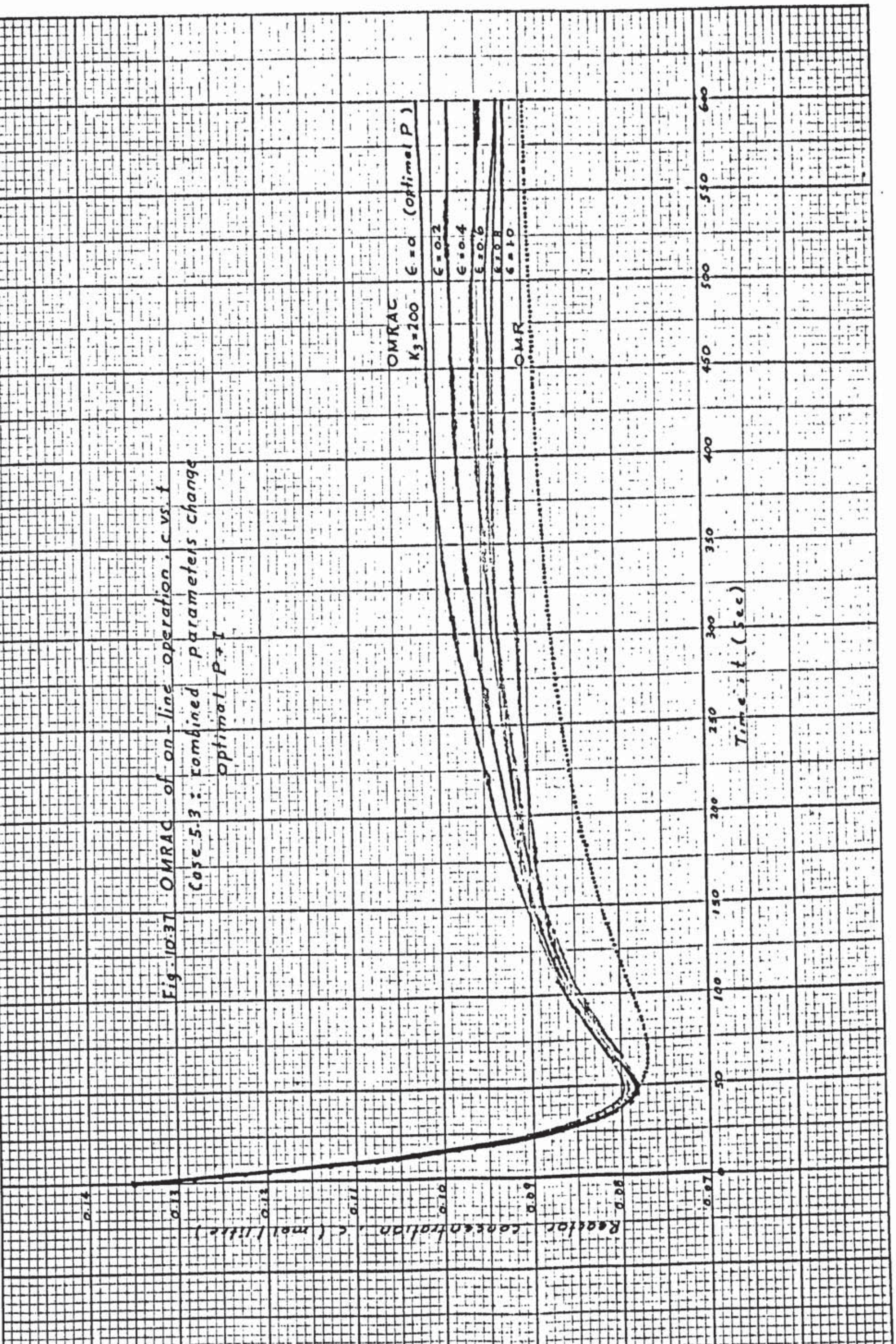

Fig 10.37 OMRAC of on-line operation, c vs. t
Case 5.3 : combined parameters change
optimal P + I

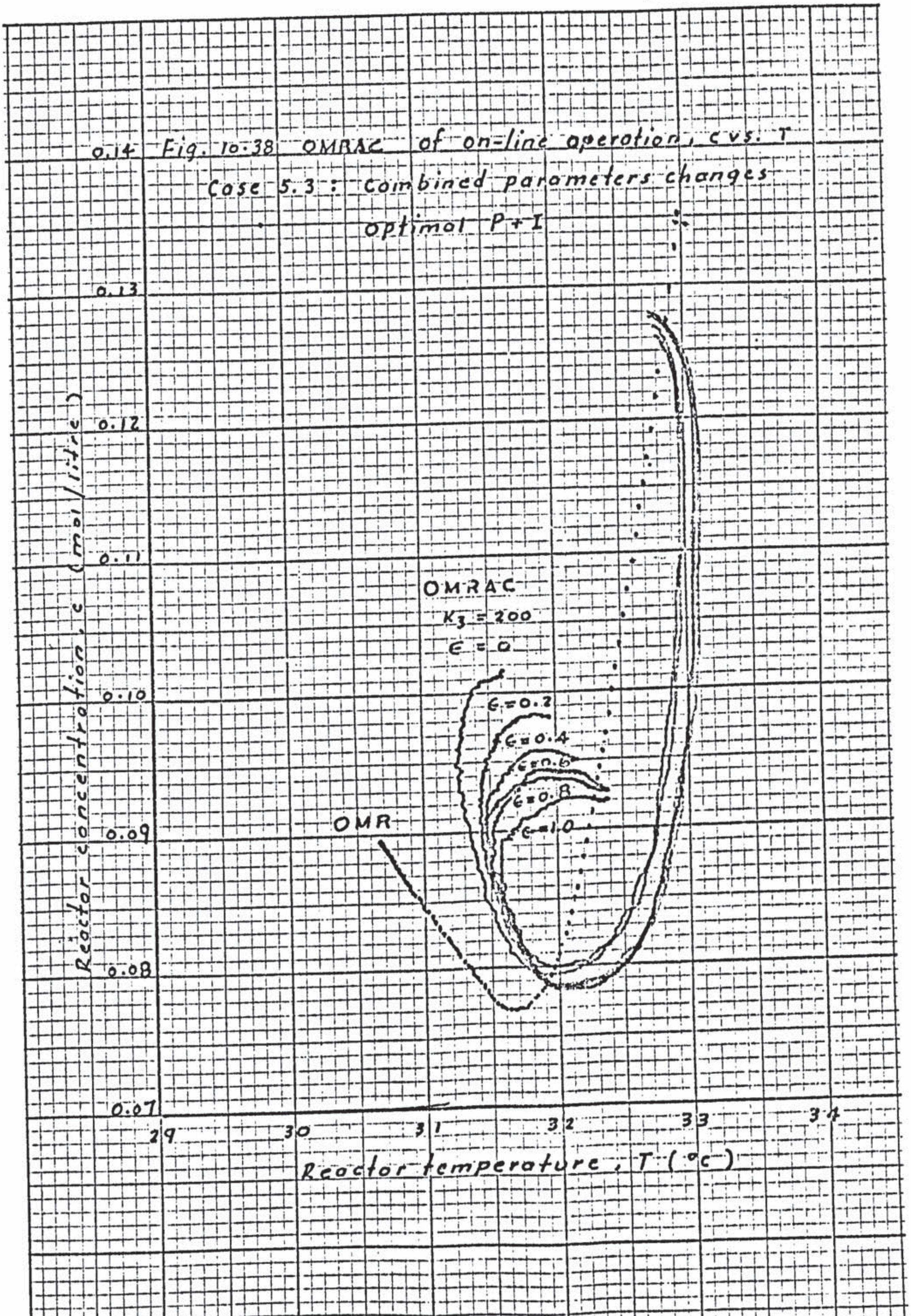
0.14
Fig. 10.38 OMRAC of on-line operation, c vs. T
Case 5.3 : combined parameters changes
optimal P+I
0.13
0.12
0.11
0.10
0.09
0.08
0.07
OMRAC
$K_3 = 200$
$\epsilon = 0$
$\epsilon = 0.2$
$\epsilon = 0.4$
$\epsilon = 0.6$
$\epsilon = 0.8$
$\epsilon = 1.0$
OMR
29
30
31
32
33
34
Reactor concentration, c (mol/litre)
Reactor temperature, T (°C)

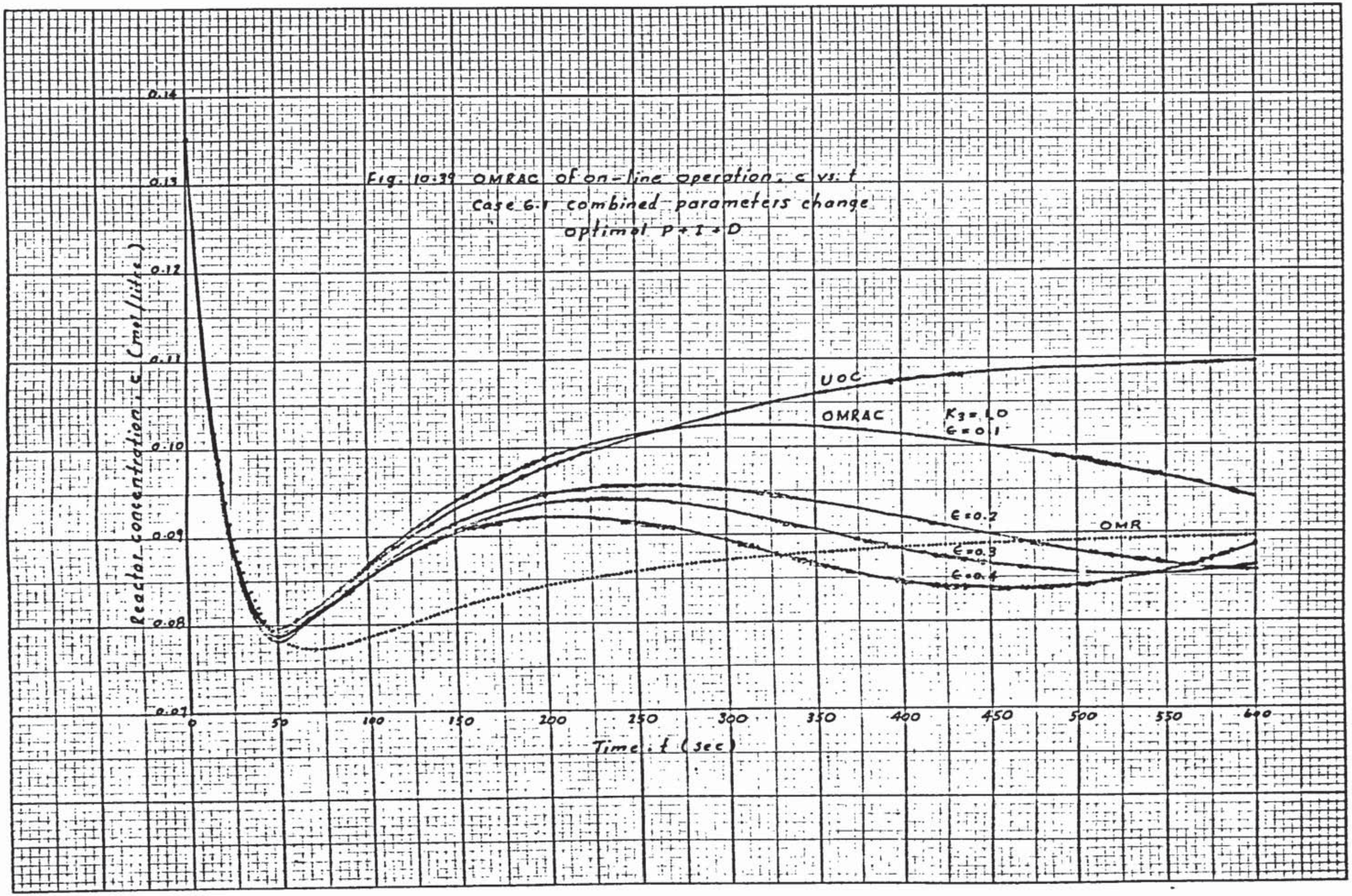

Fig. 10.39 OMRAC of on-line operation, c vs. t
Case 6.1 combined parameters change
optimal P + I + D

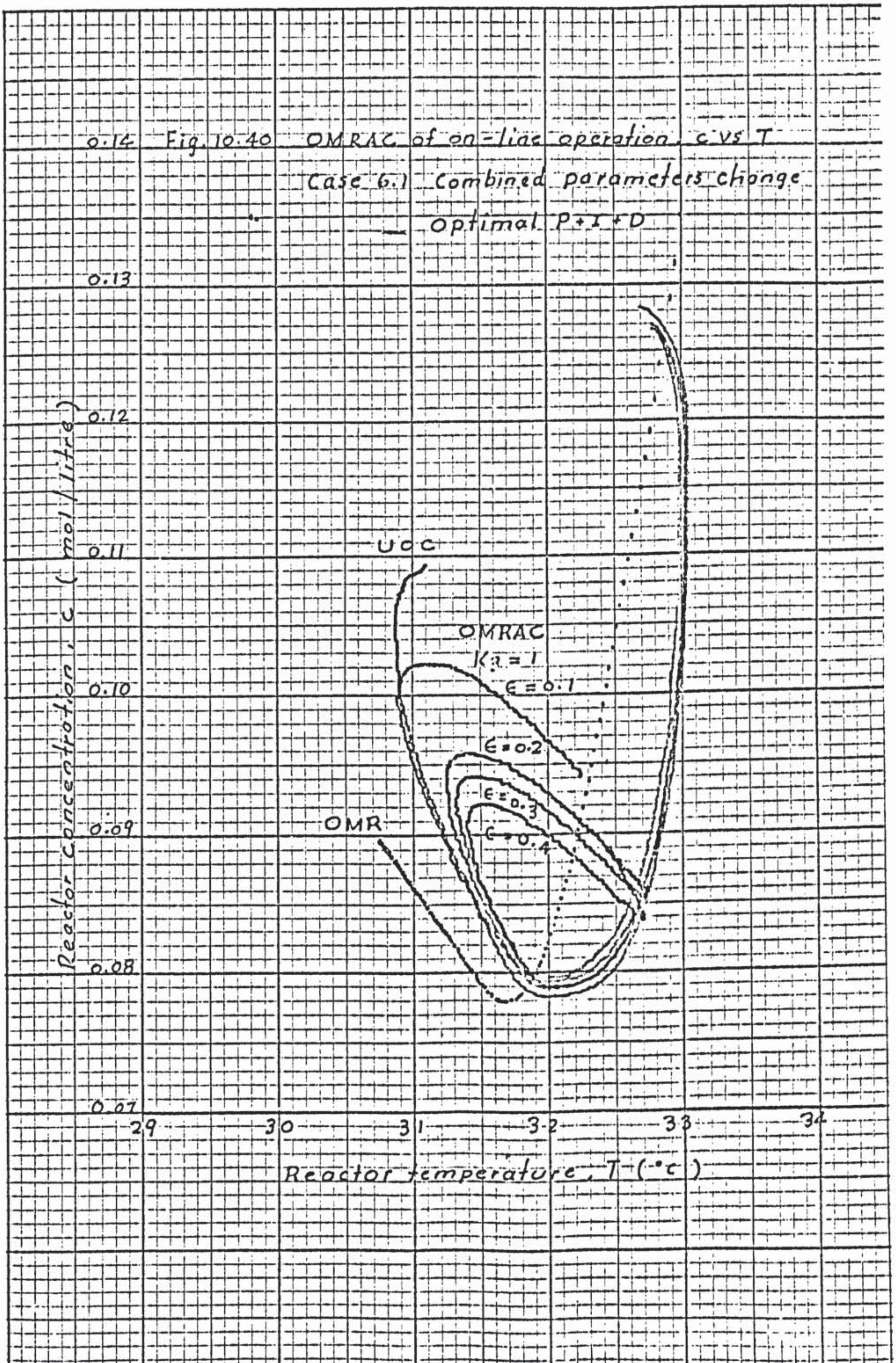

Fig. 10.40 OMRAC of on-line operation, c vs T
Case 6.1 Combined parameters change
— Optimal P+I+D
0.14
0.13
0.12
0.11
0.10
0.09
0.08
0.07
29
30
31
32
33
34
UCC
OMRAC
Kn = 1
ε = 0.1
ε = 0.2
ε = 0.3
ε = 0.4
OMR
Reactor concentration, c (mol/litre)
Reactor temperature, T (°c)

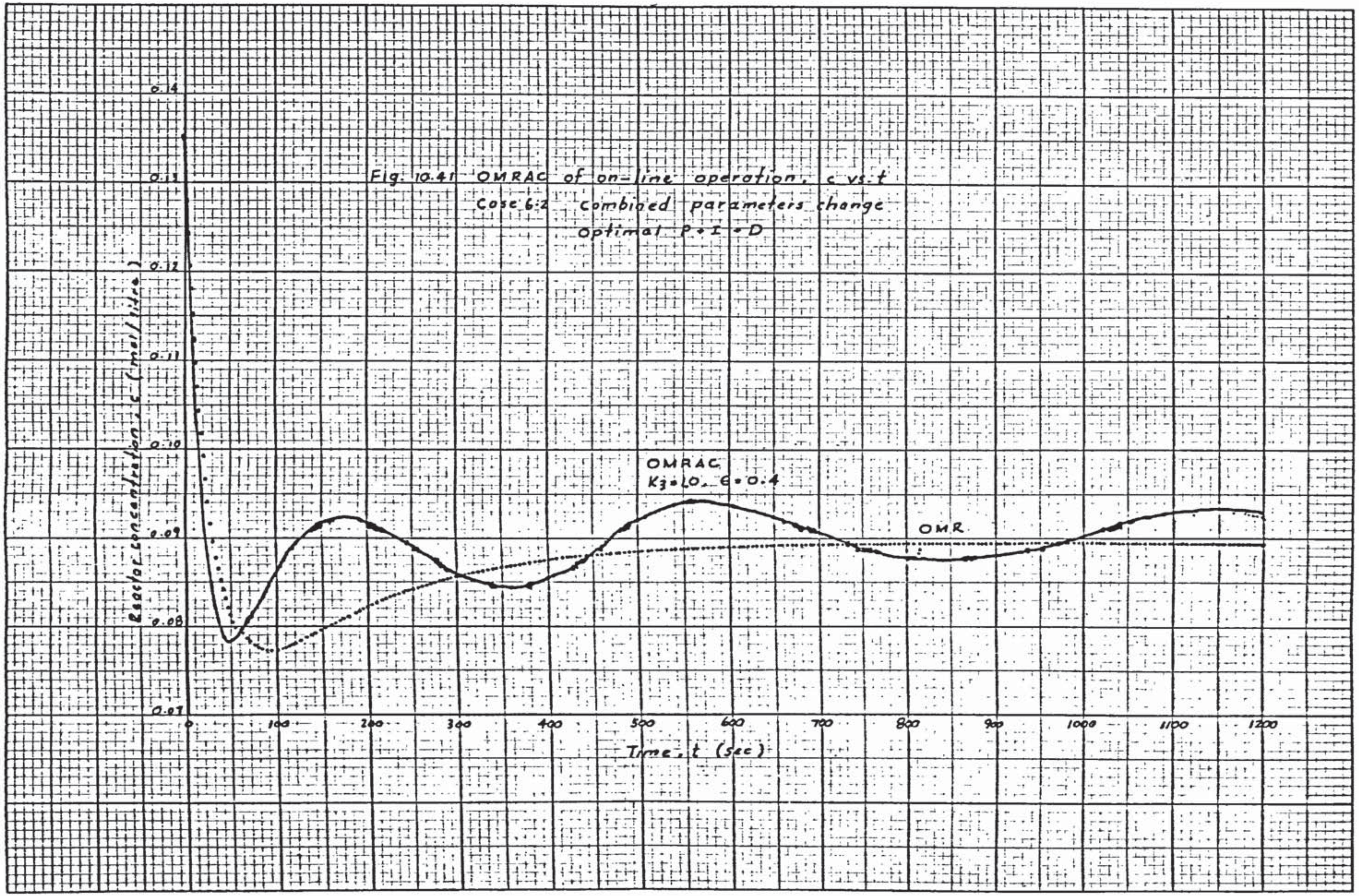

Fig. 10.41 OMRAC of on-line operation, c vs. t
Cose 6:2 Combined parameters change
Optimal P+I+D

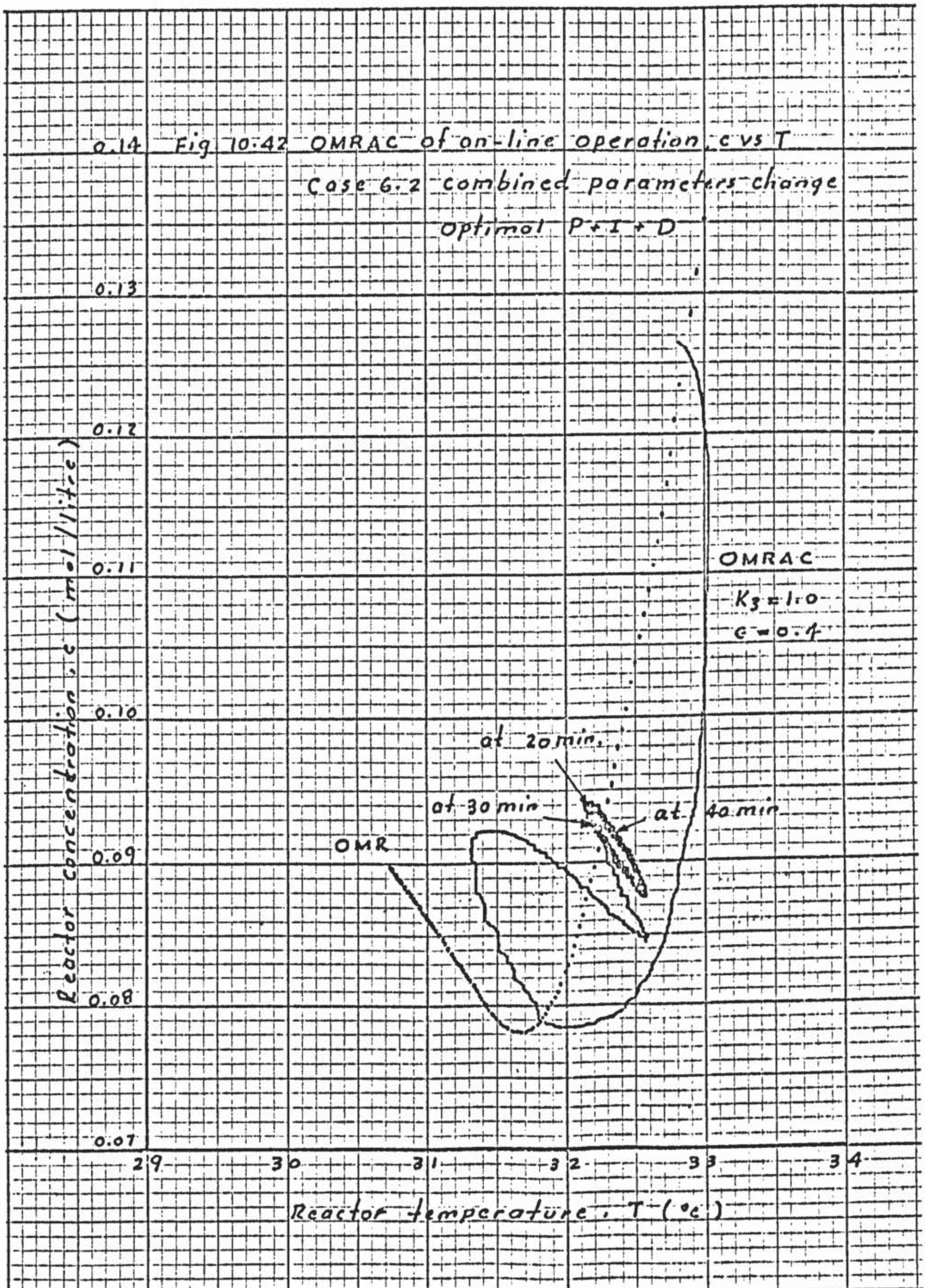
Fig 10.42 OMRAC of on-line operation, c vs T
Case 6.2 combined parameters change
optimal P+I+D
0.14
0.13
0.12
0.11
0.10
0.09
0.08
0.07
Reactor concentration, c (mol/litre)
29
30
31
32
33
34
Reactor temperature, T (°c)
OMRAC
K_3 = 1.0
c = 0.4
at 20 min.
at 30 min
at 40 min
OMR

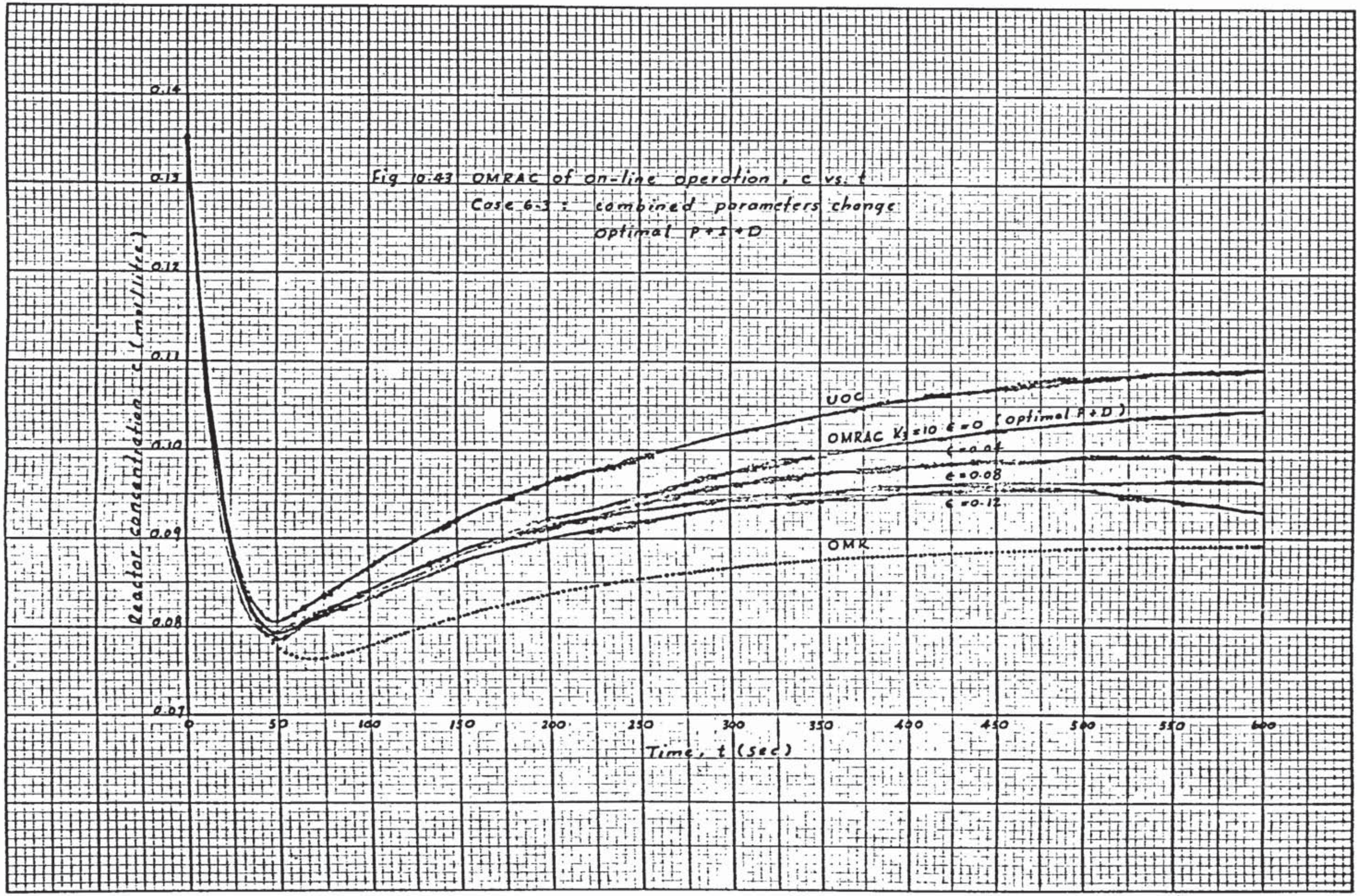

Fig 10.43 OMRAC of on-line operation, c vs. t
Case 6-3 : combined parameters change
optimal P+I+D

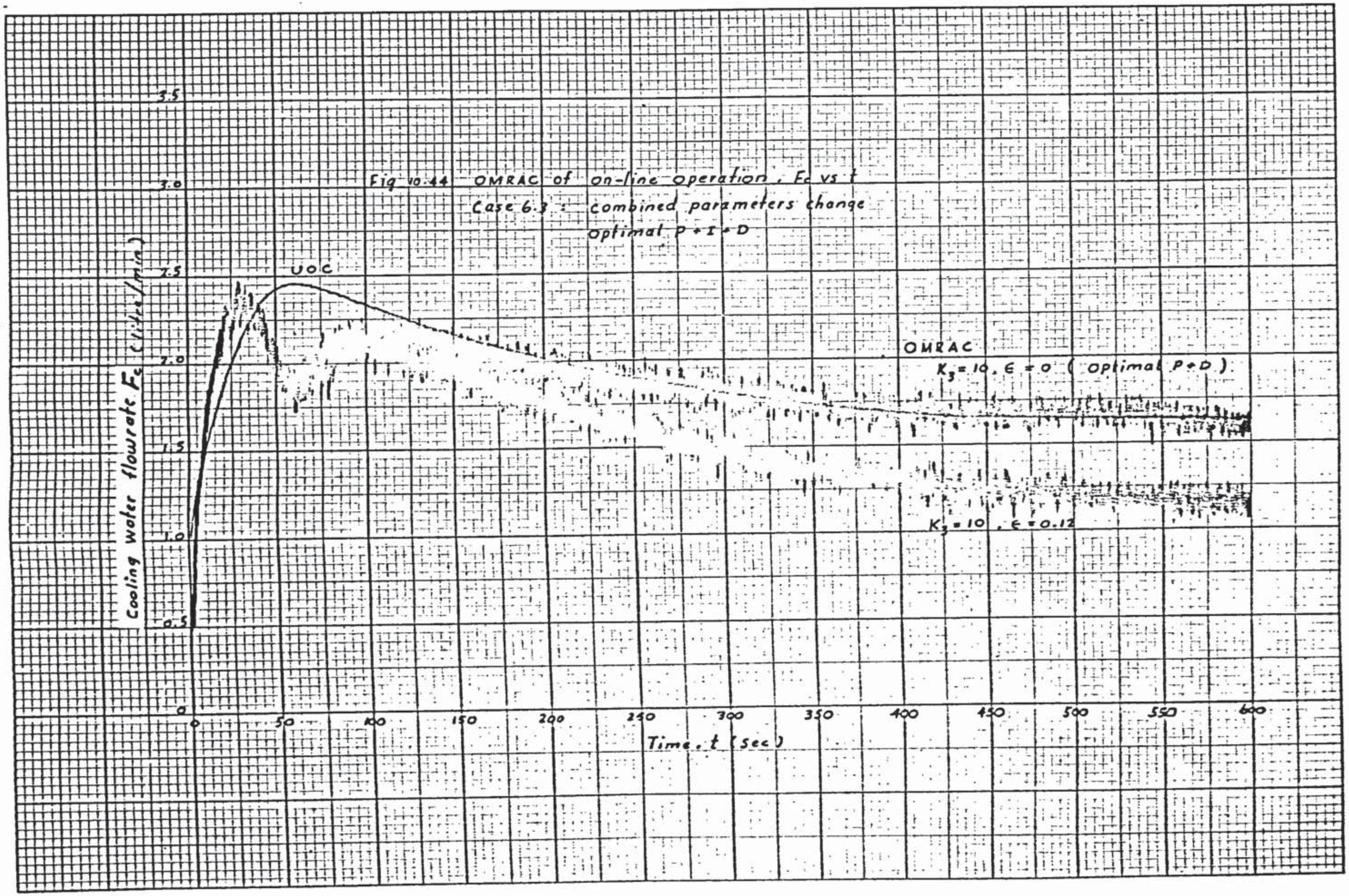

Fig 10.44 OMRAC of on-line operation, F_c vs t
Case 6.3 : combined parameters change
optimal P+I+D

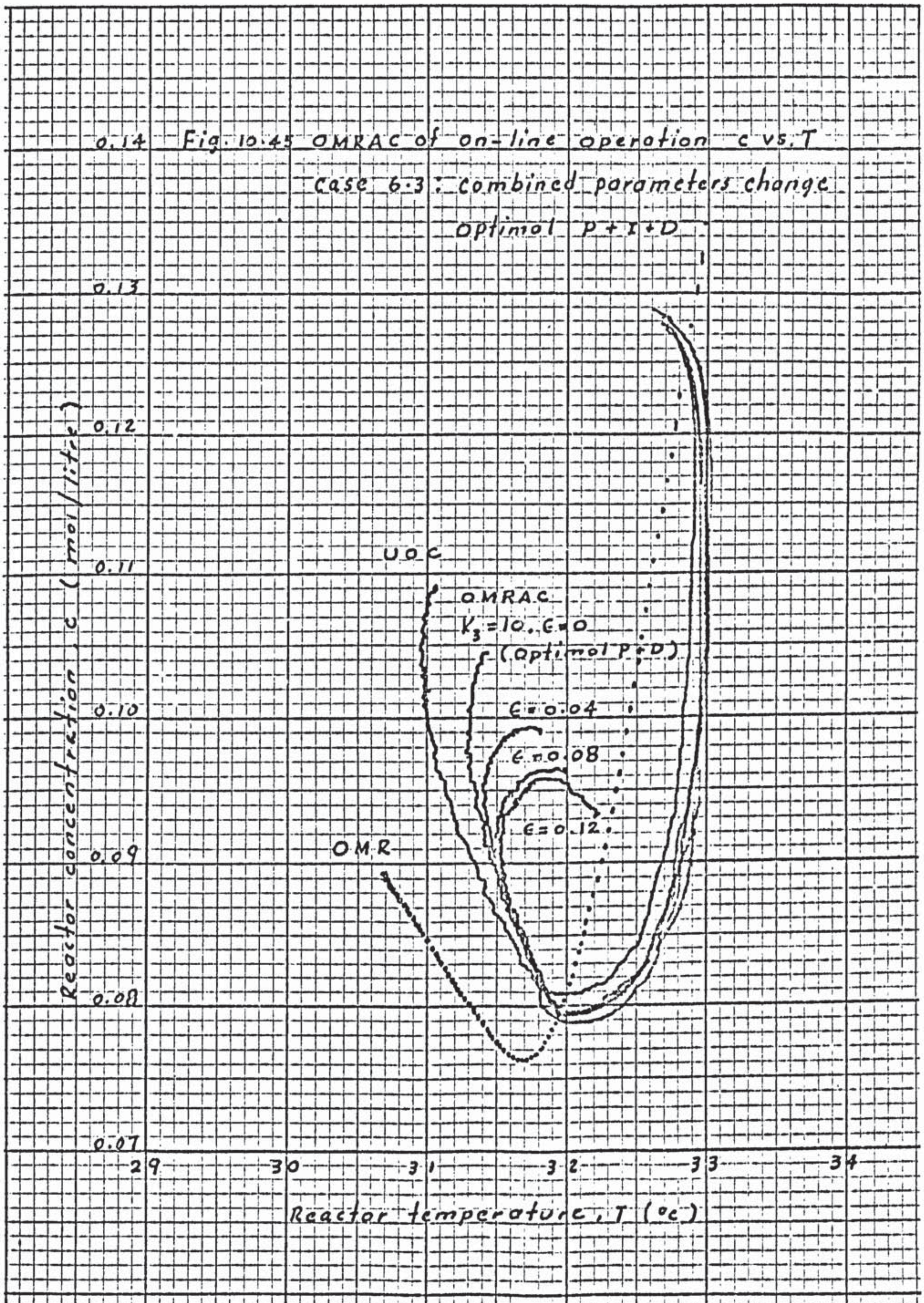

Fig. 10.45 OMRAC of on-line operation c vs. T
Case 6.3: combined parameters change
optimal P+I+D
0.14
0.13
0.12
0.11
0.10
0.09
0.08
0.07
Reactor concentration, c (mol/litre)
UOC
OMRAC
K_3=10, ε=0
(optimal P+D)
ε=0.04
ε=0.08
ε=0.12
OMR
29
30
31
32
33
34
Reactor temperature, T (°c)

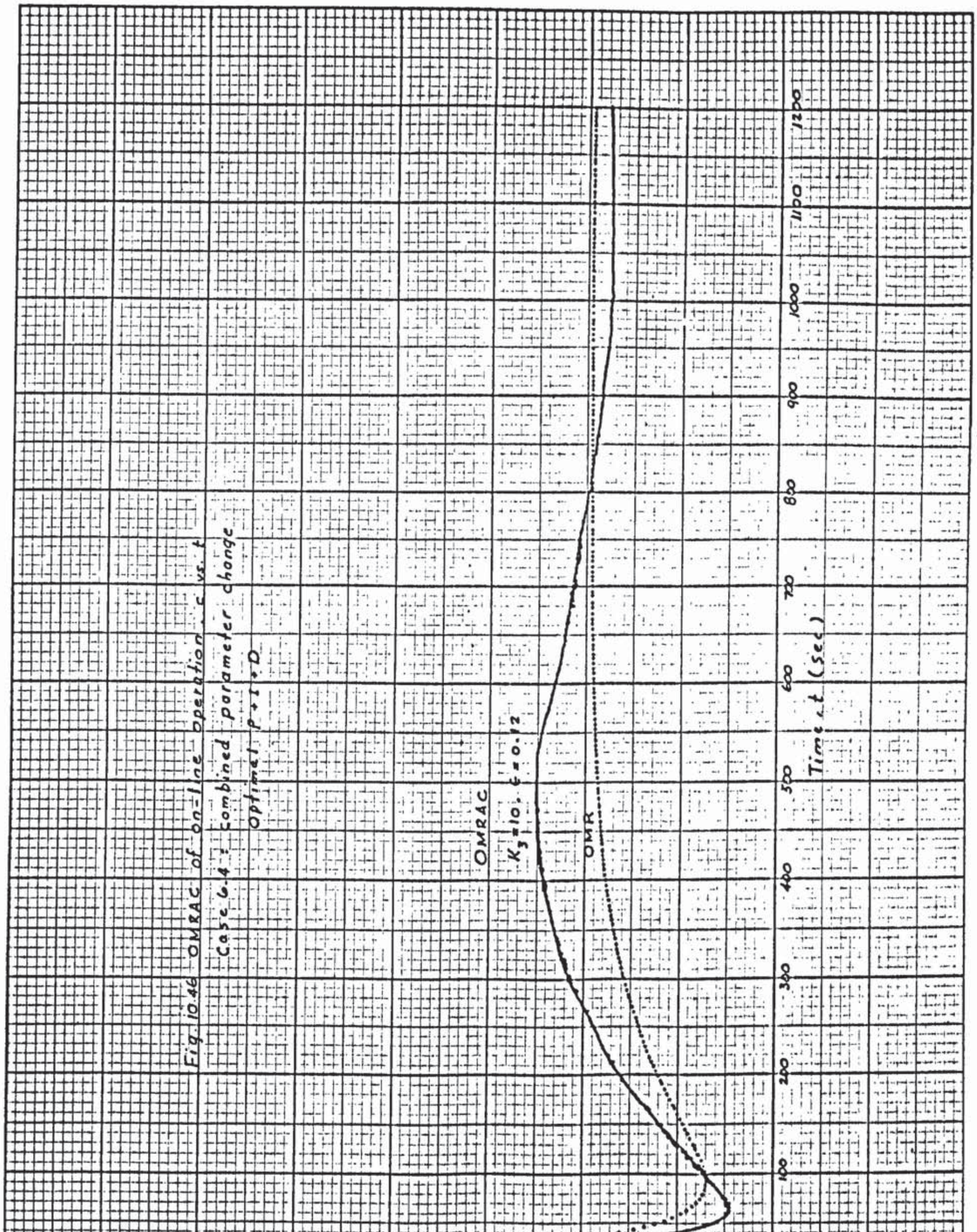

Fig. 10.46 OMRAC of on-line operation: c vs. t

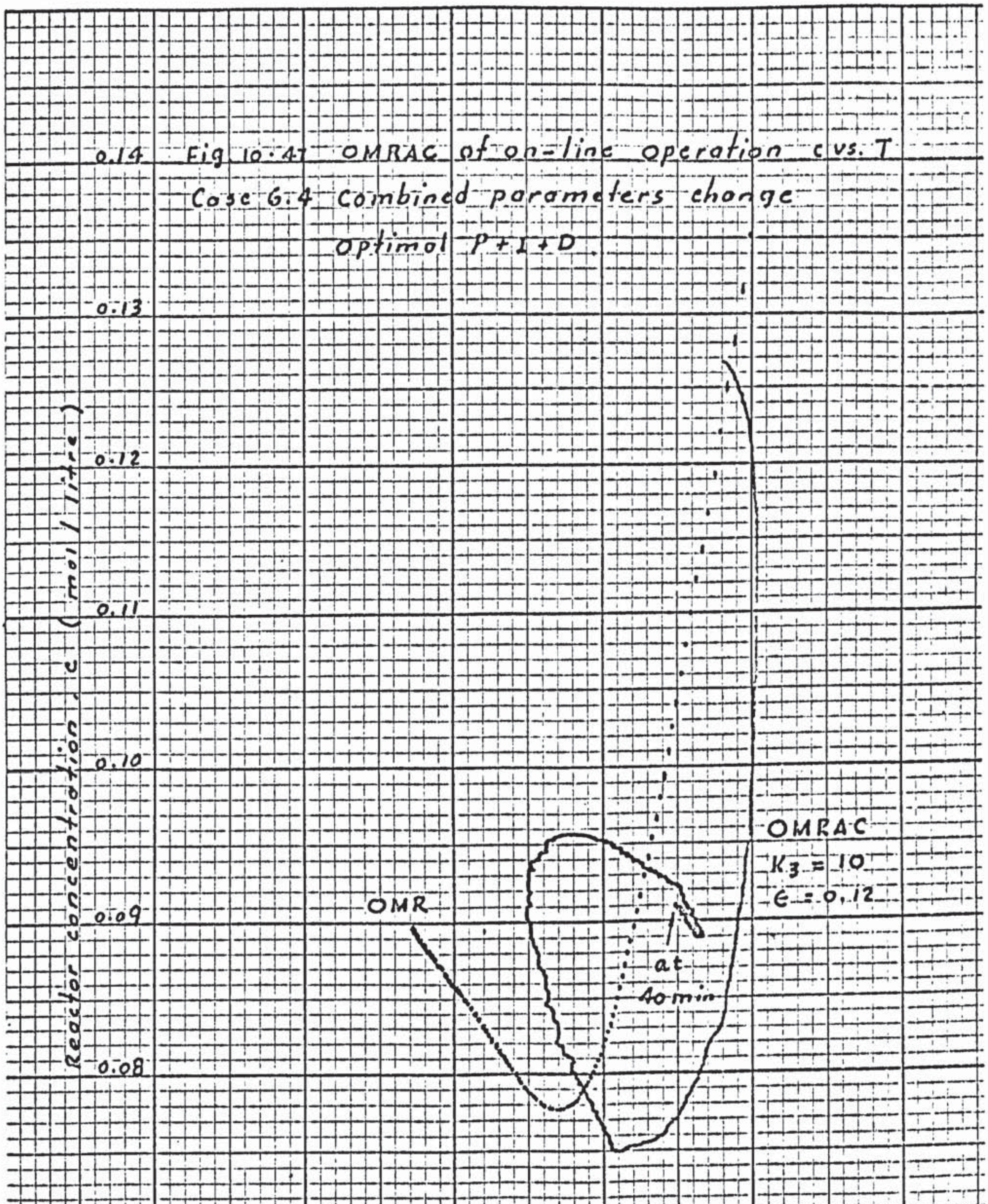
Fig 10.47 OMRAC of on-line operation c vs. T
Case 6.4 Combined parameters change
optimal P+I+D
0.14
0.13
0.12
0.11
0.10
0.09
0.08
0.07
Reactor concentration, c (mol / litre)
OMR
OMRAC
K_3 = 10
ε = 0.12
at 40 min
29
30
31
32
33
34
Reactor temperature, T (°c)

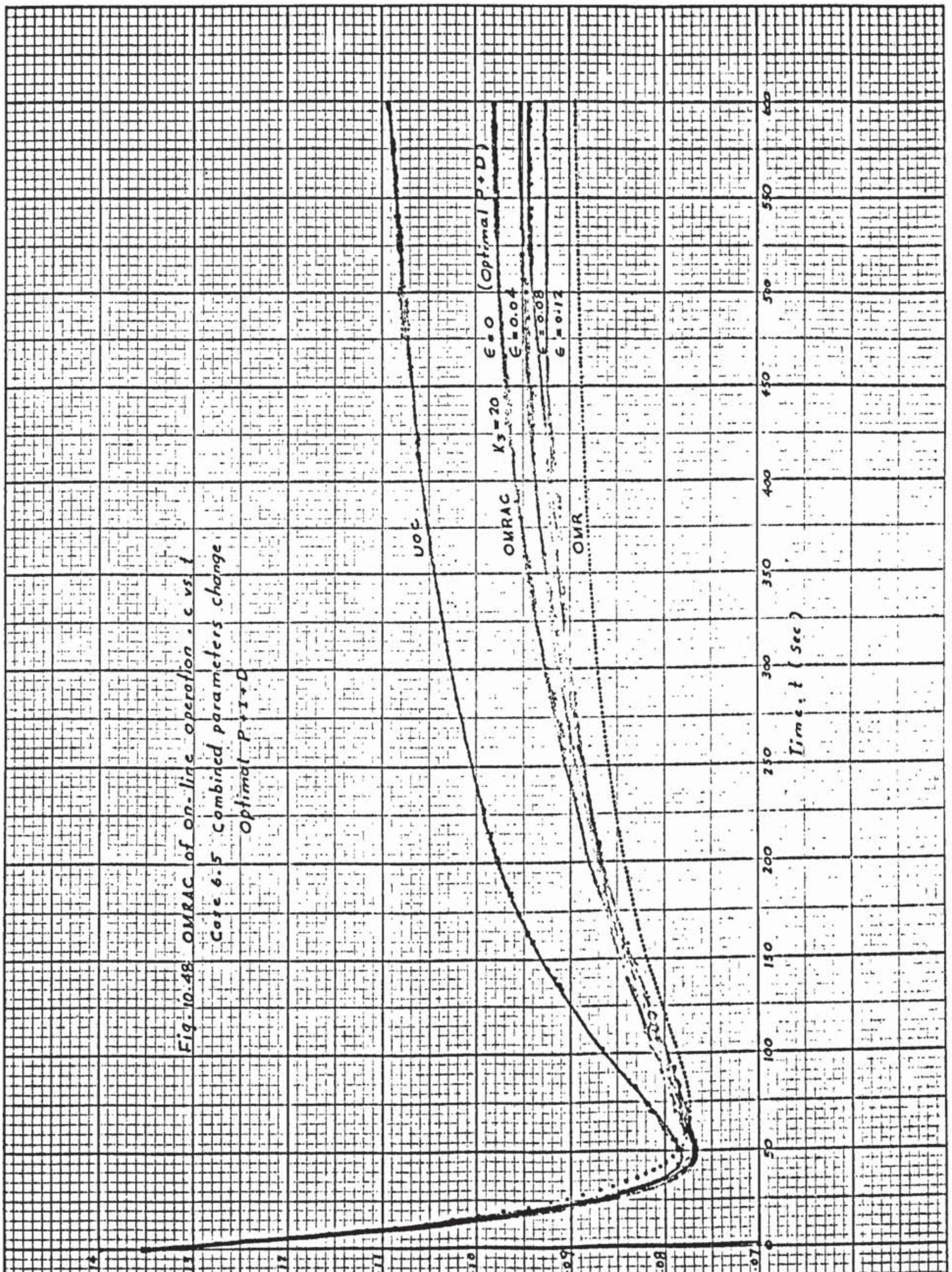
Fig. 10.48 OMRAC of on-line operation, c vs t
Case 6.5 Combined parameters change
Optimal P+I+D
UOC
OMRAC
K3 = 20
OMR
ε = 0 (Optimal P+D)
ε = 0.04
ε = 0.08
ε = 0.12
Time: t (Sec)
Reactor concentration: c (mol/liter)
0.14
0.13
0.12
0.11
0.10
0.09
0.08
0.07
0
50
100
150
200
250
300
350
400
450
500
550
600

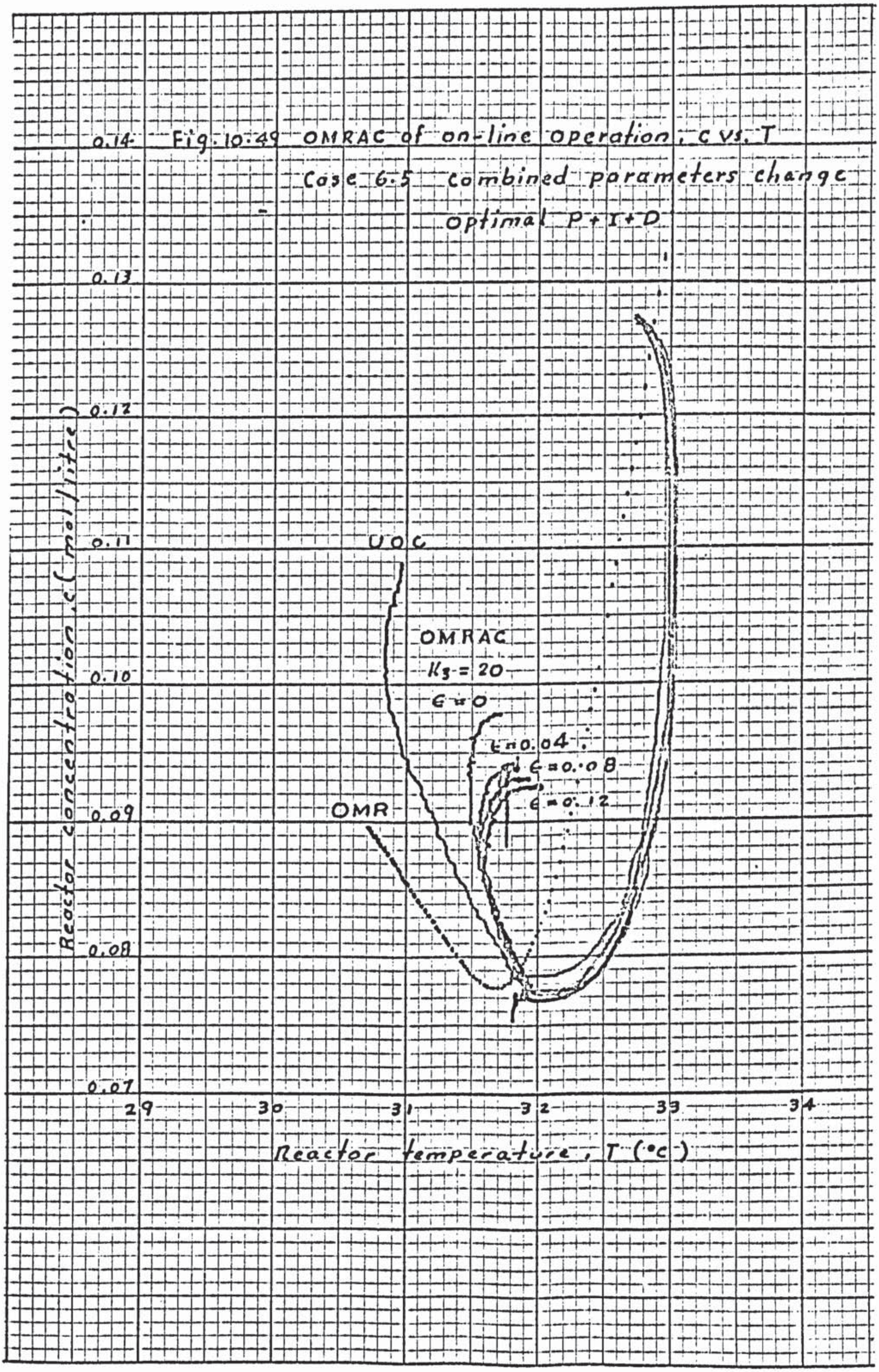
Fig. 10.49 OMRAC of on-line operation, c vs. T
Case 6.5 combined parameters change
optimal P+I+D
0.14
0.13
0.12
0.11
0.10
0.09
0.08
0.07
29
30
31
32
33
34
Reactor concentration, c (mol/litre)
Reactor temperature, T (°c)
UOC
OMRAC
K3 = 20
ϵ = 0
ϵ = 0.04
ϵ = 0.08
ϵ = 0.12
OMR

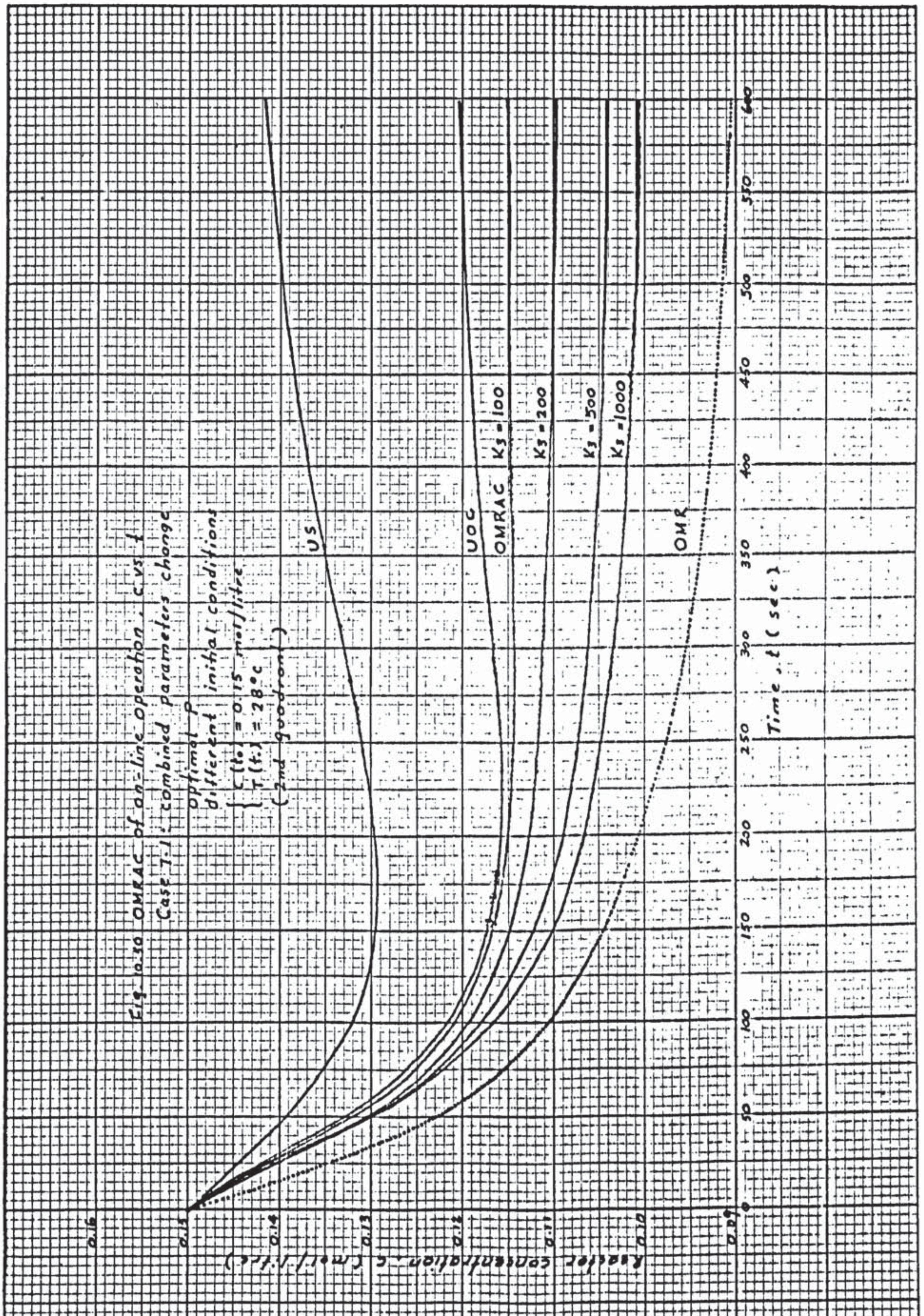
Fig. 10.30 OMRAC of on-line operation, c vs t
Case 7.1: combined parameters change
optimal ρ
different initial conditions
c(t₀) = 0.15 mol/litre
T(t₀) = 28°c
(2nd quadrant)
US
UOC
OMRAC
K3 = 100
K3 = 200
K3 = 500
K3 = 1000
OMR
Time, t (sec)
Reactor concentration, c (mol/litre)
0.16
0.15
0.14
0.13
0.12
0.11
0.10
0.09
0
50
100
150
200
250
300
350
400
450
500
550
600

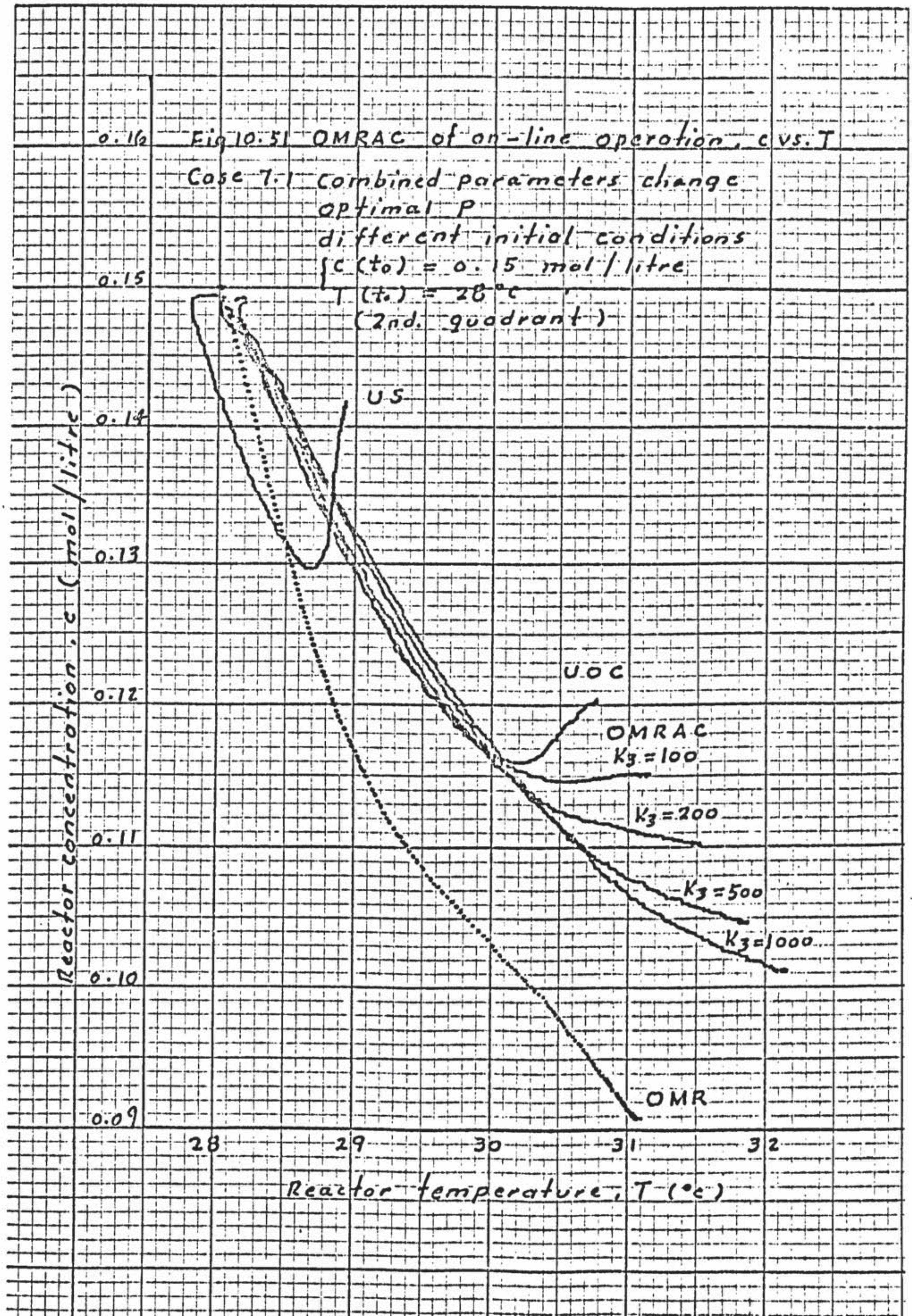

Fig 10.51 OMRAC of on-line operation, c vs. T
Case 7.1 Combined parameters change
optimal P
different initial conditions
c (t₀) = 0.15 mol/litre
T (t₀) = 28°C
(2nd. quadrant)
US
UOC
OMRAC
K3=100
K3=200
K3=500
K3=1000
OMR
0.16
0.15
0.14
0.13
0.12
0.11
0.10
0.09
28
29
30
31
32
Reactor concentration, c (mol/litre)
Reactor temperature, T (°c)

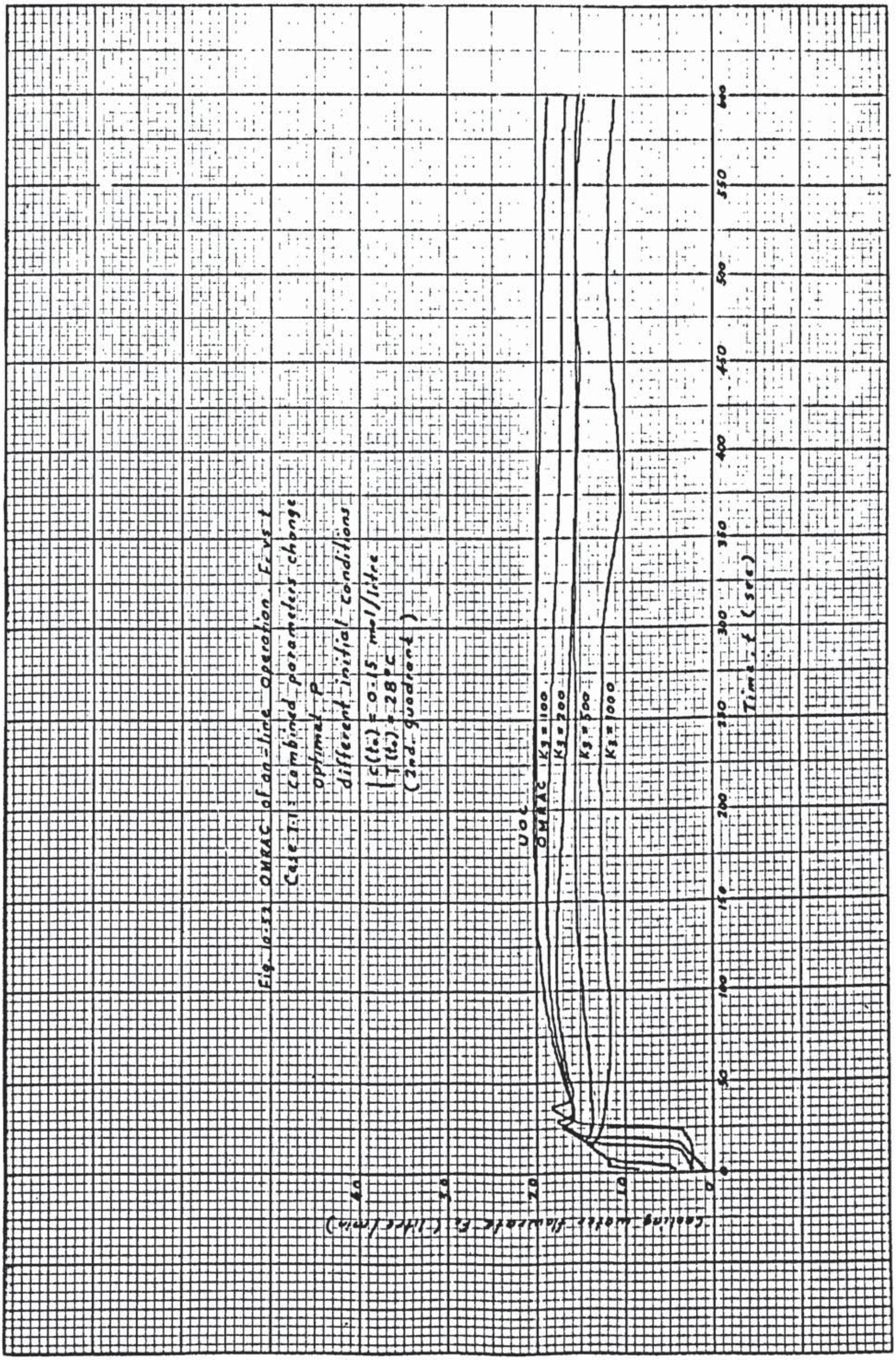
Fig. 10-53 OMRAC of on-line operation. Fc vs t
Case I-1: combined parameters change
optimal P
different initial conditions
c(t0) = 0.15 mol/litre
T(t0) = 28°C
(2nd. quadrant)
UOC
OMRAC Kg=100
Kg=200
Kg=500
Kg=1000
Time, t (sec)
Cooling water flowrate Fc (litre/min)
0
10
20
30
40
50
100
150
200
250
300
350
400
450
500
550
600

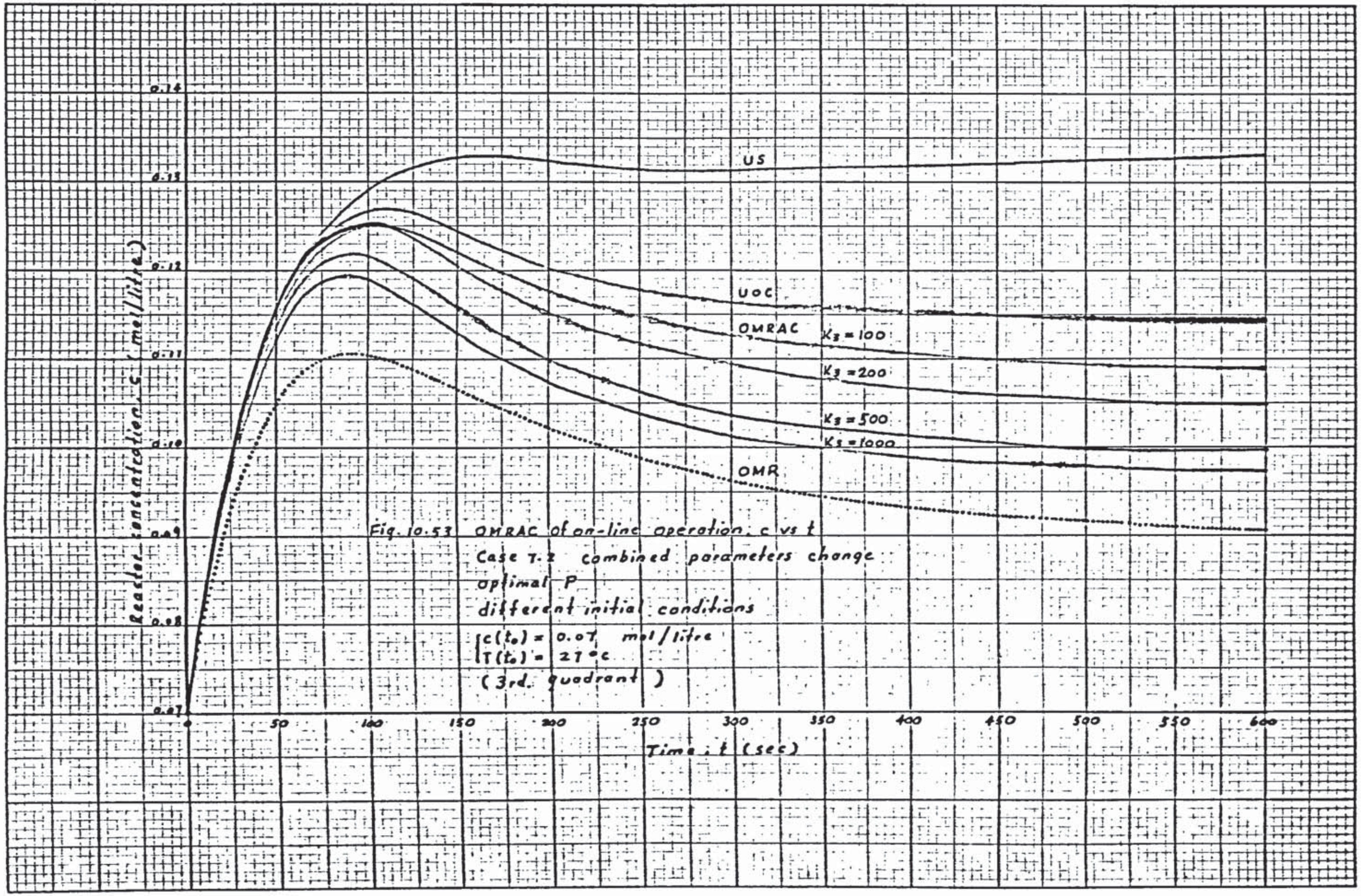

Fig. 10.53 OMRAC of on-line operation: c vs t

Case 7.2 combined parameters change

optimal P

different initial conditions

$c(t_0) = 0.07$ mol/litre

$T(t_0) = 27\,°c$

(3rd. quadrant)

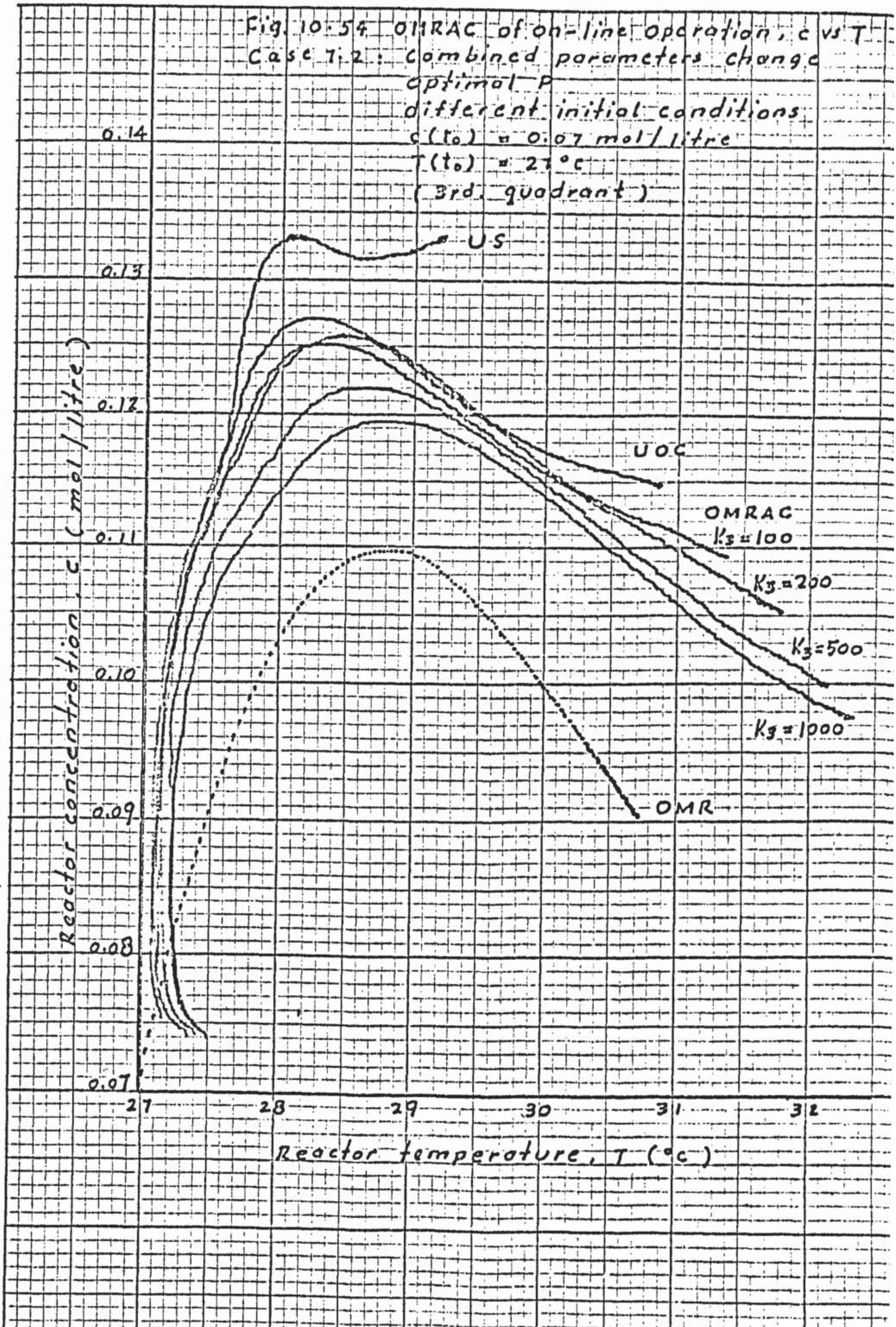
Fig. 10.54 OMRAC of on-line operation, c vs T
Case 7.2: Combined parameters change
optimal P
different initial conditions
c(t₀) = 0.07 mol/litre
T(t₀) = 27°c
(3rd. quadrant)
US
UOC
OMRAC
K3=100
K3=200
K3=500
K3=1000
OMR
0.14
0.13
0.12
0.11
0.10
0.09
0.08
0.07
27
28
29
30
31
32
Reactor concentration, c (mol/litre)
Reactor temperature, T (°c)

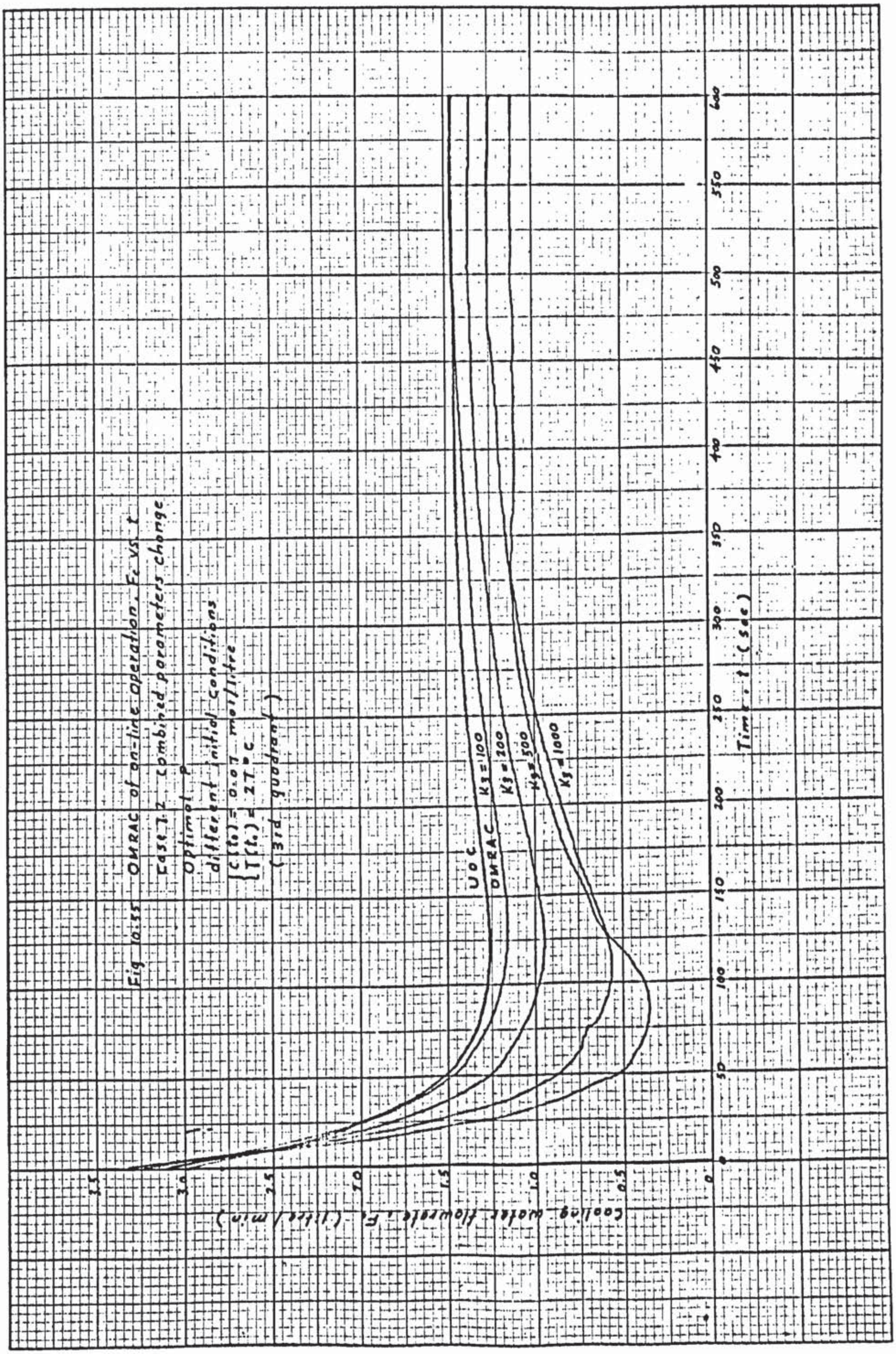
Fig 10.55 OMRAC of on-line operation, Fc vs. t
Case 3.2 Combined parameters change
Optimal P
different initial conditions
C(t0) = 0.07 mol/litre
T(t0) = 27°C
(3rd quadrant)
UOC
OMRAC
Kg=100
Kg=200
Kg=500
Kg=1000
Time, t (sec)
Cooling water flowrate, Fc (litre/min)
0
50
100
150
200
250
300
350
400
450
500
550
600
0.5
1.0
1.5
2.0
2.5
3.0
3.5

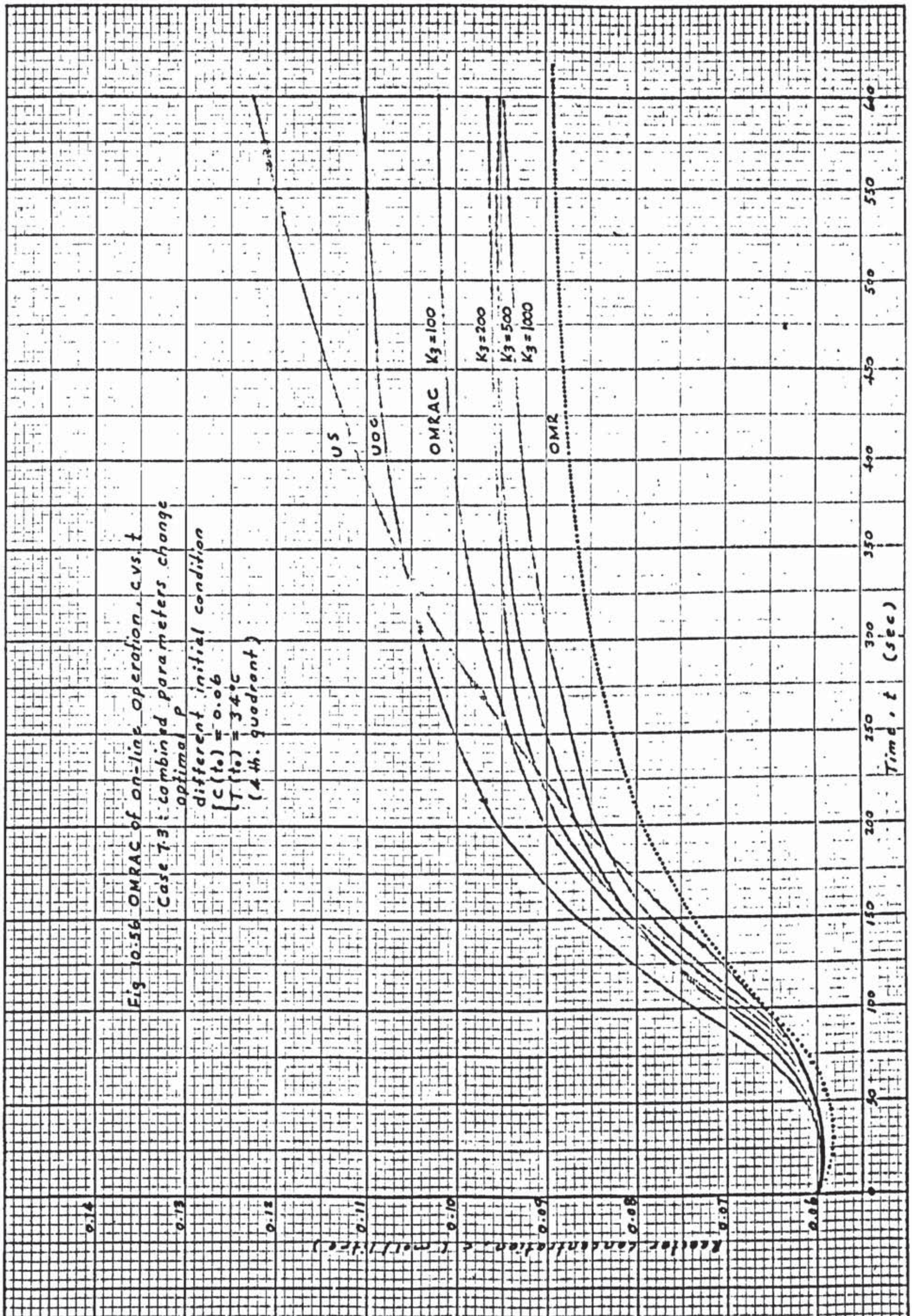

Fig 10.56 OMRAC of on-line operation, c vs. t

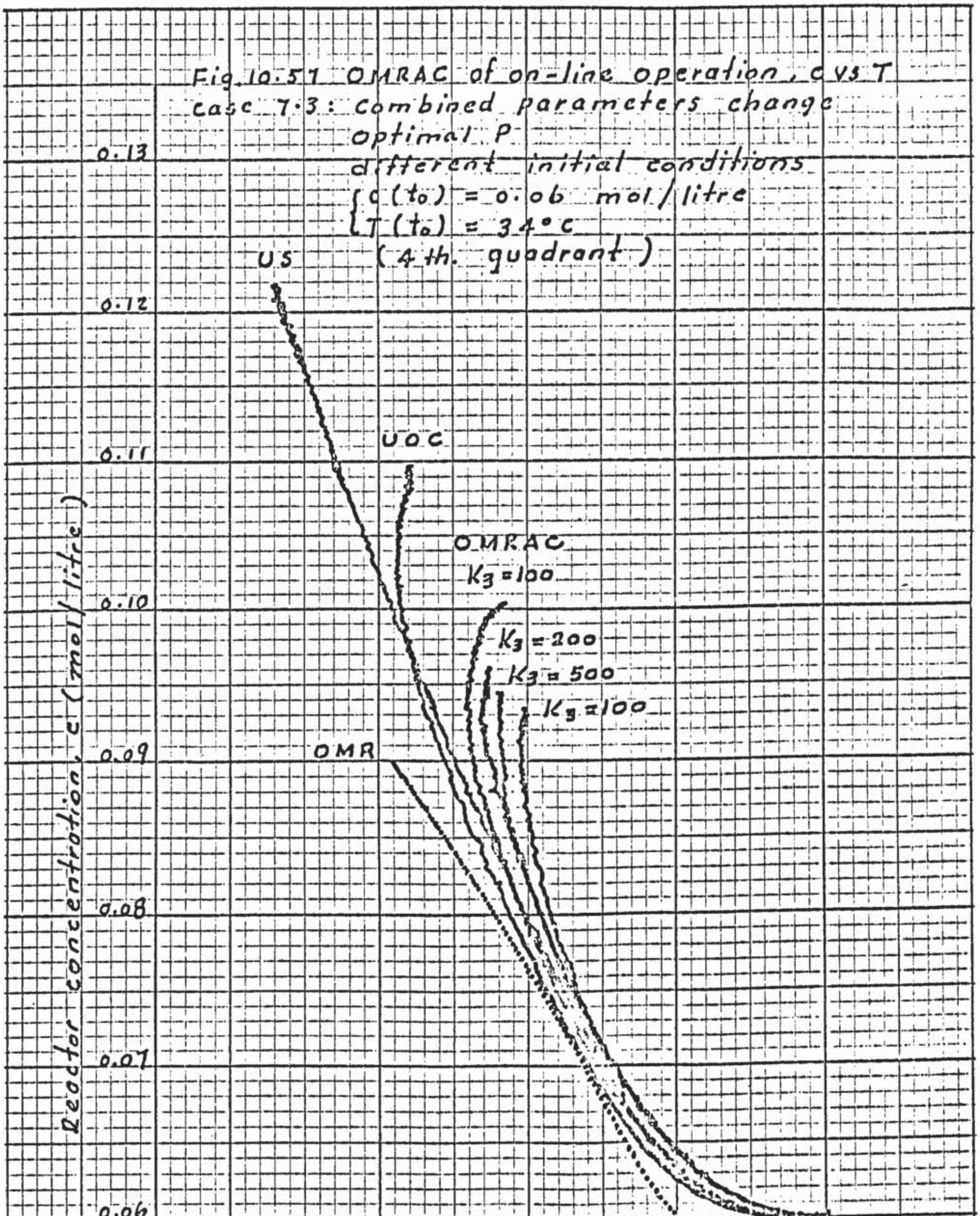

Fig. 10.51 OMRAC of on-line operation, c vs T
case 7·3: combined parameters change
optimal P
different initial conditions
$\begin{cases} c(t_0) = 0.06 \text{ mol/litre} \\ T(t_0) = 34^\circ c \end{cases}$
(4 th. quadrant)

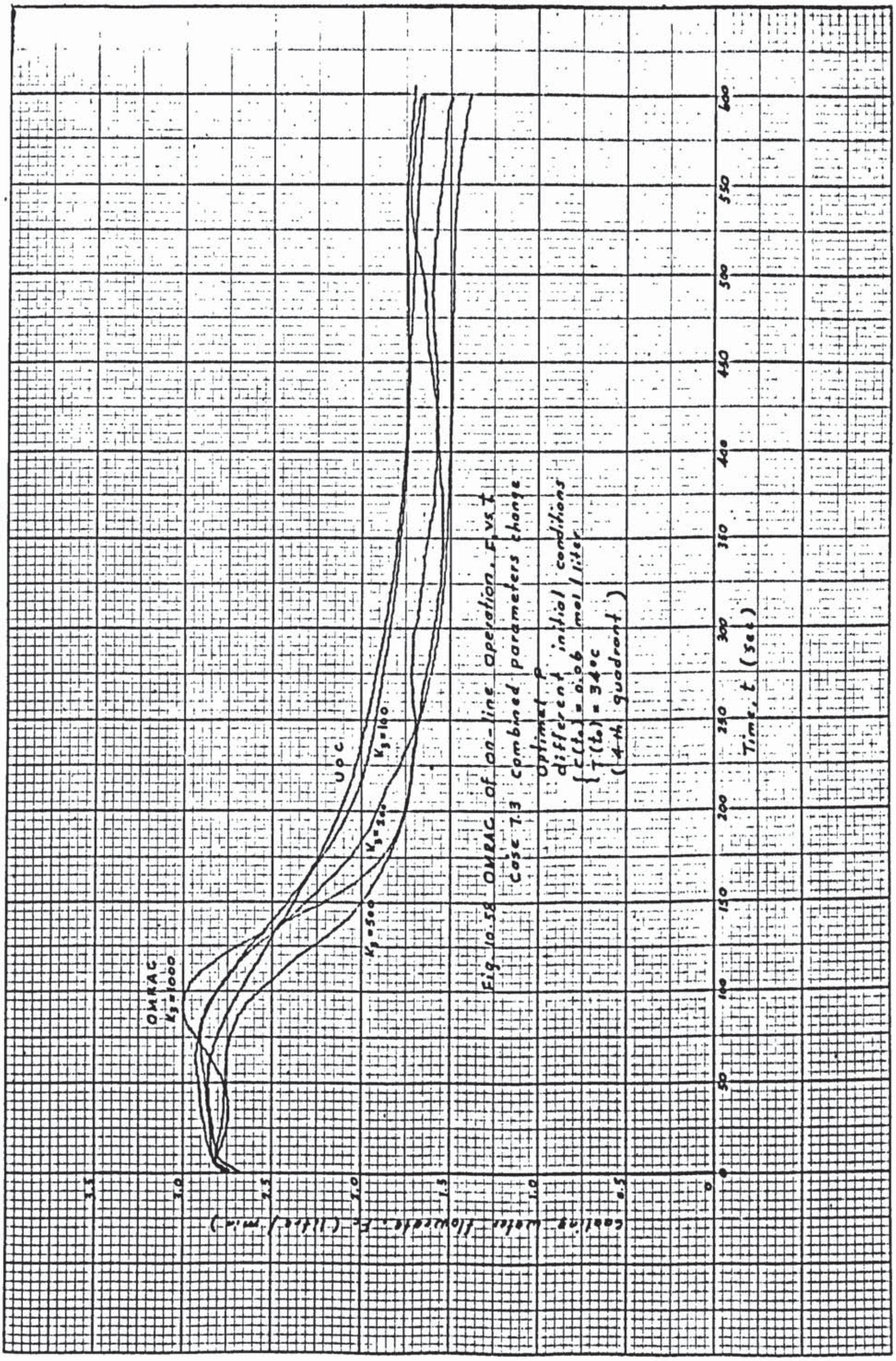

Fig 10.58 OMRAC of on-line operation, F vs. t
Case 7.3 combined parameters change
Optimal P
different initial conditions
{ $c(t_0)$ = 0.06 mol/liter
{ $T(t_0)$ = 34°C
(4th quadrant)

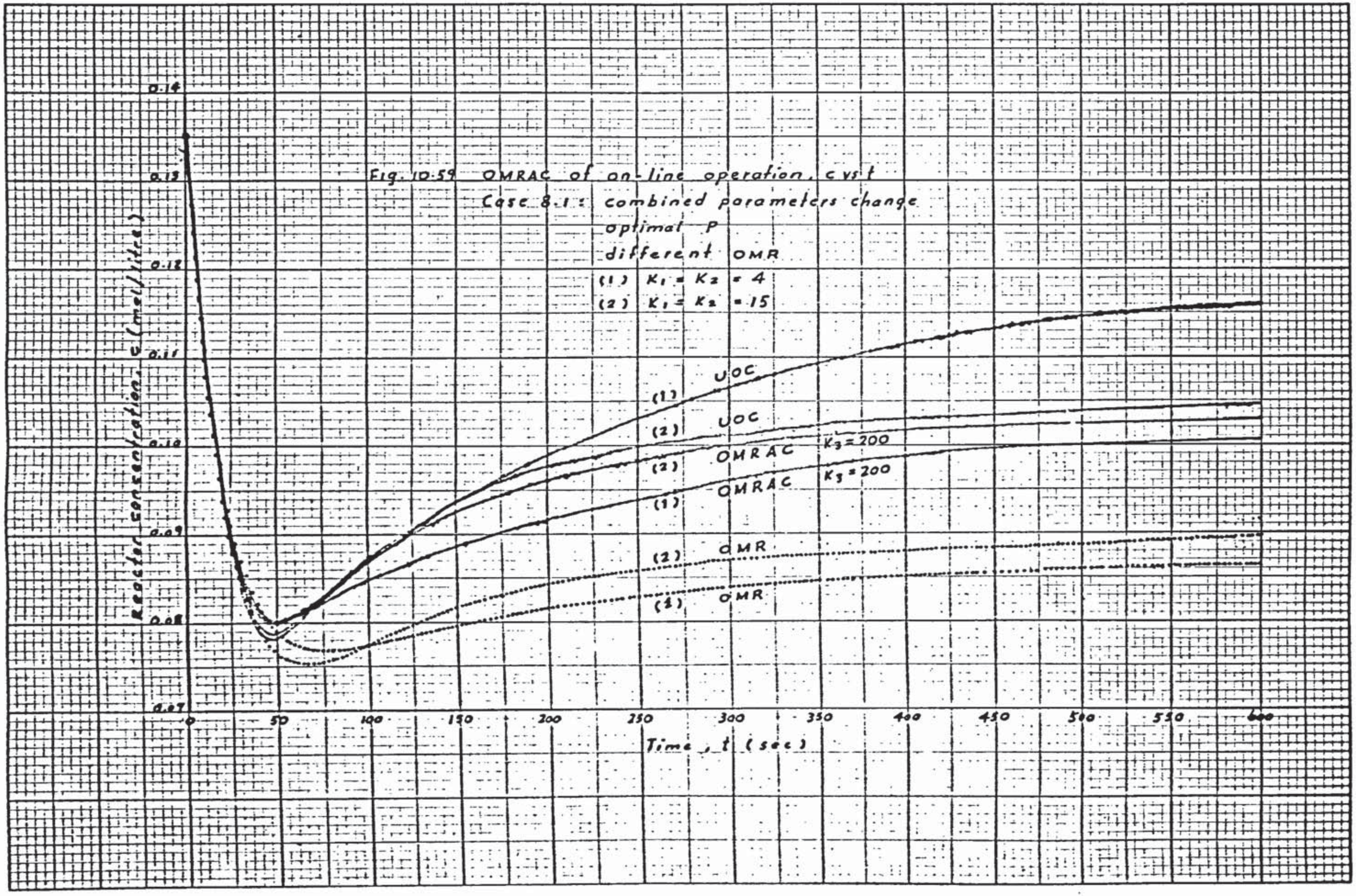

Fig. 10.59 OMRAC of on-line operation, c vs t
Case 8.1: combined parameters change
optimal P
different OMR
(1) $K_1 = K_2 = 4$
(2) $K_1 = K_2 = 15$

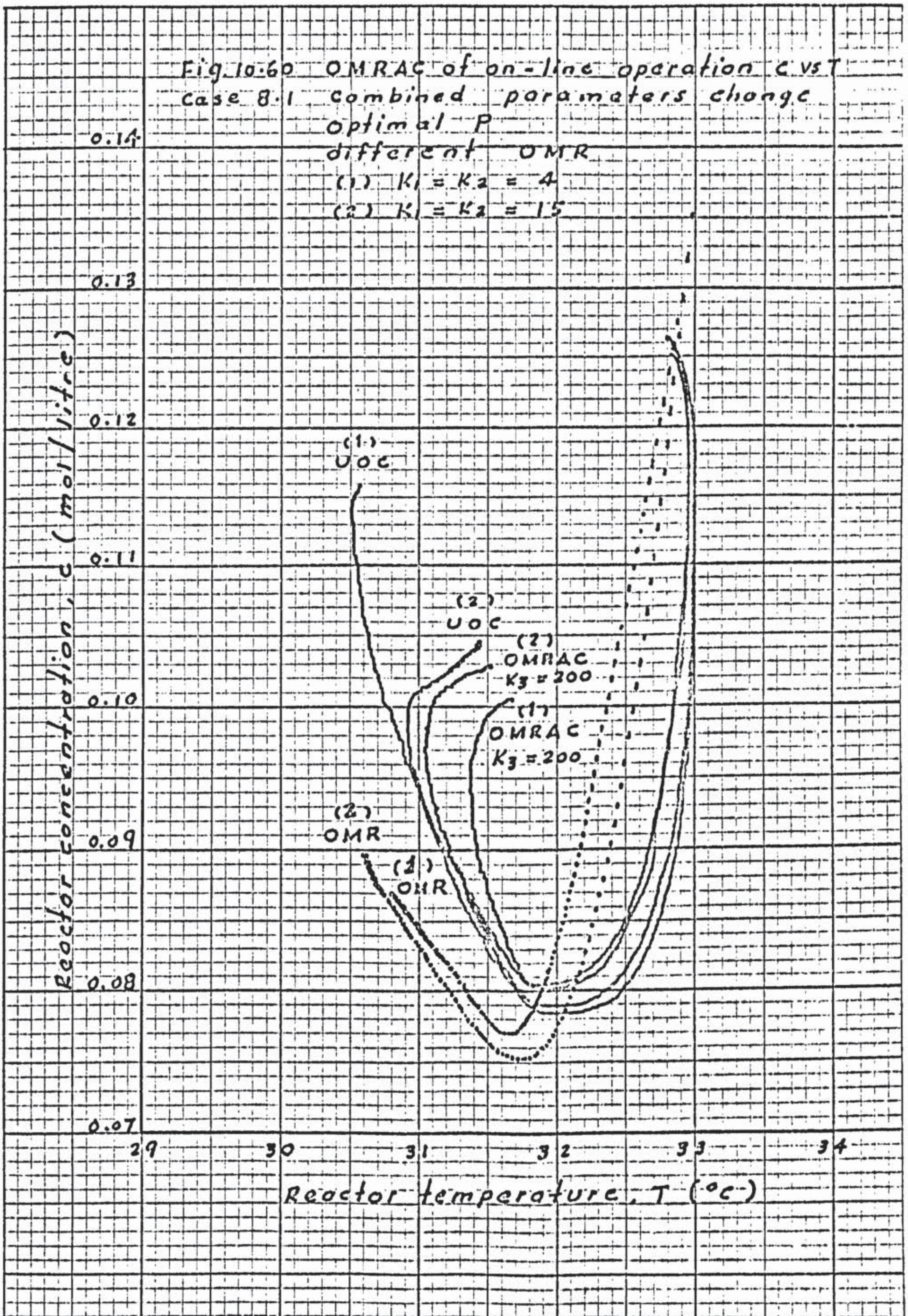
Fig. 10.60 OMRAC of on-line operation C vs T
Case 8.1 combined parameters change
optimal P
different OMR
(1) K1 = K2 = 4
(2) K1 = K2 = 15
0.14
0.13
0.12
0.11
0.10
0.09
0.08
0.07
(1) UOC
(2) UOC
(2) OMRAC K3 = 200
(1) OMRAC K3 = 200
(2) OMR
(1) OMR
29
30
31
32
33
34
Reactor concentration, c (mol/litre)
Reactor temperature, T (°C)

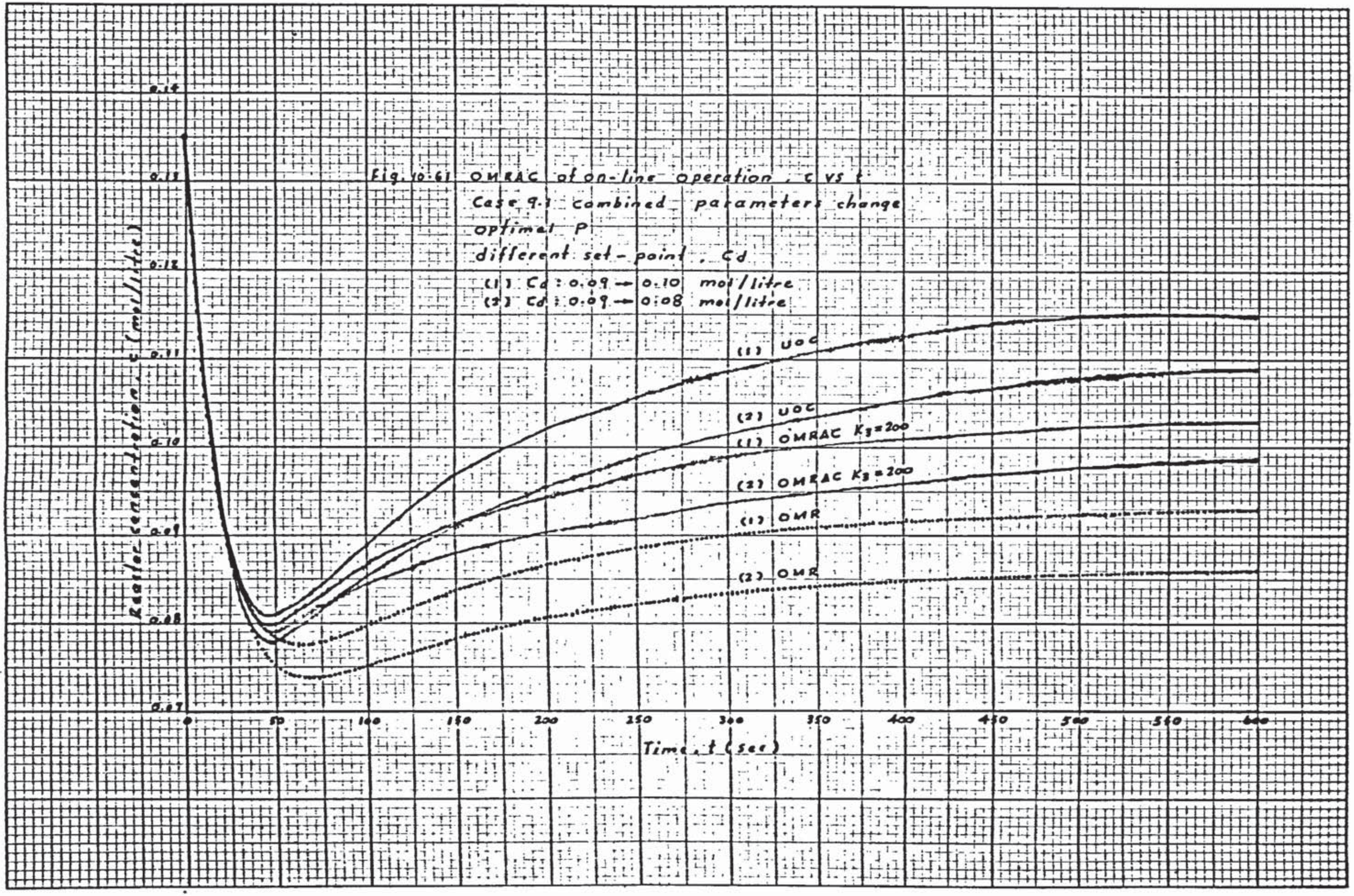

Fig. 10.61 OMRAC of on-line operation, c vs t
Case 9.1 combined parameters change
optimal P
different set-point, Cd
(1) Cd : 0.09 → 0.10 mol/litre
(2) Cd : 0.09 → 0.08 mol/litre

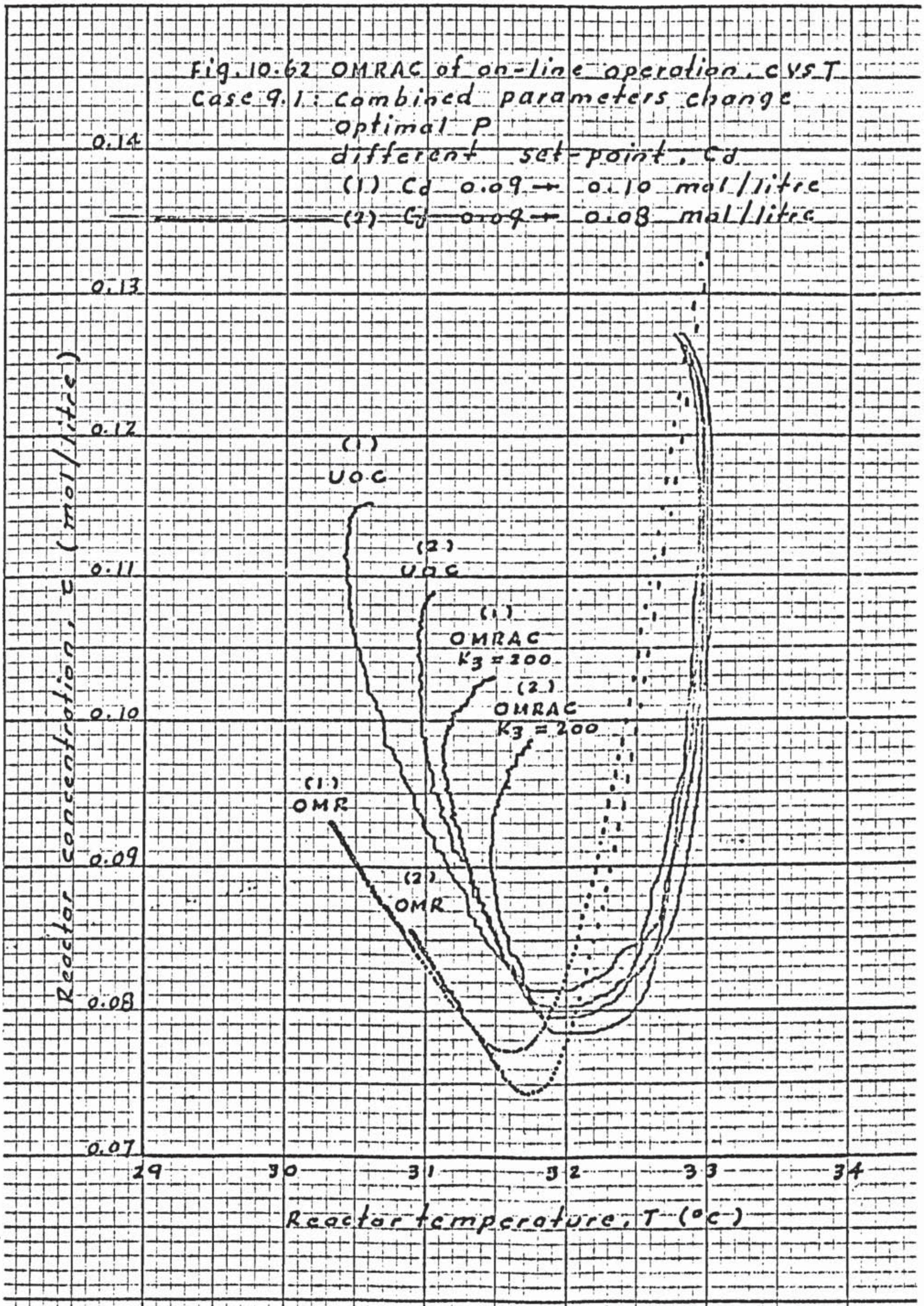

Fig. 10.62 OMRAC of on-line operation, c vs T
Case 9.1: Combined parameters change
optimal P
different set-point, Cd
(1) Cd 0.09 → 0.10 mol/litre
(2) Cd 0.09 → 0.08 mol/litre
0.14
0.13
0.12
0.11
0.10
0.09
0.08
0.07
(1) UOC
(2) UOC
(1) OMRAC K3 = 200
(2) OMRAC K3 = 200
(1) OMR
(2) OMR
29
30
31
32
33
34
Reactor temperature, T (°c)
Reactor concentration, c (mol/litre)

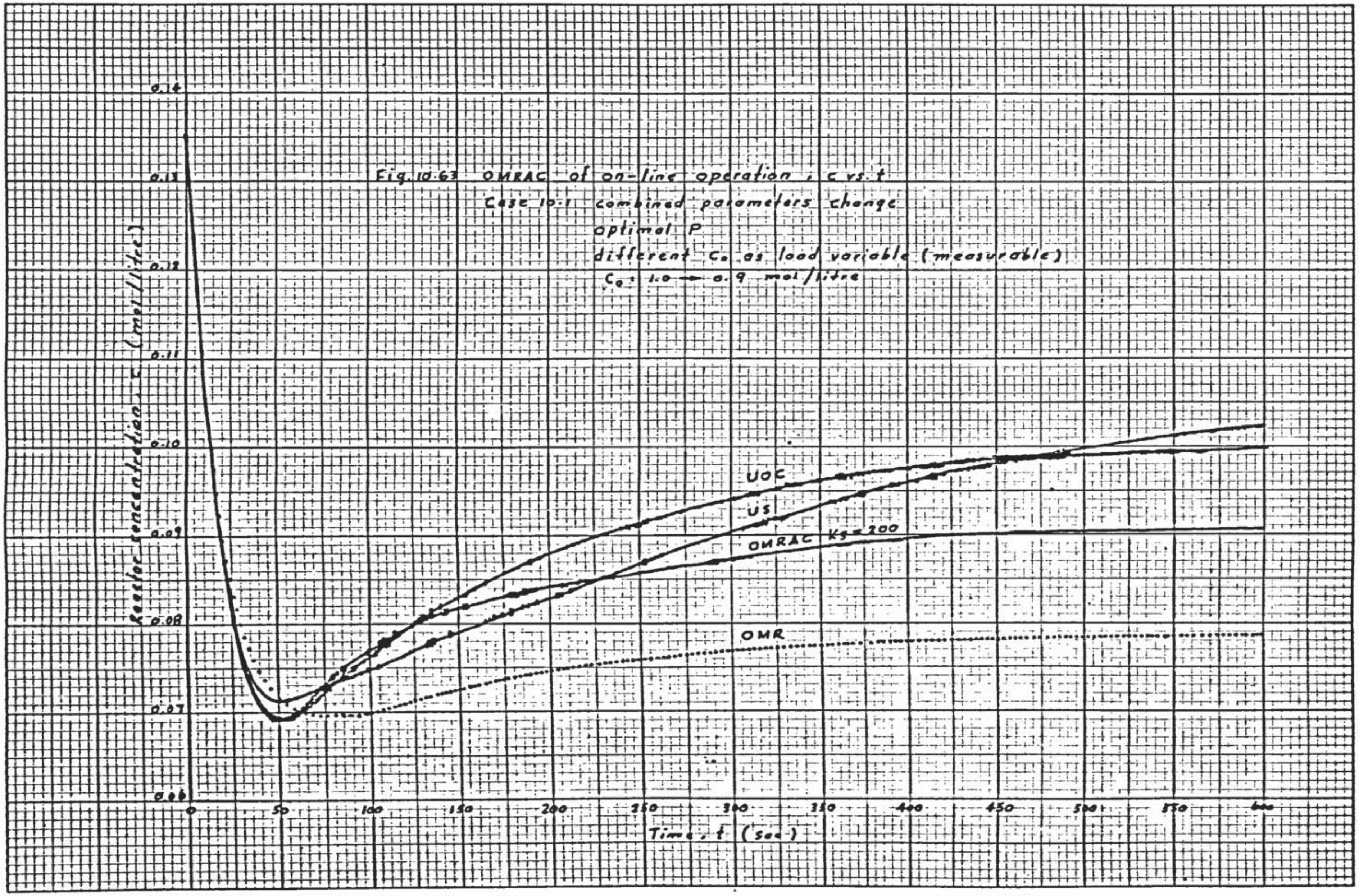

Fig. 10.63 OMRAC of on-line operation, c vs. t
Case 10.1 combined parameters change
optimal P
different C_0 as load variable (measurable)
C_0: 1.0 → 0.9 mol/litre

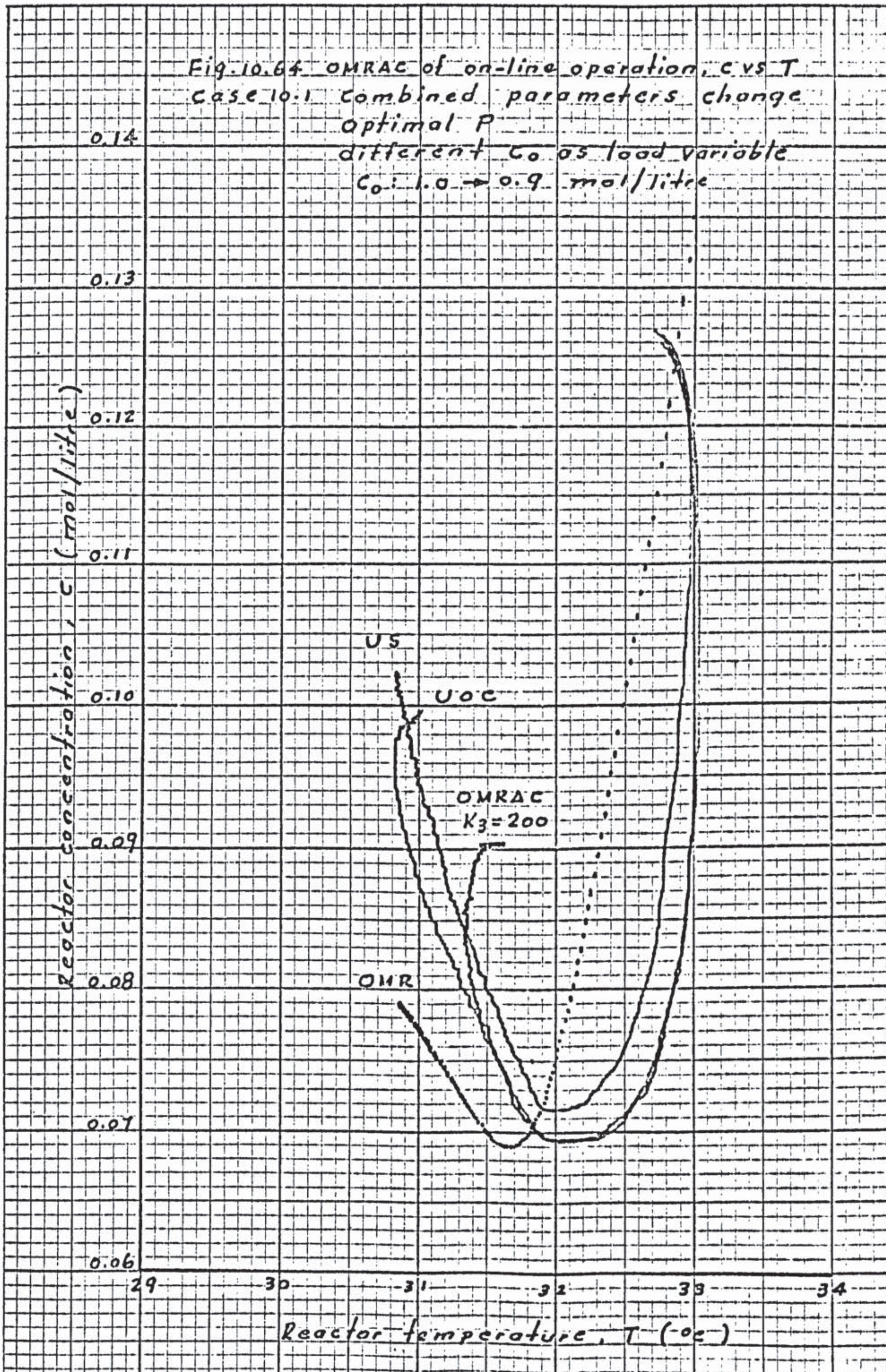

Fig. 10.64 OMRAC of on-line operation, C vs T
case 10.1 combined parameters change
optimal P
different C_o as load variable
C_o: 1.0 → 0.9 mol/litre

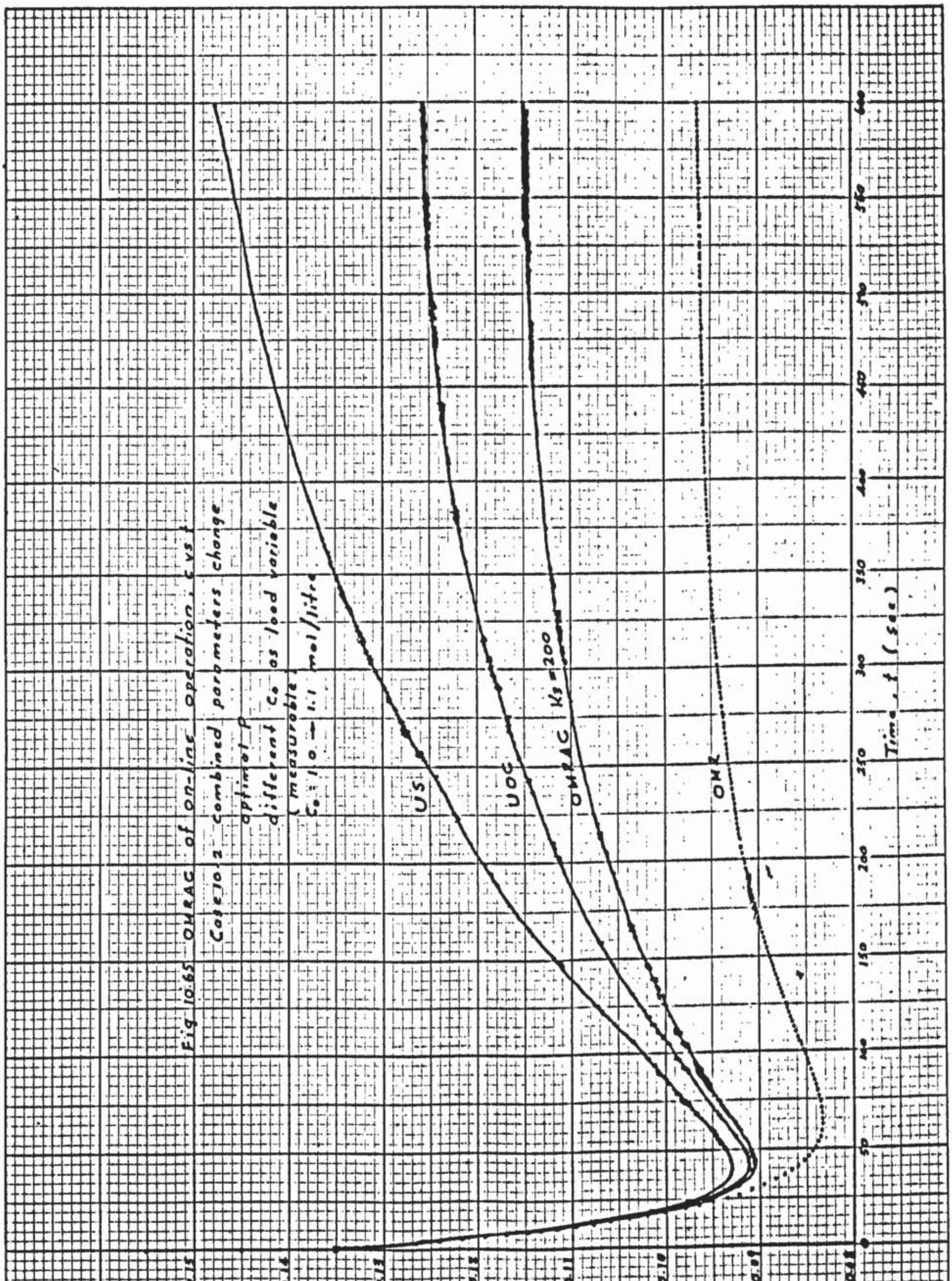

Fig 10.65 OHRAC of on-line operation, c vs t
Case 10.2 combined parameters change
optimal ρ
different C_0 as load variable
(measurable ; C_0 : 1.0 → 1.1 mol/liter

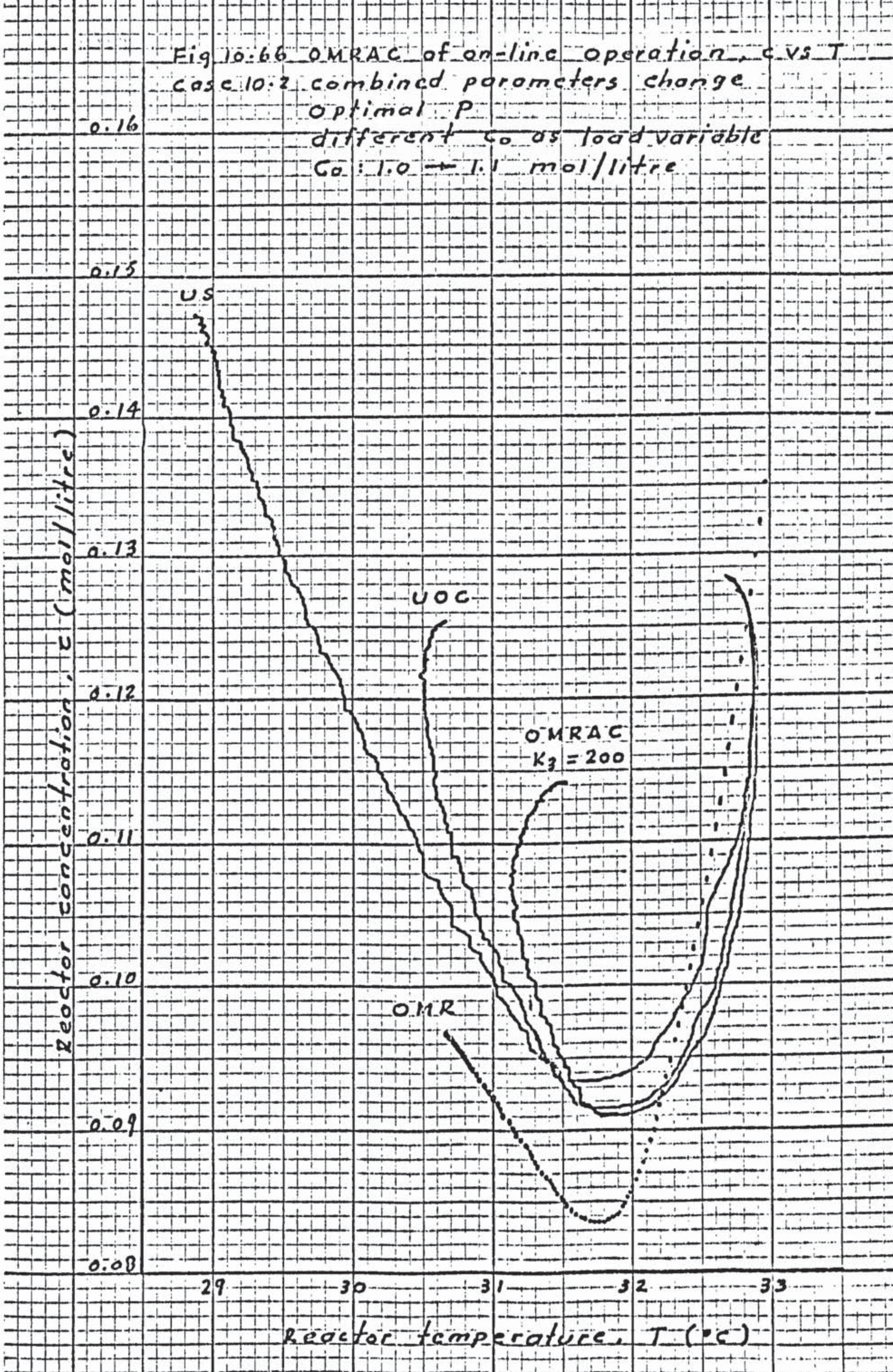

Fig 10:66 OMRAC of on-line operation, c vs T
case 10:2 combined parameters change
Optimal P
different c_0 as load variable
C_0 : 1.0 → 1.1 mol/litre
US
UOC
OMRAC
$K_3 = 200$
OMR
0.16
0.15
0.14
0.13
0.12
0.11
0.10
0.09
0.08
29
30
31
32
33
Reactor concentration, c (mol/litre)
Reactor temperature, T (°C)

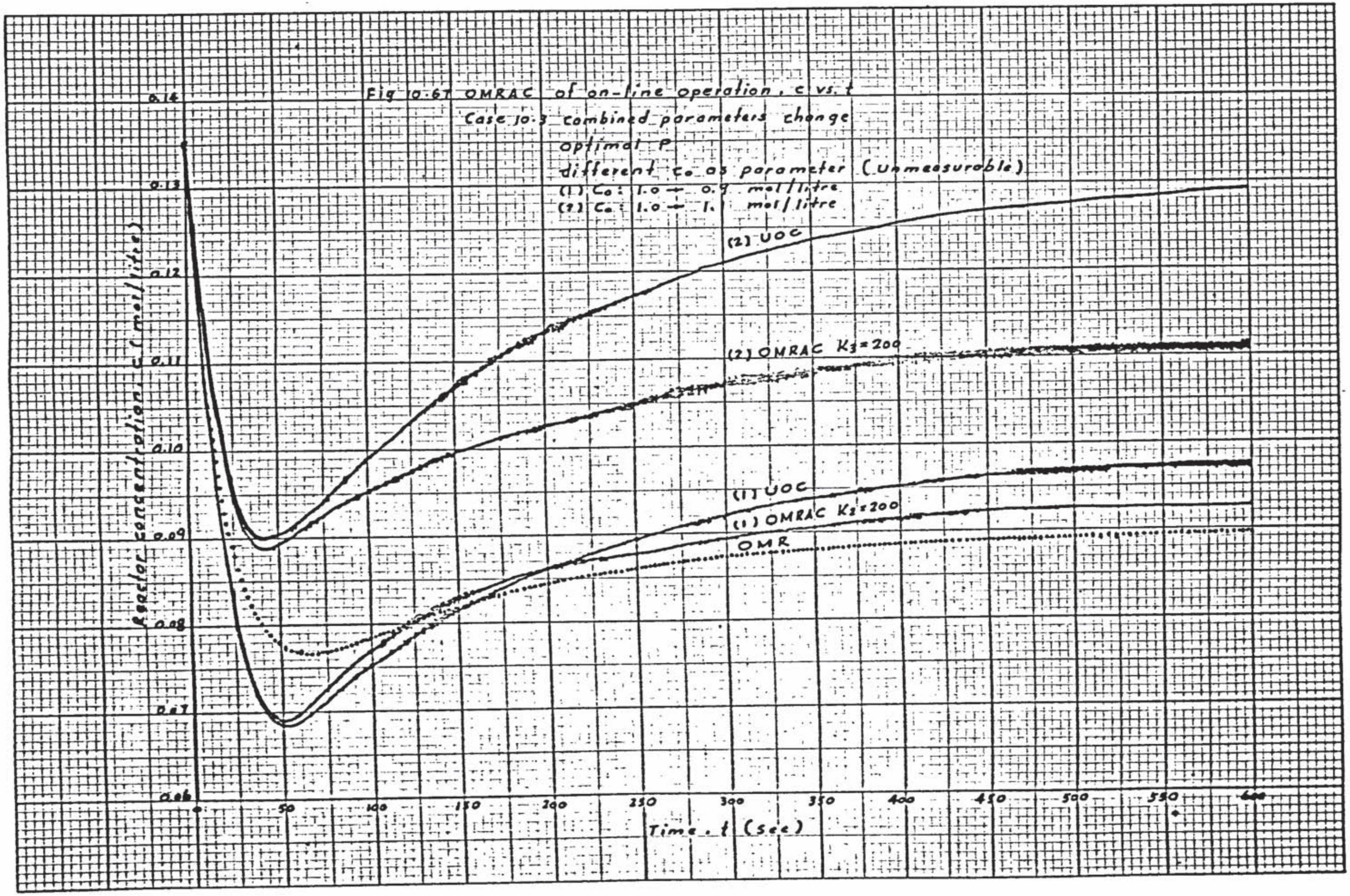
Fig 10.67 OMRAC of on-line operation, c vs. t
Case 10.3 combined parameters change
optimal P
different co as parameter (Unmeasurable)
(1) Co: 1.0 → 0.9 mol/litre
(2) Co: 1.0 → 1.1 mol/litre
(2) UOC
(2) OMRAC K3=200
(1) UOC
(1) OMRAC K3=200
OMR
Reactor concentration, c (mol/litre)
0.14
0.13
0.12
0.11
0.10
0.09
0.08
0.07
0.06
0
50
100
150
200
250
300
350
400
450
500
550
600
Time, t (sec)

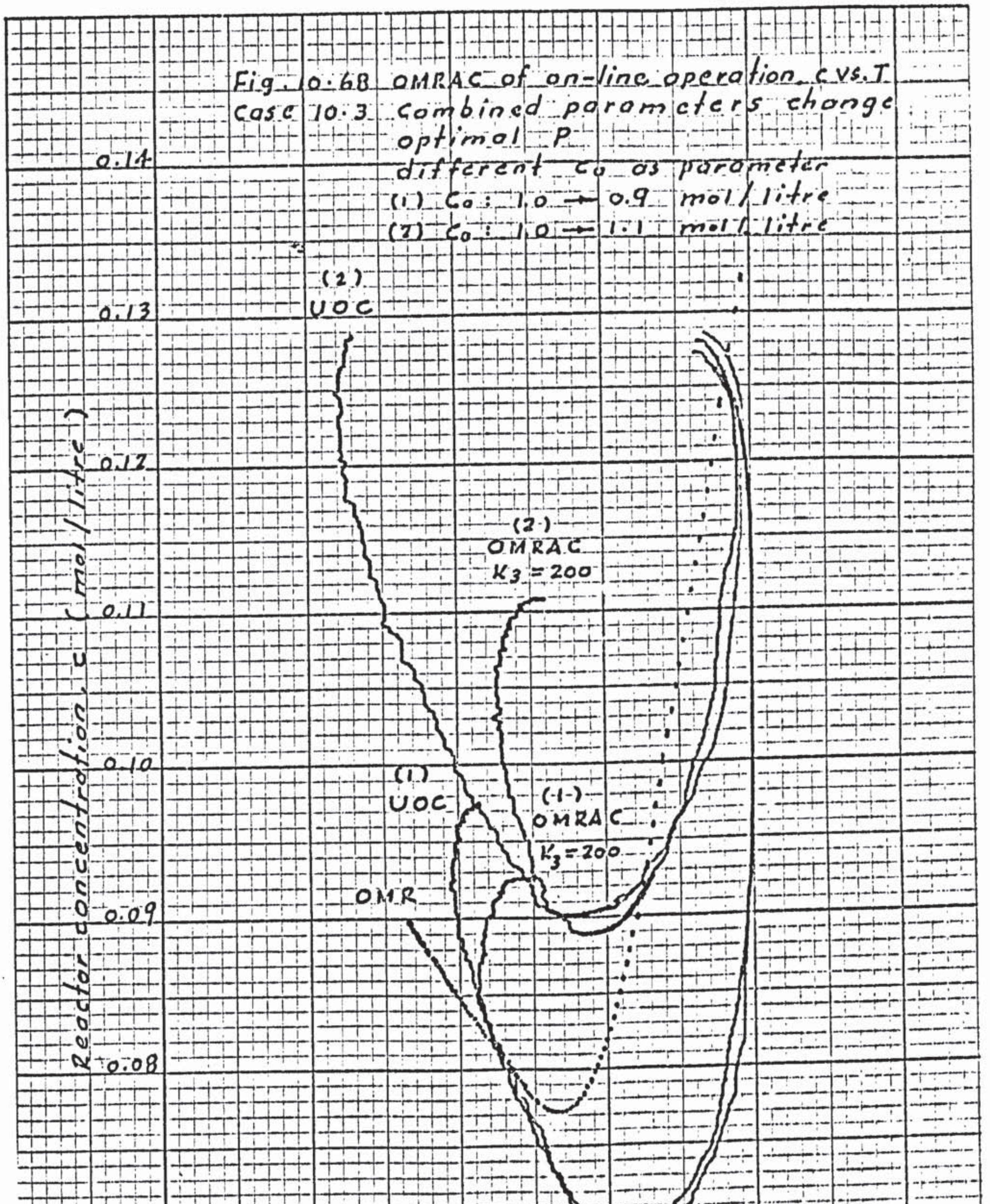

Fig. 10.68 OMRAC of on-line operation, c vs. T
case 10.3 combined parameters change
optimal P
different c_0 as parameter
(1) c_0: 1.0 → 0.9 mol/litre
(2) c_0: 1.0 → 1.1 mol/litre

CHAPTER 11

OPTIMAL ADAPTIVITY

11.1. Definition

All analysis and discussion of OMRAC both for complete simulation (Chapter 7) and on-line operation (Chapter 10) is directly based on the plotter response figures. Now for a fundamental and quantitative analysis and evaluation of OMRAC a new term "Optimal Adaptivity" is introduced and defined as follows:

$$\text{Optimal Adaptivity } \psi, \% = \frac{\left(\left[\int_0^{t_f} e^2(t)dt \right]_{UOC} - \left[\int_0^{t_f} e^2(t)dt \right]_{MRAC} \right) \times 100}{\left[\int_0^{t_f} e^2(t) \right]_{UOC}}$$

where $\int_0^{t_f} e^2(t)dt$ = Performance response, $\left(\frac{mol}{litre}\right)^2 (sec)$

$e(t) = \left(\theta_1^r(t) - \theta_1(t) \right)$

$= \left(C_r(t) - C(t) \right) \frac{mol}{litre}$

UOC = Unadapted optimal control

and MRAC = Model reference adaptive control which in this research is OMRAC

From the definition, optimal adaptivity can be used as a general term to evaluate any kind of model reference adaptive control.

By using calculated optimal adaptivity with performance response and different weighting factors (K_3) of OAC, a set of three dimensional figures both for complete simulation and for on-line operation of OMRAC can be drawn to show the overall perspective picture of the whole OMRAC system.

11.2. Optimal adaptivity of complete simulation

From Appendix 4, Figs. A.4.1. to A.4.21 obtained by the X-Y plotter, the values of optimal adaptivity for all the different cases can be calculated and are shown in Appendix 7, Tables A.7.1. to A.7.5. and the corresponding optimal adaptivity figures are drawn and shown in Figs. 11.1 to 11.8.

11.3. Optimal adaptivity of on-line operation

Performance response for on-line operation is calculated directly from all dynamic response figures by using a planimeter; the method of calculation is shown in Appendix 7.6.

The values of calculated optimal adaptivity for all the different cases of on-line operation are shown in Appendix 7, Tables A.7.6 to A.7.18, and the corresponding optimal adaptivity figures are drawn and shown in Figs. 11.9 to 11.16.

11.4. Analysis and discussion

11.4.1. From the two sets of eight optimal adaptivity figures, the overall perspective figures of the OMRAC system both for complete simulation (theoretical) and on-line operation (practical) are clearly shown to be in good agreement.

11.4.2. The optimal adaptivity always increases from $\psi \simeq 50\%$ up to $\psi \simeq 95\%$ as K_3 increases from 100 to 1000. (In case 1.3 where $K_3 = 4000$ for on-line operation optimal adaptivity is higher at 98.43%).

11.4.3. The optimal adaptivity for optimal P + I is much higher than for optimal P alone:

$\psi \simeq 95\%$ ($\epsilon = 1.0$) (Optimal P + I) $\psi \simeq 50\%$ ($\epsilon = 0$) (Optimal P)

11.4.4. The optimal adaptivity optimal P + I + D is much higher than optimal P + D:

$\psi \triangleq 90\%$ ($\epsilon = 0.12$) (Optimal P + I + D) $\psi \triangleq 50\%$ ($\epsilon = 0$) (Optimal P + D)

11.4.5. The optimal adaptivity for a constant weighting factor (K_3) of the OAC scheme increases when K_1 and K_2, the weighting factors, of the OMR scheme, decreases.

11.4.6. The optimal adaptivity for different set-point changes (or desired steady state reactor concentration) is approximately the same for complete simulation and on-line operation. Thus:

$\psi \triangleq 66\%$ in complete simulation

$\psi \triangleq 60\%$ to 75% in on-line operation.

So, optimal adaptivity of OMRAC is independent of the different set-point changes.

11.4.7. The optimal adaptivity for different inlet concentration changes is also approximately the same, or

$\psi \triangleq 66\%$ in complete simulation

$\psi \triangleq 55\% - 70\%$ in on-line operation.

So, optimal adaptivity of OMRAC is independent of the different inlet concentration changes.

11.4.8. From the above discussion and analysis, the theoretical development of OMRAC has been well established and proved with high performance both in theoretical complete simulation and in practical on-line simulation.

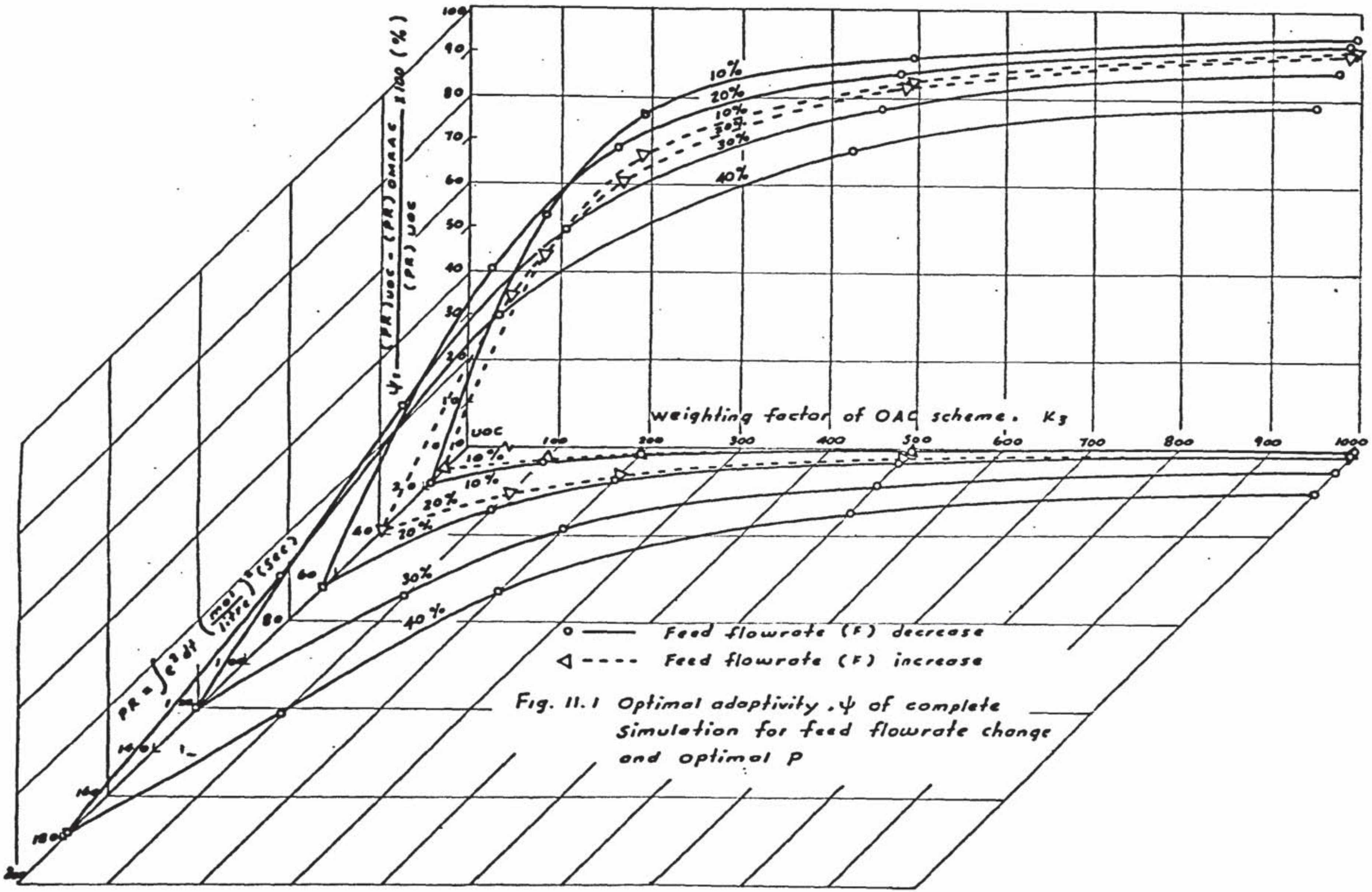

Fig. 11.1 Optimal adaptivity, ψ of complete simulation for feed flowrate change and optimal P

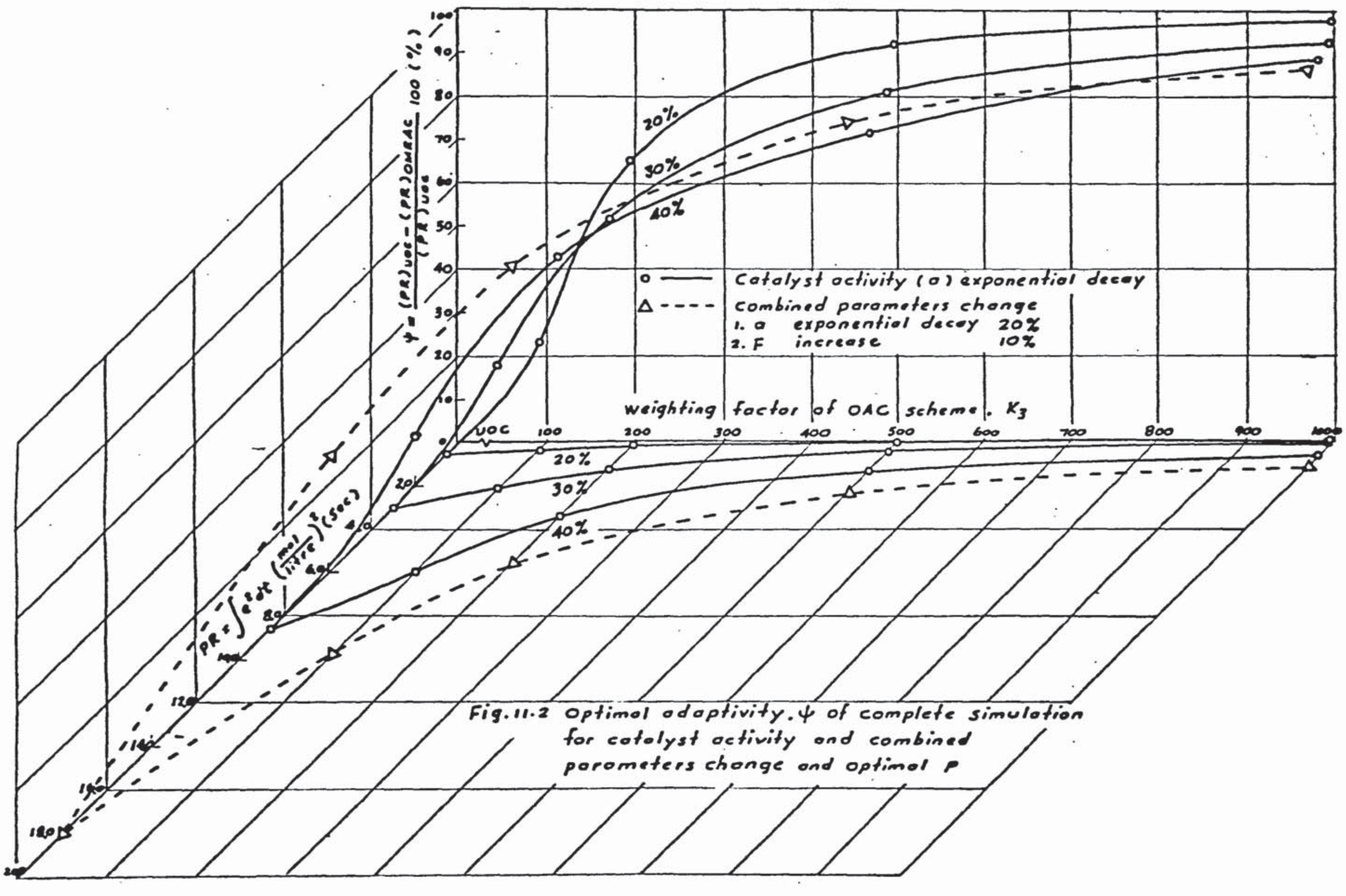

Fig. 11.2 Optimal adaptivity, ψ of complete simulation for catalyst activity and combined parameters change and optimal P

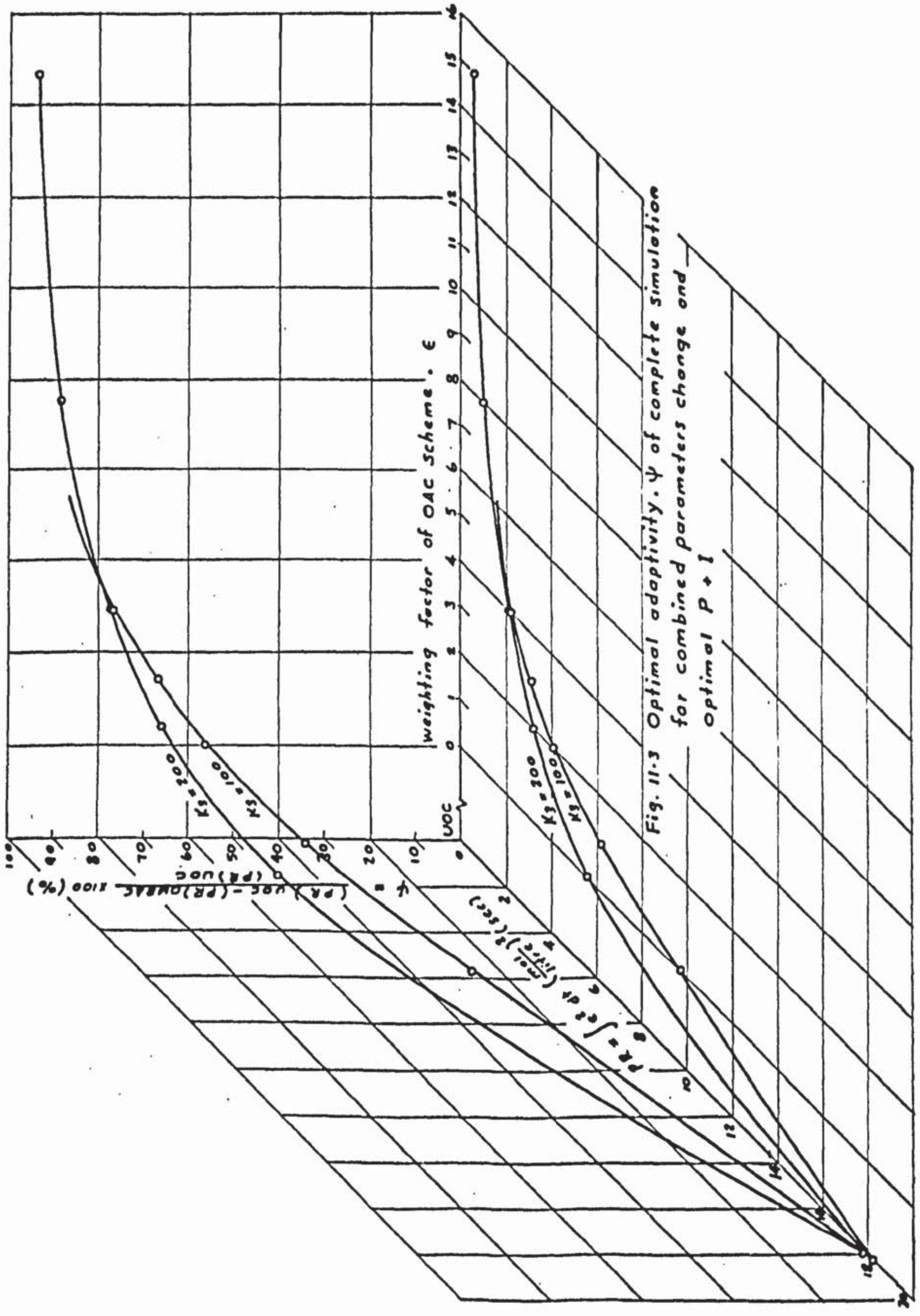

Fig. 11.3 Optimal adaptivity. Ψ of complete simulation for combined parameters change and optimal P + I

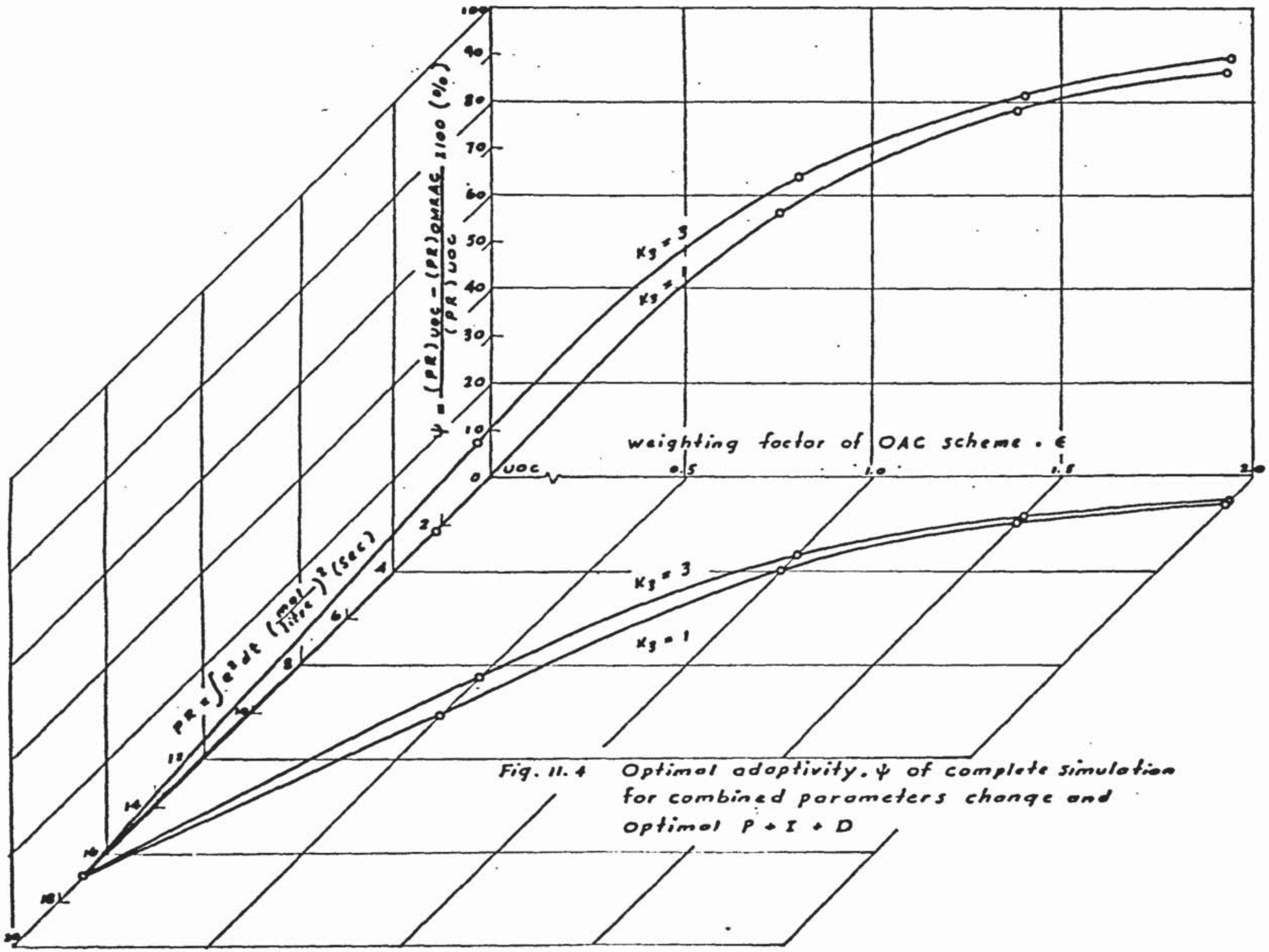

Fig. 11.4 Optimal adaptivity, ψ of complete simulation for combined parameters change and optimal P + I + D

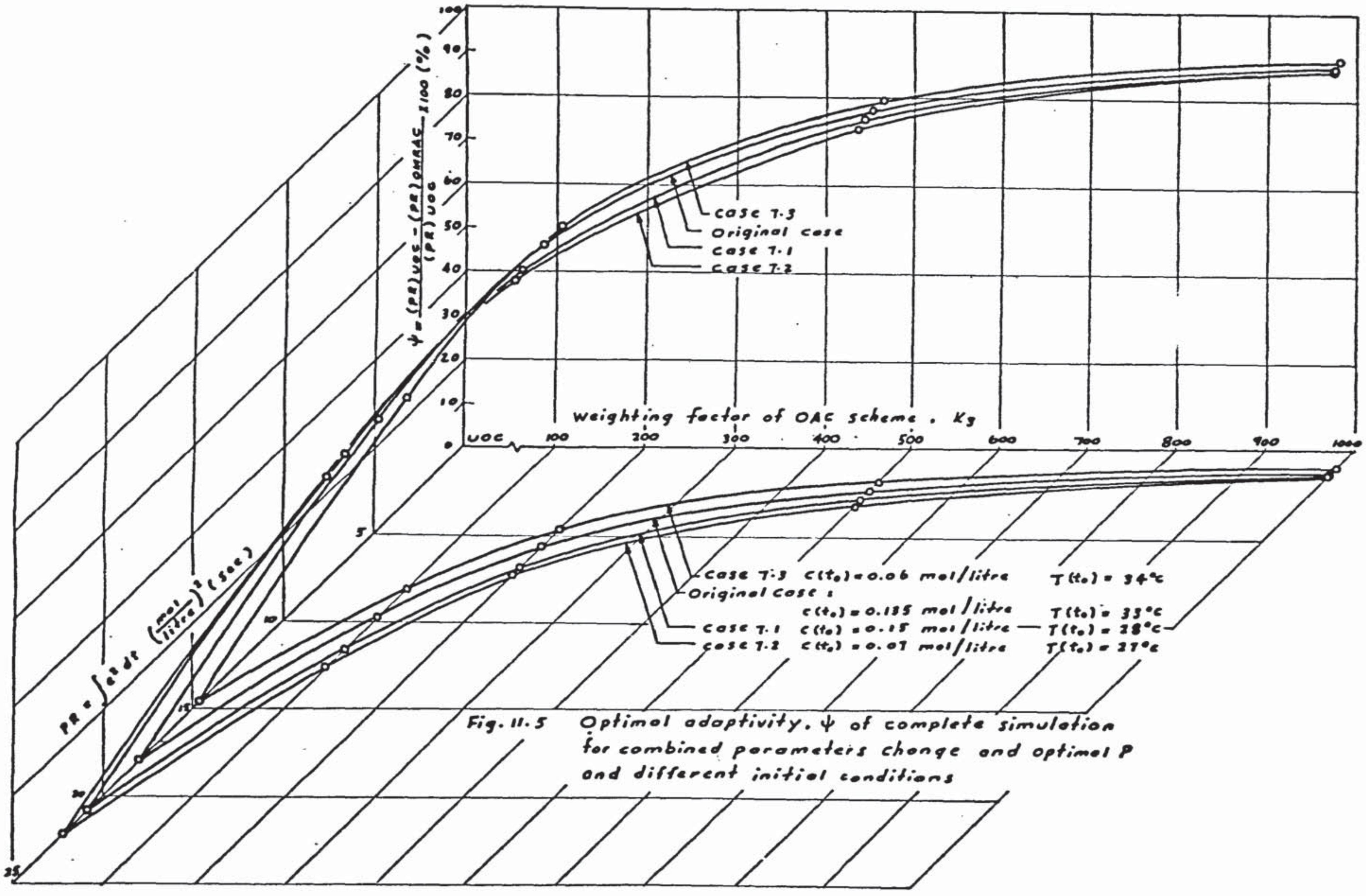

Fig. 11.5 Optimal adaptivity, ψ of complete simulation for combined parameters change and optimal P and different initial conditions

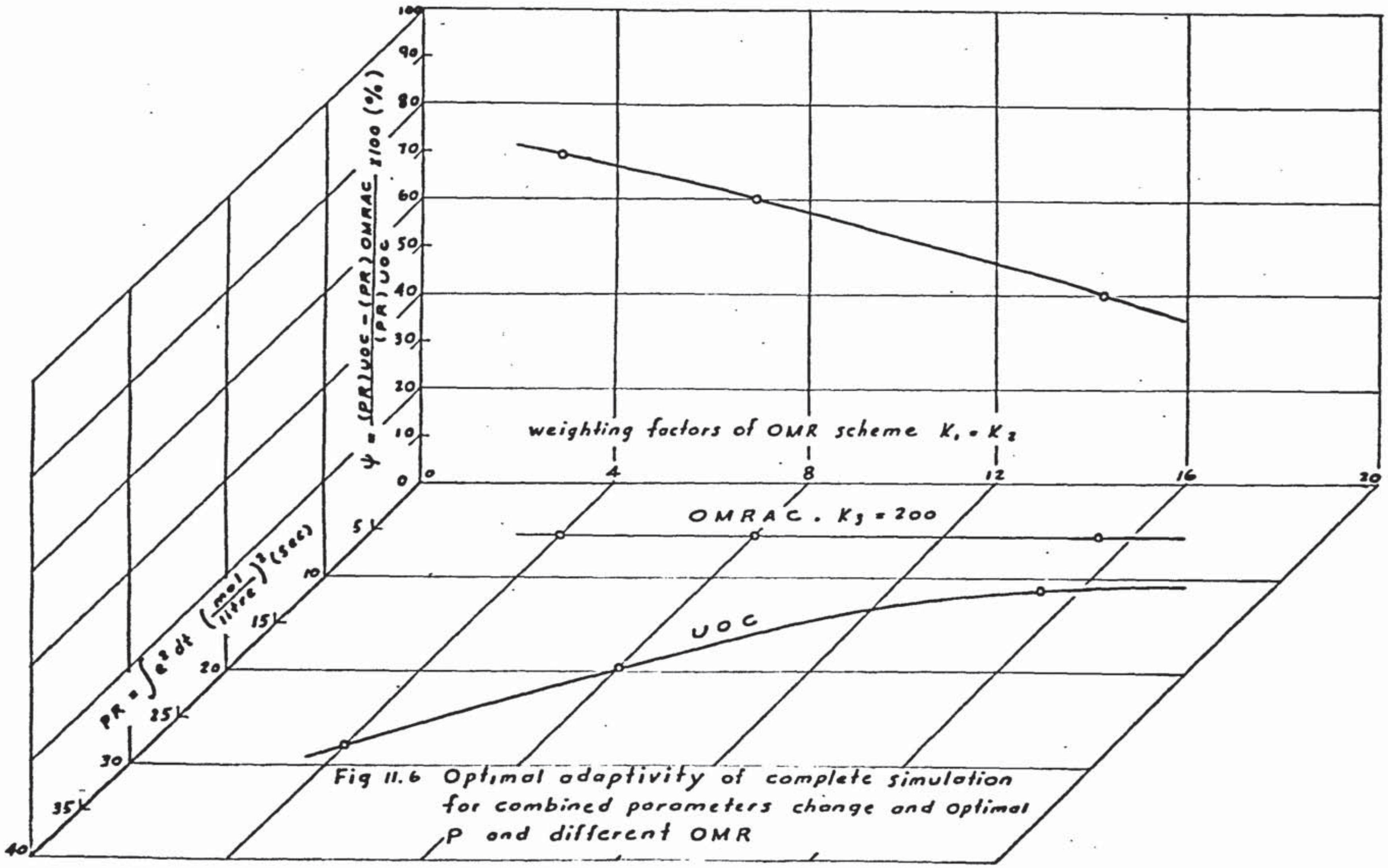

Fig 11.6 Optimal adaptivity of complete simulation for combined parameters change and optimal P and different OMR

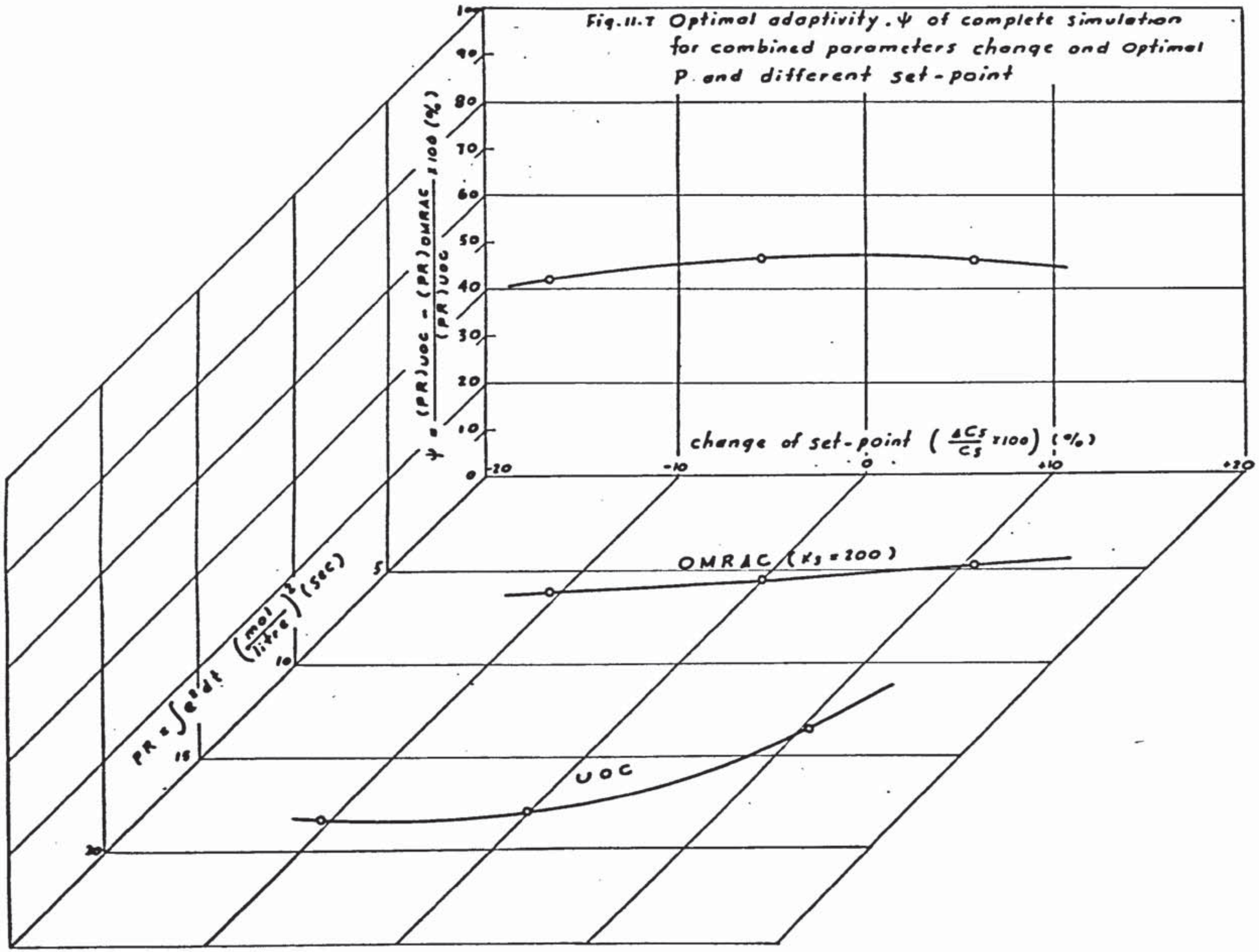

Fig. 11.7 Optimal adaptivity, ψ of complete simulation for combined parameters change and Optimal P and different set-point

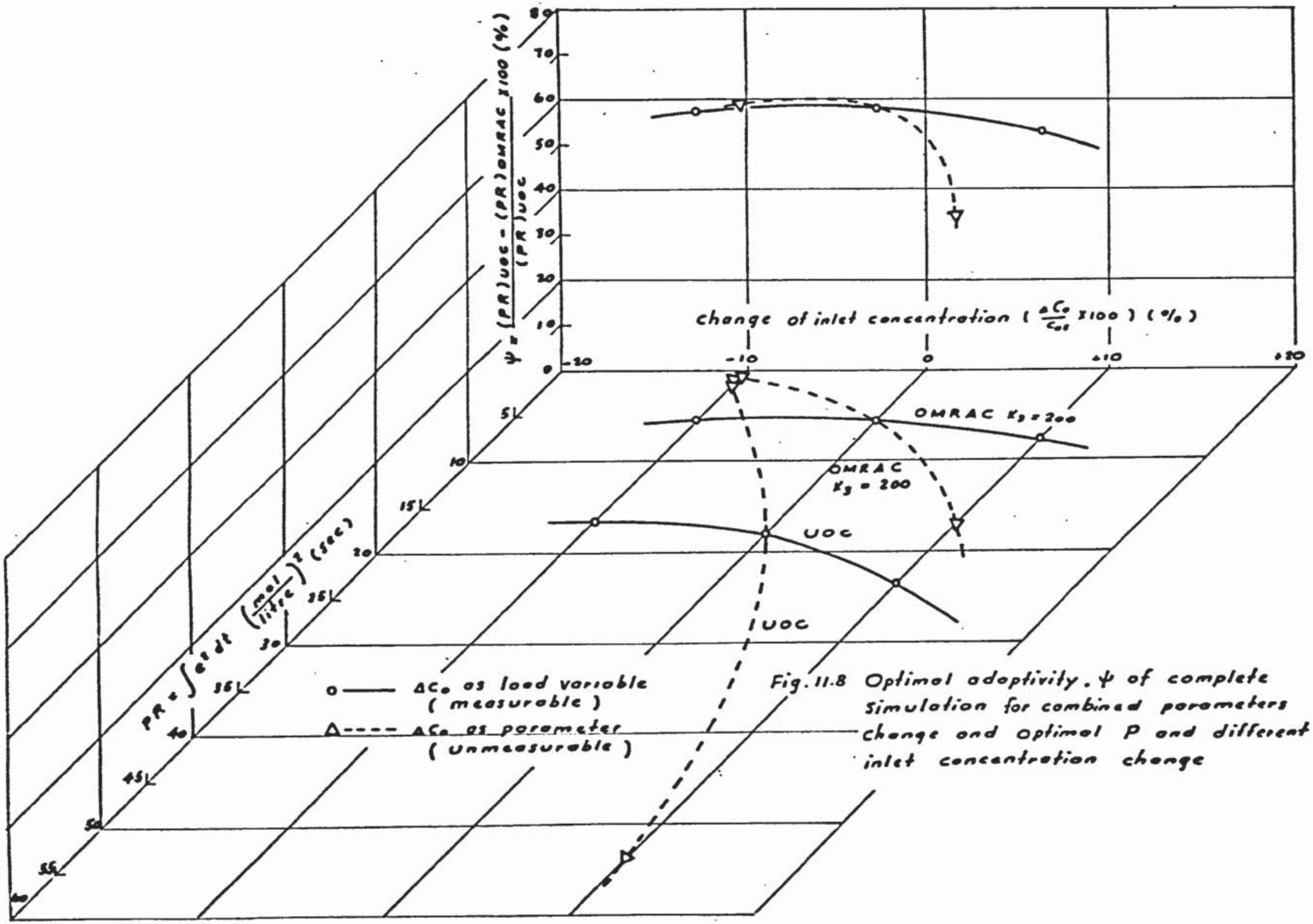

Fig. 11.8 Optimal adaptivity, ψ of complete simulation for combined parameters change and optimal P and different inlet concentration change

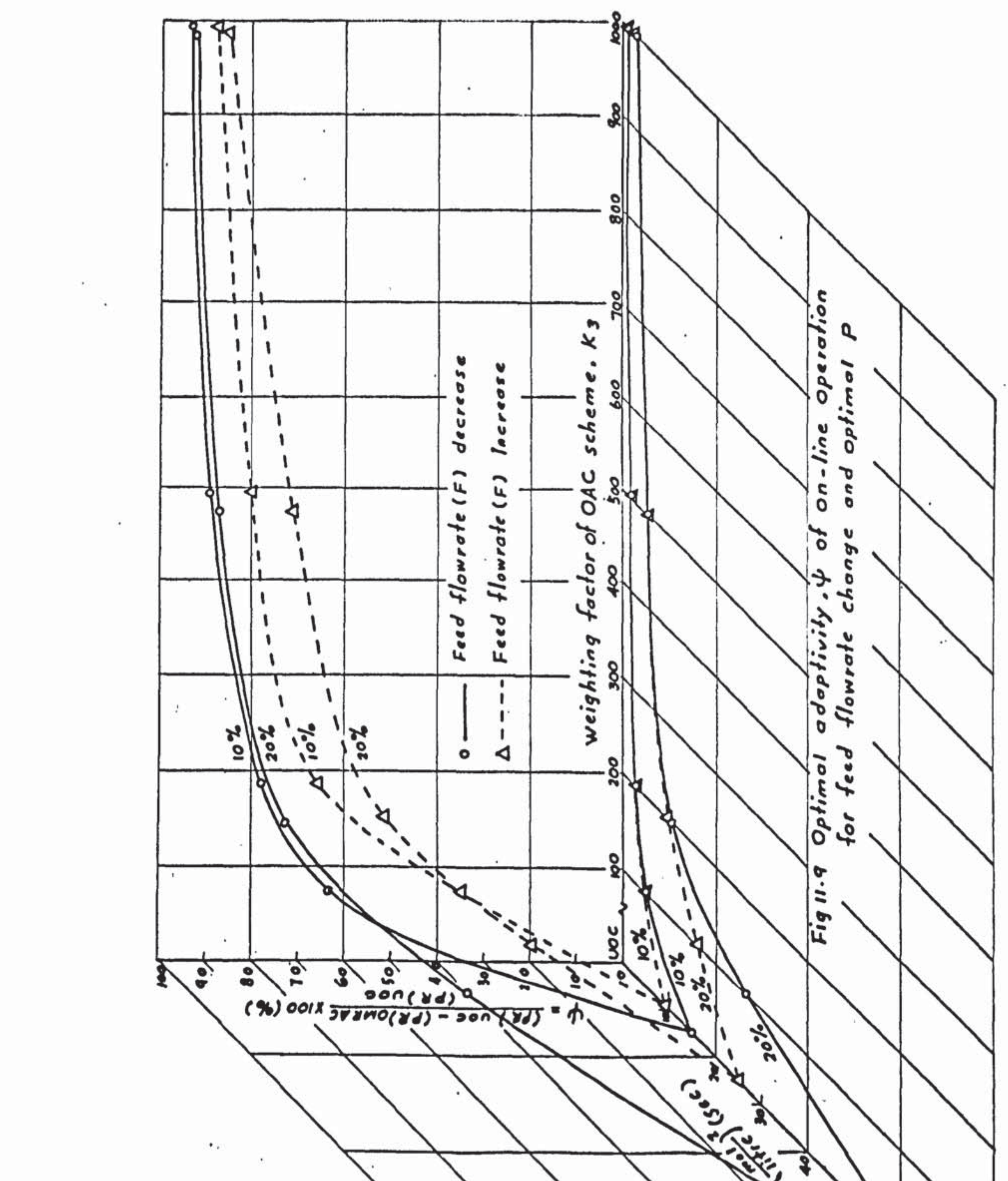

Fig 11.9 Optimal adaptivity, Ψ of on-line Operation for feed flowrate change and optimal P

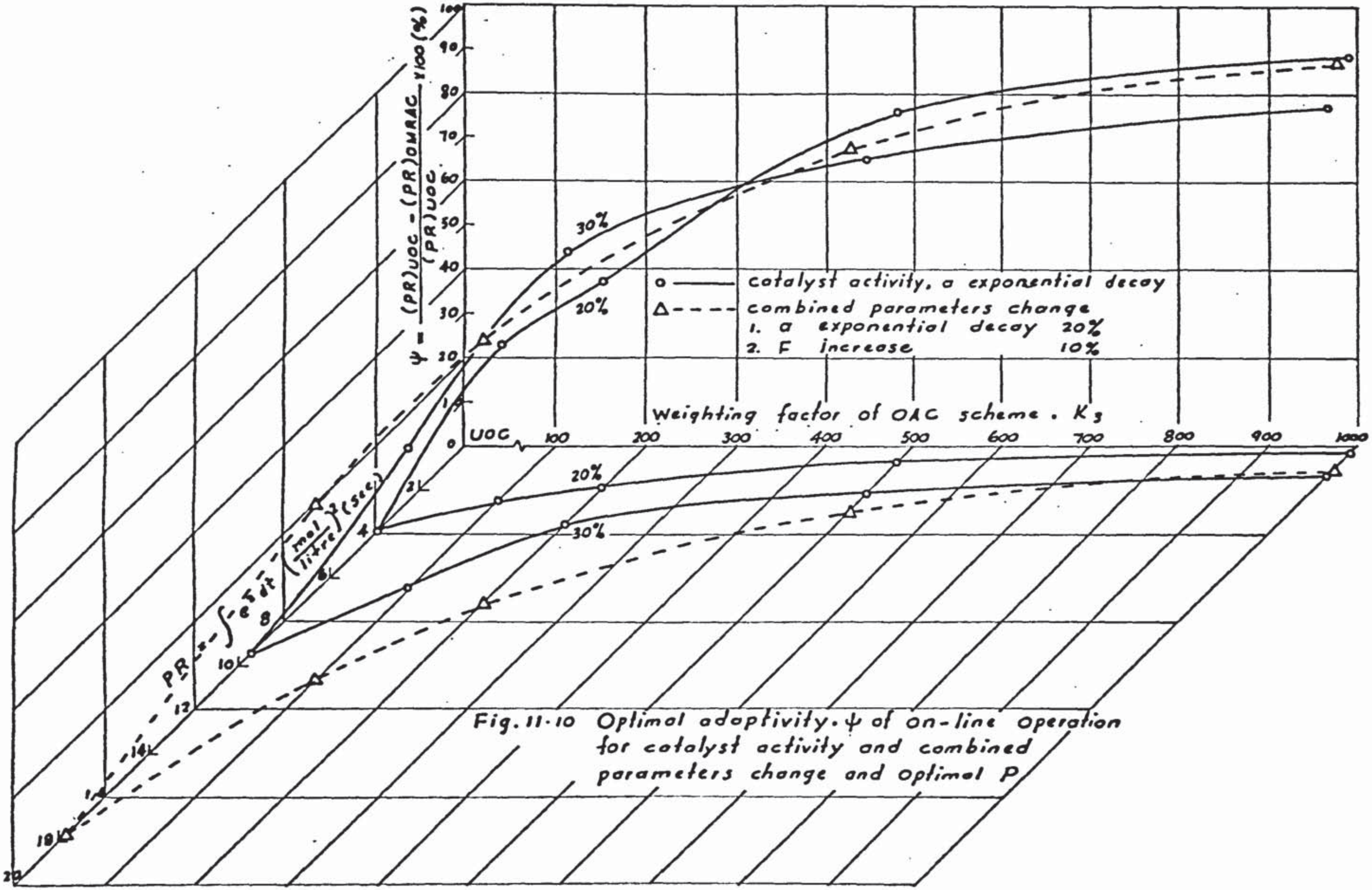

Fig. 11·10 Optimal adaptivity, ψ of on-line operation for catalyst activity and combined parameters change and optimal P

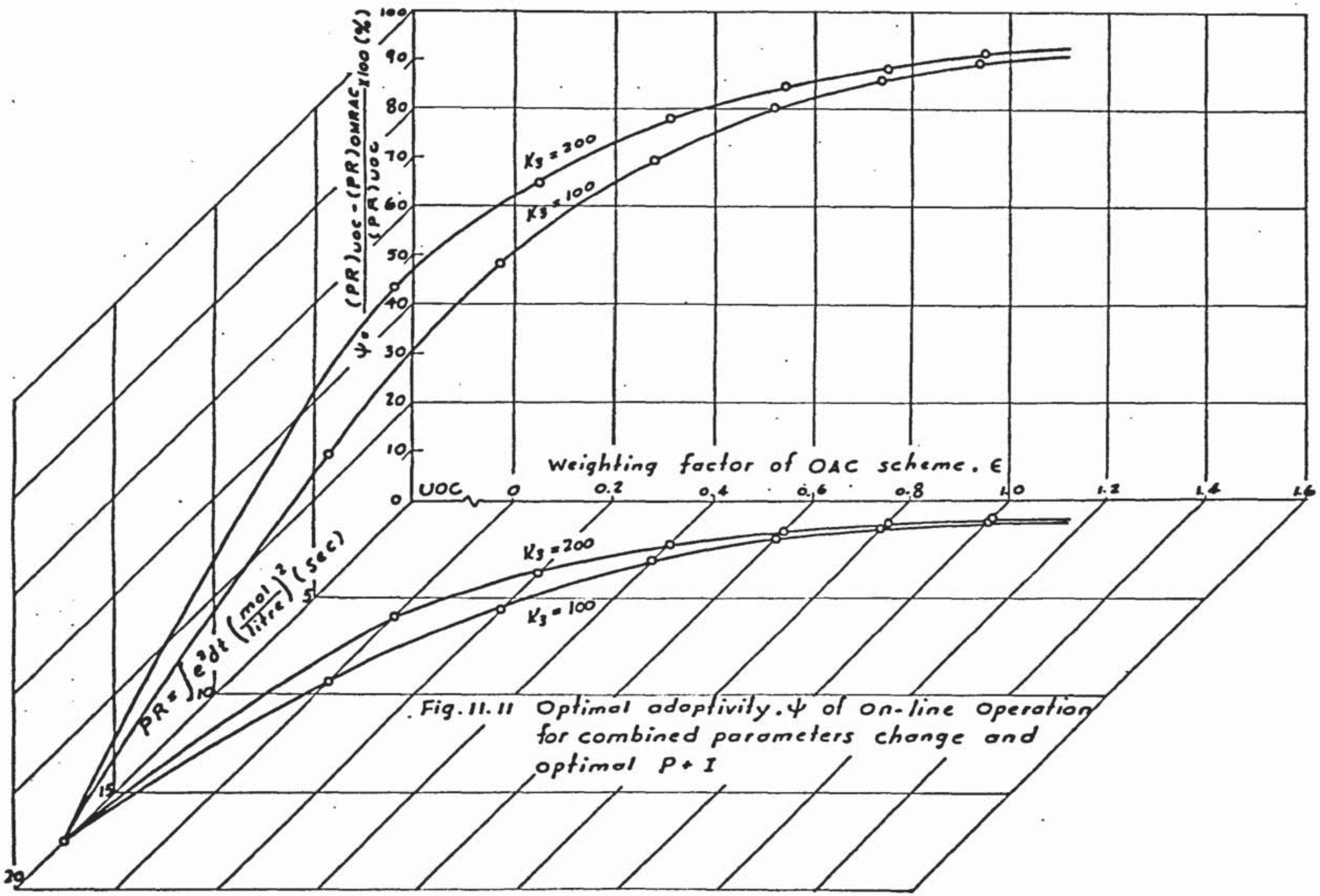

Fig. 11.11 Optimal adaptivity, ψ of On-line Operation for combined parameters change and optimal P + I

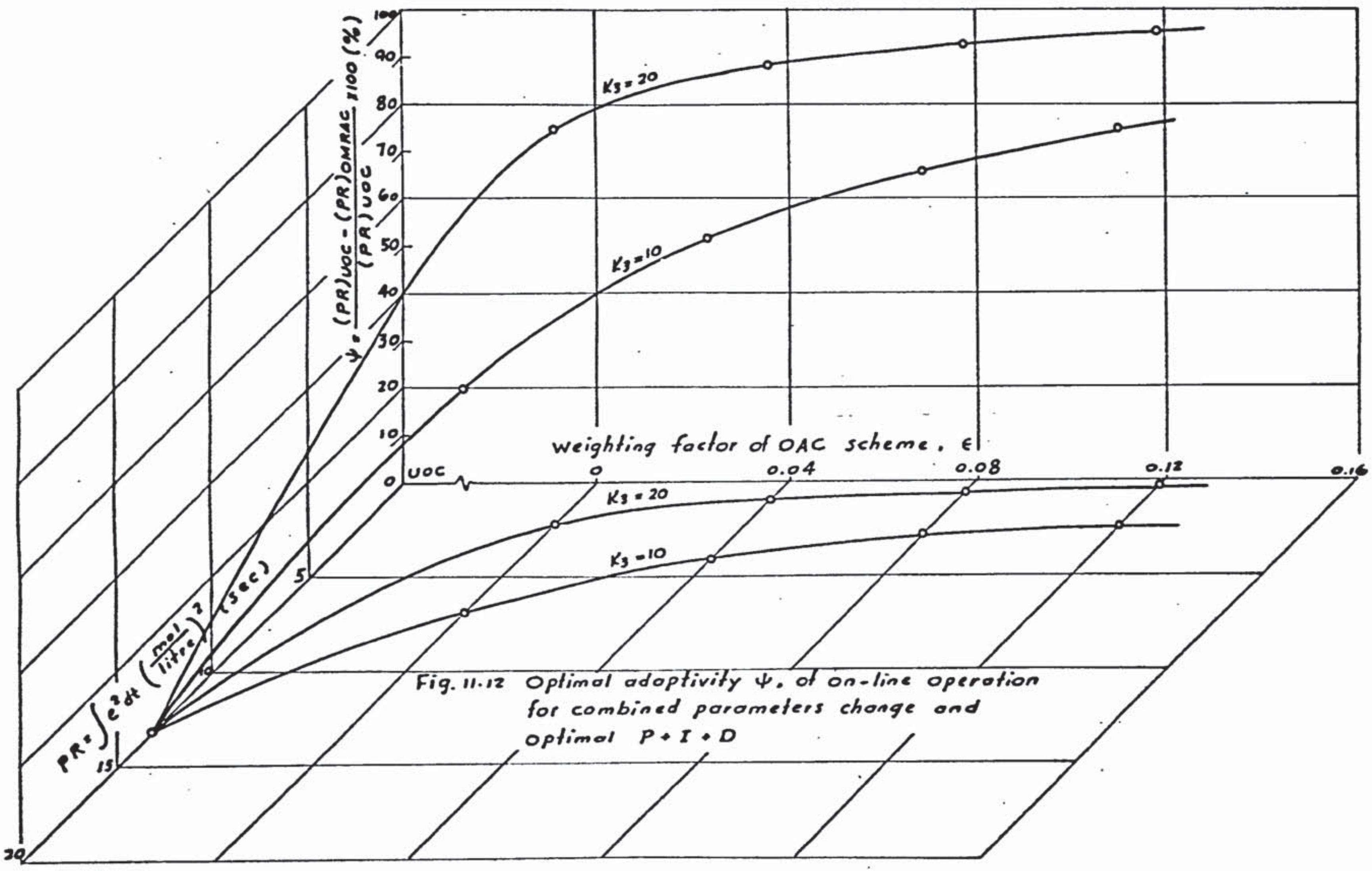

Fig. 11.12 Optimal adaptivity ψ, of on-line operation for combined parameters change and optimal P + I + D

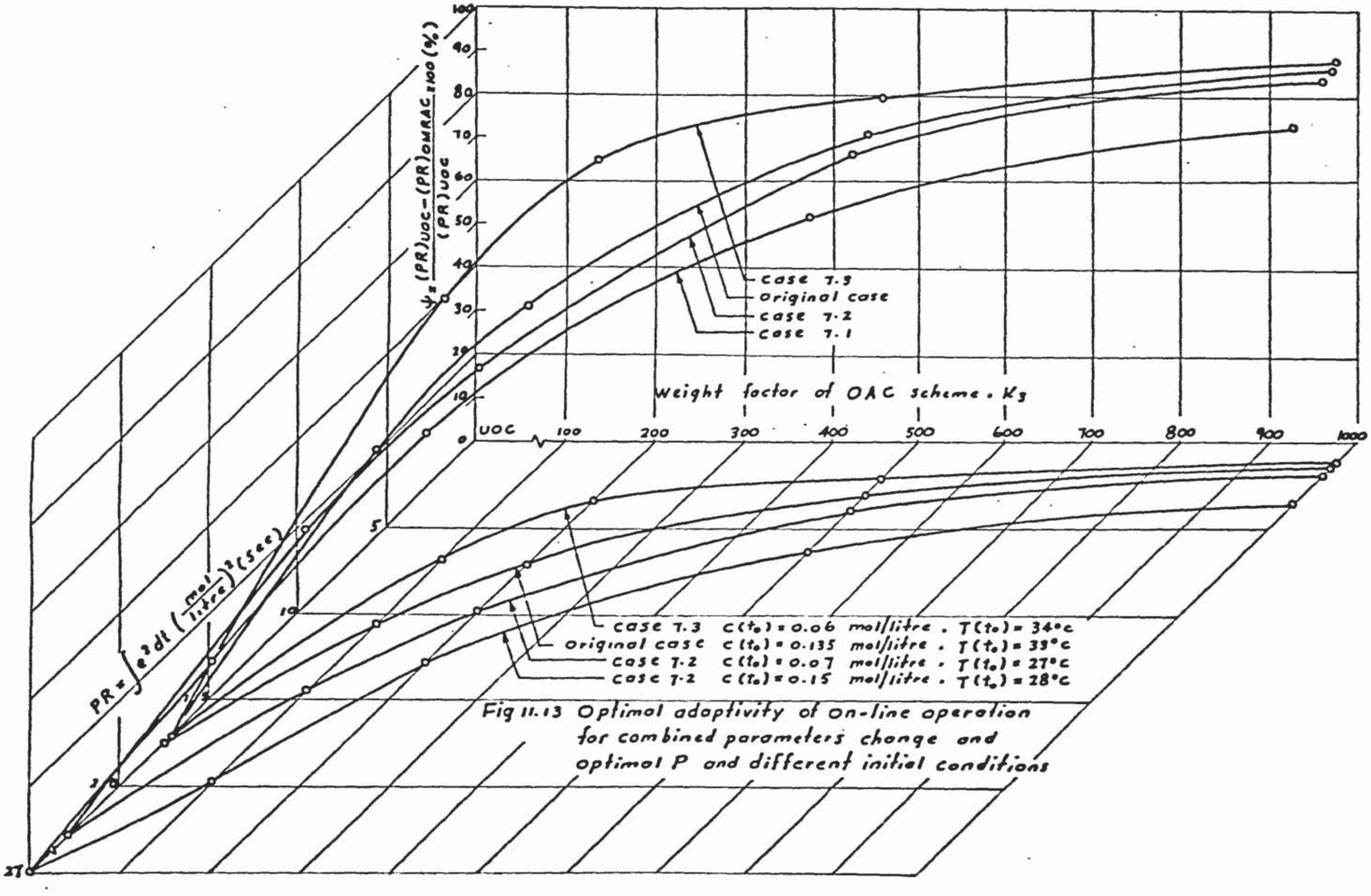

Fig 11.13 Optimal adaptivity of on-line operation for combined parameters change and optimal P and different initial conditions

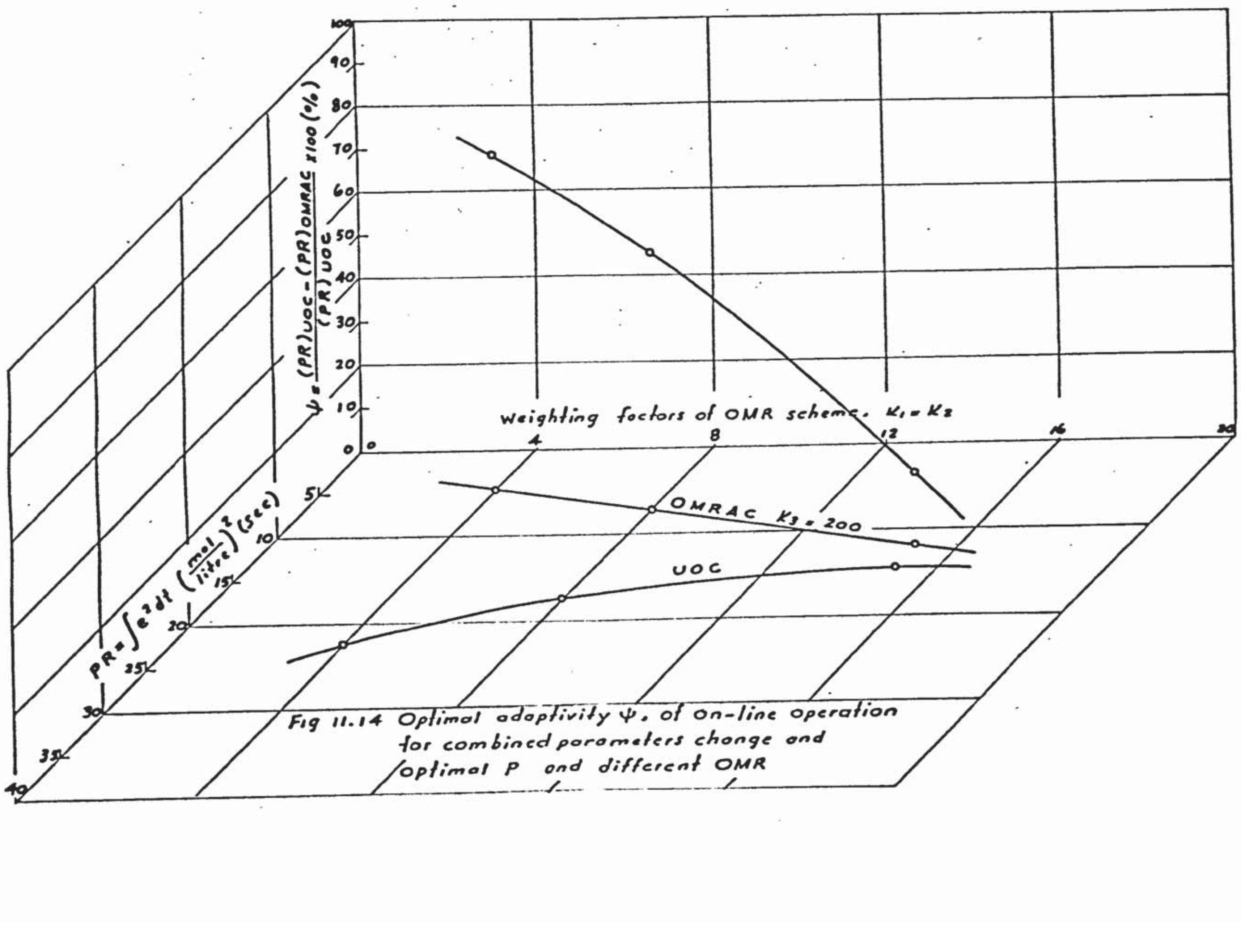

Fig 11.14 Optimal adaptivity ψ, of on-line operation for combined parameters change and optimal P and different OMR

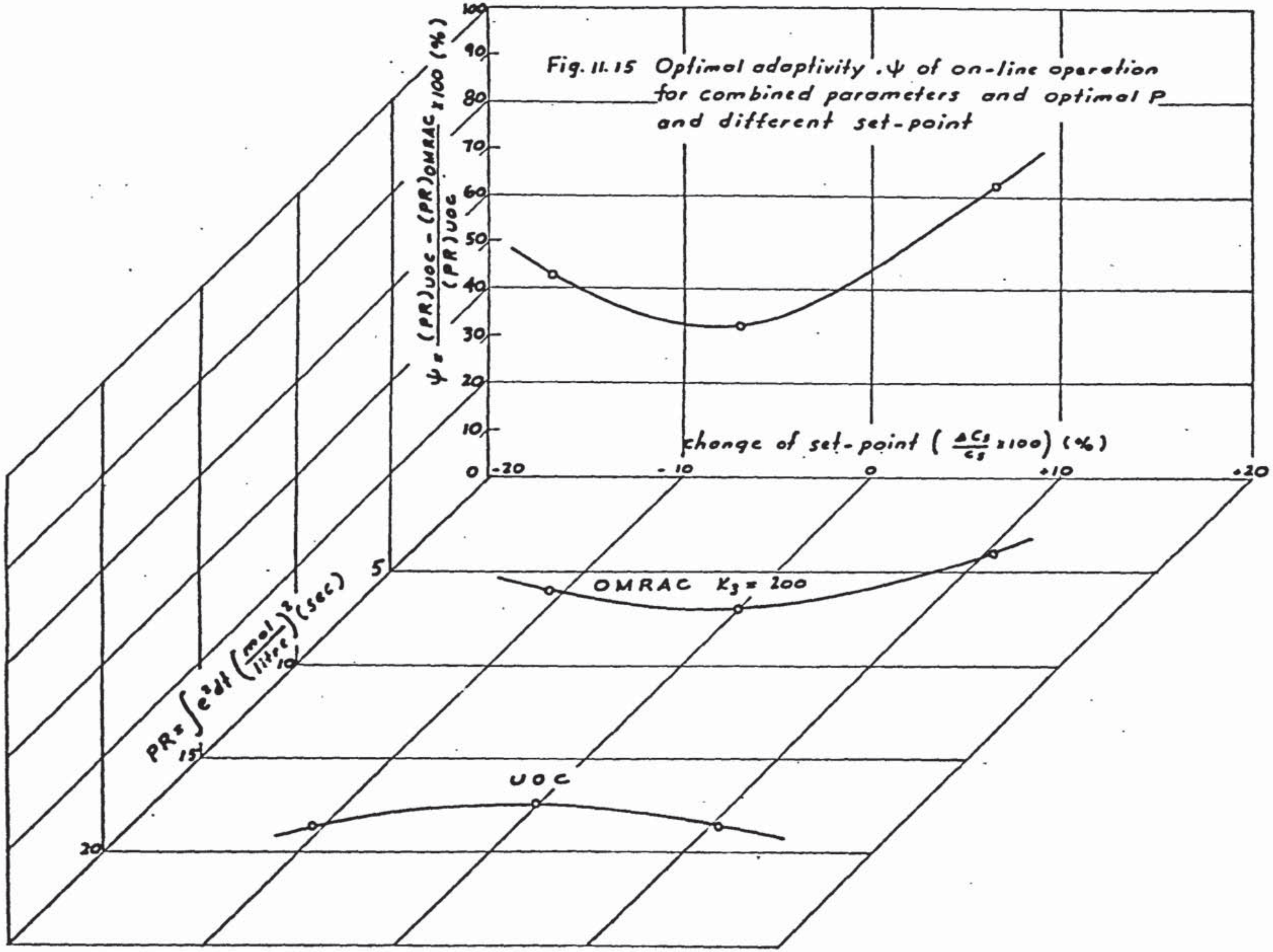

Fig. 11.15 Optimal adaptivity , ψ of on-line operation for combined parameters and optimal P and different set-point

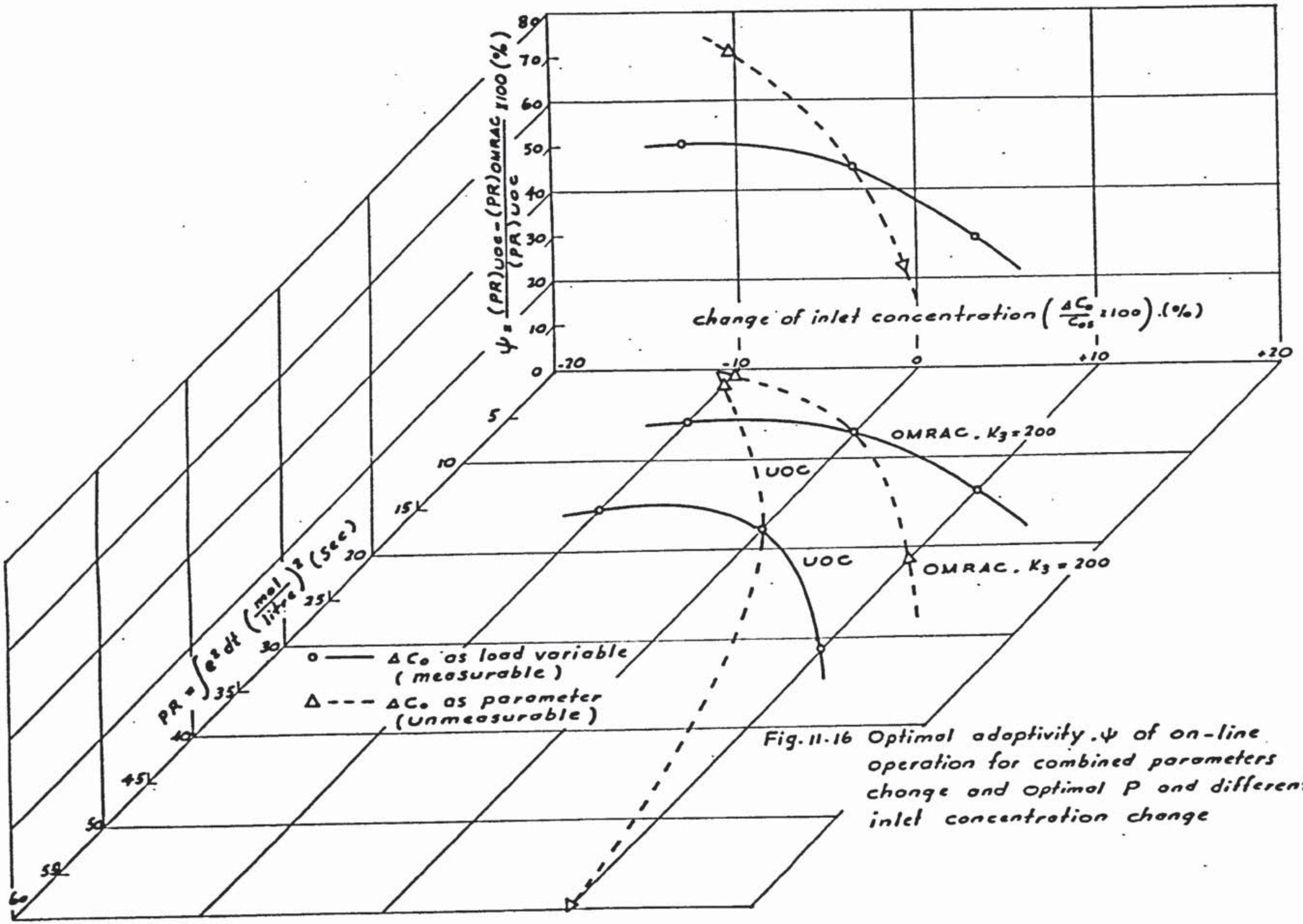

Fig. 11.16 Optimal adaptivity ψ of on-line operation for combined parameters change and optimal P and different inlet concentration change

CHAPTER 12

CONCLUSIONS

From all of the analysis and discussion of the different chapters, the overall conclusions are in the following two sections:

12.1. Overall conclusion for OMRAC system

12.1.1. Theoretical development

(1) A general algorithm and theory of the OMRAC system for an n-state variable process is developed theoretically (3.1).

(2) The general optimal PID control laws of the OAC scheme are derived in detail. (Chapter 3).

(3) All the mathematically derived equations of optimal PID control laws for a CSTR are special cases of the general equations (Chapters 4 and 5).

12.1.2. Theoretical and experimental proof

From Chapters 7, 10 and 11, all theoretical and experimental results both from complete simulation and on-line operation for a CSTR using the TR-10 analogue and the TR-48 hybrid computer are apparently in excellent agreement and are shown below:

(1) The response of OMRAC is always better than UOC and is more effective and approaches OMR more closely as a limit as the weighting factor of OAC is increased.

(2) The adaptation of OMRAC has no limitation for any operating conditions. The only limitation is the constraint of the optimal control law which corresponds to the control valve capacity for the cooling water flowrate.

(3) The response of reactor concentration and cooling water flowrate from on-line operation are more sensitive than the theoretical response from complete simulation.

(4) Optimal P + I and Optimal P + I + D of OMRAC can produce greater improvement than optimal P only, and Optimal PID has the same general properties as the conventional PID controller.

(5) Optimal PID control of on-line operation is more sensitive than complete simulation, the best value of the ratio of the two weighting factors (K_3/ε) is around 80-100.

(6) The stability of OMRAC is asymptotic stability in the large and is much better than the stability of UOC.

(7) Q_g and ($-\Delta H$) calculated from all of the experimental data at the final steady state conditions of on-line operation are in excellent agreement with operating cases and with the originally calculated theoretical values (7.1)

(8) Optimal adaptivity for a constant weighting factor (K_3) of the OAC scheme, increases when K_1 and K_2, the weighting factors of the OMR scheme, decrease.

(9) Optimal adaptivity of OMRAC is independent of the different set-point changes.

(10) Optimal adaptivity of OMRAC is independent of the different inlet concentration changes.

From the above analysis the theoretical development of OMRAC has been confirmed and proved to have high performance both from the theoretical complete simulation and experimental on-line operation for a CSTR using a hybrid computer.

12.2. Overall conclusions for on-line computer control system design and operation

From 12.1. On-line computer control system design and operation are successful with high performance in the following conditions:

12.2.1. Effective programming of the computer

Effective programming procedures were carefully followed and are shown below:

(1) Between the computer and interface, all process variables of each computer circuit diagram must be changed to scaled computer variables (Figs. 7.1 and 7.2. and Figs. 8.6 to 8.8)

(2) Careful consideration of magnitude scaling and time-scaling (7.2)

(3) Careful change of all process and related equations to the scaled computer variable equations (7.3).

(4) Careful programming of all of the necessary VDFG's (Appendix 3).

(5) Preparation of detailed assignment sheets for all potentiometers and amplifiers used for each computer diagram (Tables 7.2 to 7.7.).

(6) Careful determination of the exact relation of each interface variable on the computer side to that on the real process side, for example

$\left[\frac{Q_g}{Q_{gm}}\right]$ in volts to Q_g in Kcal x 10^3/h

and $\left[\frac{U^*}{Qcm}\right]$ in volts to F_c in litre/min

where U^* = modified optimal control law in Kcal/min. (8.33 and 8.3.4.).

(7) Application of simple rules for patching and checking the connection of the two available computers (TR-10 and TR-48) (9.2).

12.2.2. Extremely linear interface system design

In 8.2, it has been emphasised that the requirement of interface system design, as for any industrial transmitter or transducer, is that the terminal relation between the computer side and the process side must be extremely linear. To meet this requirement, an additional compensating VDFG is used, and the design procedures are shown below:

(1) Prepare complete block diagram of each individual component of interface system.

(2) Calibrate and check each block function.

(3) Combine all components of each block function to form an overall resultant function for the interface system (usually this is non-linear).

(4) From the resultant non-linear function, an additional compensating VDFG is used to compensate for the non-linearity to give an extremely linear function.

Thus, the signal from the computer is transmitted through the generated VDFG and then a series of monitoring instruments and items of equipment, give an excellent linear interface system. (8.2.1. and 8.2.2. and Appendix 5).

12.2.3. High sensitivity of on-line operation.

Since the overall sensitivity in this research work is 50 times that of Buxton's (see 9.1.) then several serious difficulties of operation on the partially simulated CSTR had to be solved and are shown below:

(1) Smooth plot of oscillating or fluctuating reactor temperature using a filter technique (see 9.3).

(2) Initial temperature setting using a switching method (see 9.4).

(3) Determination of the actual cooling water flowrate at the final steady state or $\left[\frac{F_{cs}}{F_{cm}}\right]_{final}$, by using an iteration method (9.5).

(4) Changing the feed flowrate (F), as an unmeasurable parameter, using a compensation method (9.6).

Since a very narrow operating range both for reactor concentration and temperature was used on the partially simulated CSTR, the highly sensitive performance of different types of on-line operations such as UC, UOC, OMRAC and OMR of a CSTR were plotted respectively in all Figures (Figs. 10.1 to 10.68) for comparison with the theoretical results.

Thus the partial simulation technique has been extended to give a more highly sensitive operating performance than Buxton's original design by use of a compensation technique combined with switching and iteration methods.

In the application of optimal control theory (including OMRAC) to practical real processes, Shimner(14) clearly pointed out that the optimal control theory represents an important area of research in the control field. Unfortunately a large gap has developed between research in academic and industrial organisations, i.e. between research and practice and very little has been converted into practice. This gap will undoubtedly shrink in the very near future, and the discussion (2.6.1) of Literature Survey (Chapter 2) emphasises this fact.

In a broad sense, the major effort of this research may contribute to the filling of this gap between research and practice of optimal control theory (including OMRAC).

12.3. Suggestion for future work

A proposed comparison of OMRAC for a CSTR using the on-line hybrid computer with the theoretical development of OMRAC is shown in Table 12.1.

Table 12.1

Comparison of theoretical development and application of OMRAC.

	Theoretical development of OMRAC	Application of OMRAC for a CSTR
1. Process	N-state variables (N-1) controlled variables	2-state variables 1-controlled variable (Reactor concentration)
2. Process equipment	Any type, either partially simulated or real process equipment	partially simulated CSTR
3. Optimal control techniques	Any kind of optimal control technique	maximum principle
4. On-line computer	any type of on-line hybrid or digital combined computer	TR-10 and TR-48 hybrid computers

From the above Table, for different processes with either partially simulated or real process equipment, applying different kinds of optimal control technique and using different types of on-line computer then new research on the OMRAC scheme may be developed with a sound foundation. For example: using the existing Departmental equipment, the following particular kind of OMRAC research is suggested:

"Optimal Model Reference Adaptive Control of a Cascaded two-effect evaporator using on-line Honeywell Digital Computer."

APPENDICES

(with index)

APPENDICES

INDEX TO TABLES IN THE APPENDICES

INDEX TO FIGURES IN THE APPENDICES

APPENDIX 1

DIGITAL COMPUTER COMPUTATION OF THE OPTIMAL CONTROL LAW COEFFICIENTS α_{ij} AND β_{ij} BY THE NEWTON RAPHSON ITERATION METHOD

A.1.1. General iteration algorithm

Let the simultaneous non-linear algebraic equations be shown in the following general form:

$$\left.\begin{array}{l} f_1 (x_1, x_2, \ldots\ldots\ldots\ldots, x_n) = 0 \\ f_2 (x_1, x_2, \ldots\ldots\ldots\ldots, x_n) = 0 \\ \text{-----------------------------} \\ \text{-----------------------------} \\ f_n (x_1, x_2, \ldots\ldots\ldots\ldots, x_n) = 0 \end{array}\right\} \qquad (7\text{-}1)$$

or in matrix form:

$$F (X) = 0 \qquad (7\text{-}2)$$

where

$$F = \begin{bmatrix} f_1 \\ f_2 \\ \vdots \\ f_n \end{bmatrix} \text{ and } X = \begin{bmatrix} x_1 \\ x_2 \\ \vdots \\ x_n \end{bmatrix}$$

If $\bar{X}$ are the roots of equation (7-2), expansion as a Taylor series gives:

$$F (\bar{X}) = F (X^{(1)}) + \left(\frac{\partial F}{\partial X}\right)_{X = X^{(1)}} (\bar{X} - X^{(1)}) + \ldots\ldots \qquad (7\text{-}3)$$

where:

$X^{(1)}$ = first approximated value of $\bar{X}$, or the first iteration

$$\text{and} \quad \frac{\partial F}{\partial X} = \begin{bmatrix} \frac{\partial f_1}{\partial x_1} & \frac{\partial f_1}{\partial x_2}, & \cdots\cdots\cdots, & \frac{\partial f_1}{\partial x_n} \\ \frac{\partial f_2}{\partial x_1} & \frac{\partial f_2}{\partial x_2}, & \cdots\cdots\cdots, & \frac{\partial f_2}{\partial x_2} \\ \vdots & \vdots & & \vdots \\ \frac{\partial f_n}{\partial x_1} & \frac{\partial f_n}{\partial x_2}, & \cdots\cdots\cdots, & \frac{\partial f_n}{\partial x_n} \end{bmatrix} \tag{7-4}$$

This matrix is called the Jacobi matrix.

Neglecting the high order terms, equation (7-3) becomes:

$$F(\overline{X}) \cong F(X^{(1)}) + \left(\frac{\partial F}{\partial X}\right)_{X = X^{(1)}} (\overline{X} - X^{(1)}) \tag{7-5}$$

Let the second approximation of $\overline{X}$ be $X^{(2)}$ and let $F(X^{(2)}) \cong 0$, then

$$X^{(2)} = X^{(1)} - \left[\frac{\partial F}{\partial X}\right]^{-1} F(X^{(1)}) \tag{7-6}$$

where

$\left[\frac{\partial F}{\partial X}\right]^{-1}$ is the inverse matrix of the matrix $\left(\frac{\partial F}{\partial X}\right)_{X = X^{(1)}}$

The general formula of this iteration algorithm is:

$$X^{(i+1)} = X^{(i)} - \left(\frac{\partial F}{\partial X}\right)^{-1} F(X^{(i)}) \tag{7-7}$$

where i and i+1 are the ith and (i+1)th iterations and $\left(\frac{\partial F}{\partial X}\right)^{-1}$ is the inverse matrix of $\left(\frac{\partial F}{\partial X}\right)_{X = X^{(i)}}$

For simplification in the digital computer programming, let:

$$X(I) = X \tag{7-8-1}$$

$$F(J) = F(X) \tag{7-8-2}$$

$$A(I,J) = \frac{\partial F}{\partial X} \tag{7-8-3}$$

$$B\ (I,J) = \left(\frac{\partial F}{\partial X}\right)^{-1} \qquad (7\text{-}8\text{-}4)$$

and $$R\ (I) = \left(\frac{\partial F}{\partial X}\right)^{-1} . F\ (X) = B\ (I,J) .\ F\ (J) \qquad (7\text{-}8\text{-}5)$$

where $I = 1, 2, \ldots\ldots\ldots\ldots n$

$J = 1, 2, \ldots\ldots\ldots\ldots n$

n = no. of determined coefficients

then equation (7-7) becomes:

$$X^{(i+1)}\ (I) = X^{(i)}\ (I) - B^{(i)}\ (I,J) \ .\ F^{(i)}\ (J) \qquad (7\text{-}9)$$

or

$$X^{(i+1)}\ (I) = X^{(i)}\ (I) - R^{(i)}\ (I) \qquad (7\text{-}10)$$

A.1.2. Digital computer computation for determination of the coefficients α_{12}, α_{22}, α_{23}, α_{24} and α_{25} (OMR) scheme

From Chapter 4, the derived nine simultaneous non-linear equations (4-54) $\sim$ (4-62) are rewritten below:

$$K_1 + a_{11}\alpha_{11} + a_{21}\alpha_{12} - 0.25\ b^2\alpha_{12}^2 = 0 \qquad (7\text{-}11)$$

$$a_{12}\alpha_{11} + (a_{11} + a_{22})\alpha_{12} + a_{21}\alpha_{22} - 0.5\ b^2\alpha_{12}\alpha_{22} = 0 \qquad (7\text{-}12)$$

$$-2K_1 + a_{11}\alpha_{13} + a_{21}\alpha_{23} - 0.5\ b^2\alpha_{12}\alpha_{23} = 0 \qquad (7\text{-}13)$$

$$d_{11}\alpha_{11} + a_{11}\alpha_{14} + a_{21}\alpha_{24} = 0.5\,\alpha_{12}\alpha_{24} = 0 \qquad (7\text{-}14)$$

$$d_{22}\alpha_{12} + a_{11}\alpha_{15} + a_{21}\alpha_{25} - 0.5\,\alpha_{12}\alpha_{25} = 0 \qquad (7\text{-}15)$$

$$K_2 + a_{12}\alpha_{12} + a_{22}\alpha_{22} - 0.25\ b^2\alpha_{22}^2 = 0 \qquad (7\text{-}16)$$

$$a_{12}\alpha_{13} + a_{22}\alpha_{23} - 0.5\,\alpha_{22}\alpha_{23} = 0 \qquad (7\text{-}17)$$

$$d_{11}\alpha_{12} + a_{12}\alpha_{14} + a_{22}\alpha_{24} - 0.5\,\alpha_{22}\alpha_{24} = 0 \qquad (7\text{-}18)$$

$$a_{12}\alpha_{15} + d_{22}\alpha_{22} + a_{22}\alpha_{25} - 0.5\ b^2\alpha_{22}\alpha_{25} = 0 \qquad (7\text{-}19)$$

$$\text{Let}\quad x(1) = \alpha_{11} \quad x(4) = \alpha_{14} \quad x(7) = \alpha_{23}$$
$$x(2) = \alpha_{22} \quad x(5) = \alpha_{15} \quad x(8) = \alpha_{24} \qquad (7\text{-}20)$$
$$x(3) = \alpha_{23} \quad x(6) = \alpha_{22} \quad x(9) = \alpha_{25}$$

$$P(1) = K_1 \quad P(2) = K_2 \qquad (7\text{-}21)$$

$$D(1) = a_{11} \quad D(5) = b$$
$$D(2) = a_{12} \quad D(6) = d_{11}$$
$$D(3) = a_{21} \quad D(7) = d_{22} \qquad (7\text{-}22)$$
$$D(4) = a_{22}$$

and

F(1), F(2),...... F(9) represent the above nine equations respectively.

Then equations (7-11) (7-19) become:

$$F(1) = P(1) + D(1)\,x\,(1) + D(3)\,x\,(2) - 0.25\,D^2(5)\,x^2\,(2) \qquad (7\text{-}23)$$

$$F(2) = D(2)\,x\,(1) + (D(1) + D(4))\,x\,(2) + D(3)\,x\,(6) - 0.5\,D^2(5)\,x\,(2)\,x\,(6) \qquad (7\text{-}24)$$

$$F(3) = 2P(1) + D(1)\,x\,(3) + D(3)\,x\,(7) - 0.5\,D^2(5)\,x\,(2)\,x\,(7) \qquad (7\text{-}25)$$

$$F(4) = D(6)\,x\,(1) + D(1)\,x\,(4) + D(3)\,x\,(8) - 0.5\,D^2(5)\,x\,(2)\,x\,(8) \qquad (7\text{-}26)$$

$$F(5) = D(7)\,x\,(2) + D(1)\,x\,(5) + D(3)\,x\,(9) - 0.5\,D^2(5)\,x\,(2)\,x\,(9) \qquad (7\text{-}27)$$

$$F(6) = P(2) + D(2)\,x\,(2) + D(4)\,x\,(6) - 0.25D^2(5)\,x^2\,(6) \qquad (7\text{-}28)$$

$$F(7) = D(2)\,x\,(3) + D(4)\,x\,(7) - 0.5\,D^2(5)\,x\,(6)\,x\,(7) \qquad (7\text{-}29)$$

$$F(8) = D(6)\,x\,(2) + D(2)\,x\,(4) + D(4)\,x\,(8) - 0.5\,D^2(5)\,x\,(6)\,x\,(8) \qquad (7\text{-}30)$$

$$F(9) = D(2)\,x\,(5) + D(7)\,x\,(6) + D(4)\,x\,(9) - 0.5\,D^2(5)\,x\,(6)\,x\,(9) \qquad (7\text{-}31)$$

and $$\frac{\partial F}{\partial X} =$$

$$\begin{bmatrix}
D(1) & D(3) - 0.5\,D^2(5)\,x(2) & 0 & 0 & 0 & 0 & 0 & 0 & 0 \\
D(2) & (D(1) + (D(4)) - 0.5\,D^2(5)\,x(6) & 0 & 0 & 0 & D(3) - 0.5\,D^2(5)\,x(2) & 0 & 0 & 0 \\
0 & -0.5\,D^2(5)\,x(7) & D(1) & 0 & 0 & 0 & D(3) - 0.5\,D^2(5)\,x(2) & 0 & 0 \\
D(6) & -0.5\,D^2(5)\,x(8) & 0 & D(1) & 0 & 0 & 0 & D(3) - 0.5\,D^2(5)\,x(2) & 0 \\
0 & D(7) - 0.5\,D^2(5)\,x(9) & 0 & 0 & D(1) & 0 & 0 & 0 & D(3) - 0.5\,D^2(5)\,x(2) \\
0 & D(2) & 0 & 0 & 0 & D(4) - 0.5\,D^2(5)\,x(6) & 0 & 0 & 0 \\
0 & 0 & D(2) & 0 & 0 & -0.5\,D^2(5)\,x(7) & D(4) - 0.5\,D^2(5)\,x(6) & 0 & 0 \\
0 & D(6) & 0 & D(2) & 0 & -0.5\,D^2(5)\,x(8) & 0 & D(4) - 0.5\,D^2(5)\,x(6) & 0 \\
0 & 0 & 0 & 0 & D(2) & D(7) - 0.5\,D^2(5)\,x(9) & 0 & 0 & D(4) - 0.5\,D^2(5)\,x(6)
\end{bmatrix} \tag{7.32}$$

By using the above equations (7-23) to (7-32) and the general iteration algorithm shown in equations (7-9) and (7-10), the digital computer program is shown in Appendix 2.1.

A.1.3. Digital computer computation for determination of coefficient β_{12} (Optimal P of OAC scheme)

From Chapter 5, the derived three simultaneous equations (5-42), (5-43) and (5-47) are rewritten below:

$$K_3 + a_{11}\beta_{11} + a_{21}\beta_{12} - 0.25\, b^2\beta_{12}^2 = 0 \qquad (7\text{-}33)$$

$$a_{12}\beta_{11} + (a_{11} + a_{22})\beta_{12} + a_{21}\beta_{22} - 0.5\, b^2\beta_{12}\beta_{22} = 0 \qquad (7\text{-}34)$$

$$d_{11}\beta_{12} + a_{22}\beta_{22} - 0.25\, b^2\beta_{22}^2 = 0 \qquad (7\text{-}35)$$

Let

$$\left.\begin{array}{llllll} x(1) = \beta_{11} & & P = K_3 & & D(3) = a_{21} \\ x(2) = \beta_{12} & & D(1) = a_{11} & & D(4) = a_{22} \\ x(3) = \beta_{22} & & D(2) = a_{12} & & D(5) = b \end{array}\right\} \qquad (7\text{-}36)$$

and

F(1), F(F) and F(3) represent (7-33), (7-34) and (7-35) respectively.

Then:

$$F(1) = P + D(1)\,x\,(1) + D(3)\,x\,(2) - 0.25\,D^2(5)\,x^2\,(2) \qquad (7\text{-}37)$$

$$F(1) = D(2)\,x\,(1) + (D(1) + D(4))\,x\,(2) + D(3)\,x\,(3) - 0.5\,D^2(5)\,x\,(2)\,x\,(3) \qquad (7\text{-}38)$$

$$F(3) = D(2)\,x\,(2) + D(4)\,x\,(3) - 0.25\,D^2(5)\,x^2\,(3) \qquad (7\text{-}39)$$

and $\frac{\partial F}{\partial X}$ =

$$\begin{bmatrix} D(1) & D(3) - 0.5\, D^2(5)\, x(2) & 0 \\ D(2) & D(1) + D(4) - 0.5\, D^2(5)\, x(3) & D(3) - 0.5\, D^2(5)\, x(2) \\ 0 & D(2) & D(4) - 0.5\, D^2(5)\, x(3) \end{bmatrix} \qquad (7\text{-}40)$$

By using the above equations (7-37) to (7-40) and the general iteration algorithm, the digital computer program is shown in Appendix 2.2.

A1.4 Digital computer computation for determination of the coefficients β_{21} and β_{26}. (Optimal P + I of OAC scheme)

From Chapter 5, the derived six simultaneous equations (5-77), (5-78), (5-82), (5-83), (5-84) and (5-88) are rewritten below:

$$2K_3 = 2a_{11}\beta_{11} + a_{21}\beta_{12} + a_{21}\beta_{21} - 0.5\, b^2\beta_{12}\beta_{21} + \beta_{16} = 0 \qquad (7\text{-}41)$$

$$a_{12}\beta_{11} + (a_{11} + a_{22})\beta_{12} + a_{21}\beta_{22} - 0.5\,\beta_{12}\beta_{22} = 0 \qquad (7\text{-}42)$$

$$a_{11}\beta_{16} + a_{21}\beta_{26} - 0.5\, b^2\beta_{12}\beta_{26} + \epsilon_1 = 0 \qquad (7\text{-}43)$$

$$a_{12}\beta_{11} + (a_{11} + a_{22})\beta_{21} + a_{21}\beta_{22} - 0.5\, b^2\beta_{21}\beta_{22} + \beta_{26} = 0 \qquad (7\text{-}44)$$

$$a_{12}\beta_{12} + a_{12}\beta_{21} + 2\, a_{22}\beta_{22} - 0.5\, b^2\beta_{22}^2 = 0 \qquad (7\text{-}45)$$

$$a_{12}\beta_{16} + a_{22}\beta_{26} - 0.5\, b^2\beta_{22}\beta_{26} + \epsilon_2 = 0 \qquad (7\text{-}46)$$

Let

$$\begin{aligned} x(1) &= \beta_{11} & D(1) &= a_{11} & P &= K_3 \\ x(2) &= \beta_{12} & D(2) &= a_{11} & \epsilon_1 &= \epsilon_2 = \sigma \\ x(3) &= \beta_{16} & D(3) &= a_{21} \\ x(4) &= \beta_{21} & D(4) &= a_{22} \\ x(5) &= \beta_{22} & D(5) &= b \\ x(6) &= \beta_{26} \end{aligned} \qquad (7\text{-}47)$$

and F(1), F(2),.....F(6) represent the six equations respectively, then equations(7-41) to (7-46) become:

$$F(1) = 2P + 2D(1)\,x(1) + D(3)\,x(2) + D(3)\,x(4) - 0.5\,D^2(5)\,x(2)\,x(4) + x(3) \qquad (7.48)$$

$$F(2) = D(2)\,x(1) + (D(1) + D(4))\,x(2) + D(3)\,x(5) - 0.5\,D^2(5)\,x(2)\,x(5) \qquad (7\text{-}49)$$

$$F(3) = D(1)\,x(3) + D(3)\,x(6) - 0.5\,D^2(5)\,x(2)\,x(6) + G \qquad (7\text{-}50)$$

$$F(4) = D(2)\,x(1) + (D(1) + D(4))\,x(4) + D(3)\,x(5) - 0.5\,D^2(5)\,x(4)\,x(5) + x(6) \qquad (7\text{-}51)$$

$$F(5) = D(2)\,x(2) + D(2)\,x(4) + 2D(4)\,x(5) - 0.5\,D^2(5)\,x^2(5) \qquad (7\text{-}52)$$

$$F(6) = D(2)\,x(3) + D(4)\,x(6) - 0.5\,D^2(5)\,x(6) + G \qquad (7\text{-}53)$$

and:

$$\frac{\partial F}{\partial X} = \begin{bmatrix} 2D(1) & D(3) - 0.5\,D^2(5)\,x(4) & 1 & D(3) - 0.5\,D^2(5)\,x(2) & 0 & 0 \\ D(2) & D(1) + D(4) - 0.5\,D^2(5)\,x(5) & 0 & 0 & D(3) - 0.5\,D^2(5)\,x(2) & 0 \\ 0 & -0.5\,D^2(5)\,x(6) & D(1) & 0 & 0 & D(3) - 0.5\,D^2(5)\,x(2) \\ D(2) & 0 & 0 & D(1) + D(4) - 0.5\,D^2(5)\,x(5) & D(3) - 0.5\,D^2(5)\,x(4) & 1 \\ 0 & D(2) & 0 & D(2) & 2D(4) - D^2(5)\,x(5) & 0 \\ 0 & 0 & D(2) & 0 & -0.5\,D^2(5)\,x(6) & D(4) - 0.5\,D^2(5)\,x(5) \end{bmatrix} \qquad (7\text{-}54)$$

By using the above equations (7-48) to (7-54) and the general iteration algorithm, the digital computer program is shown in Appendix 2.3.

A1.5. Digital computer computation for determination of the coefficients β_{21}, β_{26} and β_{27} (Optimal P + I + D of OAC scheme)

From Chapter 5, the derived ten simultaneous equations (5-124), (5-125), (5-126), (5-129), (5-130), (5-131), (5-132), (5-133), (5-136) and (5-137) are rewritten below:

$$2K_3 + 2a_{11}\beta_{11} + a_{21}\beta_{12} + \beta_{16} + a_{11}^2\beta_{17} + a_{21}\beta_{21} + a_{11}a_{21}\beta_{27} - 0.5\ b^2\beta_{12}\beta_{21} - 0.5\ b^2\ a_{11\ 12}\beta_{27} = 0 \qquad (7\text{-}55)$$

$$a_{12}\beta_{11} + (a_{11} + a_{22})\beta_{12} + a_{11}a_{12}\beta_{17} + a_{21}\beta_{22} + a_{12}a_{21}\beta_{27} - 0.5\ b^2\ B_{12}\beta_{22} - 0.5\ b^2a_{12}\beta_{12}\beta_{27} = 0 \qquad (7\text{-}56)$$

$$-2K_3 + a_{11}\beta_{13} - \beta_{16} + a_{21}\beta_{23} - 0.5\ b^2\beta_{12}\beta_{23} = 0 \qquad (7\text{-}57)$$

$$a_{11}\beta_{16} + a_{21}\beta_{26} - 0.5\ b^2\beta_{12}\beta_{26} + \varepsilon_1 = 0 \qquad (7\text{-}58)$$

$$\beta_{13} - a_{11}\beta_{17} - a_{21}\beta_{27} + 0.5\ b^2\beta_{12}\beta_{27} = 0 \qquad (7\text{-}59)$$

$$a_{12}\beta_{11} + a_{11}a_{12}\beta_{17} + (a_{11} + a_{22})\beta_{21} + a_{21}\beta_{22} + \beta_{26} + a_{11}a_{22}\beta_{27} - 0.5\ b^2\beta_{21}\beta_{22} - 0.5\ b^2a_{11}a_{22}\beta_{27} = 0 \qquad (7\text{-}60)$$

$$a_{12}\beta_{12} + a_{12}^2\beta_{17} + a_{12}\beta_{21} + 2a_{22}\beta_{22} + a_{12}a_{22}\beta_{27} - 0.5\ b^2\beta_{22}^2 - 0.5\ b^2a_{12}\beta_{22}\beta_{27} = 0 \qquad (7\text{-}61)$$

$$a_{12}\beta_{13} + a_{22}\beta_{23} - \beta_{26} - 0.5\ b^2\beta_{22}\beta_{23} = 0 \qquad (7\text{-}62)$$

$$a_{12}\beta_{16} + a_{22}\beta_{26} - 0.5\ b^2\beta_{22}\beta_{26} + \varepsilon_2 = 0 \qquad (7\text{-}63)$$

$$-a_{12}\beta_{17} - a_{22}\beta_{27} + \beta_{23} + 0.5\ b^2\beta_{22}\beta_{27} = 0 \qquad (7\text{-}64)$$

Let:

$$x(1) = \beta_{11} \quad x(6) = \beta_{21} \quad D(1) = a_{11} \quad P = K_3$$
$$x(2) = \beta_{12} \quad x(7) = \beta_{22} \quad D(2) = a_{12} \quad \epsilon_1 = \epsilon_2 = G$$
$$x(3) = \beta_{13} \quad x(8) = \beta_{23} \quad D(3) = a_{21}$$
$$x(4) = \beta_{16} \quad x(9) = \beta_{26} \quad D(4) = a_{22} \qquad (7\text{-}65)$$
$$x(5) = \beta_{17} \quad x(10) = \beta_{27} \quad D(5) = b$$

and let $F_1(+)$, $F_2(t)$, ... F(10) represent the above ten equations respectively.

Then equations (7-55) to (7-64) become:

$$F(1) = 2P + 2D(1)\ x\ (1) + D(3)\ x\ (2) + x(4) + D^2(1)\ x\ (5) + D(3)\ x\ (6) + D(1)D(3)\ x\ (10) - 0.5\ D^2(5)\ x\ (2)\ x\ (6) - 0.5\ D^2(5)D(1)\ x\ (2)\ x\ (10) \qquad (7\text{-}66)$$

$$F(2) = D(2)\ x\ (1) + (D(1) + D(4))\ x\ (2) + D(1)D(2)\ x\ (5) + D(3)\ x\ (7) + D(2)D(3)\ x\ (10) - 0.5\ D^2(5)\ x\ (2)\ x\ (7) - 0.5\ D^2(5)D(2)\ x\ (2)\ x\ (10) \qquad (7\text{-}67)$$

$$F(3) = -\ 2P + D(1)\ x\ (3) - x(4) + D(3)\ x\ (8) - 0.5\ D^2(5)\ x\ (2)\ x\ (8) \qquad (7\text{-}68)$$

$$F(4) = D(1)\ x\ (4) + D(3)\ x\ (9) - 0.5\ D^2(5)\ x\ (2)\ x\ (9) + G \qquad (7\text{-}69)$$

$$F(5) = x(3) - D(1)\ x\ (5) - D(3)\ x\ (10) + 0.5\ D^2(5)\ x\ (2)\ x\ (10) \qquad (7\text{-}70)$$

$$F(6) = D(2)\ x\ (1) + D(1)D(2)\ x\ (5) + (D(1) + D(4))\ x\ (6) + D(3)\ x\ (7) + x(9) + D(1)D(4)\ x\ (10) - 0.5\ D^2(5)\ x\ (6)\ x\ (7) - 0.5\ D^2(5)D(1)\ x\ (7)\ x\ (10) \qquad (7\text{-}71)$$

$$F(7) = D(2)\ x\ (2) + D^2(2)\ x\ (5) + D(2)\ x\ (6) + 2D(4)\ x\ (7) \qquad (7\text{-}72)$$
$$+ D(2)D(4)\ x\ (10) - 0.5\ B^2(5)\ x^2(7) - - 0.5\ D^2(5)D(2)\ x\ (7)\ x\ (10)$$

$$F(8) = D(2)\,x(3) + D(4)\,x(8) - x(9) - 0.5\,D^2(5)\,x(7)\,x(8) \quad (7\text{-}73)$$

$$F(9) = D(2)\,x(4) + D(4)\,x(9) - 0.5\,D^2(5)\,x(7)\,x(9) + G \quad (7\text{-}74)$$

$$F(10) = -D(2)\,x(5) - D(4)\,x(10) + x(8) + 0.5\,D^2(5)\,x(7)\,x(10) \quad (7\text{-}75)$$

and $\frac{\partial F}{\partial X} =$

$\frac{\partial F_i}{\partial x_1}$	$\frac{\partial F_i}{\partial x_2}$	$\frac{\partial F_i}{\partial x_3}$	$\frac{\partial F_i}{\partial x_4}$	$\frac{\partial F_i}{\partial x_5}$	$\frac{\partial F_i}{\partial x_6}$
$2D(1)$	$D(3)-0.5D^2(5)x(6)-0.5D^2(5)D(1)x(10)$	0	1	$D^2(1)$	$D(3)-0.5D^2(5)x(2)$
$D(2)$	$D(1)+D(4)-0.5D^2(5)x(7)-0.5D^2(5)D(2)x(10)$	0	0	$D(1)D(2)$	0
0	$-0.5D^2(5)x(8)$	$D(1)$	-1	0	0
0	$-0.5D^2(5)x(9)$	0	$D(1)$	0	0
0	$+0.5D^2(5)x(10)$	1	0	$-D(1)$	0
$D(2)$	0	0	0	$D(1)D(2)$	$D(1)+D(4)-0.5D^2(5)x(7)$
0	$o(2)$	0	0	$D^2(2)$	$D(2)$
0	0	$D(1)$	0	0	0
0	0	0	$D(2)$	0	0
0	0	0	0	$D(2)$	0

$\frac{\partial F_i}{\partial x_7}$	$\frac{\partial F_i}{\partial x_8}$	$\frac{\partial F_i}{\partial x_9}$	$\frac{\partial F_i}{\partial x_{10}}$
0	0	0	$D(1)D(3)-0.5D^2(5)D(1)x(2)$
$D(3)-0.5D^2(5)x(2)$	0	0	$D(2)D(3)-0.5D^2(5)D(2)x(2)$
0	$D(3)-0.5D^2(5)x(2)$	0	0
0	0	$D(3)-0.5D^2(5)x(2)$	0
0	0	0	$-D(3)+0.5D^2(5)x(2)$
$D(3)-0.5D^2(5)x(6)-0.5D^2(5)D(1)x(10)$	0	1	$D(1)D(4)-0.5D^2(5)D(1)x(7)$
$2D(4)-0.5D^2(5)x(7)-0.5D^2(5)D(2)x(10)$	0	0	$D(2)D(4)-0.5D^2(5)D(2)x(7)$
$-0.5D^2(5)x(8)$	$D(4)-0.5D^2(5)x(7)$	-1	0
$-0.5D^2(5)x(9)$	0	$D(4)-0.5D^2(5)x(7)$	0
$+0.5D^2(5)x(10)$	1	0	$-D(4)+0.5D^2(5)x(7)$

By using above equations (7-65) ~ (7.75) and general iteration algorithm, the digital computer programming is shown on Appendix 2-4

-374-

APPENDIX 2

Digital Computer Programming

A 2.1 Computer Programming -1
(based on A1-2)

```
      MASTER ADAPT-1
C     DETERMINATION OF OPTIMAL CONTROL LAW COEFFICIENTS X(1),X(6),X(7)
C     X(8),X(9) BY NEWTON-RAPHSON METHOD
      DIMENSION D(7),Y(9),X(9),F(9),A(9,9),B(9,9),R(9),C(81),W(81),P(2)
      READ(1,2)(D(I),I=1,7)
    2 FORMAT(7F10.5)
      WRITE(2,4)
    4 FORMAT(/3X,'P(1),P(2)ARE WEIGHTING FACTORS X1(9),X2(9),..,ARE'
     C     /2X,'IN SEQUENCE,THE FIRST NUMBERS ARE THE INITIAL GUESS',/)
      WRITE(2,5)
    5 FORMAT(/9X,'X(1)',8X,'X(2)',8X,'X(3)',8X,'X(4)',8X,'X(5)',8X,
     1'X(6)',8X,'X(7)',8X,'X(8)',8X,'X(9)',/)
      H=2.0
    6 P(1)=H
      HH=2.0
    8 P(2)=HH
      WRITE(2,10)P(1),P(2)
   10 FORMAT(/8X,'P(1)=',F5.2,5X,'P(2)=',F5.2/)
      DO 12 I=1,9
   12 Y(I)=0.0
   14 DO 16 I=1,9
   16 X(I)=Y(I)
      II=1
   18 WRITE(2,20)(X(I),I=1,9)
   20 FORMAT(/3X,9(2X,F10.5)/)
C     DEFINE VECTOR F(9) AND MATRIX A(9,9)
      F(1)=P(1)+D(1)*X(1)+D(3)*X(2)-0.250*D(5)*D(5)*X(2)*X(2)
      F(2)=D(2)*X(1)+(D(1)+D(4))*X(2)+D(3)*X(6)
     1-0.500*D(5)*D(5)*X(2)*X(6)
      F(3)=-2.*P(1)+D(1)*X(3)+D(3)*X(7)-0.500*D(5)*D(5)*X(2)*X(7)
      F(4)=D(6)*X(1)+D(1)*X(4)+D(3)*X(8)-0.500*D(5)*D(5)*X(2)*X(8)
      F(5)=D(7)*X(2)+D(1)*X(5)+D(3)*X(9)-0.500*D(5)*D(5)*X(2)*X(9)
      F(6)=P(2)+D(2)*X(2)+D(4)*X(6)-0.250*D(5)*D(5)*X(6)*X(6)
      F(7)=D(2)*X(3)+D(4)*X(7)-0.500*D(5)*D(5)*X(6)*X(7)
      F(8)=D(6)*X(2)+D(2)*X(4)+D(4)*X(8)-0.500*D(5)*D(5)*X(6)*X(8)
      F(9)=D(2)*X(5)+D(7)*X(6)+D(4)*X(9)-0.500*D(5)*D(5)*X(6)*X(9)
      A(1,1)=D(1)
      A(1,2)=D(3)-0.500*D(5)*D(5)*X(2)
      A(1,3)=0.0
      A(1,4)=0.0
      A(1,5)=0.0
      A(1,6)=0.0
      A(1,7)=0.0
      A(1,8)=0.0
      A(1,9)=0.0
      A(2,1)=D(2)
      A(2,2)=(D(1)+D(4))-0.500*D(5)*D(5)*X(6)
```

```
A(2,3)=0.0
A(2,4)=0.0
A(2,5)=0.0
A(2,6)=D(3)-0.500*D(5)*D(5)*X(2)
A(2,7)=0.0
A(2,8)=0.0
A(2,9)=0.0
A(3,1)=0.0
A(3,2)=-0.500*D(5)*D(5)*X(7)
A(3,3)=D(1)
A(3,4)=0.0
A(3,5)=0.0
A(3,6)=0.0
A(3,7)=D(3)-0.500*D(5)*D(5)*X(2)
A(3,8)=0.0
A(3,9)=0.0
A(4,1)=D(6)
A(4,2)=-0.500*D(5)*D(5)*X(8)
A(4,3)=0
A(4,4)=D(1)
A(4,5)=0.0
A(4,6)=0.0
A(4,7)=0.0
A(4,8)=D(3)-0.500*D(5)*D(5)*X(2)
A(4,9)=0.0
A(5,1)=0.0
A(5,2)=D(7)-0.500*D(5)*D(5)*X(9)
A(5,3)=0.0
A(5,4)=0.0
A(5,5)=D(1)
A(5,6)=0.0
A(5,7)=0.0
A(5,8)=0.0
A(5,9)=D(3)-0.500*D(5)*D(5)*X(2)
A(6,1)=0.0
A(6,2)=D(2)
A(6,3)=0.0
A(6,4)=0.0
A(6,5)=0.0
A(6,6)=D(4)-0.500*D(5)*D(5)*X(6)
A(6,7)=0.0
A(6,8)=0.0
A(6,9)=0.0
A(7,1)=0.0
A(7,2)=0.0
A(7,3)=D(2)
A(7,4)=0.0
A(7,5)=0.0
A(7,6)=-0.500*D(5)*D(5)*X(7)
A(7,7)=D(4)-0.500*D(5)*D(5)*X(6)
A(7,8)=0.0
A(7,9)=0.0
A(8,1)=0.0
A(8,2)=D(6)
A(8,3)=0.0
A(8,4)=D(2)
A(8,5)=0.0
A(8,6)=-0.500*D(5)*D(5)*X(8)
A(8,7)=0.0
A(8,8)=D(4)-0.500*D(5)*D(5)*X(6)
```

```
      A(8,9)=0.0
      A(9,1)=0.0
      A(9,2)=0.0
      A(9,3)=0.0
      A(9,4)=0.0
      A(9,5)=D(2)
      A(9,6)=D(7)-0.500*D(5)*D(5)*X(9)
      A(9,7)=0.0
      A(9,8)=0.0
      A(9,9)=D(4)-0.500*D(5)*D(5)*X(6)
      L=1
      DO 22 J=1,9
      DO 22 I=1,9
      C(L)=A(I,J)
   22 L=L+1
      N=9
      E=0.001
      CALL FPMGEIN(N,E,C(1),W(1),DET,IRANK,NRR)
      L=1
      DO 24 J=1,9
      DO 24 I=1,9
      B(I,J)=C(L)
   24 L=L+1
      DO 28 I=1,9
      R(I)=0.0
      DO 26 J=1,9
   26 R(I)=R(I)+B(I,J)*F(J)
      X(I)=X(I)-R(I)
   28 CONTINUE
      II=II+1
      IF(II-10) 30,30,48
   30 IF(ABS(R(1))-0.0100) 32,18,18
   32 IF(ABS(R(2))-0.0100) 34,18,18
   34 IF(ABS(R(3))-0.0100) 36,18,18
   36 IF(ABS(R(4))-0.0100) 38,18,18
   38 IF(ABS(R(5))-0.0100) 40,18,18
   40 IF(ABS(R(6))-0.0100) 42,18,18
   42 IF(ABS(R(7))-0.0100) 44,18,18
   44 IF(ABS(R(8))-0.0100) 46,18,18
   46 IF(ABS(R(9))-0.0100) 48,18,18
   48 DO 50 I=1,9
   50 Y(I)=Y(I)+1.
      IF(Y(1)-1.5) 52,52,56
   52 WRITE(2,54)
   54 FORMAT(/,3X,'USE NEW GUESS',/)
      GO TO 14
   56 HH=HH+2.0
      IF(HH-11.0) 58,58,60
   58 GO TO 8
   60 H=H+2.0
      IF(H-11.0) 62,62,64
   62 GO TO 6
   64 STOP
      END
```

A 2.2 Computer Programming -2
(based on A1-3)

```
      MASTER ADAPT-2
C     DETRRMINATION OF OPTIMAL CONTROL LAW COEFFICIENTS X(2) BY NEWTON-
C     RADHSON METHOD
      DIMENSION D(5),Y(3),X(3),F(3),A(3,3),B(3,3),R(3),C(9),W(9)
      READ(1,2)(D(I),I=1,5)
    2 FORMAT(5F10.5)
      WRITE(2,4)
    4 FORMAT(/3X,'   P ARE WEIGHTING FACTOR X1(3),X2(3),...,ARE IN'/
     C        /2X,'SEQUENCE,THE FIRST NUMBERS ARE THE INITIAL GUESS',/)
      WRITE(2,5)
    5 FORMAT(/12X,'X(1)',11X,'X(2)',11X,'X(3)',/)
      P=50.0
    6 WRITE(2,10) P
   10 FORMAT(/10X,'P=',F5.2/)
      DO 12 I=1,3
   12 Y(I)=0.0
   14 DO 16 I=1,3
   16 X(I)=Y(I)
      II=1
   18 WRITE(2,20)(X(I),I=1,3)
   20 FORMAT(/3X,3F15.5/)
C     DEFINE VECTOR F(3) AND MATRIX A(3,3)
      F(1)=P+D(1)*X(1)+D(3)*X(2)-0.250*D(5)*D(5)*X(2)*X(2)
      F(2)=D(2)*X(1)+(D(1)+D(4))*X(2)+D(3)*X(3)
     1     -0.500*D(5)*D(5)*X(2)*X(3)
      F(3)=D(2)*X(2)+D(4)*X(3)-0.250*D(5)*D(5)*X(3)*X(3)
      A(1,1)=D(1)
      A(1,2)=D(3)-0.500*D(5)*D(5)*X(2)
      A(1,3)=0.0
      A(2,1)=D(2)
      A(2,2)=D(1)+D(4)-0.500*D(5)*D(5)*X(3)
      A(2,3)=D(3)-0.500*D(5)*D(5)*X(2)
      A(3,1)=0.0
      A(3,2)=D(2)
      A(3,3)=D(4)-0.500*D(5)*D(5)*X(3)
      L=1
      DO 22 J=1,3
      DO 22 I=1,3
      C(L)=A(I,J)
   22 L=L+1
      N=3
      E=0.0001
      CALL FPMGEIN(N,E,C(1),W(1),DET,IRANK,NRR)
```

```
      L=1
      DO 24 J=1,3
      DO 24 I=1,3
      B(I,J)=C(L)
   24 L=L+1
      DO 28 I=1,3
      R(I)=0.0
      DO 26 J=1,3
   26 R(I)=R(I)+B(I,J)*F(J)
      X(I)=X(I)-R(I)
   28 CONTINUE
      II=II+1
      IF(II-15) 30,30,36
   30 IF(ABS(R(1))-0.0100) 32,18,18
   32 IF(ABS(R(2))-0.0100) 34,18,18
   34 IF(ABS(R(3))-0.0100) 36,18,18
   36 DO 38 I=1,3
   38 Y(I)=Y(I)+1.
      IF(Y(1)-1.5) 40,40,44
   40 WRITE(2,42)
   42 FORMAT(/3X,'USE NEW GUESS',/)
      GO TO 14
   44 P=P+50.0
      IF(P-1005.0) 46,46,48
   46 GO TO 6
   48 STOP
      END
```

A 2.3 Computer Programming -3
(based on A1-4)

```
      MASTER ADAPT-3
C     DETERMINATION OF OPTIMAL CONTROL LAW COEFFICIENTS X(4)AND X(6)
C     BY NEWTON-RAPHSON METHOD
      DIMENSION D(5),Y(6),X(6),F(6),A(6,6),B(6,6),R(6),C(36),W(36)
      READ(1,2)(D(I),I=1,5)
    2 FORMAT(5F10.5)
      WRITE(2,4)
    4 FORMAT(/3X,'P   ARE WEIGHTING FACTOR X1(6),X2(6),...,ARE IN'/
     C       /2X,'SEQUENCE,THE FIRST NUMBERS ARE THE INITIAL GUESS',/)
      WRITE(2,5)
    5 FORMAT(/12X,'X(1)',11X,'X(2)',11X,'X(3)',11X,'X(4)',11X,'X(5)'
     1,11X,'X(6)',/)
      P=100.0
    6 WRITE(2,8) P
    8 FORMAT(/10X,'P=',F5.2/)
      G=0.0
    9 WRITE(2,10) G
   10 FORMAT(/10X,'G=',F5.2/)
      DO 12 I=1,6
   12 Y(I)=0.0
   14 DO 16 I=1,6
   16 X(I)=Y(I)
      II=1
   18 WRITE(2,20)(X(I),I=1,6)
   20 FORMAT(/3X,6F15.5/)
C     DEFINE VECTOR F(6) AND MATRIX A(6,6)
      F(1)=2.*P   +2.*D(1)*X(1)+D(3)*X(2)+D(3)*X(4)
     1-0.500*D(5)*D(5)*X(2)*X(4)+X(3)
      F(2)=D(2)*X(1)+(D(1)+D(4))*X(2)+D(3)*X(5)
     1-0.500*D(5)*D(5)*X(2)*X(5)
      F(3)=D(1)*X(3)+D(3)*X(6)-0.500*D(5)*D(5)*X(2)*X(6)+G
      F(4)=D(2)*X(1)+(D(1)+D(4))*X(4)+D(3)*X(5)
     1-0.500*D(5)*D(5)*X(4)*X(5)+X(6)
      F(5)=D(2)*X(2)+D(2)*X(4)+2.*D(4)*X(5)-0.500*D(5)*D(5)*X(5)*X(5)
      F(6)=D(2)*X(3)+D(4)*X(6)-0.500*D(5)*D(5)*X(5)*X(6)+G
      A(1,1)=2.*D(1)
      A(1,2)=D(3)-0.500*D(5)*D(5)*X(4)
      A(1,3)=1.
      A(1,4)=D(3)-0.500*D(5)*D(5)*X(2)
      A(1,5)=0.0
      A(1,6)=0.0
      A(2,1)=D(2)
      A(2,2)=D(1)+D(4)-0.500*D(5)*D(5)*X(5)
      A(2,3)=0.0
      A(2,4)=0.0
      A(2,5)=D(3)-0.500*D(5)*D(5)*X(2)
      A(2,6)=0.0
      A(3,1)=0.0
      A(3,2)=-0.500*D(5)*D(5)*X(6)
      A(3,3)=D(1)
      A(3,4)=0.0
      A(3,5)=0.0
      A(3,6)=D(3)-0.500*D(5)*D(5)*X(2)
```

```
      A(4,1)=D(2)
      A(4,2)=0.0
      A(4,3)=0.0
      A(4,4)=D(1)+D(4)-0.500*D(5)*D(5)*X(5)
      A(4,5)=D(3)-0.500*D(5)*D(5)*X(4)
      A(4,6)=1.
      A(5,1)=0.0
      A(5,2)=D(2)
      A(5,3)=0.0
      A(5,4)=D(2)
      A(5,5)=2.*D(4)-D(5)*D(5)*X(5)
      A(5,6)=0.0
      A(6,1)=0.0
      A(6,2)=0.0
      A(6,3)=D(2)
      A(6,4)=0.0
      A(6,5)=-0.500*D(5)*D(5)*X(6)
      A(6,6)=D(4)-0.500*D(5)*D(5)*X(5)
      L=1
      DO 22 J=1,6
      DO 22 I=1,6
      C(L)=A(I,J)
   22 L=L+1
      N=6
      E=0.0001
      CALL FPMGEIN(N,E,C(1),W(1),DET,IRANK,NRR)
      L=1
      DO 24 J=1,6
      DO 24 I=1,6
      B(I,J)=C(L)
   24 L=L+1
      DO 28 I=1,6
      R(I)=0.0
      DO 26 J=1,6
   26 R(I)=R(I)+B(I,J)*F(J)
      X(I)=X(I)-R(I)
   28 CONTINUE
      II=II+1
      IF(II-30) 30,30,42
   30 IF(ABS(R(1))-0.0100) 32,18,18
   32 IF(ABS(R(2))-0.0100) 34,18,18
   34 IF(ABS(R(3))-0.0100) 36,18,18
   36 IF(ABS(R(4))-0.0100) 38,18,18
   38 IF(ABS(R(5))-0.0100) 40,18,18
   40 IF(ABS(R(6))-0.0100) 42,18,18
   42 DO 44 I=1,6
   44 Y(I)=Y(I)+1.
      IF(Y(1)-1.5) 46,46,49
   46 WRITE(2,48)
   48 FORMAT(/3X,'USE NEW GUESS',/)
      GO TO 14
   49 G=G+0.2
      IF(G-1.5) 50,50,51
   50 GO TO 9
   51 P=P+100.0
      IF(P-550.0) 52,52,54
   52 GO TO 6
   54 STOP
      END
```

A 2.4 Computer Programming -4
(based on A1-5)

```
      MASTER ADAPT-4
C     DETERMINATION OF OPTIMAL CONTROL LAW COEFFICIENTS X(6),X(9)AND
C     X(10) BY NEWTON-RAPHSON METHOD
      DIMENSION D(5),Y(10),X(10),F(10),A(10,10),B(10,10),R(10),C(100),
     CW(100)
      READ(1,2)(D(I),I=1,5)
    2 FORMAT(5F10.5)
      WRITE(2,4)
    4 FORMAT(/3X,'P ARE WEIGHTING FACTOR X1(10),X2(10),...,ARE IN'/
     C/2X,'SEQUENCE,THE FIRST NUMBERS ARE THE INITIAL GUESS',/)
      WRITE(2,5)
    5 FORMAT(/8X,'X(1)',7X,'X(2)',7X,'X(3)',7X,'X(4)',7X,'X(5)',7X,
     1'X(6)',7X,'X(7)',7X,'X(8)',7X,'X(9)',7X,'X(10)',/)
      P=5.0
    6 WRITE(2,10) P
   10 FORMAT(/10X,'P=',F5.2/)
      G=0.0
   11 WRITE(2,100) G
  100 FORMAT(/10X,'G=',F5.2/)
      DO 12 I=1,10
   12 Y(I)=0.0
   14 DO 16 I=1,10
   16 X(I)=Y(I)
      II=1
   18 WRITE(2,20)(X(I),I=1,10)
   20 FORMAT(/2X,10(1X,F10.4)/)
C     DEFINE VECTOR F(10) AND MATRIX A(10,10)
      F(1)=2.*P+2.*D(1)*X(1)+D(3)*X(2)+X(4)+D(1)*D(1)*X(5)+D(3)*X(6)
     1      +D(1)*D(3)*X(10)-0.500*D(5)*D(5)*X(2)*X(6)
     2      -0.500*D(5)*D(5)*D(1)*X(2)*X(10)
      F(2)=D(2)*X(1)+(D(1)+D(4))*X(2)+D(1)*D(2)*X(5)+D(3)*X(7)
     1      +D(2)*D(3)*X(10)-0.500*D(5)*D(5)*X(2)*X(7)
     2      -0.500*D(5)*D(5)*D(2)*X(2)*X(10)
      F(3)=-2.*P+D(1)*X(3)-X(4)+D(3)*X(8)-0.500*D(5)*D(5)*X(2)*X(8)
      F(4)=D(1)*X(4)+D(3)*X(9)-0.500*D(5)*D(5)*X(2)*X(9)+G
      F(5)=X(3)-D(1)*X(5)-D(3)*X(10)+0.500*D(5)*D(5)*X(2)*X(10)
      F(6)=D(2)*X(1)+D(1)*D(2)*X(5)+(D(1)+D(4))*X(6)+D(3)*X(7)+X(9)
     1      +D(1)*D(4)*X(10)-0.500*D(5)*D(5)*X(6)*X(7)
     2      -0.500*D(5)*D(5)*D(1)*X(7)*X(10)
      F(7)=D(2)*X(2)+D(2)*D(2)*X(5)+D(2)*X(6)+2.*D(4)*X(7)
     1      +D(2)*D(4)*X(10)-0.500*D(5)*D(5)*X(7)*X(7)
     2      -0.500*D(5)*D(5)*D(2)*X(7)*X(10)
      F(8)=D(2)*X(3)+D(4)*X(8)-X(9)-0.500*D(5)*D(5)*X(7)*X(8)
      F(9)=D(2)*X(4)+D(4)*X(9)-0.500*D(5)*D(5)*X(7)*X(9)+G
      F(10)=-D(2)*X(5)-D(4)*X(10)+X(8)+0.500*D(5)*D(5)*X(7)*X(10)
      A(1,1)=2.*D(1)
      A(1,2)=D(3)-0.500*D(5)*D(5)*X(6)-0.500*D(5)*D(5)*D(1)*X(10)
      A(1,3)=0.0
      A(1,4)=1.
      A(1,5)=D(1)*D(1)
```

```
A(1,6)=D(3)-0.500*D(5)*D(5)*X(2)
A(1,7)=0.0
A(1,8)=0.0
A(1,9)=0.0
A(1,10)=D(1)*D(3)-0.500*D(5)*D(5)*D(1)*X(2)
A(2,1)=D(2)
A(2,2)=D(1)+D(4)-0.500*D(5)*D(5)*X(7)-0.500*D(5)*D(5)*D(2)*X(10)
A(2,3)=0.0
A(2,4)=0.0
A(2,5)=D(1)*D(2)
A(2,6)=0.0
A(2,7)=D(3)-0.500*D(5)*D(5)*X(2)
A(2,8)=0.0
A(2,9)=0.0
A(2,10)=D(2)*D(3)-0.500*D(5)*D(5)*D(2)*X(2)
A(3,1)=0.0
A(3,2)=-0.500*D(5)*D(5)*X(8)
A(3,3)=D(1)
A(3,4)=-1.
A(3,5)=0.0
A(3,6)=0.0
A(3,7)=0.0
A(3,8)=D(3)-0.500*D(5)*D(5)*X(2)
A(3,9)=0.0
A(3,10)=0.0
A(4,1)=0.0
A(4,2)=-0.500*D(5)*D(5)*X(9)
A(4,3)=0.0
A(4,4)=D(1)
A(4,5)=0.0
A(4,6)=0.0
A(4,7)=0.0
A(4,8)=0.0
A(4,9)=D(3)-0.500*D(5)*D(5)*X(2)
A(4,10)=0.0
A(5,1)=0.0
A(5,2)=0.500*D(5)*D(5)*X(10)
A(5,3)=1.
A(5,4)=0.
A(5,5)=-D(1)
A(5,6)=0.0
A(5,7)=0.0
A(5,8)=0.0
A(5,9)=0.0
A(5,10)=-D(3)+0.500*D(5)*D(5)*X(2)
A(6,1)=D(2)
A(6,2)=0.0
A(6,3)=0.0
A(6,4)=0.0
A(6,5)=D(1)*D(2)
A(6,6)=D(1)+D(4)-0.500*D(5)*D(5)*X(7)
A(6,7)=D(3)-0.500*D(5)*D(5)*X(6)-0.500*D(5)*D(5)*D(1)*X(10)
A(6,8)=0.0
A(6,9)=1.
A(6,10)=D(1)*D(4)-0.500*D(5)*D(5)*D(1)*X(7)
A(7,1)=0.0
A(7,2)=D(2)
```

```
      A(7,3)=0.0
      A(7,4)=0.0
      A(7,5)=D(2)*D(2)
      A(7,6)=D(2)
      A(7,7)=2.*D(4)-0.500*D(5)*D(5)*X(7)-0.500*D(5)*D(5)*D(2)*X(10)
      A(7,8)=0.0
      A(7,9)=0.0
      A(7,10)=D(2)*D(4)-0.500*D(5)*D(5)*D(2)*X(7)
      A(8,1)=0.0
      A(8,2)=0.0
      A(8,3)=D(2)
      A(8,4)=0.0
      A(8,5)=0.0
      A(8,6)=0.0
      A(8,7)=-0.500*D(5)*D(5)*X(8)
      A(8,8)=D(4)-0.500*D(5)*D(5)*X(7)
      A(8,9)=-1.
      A(8,10)=0.0
      A(9,1)=0.0
      A(9,2)=0.0
      A(9,3)=0.0
      A(9,4)=D(2)
      A(9,5)=0.0
      A(9,6)=0.0
      A(9,7)=-0.500*D(5)*D(5)*X(9)
      A(9,8)=0.0
      A(9,9)=D(4)-0.500*D(5)*D(5)*X(7)
      A(9,10)=0.0
      A(10,1)=0.0
      A(10,2)=0.0
      A(10,3)=0.0
      A(10,4)=0.0
      A(10,5)=-D(2)
      A(10,6)=0.0
      A(10,7)=0.500*D(5)*D(5)*X(10)
      A(10,8)=1.
      A(10,9)=0.
      A(10,10)=-D(4)+0.500*D(5)*D(5)*X(7)
      L=1
      DO 22 J=1,10
      DO 22 I=1,10
      C(L)=A(I,J)
   22 L=L+1
      N=10
      E=0.0001
      CALL FPMGEIN(N,E,C(1),W(1),DET,IRANK,NRR)
      L=1
      DO 24 J=1,10
      DO 24 I=1,10
      B(I,J)=C(L)
   24 L=L+1
      DO 28 I=1,10
      R(I)=0.0
      DO 26 J=1,10
   26 R(I)=R(I)+B(I,J)*F(J)
      X(I)=X(I)-R(I)
   28 CONTINUE
      II=II+1
```

```
      IF(II-10) 30,30,50
   30 IF(ABS(R(1))-0.0100) 32,18,18
   32 IF(ABS(R(2))-0.0100) 34,18,18
   34 IF(ABS(R(3))-0.0100) 36,18,18
   36 IF(ABS(R(4))-0.0100) 38,18,18
   38 IF(ABS(R(5))-0.0100) 40,18,18
   40 IF(ABS(R(6))-0.0100) 42,18,18
   42 IF(ABS(R(7))-0.0100) 44,18,18
   44 IF(ABS(R(8))-0.0100) 46,18,18
   46 IF(ABS(R(9))-0.0100) 48,18,18
   48 IF(ABS(R(10))-0.0100) 50,18,18
   50 DO 52 I=1,10
   52 Y(I)=Y(I)+1.0
      IF(Y(1)-1.2) 54,54,57
   54 WRITE(2,56)
   56 FORMAT(/3X,'USE NEW GUESS',/)
      GO TO 14
   57 G=G+0.02
      IF(G-0.11) 58,58,59
   58 GO TO 11
   59 P=P+5.0
      IF(P-22.0) 60,60,62
   60 GO TO 6
   62 STOP
      END
```

A 2.5 Computer Programming -5

Calculation of velocity constant from Arrhenius Equation. T vs K

```
      Master Adapt-5
C     Calculation of velocity constant from Arrhenius Equation
      Write (2.5)
    5 Format(5X,'T',12X,'K',/)
      T=0.0
   10 Y=6.30*(10,0**15.0)*EXP(-24000.0/(1.987*(273.0+T)))
      Write(2.15) T.Y
   15 Format(3X,F5,1,5X,F6.4,/)
      T=T+1.0
      IF(T-100.0) 20.20.25
   20 GO TO 10
   25 STOP
      END
```

A 2.6 Computer Programming -6

Calculation of velocity constant from Arrhenius equation. T vs $\left[\frac{T}{T}\right]$ and $\left[\frac{K}{Km}\right]$

```
      Master Adapt-6
C     Calculation of velocity constant from Arrhenius Equation
      Write(2.5)
    5 Format(5X,'T', 10X,'T/TMAX',10X,'K/KMAX',/)
      T=0.0
   10 X=T/40.0
      Y=EXP((-24000.0/C1.987*(273.0+T)))+(24000.0/(1.987*3.3.0)))
      Write(2.15) T.X.Y
   15 Format(/3X,F5.1,9X,F5.3,10X,F6.4,/)
      T=T+1.0
      IF(T-40.0) 20.20.25
   20 GO TO 10
   25 STOP
      END
```

A 2.7 Tables of computed α_{ij} and β_{ij} values (Tables A 2.1 - A 2.4)

TABLE A.2.1. α_{ij} values of OMR scheme computed from A.2.1.

	α_{11}	α_{22}	α_{23}	α_{24}
$K_1 = 4$, $K_2 = 4$	28.1372	7.7681		
$K_1 = 8$, $K_2 = 8$	51.2233	14.4027	-28.4028	3.6851
$K_1 = 15$, $K_2 = 15$	85.4628	24.5025		

Table A.2.2. α_{12} value of OAC scheme for optimal P control computed from A.2.2.

	12
$K_3 = 100$	99.50
$K_3 = 200$	156.20
$K_3 = 500$	273.67
$K_3 = 1000$	410.00

Table A.2.3. β_{ij} values of OAC scheme for optimal P + I control computed from A.2.3.

$K_3 = 100$	β_{21}	β_{26}
$\epsilon = 0$	99.502	0
$\epsilon = 1$	101.470	1.667
$\epsilon = 2$	103.394	3.312
$\epsilon = 3$	105.287	4.937
$\epsilon = 4$	107.125	6.542
$K_3 = 200$		
$\epsilon = 0$	156.197	0
$\epsilon = 1$	157.238	1.215
$\epsilon = 2$	158.272	2.426
$\epsilon = 3$	159.30	3.633
$\epsilon = 4$	160.322	4.836
$\epsilon = 8$	164.509	9.709
$\epsilon = 15$	170.909	18.153
$K_3 = 100$		
$\epsilon = 0$	99.502	0
$\epsilon = 0.2$	99.899	0.335
$\epsilon = 0.4$	100.294	0.670
$\epsilon = 0.6$	100.690	1.002
$\epsilon = 0.8$	101.079	1.336
$\epsilon = 1.0$	101.470	1.667

Table A.2.3. (continued)

$K_3 = 200$	β_{21}	β_{26}
$\epsilon = 0$	156.197	0
$\epsilon = 0.2$	156.406	0.243
$\epsilon = 0.4$	156.614	0.487
$\epsilon = 0.6$	156.822	0.730
$\epsilon = 0.8$	157.030	0.973
$\epsilon = 1.0$	157.238	1.215

Table A.2.4. β_{ij} values of OAC scheme for optimal P + I + D control computed from A.2.4.

$K_3 = 1.0$	β_{21}	β_{26}	β_{27}
$\epsilon = 0.0$	5.4653	0	54.4914
$\epsilon = 0.5$	28.2819	2.6588	262.3466
$\epsilon = 1.0$	51.0984	5.3176	470.2018
$\epsilon = 1.5$	73.9150	7.9766	678.0570
$\epsilon = 2.0$	96.7316	10.6352	885.9122
$K_3 = 3.0$			
$\epsilon = 0.0$	16.3959	0	163.4743
$\epsilon = 0.5$	39.2124	2.6588	371.3295
$\epsilon = 1.0$	62.0290	5.3176	579.1847
$\epsilon = 1.5$	84.8456	7.9766	787.0399
$\epsilon = 2.0$	107.6622	10.6352	994.8951
$K_3 = 1.0$			
$\epsilon = 0.1$	10.0286	0.5318	96.0625
$\epsilon = 0.2$	14.5919	1.0635	137.6355
$\epsilon = 0.3$	19.1552	1.5953	179.2045
$\epsilon = 0.4$	23.7186	2.1270	220.7756
$K_3 = 10$			
$\epsilon = 0$	54.6529	0	544.9142
$\epsilon = 0.04$	56.4782	0.2127	561.5427
$\epsilon = 0.08$	58.3035	0.4254	578.1711
$\epsilon = 0.12$	60.1289	0.6382	594.7995

Table A.2.4. (continued)

$K_3 = 20$	β_{21}	β_{26}	β_{27}
$\epsilon = 0$	109.3035	0	1089.8285
$\epsilon = 0.04$	111.1311	0.2127	1106.4569
$\epsilon = 0.08$	112.9564	0.4254	1123.0853
$\epsilon = 0.12$	114.7817	0.6382	1139.7137

APPENDIX 3

VDFG generation curves

Figures A.3.1 to A.3.3.

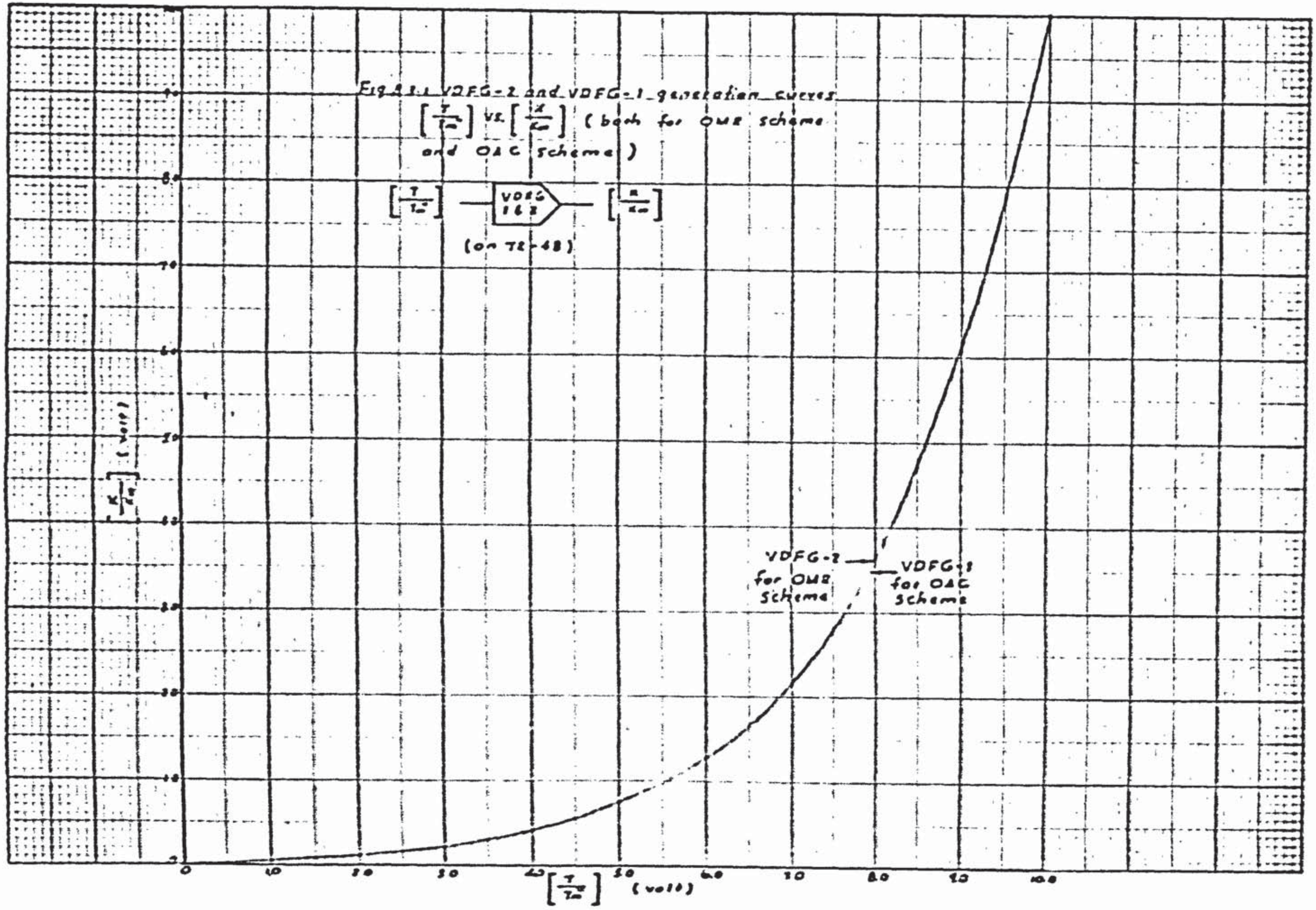
Fig 8.3.1 VDFG-2 and VDFG-1 generation curves
[T/Tm] vs [X/Xm] (both for OMR scheme and OAC scheme)
[T/Tm] — VDFG 1 & 2 — [X/Xm]
(on TR-48)
VDFG-2 for OMR Scheme
VDFG-1 for OAC Scheme
[X/Xm] (volt)
0
10
20
30
40
50
60
70
80
90
100
[T/Tm] (volt)

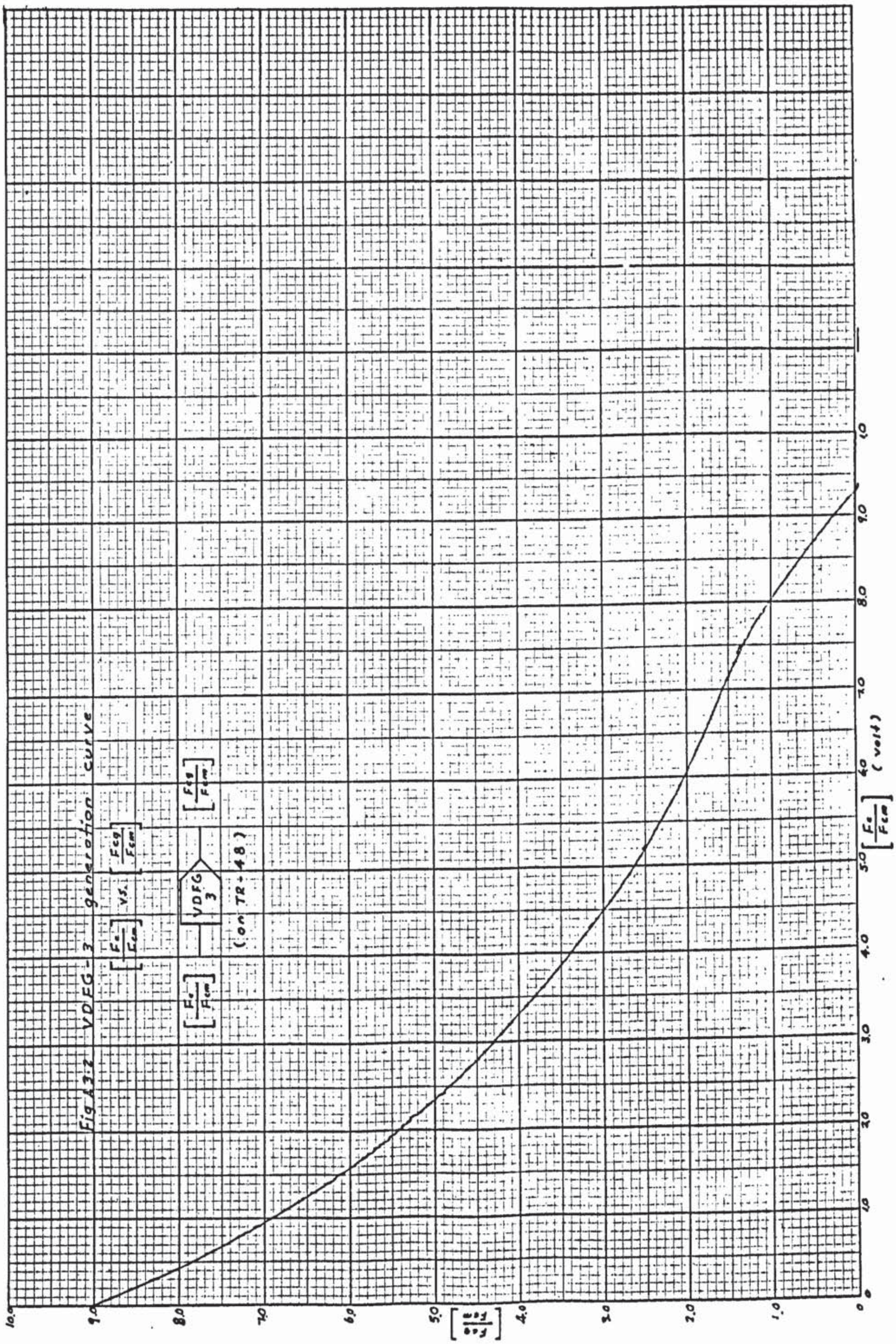

Fig A3.2 VDEG-3 generation curve
[Fe/Fcm] vs. [Fcg/Fcm]
[Fe/Fcm]
VDFG 3
[Fcg/Fcm]
(on TR-48)
10.0
9.0
8.0
7.0
6.0
5.0
4.0
3.0
2.0
1.0
0
[Fcg/Fcm]
[Fe/Fcm] (volt)

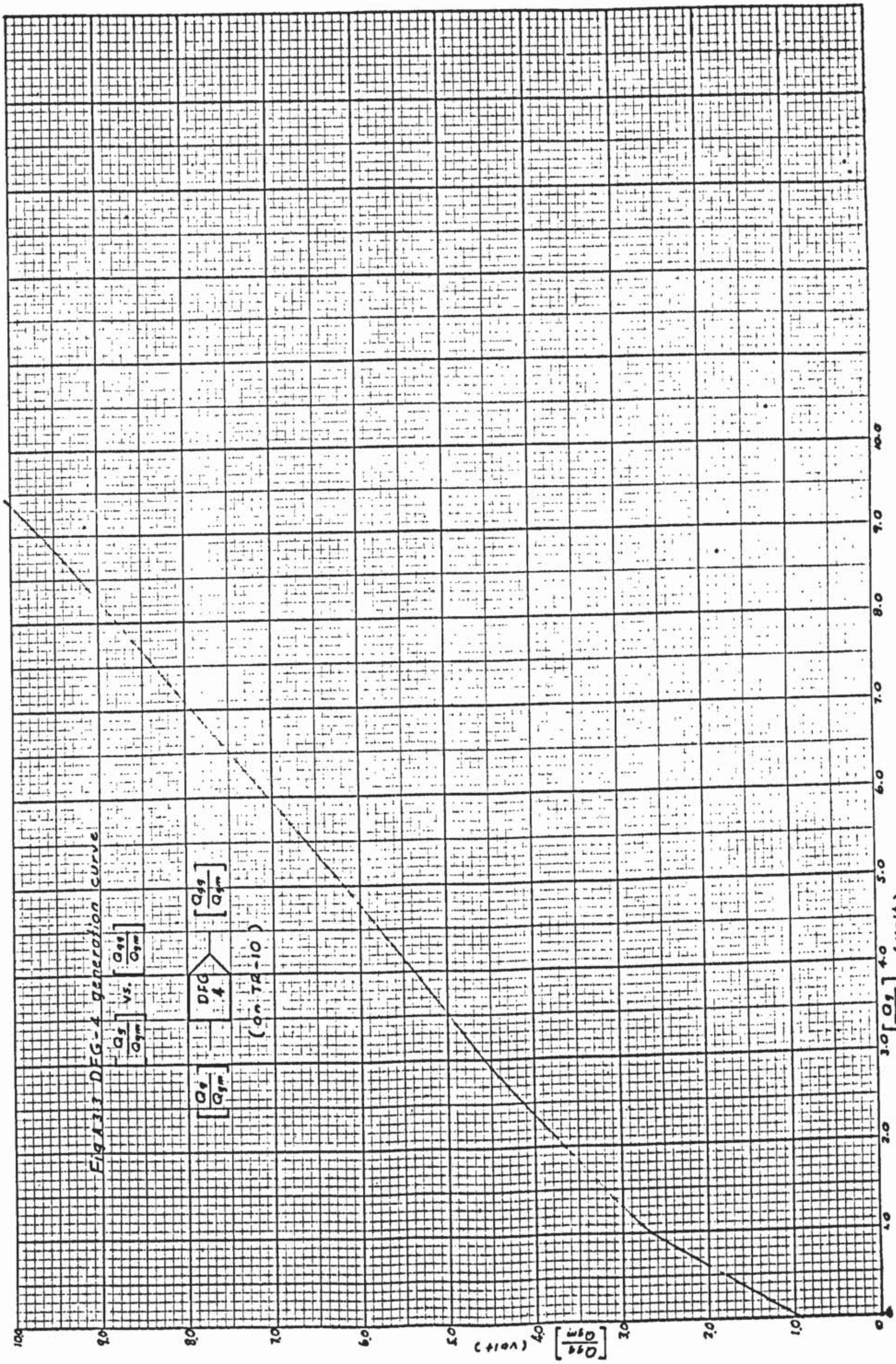
Fig.A33 DFG-4 generation curve
[Qs/Qgm] vs. [Qgg/Qgm]
DFG 4
(on TR-10)
(volt)
(volt)
0
1.0
2.0
3.0
4.0
5.0
6.0
7.0
8.0
9.0
10.0

A P P E N D I X   4

PERFORMANCE RESPONSE FIGURE OF

COMPLETE SIMULATION

Figures A.4.1. to A.4.21

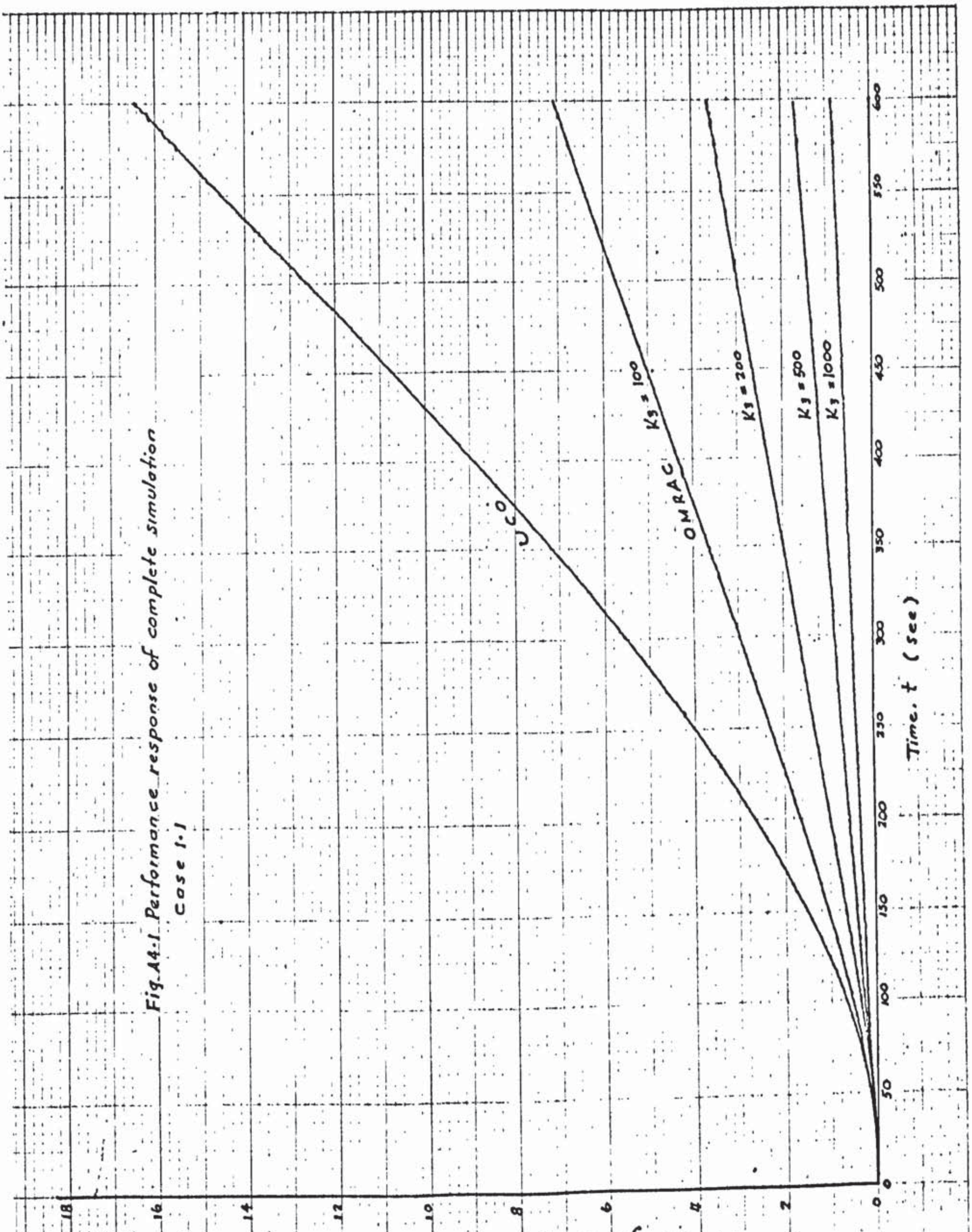

Fig. A4.1 Performance response of complete simulation
case 1.1

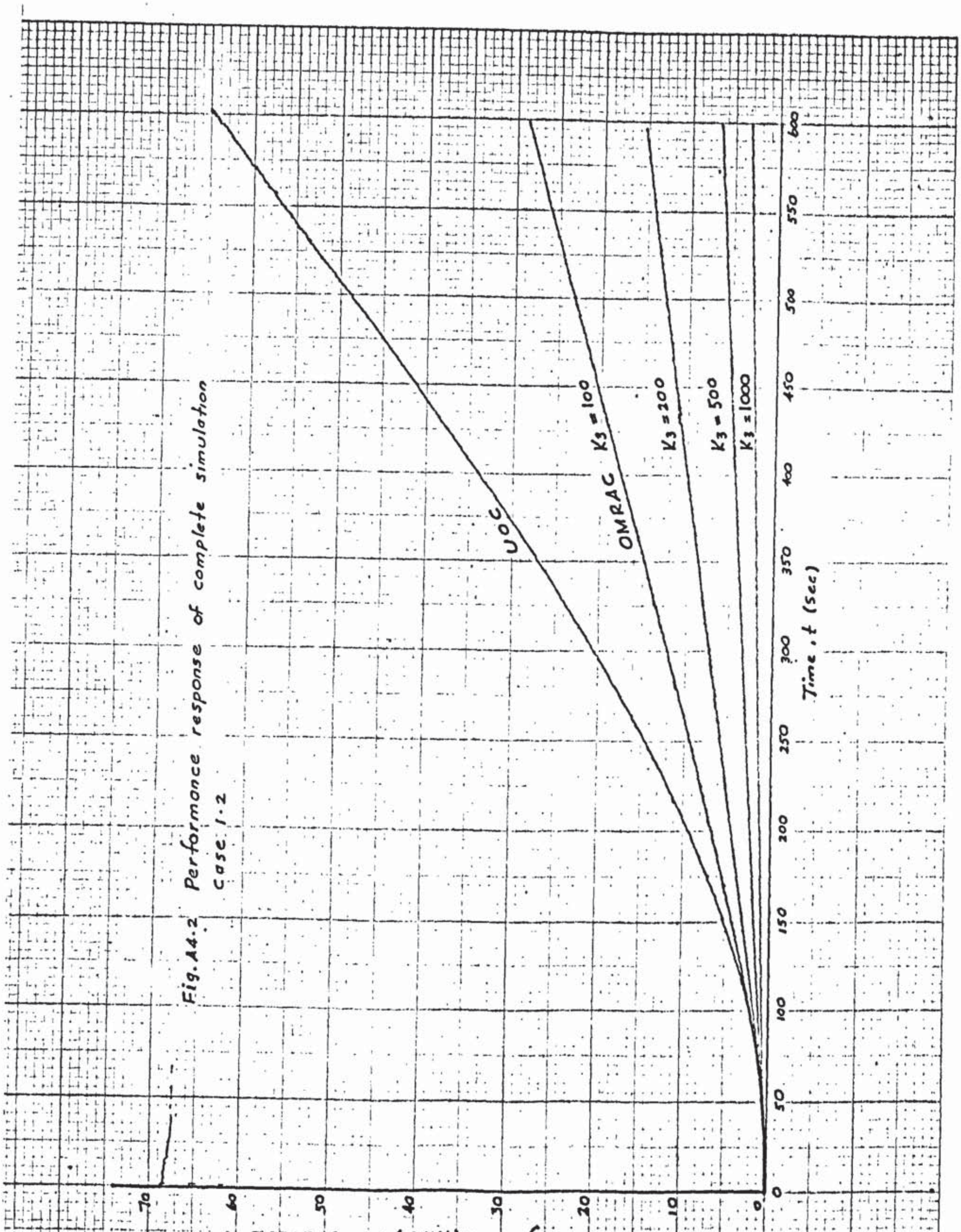

Fig. A4.2 Performance response of complete simulation case 1.2

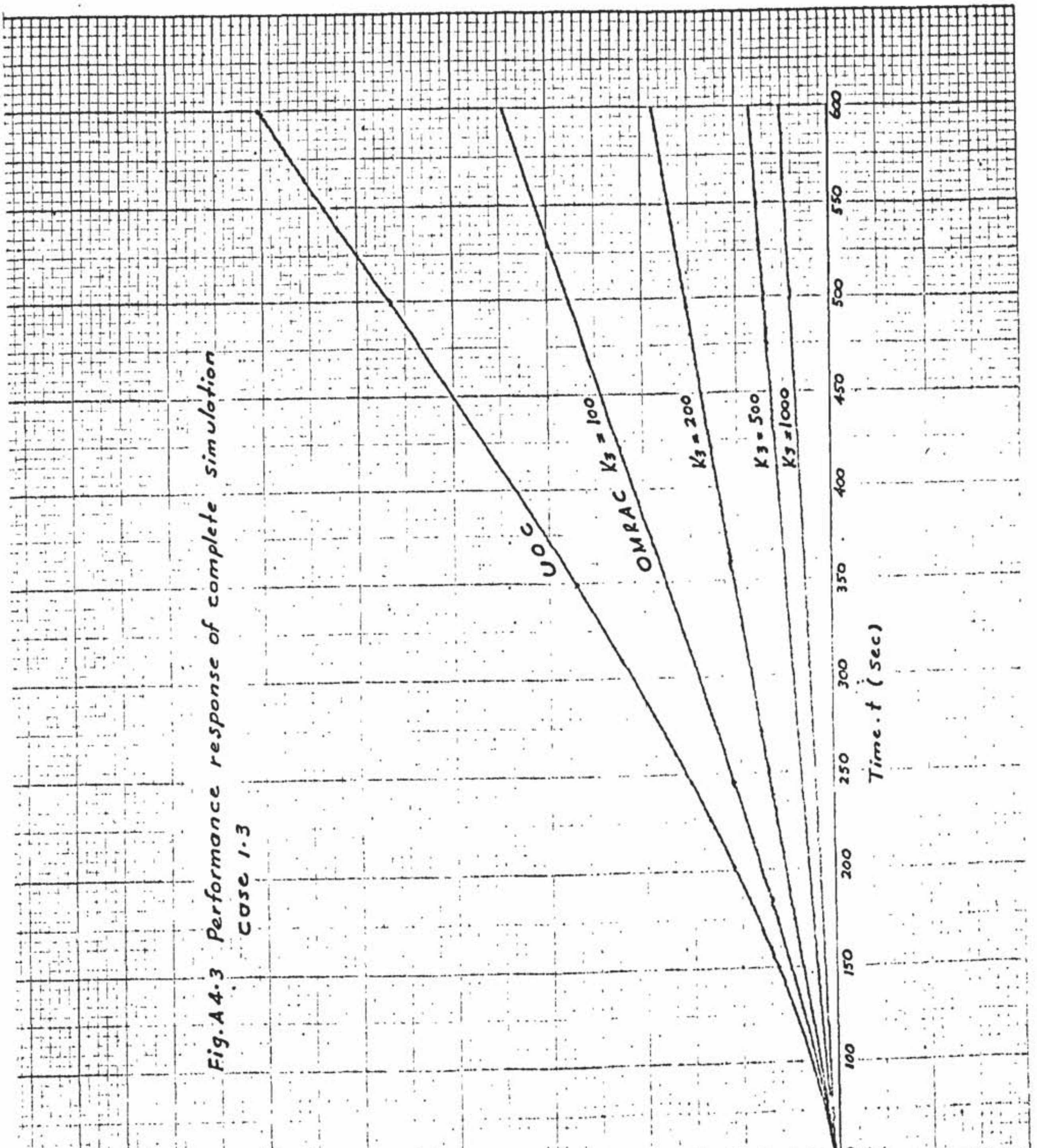

Fig. A4.3 Performance response of complete simulation case 1.3

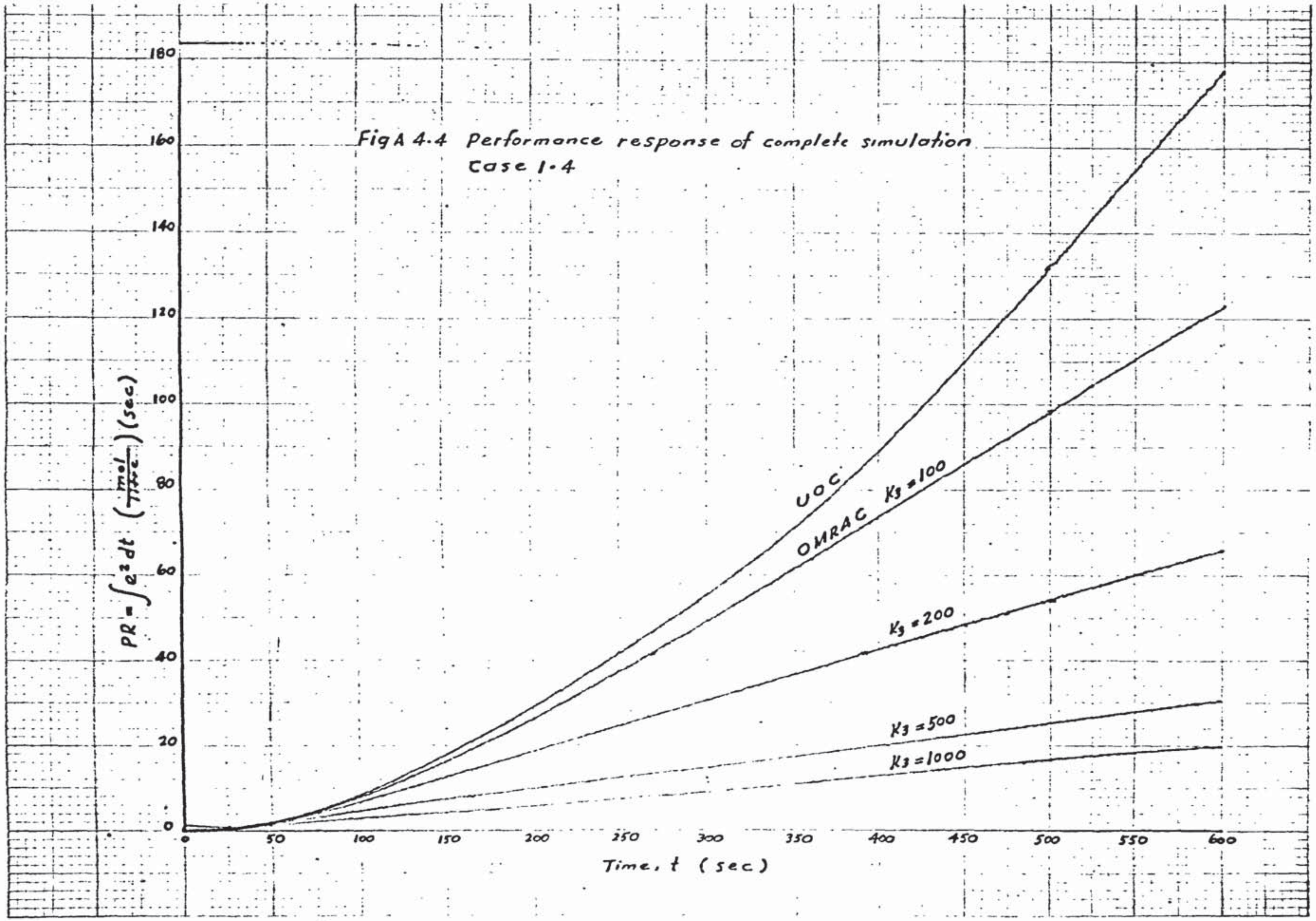

Fig A 4.4 Performance response of complete simulation
Case 1.4

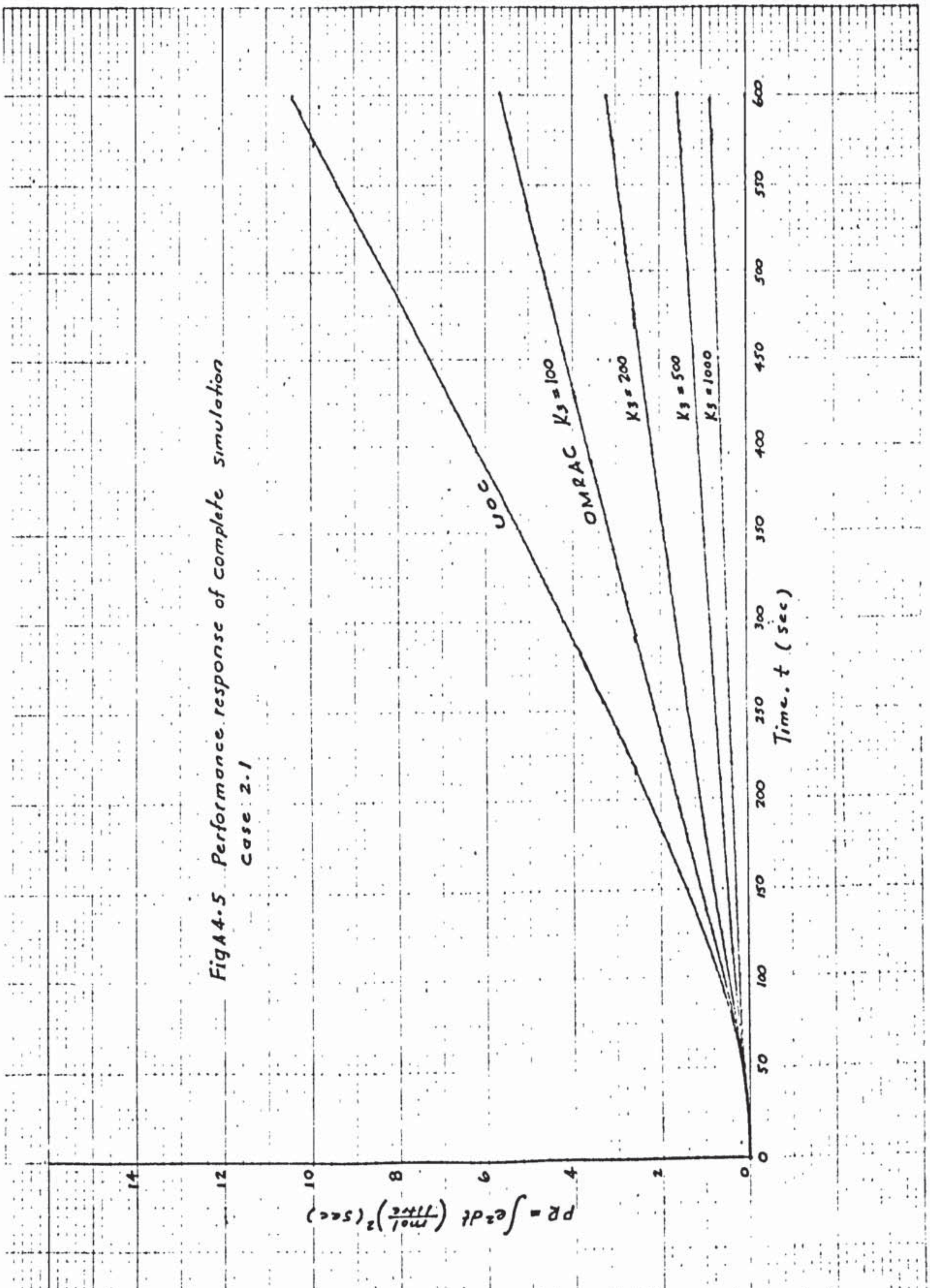

Fig A4.5 Performance response of complete simulation Case 2.1

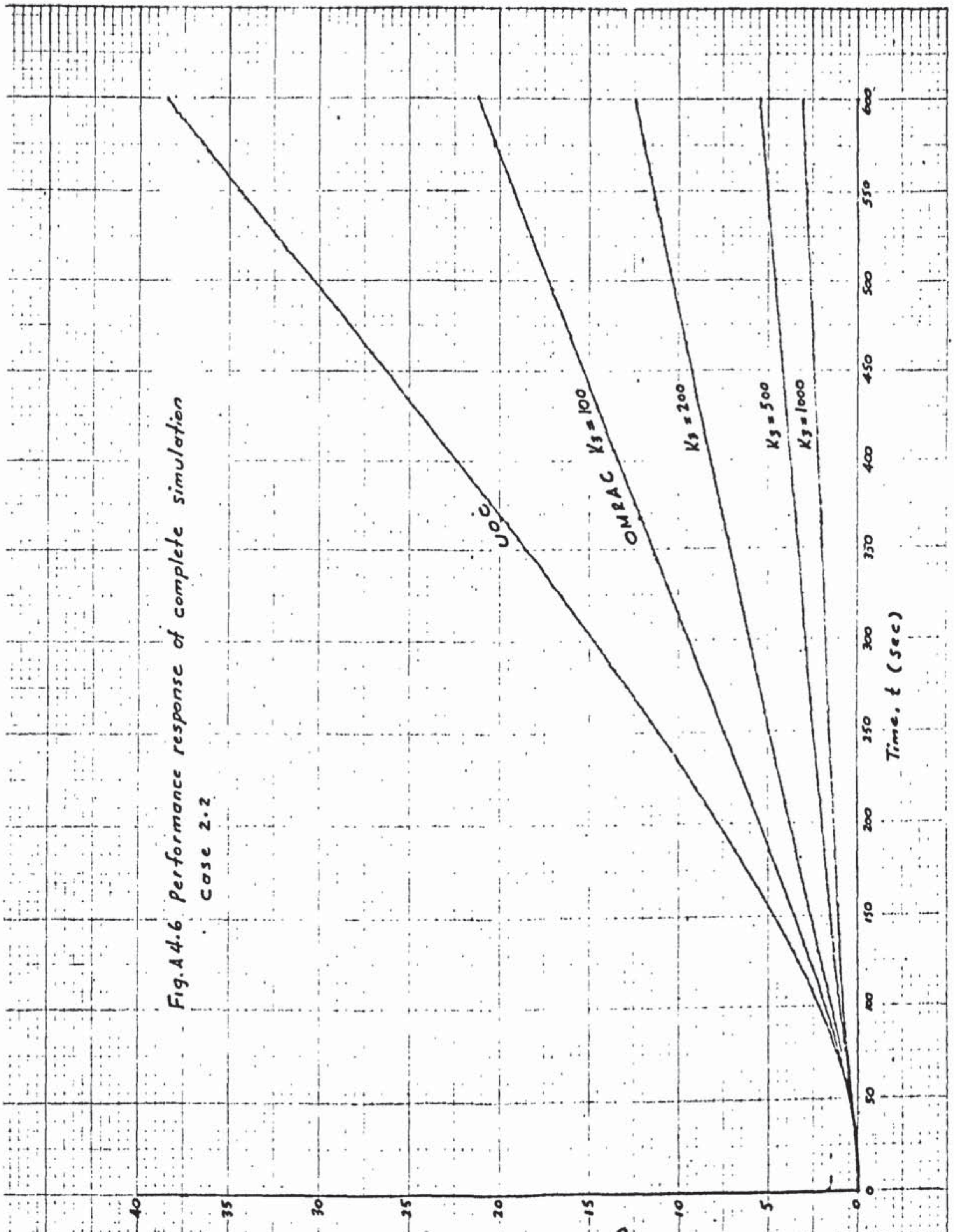

Fig. A4.6 Performance response of complete simulation case 2.2

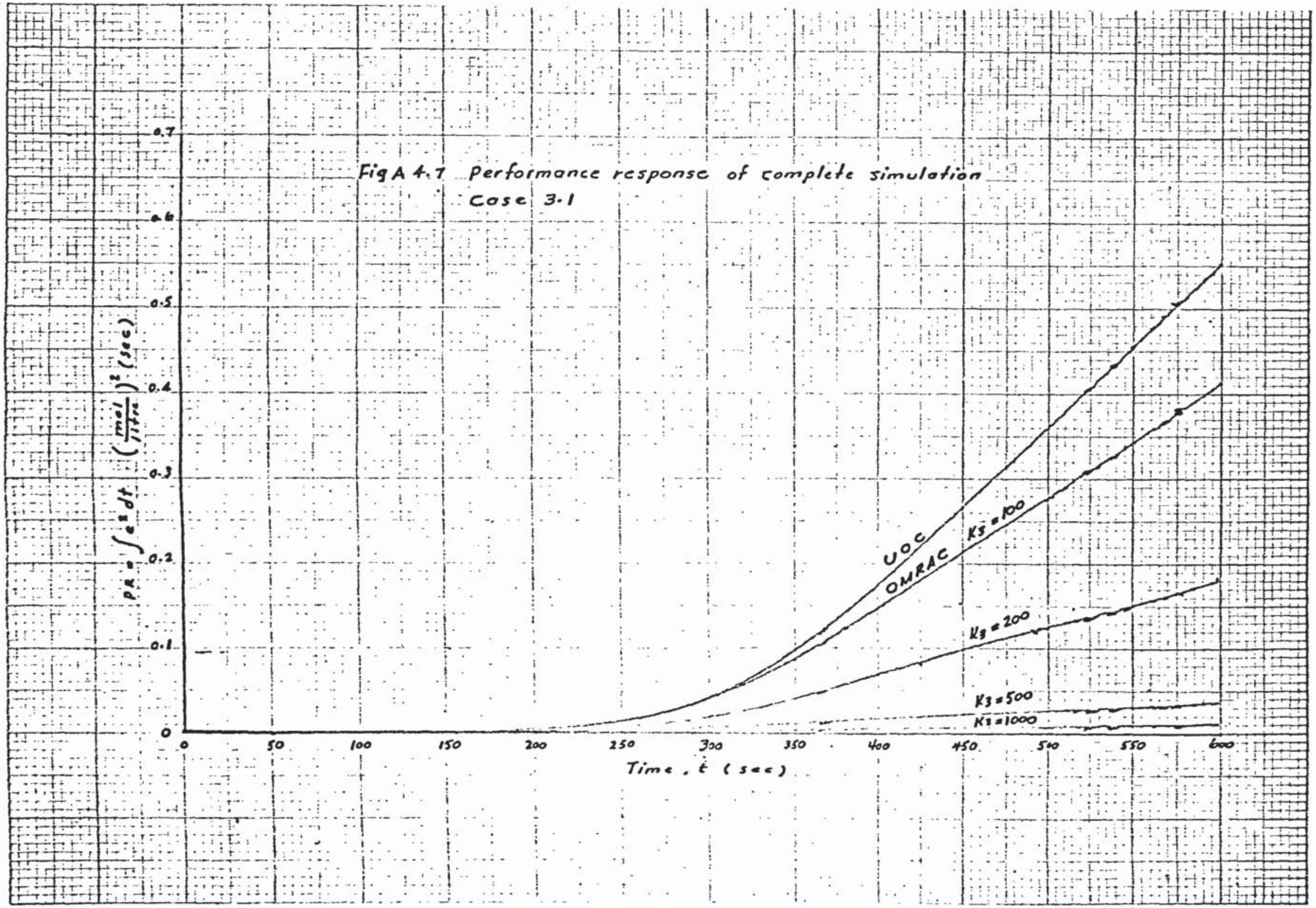

Fig A 4.7 Performance response of complete simulation
Case 3.1

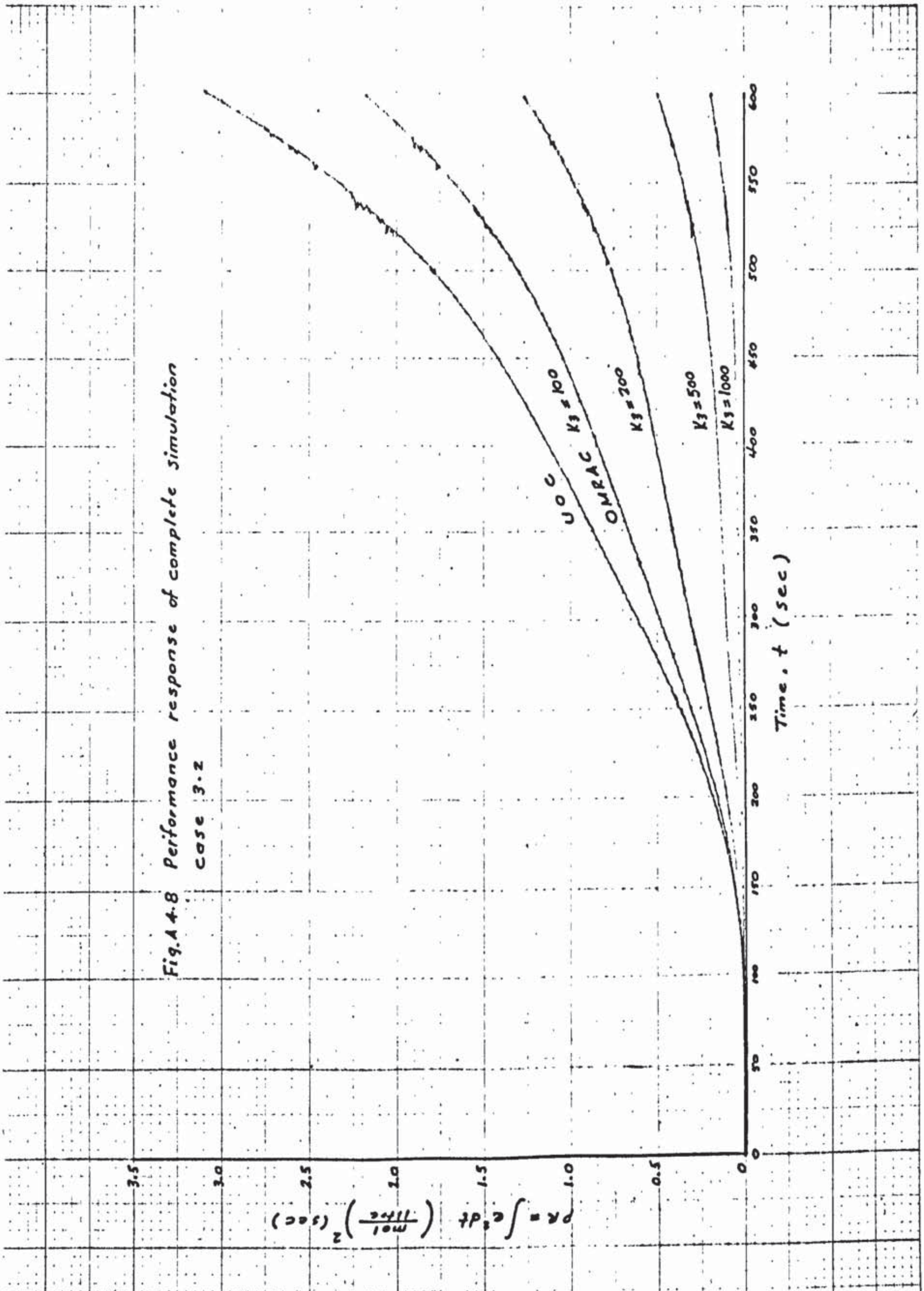

Fig. A4.8 Performance response of complete simulation case 3.2

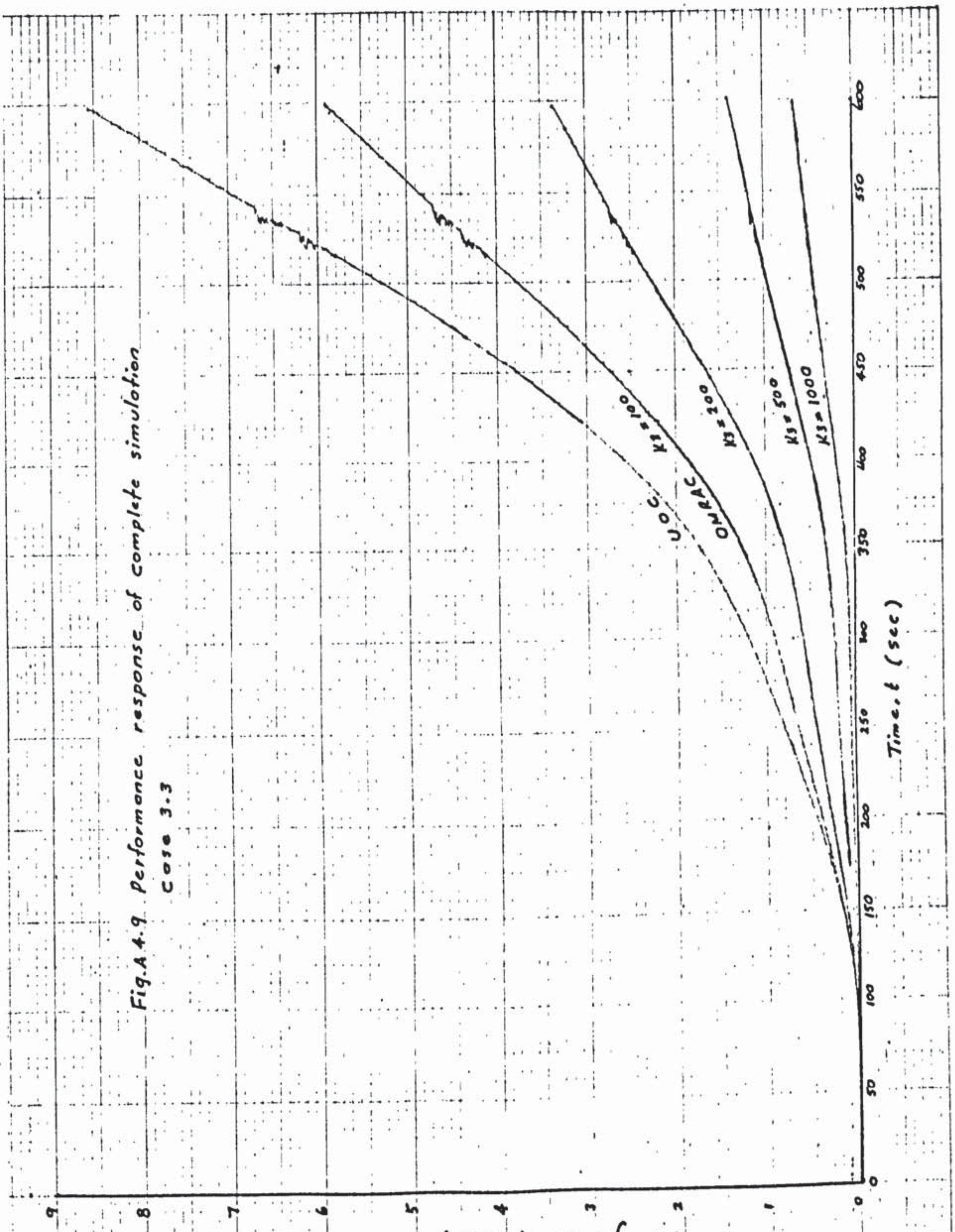

Fig.A4.9 Performance response of complete simulation
Case 3.3

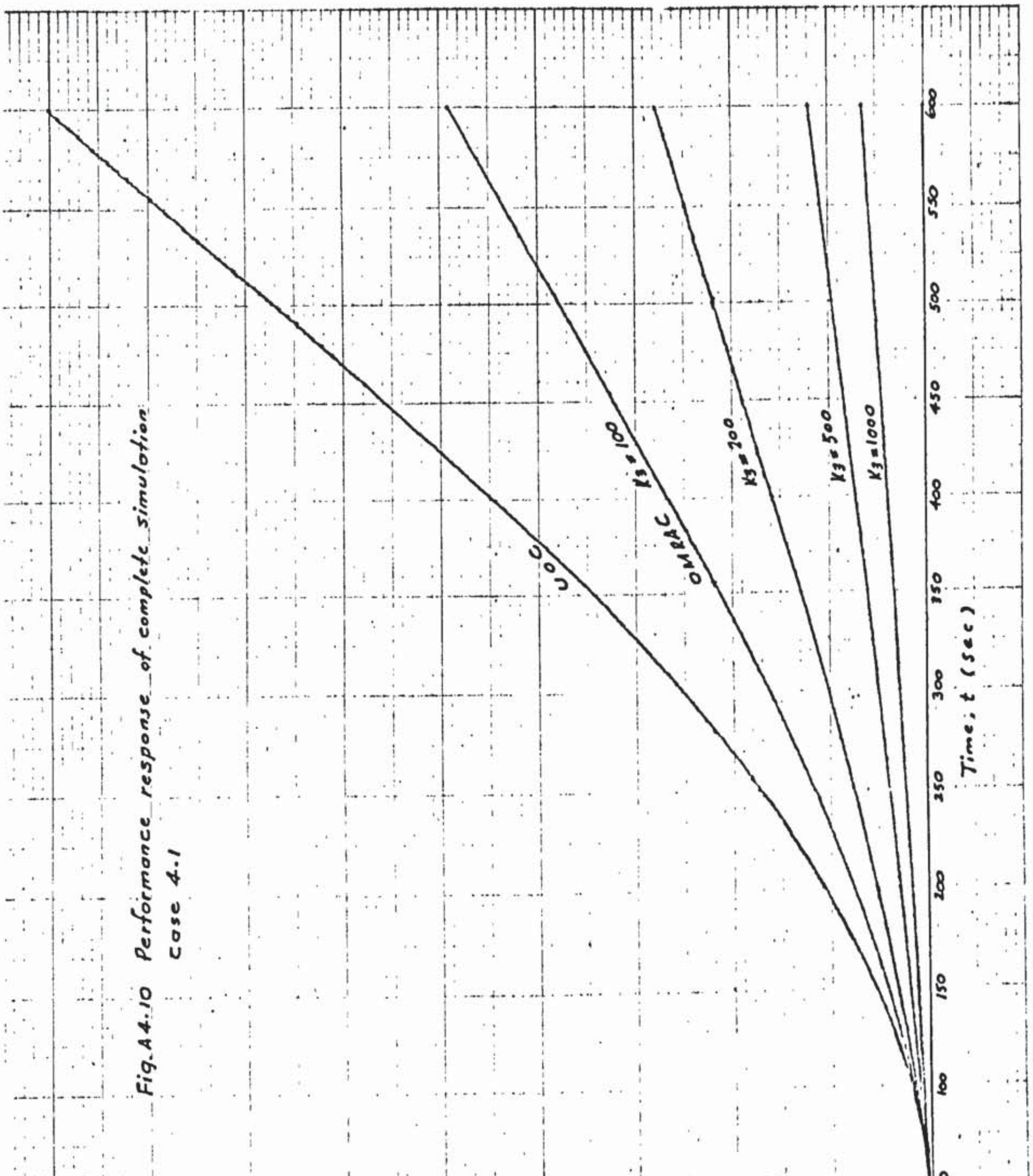

Fig. A4.10 Performance response of complete simulation
Case 4.1

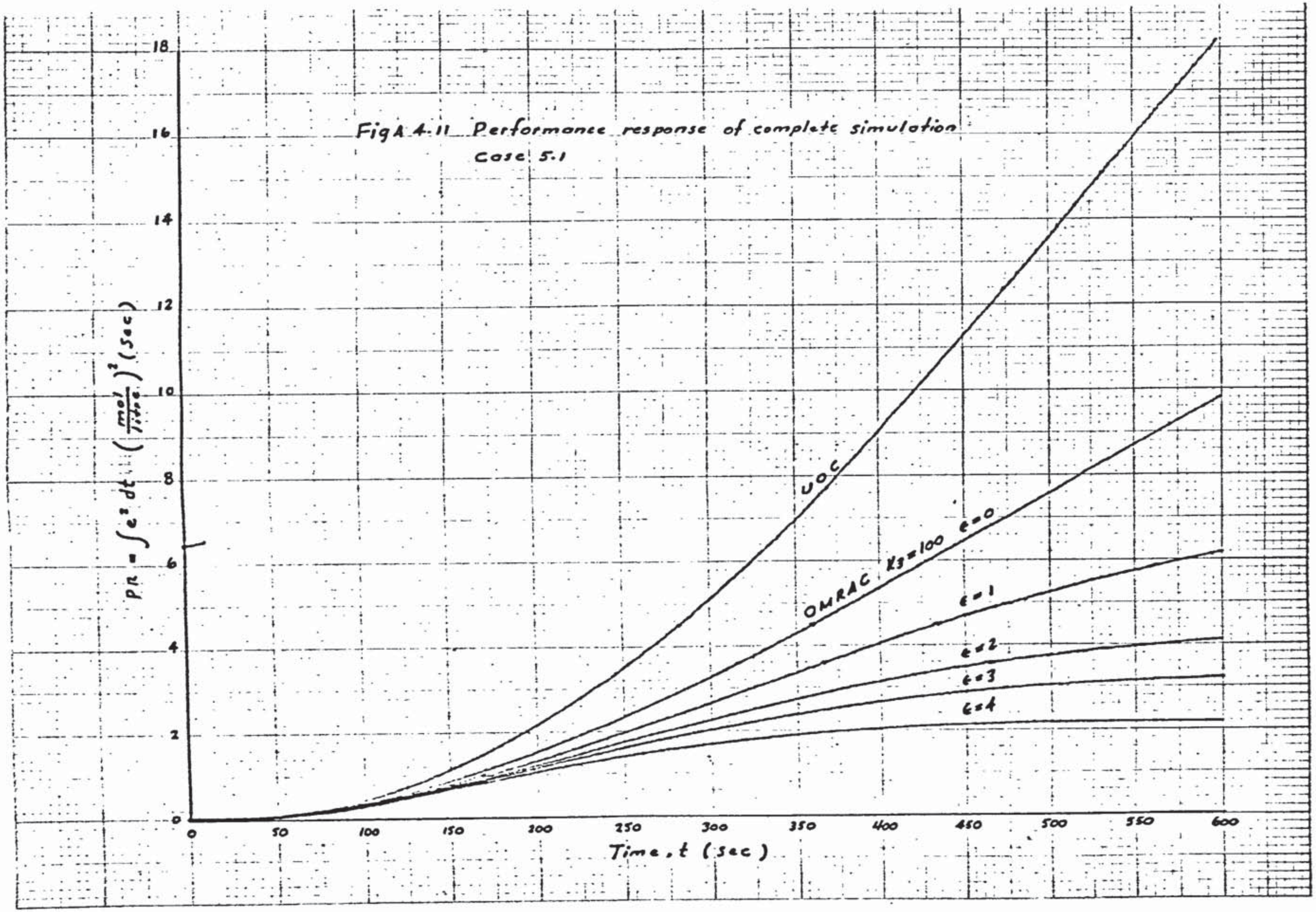

Fig A 4.11 Performance response of complete simulation
Case 5.1

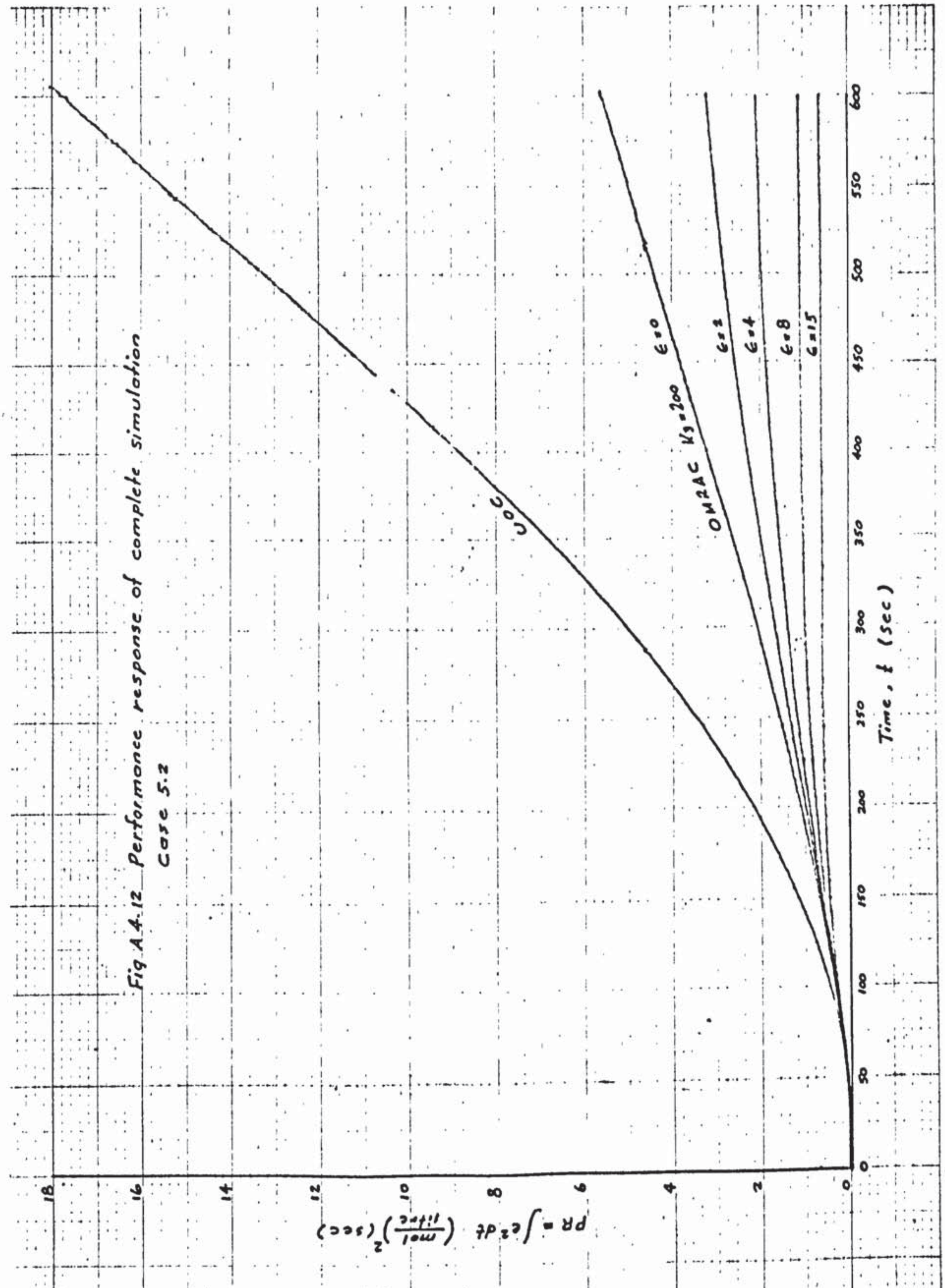

Fig A.4.12 Performance response of complete simulation
Case 5.2

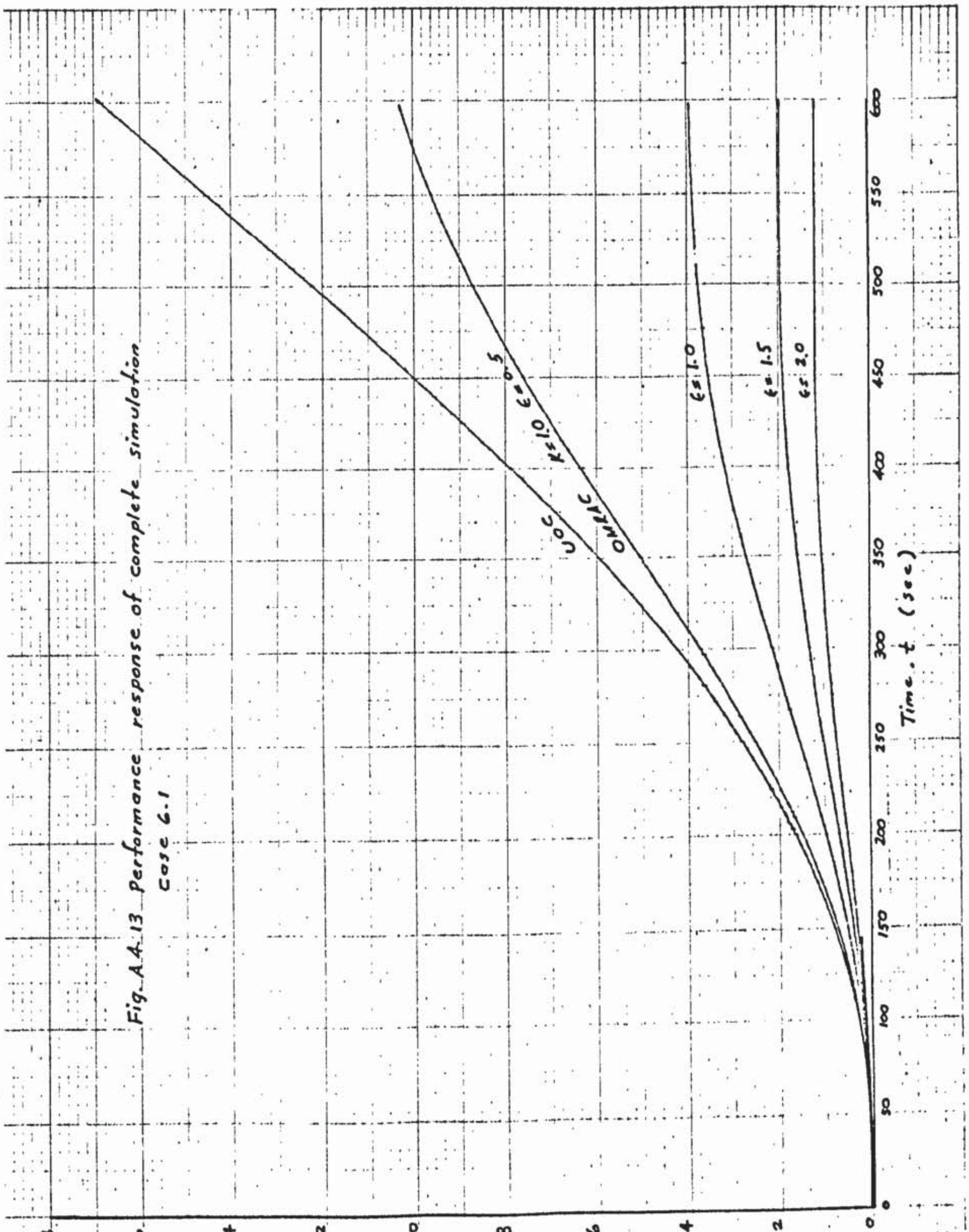

Fig. A.4.13 Performance response of complete simulation
Case 6.1

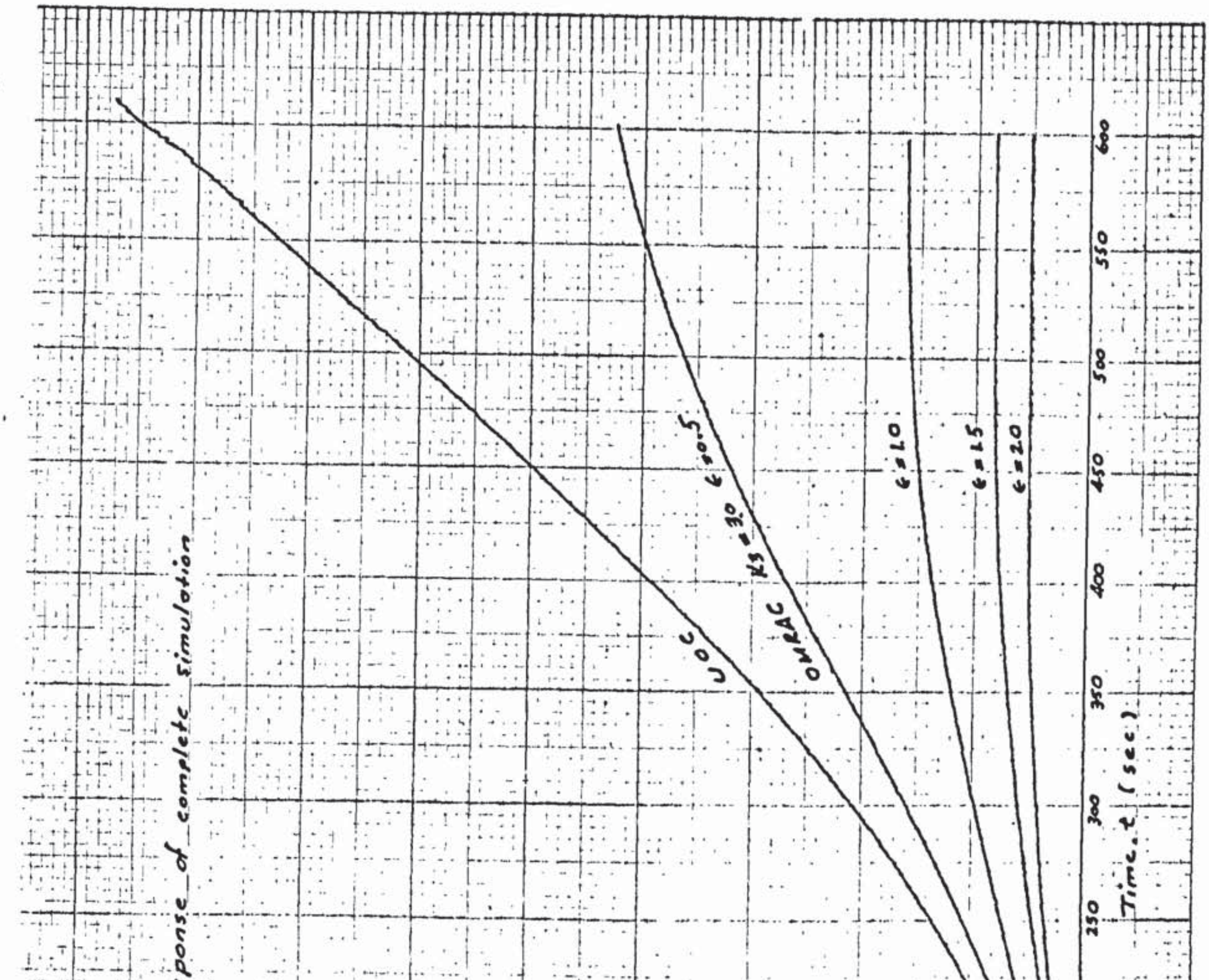

Fig. A.4.14 Performance response of complete simulation
Case 6.2

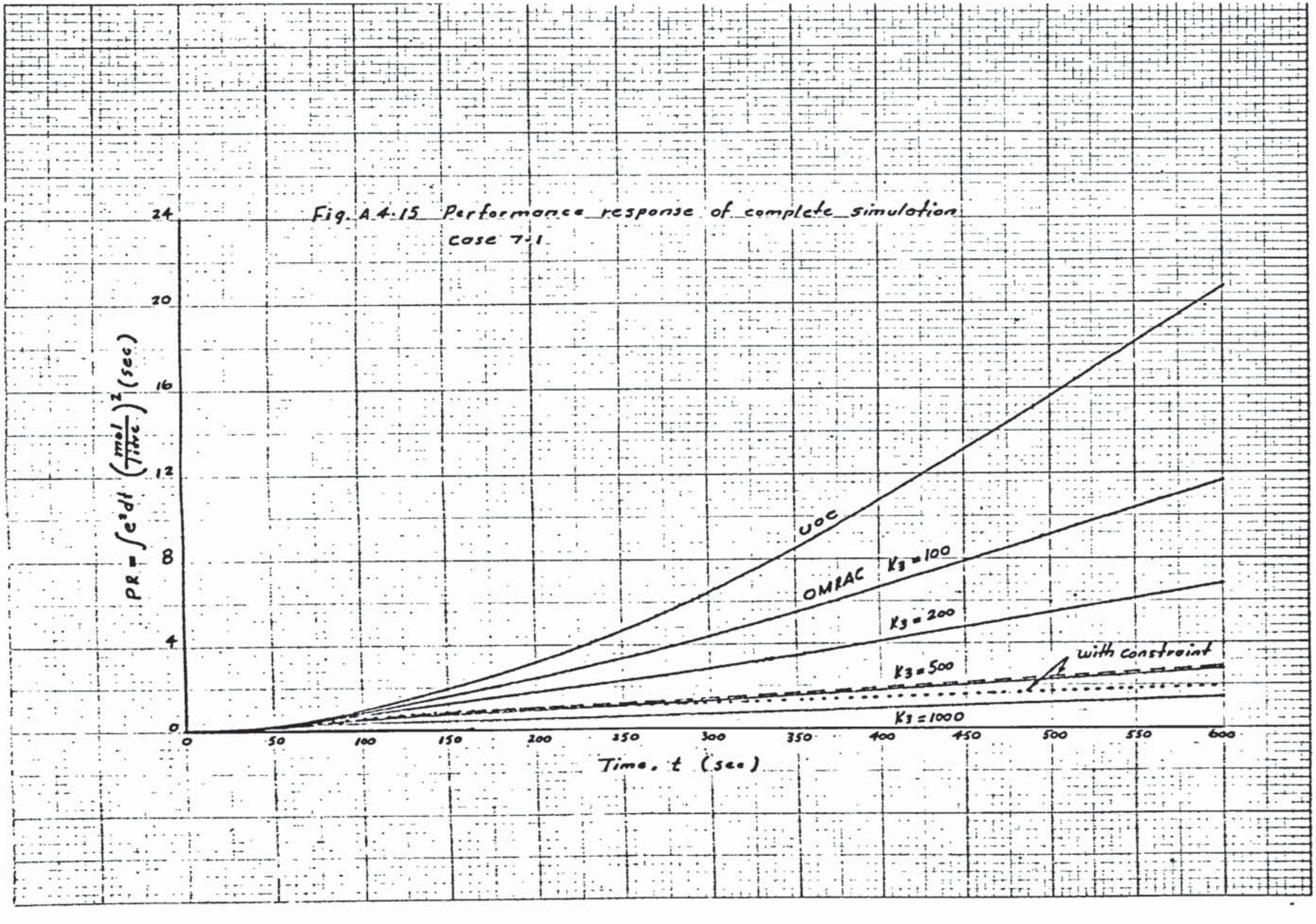

Fig. A.4.15 Performance response of complete simulation case 7.1

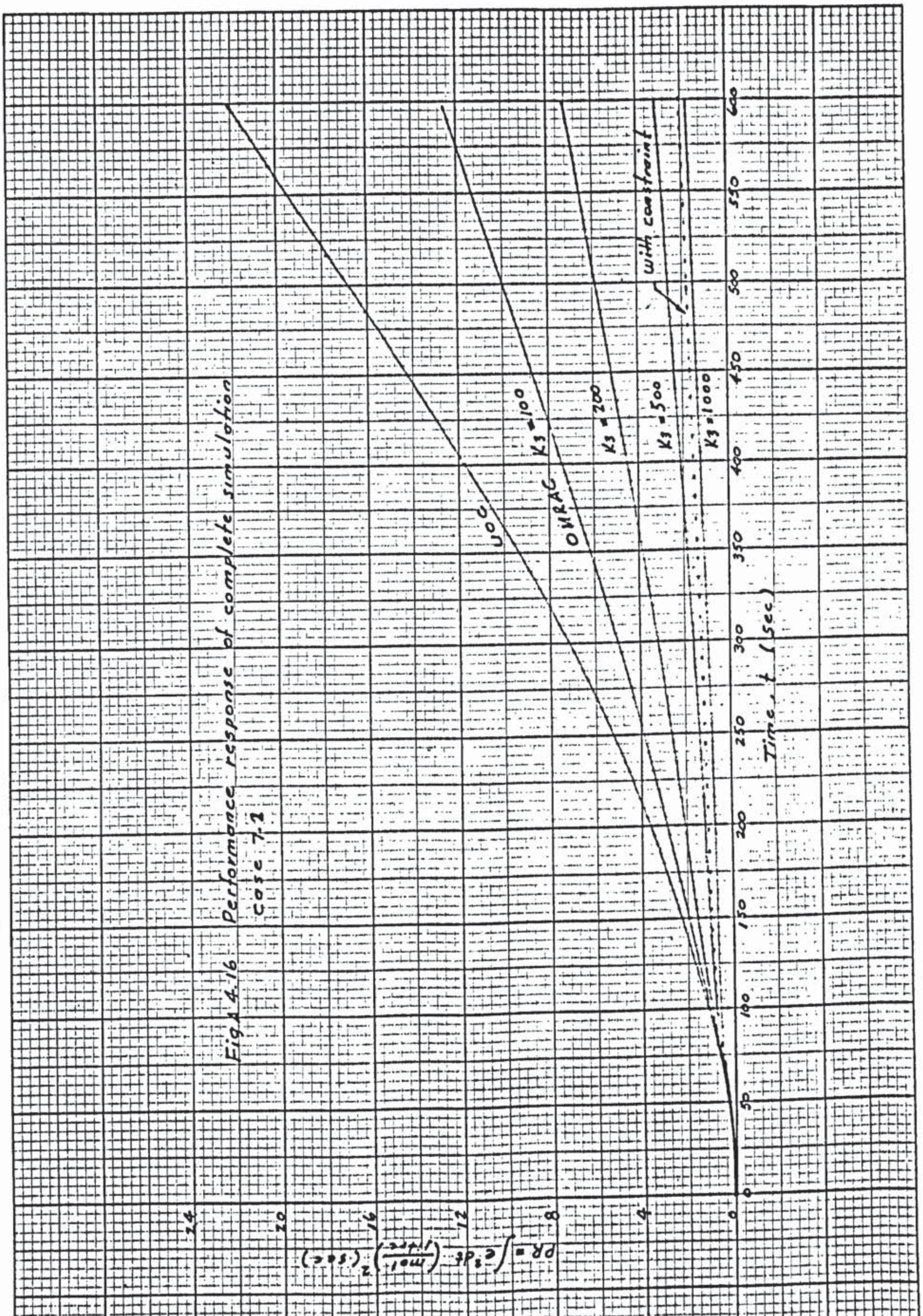

Fig 4.16 Performance response of complete simulation case 7.2

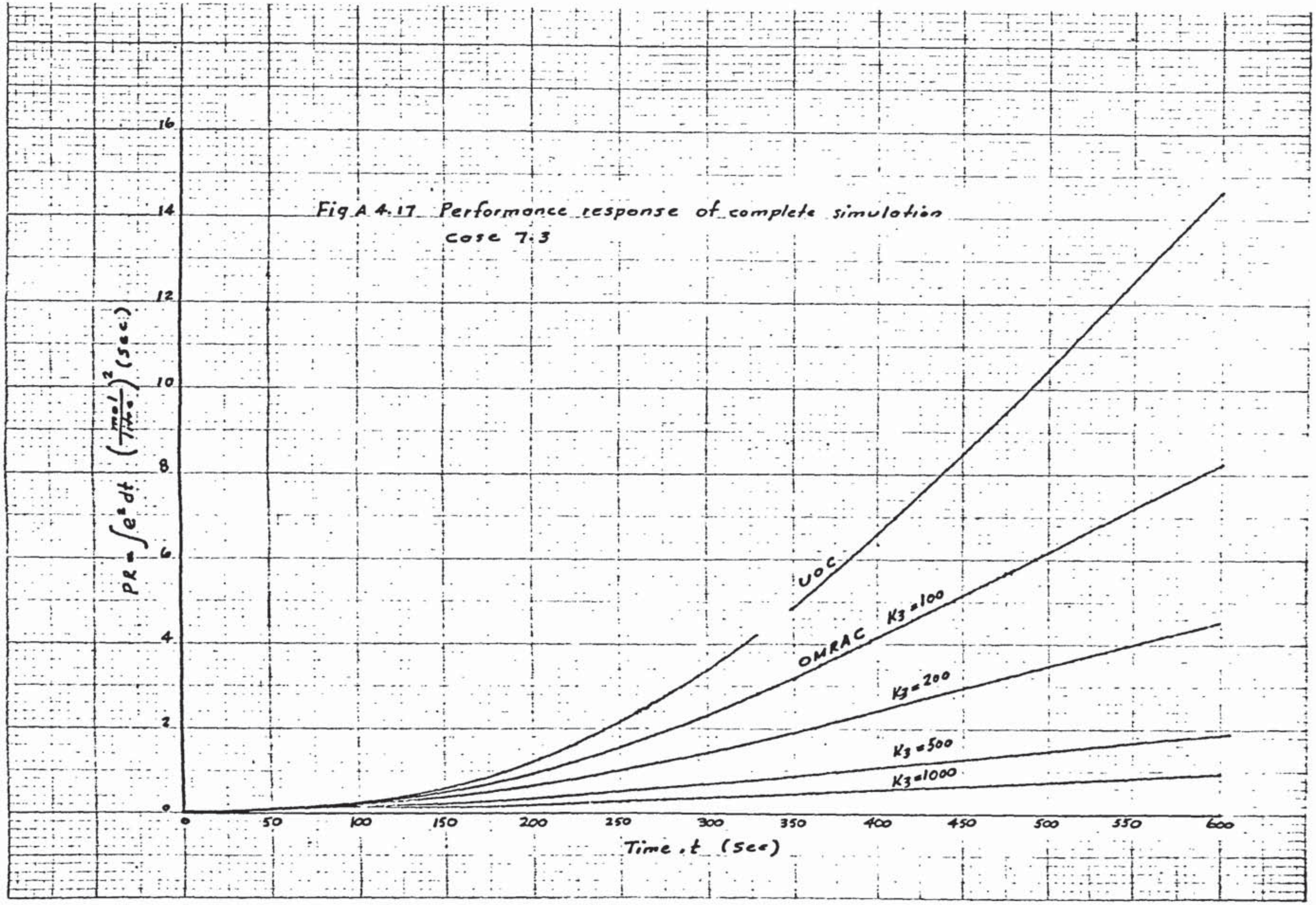

Fig A 4.17 Performance response of complete simulation
case 7.3

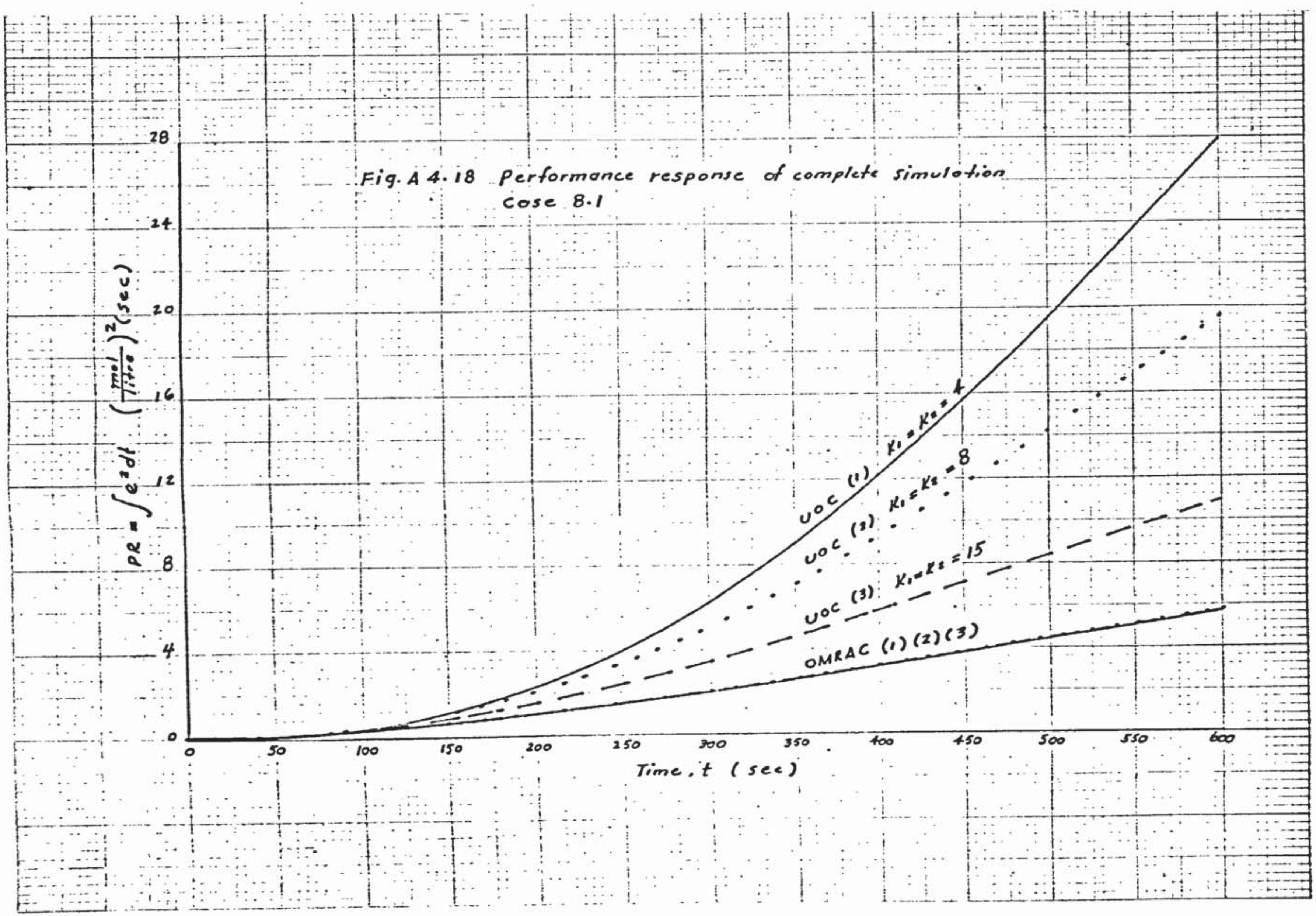
Fig. A 4.18 Performance response of complete simulation
Case B.1
PR = ∫e²dt (mol/litre)² (sec)
Time, t (sec)
0
50
100
150
200
250
300
350
400
450
500
550
600
4
8
12
16
20
24
28
UOC (1) K1 = K2 = 4
UOC (2) K1 = K2 = 8
UOC (3) K1 = K2 = 15
OMRAC (1)(2)(3)

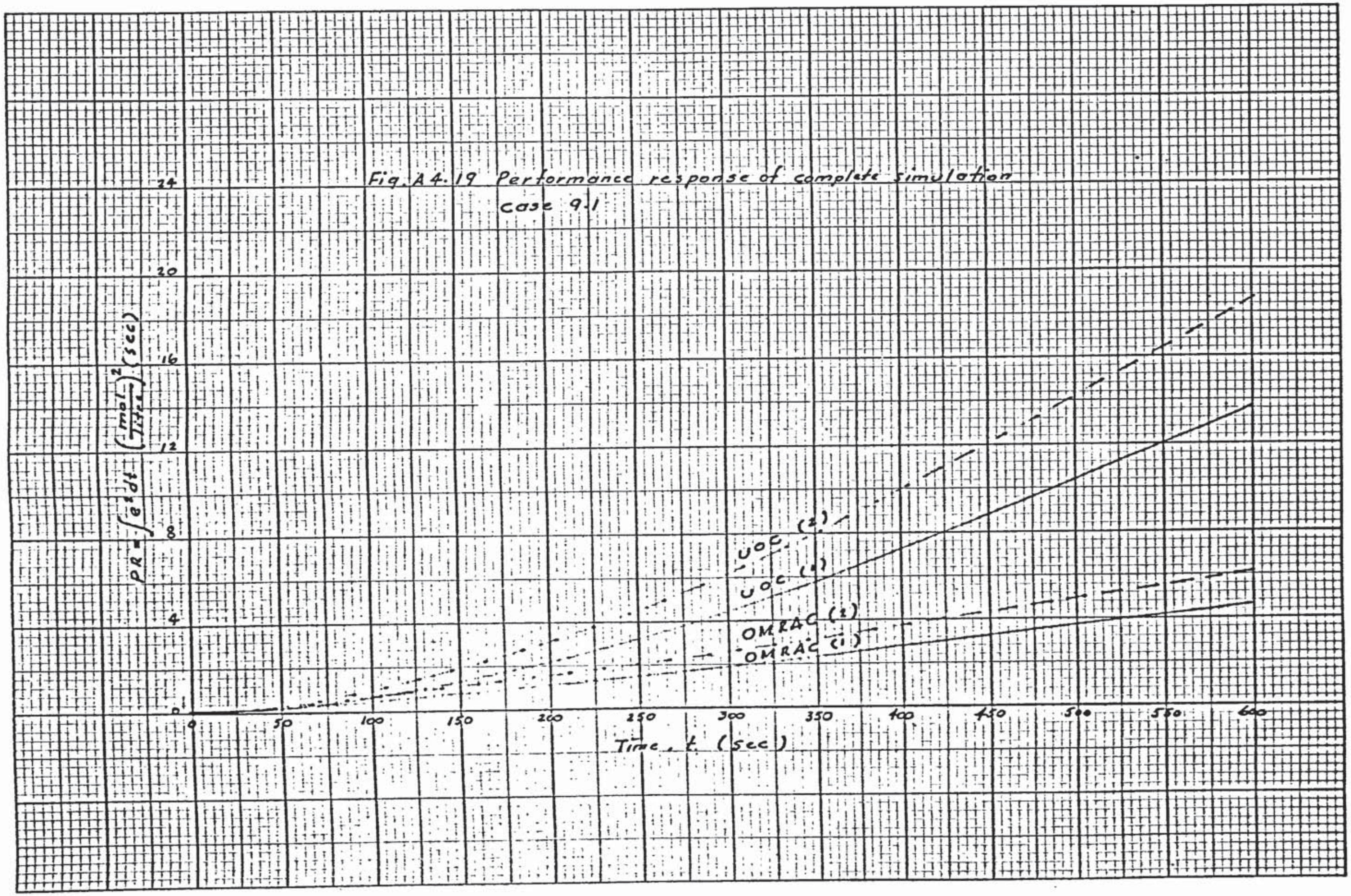

Fig. A4.19 Performance response of complete simulation
case 9.1

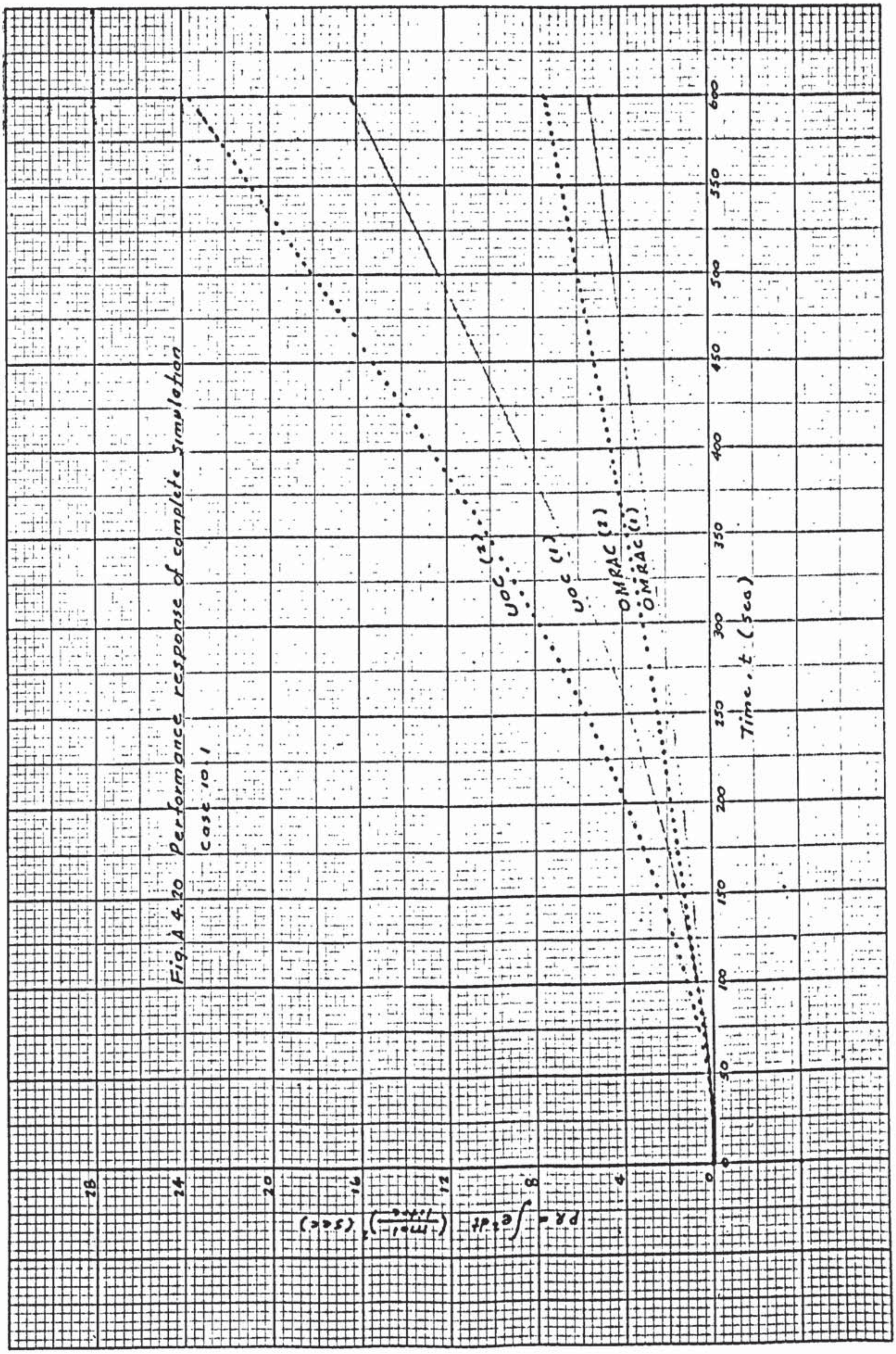

Fig. A 4.20 Performance response of complete simulation

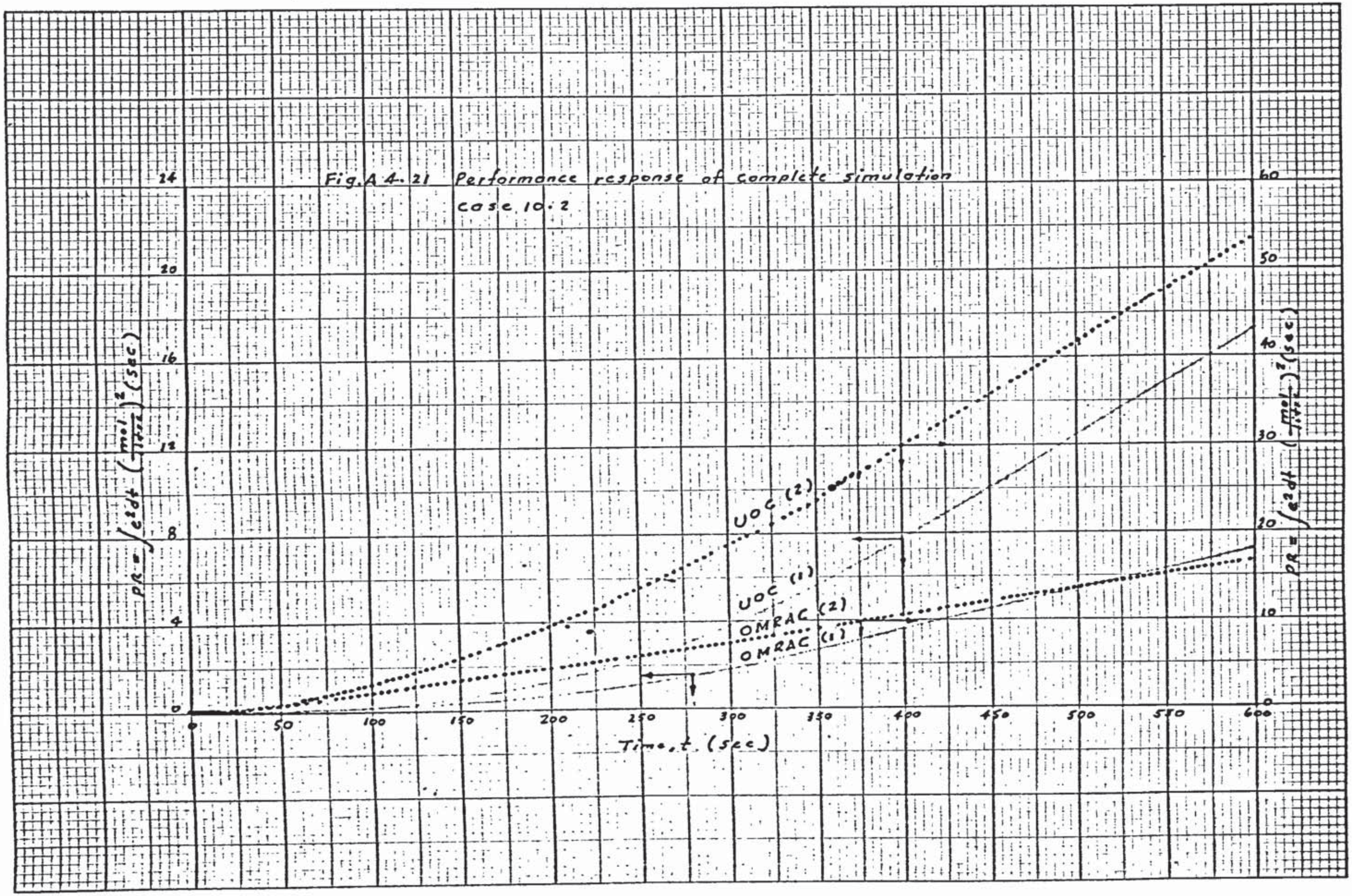

Fig. A 4.21 Performance response of complete simulation case 10.2

A P P E N D I X   5

CALIBRATION OF MONITORING EQUIPMENT AND INSTRUMENTS

Tables and corresponding Figures of calibration data:

Tables A.5.1 to A.5.16

Figures A.5.1 to A.5.19

Table A.5.1. Calibration of feed flowrate (F) rotameter

Tube size : 14s

Temperature 17°C

(see Figure A.5.1.)

Rotameter tube reading (cm)	Average flowrate litre/min
0	0.39
1	0.53
2	0.68
3	0.82
4	0.96
5	1.12
10	1.92
15	2.75
20	3.71
25	4.70

Table A.5.2. Calibration of cooling water rotameter.

Tube size : 17s

Temperature 17°C

(see Figure A.5.2)

Rotameter tube reading (cm)	Average flowrate litre/min
- 3	0.15
- 2	0.45
0	1.00
1	1.29
2	1.55
3	1.83
4	2.13
5	2.45
10	4.08
15	5.81
20	7.71
23	8.91

Table A.5.3. Calibration of flowmeter transmitter

(see Fig.A.5.3)

Feed flowrate litre/min	Theoretical $\left[\frac{F}{F_m}\right]$ volt	Experimental $\left[\frac{F}{F_m}\right]$ volt
0	0	0.0
1	2	2.20
2	4	4.10
3	6	6.00
4	8	7.90
5	10	9.75

Table A.5.4. Calibration of thermocouples

1. Feed Temperature, T_o to TR
2. Cooling water inlet temperature, T_{c1} to TR
3. Cooling water outlet temperature, T_c to TR
4. Reactor temperature, T to TRC used as TR

(see Fig. A.5.4.)

Test temperature ^oC	Thermocouples (mv) 1	2	3	4
0	0.0	0.0	0.0	0.0
25	1.0	1.0	1.0	1.0
100	4.1	4.1	4.1	4.1

Table A.5.5. Calibration of temperature transmitters

1. Reactor temperature transmitter, $\left[\frac{T}{T_m} \right]$
2. Cooling water outlet temperature transmitter, $\left[\frac{T_c}{T_m} \right]$

(see Fig. A.5.5)

Test temperature ^oC	Thermocouples (mv) 1	Thermocouples (mv) 2	$\left[\frac{T}{T_m} \right]$ volt.	$\left[\frac{T_c}{T_m} \right]$ volt.
0	0.0	0.0	0.0	0.0
25	1.0	1.0	2.5	2.5
100	4.1	4.1	10.0	10.0

Table A.5.6. Calibration of voltage to current (V/I) converter (Lec Dickens Model C5740)

(see Fig.A.5.6.)

Voltage (input) (volt)	Current (output) (ma)
0	4.0
1	5.45
2	7.05
3	8.90
4	10.50
5	12.10
6	13.80
7	15.50
8	17.00
9	18.50
10	20.00

Table A.5.7. Calibration of current to pneumatic pressure (I/P) transducer (Honeywell Model 31201/01)

(see Fig.A.5.7.)

Current (input) (ma)	Pneumatic Pressure (output) (psig)
4.0	1
5.4	2
6.7	3
8.0	4
9.3	5
10.7	6
12.0	7
13.3	8
14.6	9
16.0	10
17.3	11
18.7	12
20.0	13

Table A.5.8. Calibration of combined V/I converter and I/P transducer

(see Fig.A.5.8.)

voltage (input) (volt)	Pneumatic Pressure (output) (psig)
0	1.00
1	2.25
2	3.48
3	4.60
4	5.85
5	7.10
6	8.30
7	9.50
8	10.70
9	11.85
10	12.80

Table A.5.9. Calibration of control value flowrate vs. pneumatic pressure (without positioner) (see Fig.A.5.9).

	Pneumatic pressure increasing		Pneumatic pressure decreasing	
Pneumatic Pressure (psig)	Flowrat or reading (cm)	Flowrate (litre/min)	Flowrat or reading (cm)	Flowrate (litre/min)
0	23.8	9.30	23.8	9.30
1.0	23.8	9.30	23.6	9.20
2.0	23.8	9.30	22.0	8.50
3.0	23.6	9.20	17.9	6.90
4.0	19.1	7.30	13.3	5.20
5.0	14.5	5.60	9.6	4.05
6.0	10.6	4.25	6.5	2.90
7.0	7.5	3.22	4.0	2.12
8.0	4.8	2.30	1.6	1.40
9.0	2.7	1.70	0.0	1.00
10.0	0.9	1.22	-1.2	0.60
11.0	-0.6	1.00	-2.8	0.20
12.0	-1.9	0.45	-3.0	0.15
13.0	-3.0	0.15	-3.0	0.15

Table A.5.10. Calibration of control valve positioner

(Fig.A.5.10.)

	Pneumatic pressure increasing	Pneumatic pressure decreasing
Pneumatic pressure to positioner (psig)	Positioner output to control value (psig)	Positioner output to control valve (psig)
1.0	0	0
1.5	3.00	2.00
2.0	3.55	3.00
3.0	4.10	3.65
4.0	4.75	4.20
5.0	6.00	5.25
6.0	7.00	6.20
7.0	8.10	7.20
8.0	9.25	8.20
9.0	10.20	9.40
10.0	11.80	10.40
11.0	13.20	12.00
11.5	18.00	18.00

Table A.5.11. Calibration of control valve flowrate vs. pneumatic pressure (with positioner) (Fig.A.5.11)

	Pneumatic pressure increasing		Pneumatic pressure decreasing	
Pneumatic pressure on control valve (psig)	Flowrator reading (cm)	Flowrate (litre/min)	Flowrator reading (cm)	Flowrate (litre/min)
1.0	23.9	9.30	23.8	9.30
1.5	23.0	8.95	22.8	8.85
2.0	21.7	8.40	21.5	8.35
3.0	17.5	6.70	17.3	6.65
4.0	13.6	5.30	13.4	5.25
5.0	10.4	4.20	10.3	4.20
6.0	7.5	3.28	7.4	3.26
7.0	5.3	2.55	5.1	2.50
8.0	3.5	2.00	2.7	1.75
9.0	1.0	1.30	0.7	1.20
10.0	-0.6	0.85	-0.6	0.80
11.0	-2.5	0.30	-2.5	0.30
11.5	-4.0	0	-4.0	0

Table A.5.12. Calibration of V/I converter input from TR-48, $\left[\frac{F_{cg}}{F_{cm}}\right]$ (volt), vs. control valve flowrate, F_c (litre/min) (with positioner)

(Fig. A.5.12)

	voltage increasing		voltage decreasing	
$\left[\frac{F_{cg}}{F_{cm}}\right]$ (volt)	Rotameter reading (cm)	Flowrate F_c (litre/min)	Rotameter reading (cm)	Flowrate F_c (litre/min)
0	23.83	9.30	23.83	9.30
1.0	20.87	8.05	20.63	8.00
2.0	15.63	6.02	15.37	5.95
3.0	11.23	4.57	11.00	4.50
4.0	7.77	3.32	7.60	3.30
5.0	4.87	2.30	4.70	2.22
6.0	2.10	1.55	1.87	1.50
7.0	0.00	1.00	0.17	0.95
8.0	-2.00	0.45	-2.17	0.40
9.0	-4.00	0.0	-4.00	0.0
10.0	-4.00	0.0	-4.00	0.0

Table A.5.13. Calibration of overall F_c interface system between $\left[\frac{F_c}{F_{cm}}\right]$ (volt) from hybrid computer and F_c (litre/min) from control valve (with positioner) (Fig.A.5.14)

$\left[\frac{F_c}{F_{cm}}\right]$ before VDFG (volt)	$\left[\frac{F_{cg}}{F_{cm}}\right]$ after VDFG (volt)	Theoretical $\left[\frac{F_{cg}}{F_{cm}}\right]$ value (volt)	Rotameter reading (cm)	Control valve flowrate (litre/min)
0	8.884	9.00	-4.0	0
1.0	6.782	6.90	0.01	1.01
2.0	5.304	5.41	3.60	2.02
3.0	4.192	4.30	6.80	3.02
4.0	3.290	3.38	9.80	4.04
5.0	2.554	2.62	12.60	4.98
6.0	1.970	2.03	15.20	5.95
7.0	1.544	1.58	17.60	6.95
8.0	1.012	1.01	20.40	7.90
9.0	0.264	0.25	23.20	9.00
9.3	0.050	0.0	23.90	9.30

Table A.5.14. Calibration of computer output $\left[\frac{Q_{gg}}{Q_{gm}}\right]$ vs. variac position (Fig.A.5.15).

Variac position VR	$\left[\frac{Q_{gg}}{Q_{gm}}\right]$ volt	$\left[\frac{Q_{gg}}{Q_{gm}}\right]$ volt
10	0.80	0.064
20	1.60	0.276
30	2.46	0.605
40	3.26	1.063
50	4.11	1.689
60	5.05	2.550
70	6.13	3.756
80	7.44	5.535
85	8.23	6.773

Table A.5.15. Calibration of variac position vs heat output from immersion heater, Q_g (Fig.A.5.16)

$Q_g = 0.06\ F \Delta T\ (Kcal \times 10^3/h)$ (equation (8-2))

Feed flow-rate (litre/min)	Variac position (VR)	ΔT (^oC)	Q_g $\frac{Kcal x 10^3}{h}$	T ^oC	Q_g $\frac{Kcal x 10^3}{h}$	$(Q_g)_{av}$ $\frac{Kcal x 10^3}{h}$
3	10	0.30	0.054	0.50	0.09	0.072
3	20	1.90	0.342	2.30	0.414	0.378
3	30	4.90	0.828	5.10	0.918	0.873
3	40	8.50	1.530	9.15	1.647	1.588
3	50	13.50	2.430	14.05	2.529	2.479
3	60	19.90	3.582	20.0	3.600	3.591
5	7C	16.40	4.920	16.70	5.010	4.965
5	80	21.30	6.390	21.85	6.555	6.472
5	85	24.50	7.350	24.50	7.350	7.350

Note:

1. From columns 2 and 3 in Table A.5.14 and columns 4 and 6 in Table A.5.15 to plot Figure A.5.17.
2. From column 2 in Table A.5.14 and column 7 in Table A.5.15 to plot Figure A.5.18.

Table A.5.16. Calibration of overall heat generation, Q_g interface system between $\left[\frac{Q_g}{Q_{gm}}\right]$ (before DFG) Vs. Q_g (from immersion heater) (Fig.A.5.19)

$\left[\frac{Q_g}{Q_{gm}}\right]$ before DFG (volt)	$\left[\frac{Q_{gg}}{Q_{gm}}\right]$ after DFG (volt)	Variac position (VR)	T (^oC)	F $\frac{litre}{min}$	Q_g $\frac{Kcal x 10^3}{h}$
1.0	2.65	32.6	5.7	3	1.026
2.0	3.66	45.0	11.2	3	2.016
3.0	4.59	55.3	17.2	3	3.096
4.0	5.39	63.3	22.8	3	4.065
5.0	6.16	71.0	17.0	5	5.101
6.0	7.04	78.0	20.3	5	6.090
7.0	7.94	83.6	23.6	5	7.080
8.0	8.79	88.0	26.9	5	8.070
7.0	7.94	83.2	23.9	5	7.170
6.0	7.07	77.5	20.6	5	6.180
5.0	6.15	70.2	17.0	5	5.100
4.0	5.39	63.3	22.6	3	4.068
3.0	4.58	55.2	17.6	3	3.160
2.0	3.66	45.0	11.4	3	2.050
1.0	2.65	32.5	6.1	3	1.090

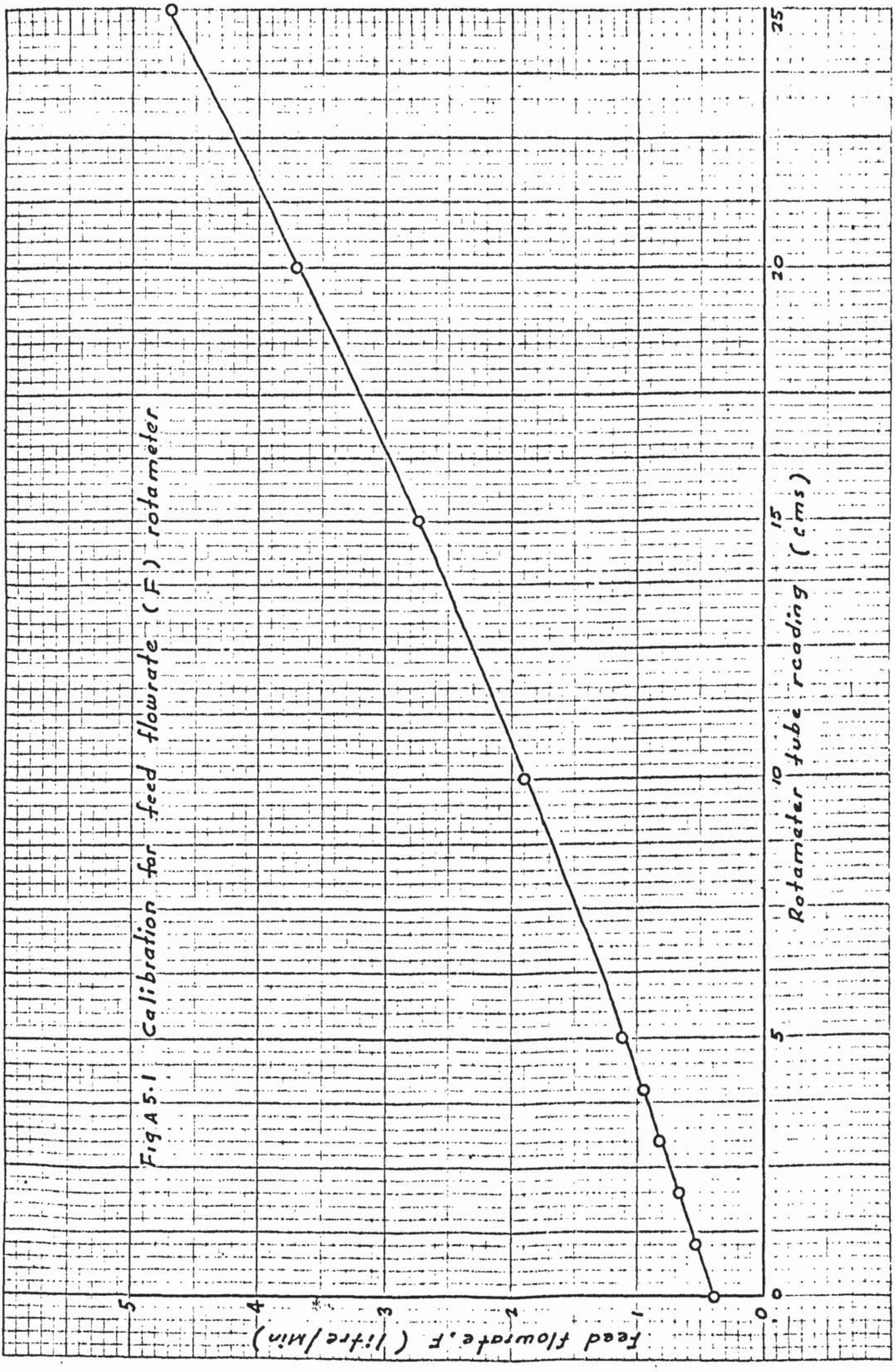

Fig.A5.1 Calibration for feed flowrate (F) rotameter
Rotameter tube reading (cms)
0
5
10
15
20
25
Feed flowrate, F (litre/min)
0
1
2
3
4
5

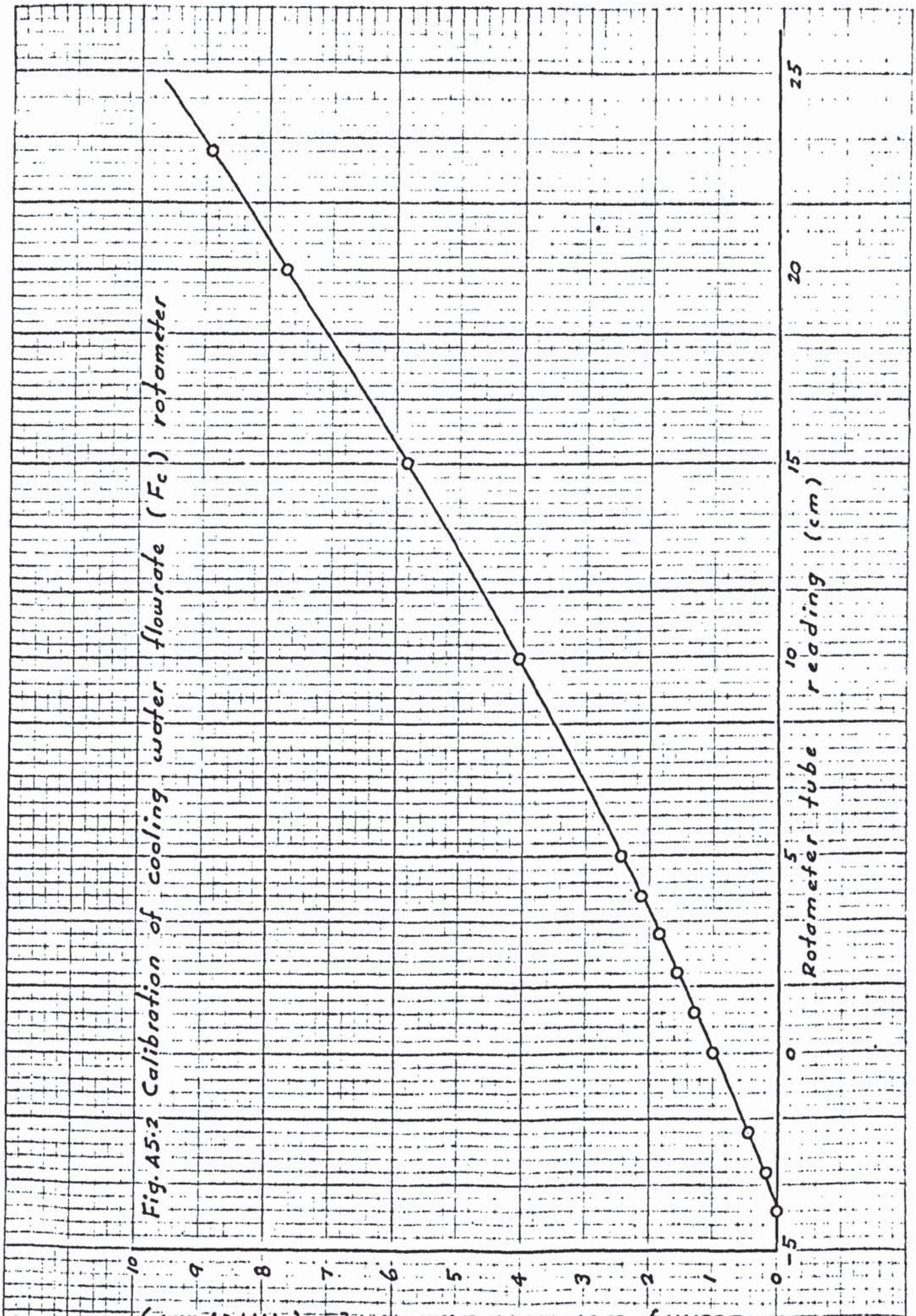

Fig. A5:2 Calibration of cooling water flowrate (F_c) rotameter

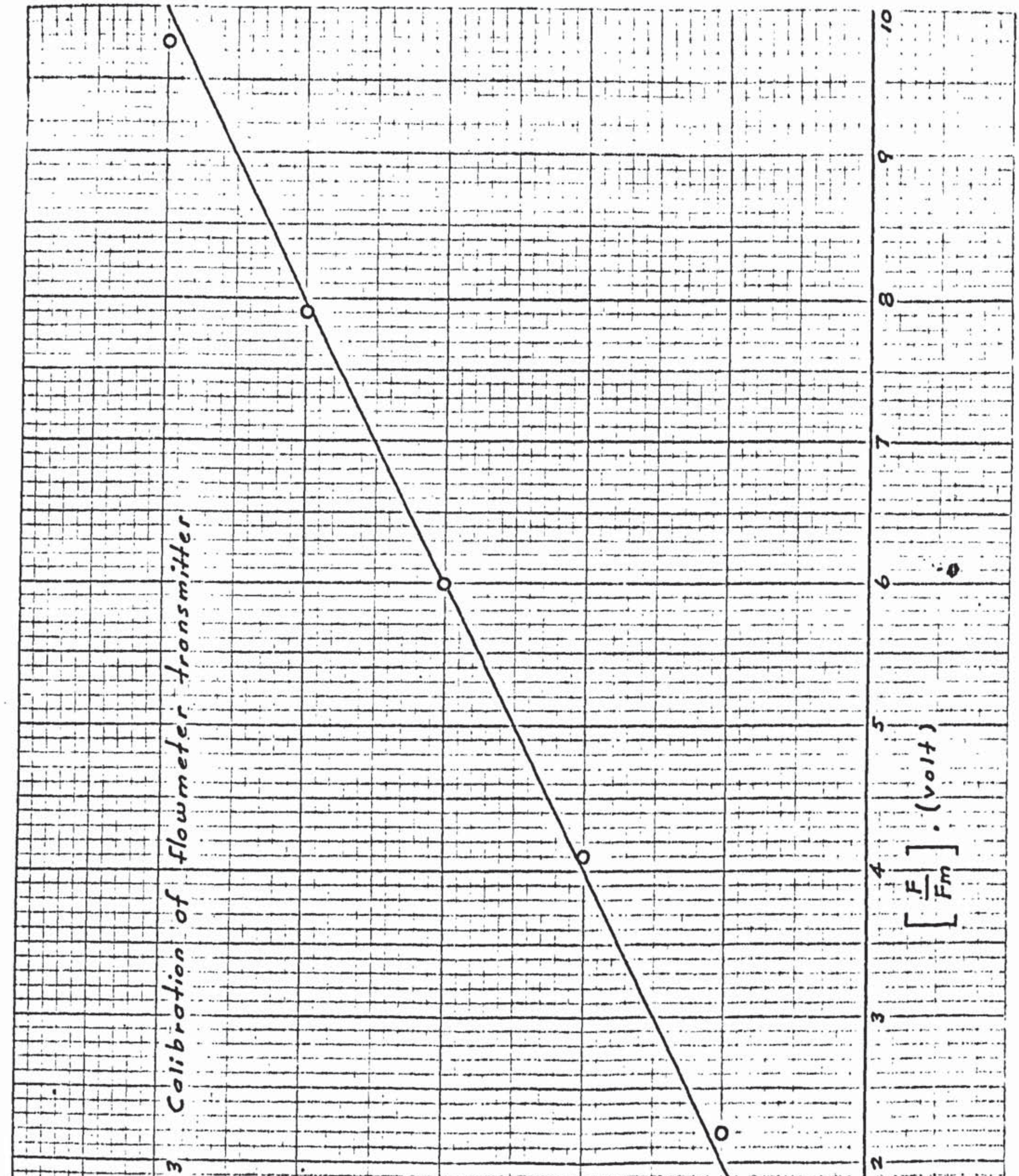

Fig. A.5.3 Calibration of flowmeter transmitter

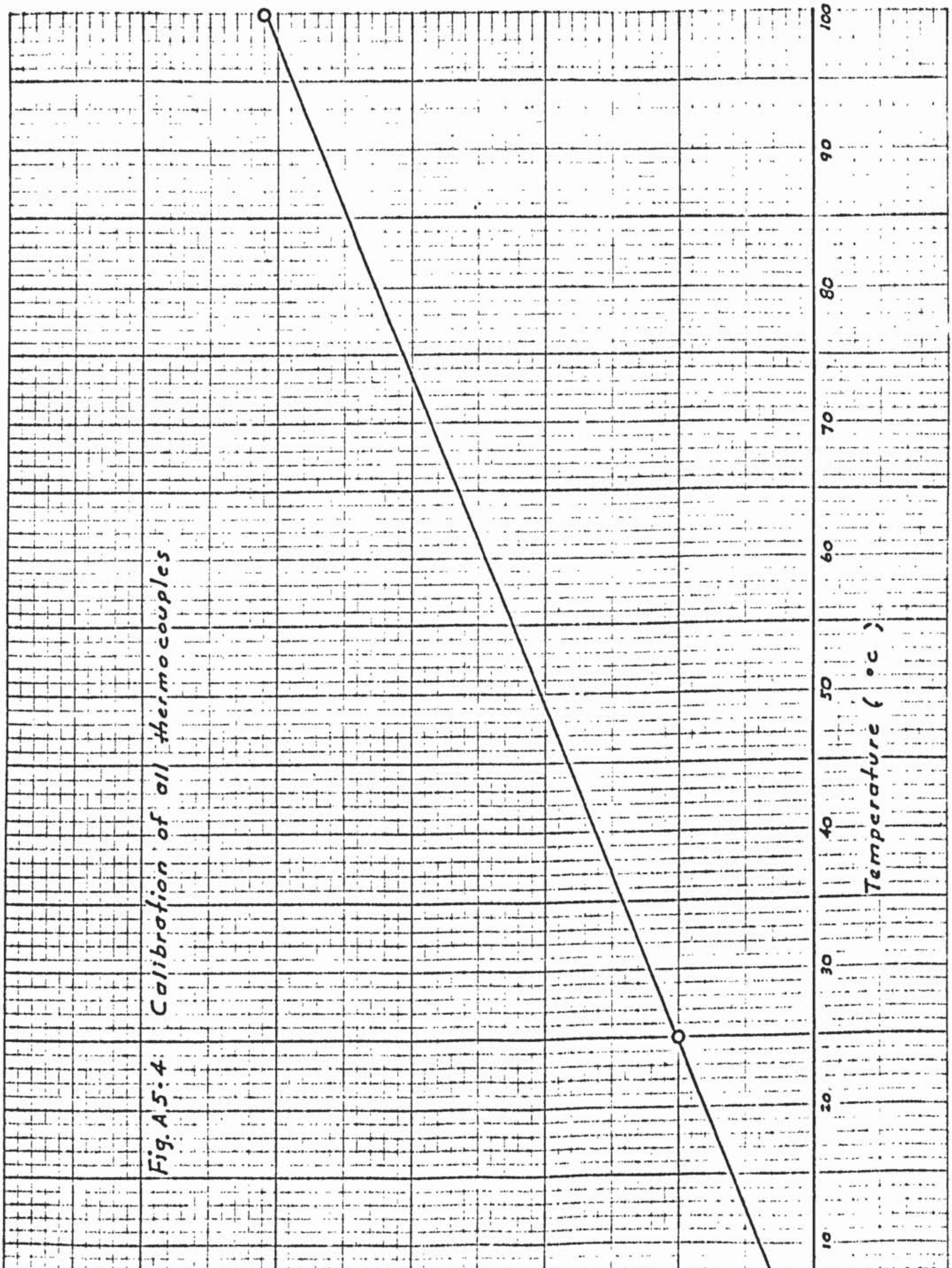

Fig. A5:4: Calibration of all thermocouples

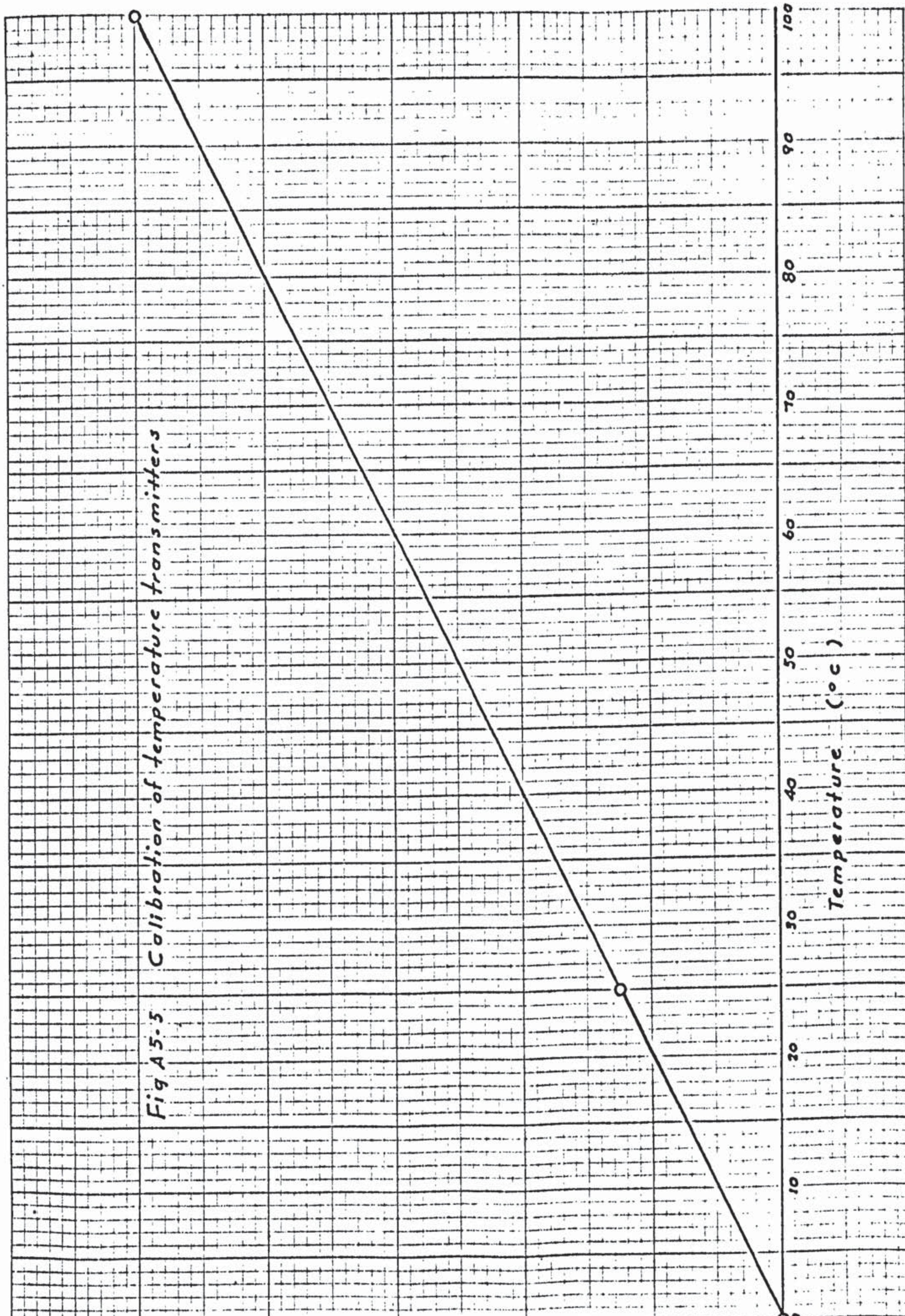

Fig A5-5 Calibration of temperature transmitters

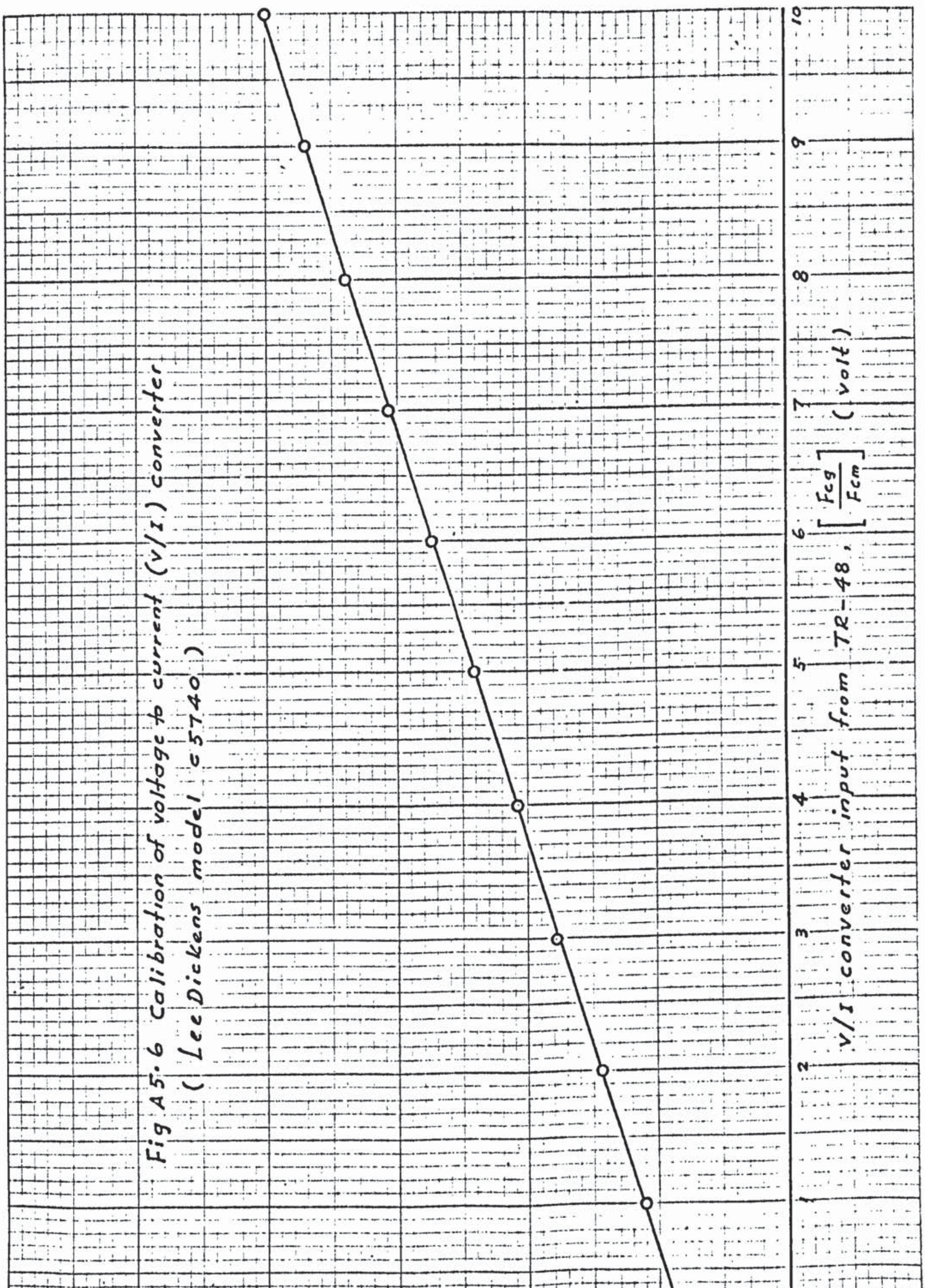

Fig A5.6 Calibration of voltage to current (V/I) converter
(Lee Dickens model C5740)

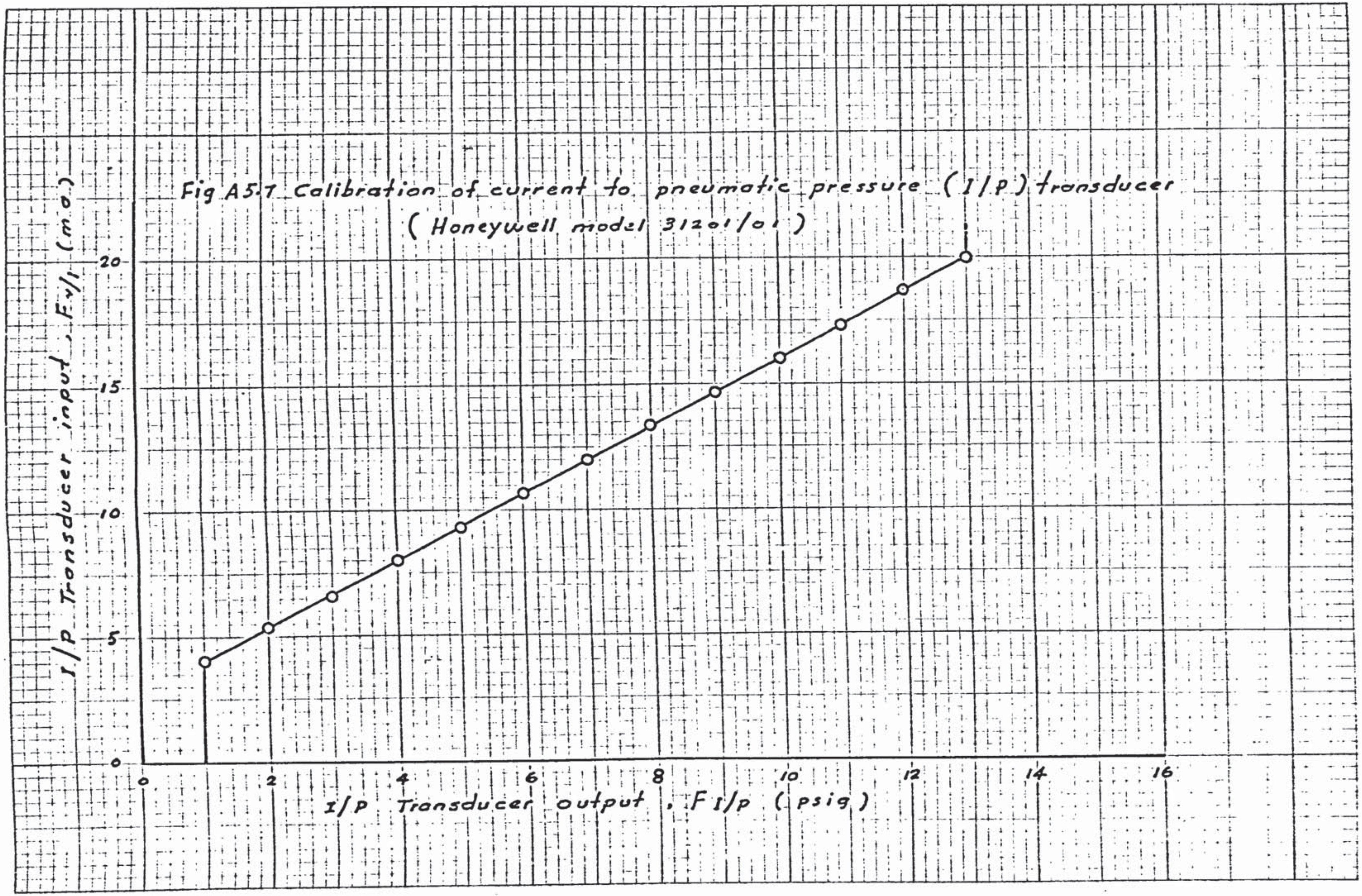

Fig A5.7 Calibration of current to pneumatic pressure (I/P) transducer
(Honeywell model 31201/01)
I/P Transducer input, $F_{v/I}$ (m a)
0
5
10
15
20
0
2
4
6
8
10
12
14
16
I/P Transducer output, $F_{I/P}$ (psig)

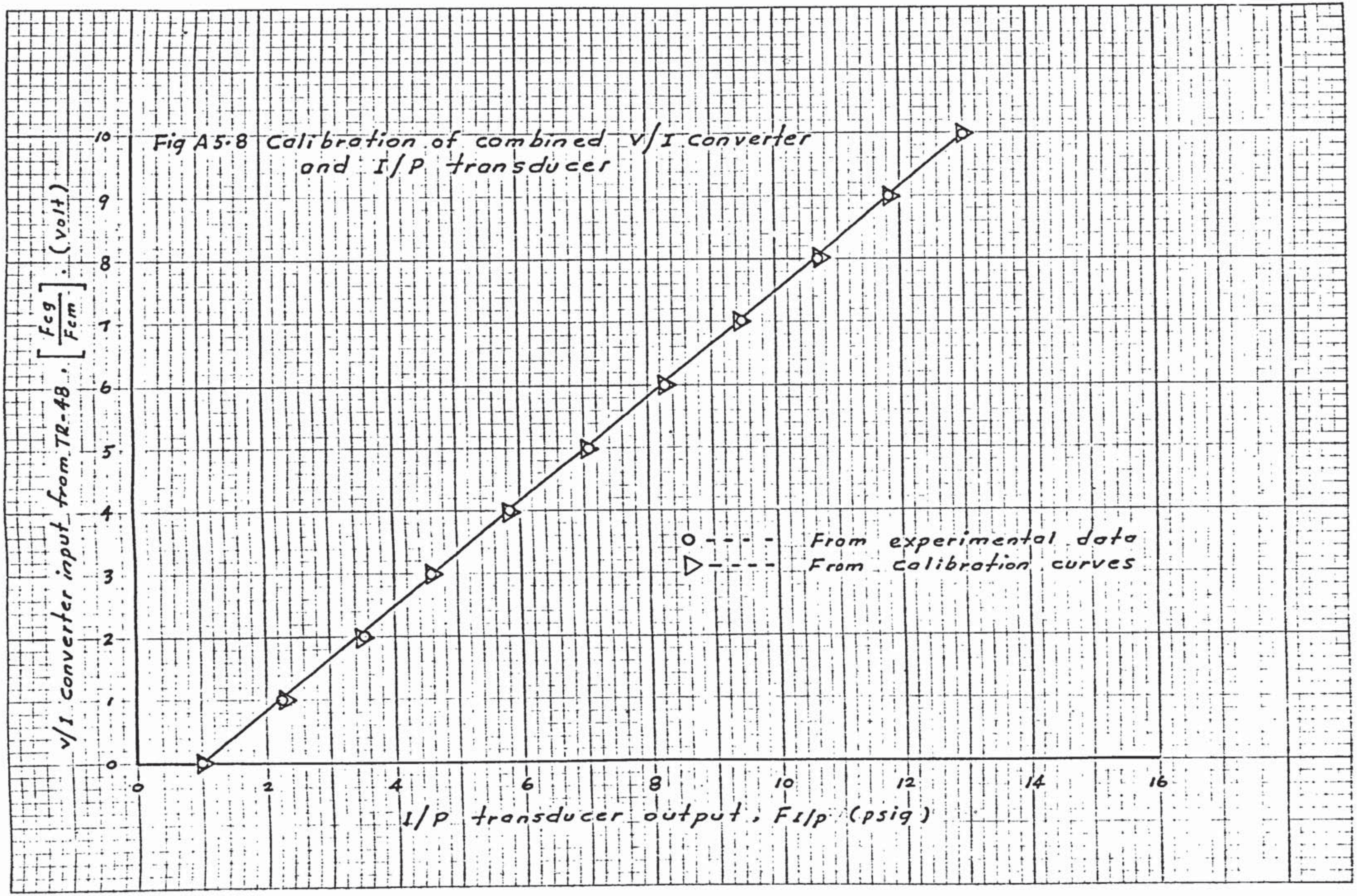

Fig A5·8 Calibration of combined V/I converter and I/P transducer

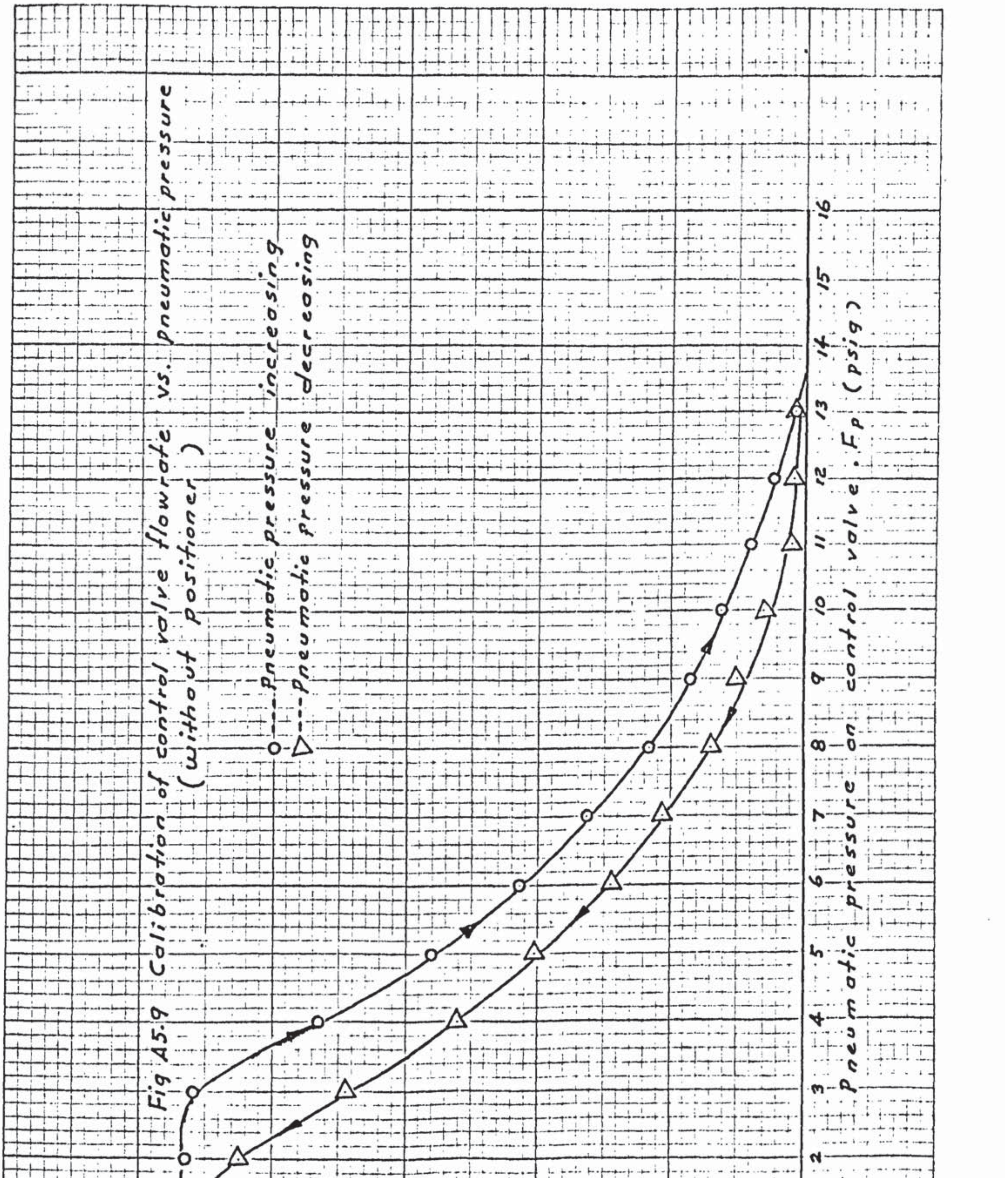

Fig A5.9 Calibration of control valve flowrate vs. pneumatic pressure (without positioner)

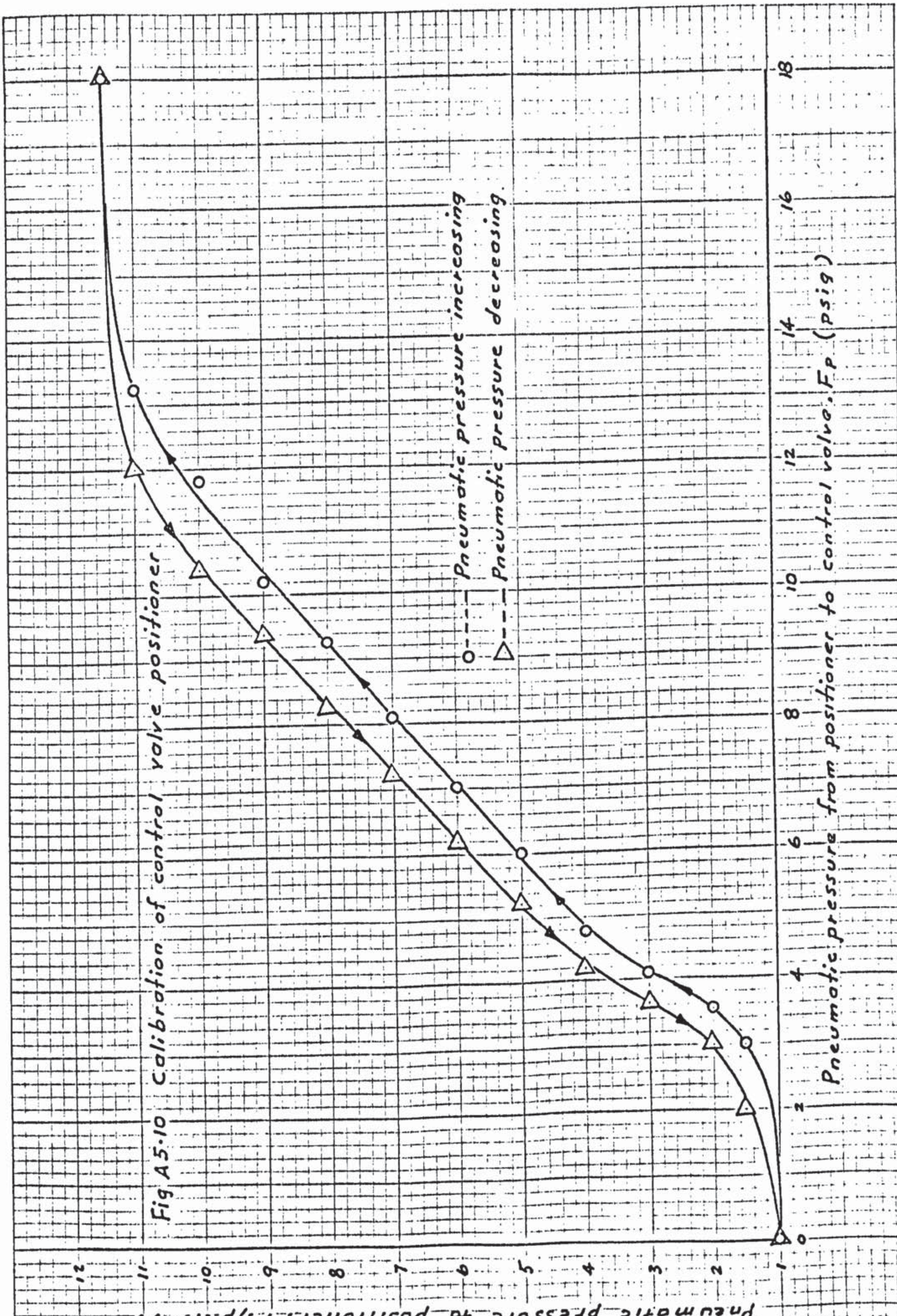

Fig A5·10 Calibration of control valve positioner

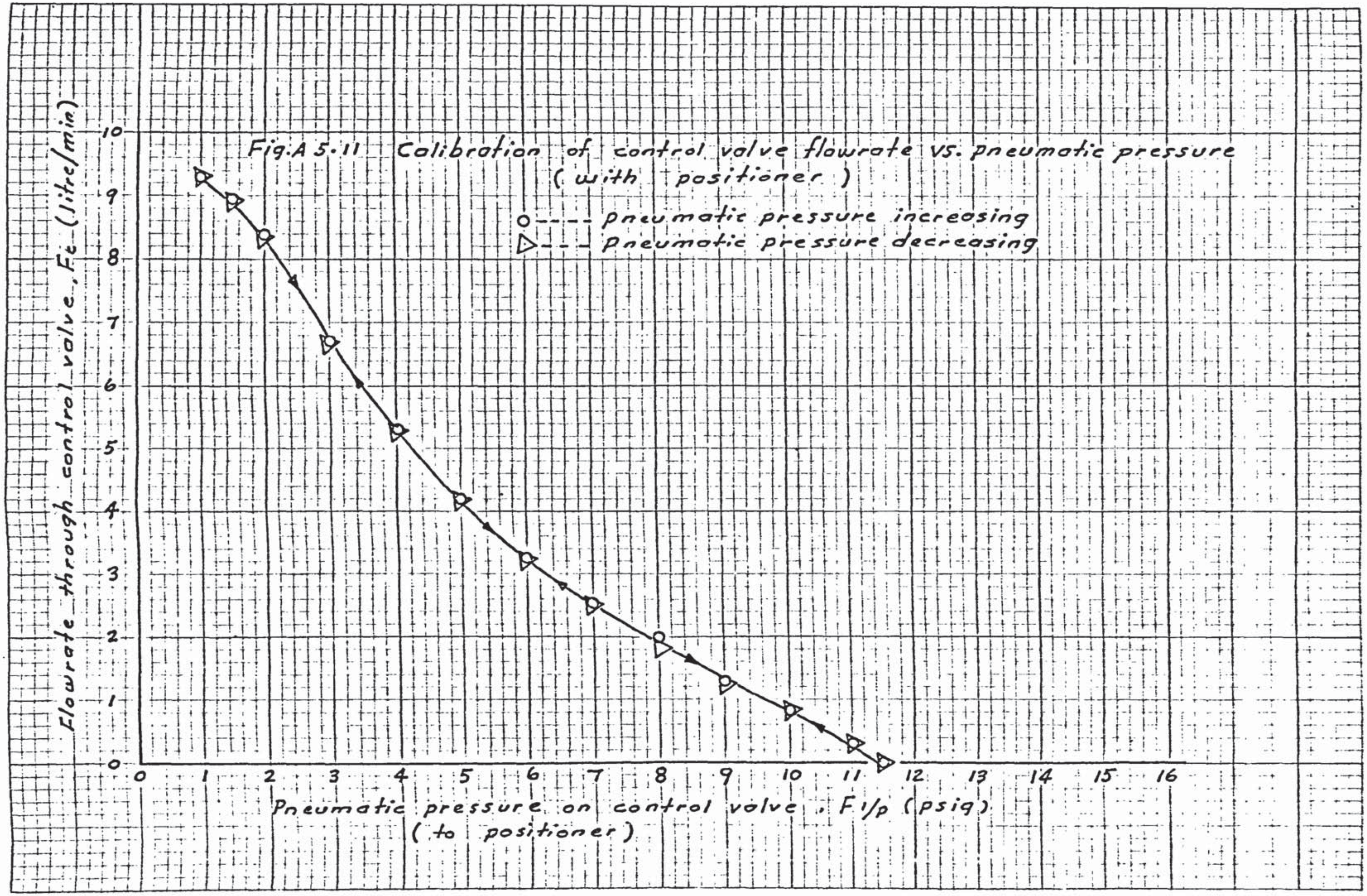

Fig.A 5.11 Calibration of control valve flowrate vs. pneumatic pressure (with positioner)

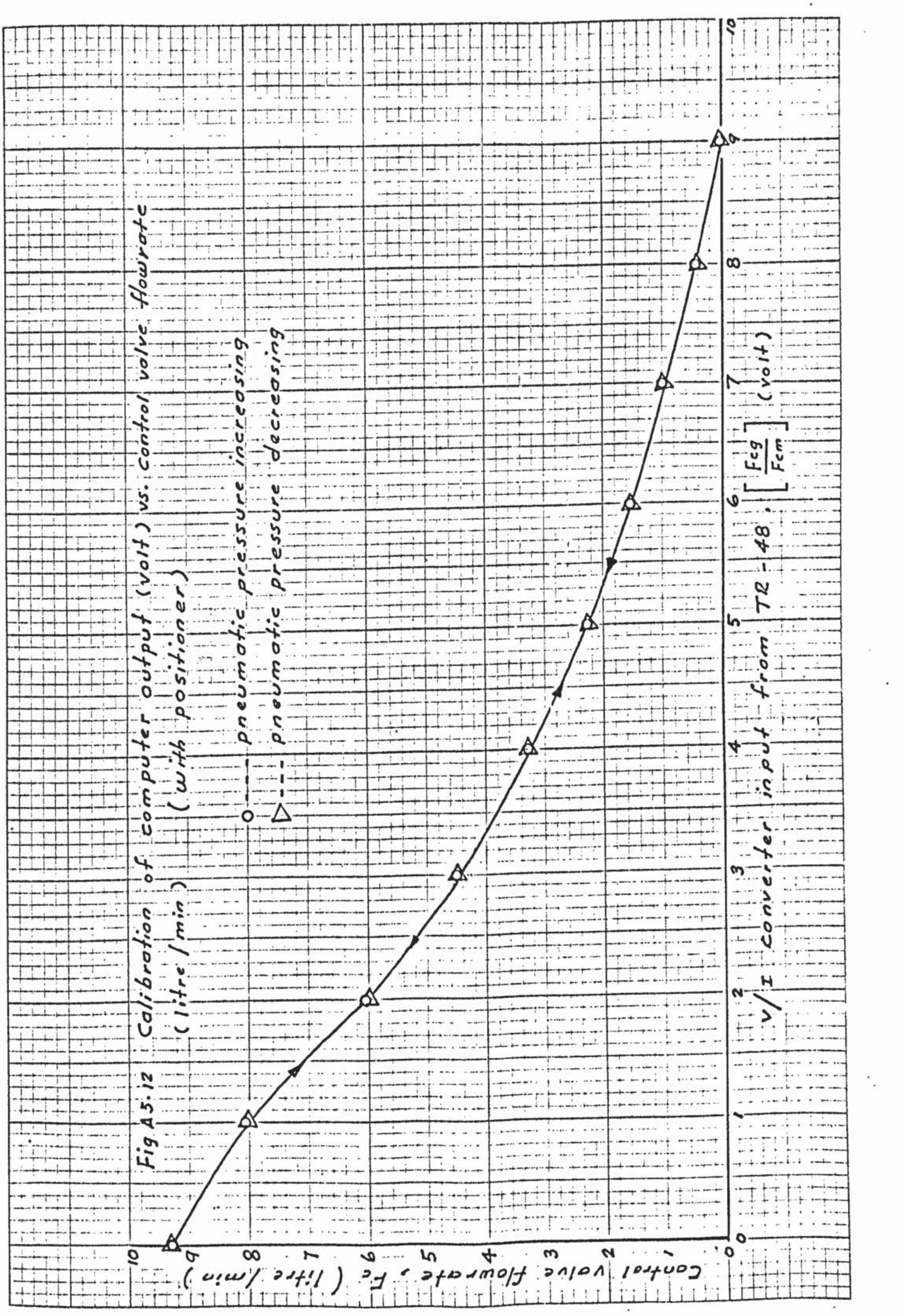

Fig A5.12 Calibration of computer output (volt) vs. control valve flowrate (litre/min) (with positioner)

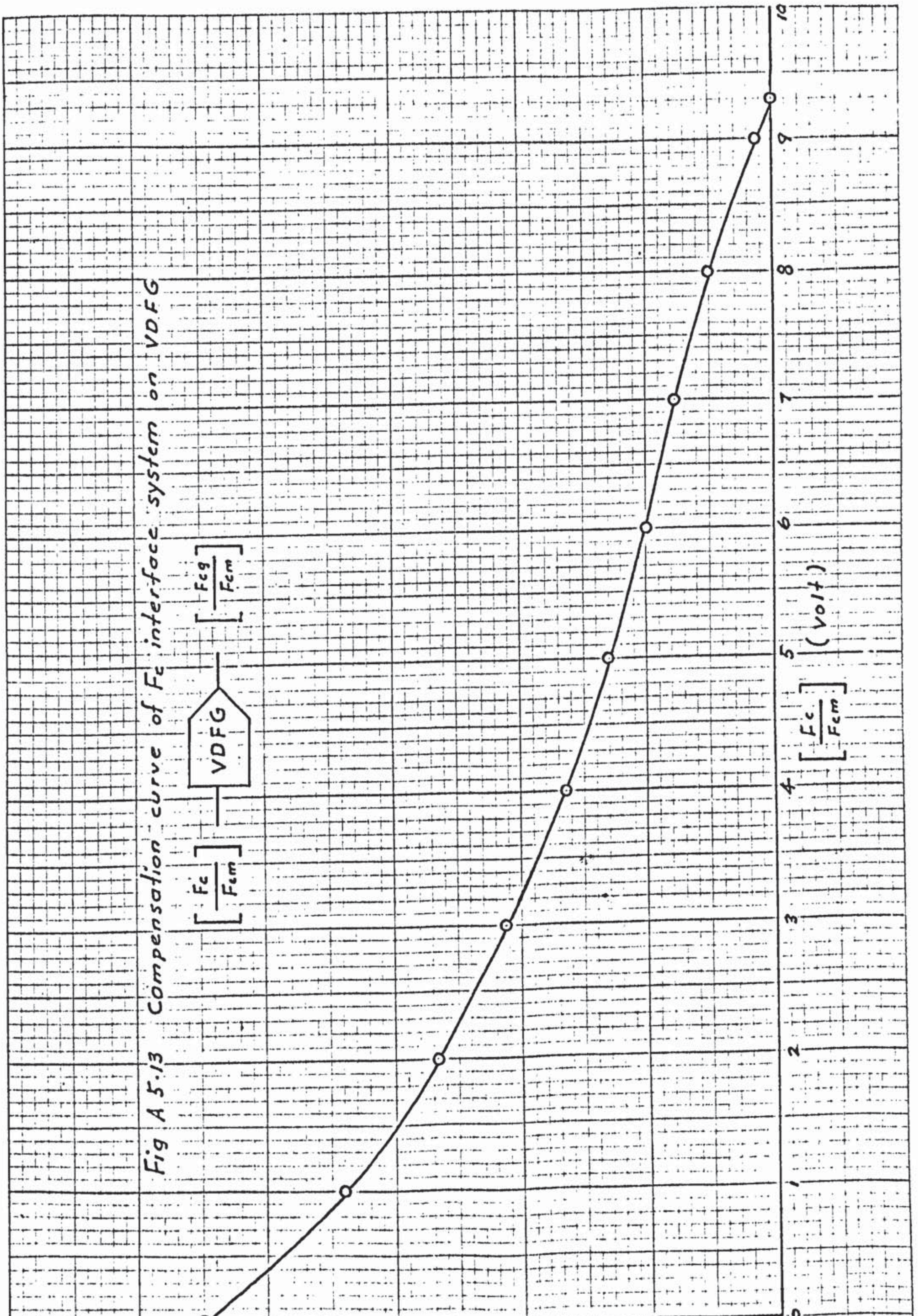

Fig A 5.13 Compensation curve of F_c interface system on VDFG

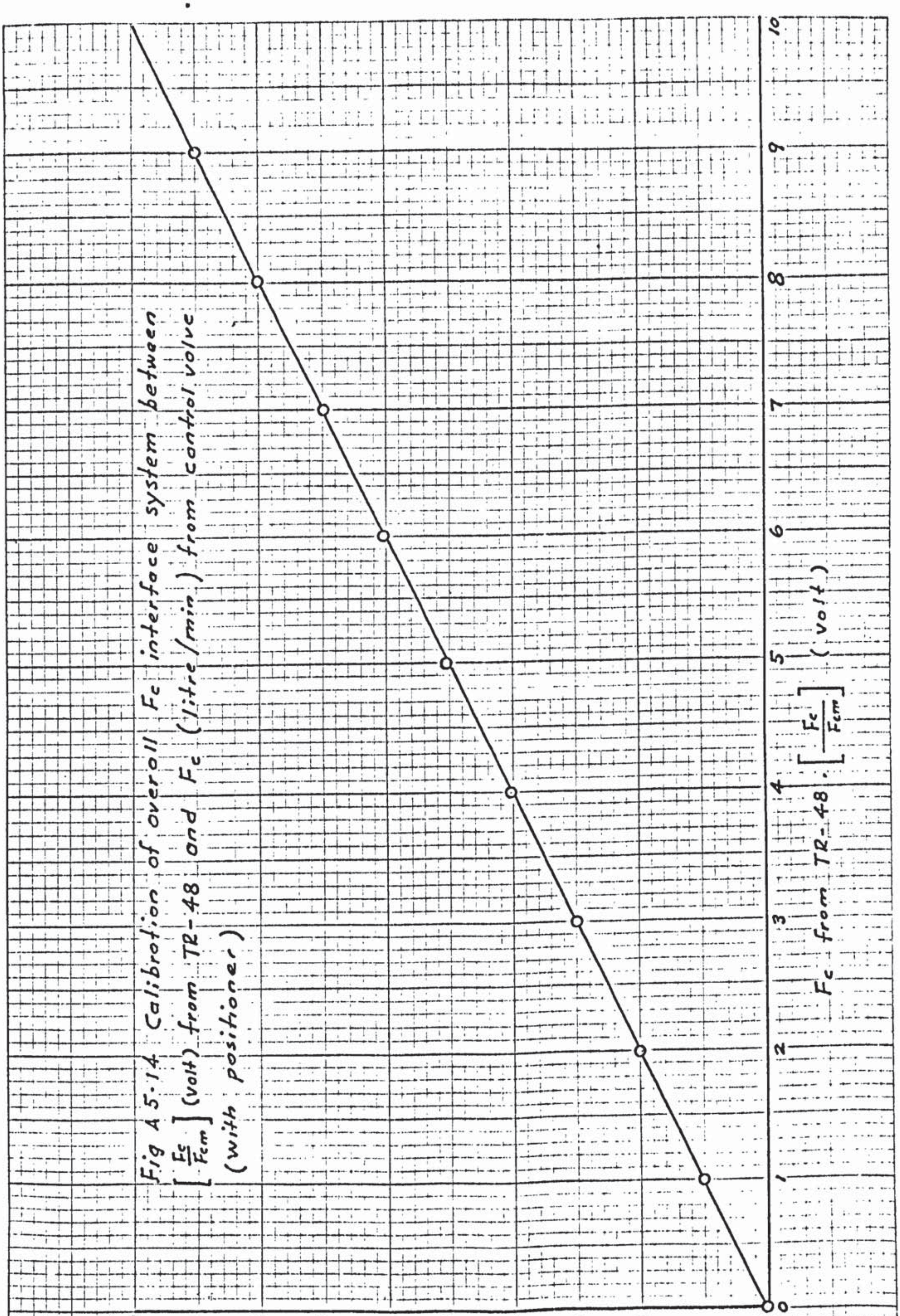

Fig A5.14 Calibration of overall F_c interface system between $\left[\frac{F_c}{F_{cm}}\right]$ (volt) from TR-48 and F_c (litre/min) from control valve (with positioner)

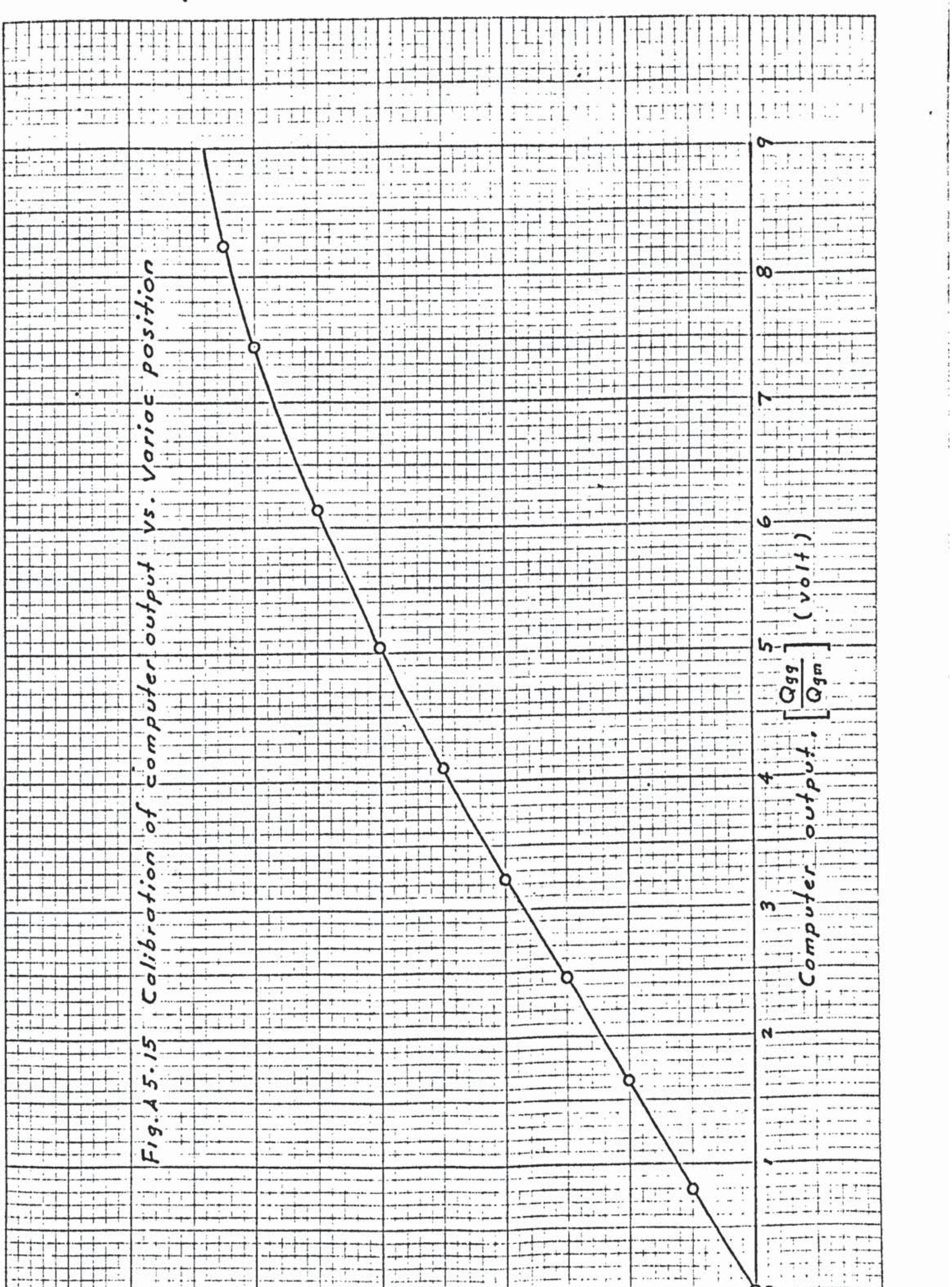

Fig. A5-15 Calibration of computer output vs. Variac position

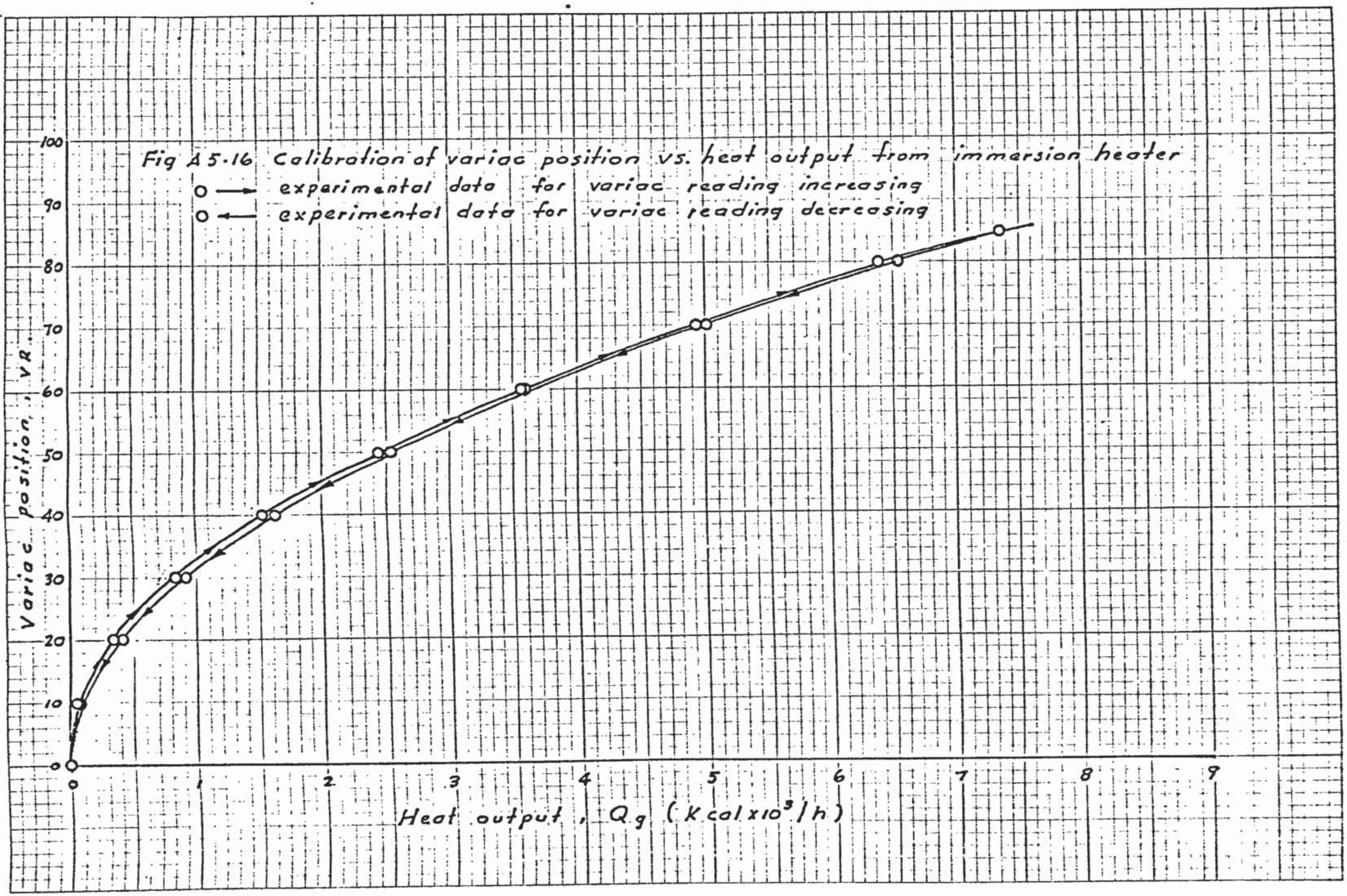

Fig A5.16 Calibration of variac position vs. heat output from immersion heater

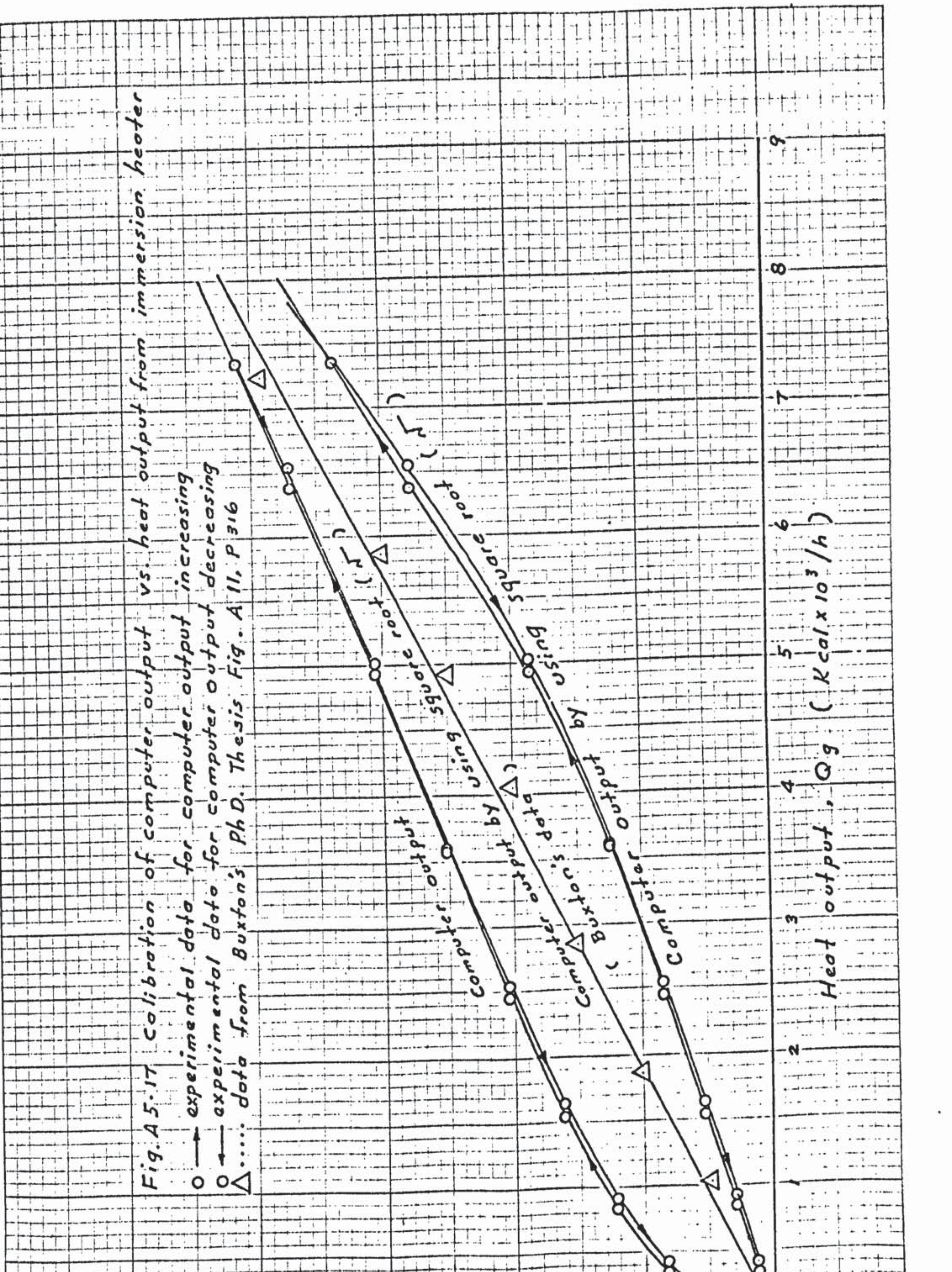

Fig. A5.17 Calibration of computer output vs. heat output from immersion heater

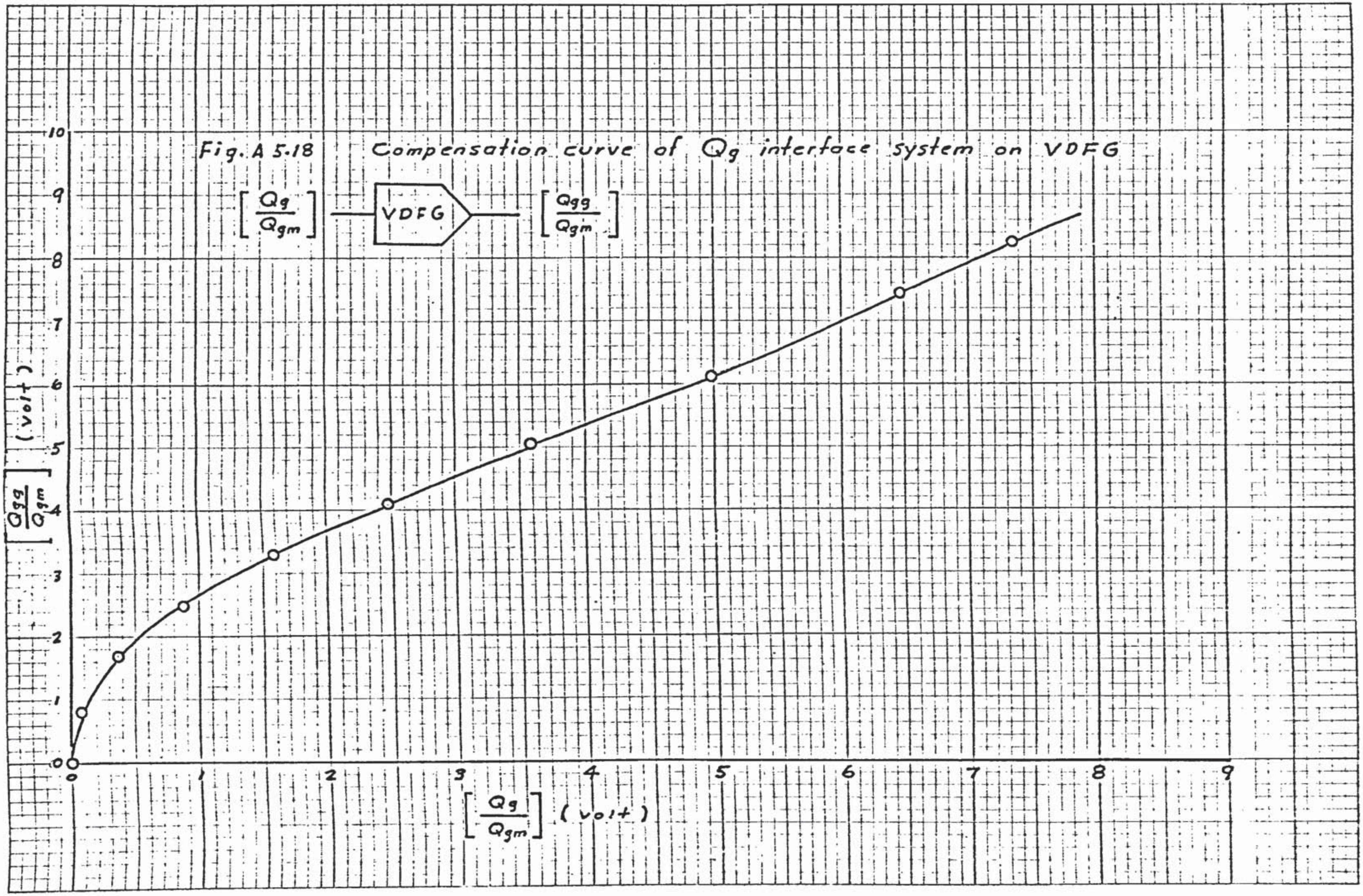

Fig. A 5.18 Compensation curve of Q_g interface system on VDFG

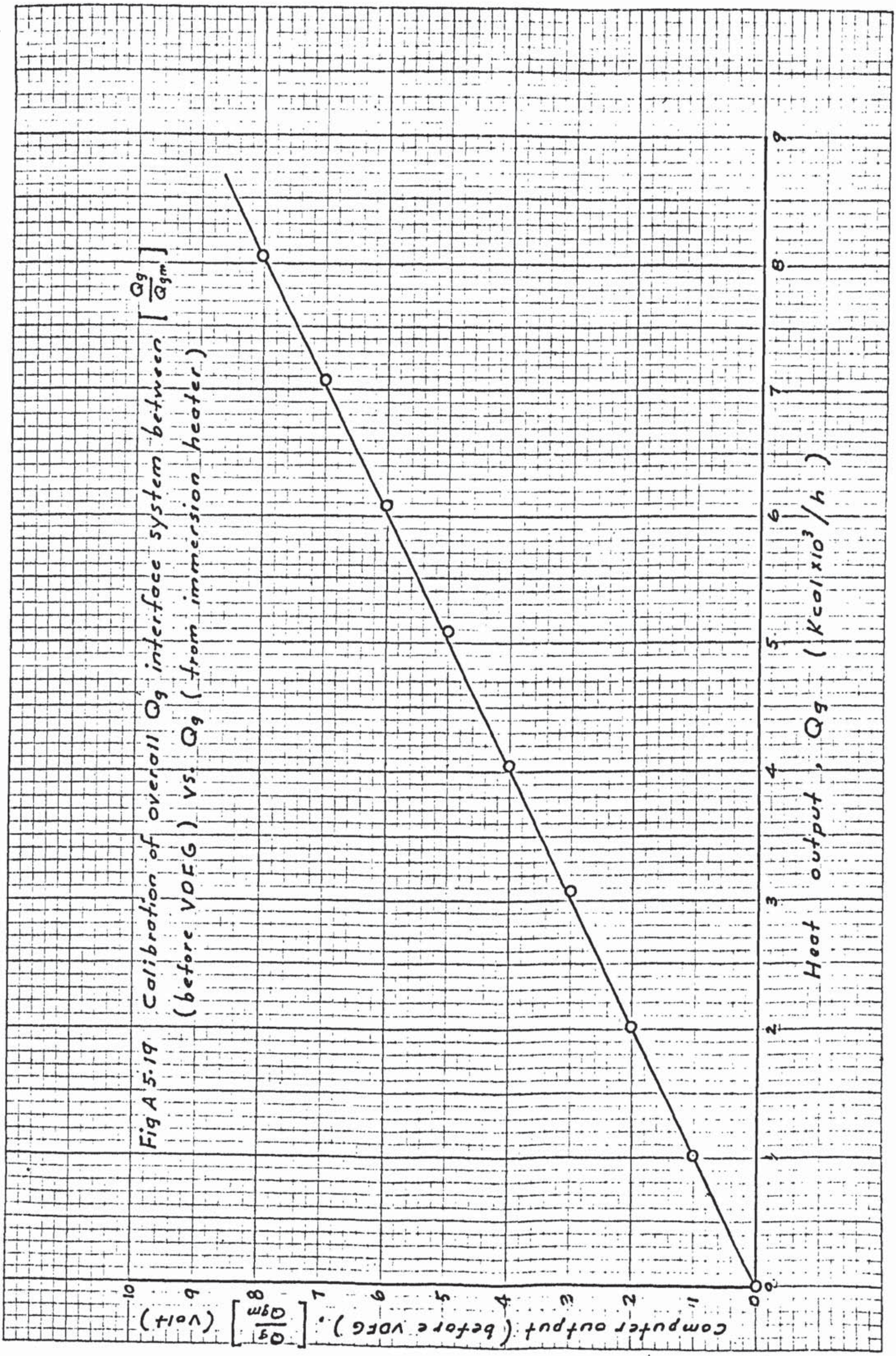
Fig A 5.19 Calibration of overall Qg interface system between [Qg/Qgm]
(before VDEG) vs. Qg (from immersion heater)
Heat output, Qg (Kcal x10^3/h)
computer output (before VDEG). [Qg/Qgm] (volt)
0
1
2
3
4
5
6
7
8
9
10

APPENDIX 6

Experimental data at final steady state of on-line operation

Tables A.6.1 to A.6.10.

Table A.6.1. Final steady state conditions of on-line operation for cases 1.1 and 1.2

	T_i °C	T °C	ΔT_c °C	F litre/min	F_c litre/min	C mol/litre	(aKC) mu	Variac VR
Case 1.1								
US	20.0	31.45	9.5	2.7	2.0	.075	.0278	54.0
UOC	20.0	30.70	10.0	2.7	2.0	.084	.0270	53.5
OMRAC								
K_3=100	20.0	30.60	10.3	2.7	2.0	.087	.0278	54.0
K_3=200	20.0	30.50	10.5	2.7	2.0	.087	.0278	54.0
K_3=500	20.0	30.40	10.2	2.7	2.1	.088	.0278	54.0
K_3=1000	20.0	30.30	10.0	2.7	2.1	.089	.0278	54.0
Case 1.2								
US	19.0	31.4	10.0	2.4	1.9	.079	.0278	54.5
UOC	19.0	30.7	10.3	2.4	2.0	.086	.0278	54.5
OMRAC								
K_3=100	19.0	30.5	10.8	2.4	2.0	.088	.0278	54.2
K_3=200	19.0	30.5	10.6	2.4	2.0	.088	.0278	54.2
K_3=500	19.0	30.4	10.5	2.4	2.1	.088	.0278	54.0
K_3=1000	19.0	30.4	10.5	2.4	2.1	.089	.0278	54.0

Notes:

1. F before change is 3.0 litre/min
2. Conditions of operating cases are shown in Table 10.1
3. (aKC) $\left[\frac{a}{a_m}\right]\left[\frac{K}{K_m}\right]\left[\frac{C}{C_m}\right]$

All above notes apply also to the following tables:

Table A.6.2. Final steady state conditions of on-line operation for Cases 1.3 and 1.4

	T_i °C	T °C	ΔT_c °C	F litre/min	F_c litre/min	C mol/litre	(aKC) mu	Variac VR
Case 1.3								
US	20.5	32.70	8.6	2.7	1.80	.0560	.0270	53.5
UOC	20.5	31.40	9.5	2.7	2.10	.0750	.0276	54.0
OMRAC:								
K_3=100	20.5	31.00	9.2	2.7	2.30	.0810	.0278	54.3
K_3=200	20.5	30.80	9.1	2.7	2.40	.0830	.0278	54.0
K_3=500	20.5	30.60	9.0	2.7	2.50	.0860	.0280	54.2
K_3=1000	20.5	30.50	8.8	2.7	2.60	.0875	.0280	54.2
K_3=4000	20.5	30.40	8.6	2.7	2.70	.0890	.0280	54.2
Case 1.4								
US	19.0	32.80	12.0	2.4	0.70	.0420	.0240	51.0
UOC	18.5	32.10	11.5	2.4	1.20	.0550	.0268	53.0
OMRAC:								
K_3=100	18.5	31.00	12.4	2.4	1.50	.0770	.0272	53.4
K_3=200	18.0	30.50	11.8	2.4	1.55	.0780	.0278	54.5
K_3=500	18.0	30.20	11.0	2.4	1.75	.0820	.0278	54.5
K_3=1000	18.0	30.00	11.0	2.4	1.78	.0840	.0280	55.0

Table A.6.3. Final steady state conditions of on-line operation for Cases 2.1, 2.2 and 2.3

	T_i °C	T °C	ΔT_c °C	F litre/min	F_c litre/min	C mol/litre	(aKC) mu	Variac VR
Case 2.1								
US	22.0	29.80	8.1	3.3	3.60	.1070	.0310	57.0
UOC	22.0	30.35	8.5	3.3	3.20	.1020	.0310	57.0
OMRAC:								
K_3=100	22.0	30.70	8.6	3.3	3.10	.0990	.0310	57.0
K_3=200	22.0	30.90	8.6	3.3	3.10	.0960	.0310	57.0
K_3=500	22.0	31.10	8.8	3.3	2.90	.0940	.0310	57.0
K_3=1000	22.0	31.20	9.2	3.3	2.70	.0930	.0310	57.0
Case 2.2								
US	21.5	29.50	8.8	3.6	3.50	.1180	.0330	59.0
UOC	21.5	30.40	9.2	3.6	3.07	.1110	.0330	59.0
OMRAC:								
K_3=100	21.5	30.70	9.2	3.6	2.90	.1050	.0330	59.0
K_3=200	21.5	31.00	9.2	3.6	2.74	.1020	.0330	59.0
K_3=500	21.5	31.10	10.3	3.6	2.40	.0990	.0330	59.0
K_3=1000	21.5	31.20	10.3	3.6	2.40	.0960	.0330	59.0
Case 2.3								
US	21.5	30.50	9.4	3.6	2.90	.1092	.0330	59.0
UOC	21.5	31.00	10.1	3.6	2.50	.1000	.0330	59.0
OMRAC:								
K = 100	21.5	31.20	10.1	3.6	2.50	.0970	.0330	59.0
K = 200	21.5	31.30	10.2	3.6	2.40	.0960	.0330	59.0
K = 500	21.5	31.40	10.2	3.6	2.40	.0940	.0330	59.0
K = 1000	21.5	31.50	10.3	3.6	2.30	.0930	.0330	59.0

Table A.6.4. Final steady state conditions of on-line operation for Cases 3.1, 3.2 and 3.3.

	T_i °C	T °C	ΔT_c °C	F litre/min	F_c litre/min	C mol/litre	(aKC) mu	Variac VR
Case 3.1.								
US	21.5	30.40	10.4	3.0	2.00	.1075	.0278	54.5
UOC	21.5	31.20	10.2	3.0	2.00	.1010	.0278	54.5
OMRAC :								
K_3=100	21.5	31.40	10.0	3.0	2.00	.0980	.0278	54.3
K_3=200	21.5	31.40	13.2	3.0	1.44	.0980	.0278	54.5
K_3=500	21.5	31.50	13.2	3.0	1.44	.0940	.0278	54.5
K_3=1000	21.5	31.60	13.3	3.0	1.40	.0932	.0278	54.5
Case 3.2.								
US	22.0	30.50	10.5	3.0	2.20	.1210	.0270	53.0
UOC	22.0	31.40	12.4	3.0	1.70	.1112	.0276	54.0
OMRAC :								
K_3=100	22.0	31.70	13.0	3.0	1.58	.1084	.0278	54.3
K_3=200	22.0	31.70	13.0	3.0	1.55	.1040	.0278	54.5
K_3=500	22.0	32.00	15.6	3.0	1.20	.1014	.0278	54.5
K_3=1000	22.0	32.40	16.1	3.0	1.11	.0990	.0278	54.5
Case 3.3.								
US	22.0	30.55	10.5	3.0	2.20	.1330	.0276	54.0
UOC	22.0	31.65	13.2	3.0	1.50	.1194	.0276	54.0
OMRAC :								
K_3=100	22.0	32.05	14.0	3.0	1.36	.1240	.0278	54.4
K_3=200	22.0	32.45	15.0	3.0	1.18	.1096	.0278	54.4
K_3=500	22.0	32.80	15.6	3.0	1.10	.1034	.0278	54.4
K_3=1000	22.0	33.25	16.0	3.0	1.00	.0988	.0280	54.9

Table A.6.5. Final steady state conditions of on-line operation for Cases 4.1 and 4.2

	T_i °C	T °C	ΔT_c °C	F litre/min	F_c litre/min	C mol/litre	(aKC) mu	Variac VR
Case 4.1								
US	21.5	31.00	11.0	3.3	2.20	.1140	.0310	57.0
UOC	21.5	31.80	12.0	3.3	1.80	.1030	.0310	57.0
OMRAC :								
K_3=100	21.5	32.00	12.0	3.3	1.70	.0980	.0310	57.2
K_3=200	21.5	32.10	12.5	3.3.	1.60	.0970	.0310	57.2
K_3=500	21.5	32.20	13.6	3.3	1.50	.0960	.0314	57.5
K_3=1000	21.5	32.30	13.6	3.3	1.50	.0940	.0314	57.5
K_3=4000	21.5	32.40	13.6	3.3	1.50	.0920	.0314	57.5
Case 4.2.								
US	21.0	29.60	11.2	3.3	2.30	.1240	.0308	57.0
UOC	21.0	30.70	13.5	3.3	1.64	.1120	.0308	57.0
OMRAC :								
K_3=100	21.0	31.20	14.0	3.3	1.50	.1058	.0310	57.0
K_3=200	21.0	31.30	14.6	3.3	1.40	.1025	.0310	57.2
K_3=500	21.0	31.50	14.8	3.3	1.30	.0980	.0310	57.2
K_3=1000	21.0	31.70	15.2	3.3	1.25	.0945	.0310	57.3
K_3=4000	21.0	31.90	15.9	3.3	1.15	.0930	.0310	57.5

Table A.6.6. Final steady state conditions of on-line operations for Cases 5.1, 5.2 and 5.3

	T_i °C	T °C	ΔT_c °C	F litre/min	F_c litre/min	C mol/litre	(aKC) mu	Variac VR
Case 5.1.								
OMRAC								
K_3 = 100								
ϵ = 0	21.0	31.50	13.0	3.3	1.60	.1050	.0310	57.0
ϵ = 1	21.0	32.30	14.5	3.3	1.30	.0980	.0310	57.0
ϵ = 2	21.0	32.40	13.4	3.3	1.40	.0924	.0310	57.0
ϵ = 3	21.0	32.50	15.5	3.3	1.20	.0890	.0310	57.0
Case 5.2								
OMRAC								
K_3 = 100								
ϵ = 0	21.0	31.60	15.0	3.3	1.30	.1050	.0310	57.5
ϵ = 0.2	21.0	31.90	15.6	3.3	1.20	.0980	.0310	57.5
ϵ = 0.4	21.0	32.20	16.3	3.3	1.10	.0930	.0310	57.5
ϵ = 0.6	21.0	32.30	16.2	3.3	1.10	.0914	.0310	57.5
ϵ = 0.8	21.0	32.40	16.8	3.3	1.00	.0910	.0310	57.5
ϵ = 1.0	21.0	32.40	16.8	3.3	1.00	.0912	.0310	57.5
Case 5.3								
OMRAC								
K_3 = 200								
ϵ = 0	21.0	31.70	13.2	3.3	1.50	.1016	.0310	57.0
ϵ = 0.2	21.0	31.95	14.2	3.3	1.40	.0980	.0310	57.0
ϵ = 0.4	21.0	32.00	14.3	3.3	1.30	.0945	.0310	57.0
ϵ = 0.6	21.0	32.40	14.5	3.3	1.30	.0934	.0310	57.0
ϵ = 0.8	21.0	32.40	15.0	3.3	1.20	.0930	.0310	57.0
ϵ = 1.0	21.0	32.50	15.2	3.3	1.20	.0920	.0310	57.0

Table A.6.7. Final steady state conditions for the on-line operations for Cases 6.1, 6.3 and 6.5

	T_i °C	T °C	ΔT_c °C	F litre/min	F_c litre/min	C mol/litre	(aKC) mu	Variac VR
Case 6.1								
UOC	22.0	31.10	14.5	3.3	1.69	.1100	.0310	57.5
OMRAC								
K_3 = 1.0								
ϵ = 0.1	22.5	32.30	15.0	3.3	1.50	.0940	.0310	57.5
ϵ = 0.2	22.5	32.70	16.0	3.3	1.38	.0860	.0310	57.5
ϵ = 0.3	22.5	32.60	16.0	3.3	1.35	.0870	.0310	57.5
ϵ = 0.4	22.5	32.50	15.0	3.3	1.48	.0890	.0310	57.5
Case 6.3								
UOC	20.0	31.20	10.7	3.3	1.65	.1090	.0310	57.2
OMRAC								
K_3 = 10								
ϵ = 0	20.0	31.50	10.7	3.3	1.60	.1050	.0310	57.4
ϵ = 0.04	20.0	31.80	11.5	3.3	1.40	.0990	.0310	57.4
ϵ = 0.08	20.0	32.00	12.3	3.3	1.30	.0970	.0310	57.4
ϵ = 0.12	20.0	32.20	12.7	3.3	1.20	.0936	.0310	57.4
Case 6.5.								
UOC	20.0	31.10	11.0	3.3	1.64	.1098	.0310	57.2
OMRAC								
K_3 = 20								
ϵ = 0	20.0	31.70	11.9	3.3	1.40	.0980	.0310	57.4
ϵ = 0.04	20.0	31.90	11.5	3.3	1.35	.0950	.0310	57.4
ϵ = 0.08	20.0	31.95	12.0	3.3	1.30	.0940	.0310	57.4
ϵ = 0.12	20.0	32.00	12.8	3.3	1.20	.0925	.0310	57.4

Table A.6.8. Final steady state conditions of the on-line operations for Cases 7.1, 7.2 and 7.3.

	T_i °C	T °C	ΔT_c °C	F litre/min	F_c litre/min	C mol/litre	(aKC) mu	Variac VR
Case 7.1								
US	21.0	28.90	9.3	3.3	3.15	.1420	.0310	57.0
UOC	21.0	30.80	11.3	3.3	1.95	.1200	.0310	57.4
OMRAC :								
K_3 = 100	21.0	31.20	12.0	3.3	1.75	.1150	.0310	57.4
K_3=200	21.0	31.50	13.0	3.3	1.55	.1100	.0310	57.4
K_3=500	21.0	31.90	13.8	3.3	1.40	.1040	.0310	57.4
K_3=1000	21.0	32.10	14.4	3.3	1.20	.1010	.0310	57.4
Case 7.2								
US	21.6	29.20	12.0	3.3	2.00	.1330	.0276	54.0
UOC	21.6	30.90	13.4	3.3	1.50	.1145	.0280	54.5
OMRAC								
K_3=100	22.0	31.30	14.7	3.3	1.45	.1090	.0290	55.5
K_3=200	22.0	31.70	15.4	3.3	1.35	.1050	.0290	55.5
K_3=500	22.0	32.10	15.9	3.3	1.25	.1000	.0290	55.5
K_3=1000	22.0	32.30	16.2	3.3	1.10	.0970	.0290	55.5
Case 7.3								
US	21.5	30.20	10.7	3.3	2.30	.1222	.0300	56.5
UOC	21.5	31.20	12.9	3.3	1.72	.1100	.0310	57.0
OMRAC								
K_3=100	21.5	31.80	13.2	3.3	1.70	.1020	.0310	57.0
K_3=200	21.5	31.72	13.5	3.3	1.65	.0960	.0310	57.0
K_3=500	21.5	31.84	14.5	3.3	1.50	.0950	.0310	57.0
K_3=1000	21.5	32.00	14.7	3.3	1.40	.0940	.0310	57.0

Table A.6.9. Final steady state conditions of on-line operations for Cases 8.1 and 9.1

	T_i °C	T °C	ΔT_c °C	F litre/min	F_c litre/min	C mol/litre	(aKC) mu	Variac VR
Case 8.1								
(I) $K_1 = K_2 = 4$								
UOC	20.5	30.50	11.1	3.3	1.74	.1162	.0300	56.4
OMRAC								
K_2=200	21.0	31.70	13.1	3.3	1.48	.1016	.0310	57.0
(II) $K_1 = K_2 = 15$								
UOC	21.0	31.50	12.8	3.3	1.54	.1046	.0310	57.0
OMRAC								
K_3 =200	21.0	31.60	13.2	3.3	1.46	.1030	.0310	57.0
Case 9.1								
(I) C_d = 0.10 g.mole/litre								
UOC	21.0	30.70	11.7	3.3	1.64	.1150	.0300	57.0
OMRAC								
K_3=200	21.0	31.50	12.5	3.3	1.58	.1030	.0310	57.0
(II) C_s = 0.08 g.mole/litre								
UOC	21.0	31.05	12.1	3.3	1.52	.1090	.0300	57.0
OMRAC								
K_3=200	21.0	31.75	13.6	3.3	1.42	.0990	.0310	57.0

Table A.6.10. Final steady state conditions of on-line operations for Cases 10.1, 10.2 and 10.3

	T_i °C	T °C	ΔT_c °C	F litre/min	F_c litre/min	C mol/litre	(aKC) mu	Variac VR
Case 10.1 C_o = 0.9 mol /litre								
US	20.5	30.80	11.6	3.3	1.40	.1030	.0280	54.4
UOC	20.5	31.00	12.7	3.3	1.30	.1006	.0290	56.0
OMRAC K_3=200	20.5	31.60	13.6	3.3	1.10	.0912	.0290	56.0
Case 10.2. C_o = 1.1 mol /litre								
US	19.5	28.90	6.8	3.3	4.10	.1480	.0330	59.5
UOC	19.5	30.70	8.3	3.3	2.80	.1260	.0340	60.0
OMRAC K_3=200	19.5	31.50	9.7	3.3	2.16	.1148	.0340	60.0
Case 10.3								
(I) C_o = 0.9 mol /litre								
UOC	19.5	31.20	13.2	3.3	1.16	.0980	.0280	54.3
OMRAC K_3=200	19.5	31.50	13.0	3.3	1.14	.0930	.0280	54.3
(II) C_o = 1.1 mol /litre								
UOC	19.5	30.30	9.8	3.3	2.78	.1298	.0340	60.0
OMRAC K_3=200	19.5	31.60	10.1	3.3	2.40	.1116	.0340	60.0

APPENDIX 7

Optimal adaptivity calculation

A.7.1. Optimal adaptivity of complete simulation

Tables A.7.1 to A.7.5.

A.7.2. Performance response calculation from dynamic response figures of on-line operation

A.7.3. Optimal adaptivity of on-line operation

Tables A.76 to A.718.

Table A.7.1. Optimal adaptivity of complete simulation for Cases 1.1, 1.2, 1.3 and 1.4

Case	Type of curves	$\int_0^{t_f} e^2 dt$	Optimal adaptivity ψ %	Figure
1.1	UOC	16.50		7.7
	OMRAC			
	K_3=100	7.10	57.00	7.7
	K_3=200	3.60	78.20	7.7
	K_3=500	1.70	89.70	7.7
	K_3=1000	0.85	94.84	7.7
1.2	UOC	65.00		7.10
	OMRAC			
	K_3=100	29.00	55.40	7.10
	K_3=200	15.50	76.15	7.10
	K_3=500	6.80	89.54	7.10
	K_3=1000	3.20	95.07	7.10
1.3	UOC	121.00		7.12
	OMRAC			
	K_3=100	69.00	43.00	7.12
	K_3=200	38.00	68.60	7.12
	K_3=500	17.00	86.00	7.12
	K_3=1000	10.00	91.73	7.12
1.4	UOC	178.00		7.14
	OMRAC			
	K_3=100	123.00	31.00	7.14
	K_3=200	66.00	63.00	7.14
	K_3=500	30.00	83.14	7.14
	K_3=1000	20.00	88.77	7.14

Table A.7.2. Optimal adaptivity of complete simulation for Cases 2.1, 2.2, 3.1, 3.2 and 3.3

Case	Type of curves	$\int_0^{t_f} e^2 dt$	Optimal adaptivity ψ %	Figure
2.1	UOC	10.40		7.16
	OMRAC			
	K_3=100	5.60	46.15	7.16
	K_3=200	3.20	69.23	7.16
	K_3=500	1.60	84.61	7.16
	K_3=1000	0.80	92.50	7.16
2.2	UOC	35.50		7.19
	OMRAC			
	K_3=100	21.20	44.93	7.19
	K_3=200	12.50	67.53	7.19
	K_3=500	5.50	85.71	7.19
	K_3=1000	3.00	92.20	7.19
3.1	UOC	0.55		7.21
	OMRAC			
	K_3=100	0.41	25.45	7.21
	K_3=200	0.18	67.27	7.21
	K_3=500	0.04	92.72	7.21
	K_3=1000	0.015	97.27	7.21

Table A.7.2. (continued)

Case	Type of curves	$\int_0^{t_f} e^2 dt$	Optimal adaptivity ψ %	Figure
3.2	UOC	3.10		7.22
	OMRAC			
	K_3=100	2.20	29.03	7.22
	K_3=200	1.30	58.06	7.22
	K_3=500	0.50	83.87	7.22
	K_3=1000	0.20	93.54	7.22
3.3	UOC	8.60		7.24
	OMRAC			
	K_3=100	5.90	31.39	7.24
	K_3=200	3.40	60.46	7.24
	K_3=500	1.40	83.72	7.24
	K_3=1000	0.70	91.86	7.24

Table 7.3. Optimal adaptivity of complete simulation for Cases 4.1, 5.1 and 5.2

Case	Type of curves	$\int_0^{t_f} e^2 dt$	Optimal adaptivity ψ %	Figure
4.1	UOC	18.0		7.26
	OMRAC			
	K_3=100	9.8	45.55	7.26
	K_3=200	5.6	68.88	7.26
	K_3=500	2.4	86.66	7.26
	K_3=1000	1.3	92.77	7.26
5.1	UOC	18.2		7.29
	OMRAC			
	K_3=100			
	= 0	9.8	46.15	7.29
	= 1.0	6.2	65.93	7.29
	= 2.0	4.1	77.47	7.29
	= 3.0	3.2	82.41	7.29
	= 4.0	2.2	87.91	7.29
5.2	UOC	17.8		7.31
	OMRAC			
	K_3=200			
	= 0	5.6	68.53	7.31
	= 2.0	3.2	82.02	7.31
	= 4.0	2.1	88.20	7.31
	= 8.0	1.1	93.82	7.31
	= 15.0	0.6	96.62	7.31

Table 7.4. Optimal adaptivity of complete simulation for Cases 6.1, 6.2, 7.1, 7.2 and 7.3.

Case	Type of curves	$\int_0^{t_f} e^2 dt$	Optimal Adaptivity ψ %	Figure
6.1	UOC	17.0		7.34
	OMRAC, $K_3 = 1$			
	$\epsilon = 0.5$	10.2	40.00	7.34
	$\epsilon = 1.0$	4.0	76.47	7.34
	$\epsilon = 1.5$	2.0	88.23	7.34
	$\epsilon = 2.0$	1.2	92.94	7.34
6.2	UOC	17.0		7.35
	OMRAC, $K_3 = 3$			
	$\epsilon = 0.5$	8.50	50.00	7.35
	$\epsilon = 1.0$	3.30	80.58	7.35
	$\epsilon = 1.5$	1.70	90.00	7.35
	$\epsilon = 2.0$	1.00	94.11	7.35
7.1	UOC	20.80		7.38
	OMRAC			
	K_3=100	11.60	44.23	7.38
	K_3=200	6.80	67.30	7.38
	K_3=500	2.80	86.53	7.38
	K_3=1000	1.50	92.78	7.38

Table 7.4. (continued)

Case	Type of curves	$\int_0^{t_f} e^2 dt$	Optimal adaptivity ψ %	Figure
7.2	UOC	22.20		7.41
	OMRAC			
	K_3=100	12.60	43.24	7.41
	K_3=200	7.20	67.56	7.41
	K_3=500	3.20	85.58	7.41
	K_3=1000	1.80	91.89	7.41
7.3.	UOC	14.60		7.44
	OMRAC			
	K_3=100	8.20	43.83	7.44
	K_3=200	4.60	68.49	7.44
	K_3=500	1.90	86.98	7.44
	K_3=1000	1.00	93.15	7.44

Table A.7.5. Optimal adaptivity of complete simulation for Cases 8.1, 9.1, 10.1 and 10.2

Case	Type of curves	$\int_{0}^{t_f} e^2 dt$	Optimal Adaptivity Ψ %	Figure
8.1	UOC	28.0		7.46
	OMRAC $K_1=K_2=4$	5.6	80.00	7.46
	UOC	19.6		7.46
	OMRAC $K_1=K_2=8$	5.6	71.42	7.46
	UOC	11.6		7.46
	OMRAC $K_1=K_2=15$	5.6	49.09	7.46
9.1	(I) UOC	13.6		7.48
	OMRAC	4.8	64.70	7.48
	(II) UOC	18.3		7.48
	OMRAC	6.2	66.12	7.48
	(Original value Ψ = 68.88%)			
10.1	(I) UOC	16.4		7.51
	OMRAC	5.4	67.07	7.51
	(II) UOC	23.6		7.51
	OMRAC	7.6	67.79	7.51
	(Original value Ψ = 68.88%)			

Table A.7.5. (Continued)

Case	Type of curves	$\int_0^{t_f} e^2 dt$	Optimal Adaptivity ψ %	Figure
10.2	(I) UOC	1.72		7.53
	OMRAC	0.72	58.13	7.53
	(II) UOC	54.00		7.53
	OMRAC	17.00	68.51	7.53

(Original value ψ = 68.88%)

A.7.2. Performance response calculation from dynamic response figures of on-line operation

From Figure A.6.1 performance response is calculated as follows:

$$\int_{o}^{t_f} e^2 dt \simeq e_1^2 \Delta t_1 + e_2^2 \Delta t_2 + - - - - e_n^2 \Delta t_n \qquad \text{(A-6-1)}$$

Set: $\Delta t_1 = \Delta t_2 = - - - - - - - t_n = \Delta t$ (A-6-2)

and: $e_1 = \frac{A_1}{\Delta t_1} = \frac{A_1}{\Delta t}$, $e_2 = \frac{A_2}{\Delta t}$, $- - - - e_n = \frac{A_n}{\Delta t}$

(A-6-3)

$$\therefore \int_{o}^{t_f} e^2 dt \simeq \frac{A_1^2 + A_2^2 + - - - - - + A_n^2}{\Delta t}$$

$$\simeq \frac{\sum_{i=1}^{n} A_i^2}{\Delta t} \qquad \text{(A-6-4)}$$

In on-line plotting curves:

t_f = 600 sec

n = 12

t = 50 sec $\Leftrightarrow$ 1 in = 2.54 cm (A-6-5)

unit of A = (0.1 x 50) $(\frac{mol}{litre})$ (sec)

$\Leftrightarrow$ 1 $in^2 = (2.54)^2$ cm^2

A_i can be obtained by using planimeter in $(cm)^2$, and equation A-6-4 then becomes:

$$\int_{o}^{t_f} e^2 dt \simeq \frac{1}{(2.54)^4} \sum_{i=1}^{12} A_i^2 \left(\frac{in^4}{in}\right) = \frac{(0.1 \times 50)^2}{(2.54)^4 (50)} \sum_{i=1}^{12} A_i^2$$

$$\text{or} \int_0^{t_f} e^2 dt \simeq 0.012 \sum_{i=1}^{12} A_i^2 \left(\frac{\text{g.mole}}{\text{L}}\right)^2 (\text{sec}) \qquad \text{(A-6-6)}$$

Performance response (PR) $= \int e^2 dt$

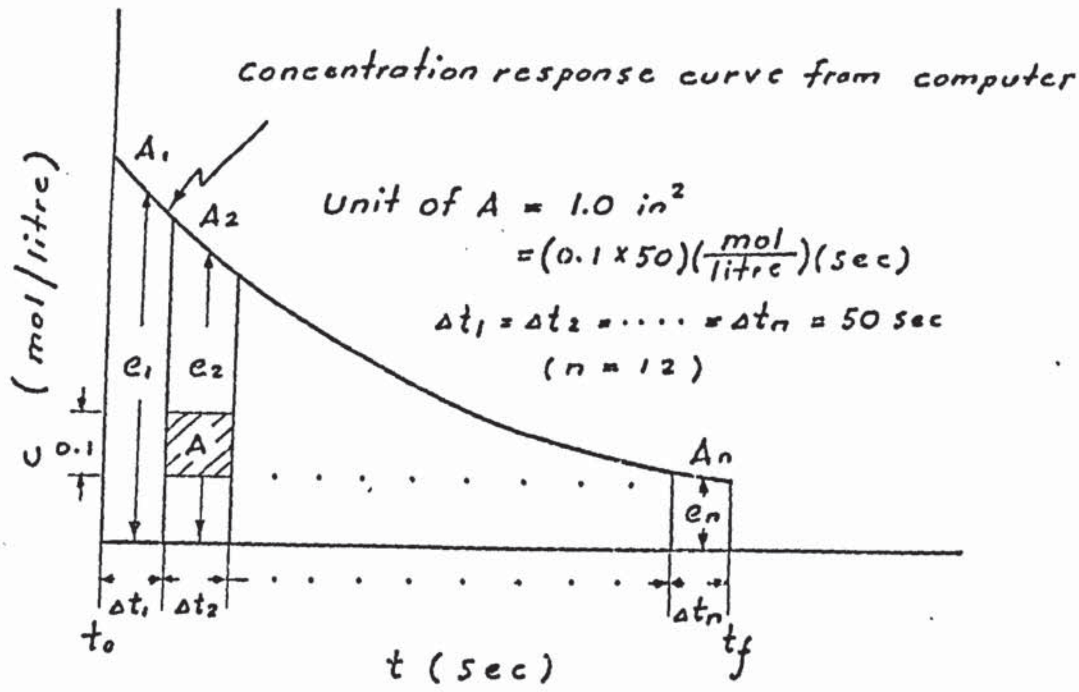

Figure A 7·1 Performance response calculation from dynamic response curve

Table A 7.6 Optimal adaptivity of On-line Operation for cases 1.1 and 1.2

	A1	A2	A3	A4	A5	A6	A7	A8	A9	A10	A11	A12	$.012\Sigma A_i^2$	Ψ %
Case 1.1	(Figure 10.1)													
U O C	5.75	8.95	7.50	5.40	4.10	3.55	3.55	3.60	3.60	3.65	3.65	3.65	3.68	
OMRAC														
K_3=100	4.90	6.75	3.75	1.00	0.65	0.89	1.20	1.40	1.50	1.60	1.80	1.60	1.20	67.39
K_3=200	4.5	6.20	2.90	0.60	0.50	0.70	1.20	1.20	1.40	1.50	1.60	1.40	0.96	73.91
K_3=500	4.00	3.50	0.70	0.85	0.40	0.55	0.80	0.90	1.10	0.80	0.80	0.60	0.41	88.86
K_3=1000	4.00	2.75	0.50	0.35	0.20	0.40	0.50	0.60	0.65	0.70	0.40	0.10	0.31	91.58
Case 1.2	(Figure 10.4)													
U O C	7.60	14.0	11.25	7.45	4.95	3.70	3.15	2.75	2.75	2.60	2.5	2.5	6.22	
OMRAC														
K_3=100	7.50	13.05	8.15	3.50	1.50	1.15	1.20	1.25	1.40	1.35	1.40	1.25	3.83	38.42
K_3=200	7.20	10.30	4.65	1.25	.80	.95	1.10	1.25	1.20	1.20	1.00	1.10	2.49	63.18
K_3=500	6.75	6.30	.70	.55	.75	.90	1.00	.85	1.20	1.20	1.00	1.10	1.13	81.83
K_3=1000	6.30	4.80	.70	.30	.30	1.10	1.00	.85	.90	.90	.70	.80	0.83	86.66

Table A 7.7 Optimal Adaptivity of On-line Operation for cases 1.3 and 1.4

	A1	A2	A3	A4	A5	A6	A7	A8	A9	A10	A11	A12	$.012\Sigma A_i^2$	ψ %
Case 1.3 (Figure 10.6)														
U O C	4.80	10.80	12.65	12.10	11.10	10.15	9.75	9.80	9.56	9.65	9.75	9.45	14.76	
OMRAC														
K_3=100	4.60	7.45	7.05	5.85	5.40	5.20	5.40	5.40	5.50	5.50	5.56	5.50	4.76	67.75
K_3=200	4.60	6.75	5.10	4.00	4.05	4.00	4.20	4.05	4.05	4.10	4.05	4.15	2.90	80.35
K_3=500	4.60	5.75	2.80	1.65	2.15	2.35	2.25	2.25	2.25	2.25	2.15	2.15	1.25	91.53
K_3=1000	4.40	4.90	1.70	1.25	1.95	1.70	1.70	1.40	1.55	1.50	1.70	1.45	0.83	94.38
K_3=4000	3.65	1.25	1.20	1.30	0.30	0.75	0.70	0.30	0.20	0.30	0.10	0	0.23	98.44
Case 1.4 (Figure 10.9)														
U O C	10.00	19.20	21.85	22.80	22.90	22.95	22.85	22.65	22.70	22.15	22.30	22.15	66.55	
OMRAC														
K_3=100	10.00	17.95	17.25	14.60	13.15	12.65	12.45	12.60	12.65	12.60	12.45	12.40	26.49	60.20
K_3=200	9.60	13.60	9.95	7.25	6.85	7.15	7.50	7.70	8.00	7.80	7.85	7.8	10.67	83.97
K_3=500	9.55	10.00	4.75	3.56	4.85	5.45	5.45	5.30	5.10	5.10	5.05	5.00	5.28	92.07
K_3=1000	9.40	6.35	0.95	2.85	4.20	3.90	3.56	3.65	3.85	3.80	3.45	3.5	3.00	95.49

Table A 7.8 Optimal Adaptivity of On-line Operation for cases 2.1 and 2.2

	A1	A2	A3	A4	A5	A6	A7	A8	A9	A10	A11	A12	$.012\Sigma A_i^2$	ψ %
Case 2.1	(Figure 10.11)													
U O C	1.85	6.85	8.45	8.50	9.20	9.10	8.05	8.60	8.45	8.25	8.15	7.75	9.38	
OMRAC														
K_3=100	1.05	6.05	6.80	7.00	6.95	6.85	6.80	6.45	6.40	6.30	6.20	6.10	5.67	39.55
K_3=200	1.50	5.45	5.40	5.15	5.00	4.80	4.60	4.35	4.35	4.30	4.10	4.05	2.96	68.44
K_3=500	1.50	5.50	4.25	3.70	3.45	3.35	3.35	3.10	3.25	3.05	3.05	3.15	1.71	81.77
K_3=1000	1.80	4.05	3.15	2.80	2.80	2.55	2.55	2.50	2.50	2.40	2.40	2.40	1.06	88.70
Case 2.2	(Figure 10.14)													
U O C	4.55	10.55	12.55	13.40	13.75	14.00	13.85	14.10	14.20	14.95	14.15	13.90	24.76	
OMRAC														
K_3=100	4.25	9.85	11.50	11.45	11.35	11.35	11.10	10.75	10.85	10.90	10.45	10.40	15.94	35.62
K_3=200	4.25	9.50	9.75	8.75	8.50	8.45	8.20	8.25	8.00	7.78	7.00	7.35	9.44	61.87
K_3=500	4.10	9.30	8.00	6.55	6.00	6.00	6.15	6.20	6.00	6.15	5.80	6.05	6.03	75.65
K_3=1000	2.70	6.15	3.80	3.20	3.70	3.90	3.95	4.00	4.25	4.10	4.45	4.55	2.47	90.02

Table A 7.9 Optimal Adaptivity of On-line Operation for cases 2.3 and 3.1

	A1	A2	A3	A4	A5	A6	A7	A8	A9	A10	A11	A12	$.012\Sigma A_i^2$	ψ %
Case 2.3	(Figure 10.16)													
U O C	3.10	7.20	8.05	7.95	8.00	7.60	7.55	7.25	7.05	6.90	6.90	6.90	7.36	
OMRAC														
K_3=100	3.20	7.85	7.60	6.85	6.60	6.20	6.15	5.75	5.90	5.30	5.25	5.20	5.35	27.31
K_3=200	3.05	6.75	5.80	5.25	5.20	4.80	4.40	4.35	4.40	4.20	4.15	4.15	3.29	55.30
K_3=500	3.00	5.40	3.00	2.15	2.25	2.20	2.25	2.35	2.30	2.35	2.55	2.35	1.14	84.51
K_3=1000	3.00	5.15	2.30	1.45	1.95	2.00	1.80	1.80	1.80	1.85	1.85	1.85	0.85	88.45
Case 3.1	(Figure 10.18)													
U O C	3.25	2.10	2.25	3.45	3.80	4.70	5.85	6.15	6.50	6.55	6.90	6.60	3.80	
OMRAC														
K_3=100	3.10	1.65	2.00	3.25	3.75	4.30	4.30	4.75	4.95	5.05	5.05	4.90	2.40	36.84
K_3=200	3.10	1.50	1.40	2.50	3.45	4.00	4.05	4.45	4.65	4.70	4.90	4.75	2.09	45.00
K_3=500	2.85	1.50	1.75	2.00	1.55	1.55	1.85	2.30	2.60	2.70	2.65	2.70	0.71	81.32
K_3=1000	2.50	1.15	1.65	1.20	1.00	1.25	1.65	1.75	1.80	1.75	1.80	1.75	0.39	89.74

Table A 7.10 Optimal Adaptivity of On-line Operation for cases 3.2 and 3.3

	A1	A2	A3	A4	A5	A6	A7	A8	A9	A10	A11	A12	$.012\Sigma A_i^2$	ψ %
Case 3.2	(Figure 10.20)													
U O C	4.55	3.00	1.65	4.75	6.90	8.15	8.65	8.75	9.25	10.00	11.15	12.60	9.47	
OMRAC														
K_3=100	3.85	1.55	2.65	5.00	6.20	6.70	6.85	6.95	7.25	8.05	9.20	10.65	6.52	31.15
K_3=200	3.85	1.55	2.25	3.95	4.85	4.85	4.65	4.70	5.00	5.70	6.80	7.75	3.51	62.94
K_3=500	3.45	1.75	3.15	3.45	3.55	3.40	3.20	3.35	3.80	4.45	5.55	6.20	2.23	76.45
K_3=1000	3.45	1.75	2.60	2.30	2.35	2.40	2.45	2.80	3.00	3.45	4.45	5.30	1.45	84.69
Case 3.3	(Figure 10.22 and 10.25)													
U O C	2.45	1.20	3.85	6.75	8.35	8.95	9.55	10.40	12.25	14.45	16.60	18.05	16.53	
OMRAC														
K_3=100	2.65	1.45	2.90	5.10	6.50	6.40	6.65	7.55	9.05	11.05	12.75	13.85	9.44	42.89
K_3=200	2.45	1.20	3.55	5.35	6.00	5.95	6.15	6.75	8.10	9.95	11.45	12.10	7.75	53.12
K_3=500	2.00	1.20	3.50	4.50	4.65	4.35	4.35	5.15	6.35	7.75	8.85	8.80	4.56	72.41
K_3=1000	2.00	1.20	2.75	2.90	2.55	2.15	2.25	2.25	4.05	5.35	5.95	6.10	1.99	87.96
K_3=4000	1.85	0.80	0.75	0.75	0.95	0.85	1.25	1.80	2.40	2.95	3.05	2.85	0.52	96.85

Table A 7.11 Optimal Adaptivity of On-line Operation for cases 4.1 and 4.2

	A1	A2	A3	A4	A5	A6	A7	A8	A9	A10	A11	A12	$.012\Sigma A_i^2$	Ψ %
Case 4.1	(Figure 10.27)													
U O C	0.20	3.50	5.00	5.50	5.90	6.35	6.9	7.25	7.50	7.50	7.95	8.05	5.80	
OMRAC														
K_3=100	0.20	2.60	3.95	4.10	4.00	4.35	4.70	5.00	5.20	5.25	5.60	5.75	2.88	50.34
K_3=200	0.10	2.50	3.35	3.05	3.35	3.85	4.30	4.65	4.85	4.85	5.00	5.00	2.27	60.86
K_3=500	0.10	2.40	2.80	2.55	2.95	3.55	3.70	3.90	4.05	4.10	4.00	4.00	1.47	74.66
K_3=1000	0.0	2.25	1.90	1.25	1.80	2.15	2.35	2.65	2.70	2.70	2.70	2.70	0.72	87.59
K_3=4000	0.0	1.65	0.50	1.15	1.25	1.35	1.40	1.40	1.50	1.45	1.25	1.45	0.24	95.86
Case 4.2	(Figure 10.29)													
U O C	1.05	4.65	7.45	9.20	10.35	11.45	12.25	12.95	13.40	13.70	13.90	14.10	17.74	
OMRAC														
K_3=100	0.40	4.05	6.55	7.55	8.20	9.20	9.65	9.85	10.35	10.40	10.15	10.40	10.61	40.19
K_3=200	0.40	4.05	6.15	6.80	7.10	7.55	7.95	8.15	8.25	8.05	7.90	7.95	7.15	59.70
K_3=500	0.20	3.65	4.60	4.30	4.30	4.75	5.05	5.15	5.25	5.30	5.20	5.25	3.08	82.64
K_3=1000	0.20	3.30	3.00	2.65	2.80	2.65	2.90	3.10	3.25	3.20	3.30	3.35	1.23	93.07
K_3= 4000	0.20	2.55	1.60	2.05	2.30	2.30	2.55	2.55	2.60	2.45	2.40	2.45	0.74	95.83

Table A 7.12 Optimal Adaptivity of On-line Operation for cases 5.1 and 5.2

	A1	A2	A3	A4	A5	A6	A7	A8	A9	A10	A11	A12	$.012\Sigma A_i^2$	ψ %
*Case 5.1	(Figure 10.32)													
OMRAC														
K_3=100														
ϵ =0.0	0.40	3.95	6.95	7.25	6.10	8.25	8.75	9.05	9.25	9.60	10.00	10.20	9.15	48.42
ϵ =1.0	0.40	4.60	5.00	3.60	5.80	2.60	1.90	1.25	1.00	0.80	0.75	0.90	1.29	92.73
ϵ =2.0	0.30	3.30	3.50	1.10	4.95	0.65	1.40	0.60	0.85	1.95	2.60	2.55	0.83	95.32
ϵ =3.0	0.30	2.95	2.00	0.60	3.80	1.65	0.80	0.90	2.70	3.25	2.50	1.10	0.68	96.17
*Case 5.2	(Figure 10.34)													
OMRAC														
K_3=100														
ϵ =0.0	0.35	3.80	6.35	7.05	7.55	8.50	9.25	9.55	9.70	9.70	9.65	9.65	9.42	46.90
ϵ =0.2	0.25	3.40	6.10	6.60	6.65	6.95	7.25	6.95	6.75	6.45	5.90	5.70	5.28	70.24
ϵ =0.4	0.20	3.10	5.80	6.60	6.35	6.05	5.45	4.95	4.35	3.60	3.10	2.40	3.18	82.07
ϵ =0.6	0.10	3.10	5.80	2.15	6.00	5.15	4.45	3.95	3.45	2.75	2.25	1.25	2.06	88.39
ϵ =0.8	0.0	2.90	4.30	5.60	4.95	4.20	3.35	2.65	2.15	1.55	1.20	1.05	1.54	91.32
ϵ =1.0	0.0	2.90	4.30	5.40	4.45	3.30	2.15	1.45	1.05	0.65	0.65	0.70	1.15	93.52

* Refer to Case 4.2 U O C $0.012\Sigma A_i^2 = 17.74$

Table A 7.13 Optimal Adaptivity of On-line Operation for cases 5.3 and 6.1

	A1	A2	A3	A4	A5	A6	A7	A8	A9	A10	A11	A12	$.012\Sigma A_i^2$	ψ %
*Case 5.3	(Figure 10.37)													
OMRAC														
K_3=200														
ϵ =0.0	0.30	3.25	5.10	5.65	6.20	6.70	7.15	7.65	7.60	7.75	7.65	7.75	5.98	66.29
ϵ =0.2	0.20	3.05	4.80	4.95	5.10	5.40	5.70	5.95	5.85	5.90	5.85	5.45	3.75	78.86
ϵ =0.4	0.20	2.80	4.80	4.70	4.45	4.20	4.30	4.45	4.35	4.30	3.85	3.45	2.31	86.98
ϵ =0.6	0.20	2.80	4.40	4.25	4.45	3.90	3.80	3.75	3.40	3.20	2.85	2.15	1.72	90.30
ϵ =0.8	0.10	2.45	4.40	4.25	3.95	3.90	3.80	3.40	3.10	2.70	2.45	2.00	1.53	91.38
ϵ =1.0	0.10	2.30	3.95	3.75	3.10	2.60	2.35	2.30	2.25	2.00	1.75	1.45	0.92	94.81
Case 6.1	(Figure 10.39)													
U O C	0.45	3.25	6.70	6.85	9.25	10.25	11.25	12.00	12.40	12.50	12.55	12.55	14.44	
OMRAC														
K_3=1.0														
ϵ =0.1	0.40	3.15	6.20	8.65	9.65	9.90	9.55	8.70	7.65	6.50	5.20	3.70	7.47	48.27
ϵ =0.2	0.30	2.85	5.40	6.40	6.65	5.75	4.45	3.00	1.35	0.50	1.30	2.25	2.32	83.93
ϵ =0.3	0.20	2.85	5.05	5.85	5.7	4.5	2.25	0.85	.85	1.95	2.55	2.40	1.74	87.95
ϵ =0.4	0.20	2.85	5.05	5.35	4.40	2.65	0.65	1.70	2.85	3.25	2.85	1.45	1.45	89.96

* Refer to Case 4.2 U O C $0.012 \Sigma A_i^2$ = 17.74

Table A 7.14 Optimal Adaptivity of On-line Operation for Cases 6.2 and 6.3

	A1	A2	A3	A4	A5	A6	A7	A8	A9	A10	A11	A12	$.012\Sigma A_i^2$	ψ %
Case 6.3	(Figure 10.43)													
U O C	0.50	4.20	6.55	7.55	8.60	9.35	10.2	11.0	11.70	12.15	12.45	12.65	13.24	
OMRAC														
K_3=10														
ϵ =0.0	0.20	3.05	4.45	5.05	5.75	6.50	7.30	7.95	8.35	9.00	9.30	9.65	6.92	47.73
ϵ =0.04	0.20	2.90	3.95	4.65	5.20	5.75	6.10	6.50	6.40	6.45	6.50	6.40	4.21	68.20
ϵ =0.08	0.10	2.90	3.95	4.65	5.10	4.95	4.80	5.95	5.10	4.75	4.60	4.70	2.96	77.64
ϵ =0.12	0.10	2.75	3.50	3.90	4.15	4.30	4.20	4.55	4.50	4.25	3.55	2.75	2.01	84.82
Case 6.3	(Figure 10.48)													
U O C	0.90	2.90	6.25	7.95	8.95	9.80	10.35	11.0	11.6	11.8	12.20	12.55	13.15	
OMRAC														
K_3=20														
ϵ =0.0	1.00	1.20	1.65	2.00	2.60	3.25	3.90	4.55	4.95	5.35	5.45	5.60	2.12	83.88
ϵ =0.04	1.00	1.05	1.25	1.65	1.90	2.35	2.80	3.25	3.50	3.60	3.75	3.75	1.05	92.02
ϵ =0.08	1.20	1.00	1.20	1.40	1.60	1.90	2.10	2.40	2.60	2.80	3.10	3.15	0.67	94.90
ϵ =0.12	1.10	0.8	0.95	1.15	1.60	1.80	1.95	2.05	2.20	2.25	2.10	2.10	0.44	96.65

Table A 7.15 Optimal Adaptivity of On-line Operation for cases 7.1 and 7.2

	A1	A2	A3	A4	A5	A6	A7	A8	A9	A10	A11	A12	$.012\Sigma A_i^2$	Ψ %
Case 7.1	(Figure 10.50)													
U O C	4.40	6.89	7.70	9.05	10.65	12.65	14.65	15.95	17.00	17.80	18.55	19.00	27.14	
OMRAC														
K_3=100	4.15	6.05	7.05	8.45	10.00	11.45	12.60	13.75	14.35	14.75	15.00	15.60	19.75	27.23
K_3=200	3.20	5.05	6.10	7.25	8.30	9.56	10.6	11.05	11.50	11.65	11.95	12.05	12.91	52.43
K_3=500	3.20	4.45	4.85	5.10	5.80	6.50	7.10	7.60	7.75	8.15	8.40	8.50	6.40	76.42
K_3=1000	3.20	41.50	3.80	3.60	4.20	4.80	5.10	5.55	5.85	5.90	6.10	6.35	3.59	86.77
Case 7.2	(Figure 10.53)													
U O C	3.55	8.70	11.00	11.65	11.80	12.75	13.35	14.1	14.45	14.9	14.85	14.95	22.79	
OMRAC														
K_3=100	3.56	7.90	9.75	10.0	9.60	10.15	10.40	11.05	11.30	11.25	11.35	11.45	14.52	36.29
K_3=200	3.45	7.75	9.15	8.65	8.35	8.45	8.50	8.55	8.60	8.75	8.80	8.95	9.90	56.56
K_3=500	2.95	6.75	6.50	5.05	4.90	4.80	4.90	5.05	5.15	5.15	5.15	5.55	3.95	82.67
K_3=1000	2.40	5.30	4.90	4.00	3.15	3.10	3.15	3.60	3.60	3.00	2.95	3.95	1.95	91.44

Table A 7.16 Optimal Adaptivity of On-line Operation for Cases 7.3 and 8.1

	A1	A2	A3	A4	A5	A6	A7	A8	A9	A10	A11	A12	$.012\Sigma A_i^2$	Ψ %
Case 7.3	(Figure 10.56)													
U O C	0.80	3.45	6.80	9.30	11.05	11.85	12.55	12.95	13.00	13.10	13.40	13.55	17.21	
OMRAC														
K_3=100	0.70	1.55	3.75	6.05	7.20	7.60	7.85	8.30	8.30	8.25	8.20	8.25	6.79	60.55
K_3=200	0.40	2.15	3.60	5.05	6.10	6.25	5.75	5.30	5.15	4.80	4.65	4.65	3.28	80.94
K_3=500	0.40	1.20	2.65	4.50	4.35	4.95	5.00	4.90	4.35	4.30	4.20	3.85	2.29	86.69
K_3=1000	0.40	0.90	1.85	3.25	3.05	3.00	3.15	3.30	3.25	3.25	3.30	3.40	1.17	93.20
*Case 8.1	(Figure 10.59)													
I. $K_1=K_2=4$														
U O C	0.75	4.45	7.05	8.55	10.3	1.20	13.35	14.60	15.80	16.45	16.90	16.95	22.53	
OMRAC														
K_3=200	0.10	4.05	4.55	4.45	4.95	5.55	6.20	6.75	6.95	7.30	7.30	7.00	4.81	78.65
II $K_1=K_2=15$														
U O C	0.20	3.60	7.75	10.2	10.55	11.1	11.25	11.55	11.35	11.5	11.55	11.6	14.35	
OMRAC														
K_3=200	0.20	3.45	7.35	8.85	9.45	10.15	10.55	10.70	10.55	10.45	10.40	10.50	12.02	16.24

* Refer to case 4.2, $K_1=K_2=8$, $K_3=200$, $\Psi = 59.67\%$

Table A 7.17 Optimal Adaptivity of On-line Operation for cases 9.1 and 10.1

	A1	A2	A3	A4	A5	A6	A7	A8	A9	A10	A11	A12	$.012\Sigma A_i^2$	Ψ %
*Case 9.1	(Figure 10.61)													
I U O C	0.30	4.15	7.25	10.4	11.7	9.25	12.75	13.40	13.85	14.45	14.55	14.25	18.70	
OMRAC														
K_3=200	0.20	3.35	4.70	5.15	5.50	4.85	5.75	6.10	6.15	6.30	6.30	6.30	4.09	78.13
II U O C	0.30	4.75	7.5	10.3	11.3	8.95	12.00	12.95	13.65	14.15	14.35	14.60	18.12	
OMRAC														
K_3=200	0.45	4.80	6.2	6.3	6.35	6.10	6.75	7.00	7.40	7.80	7.85	7.80	6.14	66.1[illegible]
*Case 10.1	(Figure 10.63)													
U O C	0.75	1.50	5.55	7.75	9.25	10.50	11.60	12.55	13.00	13.25	13.35	13.50	15.44	
OMRAC														
K_3=200	0.75	1.75	5.30	5.95	6.10	6.45	6.90	7.30	7.50	7.75	7.50	7.65	5.73	62.8[illegible]

* Refer to case 4.2 K_3=200 Ψ = 59.67%

Table A 7.18 Optimal Adaptivity of On-line Operation for cases 10.2 and 10.3

	A1	A2	A3	A4	A5	A6	A7	A8	A9	A10	A11	A12	$.012\Sigma A_i^2$	ψ %
* Case 10.2 (Figure 10.65)														
U O C	1.45	7.25	9.95	11.70	13.60	14.95	16.15	17.20	17.75	18.25	18.75	18.90	31.35	
OMRAC K_3=200	1.15	6.6	8.25	8.85	9.50	10.30	10.65	10.95	11.35	11.60	11.65	11.75	13.90	55.66
*Case 10.3 (Figure 10.67)														
I U O C	3.25	3.65	1.05	.55	1.70	2.70	3.45	4.15	4.55	4.80	5.00	4.95	1.89	
OMRAC K_3=200	3.20	2.85	0.35	0.75	1.15	1.15	1.45	1.70	2.05	2.00	2.15	1.95	0.52	72.49
II U O C	4.05	10.9	14.50	17.60	19.65	21.15	22.50	23.40	24.2	24.55	24.70	25.4	59.83	
OMRAC K_3=200	3.25	9.45	11.1	11.55	11.85	12.65	13.10	13.55	13.75	13.70	13.65	13.55	21.11	64.72

* Refer to case 4.2 K_3=200 ψ = 59.67%

NOMENCLATURE

The nomenclature in use throughout the thesis is given in the following list. Special symbols which appear from place to place are defined where they occur.

English letter symbols

A	Area
A	Constant in Arrhenius equation
A (I,J)	Matrix notation where I and J are the numbers of rows and columns respectively.
a	Catalyst activity (%)
a_i	Constants in parameter space and constraint limit
a_{ij}	Linearised coefficients of process state variable θ_i.
a'_{ij}	Modified linearisation coefficients of process state variable θ_i.
B (I,J)	Matrix notation where I and J are the numbers of rows and columns respectively
B'	Constant in Liapunov function
b	Constant in constraint limit
b	Linearised coefficient of process control variable, m.
b'	Modified linearisation coefficient of process control variable, m.
C	Concentration of reactant in the reactor (mol/litre)
C_o	Concentration of reactant in feed to reactor (mol/litre)
C_r	Optimal model reference concentration (mol/litre)
C_d	Set-point concentration
C_p	Specific heat of reactant (cal/g^{o}C)
C_{pc}	Specific heat of cooling water (cal/g^{o}C)
c_i	Constants of equations (1-1) and (1-2)

D	Derivative controlling action
D(i)	Notation for linearisation coefficients where i is an integar
d_{ij}	Linearised coefficients of process load variables θ_{Li}
d'	Modified linearisation coefficient of process load variable θ_L.
E	Activation energy, a constant (cal/mol)
e	Response error
F	Function
F	Matrix of f_i
F	Inlet flowrate to the reactor (litre/min)
F_c	Cooling water flowrate (litre/min)
F_{cg}	Signal of F_c after VDFG (volts)
$F_{V/I}$	Signal of F_c after V/I converter (ma)
$F_{I/P}$	Signal of F_c after I/P transducer (psig)
F_p	Signal of F_c after valve positioner (psig)
F(J)	Matrix notation where J are the column numbers
F(i)	Notation of function equations
f	Functional equation
f	Function
f_i	Function of simultaneous algebraic equation
G	Function
H	Function
H	Hamiltonian Function
ΔH	Change of enthalpy on reaction (cal/mol)
h	Function
I	Integral controlling action
I	Current (ma)
I	Unit matrix

J	Performance index or objective function
J'	First derivative of J
J''	Second derivative of J
K	Velocity constant (sec^{-1})
K	Gain
K_c	Controller gain
K_v	Control valve gain
K_i	Weighting factors
L	Time constant (sec)
M	Maximum value of m
m	Control variable
m	Control variables of OMR scheme
m^*	Optimal control law of OMR scheme
N	Integers
n	Integers
P	Proportional controlling action
$P(i)$	Notation of weighting factors
P_i	Parameters
P_i^*	Constant normal parameters
Q_g	Rate of heat generation (Kcal x 10^3/h)
Q_c	Rate of heat removal by water cooling coil (Kcal/min)
Q_c^*	Optimal rate of heat removal by water cooling coil (Kcal/min)
Q_{gg}	Signal of Q_g after VDFG (volt)

R	Universal gas constant (cal/ mol ^{o}K)
R	Liapunov stability region
R(I)	Matrix notation where I are the numbers of rows
S	Performance index
s	Laplace transform complex variable
T	Temperature in the reactor (^{o}C or ^{o}K)
T_o	Temperature of feed inlet to reactor (^{o}C or ^{o}K)
T_{cl}	Inlet temperature of cooling water (^{o}C or ^{o}K)
T_c	Outlet temperature of cooling water (^{o}C or ^{o}K)
t	Time (sec)
U_i	Control variables of OAC scheme
U*	Modified optimal control law of OAC scheme
V	Volumetric holdup in reactor (litres)
$\dot{V}$	Liapunov function
V	Voltage (volt)
X	Matrix of x_i
$\overline{X}$	Roots of matrix of f_i
X^i	ith no. of iteration
x_i	variables
Z	Steepest descent slope

Greek letter symbols

α_i, β_i, γ_i, δ_i and ζ_i

Optimal control law coefficients

α_{ij}	Optimal control law coefficients of the OMR scheme
β_{ij}	Optimal control law coefficients of the OAC scheme
β	Time scaling factor

ϵ_i	Weighting factor of optimal integral control
$\Delta(X)$	Change of variable
θ_i	Process state variables
θ_i^*	Optimal process state variables
θ_i^r	Optimal process state variable profiles as OMR
θ_d	Input signal of control system
θ_d	Setpoint of OMR scheme
θ_{Li}	Process load variables
λ	Constant
λ_i	Adjoint variables
Π	Product of variables
ρ	Density of process fluid (gm/cm^3)
ρ_c	Density of cooling water (gm/cm^3)
Σ	Summation
τ	Machine time of X-Y plotting (sec)
ϕ^*	Optimal PID control law
ψ	Optimal adaptivity (%)
ω	Frequency

Subscripts

f	final
i	integers
j	integers
m	maximum
s	steady state
o	initial

Abbreviations

Amp	Amplifier
CSTR	Continuous stirred tank reactor
HG	High gain
Inv	Inverter
MRAC	Model reference adaptive control
OMR	Optimal model reference
OAC	Optimal adaptive control
OMRAC	Optimal model reference adaptive control
mu	Machine unit; 1 mu = 10 volt
PI	Performance index
PR	Performance response
Pot	Potentiometer
TR	Temperature recorder
TRC	Temperature recording controller
US	Unadapted system
UOC	Unadapted optimal control
VR	Variac reading (0-100)
VDFG	Variable diode function generator
[ ]	Scaled computer variable (mu)

BIBLIOGRAPHY

1. Williams, T.J., "IEC Chemical Engineering Reviews Fundamentals Process Control and Automation" Industrial and Engineering Chemistry, 50 (3), 520-524, (March 1958).
2. Ibid., 51 (3), 432-436, (March 1959).
3. Ibid., 52 (2), 183-184, (Feb. 1960).
4. Ibid., 53 (2), 166-168, (Feb. 1961).
5. Ibid., "Annual Review: Computer, Automation, and Process Control" Industrial and Engineering Chemistry, 55,(11), 43-45, (Nov. 1963).
6. Ibid., 56,(11), 47-56, (Nov. 1964).
7. Ibid., 57 (12), 33-43, (Dec. 1965).
8. Ibid., 58 (12), 56-70, (Dec. 1966).
9. Ibid., 59 (12), 53-68, (Dec. 1967).
10. Ibid., 61 (1), 76-89, (Jan. 1969)
11. Ibid., 62 (12), 94-107, (Dec. 1970).
12. Aseltine, J.A., Manici, A.R. and Sarture, C.W., "A Survey of Adaptive Control Systems", IRE Transactions on Automatic Control, 102-108, (Dec. 1958).
13. Eveleigh, V.W., "Adaptive Control Systems", Electro-Technology, Science and Engineering Series 52, pp.79-98, (April 1963).
14. Shinners, S.M., "Optimal and Adaptive Control Systems", Electro-Technology, Science and Engineering Series 67, pp. 63-80 (July 1964).
15. Mishkin, E. and Braun, L. Jr., "Adaptive Control Systems", McGraw-Hill Book Co., (1961).

16. Eveleigh, V.W., "Adaptive Control and Optimization Techniques" Chapter 6 - Chapter 13, McGraw-Hill Book Co. (1967).

17. Oldenburger, R., (Editor), "Optimal and Self-optimizing Control" Chapter 1: Oldenburger, R., A Survey of the literature of optimal and self-optimizing control. pp.1-48. The M.I.T.Press (1966).

18. Ibid., Chapter 32: Draper, C.S. and Li, Y.T., Principles of optimalizing control systems and an application to the internal combustion engine. ASME, Sep.1951, 160pp. Pages 1-16 are reproduced here. The M.I.T.Press (1966).

19. Lee, T.H., Adams, G.E. and Gaines, "Computer Process Control: Modeling and Optimization", Chapter 8, pp.245-276, John Wiley & Sons, Inc., (1968).

20. Chang, S.L., "Synthesis of Optimum Control Systems" Chapters 10 and 11, pp.255-308. McGraw Hill Book Co. (1961).

21. Tou, J.T., "Modern Control Theory", Chapter 7, Section 7.7. pp. 323-337. McGraw-Hill Book Co. Inc. (1964)

22. Sage, A.P., "Optimum Systems Control", Chapter 15, Section 15.3. pp. 507-523. Prentice-Hall Inc. (1968)

23. Ibid., Chapter 14, Sections 14.5 and 14.6, pp.462-478.

24. Prime, H.A., "Modern Concepts in Control Theory", Chapter 6, Section 6.3, pp.161-165, McGraw Hill Book Co. (1969).

25. Whitaker, H.P., Yamron, J., and Kezer,A., "Design of Model-Reference Adaptive Control System for Aircraft", M.I.T. Instrumentation Laboratory Report R-164, September 1958.

26. Bryson, A.E. and Denham, W.F., "A Steepest Ascent Method for solving Optimum Programming Problem", Raytheon Co. Technical Report BR-1303, Aug. 1961.

27. Steinmetz, H.L., "Using the Method of Steepest Descent", Industrial Engineering Chemistry, 58 (1), 33-39, (Jan. 1966).

28. Eveleigh, V.W., "A Comparison of Two Approaches to Extrema Searching Adaptive System", Ph.D. Thesis, Purdue University, Lafayette, Ind., June 1961.

29. Eveleigh, V.W., "General Stability Analysis of Sinusoidal Perturbation Extrema Searching Adaptive System", Proc. 1963 IFAC Conf., Butterworth & Co. (Publishers) Ltd., London.

30. Chao, Y.C., "New Approach to Response Surface Generation by Analogue Computer", British Chemical Engineering, 14 (10), 549-551, (Oct. 1969).

31. Halbert, P.W., "Hybrid Simulation of an Aircraft Adaptive Control System", EAI Applications Reference Library, Application study 3.4.5h. 1963.

32. Kwai, W.H., "A Two-Mode Reference Self-Adaptive Control System", ISA Transaction, 3 (2), 184-192, (April 1964).

33. White, A.J., "Analysis and Design of Model Reference Adaptive Control System", Proceedings IEE, 113 (1), 175-184, (Jan.1966)

34. Drassler, R.M., "An Approach to Model Reference Adaptive Control System", IEEE Trans. Autom.Contr., 12 (1), 75-80, (Feb. 1967).

35. Graupe, D. and Cassir, G.R., "Adaptive Control by Predictive Identification and Optimization", IEEE Trans.Autom.Contr., 12 (2), 191-194, (April 1967).

36. Pearson, A.E. and Noonan, F., "On the Model Reference Adaptive Control Problem", Joint Automatic Control Conference, pp.538-545, (1968).

37. Wilkie, D.F. and Perkins, W.R., "Design of Model Reference System Using the Companion Transformation", Joint Automatic Control Conference, pp.594-595, (1969).

38. Bristal, E.H., Inaloglu, C.F. and Steadman, J.F., "Dynamic Adaptation of Process Controllers by Pattern Recognition" Instru.Contr.System, 43 (3), 101-105, (March 1970).

39. Powell, F.D., "Predictive Adaptive Control", IEEE Trans.Autom. Contr., 14 (5), 550-552, (Oct. 1969).

40. Price, C.F., "An accelerated Gradient Method for Adaptive Control", IEEE Symposium on Adaptive Processes (9th), Decision and Control, pp. lV. 4.1. - lV. 4.10, (1970).

41. Buxton, W.D.T. and Powell, F.D., "A Self-Adaptive Automatic Carrier Landing System (ACLS)", IEEE Symposium of Adaptive Processes (9th), Decision and Control, pp. viii, 5.1 - viii. 5.5. (1970).

42. Monopoli, R.V., "Control of Linear Plants with Zeros and Slowly Varying Parameters", IEEE Trans.Autom.Contr., 12 (1), 80-83, (Feb. 1967).

43. Parks, P.C., "Liapunov Redesign of Model Reference Adaptive Control", IEEE Trans.Autom.Contr., 11 (3), 362-367, (July 1966).

44. Monopoli, R.V., "Liapunov Method for Adaptive Control System Design", IEEE Trans.Autom.Contr., 12 (3), 334-335, (June 1967).

45. Osburn, P.V., Whitaker, H.P. and Kezar, A., "New Development in the Design of Adaptive Control System", Instru. of Aeronautical Science, Paper 61-39.

46. Winsor, C.A. and Roy, R.J., "Design of Model Reference Adaptive Control System by Liapunov's Second Method", IEEE Trans.Autom. Contr., 13 (2), 204, (April 1968).

47. Landau, I.D., "A Hyperstability Criterion for model Reference Adaptive Control Systems", IEEE Trans.Autom. Contr., 14 (5) 552-555, (Oct. 1969).

48. Gromyko, V.P. and Sankovskii, E.A., "Adaptive System with Model and Combined Adjustment", Autom.Remote Contr. (USSR), 30, 1959-64, (1969).

49. Gilbart, J.W., Monopoli, R.V. and Price, C.F., "Improved Convergence and Increased Flexibility in the design on Model Reference Adaptive Control Systems", IEEE Symposium on Adaptive Processes (9th), Decision and Control, pp. iv. 3.1 to iv. 3.10, (1970).

50. Shanein, H.I.H., Ghonaimy, M.A.R. and Shen, D.W.C., "Accelerated Model-Reference Adaptation Via Liapunov and Steepest Descent Design Techniques", IEEE Trans.Autom.Contr. 17 (1), 125-128, (Feb.1972).

51. Womack, B?F., and Watt, J.T., Jr., "A Two Parameter Adaptive System Using a Sinusoidal Test Signal", IEEE Trans. Autom.Contr., 10 (2), 194-197, (April 1965).

52. Kershow, W.V., "Adaptive Control by Plant Identification" Contr.Eng., 12 (9), 103-110, (Sep. 1965).

53. Puri, N.N., "Design of Optimal Adaptive Digital Autopilot" Joint Automatic Control Conference of the American Automatic Control Council, pp.96-107, Section 3E, (1970).

54. Obradovic, I.J., "A New Adaptive Control System Based upon the Areas Enclosed Between the Input and Output Plots", Joint Automatic Control Conference of the American Automatic Control Council, pp.227-236, Section 9E, (1970).

55. Banham, J.W., Jr. and Smith, W.L., "A Practical Approach to Adaptive Control", Control Eng., 13 (5), 97-102, (May 1966).

56. Aoki, M., "On Performance Losses in Some Adaptive Control Systems", Trans.ASME., Ser.D.J. Basic Eng., 87 (1), 90-94 (March 1965).

57. Pearson, A.E. and Sarachik, P.E., "On the Formulation of Adaptive Optimal Control Problems", Trans.ASME, Ser.D.J. Basic Eng., 87 (1), 125-134, (March 1965).

58. Kulikouski, R., "Optimization of Non-linear Random Control Processes", Second IFAC Congress, Butterworths, London, 1965.

59. Pearson, A.E., "Aspects of Adaptive Optimal Steady State Control", Trans.ASME. Ser.D.J. Basic Eng., 90 (2), 201-207, (June 1968).

60. Pearson, A.E., "A Modified Gradient Procedure for Adaptation in Non-linear Control System", Trans.ASME, Ser.D.J. Basic Eng., 92 (2), 322-327, (June 1970).

61. Marcus, R.H. and Hougen, J.O., "An Approach to Adaptive Process Control", CEP Symposium series 46, Vol.59, pp.70-83, (1963).

62. Crandall, E.D. and Stevens, W.F., "An Application of Adaptive Control to a Continuous Stirred Tank Reactor", AIChE.J., 11 (5) 930-936, (Sep. 1965).

63. Casciano, R.M. and Staffin, H.K., "Model Reference Adaptive Control System", AIChE.J., 13 (3), 485-491, (May 1967).

64. Ryan, P.J. and Crandall, E.D., "Multiparameter Adaptive Process via Constrained Objective Functions", AIChE.J., 17 (2), 326-335, (March 1971).

65. Ahlgren, T.D. and Stevens, W.F., "Adaptive Control of a Chemical Process System", AIChE.J., 17 (2), 428-435, (March 1971).

66. Mellichamp, D.A., Coughanowr, D.R. and Koppel, L.B., "Identification and Adaptation in Control Loops with time varying Gain", AIChE.J., 12 (1), 83-89, (Jan. 1966).

67. Chao, Y.C. and Huang, T.S., "Optimal Adaptive Control by Identification", Research Report on Department of Chemical Engineering, National Taiwan University, 1969, (not published).

68. Box, G.E.P. and Chanmugam, E., "Adaptive Optimization of Continuous Processes", I.& E.C. Fundamentals, 1 (1), 2-16, (Feb. 1962).

69. Hoyer, G.G., White, J.W., Foley, G.J. and Altpeter, R.J., "Application of Sinusoidal Perturbation Adaptive Optimization to Chemical Processes", CEP Technical Manual: Systems and process Control, pp.51-64, 1967.

70. Price, R.J. and Rippin, D.W.T., "Single Variable On-Line Adaptive Optimization of Water Gas Shift Reactor", Chem.Eng.Science, 23 (6), 593-617, (Aug. 1968)

71. Weinrich, S.W. and Lapidus, L., "Optimally Sensitive and Adaptive Control System", AIChE.J., 17 (6), 1471-1480, (Nov.1971).

72. Fan, L.T. and co-authors, "The continuous maximum principle" John Wiley & Son Inc. (1966)

73. Koppel, L.B., "Introduction to control Theory", Prentice-Hall Inc. (1968)

74. Lapidus, L. and Luus, R., "Optimal Control of Engineering Process" Balisdell Publishing Co. (1967)

75. Roberts, S.M., "Dynamic Programming in Chemical Engineering and Process Control."
Academic Press Inc. (1964)

76. Chao, Y.C., "Optimal Design of Process Control System by Dynamic Programming", National Science Council, Engineering Science Research Center, Republic of China, 1969

77. Denn, M.M., and Douglas, J.M., "Optimal Design and Control by Variational method", Ind.and Eng.Chem., 57 (11), 18-31, (Nov. 1965).

78. Tou, Julius T., "Modern control Theory", pp.225-259, McGraw Hill Book Co. Inc., 1964.

79. Shih, Y.P., "Integral Action in the Optimal Control of linear Systems with Quadratic Performance Index", Ind. and Eng.Chem. Fundamentals, 9 (1), 35-37, (Feb.1970).

80. Buxton, B., "The Study of the Process Dynamics and Control of a continuous stirred tank reactor using a partial simulation technique", Ph.D.Thesis, March 1971, The University of Aston in Birmingham.

81. Ogata, K., "Modern Control Engineering", pp.96-105, Prentice-Hall Inc., 1970.